Étude de l'influence de la glutaminolyse des macrophages dans les maladies cardio-métaboliques

Johanna Merlin

UNIVERSITÉ CÔTE D'AZUR

ÉCOLE DOCTORALE
SCIENCES DE LA VIE ET DE LA SANTÉ

THÈSE DE DOCTORAT

Étude de l'influence de la glutaminolyse des macrophages dans les maladies cardio-métaboliques

Johanna MERLIN

Centre Méditerranéen de Médecine Moléculaire (C3M)

Présentée en vue de l'obtention du grade de docteur en Sciences de la Vie et de la Santé. Spécialité : Interactions Moléculaires et Cellulaires **d'**Université Côte d'Azur

Dirigée par : Dr. **Laurent YVAN-CHARVET** et Dr. **Stoyan IVANOV**

Soutenue le : 25 Septembre 2020

Devant le jury, composé de :

Dr. **Myriam AOUADI**, DR, KI

Dr. **Fabienne FOUFELLE**, DR INSERM, CRC

Dr. **Xavier PRIEUR**, MCU, IRS-UN

Dr. **Jean-Ehrland RICCI**, DR INSERM, C3M

Pr. **Bart STAELS**, PR INSERM, IPL

erc

Étude de l'influence de la glutaminolyse des macrophages dans les maladies cardio-métaboliques

Jury:

Président du jury :

Dr. Jean-Ehrland RICCI, Directeur de recherche INSERM, Centre Méditerranéen de Médecine Moléculaire, Université Côte d'Azur

Rapporteurs :

Dr. Myriam AOUADI, Principal Investigator, Institut Karolinska

Dr. Xavier PRIEUR, Maître de Conférences, HDR, Institut du thorax IRS – UN, Université de Nantes

Examinateurs :

Dr. Fabienne FOUFELLE, Directeur de recherche INSERM, Centre de Recherche des Cordeliers, Sorbonne université

Pr. Bart STAELS, Professeur INSERM, Institut Pasteur de Lille, Université Lille Nord de France

Directeurs de thèse :

Dr. Laurent YVAN-CHARVET, Directeur de recherche INSERM, Centre Méditerranéen de Médecine Moléculaire, Université Côte d'Azur

Dr. Stoyan IVANOV, Chargé de recherche INSERM, Centre Méditerranéen de Médecine Moléculaire, Université Côte d'Azur

Résumé

Les maladies chroniques inflammatoires telles que l'obésité ou l'athérosclérose constituent un problème majeur de santé publique dans les pays occidentaux. Il est désormais bien établi que les cellules immunitaires, et en particulier les macrophages, jouent un rôle essentiel dans l'initiation et la progression de ces maladies métaboliques. En effet, les macrophages résidents au sein des tissus contrôlent leur homéostasie comme par exemple l'expansion du tissu adipeux viscéral ou la thermogenèse du tissu adipeux brun. Cependant, les mécanismes restent mal compris. L'immuno-métabolisme est un nouveau domaine de recherche qui illustre l'adaptabilité des macrophages à leur environnement nutritionnel pour le maintien de leurs fonctions. Nous nous sommes ainsi intéressés au rôle de la glutamine dans l'homéostasie des macrophages et son impact sur l'obésité et l'athérosclérose. Pour cela, nous avons génétiquement supprimé l'enzyme limitante hydrolysant la glutamine en glutamate, appelée glutaminase 1 (Gls1), spécifiquement au sein des cellules myéloïdes.

Dans notre première étude, nos données démontrent que l'absence de Gls1 dans les cellules myéloïdes conduit à une intolérance au glucose sous régime riche en graisses, associée à une diminution des niveaux de norépinephrine dans le tissu adipeux brun conduisant alors à un défaut de thermogenèse. Nos résultats mettent en évidence une diminution de l'adhésion des macrophages de la moelle épinière aux neurones glutamatergiques et diminuant ainsi l'activation de ces derniers. Notre étude démontre donc le rôle de la glutaminolyse des macrophages dans le contrôle du tonus sympathique des tissus adipeux thermogéniques.

Dans un second temps nous avons étudié l'impact la glutaminolyse des cellules myéloïdes sur le développement de l'athérosclérose. L'invalidation de la glutaminolyse des cellules myéloïdes entraîne une augmentation de la surface de la plaque athéromateuse. En particulier, nous avons pu observer une augmentation de la nécrose des plaques suggérant une nouvelle fonction de la glutaminolyse des macrophages. Nous avons également pu valider cette association dans des plaques athéromateuses humaines. Bien que la déficience en Gls1 dans les macrophages n'altère pas leur survie, nous avons pu mettre en évidence un rôle clé de cette voie dans le processus d'efférocytose. L'analyse des mécanismes en aval a révélé une altération de la polarisation alternative des macrophages chez ces souris associée à une reprogrammation du métabolisme mitochondrial. La modulation de ces voies conduit à une baisse d'activité de Rac1 expliquant ainsi le défaut d'efférocytose. Ainsi, notre seconde étude identifie la glutaminolyse des cellules myéloïdes comme un acteur essentiel dans le développement des maladies cardiovasculaires.

Mots clés : Macrophage, Glutamine, Glutaminolyse, Obésité, Athérosclérose

Summary

Chronic inflammatory diseases such as obesity or atherosclerosis are a major public health concern in the western countries. It is now well established that immune cells, and in particular macrophages, play a critical role in the initiation and progression of cardiometabolic diseases. Indeed, tissue resident macrophages control tissue homeostasis such as visceral adipose tissue expansion and brown adipose tissue thermogenesis. However, the underlying mechanisms remain unknown. Immuno-metabolism is a new research area that illustrates macrophage adaptability to their nutritional environment for their function maintenance. We therefore looked at the role of glutamine in macrophage homeostasis and its impact on obesity and atherosclerosis. Therefore, we genetically abolished the limiting enzyme hydrolyzing glutamine to glutamate, called glutaminase 1 (Gls1), specifically in myeloid cells.

In our first study, our data demonstrate that Gls1 deficiency in myeloid cells leads to glucose intolerance on a high-fat diet. This is associated with a decrease in norepinephrine levels in brown adipose tissue leading to defective thermogenesis. Our results highlight a decrease in spinal cord macrophage adhesion to glutamatergic neurons leading therefore to a decrease in neuron activation. Thus, our study demonstrates the role of macrophage glutaminolysis in controlling the sympathetic tone of thermogenic adipose tissue.

Secondly, we studied the impact of myeloid cell glutaminolysis on atherosclerosis development. Glutaminolysis invalidation in myeloid cells leads to an increase atherosclerotic plaque area. In particular, we observed an increase in plaque necrosis suggesting a new function for macrophage glutaminolysis. We also validated this association in human atheromatous plaques. Although Gls1 deficiency in macrophages does not affect their survival, we showed a key role of this pathway in efferocytosis. Further analyses of the downstream mechanisms revealed an alteration in macrophage alternative polarization associated with mitochondrial metabolism reprogramming. Modulation of these pathways leads to a drop in Rac1 activity, thus explaining the efferocytosis defect. Therefore, our second study identifies myeloid cell glutaminolysis as an essential actor in atherosclerosis development.

Key words: Macrophage, Glutamine, Glutaminolysis, Obesity, Atherosclerosis

Je suis de ceux qui pensent que la science est d'une grande beauté.
Un scientifique dans son laboratoire est non seulement un technicien :
il est aussi un enfant placé devant des phénomènes naturels
qui l'impressionnent comme des contes de fées.
- Marie Curie

Aucun de nous, en agissant seul, ne peut atteindre le succès.
- Nelson Mandela

Ce n'est pas la fin. Ce n'est même pas le commencement de la fin.
Mais, c'est peut-être la fin du commencement.
- Winston Churchill

Remerciements

Aux membres du jury,

Je tiens tout d'abord à remercier l'ensemble des membres du jury d'avoir accepté de juger mon travail de thèse. Un grand merci au **Dr. Jean-Ehrland Ricci** pour avoir accepté de présider mon jury. **Dr. Myriam Aouadi** et **Dr. Xavier prieur**, merci pour votre temps, vos remarques pertinentes et vos conseils. **Dr. Fabienne Foufelle** et **Pr. Bart Staels**, merci d'avoir accepté d'examiner mon travail de thèse.

A mon comité de suivi de thèse,

Je remercie sincèrement les membres de mon comité de suivi de thèse d'avoir accepté d'évaluer mes travaux au cours de ces trois années. **Laurent,** merci pour tes retours, tes nombreux conseils et tes encouragements. **Dr. Emmanuel Gauthier**, merci pour tout le temps consacré à l'avancée de ce projet, les critiques constructives et les conseils.

A mes directeurs de thèse,

Laurent, je te remercie de m'avoir fait confiance dès le master avec ce projet ambitieux que j'affectionne tant. Ta manière d'expliquer si simplement la complexité de la science m'a conquise dès le premier entretien de master. Je te remercie pour ta patience, tes conseils, ton soutien, ton implication et ta disponibilité depuis mes débuts dans l'équipe. Tout simplement, merci pour tout.

Stoyan, Stojean, merci de m'avoir formé depuis mes débuts en master quand tout me semblait encore impossible à réaliser. Tu as été mon mentor et je suis plus que reconnaissante d'avoir appris aux côtés d'une personne si brillante. Merci pour ta formation, ton aide, tes conseils, tes corrections, ta disponibilité, tes musiques en boucle, tes blagues et pour la bonne ambiance que tu sais mettre dans le bureau. Je te dois beaucoup, merci.

A ceux qui ont pu travailler à mes côtés,

Rodolphe, je tiens à te remercier pour tes nombreuses discussions qui ont permis de faire avancer le projet. Merci pour ton aide précieuse depuis le master et tes conseils avisés. Ta passion pour la science m'a toujours inspirée ! Je te souhaite plein de bonheur pour la suite !

Alexandre, tu as commencé en étant mon master 1 et aujourd'hui tu es devenu un thésard hors norme. Ton implication dans les projets et ta réflexion te promettent une réussite certaine. Merci pour ton aide, ta discographie, tes blagues et ta bonne humeur.

Manon, merci de ton accueil et de ton aide quand je suis arrivée au labo en master. Ce fut un plaisir de travailler à tes côtés.

Julie, je te remercie pour ton aide sur les manips ou je n'en voyais pas le bout. Je te souhaite du succès dans ta nouvelle aventure professionnelle.

Nathalie, merci pour ton aide, ta gentillesse et ta bonne humeur au quotidien.

Bastien, merci pour ta bonne humeur et ta motivation. Je te souhaite une thèse fructueuse !

Emma, **Gaël**, **Florent**, **Narges**, même si nous n'avons pas vraiment travaillé ensemble sur les projets, je vous remercie pour le temps que nous avons passé ensemble. Je vous souhaite le meilleur pour la suite.

A ceux qui sont devenus plus que des collègues,

Marion A, merci pour l'aide précieuse que tu as su m'apporter quand tu faisais encore parti de la Team 13. Mais aussi après, quand tu nous as quitté mais que rien n'a changé. Merci pour ta bonne humeur, tes rires, tes bruits de bouche improbables et tes sursauts inappropriés.

Marion S, stunette, nous avons parcouru cette expérience côte à côte, et j'en suis reconnaissante. Et n'oublie pas, « quand on commence à aimer les fusées, on finit souvent sur la lune ». Tu es dans la dernière ligne droite, ne lâche rien !

Sébastien, je te remercie pour tous les complexes que tu as su m'apporter. Plus sérieusement, merci de me pousser toujours plus haut dans la vie comme dans la science. Merci pour tes rires, ta bonne humeur et tous tes conseils.

Adélie, merci de m'avoir toujours encouragée et aidée au labo. Tu m'as beaucoup appris, notamment à réussir un western blot et ce n'était pas gagné !! Encore merci pour tes corrections du manuscrit et ton aide pour la soutenance. Je te dois beaucoup. Merci pour tous les moments partagés ensemble et bien sûr, merci de me faire découvrir chaque jour de nouvelles bières au goût fantastique !

Alexia, 647, quand tu es arrivée tu nous as soulagé d'un travail monstre. Je te remercie pour ton aide au quotidien depuis ton arrivée. Je te remercie pour tous les bons moments que l'on a pu passer en dehors du labo, à boire, à manger, à rire. J'espère qu'il y en aura encore plein d'autres à venir.

Alexandre B., même si nous n'avons pas travaillé longtemps ensemble à cause des conditions, j'ai été très heureuse de te connaître. Merci pour ta bonne humeur et pour tous les moments passés ensemble. Je te souhaite plein de bonheur et de réussite pour la suite.

A tous ceux du centre avec qui j'ai pu partager,

Je tiens sincèrement à remercier **l'équipe de la gestion**, en particulier **Carole** pour ton aide durant ces nombreuses années et **Dominique** pour toutes tes blagues du Vendredi. De même, merci **Émilie** pour ta gentillesse et **Jean** pour ta bonne humeur au quotidien. Merci aux responsables de plateformes, **Marie** pour ton aide en microscopie ainsi que **Véronique** et l'ensemble de l'**équipe animalerie** pour votre bienveillance.

Merci à **Philippe G.** pour m'avoir soutenue depuis mes débuts en master, **Mireille** pour tes discussions et tes conseils, **Stéphan** pour ton aide en microscopie. Je tiens à remercier tous les autres membres du C3M avec qui j'ai pu travailler et discuter : **Pierre**, **Elodie**, **Marina**, **Marion**, **Manon**, **Stephie**, **Déborah R**, **Déborah V**, **Carmelo**, **Océane**, **Victor**, **Julie**, **Fred**, **Karine**, **Jérôme**, **Sophia**, **Mélanie**, **Sophie**, **Jennifer**, **Adriana**.

A mes amis,

Marie, je te remercie pour ton aide depuis le master. Tu m'as toujours poussée plus haut que je ne pouvais m'imaginer, et si aujourd'hui j'ai une thèse, c'est en partie grâce à toi. Merci pour tous ces bons moments passés ensemble, au restaurant, au bar, à me faire découvrir tous les jolis spots autour de Nice, à rire, à profiter de la vie tout simplement.

Coraline, ça n'a pas toujours été facile entre la thèse et la distance mais tu as toujours été là. Merci à toi et **Fabien** pour tous les moments que nous avons passés ensemble.

Andréa, **Pauline**, **Manon**, **Johanna**, je vous remercie pour tous vos encouragements et pour tous nos moments inoubliables passés ensemble depuis la licence. Merci d'être qui vous êtes.

A ma famille,

Je remercie avant tout mon **grand-père**, ce n'est pas toujours facile d'expliquer ce que l'on fait mais tu as toujours cherché à comprendre, jusqu'à lire ma thèse en détail, et ce n'était pas rien ! Merci pour tes discussions, tes conseils et tes encouragements. A ma **grand-mère**, bien que je ne sois que peu présente tu es toujours là pour moi quand j'en ai besoin. A mes **parents**, vous m'avez toujours poussé vers le haut, et j'espère vous avoir rendu fiers aujourd'hui. Merci à tous les membres de ma famille, **Benjamin**, **Jordan**, **Elodie**, pour tout ce que vous faites au quotidien pour moi. Enfin, **Alexis**, merci pour ton soutien dans les moments de stress, de fatigue, tout autant que dans les moments de joie. Merci de toujours me pousser à voir plus grand.

Valorisation

A. Publications

- **Biology and function of adipose tissue macrophages, dendritic cells and B cells.** Ivanov S, **Merlin J**, Lee MKS, Murphy AJ, Guinamard RR. Atherosclerosis. 2018 Apr;271:102-110. doi: 10.1016/j.atherosclerosis.2018.01.018.

- **Mesothelial cell CSF1 sustains peritoneal macrophage proliferation.** Ivanov S, Gallerand A, Gros M, Stunault MI, **Merlin J**, Vaillant N, Yvan-Charvet L, Guinamard RR. Eur J Immunol. 2019 Nov;49(11):2012-2018. doi: 10.1002/eji.201948164.

- **Le sommeil protège-t-il nos vaisseaux sanguins ?** Yvan-Charvet L, **Merlin J**. Med Sci (Paris). 2019 Oct;35(10):743-746. doi: 10.1051/medsci/2019147.

- **ABCA1 Exerts Tumor-Suppressor Function in Myeloproliferative Neoplasms**. Viaud M, Abdel-wahab OO, Gall J, Ivanov S, Guinarmard RR, Sore S, **Merlin J**, Ayrault M, Guilbaud E, Jacquel A, Auberger P, Wang N, Levine RL, Tall AR, Yvan charvet L. 2020 Mar 10;30(10):3397-3410.e5. doi: 10.1016/j.celrep.2020.02.056.

- **Myeloid Cell Diversity and Impact of Metabolic Cues during Atherosclerosis.** Gallerand A*, Stunault MI*, **Merlin J*,** Guinamard RR, Yvan-Charvet L, Ivanov S. Immunometabolism.2020;2(4):e200028. doi: 10.20900/immunometab20200028.

- **Spinal cord macrophage glutaminolysis controls glucose homeostasis by supporting sympathetic tone of thermogenic adipose depots. Merlin J***, Ivanov S*, Sergushichev A, Ayrault M, Vaillant N, Gilleron J, Cormont M, Tanti JF, Dumas K, Ohanna M, Masson J, Gaisler-Salomon I, Rayport S, Re DB, Gautier EL, Guinamard RR, Artyomov MN, Yvan-Charvet L.. En préparation.

- **Non-canonical transamination metabolism of glutamine sustains efferocytosis by coupling oxidative stress buffering to oxidative phosphorylation. Merlin J***, Ivanov S*, Sergushichev A, Gall J, Stunault MI, Ayrault M, Swain A, Orange F, Gallerand A, Gautier EL, Berton T, Martin JC, Carobbio S, Masson J, Gaisler-Salomon I, Maechler P, Rayport S, Sluimer JC, Biessen EAL, Guinamard RR, Thorp EB, Artyomov MN, Yvan-Charvet L. En préparation.

- **Adipose Tissue Lipolysis Regulates Monocyte Pool Dynamics in a Circadian Manner.** Stunault MI, Gallerand A, **Merlin J**, Luehmann HP, Khedher N, Jalil A, Dolfi B, Castiglione A, Ayrault M, Vaillant N, Gilleron J, Mack M, Masson D, Liu Y, Guinamard RR, Yvan-Charvet L, Ivanov S. En préparation.

B. Communications orales

- **Myeloid cell glutaminolysis controls monocyte numbers and macrophage efferocytosis during atherosclerosis. Johanna Merlin**, Stoyan Ivanov, Rodolphe R. Guinamard and Laurent Yvan-Charvet. Symposium Inflammation and Disease. Avril 2018, Nice, France.

- **Myeloid cell glutaminolysis controls monocyte numbers and macrophage efferocytosis during atherosclerosis. Johanna Merlin**, Stoyan Ivanov, Rodolphe R. Guinamard and Laurent Yvan-Charvet. Nouvelle Société Française d'Athérosclérose (NSFA). Juin 2019, Biarritz, France.

- **Myeloid cell glutaminolysis controls monocyte numbers and macrophage efferocytosis during atherosclerosis. Johanna Merlin**, Stoyan Ivanov, Marion I. Stunault, Marion Ayrault, Rodolphe R. Guinamard, and Laurent Yvan-Charvet. 3rd Symposium of the Occitanie network on Monocytes-Macrophages (SOMM). Novembre 2019, Montpellier, France.

- **How a Seahorse helped me understand macrophage glutaminolysis. Johanna Merlin**. Agilent Cell Analysis Seminar and Seahorse XF Workshop. Mars 2020, Nice, France.

C. Communications affichées

- **Myeloid cell glutaminolysis controls monocyte numbers and macrophage efferocytosis during atherosclerosis. Johanna Merlin**, Stoyan Ivanov, Alexey Sergushichev, Rodolphe R. Guinamard, Maxim N. Artyomov and Laurent Yvan-Charvet. European Atherosclerosis Society (EAS). Mai 2018. Lisbonne, Portugal. ePoster.

- **Myeloid cell glutaminolysis controls macrophage functions during obesity**. **Johanna Merlin**, Stoyan Ivanov, Rodolphe R. Guinamard and Laurent Yvan-Charvet. Nouvelle Société Française d'Athérosclérose (NSFA). Juin 2018, Biarritz, France.

- **Myeloid cell glutaminolysis controls monocyte numbers and macrophage efferocytosis during atherosclerosis. Johanna Merlin**, Stoyan Ivanov, Rodolphe R. Guinamard and Laurent Yvan-Charvet. Journées de l'écolde doctorale (JEDNs). Mai 2019, Nice, France.

- **Myeloid cell glutaminolysis controls monocyte numbers and macrophage efferocytosis during atherosclerosis. Johanna Merlin**, Stoyan Ivanov, Rodolphe R. Guinamard and Laurent Yvan-Charvet. Nouvelle Société Française d'Athérosclérose (NSFA). Juin 2018, Biarritz, France.

- **Dormir pour un corps en bonne santé. Johanna Merlin**, Sébastien Le Garf, Marion Stunault. Fête de la sciences 2019. Nice, France.

Table des matières

Liste des illustrations

Liste des tables

Liste des abréviations

A

α-KG : alpha-kétoglutarate
AAV : Virus Adéno-Associé
ABCA1/G1 : Cassette de liaison à l'ATP A1/G1
ACC1 : Acétyl-CoA Carboxylase 1
ACLY : ATP Citrate Lyase
AdExos : Exosomes adipocytaires
AG : Acide Gras
AGPAT : AcylGlycérol Phosphate AcylTransférase
AMPc : Adénosine Monophosphate Cyclique
AMPK : AMP-activated Protein Kinase
ApoA1 : Apolipoprotéine A1
ApoE : Apolipoprotéine E
ApoER2 : Apolipoprotéine Receptor-2
Arg1 : Arginase 1
ARN : Acide Ribonucléique
ASL : Argininosuccinate Lyase
Atf2 : Activating transcription factor 2
ATGL : Adipose Triglyceride Lipase
ATM : Macrophage du Tissu Adipeux
ATP : Adénosine Triphosphate

B

BMDM : Macrophage dérivé de la moelle osseuse

C

CANTOS : Canakinumab Anti-inflammatory Thrombosis Outcome Study
CAR : Cellules Réticulaires Abondantes en CXCL12
CARKL : Carbohydrate Kinase-Like
CCL : C-C Motif Chemokine Ligand
CCR : C-C Chemokine Receptor
CD : Cluster de Différentiation
Cdc42 : Cell division cycle 42
CDP : Précurseur de Cellules Dendritiques Communes
CETP : Protéine de Transfert des Esters de Cholestérol
Cidea : Cell Death Inducing DFFA Like Effector A
CLP : Progéniteur Commun Lymphoïde
CLS : Crown Like Structures
CM : Chilomicrons
CML : Cellule Musculaire Lisse
cMop : Précurseur de Monocytes Communs
CMP : Progéniteur Commun Myéloïde
Cpt1 : Carnitine palmitoyl-transferase
CREB : C-AMP Response Element-Binding Protein
CRP : Protéine C Réactive
CSF-1 : Colony Stimulating Factor 1
CSF1R : Colony Stimulating Factor 1 Receptor
CSH : Cellule Souche Hématopoïétique
CXCL : C-X-C Motif Chemokine Ligand
CXCR : C-X-C Motif Chemokine Receptor

D

DAG : DiAcylglycérol
DGAT : Diacylglycérol Acyltransférase

E

E : jour Embryonnaire
EMP : Précurseur Érythro-Myéloïde
ETC : Chaine de Transport d'Électrons

F

FAS : Fatty Acid Synthase
FATP1 : Fatty Acid Transport Protein 1
FDA : Food and Drug Administration
Fructose-6P : Fructose-6-Phosphate
FSV : Fraction Stroma-Vasculaire

G

G-3-P : Glycérol-3-Phosphate
GFAT : Glutamine-Fructose-6-Phosphate Amidotransférase
Gln : Glutamine
Gls : Glutaminase
Glu : Glutamate
Glud1 : Glutamate déhydrogénase
GLUT : Glucose Transporter
GM-CSF : Granulocyte-Macrophage Colony-Stimulating Factor
GMP : Progéniteur des Granulocytes/Macrophages
GOT : Glutamate-Oxaloacétate Transaminases
GPAT : Glycérol Phosphate AcylTransférase

GS : Glutamine Synthétase
GSH : Glutathion réduit
GSSG : Glutathion oxydé

H

HDL : Lipoprotéine de Haute Densité
HDL-c : HDL cholestérol
HIF-1α : Hypoxia-Inducible Factor 1 alpha
HL : Lipase Hépatique
HSPC : Cellules Souches et Progénitrices Hématopoïétiques

I

ICAM : Intracellular Adhesion Molecule
IDH : Isocitrate Déshydrogénase
IDL : Lipoprotéine de Densité Intermédiaire
IFNAR : Interferon-alpha/beta Receptor
IFNγ : Interféron gamma
IGF : Insulin-like Growth Factor
IL : Interleukine
IL-1R : Interleukin-1 Receptor
ILC : Cellule Lymphoïde Innée
IMC : Indice de Masse Corporelle
iMo : Monocyte inflammatoire
IRS1 : Insulin Receptor Substrate 1

J

JMJ : Jumonji

K

KGA : Kidney-type Glutaminase

L

LAL : Lipase Acide Lysosomale
LAPV : Low Attenuation Plaque Volume
LDL : Lipoprotéine de Basse Densité
LDL-c : LDL cholestérol
LDLR : Récepteur aux Lipoprotéines de Basse Densité
LGA : Liver-type Glutaminase
LHS : Lipase Hormono-Sensible
LOX-1 : Lectin-type Oxidized LDL Receptor 1
LPA : Acide Lysophosphatidique
LPL : Lipoprotéine Lipase
LPS : Lipopolysaccharides
LT-CSH : CSH à Long Terme
LysoPC : Lysophosphatidylcholine

M

M-CSF : Macrophage Colony-Stimulating Factor
MCP-1 : Macrophage Chemoattractant Protein 1
MCV : Maladies Cardiovasculaires
MDP : Progéniteur Monocytes-Macrophages/Cellules Dendritiques
MerTK : Myeloid-epithelial-reproductive Tyrosine Kinase
MGL : MonoGlycéride Lipase
Mgl1/2 : Macrophage galactose N-acetyl-galactosamine–specific lectins 1/2
Mme : Macrophage activé métaboliquement
MPP : Progéniteur multipotent
Mrc1/2 : Mannose receptor C type 1/2
mTOR : mammalian Target of Rapamycin

N

NAFLD : Non Alcoholic Fatty Liver Disease
NE : Norépinephrine
NF-κb : Facteur nucléaire-kappa B
NLRP3 : NOD-like Receptor family, Pyrin domain containing 3
NO : Oxyde Nitrique
NR4A1 : Nuclear Receptor Subfamily 4 Group A Member 1

O

OAT : Ornithine Aminotransferase
OCDE : Organisation de Coopération et de Développement Économiques
OMS : Organisation Mondiale de la Santé
OOA : Oxaloacétate
oxLDL : LDL oxydé

P

P2RX5 : Purinergic Receptor P2X 5
PA : Acide Phosphatidique
PAK1 : P21-Activated Kinase 1
PAMPs : Motifs Moléculaires Associés aux Pathogènes
PAP : Phosphate de l'Acide Phosphatidique
PCSK9 : Proprotéine Convertase Subtilisine/Kexine de type 9
PFK-2 : Phosphofructokinase-2
PGC-1β : Peroxisome proliferator-activated receptor Gamma Coactivator 1 beta
PKA : Protéine Kinase A

pMo : Monocytes patrouilleurs
PPAR : Peroxisome Proliferator-Activated Receptor
Ppargc1-α : Peroxisome proliferator activated receptor gamma coactivator 1-alpha
Prdm16 : PR-domain containing 16
PS : Phosphatidylsérine

R

R5P : Ribose-5-Phosphate
Rac1 : Ras-Related C3 Botulinum Toxin Substrate 1
RE : Réticulum Endoplasmique
RNI : Intermédiaires Réactifs de l'Azote
ROS : Espèces Réactives de l'Oxygène

S

SCF : Stem-Cell Factor
SDH : Succinate Déshydrogénase
Sema : Sémaphorine
SLC : Solute Carrier
SR-A : Scavenger Receptor-A
SR-BI : Scavenger Receptor class B type I
ST-CSH : CSH à Court Terme
STAT6 : Signal Transducer and Activator of Transcription 6

T

TA : Tissu Adipeux
TAM : Tyr3, Axl, MerTK
TET : Ten-Eleven Translocation
TG : Triglycéride
TGF-β : Transforming Growth Factor beta
Th : Tyrosine hydroxylase
Th1 : T helper de type 1
TIM : T cell Immunoglobulin Mucin domain 1
TLR : Récepteur de type Toll
TNF-α : Facteur de Nécrose Tumorale alpha
TPO : Thrombopoïétine

U

UCP1 : Uncoupling Protein 1
UDP-GlcNAc : Uridine Diphosphate N-acetylglucosamine

V

VCAM-1 : Vascular Cell Adhesion Molecule
VEGF : Vascular Endothelial Growth Factor
VLDL : Lipoprotéine de Très Basse Densité
VLDLR : Récepteur aux VLDL

Introduction

Chapitre I : L'obésité, un problème de santé publique

A. Définition

L'obésité est une maladie qui se caractérise par une accumulation anormale ou excessive de graisse corporelle pouvant nuire à la santé. L'indice de masse corporelle (IMC) est une métrique internationale utilisée pour estimer la quantité de masse grasse corporelle chez les adultes. L'IMC est calculée en divisant le poids (en kilogrammes) par la taille (en mètres) au carré. La classification en fonction des valeurs de l'IMC est présentée ci-dessous (Table 1).

Table 1 : Classification de l'IMC selon l'OMS.

Valeur de l'IMC (en Kg/m²)	**Classification**
<18.5	Insuffisance pondérale
18-24.9	Corpulence normale
25-29.9	Surpoids
30-34.9	Obésité de classe I (modérée)
35-39.9	Obésité de classe II (sévère)
>40	Obésité de classe III (morbide)

Cette classification n'est cependant pas toujours optimale. Elle ne peut pas s'appliquer aux enfants (0-18 ans) et ne prend pas en compte la composition corporelle (masse maigre/masse grasse) ni la répartition du tissu adipeux. On distingue deux types d'obésité selon la répartition des graisses, l'obésité gynoïde où l'excès de graisse se situe sur le bas du corps généralement au niveau des fesses et des cuisses, et l'obésité androïde où l'excès de masse graisseuse se trouve au niveau de l'abdomen. De récentes études ont montré que l'obésité androïde était associée à de nombreuses pathologies indépendamment de l'IMC. C'est pourquoi le tour de taille des patients est un second critère pris en compte lors de l'estimation de l'obésité. Un tour de taille supérieur à 100 cm chez l'homme et 88 cm chez la femme est ainsi considéré comme une obésité abdominale.

B. Épidémiologie

L'obésité est aujourd'hui considérée comme un problème majeur de santé publique. En effet, la prévalence de l'obésité a considérablement augmenté ces dernières années, en particulier dans les pays industrialisés. D'après l'organisation mondiale de la santé (OMS), le nombre de cas d'obésité a presque triplé depuis 1975. En 2016, 1,9 milliards de personnes de plus de 18 ans étaient en surpoids ou obèses dans le monde représentant respectivement 39% et 13% de la population. En France, l'étude Esteban-2015 indique que 32% de la population adulte est en surpoids et que 17% des adultes sont concernés par l'obésité sans distinction entre hommes et femmes. L'OCDE (Organisation de Coopération et de Développement Économiques) estime que d'ici 2030, 47% des adultes américains pourraient être obèses contre 21% des adultes français.

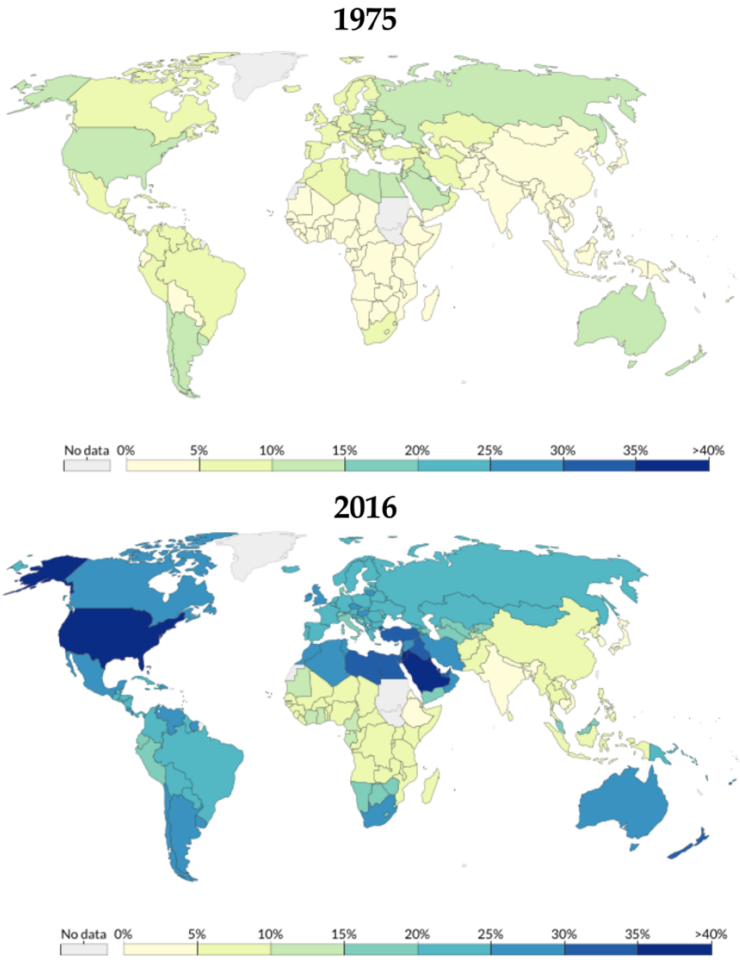

Figure 1 : Pourcentage d'adultes obèses dans le monde en 1975 et en 2016 selon L'OMS

C. Morphologie des différents tissus adipeux

Chez les mammifères, il existe plusieurs types de tissus adipeux (TA) qui se distinguent par leurs morphologies, localisations, origines développementales et fonctions distinctes : le TA blanc, brun et beige.

1. *Le tissu adipeux blanc*

Chez l'Homme, le TA blanc constitue la majorité du TA total. Cet organe représente 10 à 20% du poids corporel chez un individu sain. Chez la plupart des espèces, le TA blanc est divisé en deux sous-groupes : le TA sous-cutané et le TA viscéral (Pond, 1992). Le TA sous-cutané est distribué différemment selon l'âge et le sexe des individus. Chez l'homme le TA sous-cutané est retrouvé au niveau de la nuque, des épaules et du ventre, tandis que chez la femme ce tissu prédomine au niveau des hanches, des fesses et des cuisses. Le TA viscéral, quant à lui, est un tissu profond qui entoure les viscères. Le TA viscéral est lui-même constitué du TA mésentérique, qui entoure l'intestin, du TA omental, qui couvre l'abdomen et, chez les rongeurs du TA périgonadal, qui entoure les gonades. Chez la souris, les dépôts adipeux blancs se développent à différents stades de la vie (Han et al., 2011). En effet, les adipocytes sous-cutanés se forment pendant la période périnatale, tandis que les TA viscéraux se développent après la naissance (Wang et al., 2013). En revanche, chez l'Homme, les TA blancs sont totalement développés à la naissance (Feng et al., 2013; Poissonnet et al., 1984).

Morphologiquement, le tissu adipeux blanc est essentiellement composé d'adipocytes qualifiés d'adipocytes blancs puisqu'ils contiennent une seule grosse gouttelette lipidique qui occupe 90% du cytoplasme, un noyau périphérique, peu de mitochondries et un petit réticulum endoplasmique (RE). Les adipocytes blancs sont maintenus ensemble par un tissu conjonctif peu vascularisé et innervé (Mattson, 2010). En plus des adipocytes, le TA blanc contient également des cellules immunitaires, des fibroblastes et des cellules endothéliales. Cet ensemble de cellules, nécessaire à l'homéostasie du tissu est appelé la fraction stroma-vasculaire (FSV). Le TA blanc est caractérisé par une grande capacité de stockage. Il permet le stockage d'énergie sous forme de triglycérides (TG), qui peuvent être libérés sous forme d'acides gras (AG) en cas de besoin énergétique.

2. *Le tissu adipeux brun*

Le TA brun est présent principalement chez les mammifères hibernants. Chez l'Homme, il est retrouvé chez les nouveau-nés, et devient moins développé à l'âge adulte (Chechi et al., 2014). Chez l'adulte le TA brun peut être détecté dans la région supra-claviculaire, cervicale, périrénale et médiastinale (Cypess et al., 2009; Nedergaard et al., 2007; van Marken Lichtenbelt et al., 2009). Chez les rongeurs, le TA brun est le premier TA à se former. Il se développe durant l'embryogenèse, permettant ainsi une thermogenèse fonctionnelle dès la naissance (Wang and Seale, 2016). Pendant longtemps, il était pensé que les adipocytes bruns et blancs dérivaient d'un adipoblaste commun. Cependant, les adipocytes bruns dérivent d'une population progénitrice multipotente qui exprime En1 (Engrailed Homeobox 1), Pax7 (Paired Box 7) et Myf5 (Myogenic factor 5) (Lepper and Fan, 2010; Seale et al., 2008). En effet, pendant l'embryogenèse, ces progéniteurs se différencient en pré-adipocytes bruns qui eux-mêmes vont se différencier en adipocytes bruns matures et exprimer les marqueurs caractéristiques Ucp1 (Uncoupling Protein 1), Cidea (Cell Death Inducing DFFA Like Effector A), Ppargc1-α (Peroxisome proliferator activated receptor gamma coactivator 1-α), Prdm16 (PR-domain containing 16), Dio2 (type II deiodinase) ou encore P2RX5 (Purinergic Receptor P2X 5) (Harms and Seale, 2013; Ussar et al., 2014).

Le TA brun joue un rôle crucial dans la génération de chaleur par la thermogenèse non frissonnante en réponse à un environnement froid par l'intermédiaire d'Ucp1. Le TA brun est constitué d'adipocytes bruns et de la FSV. Les adipocytes bruns sont morphologiquement différents des adipocytes blancs. En effet, ils contiennent de nombreuses petites gouttelettes lipidiques, un noyau central, un RE sous développé et de nombreuses mitochondries, ce qui leur donnent une apparence histologique multiloculaire et brune. De plus, le TA brun est hautement vascularisé et innervé (Mattson, 2010). Bien que l'innervation du TA brun par le système nerveux sympathique soit validée (Bartness TJ, 2005), l'innervation de ce tissu par le système parasympathique reste controversée.

3. *Le tissu adipeux beige*

En réponse à une exposition au froid, le TA blanc sous-cutané peut, lui aussi, adopter un phénotype brun par un processus nommé le « beiging ». Suite à un stimulus, les adipocytes blancs sous-cutanés acquièrent les caractéristiques morphologiques et fonctionnelles des adipocytes bruns, c'est pourquoi ils sont appelés adipocytes beiges (Barreau et al., 2016). Après le processus de beiging, les adipocytes beiges se retrouvent avec un grand nombre de mitochondries et de gouttelettes lipidiques dans leur cytoplasme et expriment les marqueurs caractéristiques des adipocytes bruns (Chen et al., 2016; Harms and Seale, 2013; Lo and Sun, 2013). Bien que les adipocytes bruns et beiges partagent de nombreuses caractéristiques, ces deux types d'adipocytes possèdent des caractéristiques phénotypiques et fonctionnelles distinctes. Cependant, l'origine cellulaire des adipocytes beiges reste encore incertaine. Une fois l'exposition au froid terminée, les adipocytes beiges peuvent de nouveau changer de phénotype et présenter les caractéristiques d'un adipocyte blanc (Rosenwald et al., 2013). Ainsi, les adipocytes beiges sont dotés d'un phénotype flexible selon leur environnement, leur permettant à la fois de stocker de l'énergie tels les adipocytes blancs et de générer de la chaleur tels les adipocytes bruns.

D. Fonction des tissus adipeux

1. *Un organe de stockage d'énergie*

Pour pouvoir survivre, les êtres vivants ont besoin d'énergie, apportée à l'organisme par l'alimentation. Les adipocytes permettent de stocker l'excès de calories sous forme de lipides par un processus nommé la lipogenèse *de novo* (Bjorntorp and Sjostrom, 1978). En situation de jeûne, les adipocytes peuvent relarguer ces lipides sous forme d'AG par la lipolyse, permettant ainsi de fournir de l'énergie à l'organisme. Cependant, quand les apports énergétiques sont plus importants que les dépenses énergétiques, le tissu adipeux blanc prend du volume ce qui conduit à l'obésité.

i. La lipogenèse

La lipogenèse *de novo* est une voie métabolique qui permet le stockage des glucides en excès issus de l'alimentation sous forme d'AG. Ces AG synthétisés vont pouvoir être transformés en TG qui seront stockés dans les adipocytes. Dans des conditions physiologiques, la lipogenèse *de novo* est active majoritairement au niveau du foie et du tissu adipeux (Hollands and Cawthorne, 1981). La lipogenèse est réalisée au cours d'une successions de réactions enzymatiques permettant la conversion du flux de carbones du glucose en AG (Ameer et al., 2014). Pour commencer, le glucose issu de l'alimentation va entrer dans la cellule par l'intermédiaire du transporteur GLUT4 (Glucose transporter type 4), qui est sous le contrôle de l'insuline (Leto and Saltiel, 2012). Puis, le glucose va être transformé en pyruvate par la glycolyse, qui entrera dans la mitochondrie, puis dans le cycle de Krebs pour donner du citrate. Ce citrate est transporté vers le cytosol puis converti en acétyl-CoA par l'ATP citrate lyase (ACLY). Ensuite, l'acétyl-CoA carboxylase 1 (ACC1) va permettre la conversion de l'acétyl-CoA en malonyl-CoA qui est lui-même converti en palmitate en sept cycles réactionnels par l'acide gras synthase (FAS : fatty acid synthase), l'enzyme limitante de la lipogenèse *de novo*. Enfin, le palmitate va subir des réactions d'élongation et de désaturation pour générer des acides gras complexes (Ameer et al., 2014).

En parallèle, la réaction de glycolyse permet la génération de glycérol-3-phosphate (G-3-P) nécessaire à la synthèse de triglycérides. Grâce aux acyl-CoA produits par l'activation des acides gras lors de la lipogenèse, le G-3-P est transformé en acide lysophosphatidique (LPA) par l'enzyme glycérol phosphate acyltransférase (GPAT) au sein du réticulum endoplasmique. Le LPA est ensuite converti en acide phosphatidique (PA) par l'acylglycérol phosphate acyltransférase (AGPAT). Le phosphate de l'acide phosphatidique (PAP) déphosphoryle la PA et forme du diacylglycérol (DAG). Pour finir, le DAG est converti en triglycérides par la diacylglycérol acyltransférase (DGAT) (Ahmadian et al., 2007). Ces réactions régulées positivement par l'insuline sont essentielles pour permettre le stockage d'énergie dans l'organisme.

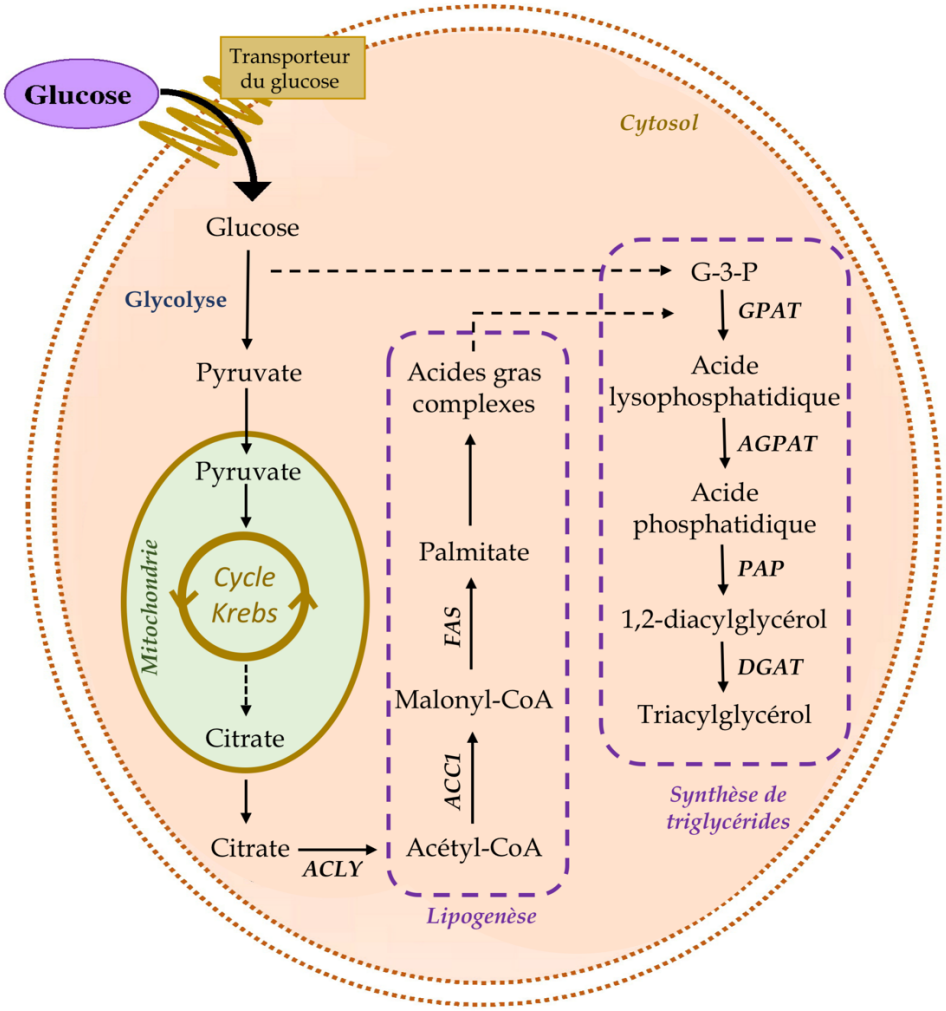

Figure 2 : La lipogenèse *de novo* et la synthèse de triglycérides

Adapté de Ameer et al., 2014 (Ameer et al., 2014) et Ahmadian et al., 2007. (Ahmadian et al., 2007)

ii. La lipolyse

En période de besoin énergétique, comme pendant le jeûne ou pendant une activité physique, le corps puise dans les réserves de graisses pour fournir de l'énergie à l'organisme. Pour ce faire, les TG stockés au sein des adipocytes peuvent être rapidement mobilisés sous forme d'acides gras et de glycérol durant le processus de lipolyse. Ce processus fait intervenir trois enzymes différentes : l'adipose triglyceride lipase (ATGL), qui est l'enzyme limitante de la lipolyse, la lipase hormono-sensible (HSL) et la monoglycéride lipase (MGL). Les TG sont hydrolysés en réponse à des signaux cataboliques tels que la noradrénaline, l'adrénaline et le glucagon. Au cours de ce processus, les TG sont transformés en diglycérides par l'ATGL, puis

en monoglycérides par la HSL et enfin en AG et en glycérol par la MGL (Bolsoni-Lopes and Alonso-Vale, 2015). Le glycérol est redirigé vers le foie pour être métabolisé en glucose par la néoglucogenèse. Les AG libérés dans le sang sont transportés par l'albumine (Jeppesen and Kiens, 2012) vers des tissus périphériques, notamment le foie et les muscles pour subvenir à leurs besoins métaboliques.

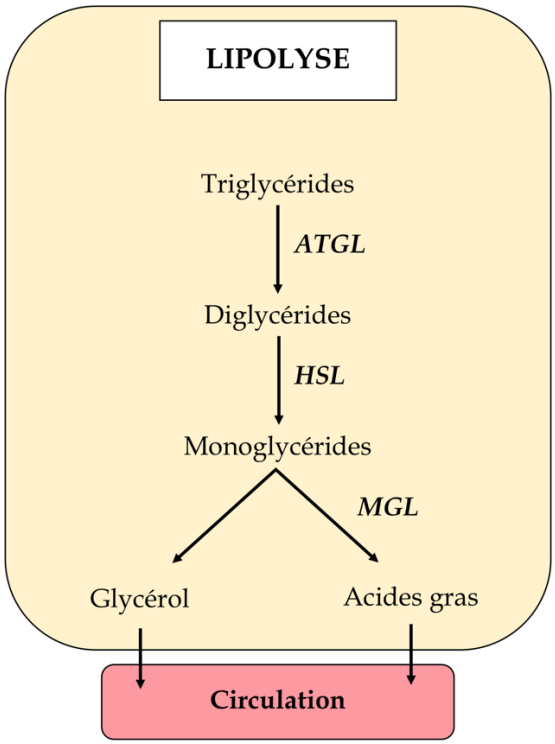

Figure 3 : La voie de la lipolyse
Adapté de Townsend et al., 2017. (Townsend et al., 2017)

Cependant, la lipolyse adipocytaire ATGL dépendante n'est pas la seule forme de lipolyse existante. En effet, plusieurs autres sortes de lipolyse sont caractérisées : la lipolyse endothéliale, la lipolyse hépatique, la lipolyse lysosomale et enfin la production d'acide gras de manière lipolyse indépendante (Figure 4).

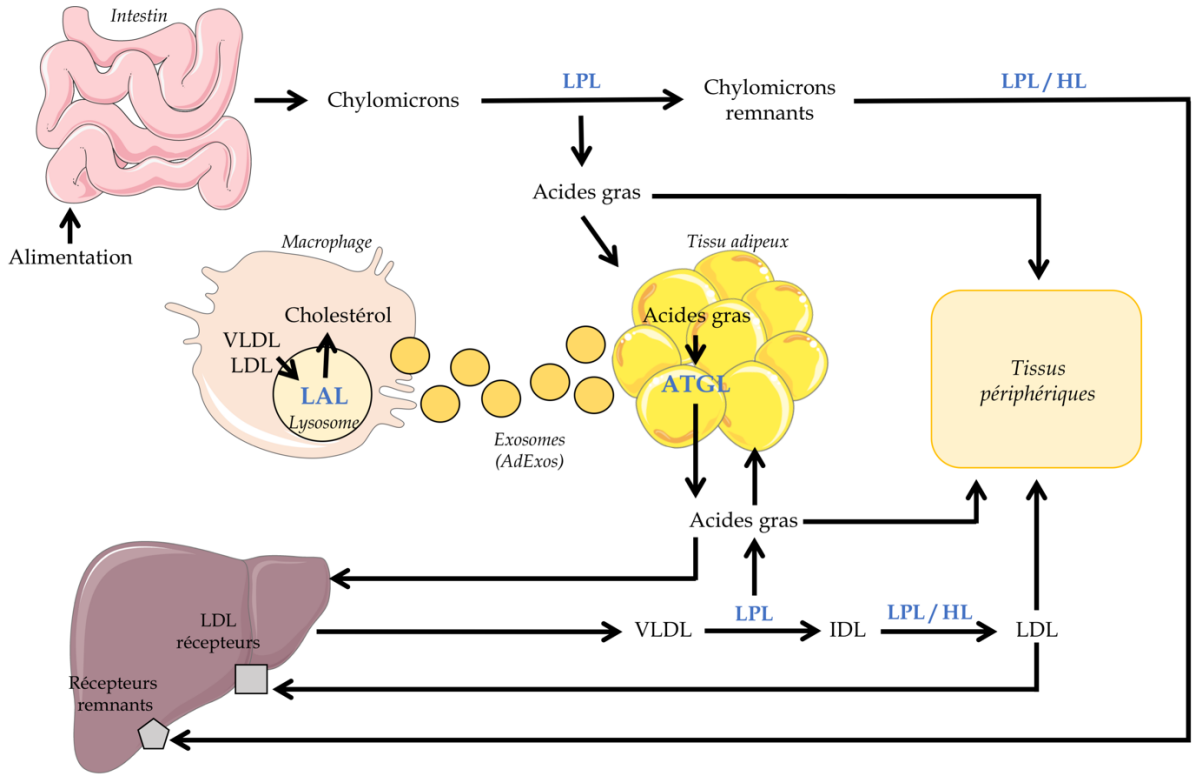

Figure 4 : Les différentes forme de lipolyse

Adapté de Kobayashi et al., 2015. (Kobayashi et al., 2015)

La lipolyse endothéliale est médiée par la lipoprotéine lipase (LPL) qui se trouve du côté luminal des capillaires sanguins. La LPL hydrolyse les TG contenus dans les lipoprotéines de très basse densité (VLDL) et les chylomicrons (CM), libérant ainsi des acides gras et générant des lipoprotéines de basse densité (LDL) (Basu and Goldberg, 2020). La lipase hépatique (HL) est une enzyme catalysant l'hydrolyse des TG et des phospholipides dans les lipoprotéines de haute densité (HDL) et les lipoprotéines riches en TG. L'une des principales fonctions de la HL est la conversion des lipoprotéines de densité intermédiaire (IDL) en LDL. La déficience en HL entraine une hyperlipidémie, avec de taux plasmatiques élevés de HDL enrichis en phospholipides et TG (Carmena, 2019). La lipolyse lysosomale est, quant à elle, médiée par la lipase acide lysosomale (LAL). Cette enzyme hydrolyse, au sein du lysosome, les esters de cholestérol et les TG contenus dans les VLDL et Les LDL endocytés, permettant ainsi l'exportation du cholestérol libre produit (Gomaraschi et al., 2019; Ouimet et al., 2011). La mutation perte de fonction de LIPA, le gène codant pour la LAL, engendre des troubles sévères avec une accumulation d'esters de cholestérol et de TG dans les hépatocytes et les

macrophages, provoquant des lésions tissulaires importantes (Bernstein et al., 2013; Reiner et al., 2014). Enfin, les adipocytes peuvent libérer des exosomes remplis de lipides (AdExos) qui sont capturés localement par les macrophages du tissu adipeux (ATM). Ces AdExos fournissent des acides gras qui sont alors hydrolysés par les macrophages et conduisent à leur différenciation au sein du tissu (Flaherty et al., 2019).

iii. L'hypertrophie et l'hyperplasie des adipocytes

La quantité de TG stockés au sein des adipocytes dépend de l'équilibre entre la lipogenèse et la lipolyse. Lorsque les adipocytes stockent plus de TG qu'ils n'en libèrent, lors d'une augmentation des apports caloriques et/ou d'une diminution de l'activité physique, le bilan énergétique est positif. Un bilan énergétique positif prolongé induit une augmentation de l'adiposité et conduit au développement de l'obésité (Guyenet and Schwartz, 2012). L'expansion du tissu adipeux peut être médiée à la fois par une hypertrophie des adipocytes, c'est à dire une augmentation de la taille des adipocytes et une hyperplasie des adipocytes, c'est à dire une augmentation du nombre d'adipocytes (Haczeyni et al., 2018). Cependant, les nombreux mécanismes moléculaires contrôlant l'expansion des adipocytes ne sont toujours pas complètement connus. Dans un premier temps, les souris nourries avec un régime riche en graisses vont favoriser l'hypertrophie. En cas de régime prolongé, une fois la limite de volume atteinte par les adipocytes, l'adipogenèse *de novo* commence et permet la formation de nouveaux adipocytes permettant d'augmenter la capacité de stockage (Joe et al., 2009; Wang et al., 2013). Chez l'Homme, les troubles métaboliques sont principalement déclenchés par l'hypertrophie des adipocytes et le nombre d'adipocytes entre des personne saines et obèses reste le même (Spalding et al., 2008). En effet, l'hypertrophie adipocytaire est généralement associée aux complications métaboliques et à un risque accru de développer un diabète de type 2 (Longo et al., 2019). L'hypertrophie adipocytaire est ainsi considérée comme le principal mode d'expansion du TA chez l'adulte (Kim et al., 2014).

2. *Un organe endocrinien*

Historiquement, le tissu adipeux était considéré comme un simple organe de stockage d'énergie. Cependant, la découverte de la leptine, une cytokine sécrétée par les adipocytes, a révolutionné ce domaine. En effet, il est maintenant démontré que les adipocytes peuvent sécréter un grand nombre de peptides et de lipides régulateurs, nommé adipokines et lipokines respectivement. Ces molécules, sécrétées à la fois par les adipocytes et les cellules de la FSV, peuvent agir sur les cellules voisines ou les cellules d'autres organes par des actions endocrines, paracrines et autocrines. Ces facteurs régulent l'équilibre énergétique, l'homéostasie lipidique et glucidique, mais aussi l'inflammation au sein du tissu adipeux (Trayhurn and Wood, 2004). Les adipocytes sécrètent de nombreuses hormones endocrines ayant des effets sur d'autres organes (Figure 5). Les deux hormones principales sécrétées par les adipocytes sont la leptine et l'adiponectine. La leptine, sécrétée en réponse à l'apport alimentaire, inhibe l'appétit et stimule la satiété *via* les récepteurs du système nerveux central (Friedman, 2016). Les souris déficientes pour la leptine (ob/ob) ou pour le récepteur à la leptine (db/db) sont extrêmement obèses en raison de leur appétit incontrôlé (Chen et al., 1996; Pelleymounter et al., 1995). De plus, la leptine augmente la température corporelle, améliore la résistance périphérique à l'insuline (Scheja and Heeren, 2019) et stimule l'inflammation (Fantuzzi and Faggioni, 2000). Les niveaux de leptine circulante sont en corrélation positive avec la masse du TA. Ainsi, au cours de l'obésité, les niveaux de leptine circulante sont élevés mais la résistance à la leptine hypothalamique aggrave l'obésité en inhibant le contrôle de l'appétit et l'oxydation des lipides (Munzberg et al., 2004; Myers et al., 2010). L'adiponectine, quant à elle, est une adipokine retrouvée en abondance dans le sang (Scherer et al., 1995). Cette adipokine a des propriétés anti-obésité et antidiabétique et atténue la résistance à l'insuline en stimulant l'oxydation des lipides et les réponses anti-inflammatoires (Berg et al., 2001; Folco et al., 2009; Yamauchi et al., 2002). De plus, l'adiponectine régule l'expression des molécules d'adhésion à la surface de l'endothélium et permet ainsi d'inhiber le recrutement des monocytes (Tilg and Moschen, 2006). En effet, les souris déficientes pour l'adiponectine sont résistantes à l'insuline et au glucose, et présentent une augmentation des taux de TNF-α (Tumor Necrosis Factor-α) plasmatiques et une diminution des taux d'IRS1 (Insulin Receptor Substrate 1) et FATP1 (Fatty Acid Transport

Protein 1) dans les muscles (Kubota et al., 2002; Maeda et al., 2002; Nawrocki et al., 2006). De plus, les souris déficientes pour l'adiponectine présentent plus de formations néointimales au sein des artères fémorales, prouvant le rôle protecteur de l'adiponectine dans l'athérosclérose (Kubota et al., 2002; Maeda et al., 2002). Chez les personnes obèses, l'adiponectine est grandement diminuée et ceci contribue au développement des maladies cardio-métaboliques liées à l'obésité (Fang and Judd, 2018).

Enfin, d'autres adipokines et lipokines sécrétées par les adipocytes agissent également sur les différents organes du corps, comme nous pouvons le voir dans la Figure 5. Ainsi, l'identification des nombreuses adipokines et lipokines a révélé le rôle majeur de la fonction sécrétoire du TA dans la régulation de l'inflammation et du métabolisme.

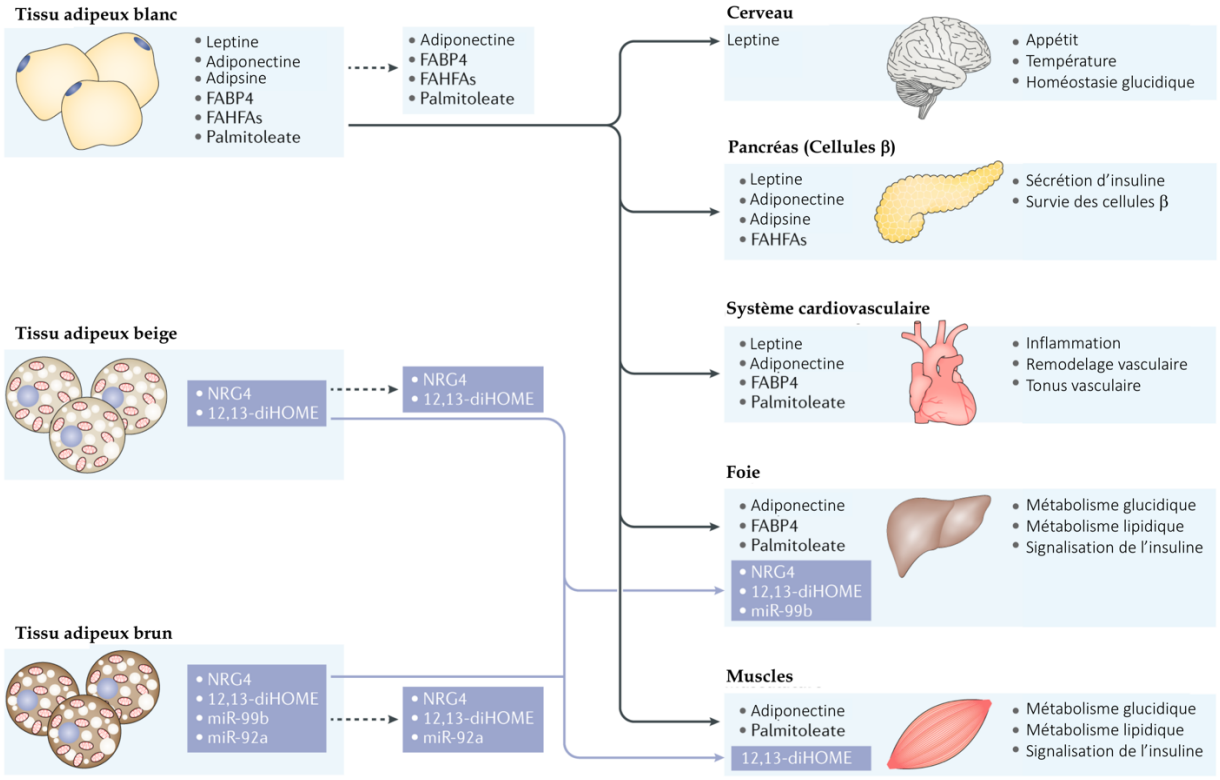

Figure 5 : Effets endocriniens des facteurs sécrétés par les adipocytes.

Adapté de Scheja et al., 2019. (Scheja and Heeren, 2019)

3. *Un organe thermique*

Suite à une exposition à un environnement froid, ou à la baisse de la température corporelle, la thermogenèse non frissonnante peut avoir lieu au sein du tissu adipeux brun et beige. La thermogenèse est médiée par une protéine de la membrane mitochondriale, fortement exprimée dans le TA brun : l'UCP1 (Ricquier and Kader, 1976). L'UCP1 est un découpleur de la respiration mitochondriale qui dissipe le gradient de protons généré par la chaine respiratoire en permettant l'entrée des protons dans la matrice mitochondriale sans synthèse d'ATP (Adénosine Triphosphate). Le principal régulateur de la thermogenèse est le système nerveux sympathique. En effet, les neurones sensoriels à la surface du corps, activés par le froid, transmettent le message au cerveau. Les terminaisons nerveuses sympathiques présentes dans le tissu adipeux bruns vont ainsi libérer de la noradrénaline qui se fixe au niveau des récepteurs β-adrénergiques. La liaison de la noradrénaline avec les récepteurs adrénergiques active la voie du récepteur couplé aux protéines G qui implique une élévation de l'adénosine monophosphate cyclique (AMPc) puis de la protéine kinase A (PKA) (Figure 6). La PKA va d'une part activer HSL qui va permettre la lipolyse des TG et la libération d'AG libres, et d'autre part phosphoryler les protéines CREB (C-AMP Response Element-Binding Protein) et P38. La phosphorylation de P38 entraine à son tour la phosphorylation de ATF2 (Activating Transcription Factor 2) et de PGC1α. CREB et ATF2 favorisent directement l'expression de PGC1α qui est aussi, une fois phosphorylé, le co-activateur de PPARγ (Peroxisome Proliferator-Activated Receptor) et de PPARα pour la transcription d'UCP1. UCP1 migre vers la mitochondrie où l'oxydation des lipides permet l'augmentation de la fuite de protons à travers UCP1 sur la membrane interne des mitochondries, afin d'augmenter la génération de chaleur (Wang et al., 2019). La souris déficiente pour UCP1 (UCP1 KO) a été développé en 1997 (Enerback et al., 1997). Les souris UCP1 KO sont sensibles à l'exposition aigüe au froid, prouvant ainsi le rôle d'UCP1 dans la thermogenèse non frissonnante (Enerback et al., 1997). Cependant, si la température est progressivement diminuée, les souris UCP1 KO s'acclimatent et deviennent tolérantes au froid (Golozoubova et al., 2001; Keipert et al., 2017; Meyer et al., 2010; Ukropec et al., 2006). Des mécanismes compensatoires ou indépendants d'UCP1 peuvent donc avoir lieu pour maintenir la thermogenèse. L'une des hypothèses est que le tremblement musculaire permet la génération de chaleur suite à une activité contractile

chronique chez ces souris. Cependant, les données sur la hausse de l'activité métabolique du muscle squelettique chez les souris UCP1 KO sont contradictoires (Golozoubova et al., 2001; Meyer et al., 2010; Mineo et al., 2012; Monemdjou et al., 2000; Shabalina et al., 2010; Ukropec et al., 2006). De plus, le degré de frisson entre les souris sauvage et UCP1 KO est relativement identique, que les souris soient exposées au froid de manière aigüe ou progressive (Golozoubova et al., 2001). Le tremblement musculaire ne peut donc pas être le seul mécanisme permettant l'adaptation des souris UCP1 KO. L'une des particularités des souris UCP1 KO est leur résistance à l'obésité suite à un régime riche en graisse dans des contions d'hébergement à des températures standards (20-24°C) (Enerback et al., 1997). Les souris UCP1 KO sont protégées de l'obésité induite par l'alimentions puisqu'elles utilisent des voies thermogéniques alternatives qui nécessitent la dissipation de plus de calories pour produire la même quantité de chaleur, et maintenir leur température corporelle (Anunciado-Koza et al., 2008). Au fil des années, plusieurs mécanismes de thermogenèse indépendant d'UCP1 ont pu être mis en lumière. La phosphocréatine est une source d'énergie permettant de générer de l'ATP au sein du muscle squelettique au cours de l'activité physique (Bogdanis et al., 1996). Ce cycle futile, retrouvé au sein des mitochondries des adipocyte beiges (Kazak et al., 2015), est capable d'induire la thermogenèse même en absence d'UCP1 (Bertholet et al., 2017). La suppression de la glycine amidinotransférase, l'enzyme permettant la synthèse de créatine, diminue les niveaux de créatine dans le TA brun et entraine une intolérance au froid sans changement d'UCP1 au sein du TA brun (Kazak et al., 2017). De plus, un rôle du transport du calcium dans la thermogenèse non frissonnante a été proposé à la fois dans les muscles et le TA brun. En effet, la libération du calcium du réticulum endoplasmique (ou sarcoplasmique pour le muscle) permettrait la thermogenèse par l'ATPase SARCA (de Meis, 2003; de Meis et al., 2006; Periasamy et al., 2017). Le cycle du calcium peut être régulé par le phospholamban, qui est surexprimé dans le TA beige des souris UCP1 KO (Ukropec et al., 2006). De même, un cycle futile de lipolyse et ré-estérification permet le processus de thermogenèse indépendamment d'UCP1. Au cours de ce cycle, la lipolyse permet la formation d'AG et de glycérol à partir des TG stockés dans les adipocytes et est suivie simultanément d'une ré-estérification des AG par le G-3-P permettant ainsi la libération d'ATP (Mottillo et al., 2014). Enfin, les mitochondries sont capables de faire circuler les protons indépendamment d'UCP1 et pourraient donc permettre la thermogenèse indépendamment d'UCP1 (Smith et al., 2002).

Ainsi, la régulation de la thermogène est un processus complexe réalisé par plusieurs voies de régulation qui se compensent pour maintenir la chaleur corporelle.

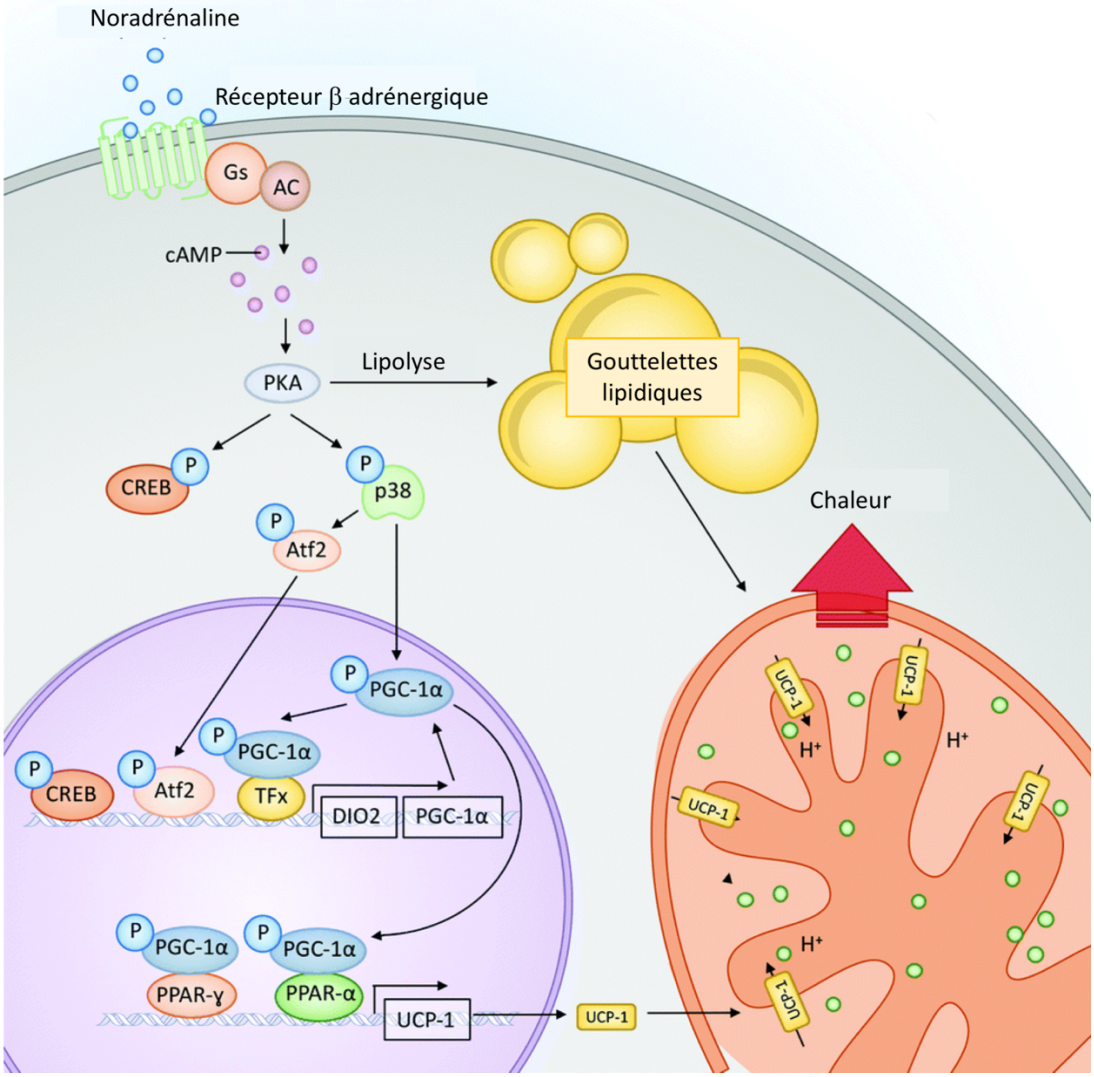

Figure 6 : Principe de la thermogenèse dépendante d'UCP1 dans les adipocytes

Adapté de Wang et al., 2019. (Wang et al., 2019)

E. Complications liées à l'obésité

L'obésité contribue au développement de nombreuses complications métaboliques et physiologiques comme l'arthrite, les maladies du foie gras non alcoolique (NAFLD) et certains types de cancers (colorectaux, prostate, rein, sein, col de l'utérus, ovaires). La principale conséquence de l'obésité est le développement du syndrome métabolique. Le syndrome métabolique est défini comme une combinaison de troubles médicaux tels qu'une obésité abdominale, une hypertriglycéridémie, une résistance à l'insuline, une intolérance au glucose, une augmentation de la pression artérielle, une augmentation de mauvais cholestérol (LDL-c) et des niveaux réduits de bon cholestérol (HDL-c) (Wilborn et al., 2005). La présence d'au moins trois de ces troubles médicaux constitue un diagnostic clinique (Alberti et al., 2009). Les dyslipidémies observées au cours de l'obésité jouent un rôle majeur pour le développement des maladies cardiovasculaires. Il est maintenant démontré que plus l'IMC est haut, plus le risque de développer un diabète de type 2 augmente (Williams and Kelley, 2000). Le diabète de type 2 est induit par la mauvaise utilisation des sucres au sein de l'organisme. Il est estimé que 75% des personnes diabétiques sont obèses. Le diabète peut lui-même conduire à différentes pathologies comme des maladies rénales, ophtalmologiques et cardiovasculaires (Bailes, 2002). Le développement des maladies cardiovasculaires est fortement corrélé avec l'augmentation de l'adiposité viscérale (Buchholz and Bugaresti, 2005). L'hypercholestérolémie et l'hypertriglycéridémie chronique conduisent au développement de l'athérosclérose en formant des plaques d'athéromes au sein des artères (Williams and Kelley, 2000).

Chapitre II : L'athérosclérose, la maladie des artères

L'athérosclérose est une maladie inflammatoire chronique qui se caractérise par l'accumulation progressive de lipides et de cellules inflammatoires dans l'intima des artères de moyen et gros calibre (Badimon et al., 2009). L'athérosclérose implique en premier lieu une expansion sur plusieurs décennies de l'intima artérielle. Bien que ce processus initial n'entraine généralement aucun symptôme, lorsque la maladie évolue, ces lésions peuvent entrainer divers évènements vasculaires nuisibles tels que des maladies coronariennes, des accidents vasculaires cérébraux, des maladies artérielles périphériques ou encore des problèmes rénaux selon les artères touchées (Hansson, 2005).

A. Épidémiologie

Bien que les causes exactes du développement de l'athérosclérose restent inconnues, certains facteurs de risque peuvent augmenter le risque de développer la maladie. Parmi les facteurs de risque les plus connus tels que l'hypertension, le tabagisme, l'obésité ou encore l'âge, le plus important reste le taux élevé de mauvais cholestérol (LDL) et la diminution du bon cholestérol (HDL) dans le sang (Rafieian-Kopaei et al., 2014). Dans la circulation sanguine, 70% du cholestérol se retrouve sous une forme estérifiée au sein des lipoprotéines. La classification des lipoprotéines est basée sur leur densité. Nous retrouvons les lipoprotéines de haute densité (HDL) appelées bon cholestérol, qui captent l'excès de cholestérol des cellules périphériques afin de le transporter jusqu'au foie pour sa dégradation. Les lipoprotéines de basse densité (LDL), appelées mauvais cholestérol, sont captées par les organes extra-hépatiques et peuvent, selon l'environnement, s'oxyder (LDLox). Les lipoprotéines de très basse densité (VLDL) permettent le transport des TG et du cholestérol synthétisés par le foie vers les tissus périphériques. Les lipoprotéines de densité intermédiaire (IDL) issues des VLDL, sont métabolisées par les tissus ou forment des LDL. Enfin, les chylomicrons (CM) transportent les TG et le cholestérol issus de l'alimentation vers les tissus périphériques (Rafieian-Kopaei et al., 2014). L'excès de cholestérol total et de LDL, ainsi que la carence en HDL constitue un facteur de risque pour l'athérosclérose (Table 2).

Table 2 : Taux de cholestérol circulant chez les personnes saines ou à risque.
D'après Hao et Friedman, 2014. (Hao and Friedman, 2014)

Classe	Taux chez personnes saines	Taux chez personnes à haut risque
HDL	> 50 mg/dL	< 40 mg/dL
LDL	< 100 mg/dL	≥ 190 mg/dL
Cholestérol total	< 200 mg/dL	≥ 240 mg/dL

Au cours des 50 dernières années, l'identification de facteurs de risque, les progrès cliniques et les avancées scientifiques ont contribué à la diminution de l'incidence des maladies cardio-vasculaires (MCV) malgré l'augmentation de l'espérance de vie (Elizabeth G. Nabel, 2012). Cependant, malgré cette diminution de la mortalité par MCV dans les pays développés, les MCV restent la principale cause de décès dans le monde devant les cancers. Selon l'OMS, en 2017 on estimait à 17,7 millions le nombre de décès dus aux MCV, soit 31% de la mortalité mondiale totale. Les prédictions tendent même à penser que les MCV resteront la première cause de mortalité d'ici 2030, avec près de 23,6 millions de morts par an.

B. Description de la pathologie

1. *Initiation*

L'implication de l'endothélium vasculaire dans le développement de l'athérosclérose est connue depuis maintenant longtemps (Virchow, 1856). De par son activité métabolique, l'endothélium vasculaire joue un rôle déterminant dans le contrôle de l'homéostasie vasculaire, le tonus vasculaire, la fluidité, la coagulabilité du sang et dans l'adhésion cellulaire (Born GVR, 1997). L'endothélium vasculaire est contraint à des forces mécaniques hémodynamiques conférées par le flux sanguin, avec lequel il est en contact direct, qui peuvent altérer la structure et la fonction des cellules endothéliales (Gimbrone et al., 2000; Williams and Tabas, 1995). Les LDL sont les transporteurs du cholestérol dans la paroi artérielle. Le point initiateur de l'athérosclérose est la rétention sous-endothéliale de LDL contenant de l'apolipoprotéine-B au niveau de zones de turbulences, comme les coudures et les bifurcations des artères. Dans le microenvironnement de la paroi artérielle, les

lipoprotéines retenues vont alors être sensibles à diverses modifications. Les LDL seront biochimiquement modifiées par des protéases et des lipases entrainant ainsi leur agrégation et une liaison accrue aux protéoglycanes empêchant leur retour du tissu vers la circulation sanguine (Pentikainen et al., 2000). Ces lipoprotéines vont aussi subir des modifications oxydatives par la myéloperoxydase, la lipoxygénase et les espèces réactives de l'oxygène conduisant à la formation de LDLox, rendant ainsi les particules de lipoprotéines pro-inflammatoires (Hansson and Hermansson, 2011).

L'accumulation des LDL déclenche l'activation des cellules endothéliales qui vont alors exprimer et sécréter différentes sortes de molécules, telles que des sélectines (Sélectine E/P) (Gebuhrer et al., 1995), des molécules d'adhésions (Intracellular Adhesion Molecule 1 : ICAM-1 (Collins et al., 2000), Vascular Cell Adhesion Molecule : VCAM-1 (Cybulsky and Gimbrone, 1991; Dansky et al., 2001; Khan et al., 1995)) et des facteurs chémoattractants (Macrophage Chemoattractant Protein 1 : MCP-1 (Gosling et al., 1999; Gu et al., 1998), Interleukine-8 : IL-8 (Subbanagounder et al., 2002)) permettant l'entrée et la rétention des monocytes au sein de l'intima (Figure 7). Une fois la barrière endothéliale passée, les monocytes infiltrés se différencient en macrophages en réponse à la production locale de M-CSF (Macrophage Colony-Stimulating Factor) (Qiao et al., 1997). Ce programme de différenciation entraine une augmentation de l'expression de récepteurs dits « scavengers » tels que CD36 (Cluster de différentiation 36) (Febbraio et al., 2000; Kunjathoor et al., 2002), SR-A (Scavenger Receptor-A) (Suzuki et al., 1997), LOX-1 (Lectin-type Oxidized LDL Receptor 1) (Oka et al., 1998) et d'autres récepteurs aux LDL qui entrainent l'internalisation des LDLox par les macrophages.

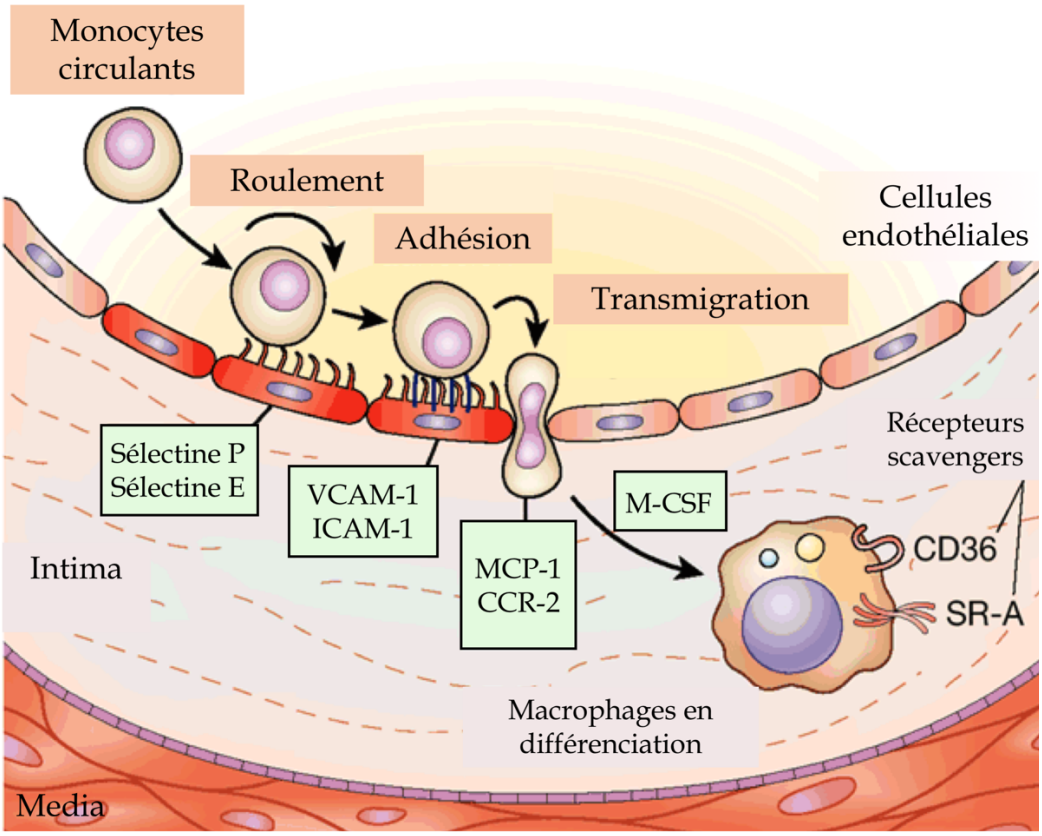

Figure 7 : Mécanismes contribuant au recrutement des monocytes dans la paroi artérielle et à leur différenciation en macrophages.

Adapté de Li et Glass, 2002. (Li and Glass, 2002)

En raison du recrutement continu de monocytes, de leur différenciation et de la prolifération locale des macrophages, les macrophages représentent la population cellulaire prédominante dans les plaques athéromateuses (Robbins et al., 2013). De nombreux autres types cellulaires sont présents au sein de la plaque (Cochain et al., 2018; Cole et al., 2018; Fernandez et al., 2019; Winkels et al., 2018; Zernecke et al., 2020) et contribuent au développement de la plaque d'athérosclérose comme les mastocytes, les cellules dendritiques (Paulson et al., 2010), les lymphocytes T et B (Baardman and Lutgens, 2020; Sage et al., 2019; Taleb et al., 2015; Winkels et al., 2018) ainsi que les neutrophiles (An et al., 2019; Doring et al., 2020; Franck et al., 2018; van Leeuwen et al., 2008).

L'infiltration des monocytes est un mécanisme de défense pour éliminer les LDLox, qui endommagent la paroi vasculaire. Cependant, l'accumulation incontrôlée de monocytes et leur différenciation en macrophages au sein de la plaque peut contribuer à la progression de la maladie. En effet, dans cette première phase de l'athérosclérose, les macrophages internalisent plus de lipoprotéines présentes dans l'intima qu'ils n'en libèrent. L'engloutissement continu des lipoprotéines conduit à la transformation des macrophages en cellules spumeuses (Goldstein et al., 1979). L'efflux du cholestérol des cellules spumeuses est médié par les HDL. En effet, les HDL sont capables de capter l'excès de cholestérol présent au sein des macrophages de la paroi artérielle puis de rejoindre la circulation sanguine afin de transporter le cholestérol au niveau du foie pour l'excréter dans la bile (Fielding and Fielding, 1995) (Figure 8).

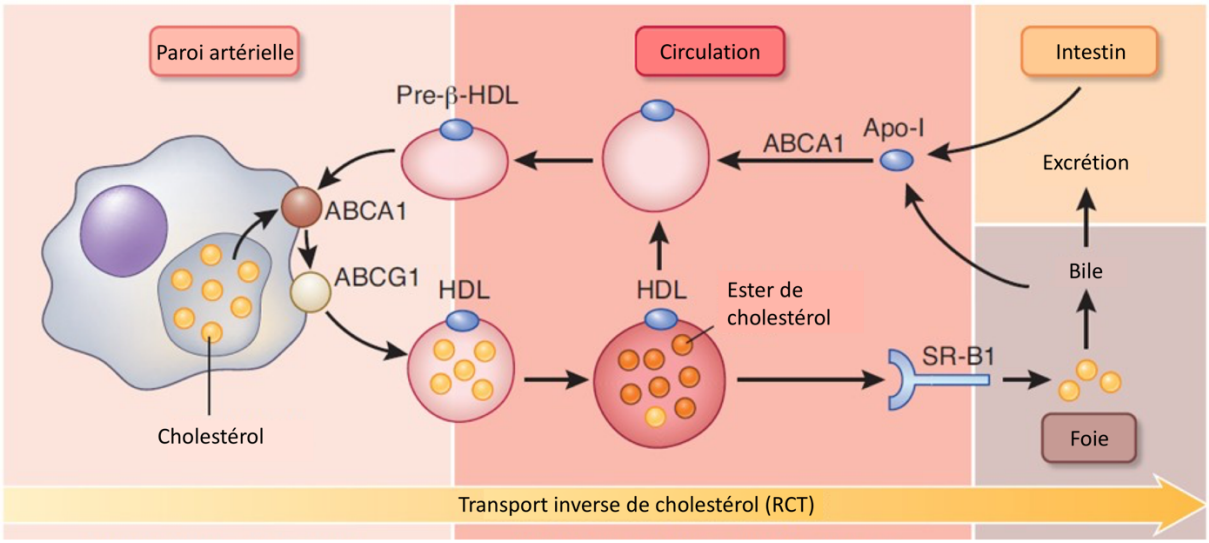

Figure 8 : Le transport inverse du cholestérol par les HDL.
Adapté de Heinecke et al., 2012. (Heinecke, 2012)

La première étape de synthèse des HDL est la sécrétion de l'apoA1 (Apolipoprotéine A1) par le foie et l'intestin (Zannis and Breslow, 1985). Les HDL sont tout d'abord synthétisés sous forme de pré-β-HDL, des particules pauvres en lipides et riches en apoA1 (Zannis et al., 2004). Durant le processus de transport inverse du cholestérol, l'apoA1, à la surface des pré-β-HDL, se lie aux transporteurs membranaires ABCA1 et ABCG1 (cassette de liaison à l'ATP A1 et G1) et au récepteur scavenger SR-BI (Scavenger Receptor class B type I) des cellules spumeuses afin de transporter le cholestérol hors de la cellule (Westerterp et al., 2013; Yvan-Charvet et

al., 2010). Au sein des HDL le cholestérol est estérifié par la lécithine-cholestérol acyltransférase (Jonas, 2000). Ces HDL contenant des esters de cholestérol sont appelés HDL matures. Ensuite, les HDL matures peuvent retourner au niveau du foie et transférer leur contenu *via* le récepteur SR-BI à la surface des hépatocytes (Krieger, 1999; Pagler et al., 2006). Enfin, le cholestérol peut être réutilisé ou éliminé dans la bile puis au niveau des fèces. Cependant, le développement de l'athérosclérose altère le transport inverse de cholestérol qui diminue au fur et à mesure que la maladie progresse. Ainsi, l'accumulation de cellules spumeuses conduit à la formation d'une strie lipidique, qui est la première caractéristique de l'athérosclérose. A ce stade précoce, qui peut commencer dans l'enfance ou l'adolescence (Strong et al., 1999), les stries lipidiques peuvent se résorber ou bien évoluer vers des stades plus pathologiques.

2. *Progression*

Les macrophages qui s'accumulent dans les plaques athéromateuses ont une capacité migratoire compromise, contribuant à l'échec de la résolution de l'inflammation et entrainant la formation de plaques de plus en plus complexes et avancées (Park et al., 2009; Randolph, 2008). Les macrophages contribuent à la différenciation, la prolifération et la migration des cellules musculaires lisses (CML) de la media vers l'intima (Campbell and Campbell, 1994). Ces CML deviennent alors capables de capter les LDLox et se transforment par la suite en cellules spumeuses qui participent à la formation du cœur lipidique (Stary et al., 1995). Au sein de l'intima artérielle, l'absorption excessive de cholestérol par les cellules spumeuses dérégule leur métabolisme lipidique entrainant ainsi leur mort cellulaire (Feng et al., 2003). Les cellules spumeuses apoptotiques qui ne sont pas correctement éliminées peuvent libérer leur contenu lipidique et leurs composantes cellulaires donnant lieu à la formation d'un cœur nécrotique. Nous parlons alors de plaque fibroathéromatheuse, avec la formation d'une chape fibreuse riche en collagène, en CML et en protéines de structure, dont l'intégrité est essentielle à la cohésion et à la stabilité de la plaque. Cette chape fibreuse entoure le noyau lipidique, une zone dans la plaque qui se compose de débris, de cellules apoptotiques, nécrotiques, de lipides et de cristaux de cholestérol.

3. *Lésions avancées*

L'inflammation non résolue est la principale cause de la plaque avancée, conduisant à la formation d'une plaque dite vulnérable, instable ou encore fibroathéromateuse à chape fine. La plaque vulnérable est caractérisée par un cœur nécrotique important et une fine chape fibreuse (Figure 9) (Naghavi et al., 2003; van der Wal et al., 1994). Ce type de plaque représente le stade le plus complexe de l'athérosclérose et est associé à de graves manifestations cliniques. Nous parlons de plaque vulnérable, en raison du risque de rupture et de thrombose menaçant le pronostic vital (Virmani et al., 2002). Contrairement aux premiers stades de l'athérosclérose, la rupture de la plaque est un évènement rapide, imprévisible et sans retour. La progression de l'athérome vers une plaque vulnérable survient généralement chez les personnes de plus de 55 ans (Cheruvu et al., 2007) . On estime que les ruptures de plaque représentent environ 70% des événements de thrombose coronaire (Kubo et al., 2007).

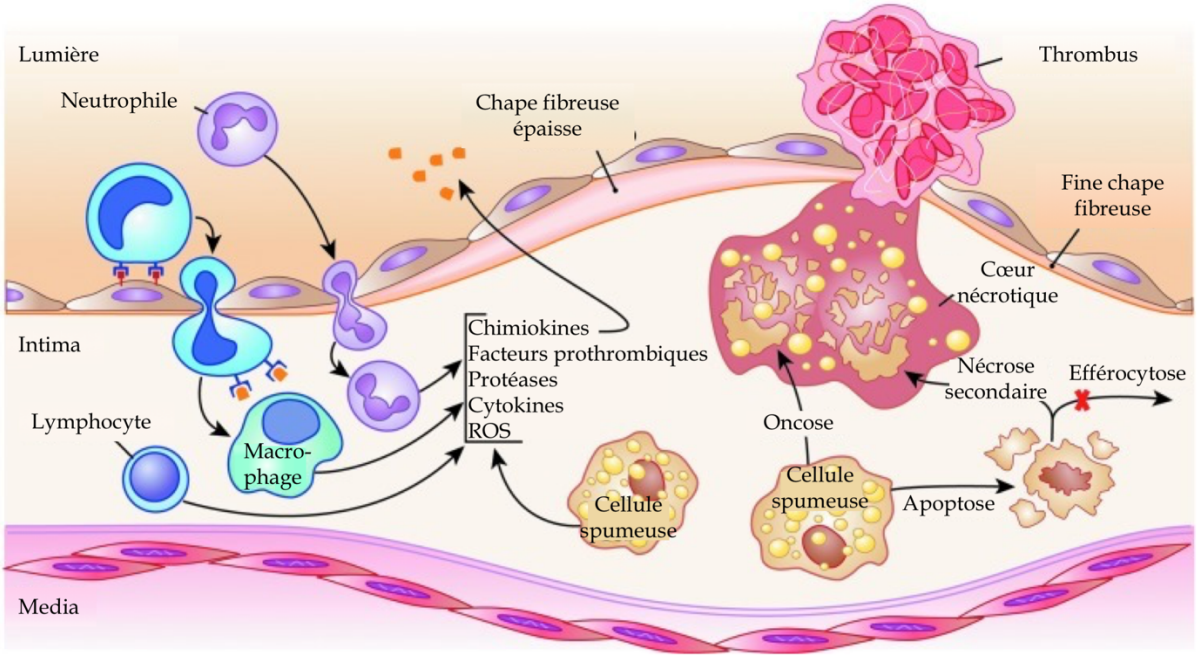

Figure 9 : Vue d'ensemble de l'athérogenèse dans les plaques avancées.
Adapté de Tavakoli et al., 2012. (Tavakoli and Asmis, 2012)

C. Modèles d'études murins

L'athérosclérose est étudiée chez les animaux depuis le début des années 1900, à commencer par les travaux d'Ignatowski (Ignatowski, 1909). Cependant, les souris sont résistantes à l'athérosclérose en raison de leur profil lipidique différent de celui des humains. En effet, les souris sauvages ont des taux élevés de HDL et faibles de LDL tandis qu'à l'inverse, l'Homme a des niveaux élevés de LDL et faibles de HDL. La différence entre les profils lipidiques de la souris et de l'Homme est due à l'absence de la protéine de transfert des esters de cholestérol (CETP) chez la souris (Jiang et al., 1993; Marotti et al., 1992). Chez les souris sauvages, plus de 80% du cholestérol plasmatique est transporté par les HDL, les rendant donc résistantes à l'hypercholestérolémie et à l'athérosclérose (Chan, 2015). C'est pourquoi des modifications génétiques de leur métabolisme lipidique sont obligatoires afin d'étudier la pathologie.

1. *ApoE-/-*

L'apolipoprotéine E (ApoE) est une lipoprotéine jouant un rôle protecteur clé dans l'athérosclérose. Dans des conditions physiologiques, l'ApoE est produite par le foie et les macrophages et sert d'intermédiaire dans le métabolisme du cholestérol. L'ApoE est présente dans la circulation à la surface des chylomicrons, VLDL et IDL et, participe au métabolisme de ces lipoprotéines. En effet, l'ApoE est essentielle pour le catabolisme des lipoprotéines riches en TG et facilite l'interaction des lipoprotéines et de leurs cellules cibles. Chez l'Homme, une diminution de l'expression de l'ApoE causée par certains types de maladies génétiques (hyperlipoprotéinémie de type III associée à une carence familiale en ApoE) entraine un changement du profil lipidique et une augmentation de la prévalence de l'athérosclérose chez ces patients (Ghiselli et al., 1981; Schaefer et al., 1986). La première lignée de souris ApoE déficientes ($ApoE^{-/-}$) a été développée en 1992 par Piedrahita *et al.* (Piedrahita et al., 1992). Les souris $ApoE^{-/-}$ sont le modèle de souris le plus utilisé pour l'étude de l'athérosclérose en raison de leur développement spontané de lésions vasculaires complexes, même sous régime normal. La capacité des souris $ApoE^{-/-}$ à éliminer les lipoprotéines plasmatiques est gravement altérée, ce qui entraîne une augmentation des taux de VLDL, IDL et LDL et une diminution du taux de HDL (Plump et al., 1992). Un régime riche en graisses et en cholestérol permet

d'accélérer la pathologie en entrainant des lésions riches en cellules spumeuses (Nakashima et al., 1994). Les souris ApoE$^{-/-}$ âgées présentent également des hémorragies suggérant une instabilité de la plaque (Rosenfeld et al., 2000). Néanmoins, l'utilisation de ces souris comporte certains inconvénients. En effet, l'ApoE est une protéine multifonctionnelle qui a un impact sur l'inflammation, l'oxydation, le transport inverse du cholestérol par les macrophages et la prolifération et la migration des muscles lisses (Getz and Reardon, 2009). Cela pourrait donc affecter la progression de la plaque indépendamment des niveaux lipidiques plasmatiques (Fazio et al., 1997; Van Eck et al., 2000).

2. *Ldlr-/-*

Le récepteur aux LDL (LDLR) est un récepteur membranaire intervenant dans l'endocytose des LDL riches en cholestérol, permettant ainsi le maintien du niveau plasmatique des LDL. C'est en 1993 qu'Ishibashi *et al.* ont généré les souris LDLR déficientes (Ldlr$^{-/-}$) (Ishibashi et al., 1993). Ce modèle de souris présente les mêmes caractéristiques que celles observées dans l'hypercholestérolémie familiale humaine, causée par une mutation du récepteur aux LDL (Hobbs et al., 1990; Lee et al., 2017). A l'inverse des souris ApoE$^{-/-}$, les souris Ldlr$^{-/-}$ ne développent pas de plaque d'athérome sous un régime normal (Ishibashi et al., 1994). En revanche, lorsqu'elles sont soumises à un régime riche en graisses et en cholestérol, les souris Ldlr$^{-/-}$ sont capables de développer des lésions athéromateuses importantes et de l'hypercholestérolémie proche du profil lipidique humain (accumulation de VLDL et de LDL) (Knowles and Maeda, 2000).

3. *PCSK9-AAV*

En 2014, le virus adéno-associé (AAV) codant pour la proprotéine convertase subtilisine/kexine de type 9 (PCSK9) a été mis en lumière par deux groupes comme un nouveau modèle d'étude de l'athérosclérose (Bjorklund et al., 2014; Roche-Molina et al., 2015). La PCSK9 est une enzyme qui se fixe aux récepteurs lipidiques de basse densité tels que les LDLR, les VLDLR (récepteurs aux VLDL) et l'apolipoprotéine receptor-2 (ApoER2) (Shan et al., 2008) et qui induit leur dégradation (Poirier et al., 2008). L'induction d'un gain de fonction

de PCSK9 au niveau hépatique par injection intraveineuse du PCSK9-AAV associée à un régime riche en graisse induit le développement de l'athérosclérose chez la souris. De plus, les souris PCSK9-AAV présentent une hausse du cholestérol plasmatique ainsi que des VLDL et LDL. Un an après l'injection, les souris PCSK9-AAV présentent toujours une hyperlipidémie (Roche-Molina et al., 2015).

4. *ApoE * 3-Leiden.CETP*

La CETP permet l'échange d'esters de cholestérol et de TG entre les lipoprotéines contenant de l'apoB (chylomicrons, VLDL, LDL) et les HDL dans le plasma (Ha et al., 1981). Chez les personnes atteintes de maladies cardiovasculaires, une forte concentration de CETP accroit la progression de l'athérosclérose (Klerkx et al., 2004). De plus, l'expression de l'ApoE3-Leiden, un rare variant mutant de la forme ApoE humaine, est associée à une forme héréditaire dominante d'hyperlipoprotéinémie familiale de type III (Havekes et al., 1986). La combinaison de ces deux modèles par Westerterp *et al.* a permis la création des souris ApoE*3-Leiden.CETP. Ces souris montrent une augmentation des VLDL et des LDL au détriment des HDL, ce qui engendre une forme sévère d'athérosclérose (Westerterp et al., 2006). De même, le profil lipidique des souris ApoE*3-Leiden.CETP sous régime riche en graisse pendant 6 mois imitent les profils lipidiques observés chez les personnes souffrant du syndrome métabolique (Kuhnast et al., 2015; Paalvast et al., 2017). L'utilisation de ce modèle est donc intéressante afin d'étudier les variations du métabolisme lipidique et le transport inverse du cholestérol durant les maladies cardiovasculaires.

5. *ApoE$^{-/-}$ Fbn1$^{C1039G+/-}$*

Bien que tous les modèles présentés ci-dessus entrainent le développement de l'athérosclérose, aucun de ces modèles ne permet d'étudier les stades avancés de la pathologie, notamment la rupture spontanée de la plaque qui peut être observée chez l'Homme. Ainsi, le modèle de souris ApoE$^{-/-}$ Fbn1$^{C1039G\ +/-}$ a été développé afin d'étudier les plaques athéromateuses avancées (Van Herck et al., 2009).

La fibrilline 1 (Fbn1) est essentielle dans la formation de la matrice extracellulaire et plus précisément dans la génération et la maintenance des fibres élastiques. En effet, la déficience en Fbn1 par la mutation hétérozygote au niveau du gène de la Fbn1 ($Fbn1^{C1039G+/-}$) entraine le syndrome de Marfan, une maladie génétique caractérisée par la fragmentation des fibres élastiques (Judge et al., 2004). De plus, la déficience en Fbn1 entraine un raidissement artériel et conduit au développement de plaques athéromateuses vulnérables et à la rupture des plaques chez la souris (Van der Donckt et al., 2015b). Après un régime riche en graisses, les souris $ApoE^{-/-}$ $Fbn1^{C1039G+/-}$ montrent une perméabilité de la barrière hémato-encéphalique conduisant à des xanthomes dans le cerveau (Van der Donckt et al., 2015a). Ce modèle n'étant pas parfait, de nombreux laboratoires sont toujours à la recherche de modèles complémentaires afin d'étudier les mécanismes complexes des plaques avancées.

D. Traitements actuels

L'athérosclérose étant un trouble inflammatoire chronique des artères entraîné par les lipides, le traitement de l'athérosclérose est à ce jour encore principalement axé sur la réduction des concentrations de lipides sanguins, réduisant ainsi partiellement le risque de maladie cardiovasculaire. Cependant, de nouveaux traitements prometteurs visant les voies inflammatoires sont en train de voir le jour.

1. *Modulation des lipoprotéines*

Les statines. Le développement des statines en 1988 a été une grande avancée pour les maladies cardiovasculaires (Alberts, 1988). Ce sont les molécules les plus utilisées pour diminuer le taux de cholestérol à la fois pour les préventions primaires et secondaires. Les statines sont des inhibiteurs compétitifs de l'hydroxyméthylglutaryl-CoA réductase permettant une inhibition de la synthèse de cholestérol. La diminution du taux intracellulaire de cholestérol entraine une augmentation de l'expression du LDLR à la surface des hépatocytes favorisant alors la clairance des LDL. Les statines permettent ainsi d'abaisser le taux de LDL-c d'environ 30% et de réduire de 30 à 40% le risque d'accident cardiovasculaire. Plusieurs études montrent l'effet bénéfique des statines sur les patients présentant des

facteurs de risque ou des maladies cardiovasculaires (1994; Cannon et al., 2004; Jukema et al., 1995; Nicholls et al., 2011; Nissen et al., 2006; Sacks et al., 1996; Shepherd et al., 1995). Néanmoins, des effets secondaires importants comme le développement du diabète de type 1, des dysfonctions hépatiques, des troubles musculaires, rénaux ou encore neurologiques (Ramkumar et al., 2016) peuvent survenir, rendant le composé inadapté à certains patients. En effet, de nombreux patients ne tolèrent pas les statines ou ne peuvent pas atteindre des niveaux adéquats de LDL-c malgré le traitement.

L'Ézétimibe. L'ézétimibe est une molécule hypocholestérolémiante qui diminue l'absorption du cholestérol par l'intestin grêle. L'ézétimibe est utilisée comme un traitement de deuxième intention soit en association avec des statines, lorsque le taux de LDL-c ciblé n'est pas atteint avec les statines seules, soit en monothérapie chez les patients présentant une contre-indication aux statines. Cette molécule réduit ainsi les taux de LDL-c de 15 à 20% en monothérapie et contribue à une diminution des évènements cardiovasculaires (Cannon et al., 2015; Tsujita et al., 2015).

Les inhibiteurs de PCSK9. Une nouvelle classe de médicament visant à diminuer le taux de cholestérol a récemment vu le jour, les inhibiteurs de la PCSK9. Comme discuté ci-dessus, la PCSK9 est une protéine participant à l'homéostasie du cholestérol en régulant l'expression des LDLR par endocytose. (Lopez, 2008). L'inhibition de la PCSK9 empêche la dégradation du LDLR à la surface des hépatocytes conduisant ainsi à une augmentation de l'absorption du LDL-c par le foie et donc à une diminution des taux plasmatiques de LDL-c plus importante que la combinaison statines/ézétimibe. Cependant, malgré leurs effets majeurs sur la diminution des LDL plasmatiques, les inhibiteurs de la PCSK9 n'ont montré à ce jour aucun résultat frappant concernant la diminution des maladies cardiovasculaires (Bittner et al., 2020; Ray et al., 2019; Ridker et al., 2018; Sabatine et al., 2016) .

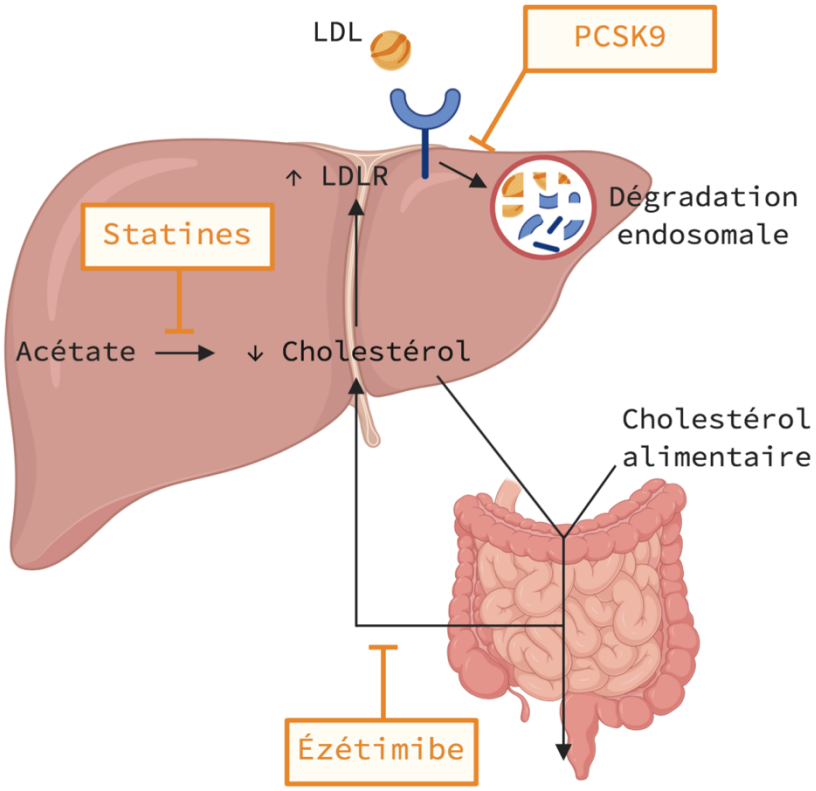

Figure 10 : Principaux traitements modulant les lipoprotéines.
Adapté de Grundy et al., 2016 (Grundy, 2016)

2. *Traitements anti-inflammatoires*

La Colchicine. Cet anti-inflammatoire initialement utilisé pour le traitement de la goutte présente de nombreux avantages. La colchicine permet d'inhiber la chimiotaxie des neutrophiles et bloque l'inflammasome NLRP3 (NOD-like receptor family, pyrin domain containing 3), inhibant ainsi la production de cytokines comme l'IL-1β ou encore l'IL-18 conduisant ainsi à la réduction en aval de l'IL-6 et de la CRP (Protéine C réactive) (Leung et al., 2015; Solomon et al., 2016). Une étude récente a démontré l'effet bénéfique d'une thérapie à base de faible dose de colchicine. En effet, la colchicine diminue significativement la LAPV (Low Attenuation Plaque Volume) et la CRP, tout cela indépendamment de la thérapie aux statines et de la réduction des LDL-c (Vaidya et al., 2018). Enfin, le traitement à faible dose de

colchicine est significativement bénéfique dans la revascularisation coronarienne et l'AVC (Tardif et al., 2019).

Le Méthotrexate. Ce médicament est un anti-inflammatoire utilisé pour le traitement des troubles inflammatoires chroniques comme la polyarthrite rhumatoïde ou encore le psoriasis. Le méthotrexate inhibe la production de cytokines (IL-6, IL-8, IL-1β and TNF-α) par les cellules T activées (Cutolo et al., 2001; Gerards et al., 2003). Cependant, après 2-3 ans de suivi des patients, l'essai clinique a été stoppé car il n'y avait pas de réduction de l'IL-1β, de l'IL-6 de la CRP ou encore des évènements cardiovasculaires (Ridker et al., 2019).

Le Canakinumab. En septembre 2017, l'étude CANTOS (Canakinumab Anti-inflammatory Thrombosis Outcome Study) a pour la première fois mis en évidence que le ciblage spécifique de l'inflammation médiée par l'IL-1β, pouvait avoir des effets bénéfiques sur l'athérosclérose (Ridker et al., 2017). L'IL-1β est une cytokine qui est au cœur de la réponse inflammatoire et qui pilote la voie de signalisation de l'IL-6. Le Canakinumab est un anticorps monoclonal bloquant l'IL-1β, ayant ainsi des effets anti-inflammatoires qui ont été approuvés pour une utilisation clinique dans les troubles rhumatologiques (Lachmann et al., 2009; Ruperto et al., 2012). Chez les patients atteints de maladies cardiovasculaires, le traitement avec une dose de 150mg de canakinumab a entraîné une réduction statistiquement significative de 15% du critère d'évaluation principal et de 17% du critère d'évaluation secondaire, par rapport au placebo. En revanche, davantage de décès dus à des infections ont été détectés dans le groupe traité au canakinumab (Ridker et al., 2017). Cette étude met en évidence que l'athérosclérose est une maladie inflammatoire pouvant être ciblée par une thérapie anti-inflammatoire spécifique. De nouvelles études visant à inhiber l'inflammasome, par l'inhibiteur MCC950, afin de diminuer l'athérosclérose sont en cours (Gao et al., 2019; van Hout et al., 2017).

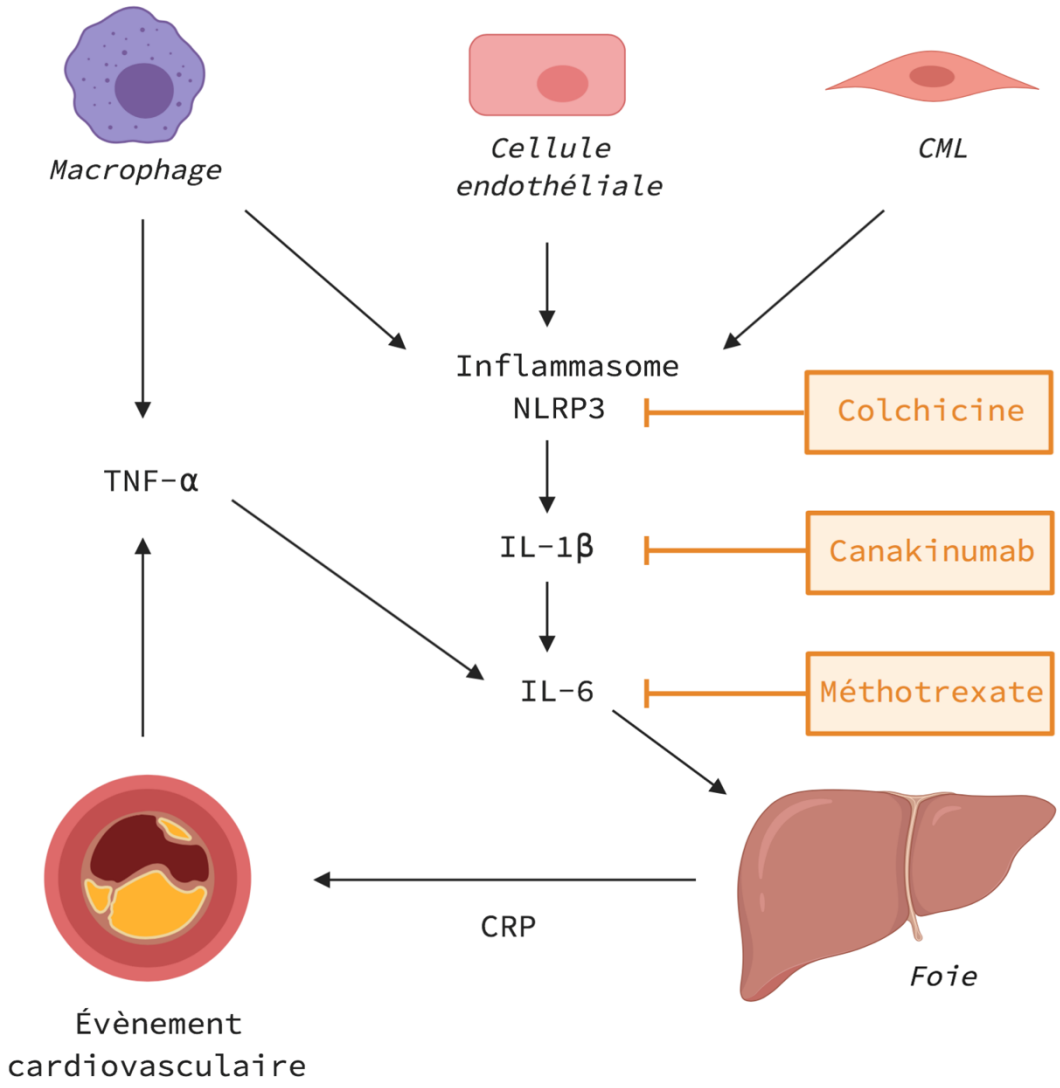

Figure 11 : Principaux traitements anti-inflammatoires.

Adapté de Lorenzatti et al., 2018 et Libby et al., 2019 (Libby and Everett, 2019; Lorenzatti and Servato, 2018)

Chapitre III : Les cellules myéloïdes, acteurs clés de l'immunité innée

Les granulocytes, les monocytes, les macrophages et les cellules dendritiques représentent un sous-groupe de leucocytes appelés cellules myéloïdes. Les cellules myéloïdes jouent un rôle primordial en tant que première barrière de défense contre les pathogènes, mais ces cellules jouent aussi un rôle majeur dans de nombreuses pathologies comme l'obésité ou l'athérosclérose. Lors de l'inflammation, les cellules myéloïdes sont rapidement recrutées au niveau des tissus lésés *via* des récepteurs aux chimiokines exprimés à leur surface. C'est au niveau de ces tissus que les cellules myéloïdes vont jouer un rôle clé dans l'immunité innée en phagocytant les pathogènes, les débris cellulaires et en sécrétant des cytokines pro- ou anti-inflammatoires. De cette manière, ces cellules jouent divers rôles, bénéfiques et délétères, dans le corps notamment dans le développement, l'homéostasie et la réparation des tissus mais aussi dans la défense de l'hôte, l'initiation et la résolution de l'inflammation.

A. La myélopoïèse

La moelle osseuse est un organe lymphoïde primaire dans lequel se déroule l'hématopoïèse, un processus finement régulé conduisant à la formation de toutes les cellules du sang. Alexander Maximow est le premier, il y a maintenant plus d'un siècle, à avoir postulé l'idée que l'hématopoïèse résulte de précurseurs communs devenant progressivement plus restreints et finissant par donner naissance à diverses populations de cellules sanguines (Maximow, 1909). Il est de nos jour bien connu que les cellules souches hématopoïétiques (CSH), également appelées CSH à long terme (LT-CSH), sont au sommet de cette hiérarchie. Ces cellules multipotentes (dites dormantes) sont capables, une fois activées par des interactions juxtacrines (cellule-cellule ou cellule-matrice extracellulaire) ou paracrines (facteurs de croissance, cytokines, chimiokines) (Cordeiro Gomes et al., 2016; Wei and Frenette, 2018), de s'auto-renouveler (Seita and Weissman, 2010). Les facteurs de survie ou de prolifération tels Runx-1 (Runt-related transcription factor 1), Slc (Stem cell leukemia)/ tal-1 (T-cell acute leukemia 1), Lmo-2 (LIM domain only 2), ETV6 (ETS Variant Transcription Factor

6), Gfi-1 (Growth Factor Independent 1 Transcriptional Repressor) et GATA-2, sont essentiels pour le maintien des LT-CSH (Orkin and Zon, 2008). Le maintien des LT-CSH dans la niche est régulé par un micro-environnent composé de différents types cellulaires tels que des cellules stromales mésenchymateuses, des cellules endothéliales mais aussi de mégacaryocytes (Wei and Frenette, 2018).

Les LT-CSH peuvent par la suite se différencier en CSH à court terme (ST-CSH) puis en progéniteurs multipotents (MPP). La différenciation des CSH en MPP est la première étape d'une cascade d'événements aboutissant à la génération des cellules hématopoïétiques matures (Figure 12), bien que les macrophages résidant dans les tissus puissent dériver de progéniteurs embryonnaires (Hoeffel and Ginhoux, 2018; McGrath et al., 2015). Les MPP se différencient ensuite en deux types de progéniteurs, les progéniteurs communs myéloïdes (CMP) en présence de TPO (thrombopoïétine) et de SCF (stem-cell factor), et les progéniteurs communs lymphoïdes (CLP) en présence d' IL-7 (Bennett et al., 2013; Seita and Weissman, 2010).

Toutefois, il existe un déséquilibre entre la production myéloïde et lymphoïde par les MPP en faveur des CMP (Busch et al., 2015). Les CMP peuvent, entre autres, se différencier en progéniteurs des granulocytes/macrophages (GMP) qui vont pouvoir donner lieu soit à la lignée granulocytaire, soit se différencier de nouveau en progéniteurs monocytes-macrophages/cellules dendritiques (MDP). Les MDP donnent lieu soit à des précurseurs de cellules dendritiques communes (CDP), soit à des précurseurs de monocytes communs (cMoP). Les cMoP se différencient enfin en monocytes Ly6C^{hi} matures qui vont pouvoir être libérés dans la circulation sanguine. Le développement et la survie des monocytes vont dépendre de la cytokine CSF-1 (aussi appelée M-CSF ; colony stimulating factor 1) et de son récepteur CSF1R (aussi connu sous le nom CD115 ; colony stimulating factor 1 receptor) (Cecchini et al., 1994; Dai et al., 2002; Wiktor-Jedrzejczak and Gordon, 1996).

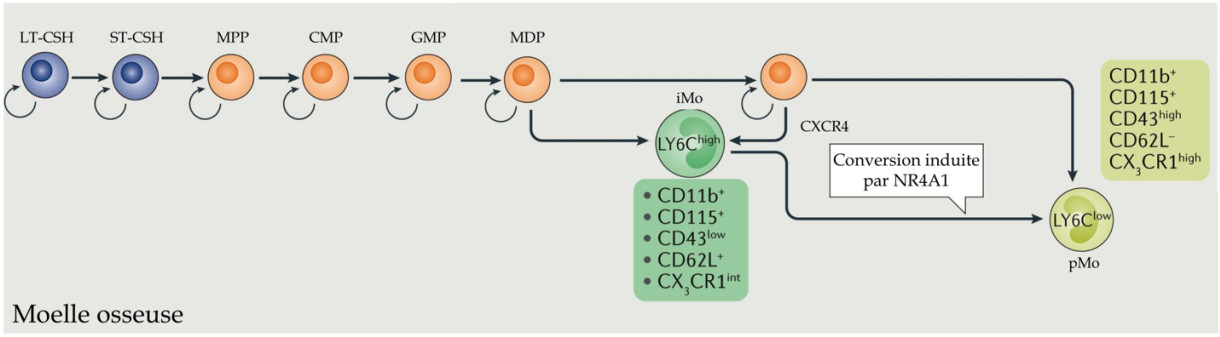

Figure 12 : La myélopoïèse au sein de la moelle osseuse

Adapté de Rahman et al. 2017. (Rahman et al., 2017)

Dans des conditions pathologiques ou de stress, les CSH peuvent contourner plusieurs étapes de l'hématopoïèse traditionnelle *via* une différenciation directe en progéniteurs myéloïdes par division asymétrique (Yamamoto et al., 2013). Ce processus rapide est nommé « myélopoïèse d'urgence » (Schultze et al., 2019) et permet l'approvisionnement adéquat des cellules myéloïdes face à une demande accrue (Ueha et al., 2011). D'autres part, en cas d'hypercholestérolémie, notamment au cours de l'athérosclérose, les cellules souches et progénitrices hématopoïétiques (HSPC) (terme combinant les CSH et les MPP) sont libérées de la moelle osseuse pour rejoindre la rate. Au niveau de la rate va alors avoir lieu l'hématopoïèse extramédullaire, processus pendant lequel les HSPC spléniques se différencient en monocytes *via* des interactions avec le GM-CSF (Granulocyte-macrophage colony-stimulating factor), l'IL-3 (Interleukine-3) et le microenvironnement hématopoïétique extramédullaire (Robbins et al., 2012; Swirski et al., 2009).

B. Les monocytes

Les monocytes sont des phagocytes mononucléaires qui sont générés durant l'hématopoïèse à partir de précurseurs myéloïdes présents dans les organes lymphoïdes primaires comme le foie fœtal, la moelle osseuse ou dans des conditions inflammatoires, dans la rate.

1. *Sortie des monocytes de la moelle*

Une fois matures, les monocytes peuvent quitter la moelle osseuse pour rejoindre la circulation sanguine, dans laquelle les monocytes représentent 5 à 10% des leucocytes chez l'Homme et environ 2% chez la souris. Les monocytes présents dans la moelle osseuses co-expriment les récepteurs de surface CXCR4 (C-X-C Motif Chemokine Receptor 4) et CCR2 (C-C chemokine receptor type 2), deux récepteurs qui vont jouer des rôles contraires. Dans des conditions physiologiques, la rétention des monocytes au sein de la moelle osseuse va être possible grâce à la liaison de de la chimiokine CXCL12 (C-X-C Motif Chemokine Ligand 12), constitutivement sécrétée par les cellules stromales mésenchymateuses de la moelle osseuse, à son récepteur CXCR4 (Jung et al., 2015). Néanmoins, dans des conditions d'inflammation, les cellules stromales mésenchymateuses de la moelle osseuse et les cellules CAR (cellules réticulaires abondantes en CXCL12), vont alors rapidement libérer la cytokine CCL2 (C-C Motif Chemokine Ligand 2) (Jung et al., 2009; Shi et al., 2011) et CCL7 (Jia et al., 2008; Tsou et al., 2007) qui vont se lier et activer CCR2 à la surface des monocytes et désensibiliser CXCR4, favorisant ainsi l'émigration des monocytes vers la circulation (Serbina and Pamer, 2006).

2. *Circulation des monocytes dans le sang*

Des études au cours des deux dernières décennies ont mis en évidence la présence d'une population hétérogène de monocytes sanguins chez la souris et chez l'Homme. Chez la souris, deux sous-ensembles majeurs de monocytes ont été identifiés, les monocytes classiques dits inflammatoires et les monocytes non classiques dits patrouilleurs tandis que chez l'Homme, trois sous-ensembles ont été décrit, les monocytes classiques (correspondant à 80% des monocytes totaux), les monocytes intermédiaires et les monocytes non classiques.

Chez la souris, les monocytes sont identifiés par l'expression de leur marqueur de surface CD115, F4/80 et CD11b. Les sous-groupes de monocytes se basent ensuite sur le niveau d'expression de différents marqueurs de surface tels que Ly6C, CCR2, CD43, CD62L et CX3CR1 (CX3C Chemokine Receptor 1) (Figure 13) (Geissmann et al., 2010a; Geissmann et al., 2003; Ingersoll et al., 2010).

Les monocytes inflammatoires (iMo) sont caractérisés par une forte expression de Ly6C (Ly6C^{hi}), de CCR2 (CCR2^{+}) et de CD62L (CD62L^{+}) et par une expression intermédiaire du récepteur CX3CR1 (CX3CR1^{int}). Chez l'Homme, les iMos correspondent au sous-ensemble de monocytes CD14^{hi} CD16^{low} (Ingersoll et al., 2010). En réponse à des signaux inflammatoires, les iMos sont rapidement recrutés et ont la capacité de transmigrer à travers l'endothélium et d'entrer dans les tissus où ils se différencient localement en macrophages inflammatoires (Jakubzick et al., 2013). Une fois de plus, l'axe CCL2/7-CCR2 est critique pour le recrutement des iMos au sein des tissus périphériques pendant l'inflammation (Tacke et al., 2007).

En revanche, les monocytes patrouilleurs (pMo) qui expriment faiblement le marqueur Ly6C (Ly6C^{low}) sont marqués par une expression de surface élevée de CX3CR1 (CX3CR1^{hi}) et CD43 (CD43^{+}) (Geissmann et al., 2010a; Geissmann et al., 2003). Les pMos de souris, tout comme leurs équivalents humains CD14^{low} CD16^{hi}, sont fortement dépendants du facteur de transcription NR4A1 (Nuclear Receptor Subfamily 4 Group A Member 1) (Hanna et al., 2011; Thomas et al., 2016). En effet, en l'absence de NR4A1, les pMos sont quasiment absents du sang, laissant donc penser que les pMos se développent à partir d'un progéniteur différent des iMos (Geissmann et al., 2010b; Hanna et al., 2011). Le rôle des pMos, comme leur nom l'indique, est de patrouiller dans les vaisseaux sanguins. Les pMos restent à proximité de l'endothélium et surveillent l'intégrité des cellules endothéliales tout en éliminant celles qui sont mortes ou stressées (Auffray et al., 2007; Carlin et al., 2013). De plus, les pMos contribuent à l'immunosurveillance du cancer et permettent de diminuer les métastases pulmonaires chez la souris (Hanna et al., 2015).

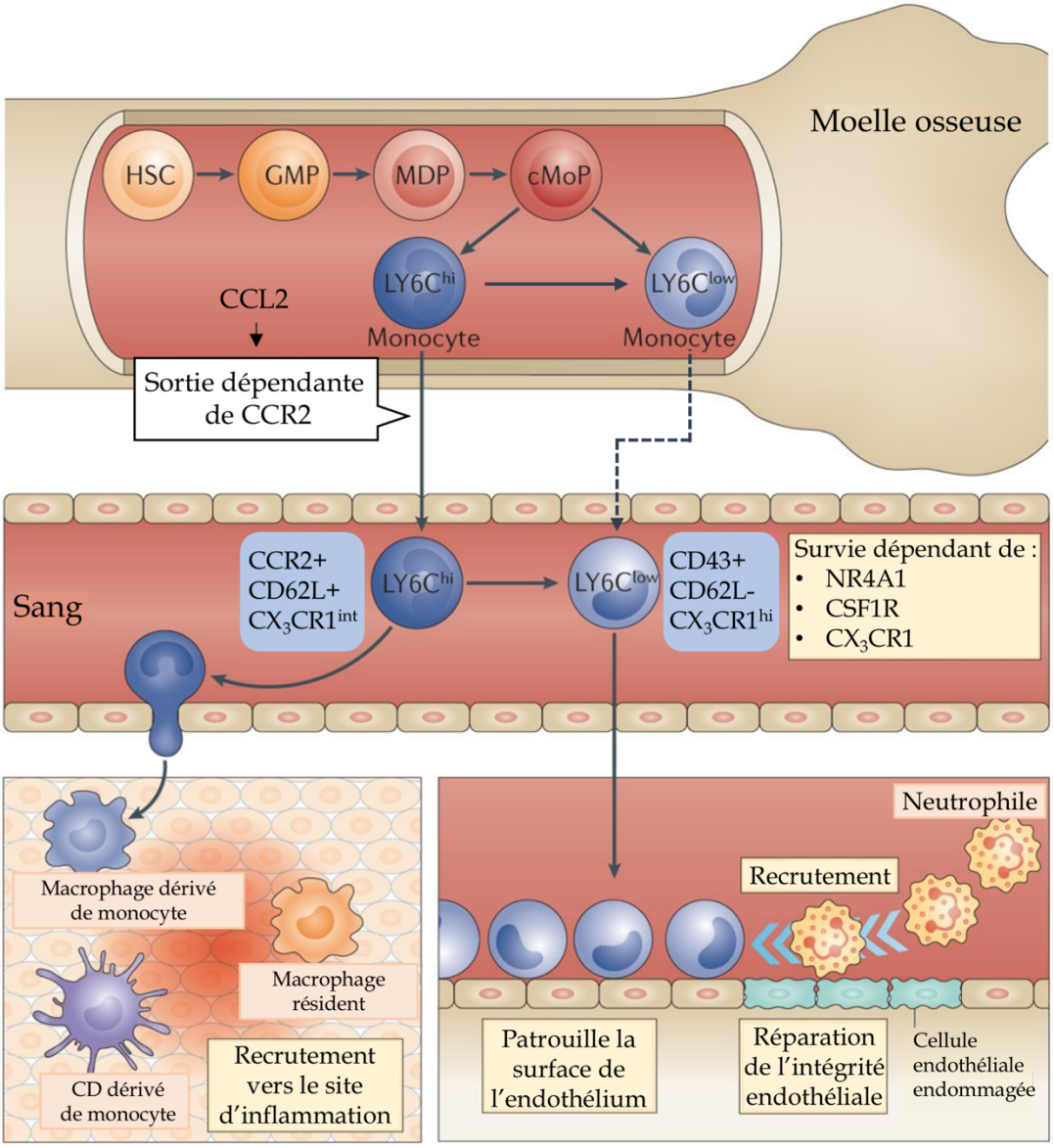

Figure 13 : Rôle des deux sous-groupes de monocytes

Adapté de Ginhoux et al., 2014. (Ginhoux and Jung, 2014)

C. Les macrophages au sein des tissus

Historiquement, les macrophages ont été observés et décrits pour la première fois à la fin du 19ème siècle par Ilya Metchnikoff. Les macrophages sont des cellules spécialisées dans la phagocytose qui jouent un rôle central dans le développement, l'homéostasie et la réparation des tissus ainsi que dans la résolution de l'inflammation et des infections. Ces cellules de l'immunité innée assurent une défense immédiate contre les agents pathogènes étrangers et

coordonnent l'infiltration des leucocytes, ils contribuent à l'homéostasie des tissus en phagocytant les cellules apoptotiques et les microbes, en participant à la clairance des antigènes, et enfin, ils collaborent avec les lymphocytes T et B, pour permettre la libération de cytokines et de chimiokines pro-inflammatoires. Les macrophages, *via* leur expression du complexe majeur d'histocompatibilité de classe II (MHC II), participent également à la présentation d'antigènes et la stimulation de la réponse lymphocyte T-dépendante.

1. *Origine des macrophages : résidents ou différenciés ?*

Il est maintenant bien établi que les tissus sains contiennent des macrophages résidents dont le nom et les fonctions diffèrent selon leur localisation (Caputa et al., 2019). Pendant de nombreuses décennies, il a été pensé que les macrophages résidents dans les tissus étaient constamment repeuplés à partir des monocytes circulants dans le sang. Ce concept linéaire, établi par Van Furth en 1972, regroupait les précurseurs hématopoïétiques dans la moelle osseuse, les monocytes dans le sang et les macrophages ainsi différenciés dans les tissus (van Furth et al., 1972). Cependant, au cours des dernières années, de nombreuses publications ont permis de radicalement changer notre vision du développement des macrophages en démontrant que de nombreux macrophages tissulaires étaient établis au cours du développement embryonnaire et persistaient à l'état adulte par un auto-renouvèlement indépendant des monocytes (Ginhoux et al., 2010; Guilliams et al., 2013; Hashimoto et al., 2013; Hoeffel et al., 2012; Schulz et al., 2012).

Le recrutement des macrophages au sein des tissus pendant l'embryogenèse se fait en trois vagues distinctes (Figure 14). La première vague conduisant à une différenciation des macrophages chez la souris débute au jour embryonnaire E7.0 au niveau des ilots de sang présents dans le sac vitellin (Palis and Yoder, 2001; Samokhvalov et al., 2007). A cette période, les cellules progénitrices sont dérivées du mésoderme de la plaque postérieure, et vont permettre la formation d'un pool de macrophages, d'érythroblastes et de mégacaryocytes (Palis et al., 1999), c'est ce que l'on appelle l'hématopoïèse primitive. Contrairement aux macrophages dérivés des monocytes de la moelle osseuse, les macrophages dérivés du sac vitellin se développent indépendamment du facteur de transcription myb (Schulz et al., 2012). La vague définitive transitoire, la deuxième vague de production de progéniteurs

hématopoïétiques, se fait entre les E8.0 et E8.5. Ces progéniteurs hématopoïétiques proviennent de l'endothélium hémogène du sac vitellin et sont appelés précurseurs érythro-myéloïdes (EMP). A partir de l'E8.5, les EMP peuvent migrer vers le foie fœtal (Palis and Yoder, 2001) par le système vasculaire sanguin nouvellement formé, où ils sont capables de se différencier en cellules de différentes lignées, notamment en monocytes, ressemblant étroitement aux monocytes de la moelle osseuse adulte. De même, à ce stade, des macrophages sont aussi formés par les EMP et peuvent migrer vers les tissus dès que le système vasculaire le permet.

Le foie fœtal contient dès lors, des cellules progénitrices des monocytes et ce, jusqu'au développement de la moelle osseuse. Ces cellules sont considérées comme la principale source des macrophages tissulaires (Hoeffel et al., 2015). A E8.5, en même temps que l'émergence des EMP tardifs, une troisième vague de progéniteurs hématopoïétiques émerge donnant lieu à des CSH immatures dans la région splanchnopleure para-aortique et générant ainsi à E10.5 des CSH fœtales dans l'aorte, les gonades et le mésonéphros (Cumano and Godin, 2007).

Ces précurseurs colonisent ainsi le foie fœtal et la moelle osseuse fœtale où l'hématopoïèse définitive se met en place. Les macrophages tissulaires résidents peuvent ainsi être composés de macrophages du sac vitellin, ou de macrophages dérivés de monocytes du foie fœtal selon le tissu (Figure 3). Ces macrophages d'origine embryonnaire possèdent des fonctions communes avec les macrophages dérivés des monocytes mais ils ont aussi des fonctions et des propriétés qui leurs sont propres et qui dépendent de leur localisation tissulaire (Bleriot et al., 2020).

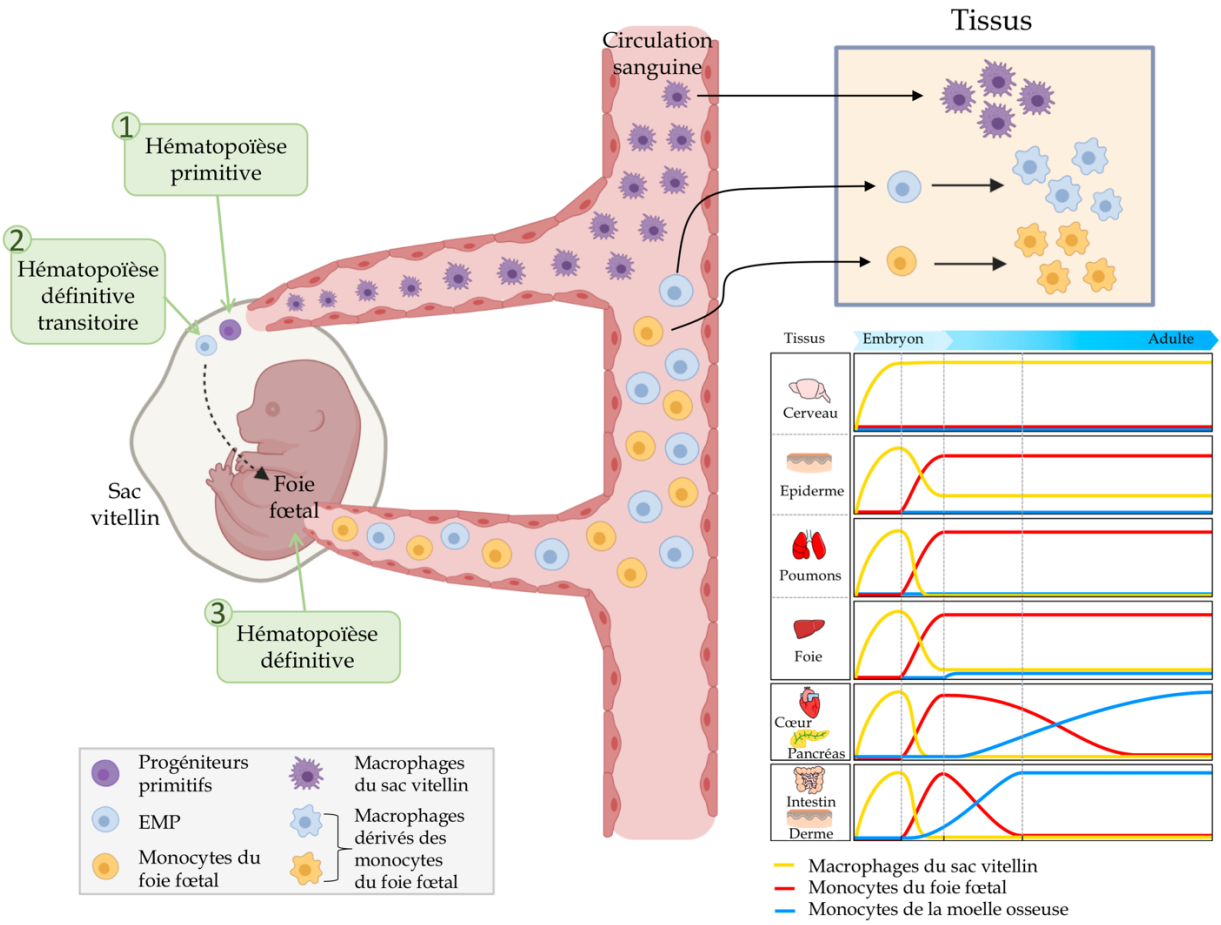

Figure 14 : L'hématopoïèse embryonnaire et les macrophages au sein des tissus
Adapté de Ginhoux et al., 2014, 2016. (Ginhoux and Guilliams, 2016; Ginhoux and Jung, 2014)

2. *Fonction des macrophages au sein des tissus*

Il est maintenant bien reconnu que la fonction des macrophages est étroitement liée à leur métabolisme et leur microenvironnement. En réponse à des signaux environnementaux, les macrophages subissent une reprogrammation avec un spectre de phénotypes fonctionnels distincts. Ainsi, l'activation des macrophages peut être pro-inflammatoire ou anti-inflammatoire, et selon le phénotype, ils peuvent contribuer à la destruction ou à la régénération des tissus et à la cicatrisation des plaies. Nous savons maintenant que les macrophages peuvent être activés différemment en réponse aux signaux tissulaires présents au sein du microenvironnement tissulaire et présentent ainsi un éventail de phénotypes

différents. Malgré cette diversité, aux extrêmes du spectre, deux états de polarisation des macrophages ont été classifiés, les macrophages dits pro-inflammatoires ou M1 qui présentent une activation classique, et les macrophages dits anti-inflammatoires ou M2 qui sont alternativement activés (Biswas and Mantovani, 2010).

i. Polarisation classique

La polarisation des macrophages en phénotype M1 est induite par la sécrétion de cytokines de type T helper de type 1 (Th1) telles que l'interféron gamma (IFNγ), TNF-α ou par des motifs moléculaires associés aux pathogènes (PAMPs) comme les lipopolysaccharides (LPS), agonistes du TLR4 (Colin et al., 2014). Les macrophages M1 vont contribuer à l'augmentation de la réponse inflammatoire en sécrétant une quantité accrue de cytokines pro-inflammatoires telles que l'IL-1β, IL-6, TNF-α, IL-23 et IL-12 (Mosser, 2003; Verreck et al., 2004). Les macrophages M1 produisent aussi d'importantes quantités d'espèces réactives de l'oxygène (ROS), d'oxyde nitrique (NO) et d'intermédiaires réactifs de l'azote (RNI), permettant ainsi aux macrophages d'accroitre leurs fonctions endocytaires et leurs capacités à détruire les agents pathogènes intracellulaires (Biswas and Mantovani, 2010). Grâce à leur forte activité microbicide, les macrophages M1 jouent un rôle clé lors de maladies infectieuses aiguës.

ii. Polarisation alternative

A l'extrême opposé du spectre d'activation, nous pouvons retrouver les macrophages M2 alternativement activés principalement appelés macrophages anti-inflammatoires. Ces macrophages sont initialement décrits comme activés par l'IL-4 et l'IL-13, deux cytokines produites par les cellules Th2, d'où leur nom « macrophage M2 » qui reflète la nomenclature Th2 (Gordon, 2003). Cependant, au fil des années, la classification des macrophages M2 s'est étendue et se subdivise maintenant en quatre sous-groupes, les macrophages M2a, M2b, M2c et M2d. Les macrophages M2a sont activés en réponse à l'IL-4 et à l'IL-13 et se caractérisent par une activité phagocytaire élevée, une forte expression des récepteurs du mannose (Stein

et al., 1992) et du galactose, une production d'ornithine et de polyamines par la voie de l'arginase et la sécrétion d'IGF (Insulin-like Growth Factor) et de TGF-β (Transforming Growth Factor beta 1) contribuant à la réparation tissulaire (Biswas and Mantovani, 2010). Ces macrophages dits « cicatrisants » aident à éliminer les parasites, à diminuer l'inflammation et favorisent le remodelage des tissus. Les macrophages M2b sont induits lors d'une exposition combinée à des complexes immuns et des ligands des récepteurs de type Toll (TLR) ou des agonistes de l'IL-1R (Interleukin-1 Receptor) (Mosser and Edwards, 2008). Ce sous-groupe de macrophages anti-inflammatoires est le seul à produire des doses élevées de cytokines anti-inflammatoires, d'IL-10 mais peu d'IL-12 qui est une cytokine à fort potentiel inflammatoire (Mosser, 2003). Les macrophages M2c, eux, sont activés par L'IL-10 et les glucocorticoïdes. Les macrophages M2b et M2c expriment fortement le récepteur MerTK (Myeloid-epithelial-reproductive Tyrosine Kinase), leurs conférant ainsi une capacité d'efférocytose accrue (Zizzo and Cohen, 2013; Zizzo et al., 2012). Ces deux sous-groupes de macrophages sont, de ce fait, appelés macrophages régulateurs (Mosser and Edwards, 2008). Pour finir, les macrophages M2d sont activés par une co-stimulation par des agonistes des TLR et des récepteurs à l'adénosine de type A2. Ces macrophages sont majoritairement connus pour sécréter de l'IL-10 et du VEGF (Vascular Endothelial Growth Factor). Les macrophages M2d sont pro-tumoraux et pro-angiogéniques et jouent ainsi un rôle néfastes à la fois dans les cancers et l'athérosclérose (Xu et al., 2019).

iii. Métabolisme des macrophages M1 et M2

Les macrophages M1 et M2 sont métaboliquement bien différents. Les macrophages M1 font partie de la première ligne de défense du système immunitaire, jouant donc un rôle inflammatoire très rapidement, en revanche, les macrophages M2 sont importants dans la phase de résolution de l'inflammation. Leur métabolisme se distingue pour permettre de mettre en place des fonctions différentes à des temps précis de l'inflammation.

Les macrophages M1.

L'activation des macrophage M1 entraine une absorption accrue de glucose au sein de la cellule médiée par la forte expression des transporteurs du glucose GLUT1 et GLUT3 à la

surface des macrophages (Freemerman et al., 2014). De plus, les macrophages pro-inflammatoires ont une activité glycolytique augmentée qui résulte du changement d'expression des isoformes de la phosphofructokinase-2 (PFK-2) de type hépatique vers un isoforme de PFK-2 ubiquitaire plus actif conduisant à une accumulation de fructose-2,6-bisphosphaste, qui pousse le flux glycolytique (Rodriguez-Prados et al., 2010). De plus, au sein de ces macrophages, le cycle de Krebs est altéré et conduit à une diminution de l'activité de la chaine respiratoire, permettant ainsi la production de ROS.

La stimulation par LPS lors de l'activation classique va avoir un double effet sur le macrophage. Elle va d'une part induire la production du facteur nucléaire-kappa B (NF-κb) au sein du macrophage et d'autre part diminuer l'expression de CARKL (Carbohydrate Kinase-Like). NF-κb peut à son tour induire HIF-1α (Hypoxia-Inducible Factor 1 alpha) (Rius et al., 2008), qui régule la glycolyse en induisant la transcription de plusieurs gènes glycolytiques dont le transporteur GLUT1, et qui favorise la conversion du pyruvate en lactate en induisant l'expression de la lactate déshydrogénase et de la pyruvate déshydrogénase kinase, inhibant ainsi l'utilisation du pyruvate dans le cycle de Krebs (Kim et al., 2006; Papandreou et al., 2006). De plus la diminution de l'expression de CARKL entraine une activité accrue de la voie du pentose phosphate, une voie essentielle pour la génération de NADPH et pour la production de ROS, mais aussi pour la synthèse d'oxyde nitrique (Aktan, 2004; Haschemi et al., 2012). Enfin, deux coupures sont présentes dans le cycle de Krebs au sein des macrophages M1 (O'Neill, 2015). La première coupure se produit au niveau de l'isocitrate déshydrogénase (IDH) qui conduit à l'accumulation de citrate et d'itaconate au sein de la cellule (Lampropoulou et al., 2016). Le citrate alimente la synthèse des acides gras pour la production de prostaglandine et d'oxyde nitrique, tandis que l'itaconate possède une fonction antibactérienne et anti-inflammatoire (Michelucci et al., 2013). La deuxième coupure se produit au niveau de l'enzyme succinate déshydrogénase (SDH), ce qui conduit à une accumulation de succinate. Le succinate stabilise HIF-1α qui contribue à l'expression de la cytokine pro-inflammatoire IL-1β (Tannahill et al., 2013). Plus récemment, il a été mis en évidence que la production accrue de succinate dans les macrophages traités au LPS pouvait réguler la production de ROS et limiter la production des cytokines anti-inflammatoires IL-1RA, un récepteur leur permettant de baisser le niveau d'IL-1β, et IL-10 (Mills et al., 2016). Dans l'ensemble, ces événements

métaboliques (Figure 15) peuvent fournir à la cellule une énergie rapide et des fonctions nécessaires à l'activité bactéricide.

Les macrophages M2.

Le profil métabolique des macrophages M2 diffère complètement de celui des macrophages M1. En effet, les macrophages M2 tirent une grande partie de leur énergie de l'oxydation des AG et de la phosphorylation oxydative (O'Neill, 2016; Vats et al., 2006). Ces voies métaboliques permettent une génération d'énergie soutenue nécessaire dans les fonctions de réparation et de remodelage des tissus par les macrophages M2. L'augmentation de la phosphorylation oxydative est permise en raison d'une faible production d'oxyde nitrique et d'une forte activité de l'AMPK (AMP-activated protein kinase) au sein de la cellule. De même, l'activité de l'arginase 1 est augmentée au sein des macrophages M2 ce qui favorise la formation d'ornithine et de proline permettant non seulement la prolifération de la cellule mais aussi la production de collagène, nécessaire à la réparation tissulaire (Gordon, 2003). L'ornithine permet aussi la production de putrescine puis de spermidine, qui favorise l'hypunisation de l'eIF5A et ainsi la phosphorylation oxydation au cours de l'activation M2 (Puleston et al., 2019). De plus, lors de l'activation alternative, le facteur de transcription STAT6 (Signal Transducer and Activator of Transcription 6) est activé et induit à son tour l'expression de PGC-1β (Peroxisome proliferator-activated receptor gamma coactivator 1 beta) (Wu et al., 1999). La PGC-1β augmente l'activité de la β-oxydation en activant PPARγ (Peroxisome Proliferator-Activated Receptor gamma) et PPARδ ce qui permet l'induction de la respiration mitochondriale (Kang et al., 2008; Odegaard et al., 2007). Cette reprogrammation métabolique favorise l'oxydation des acides gras qui doivent être générés ou internalisés au sein de la cellule pour un polarisation M2 efficace. L'analyse métabolomique des macrophages classiquement ou alternativement polarisés montre une accumulation de monoacylglycérol au sein des macrophages M2, suggérant une lipolyse accrue au sein de ces cellules (Huang et al., 2014). De même, l'activité de LIPA, qui utilise des AG comme substrat, est augmentée dans les macrophages M2 (Viaud et al., 2018) et sa déficience entraine une diminution de l'oxydation des AG et altère la polarisation alternative (Huang et al., 2014). Enfin, l'entrée des AG par le récepteur CD36 joue un rôle clé au cours de la polarisation M2 des macrophages. En effet, la déficience de CD36 dans les macrophages conduit à un défaut

de polarisation alternative des macrophages (Huang et al., 2014). Les macrophages M2 expriment également un isoforme particulier de la PFK-2, la PFKFB1. L'isoforme PFKFB1 a une activité élevée et catalyse efficacement le fructose-2,6-bisphosphate en fructose-6-phosphate, abaissant ainsi le taux glycolytique. De plus, les niveaux élevés d'expression de CARKL permettent la diminution du flux par la voie du pentose phosphate (Figure 15) (Nagy and Haschemi, 2015).

Le métabolisme joue donc un rôle majeur sur le changement de phénotype des macrophages. Par ailleurs, il avait été montré que bloquer le métabolisme oxydatif par l'inhibiteur étomoxir bloquait non seulement le phénotype M2 mais entrainait également le macrophage dans un état M1. De même, forcer le métabolisme oxydatif dans un macrophage M1 potentialisait le phénotype M2 (Rodriguez-Prados et al., 2010; Vats et al., 2006). Cependant, l'analyse des macrophages déficients pour Cpt1 (carnitine palmitoyl-transferase) ou Cpt2, les deux enzymes cibles de l'étomoxir, a permis de démontrer que l'inhibition du métabolisme oxydatif n'avait aucun effet sur la polarisation M2 des macrophages (Divakaruni et al., 2018; Nomura et al., 2016). L'étude des doses d'étomoxir précédemment utilisées a montré que les doses choisies étaient trop fortes (200µM contre 3µM pour une dose spécifique et saturante) et que cela entrainait ainsi un effet non spécifique. En effet, à forte dose, la CoA libre intracellulaire est diminuée et induit alors le défaut de polarisation M2 indépendamment du métabolisme oxydatif (Divakaruni et al., 2018).

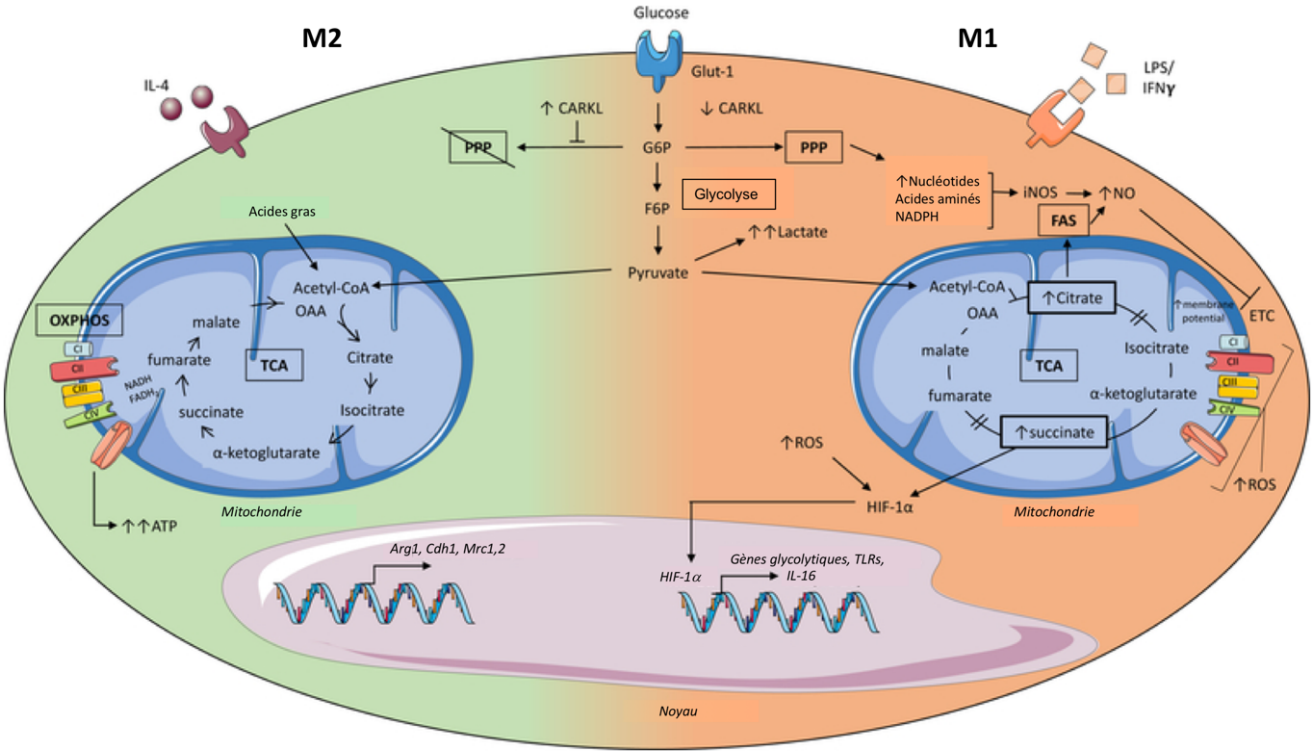

Figure 15 : Reprogrammation métabolique pendant la polarisation des macrophages

Adapté de Koelwyn et al., 2018. (Koelwyn et al., 2018)

Vue d'ensemble simplifiée des voies métaboliques dans les macrophages activés classiquement ou alternativement. Les macrophages M1 utilisent majoritairement la glycolyse aérobie (effet Warburg) pour produire de l'énergie sous forme de 4 molécules d'ATP. À partir d'une molécule de glucose, environ 5% seulement passent par le cycle de Krebs, tandis que la majorité est convertie en lactate. Cela permet à la cellule de produire à la fois de l'énergie et des substrats (biosynthèse des macromolécules) pour maximiser les taux de croissance et de prolifération. A l'inverse, les macrophages M2 utilisent le cycle de Krebs et la phosphorylation oxydative pour générer de l'ATP. Dans ce cas, la conversion d'une molécule de glucose est très efficace et génère 36 molécules d'ATP.

D. Les macrophages au cours des maladies cardio-métaboliques

1. *Durant l'obésité*

L'obésité, caractérisée comme une inflammation chronique à bas grade, est accompagnée de l'infiltration progressive de cellules immunitaire, notamment de macrophages, dans le tissu adipeux. Les ATM jouent un rôle clé dans l'établissement de l'inflammation chronique et des dérégulations métaboliques. La première observation de macrophages au sein du TA a été faite au début des années 2000 (Bornstein et al., 2000; Weisberg et al., 2003; Xu et al., 2003). Lors d'une prise de poids excessive, la taille des adipocytes augmente de manière extrême et conduit au recrutement et à la prolifération des macrophages au sein du tissu (Amano et al., 2014; Cinti et al., 2005; Fink and Cookson, 2005; Zheng et al., 2016). L'accumulation de macrophages dans le TA conduit à un état inflammatoire chronique qui altère la fonction adipocytaire et peut contribuer au développement de la résistance à l'insuline (Amano et al., 2014). Les ATM recrutés peuvent entourer les adipocytes endommagés dans une configuration en forme de couronne bien reconnaissable, c'est ce que l'on appelle les « crown like structures » (CLS) (Cinti et al., 2005). L'augmentation des CLS, considérées comme des lésions pathologiques, est corrélée à l'inflammation et à l'apparition de troubles métaboliques (Aouadi et al., 2013). Néanmoins, il reste encore à déterminer si cette augmentation des macrophages est due à la prolifération locale des ATM résidents ou au recrutement accru de monocytes par la circulation sanguine. L'axe CCR2-CCL2 contrôlant à la fois la sortie des monocytes de la moelle osseuse et la prolifération des ATM résidents, il semblerait que le recrutement et la prolifération soit interconnectés (Amano et al., 2014; Serbina and Pamer, 2006) et contribuent tous deux à la progression de la maladie.

i. Polarisation des macrophages au cours de l'obésité

En 2007, Lumeng et al. ont mis en évidence un changement phénotypique des macrophages lors de l'obésité (Lumeng et al., 2007a). En effet, les macrophages au sein du TA sain expriment les marqueurs IL-10, Arg1 (arginase I), Mrc2 (mannose receptor C type 2), Ym1/Chi3l3

(Ym1/chitinase 3–like 3), et Mgl1/2 (macrophage galactose N-acetyl-galactosamine–specific lectins 1 and 2), associés à la polarisation alternative. Cependant, dans les cas d'obésité, les macrophages changent de profil et acquièrent une signature pro-inflammatoire qui contribue à une augmentation de l'inflammation et des lésions tissulaires (Lumeng et al., 2007a; Lumeng et al., 2008). Durant l'obésité, la lipolyse du tissu adipeux est augmentée, ainsi les adipocytes génèrent des acides gras libres auxquels les macrophages sont localement exposés. Les AG libres peuvent être internalisés au sein des ATM *via* le récepteur de surface CD36. Comme nous l'avons vu précédemment, les macrophages M1 utilisent préférentiellement la glycolyse à l'inverse des macrophages M2 qui utilisent à la fois le glucose et les acides gras pour la phosphorylation oxydative. Dans les premiers stades de l'expansion du tissu adipeux, les ATM arborent un phénotype M2 avec une surexpression des marqueurs Arg1 et CD209e. Cependant, l'accumulation progressive de lipides dans les ATM induit une surexpression des marqueurs MCP-1 (CCL-2), TNF-α, INFβ et IFNAR (interferon-α/β receptor) démontrant ainsi le changement de polarisation des macrophages vers un profil M1. L'alimentation des souris au Rosiglitazone, un procédé permettant d'augmenter la capacité des adipocytes à stocker des lipides, permet le maintien de la polarisation M2 des macrophages. Ainsi, le changement de polarisation M1 des macrophages accumulant des lipides, telles les cellules spumeuses, laisse à penser que la lipotoxicité est un acteur clé dans la génération d'une inflammation dans le TA (Prieur et al., 2011). Cependant, une étude *in vivo* et *in vitro* a montré qu'au cours de l'obésité, ou après stimulation avec du palmitate, les macrophages ne se différenciaient pas en M1 comme durant les infections mais en Mme (macrophages activés métaboliquement) (Kratz et al., 2014). Ces macrophages sont distincts car ils ne présentent pas les marqueurs de surface des macrophages M1 tels que CD38, CD319 ou CD274. Le palmitate va se lier aux TLR et conduire à la production des cytokines pro-inflammatoires TNF-α, IL-1b, et IL-6. En parallèle, l'internalisation du palmitate active p62 et PPARγ et favorise le métabolisme lipidique tout en limitant l'inflammation. Ainsi, au cours de l'obésité, l'équilibre entre ces deux voies parallèles peut être modulé et entrainer des phénotypes complexes (Kratz et al., 2014).

ii. *Rôle des macrophages dans le tissu adipeux viscéral*

En condition physiologique ou d'obésité, les ATM sont essentiels pour l'homéostasie du tissu. Le tissu adipeux contient des populations de macrophages hétérogènes définies par des fonctions inflammatoires et métaboliques distinctes telles que les macrophages résidents, les macrophages activés ou encore les macrophages favorisant la phagocytose (Weinstock et al., 2019). Les macrophages permettent le bon développement du tissu adipeux (Pridans et al., 2018), stimulent le stockage des lipides en empêchant leur stockage ectopique, promeuvent l'angiogenèse et favorisent l'élimination des adipocytes morts par l'efférocytose (Thomas and Apovian, 2017). Cependant l'interaction entre les adipocytes et les ATM aggrave l'inflammation chronique chez les personnes obèses (Wellen and Hotamisligil, 2003). Lors de l'obésité, les adipocytes libèrent des cytokines pro-inflammatoires telles que MCP-1 et TNF-α (Schmoker et al., 2009) et des AG libres qui interagissent avec le récepteur TLR4 des ATM résidents, conduisant alors à une libération d'IL-1β dépendante de l'inflammasome (Shi et al., 2006). Ceci conduit à une production et une mobilisation accrue de monocytes et neutrophiles à partir de la moelle osseuse (Nagareddy et al., 2014; Scott and Owens, 2008; Suganami et al., 2005). De même, les macrophages activés vont sécréter des chimiokines pro-inflammatoires comme MCP-1, engendrant par la suite le recrutement des monocytes par la circulation sanguine au niveau du TA (Kamei et al., 2006). Une fois dans le TA, les monocytes vont se différencier en macrophages et augmenter le nombre de macrophages inflammatoires au sein du tissu adipeux, en parallèle de la prolifération locale des ATM. Ces macrophages interagissent avec les adipocytes en produisant du TNF-α, qui permet l'augmentation de la production des adipokines pro-inflammatoires et à l'inverse la diminution de la production d'adipokines anti-inflammatoires (Suganami et al., 2005). L'interaction entre les macrophages et les adipocytes entraine ainsi un cercle vicieux maintenant l'état d'inflammation chronique en recrutant constamment de nouveaux monocytes (Figure 16).

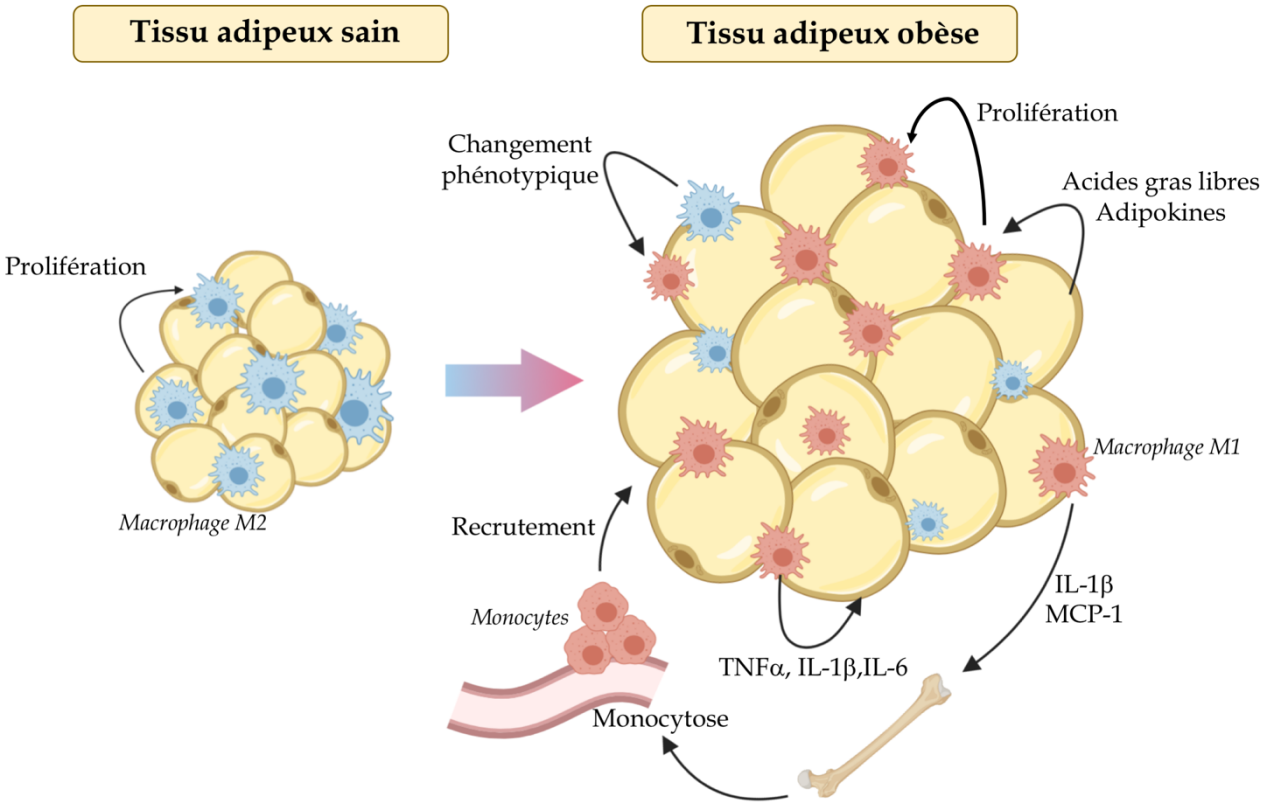

Figure 16 : Modulation des ATMs durant l'obésité
Adapté de Kraakman et al., 2014. (Kraakman et al., 2014)

iii. Rôle des macrophages dans le tissu adipeux brun et sous-cutané

Le tissu adipeux brun, comme nous avons pu le voir auparavant, est un organe essentiel où s'effectue la thermogenèse, caractérisée par une augmentation d'UCP1 dans les adipocytes. La thermogenèse est induite par des températures froides et dépend de la sécrétion des cytokines IL-4 et IL-13 par les cellules lymphoïdes innées (ILC) et les éosinophiles (Lee et al., 2015; Qiu et al., 2014; Rao et al., 2014). Les macrophages jouent un rôle majeur dans l'induction de cette thermogenèse. En effet, la sécrétion d'IL-4 et d'IL-13 va avoir un impact sur les ATM en favorisant leur phénotype M2. Ces macrophages M2 vont ainsi permettre la sécrétion de noradrénaline pour induire l'expression de gènes thermogéniques dans le tissu adipeux (Nguyen et al., 2011). La tyrosine hydroxylase (Th), l'enzyme limitante dans la production des catécholamines, n'étant pas exprimé dans les ATM (Fischer et al., 2017), la

production de noradrénaline ne peut pas venir des macrophages. Cependant, certains ATM du TA brun sont en étroite connexion avec des neurones au sein même du tissu (Wolf et al., 2017). Bien que les facteurs requis pour cette interaction restent à élucider, les macrophages, *via* la plexinA4, peuvent contribuer au phénomène d'attraction et de répulsion avec les axones sympathiques exprimant la Sema6A (Semaphorin 6A). Ainsi, les macrophages activés par l'IL-4 et l'IL-13 peuvent interagir avec les axones sympathiques présents au sein du TA brun, et permettre la sécrétion de noradrénaline par ces mêmes axones. De plus, une population de macrophages associés aux neurones (SAM) a été montré pour s'accumuler pathologiquement dans les nerfs du système nerveux sympathique chez les animaux obèses (Pirzgalska et al., 2017). Les SAM médient la clairance de la norépinephrine *via* le transporteur SLC6A2 et l 'enzyme de dégradation MAOA présente au sein des macrophages conduisant à un état pro-inflammatoire. L'ablation du transporteur SLC6A2 conduit à une augmentation de la thermogenèse et à une perte de poids chez les animaux obèses (Pirzgalska et al., 2017). De plus, les ATM possèdent un ensemble de gènes qui contrôle les niveaux de noradrénaline et qui régule sa dégradation (Camell et al., 2017). Enfin, les ATM peuvent directement interagir avec les adipocytes *via* VCAM1 et son ligand ITGA4, contrôlant ainsi l'expression de UCP1 indépendamment des neurones (Figure 17).

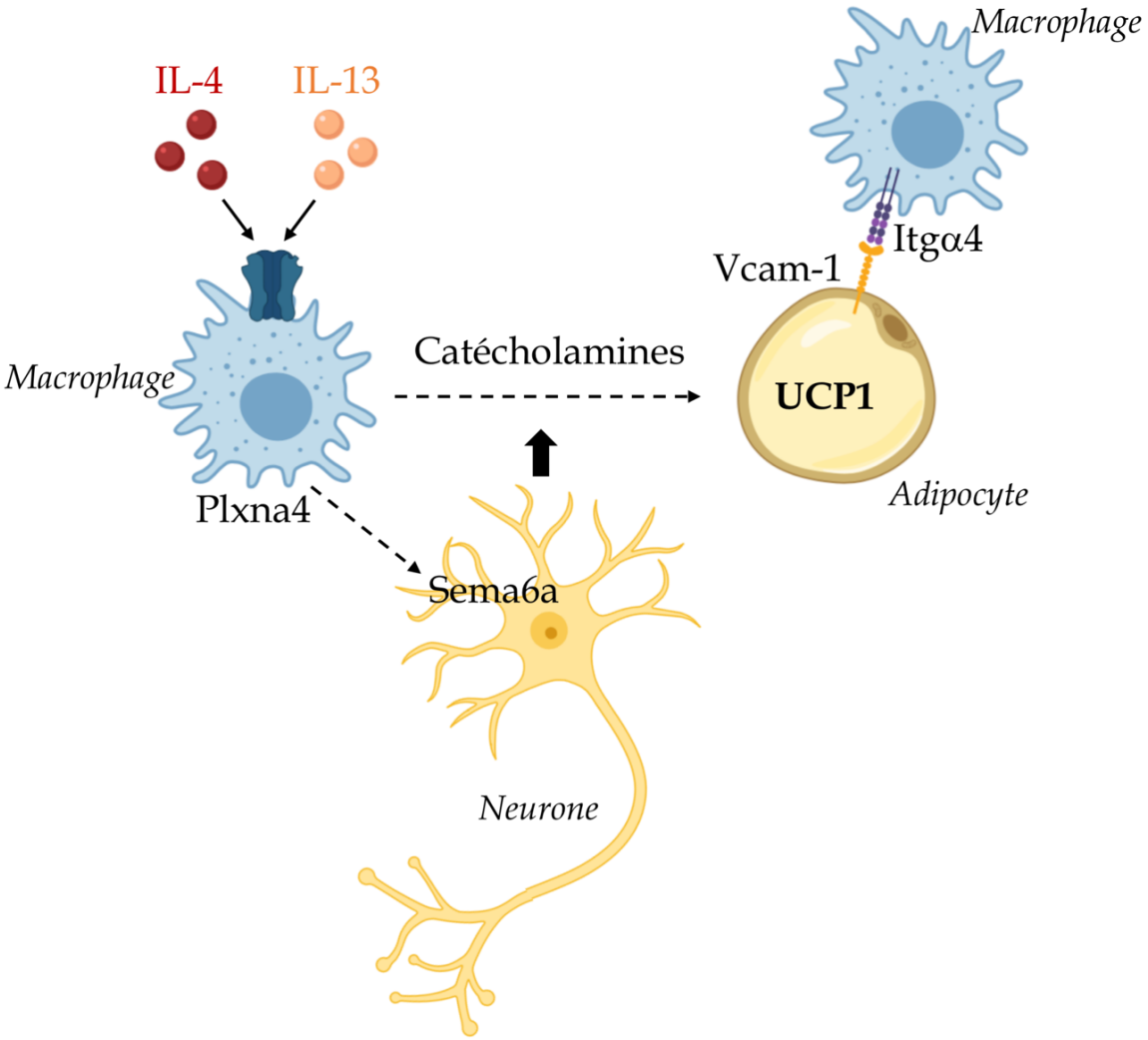

Figure 17 : Mécanismes induisant la thermogenèse du tissu adipeux
Adapté d'Ivanov et al., 2018. (Ivanov et al., 2018)

2. *Durant l'athérosclérose*

i. Origine et maintien des macrophages de la plaque

Les macrophages sont les cellules immunes les plus abondantes dans la plaque athéromateuse. Comme nous l'avons vu, le recrutement des monocytes est une étape importante dans le développement de la plaque. Pendant de nombreuses années, les monocytes ont été considérés à l'origine de tous les macrophages de la plaque (Swirski et al., 2006). En effet, le nombre de monocytes circulants corrèle avec le nombre de macrophages

dans la plaque (Combadiere et al., 2008). Il était de plus pensé que les iMos se différenciaient au niveau de la plaque en macrophages M1 tandis que les pMos infiltrant la plaque se différenciaient plutôt en macrophages M2. Cependant, l'origine des macrophages dans la plaque s'est avéré être bien plus complexe. A la fin des années 90, des études ont pu montrer que la présence de oxLDL pouvait favoriser la prolifération des macrophages *in vitro* (Hamilton et al., 1999; Martens et al., 1998). De plus, plusieurs études ont révélé que dans certaines conditions inflammatoires, les macrophages résidents pouvaient proliférer et ainsi contribuer à l'accumulation d'environ 87% des macrophages dans la plaque (Guo et al., 2005; Robbins et al., 2013; Schulz et al., 2012). Cependant, la prolifération *in situ* des macrophages est plus faible dans les lésions précoces que dans les lésions avancées (Lhotak et al., 2016).

ii. Fonction des macrophages dans la plaque

Comme nous avons pu le voir dans le chapitre précédent, les macrophages jouent un rôle clé dans l'initiation et la progression de l'athérosclérose. Principalement dérivés des monocytes et puis de la prolifération locale, le nombre de macrophages augmente jusqu'à 20 fois dans les aortes de souris athérogéniques (Moore et al., 2018). Durant le développement de l'athérosclérose, l'ingestion et l'accumulation de lipoprotéines par les macrophages entraine un changement de phénotype des macrophages vers des macrophages spumeux. L'accumulation des cellules spumeuses contribue à la croissance de la plaque et au stockage des lipides (Moore et al., 2018). De plus, les macrophages, en association avec les CLM, amplifient l'inflammation en produisant des cytokines pro-inflammatoires et des composants de la matrice extracellulaire, favorisant davantage la rétention des lipoprotéines au sein de la plaque. En raison de l'accumulation excessive de cholestérol libre dans les macrophages, la cellule active des réponses au stress du réticulum endoplasmique qui conduit, sur le long terme, à l'apoptose des macrophages. Dans les plaques avancées, la capacité des macrophages à éliminer les débris et les cellules apoptotique est altérée en raison de l'excès de cholestérol dans les cellules (Yvan-Charvet et al., 2010). Les macrophages au sein de la plaque dépendent fortement du glucose et ainsi du récepteur GLUT1, codé par le gène SLC2A1, qui permet son entrée. Les souris déficientes pour SLC2A1 spécifiquement dans les cellules myéloïdes (Lyz2cre) présentent une diminution de la glycolyse et du PPP. La déficience

pour SLC2A1 au niveau des cellules myéloïdes dans les souris athérogène Ldlr-/- conduit à une augmentation du cœur nécrotique, bien que la plaque soit de taille similaire (Freemerman et al., 2019; Morioka et al., 2018). De même, chez ces souris, la clairance des cellules apoptotiques est altérée et cela explique l'augmentation de l'instabilité de la plaque (Morioka et al., 2018). En effet, les défauts d'efférocytose contribuent à la nécrose secondaire et à la formation puis à l'expansion du cœur nécrotique, qui contribue à la vulnérabilité de la plaque (Moore et al., 2018). De plus, dans les plaques avancées, les macrophages spumeux expriment des molécules de rétention telles que la nétrine 1 ou la sémaphorine 3E, qui favorisent la rétention des macrophages au sein de la plaque et conduisent ainsi à leur accumulation (van Gils et al., 2012; Wanschel et al., 2013). Enfin, sous régime riche en graisses, les souris $Ldlr^{-/-}$ déficientes pour SLC2A1 dans les cellules myéloïdes présentent une diminution de la myélopoïèse et de l'infiltration des macrophages dans la plaque après induction d'une hyperglycémie transitoire intermittente (Flynn et al., 2020). Cela permet ainsi d'expliquer pourquoi l'hyperglycémie transitoire intermittente, présente chez les personnes diabétiques, est un facteur de risque indépendant des maladies cardiovasculaires (Flynn et al., 2020).

iii. Plasticité des macrophages de la plaque

Une des caractéristiques majeures des macrophage est leur plasticité, qui leur permet de produire une réponse adaptée aux stimuli du microenvironnement (Sica and Mantovani, 2012). Au sein de la plaque, des macrophages M1 et M2 coexistent, avec une majorité de macrophages M1 (Chistiakov et al., 2015). Chez l'Homme, les marqueurs cellulaires spécifiques des macrophages M1 ont été détectés dans les régions de la plaque sujettes à la rupture et instables tandis que les macrophages M2 prédominent dans les régions stables de la plaque et dans l'adventice, hors du cœur lipidique (Chinetti-Gbaguidi et al., 2011).

Le microenvironnement au sein des lésions est assez complexe. De ce fait, nous pouvons retrouver plusieurs sous-groupes de macrophages anti-inflammatoires dans la plaque. Les macrophages en conditions hémorragiques, les Mhem, résident dans les hémorragies intra-plaque et phagocytent les résidus érythrocytaires et les dépôts d'hémoglobines (Finn et al., 2012). Ces macrophages ont une surexpression des transporteurs du cholestérol ABCA1 et ABCG1 ainsi que de l'activité des LXR. Les Mhem ont donc une capacité accrue d'efflux du

cholestérol et participent ainsi à la prévention de la formation des macrophages spumeux (Boyle et al., 2012). Ce sous-ensemble qui participe au maintien de l'homéostasie au sein de la plaque athéromateuse est donc athéro-protecteur. Les macrophages Mox, vont être induits après exposition avec des lipides oxydés. Ces macrophages présentent une capacité réduite de phagocytose et de chimiotactisme. De plus, les Mox protègent du stress oxydatif grâce à l'expression de gènes tels que Hmox1 (Heme Oxygenase 1), Srxn1 (Sulfiredoxin 1), Txnrd1 (Thioredoxin Reductase 1) et Gsr (Glutathione Reductase) (Kadl et al., 2010). De même, les Mox sont capables de produire des cytokines pro-inflammatoires comme l'IL-1β ou la cyclooxygénase 2, de manière dépendante de l'activation de la voie TLR2 (Kadl et al., 2010).
Chez les souris présentant des plaques avancées, ce sous-groupe pro-athérogène représenterait 30% des macrophages de la plaque (Gleissner et al., 2008). Enfin, les M4 sont un sous-groupe polarisé par le facteur PF4 ou CXCL4, produits non seulement par les plaquettes sanguines mais aussi par les cellules endothéliales, les monocytes et les macrophages (Gleissner et al., 2010a). Ces macrophages M4 expriment la métalloprotéinase 7 (MMP7) et une protéine de liaison au calcium appelée S100A8 (Erbel et al., 2015). Les macrophages M4 sont définis comme athérogènes aux vues de leur production de cytokines pro-inflammatoires telles que l'IL-6 et le TNF-α et de leur défaut de phagocytose au sein de la plaque (Gleissner et al., 2010a; Gleissner et al., 2010b). Il faut noter qu'au cours de l'évolution de la pathologie, le microenvironnement et les signaux varient, renforçant le fait que la polarisation des macrophages est un processus dynamique qui varie au cours du temps (Gosselin et al., 2014; Lavin et al., 2014). Cependant, la dynamique et la distinction de ces populations restent à établir *in vivo*. En effet, des études récentes ont démontré par une technologie de séquençage Single-Cell la présence de multiples populations de macrophages au sein de la plaque (Cochain et al., 2018; Cole et al., 2018; Kim et al., 2018; Winkels et al., 2018). Néanmoins, des différences importantes existent dans ces études, notamment la fréquence des macrophages au sein de la plaque varie de manière significative. Une méta-analyse a récemment apparu proposant une unification de la nomenclature des cellules myéloïdes identifiées dans les études décrites ci-dessus (Zernecke et al., 2020).

E. Rôle de l'efférocytose dans l'athérosclérose

La clairance efficace des cellules apoptotiques au sein des tissus, un processus nommé efférocytose, régule de manière critique l'homéostasie tissulaire. Cependant, au cours des maladies chroniques inflammatoires comme l'athérosclérose, l'efférocytose devient défectueuse. Au sein des lésions athéromateuses, les macrophages présentent initialement une efférocytose efficace qui limite la progression de la plaque et l'accumulation de cellules mortes et débris cellulaires. Toutefois, au cours du développent de la pathologie, les macrophages subissent une reprogrammation cellulaire qui diminue la capacité efférocytique et entraine l'accumulation de cellules apoptotiques et une inflammation au sein de la plaque. L'efférocytose joue ainsi un rôle primordial au sein de la plaque et sa défaillance stimule la formatons du cœur nécrotique et peut déclencher la rupture de la plaque.

1. *Efférocytose et régulation de l'inflammation : généralités*

La détection et l'élimination des cellules apoptotiques sont deux fonctions physiologiques importantes permettant d'éliminer des millions de cellules endommagées ou mortes dans le corps (Thorp, 2010). Ce processus de clairance, nommé l'efférocytose, permet par la suite, la génération et la croissance de nouvelles cellules viables afin de remplacer les cellules sénescentes. L'efférocytose joue donc un rôle essentiel dans le maintien de l'homéostasie tissulaire (Fadok et al., 1992). En raison de ses mécanismes d'action qui n'entrainent pas la libération de cytokines ou chimiokines pro-inflammatoires, l'efférocytose est considérée comme une forme de phagocytose immunologiquement silencieuse. En effet, durant ce processus, les cellules apoptotiques sont éliminées avant de devenir nécrotiques. Ainsi, des cytokines anti-inflammatoires et des médiateurs lipidiques pro-résolvants sont sécrétés, empêchant la libération d'antigènes immunogènes (Hoffmann et al., 2001; Ravichandran and Lorenz, 2007). Afin de mieux comprendre le déroulement de l'efférocytose, nous allons nous intéresser aux différentes étapes de ce processus (Figure 18).

Le nombre de cellules apoptotiques dans un tissu sain est très faible, ce qui indique que les macrophages se mobilisent rapidement vers les cellules mortes afin de les éliminer

(Hochreiter-Hufford and Ravichandran, 2013). La migration des macrophages vers les cellules apoptotiques est menée par des facteurs chimiotactiques, les signaux « find-me », sécrétés par les cellules apoptotiques. Les nucléotides triphosphates ATP et UTP (Uridine Triphosphate) sont les signaux de détection les plus connus. Ils vont être libérés par les cellules apoptotiques via le canal Pannexin-1, et se lier aux récepteurs purinergiques P2Y à la surface des phagocytes (Elliott et al., 2009). De plus, la sécrétion de la chimiokine CX_3CL_1 par les cellules apoptotiques favorise le recrutement des phagocytes exprimant le récepteur de surface CX_3CR_1 (Truman et al., 2008). De même, la sphingosine-1-phosphate (S1P) est un signal « find-me » qui interagit avec ses récepteurs S1PR1 à S1PR5 et qui augmente l'érythropoïétine au sein des macrophages et améliore l'expression de nombreux récepteurs des phagocytes comme MerTK, MFGE8 (Milk fat globule-EGF factor 8 protein), Gas6 (Growth Arrest Specific 6) ou encore CD36 (Gude et al., 2008). Enfin, la lysophosphatidylcholine (LysoPC) est un puissant chimio-attractant qui réagit avec le récepteur G2A des monocytes et macrophages pendant l'efférocytose, cependant son rôle n'est pas encore clair (Lauber et al., 2003).

Bien que les signaux « find-me » permettent de guider les macrophages jusqu'aux zones riches en cellules apoptotiques, ce sont les signaux « eat-me » qui vont permettre l'identification et l'élimination spécifique des cellules apoptotiques (Gardai et al., 2006).

Les signaux « eat-me » sont présents à la surface des cellules apoptotiques et vont être reconnus par une panoplie de récepteurs à la surface des macrophages engendrant des cascades de signalisation et permettant ainsi le réarrangement du cytosquelette et l'engloutissement des cellules apoptotiques. Bien que de nombreux signaux aient été identifiés, la phosphatidylsérine (PS) est le signal « eat-me » le plus caractérisé (Fadok et al., 2001; Fadok et al., 1992). La PS est naturellement présente sur la surface interne de la membrane plasmique des cellules, cependant, lors de l'apoptose, la PS va se retrouver sur la surface externe de la membrane plasmique (Fadok et al., 1998). Les macrophages se lient à la PS présente à la surface des cellules apoptotiques *via* des récepteurs tels que la stabiline, BAI1, TIM (T cell Immunoglobulin Mucin domain 1), TAM (Tyr3, Axl, MerTK) ou CD300.

Le récepteur BAI1 se lie directement sur la PS et induit la polymérisation de l'actine et la phagocytose *via* le recrutement et l'activation des protéines Elmo-Dock-Rac (Park et al., 2007). La signalisation Elmo-Dock régule d'une part la dynamique de l'actine et d'autre part modifie l'expression de gènes inflammatoires, même si ce mécanisme reste à ce jour peu compris (Lee

et al., 2016). Les récepteurs TIM sont des glycoprotéines de surface qui se lient à la PS. Les récepteurs TIM-1 et TIM-3 sont les deux récepteurs majeurs impliqués dans la reconnaissance de la PS. La liaison de TIM-1 avec la PS est requise pour que les cellules apoptotiques inhibent NFκB et la production de cytokines inflammatoires (Ocana-Guzman et al., 2016; Yang et al., 2015). De plus, sur les sept gènes humains de CD300, trois ont été montrés pour se lier à la PS et moduler l'efférocytose : CD300A, CD300B et CD300F (84). Ces récepteurs peuvent entrainer des réponses activatrices ou inhibitrices selon leur association avec différents modules de signalisation cytoplasmique. Contrairement aux récepteurs que nous venons de voir, certains récepteurs peuvent reconnaître la PS des cellules apoptotique de manière indirecte *via* des protéines intermédiaires comme Gas6, la protéine S (ProS) ou encore MFG-E8. Les récepteurs TAM peuvent être activés par les protéines intermédiaires Gas6 et ProS, ce qui induit leur dimérisation et l'activation de Rac, permettant ainsi l'efférocytose (van der Vorst et al., 2015). Enfin, la protéine MFG-E8 peut se connecter à la fois à la PS à la surface des cellules apoptotiques et aux intégrines αvβ3 / αvβ5 à la surface des macrophages permettant ainsi la fixation indirecte des deux types cellulaires. Cette fixation va induire une activation de Rac1 et le réarrangement du cytosquelette afin de permettre la phagocytose des cellules apoptotiques (Akakura et al., 2004; Albert et al., 2000). Les cellules vivantes peuvent aussi exprimer la PS à la surface de leur membrane cellulaire tout en étant épargnées de leur efférocytose. Cette distinction entre les cellules apoptotiques et les cellules vivantes est possible grâce à la présence de signaux « don't eat-me » à la surface des cellules vivantes. En effet, l'expression de CD31 et de CD47 à la surface des cellules protège les cellules saines de l'efférocytose. Le récepteur CD31 provoque une répulsion ou un détachement des macrophages et inhibe ainsi leur engloutissement (Brown et al., 2002). Le récepteur CD47, quant à lui, est un marqueur du « soi » qui se lie à la protéine régulatrice α (SIRPα) à la surface des macrophages et inactive le réarrangement du cytosquelette (Lv et al., 2015; Oldenborg et al., 2001; Tsai and Discher, 2008).

Une fois le contact établi entre les cellules apoptotiques et les macrophages, les macrophages doivent réorganiser les réseaux de filaments d'actine pour former une coupe et permettre l'engloutissement des cellules apoptotiques. Les facteurs impliqués dans ce processus sont les GTPases RhoA, Cdc42 (Cell Division Cycle 42) et Rac1 (Ras-Related C3 Botulinum Toxin Substrate 1) (Mao and Finnemann, 2015). L'engloutissement des cellules apoptotiques par

les macrophages est inhibé lorsque RhoA est activée mais est au contraire augmenté par Cdc42 et Rac1.

La phagocytose des cellules apoptotiques par les macrophages entraine l'accumulation de matériaux cellulaires en excès tels que des lipides, des glucides, des protéines et des acides aminés. C'est pourquoi les macrophages adaptent leur métabolisme pour permettre la dégradation ou l'efflux de ce matériel. En effet, le cholestérol accumulé va être efflué *via* les transporteurs de cassette de liaison à l'ATP (ABC) vers des accepteurs de cholestérol extracellulaires. De plus, les macromolécules digérées fournissent de l'énergie à la cellule et induisent des changements cellulaires nécessaires pour continuer l'efférocytose à long terme. Ces changements incluent l'activation des PPAR δ/γ et des récepteurs LXR α/β qui vont non seulement stimuler l'expression de ABCA1 et ABCG1 pour effluer le cholestérol de la cellule, mais aussi vont améliorer l'efférocytose (Kidani and Bensinger, 2012; Lea et al., 2014; N et al., 2009). De plus, lorsqu'un macrophage dégrade efficacement une cellule apoptotique, il sécrète des facteurs bénéfiques tels que l'IL-10 et le TGF-β afin de bloquer le recrutement des cellules inflammatoires (Fadok et al., 1998).

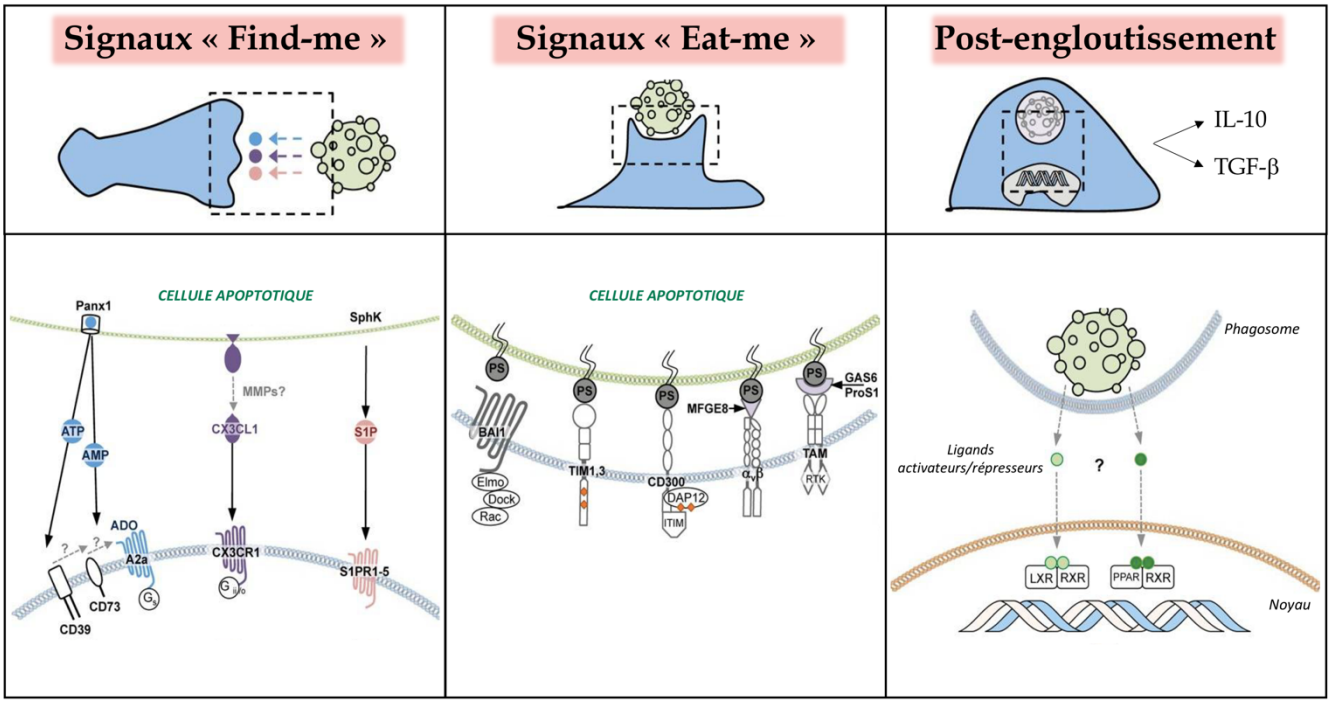

Figure 18 : Les différentes étapes de l'efférocytose

Adapté de Elliott et al., 2017. (Elliott et al., 2017)

2. *Dans les plaques précoces*

Dans les lésions précoces, l'apoptose des macrophages est associée à une diminution de la taille de la plaque et à une plus faible progression de la pathologie (Liu et al., 2005). L'efférocytose semble donc fonctionnelle au sein des lésions précoces et permettrait grâce à l'élimination des cellules apoptotiques ainsi qu'à la sécrétion de médiateurs anti-inflammatoires, de diminuer la taille de la plaque athéromateuse. De plus, il a été démontré que plus les macrophages entrent rapidement en apoptose plus les lésions sont petites (Arai et al., 2005). Ces données indiquent, qu'au début de la pathologie, les processus d'efférocytose et de résolution de l'inflammation ne sont pas encore défectueux (Figure 19).

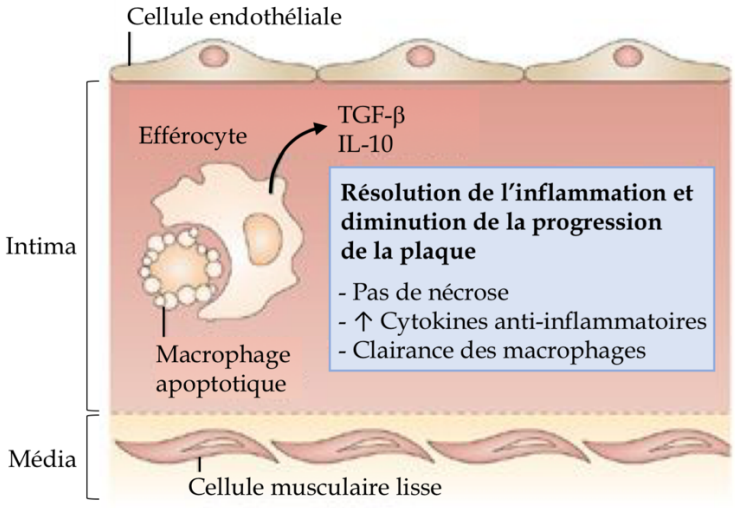

Figure 19 : L'efférocytose dans les lésions précoces
Adapté de Tabas, 2010. (Tabas, 2010)

3. *Dans les plaques avancées*

Contrairement aux premiers stades de l'athérosclérose où l'efférocytose permet la clairance rapide des cellules apoptotiques, dans les lésions avancées, le nombre de cellules apoptotiques augmente en raison d'un défaut des capacités efférocytiques au sein de la plaque (Kockx and Herman, 2000). Ce défaut d'efférocytose peut être dû à plusieurs mécanismes. Les lésions athéromateuses contiennent une grande quantité de lipides oxydés,

qui, à mesure que la pathologie progresse, s'accumulent. Ces lipides oxydés vont avoir plusieurs effets néfastes sur l'efférocytose. D'une part, ils peuvent se lier au récepteur CD14 et augmenter de ce fait l'activité de la GTPase RhoA, qui comme nous l'avons vu, inhibe l'engloutissement des cellules apoptotiques. D'autre part, ces lipides peuvent se lier aux récepteurs de reconnaissance des cellules apoptotiques et ainsi concurrencer avec les cellules apoptotiques (Gillotte-Taylor et al., 2001). De même, les auto-anticorps dirigés conte les lipides oxydés peuvent se lier aux signaux « eat-me » à la surface de cellules apoptotiques et ainsi masquer leur présence (Chang et al., 1999; Shaw et al., 2001). Enfin, les oxLDL augmentent la signalisation inflammatoire par le TLR4, ce qui conduit à la sécrétion accrue de cytokines pro-athérogènes telles que le TNF-α et l'IL-1β tout en inhibant la sécrétion des cytokines anti-inflammatoires TGFβ et IL-10 (Bae et al., 2009). Cet environnement pro-inflammatoire inhibe l'expression du récepteur MFGE8, connu comme un récepteur pro-efférocytique (Komura et al., 2009). De plus, la sécrétion de TNF-α induit l'expression de CD47, un signal « don't eat-me », à la surface des cellules de la plaque, empêchant donc l'internalisation des cellules apoptotiques (Kojima et al., 2016). Par ailleurs, au sein des lésions avancées, les récepteurs et les protéines intermédiaires permettant la reconnaissance des cellules apoptotiques par les macrophages sont altérés. En effet, quand les lésions progressent, la métalloprotéinase ADAM17 est capable de cliver le récepteur MertTK à la surface des macrophages, générant ainsi l'accumulation du fragment soluble du récepteur MerTK, solMer, qui a son tour inhibe l'efférocytose en compétant avec Gas6 (Cai et al., 2017; Sather et al., 2007). Enfin, le récepteur LRP1 des macrophages peut lui aussi être régulé à la baisse par l'activation de TLR4 et inactivé par son clivage médié par ADAM17 (Costales et al., 2013; Gardai et al., 2005).

En conséquence de ces différentes modifications cellulaires, les macrophages sont incapables de dégrader efficacement les cellules apoptotiques dans la plaque et se transforment eux même en cellules spumeuses favorisant par la suite les réponses inflammatoires par la sécrétion de cytokines pro-inflammatoires et de ROS. De plus, la diminution de la clairance des cellules apoptotiques entraine leur nécrose qui conduit à la progression de l'athérosclérose et à ses complications (Randolph, 2014). En effet, les cellules apoptotiques non phagocytées vont subir une dégradation de leurs membranes cellulaires, ce qui conduit à la libération de leur contenu intracellulaire dans l'intima. Parmi ces facteurs libérés on

retrouve des protéases, des cytokines favorisant l'inflammation locale et l'angiogenèse telles que TNF-α, IL-1β et IL-6 ou encore des facteurs tissulaires thrombogènes qui peuvent accélérer la pathologie et favoriser la vulnérabilité de la plaque (Figure 20) (Gautier et al., 2009; Martinet et al., 2011). L'efférocytose joue donc un rôle majeur dans le développement de l'athérosclérose, et le défaut de ce processus peut entrainer l'accélération de la pathologie.

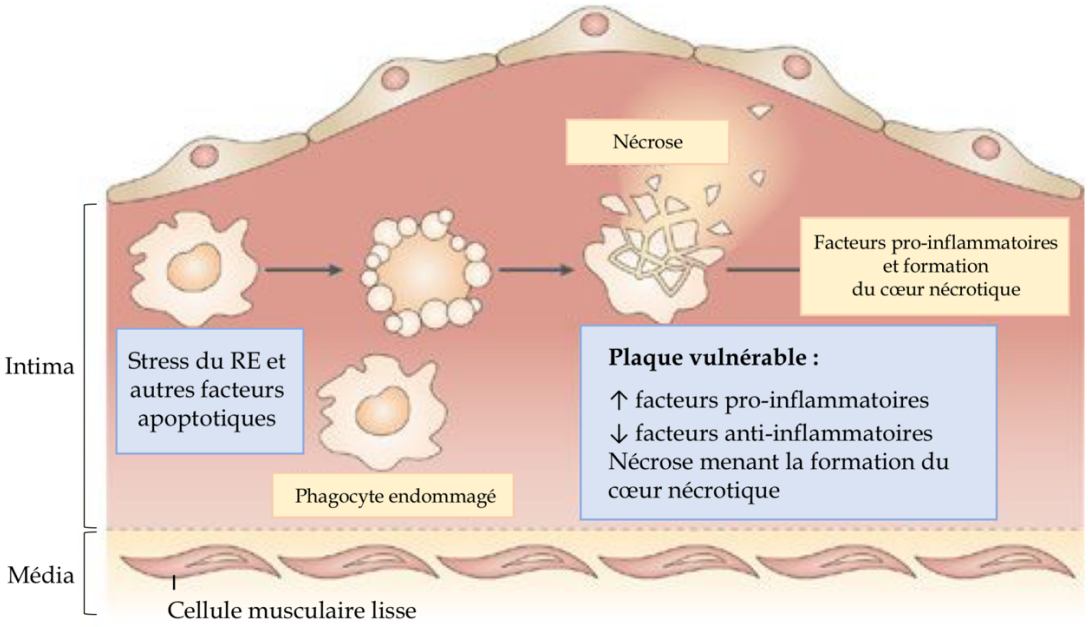

Figure 20 : L'efférocytose dans les lésions avancées
Adapté de Tabas, 2010. (Tabas, 2010)

Chapitre IV : La glutamine, un biomarqueur émergent dans les maladies cardio-métaboliques

A. Généralités

Tout comme le glucose, la glutamine est un nutriment essentiel pour le maintien de l'homéostasie corporelle (Bode, 2001; Newsholme et al., 2003b). La glutamine (Gln) est l'acide aminé le plus abondant de l'organisme. En effet, dans le plasma ou les tissus, la concentration de Gln est 10 à 100 fois supérieure à tout autre acide aminé. La concentration de Gln dans le plasma varie de 200 à 800 µM/L, représentant ainsi 20% des acides aminés totaux dans le sang (Newsholme et al., 2003b; Roth, 2008). Dans le foie et les muscles squelettiques la concentration de Gln représente 40 à 60% des acides aminés totaux (Labow et al., 2001). La Gln joue différents rôles essentiels au niveau des tissus. En effet, elle favorise la synthèse protéique ainsi que des sucres aminés et des nucléotides (Blomqvist et al., 1995), permet le maintien de la balance acide/base et participe à la croissance cellulaire (Duran et al., 2012). En effet, la glutamine sert de substrat dans de nombreuses voies métaboliques et régule également la balance redox en stimulant la synthèse du glutathion (Newsholme et al., 2003b). Au niveau du cerveau, la glutamine contribue au cycle glutamine/glutamate contrôlant de nombreux influx nerveux (Bak et al., 2006). La Gln est un acide aminé classé comme non essentiel. En effet, dans des conditions physiologiques, le corps est capable de synthétiser de la glutamine par l'enzyme glutamine synthétase (GS) de manière endogène. Cependant, il devient conditionnellement essentiel au cours des maladies inflammatoire notamment dans les cancers (Carey et al., 2015). En effet, la demande en Gln par les cellules devient accrue, et la synthèse endogène de cet acide aminé n'est pas suffisante. La disponibilité de la Gln dans l'organisme dépend de l'équilibre entre sa synthèse (ou son apport par l'alimentation) et de sa dégradation au sein des tissus.

B. Synthèse de glutamine

La synthèse *de novo* de Gln est réalisée par la GS, l'unique enzyme permettant la formation de glutamine dans l'organisme. Au sein du cytoplasme des cellules, la GS convertie, en présence d'ATP, le glutamate et l'ammoniac en glutamine (Figure 21). Cette enzyme, codée par le gène GLUL (glutamate amonia ligase), est principalement active dans les muscles squelettiques, les poumons, le foie, le tissu adipeux et le cerveau. L'expression de la GS est majoritairement régulée par les glucocorticoïdes, l'insuline et la concentration intracellulaire de glutamine (Labow et al., 2001; Wang and Watford, 2007) et a été montrée pour diminuer au cours de l'âge (Pinel et al., 2006). De très rares cas de mutations congénitales du gène GLUL entrainant une déficience pour la GS ont été rapportés, tous conduisant à des encéphalopathie épileptiques sévères le plus souvent létales (Haberle et al., 2005; Haberle et al., 2006; Haberle et al., 2011).

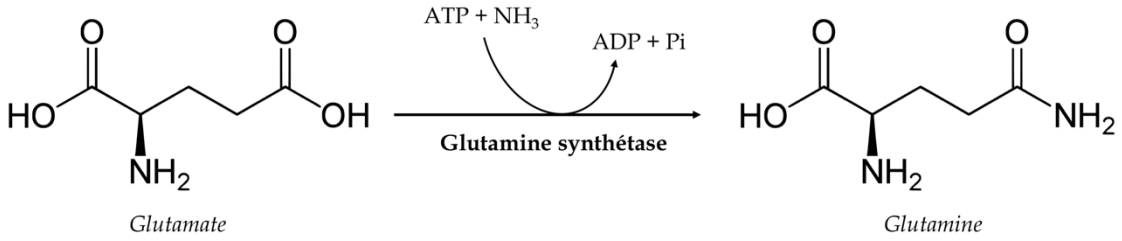

Figure 21 : Synthèse de glutamine par la glutamine synthétase

C. Transport de la glutamine au sein de la cellule

Une fois la Gln synthétisée ou apportée par l'alimentation, elle est livrée aux différents tissus de l'organisme. L'entrée de la Gln au sein des cellules est contrôlée par des transporteurs localisés au niveau de la membrane plasmique des cellules. Il existe plusieurs classes de transporteurs ayant de l'affinité pour la Gln. En effet, un transporteur peut permettre l'entrée ou la sortie de plusieurs acides aminés, et inversement, un acide aminé peut utiliser plusieurs transporteurs différents. Les transporteurs de la Gln sont classifiés en deux grands groupes :

les transporteurs dépendants de l'ion sodium, et les transporteurs indépendants de l'ion sodium (Bode, 2001). A l'origine, les transporteurs de la Gln étaient classifiés en « systèmes » basés sur la spécificité du substrat. Les systèmes les plus décrits sont : le système A (nommé pour préférer l'alanine) (Oxender and Christensen, 1963), le système N (nommé pour préférer les acides aminés contenant de l'azote au sein de leurs chaînes latérales) (Schioth et al., 2013), le système ASC (nommé pour préférer l'alanine, la sérine et la cystéine) et le système B0, qui appartiennent tous quatre au groupe des transporteurs dépendant de l'ion sodium, et enfin le système L (nommé pour préférer la leucine) qui appartient aux transporteurs indépendants de l'ion sodium (Oxender and Christensen, 1963). Plus récemment, la nomenclature des transporteurs a été standardisée sur la base de leurs similitudes de séquences en rapport avec les familles de gènes et de protéines. Cette nomenclature nommée SLC (Solute Carrier) permet ainsi un regroupement plus structuré des transporteurs (McGivan and Bungard, 2007) (Table 2).

Table 3 : Nomenclature des principales protéines utilisées dans le transport de la Gln.

Famille	Membre	Nom commun	Système
SLC1	A5	ASCT2	ASC
SLC6	A19	B0AT1	B0
SLC7	A5	LAT1	L
	A8	LAT2	
SLC38	A19	SNAT1	A
	A2	SNAT2	
	A3	SNAT3	N
	A5	SNAT5	
	A7	SNAT7	
	A9	-	-

Enfin, au sein de la cellule, la glutamine est essentielle au niveau de la mitochondrie où de nombreuses voies métaboliques se produisent. Malgré de nombreuses années de recherche, le transporteur de la glutamine au niveau de la membrane mitochondriale reste non identifié.

Des études préliminaires sur la fonction du transporteur mitochondrial de la Gln ont été réalisées (Sastrasinh and Sastrasinh, 1989) et quelques années plus tard la protéine responsable de cette fonction a pu être isolée et purifiée (Indiveri et al., 1998). Cependant, aucune nouvelle avancée scientifique dans l'identification de la protéine et de son gène n'a été réalisée.

1. *Le transporteur SLC1A5 : ASCT2*

Le transporteur SLC1A5, anciennement connu sous le nom ASCT2, est un transporter de la Gln appartenant à la famille SLC1 (Kanai et al., 2013). C'est le premier transporteur de la Gln à avoir été isolé en 1996 à partir de placenta humain (Kekuda et al., 1996). Ce transporteur, formé de huit domaines transmembranaires et 2 boucles en épingle à cheveux, permet l'échange antiport d'acides aminés neutres de manière dépendante du sodium (Utsunomiya-Tate et al., 1996). Le transport des acides aminés est fonctionnellement asymétrique. En effet, la glutamine, la sérine, l'asparagine et la thréonine peuvent être transportées dans les deux sens tandis que l'alanine, la valine et la méthionine ne peuvent être transportées que vers l'intérieur de la cellule (Pingitore et al., 2013). Le gène SLC1A5 est exprimé dans plusieurs tissus tels que le rein, l'intestin, le cerveau, le poumon, le muscle squelettique, le placenta et le pancréas (Deitmer et al., 2003; Kekuda et al., 1996; Utsunomiya-Tate et al., 1996). Le transporteur SLC1A5 est impliqué dans le cycle glutamine/glutamate au niveau du cerveau. En effet, il permet l'efflux de la glutamine vers la fente synaptique et permet ainsi, via d'autres transporteurs de la Gln, l'élimination de l'excès de glutamate (Glu) alors libéré (Broer et al., 1999). Au niveau du placenta, il permet l'entrée de la glutamine au sein du foie fœtal afin qu'elle soit utilisée au cours du métabolisme du fœtus (Torres-Zamorano et al., 1998).

2. *Le transporteur SLC6A19 : B0AT1*

Le transporteur SLC6A19, anciennement nommé B0AT1, appartient à la famille des SLC6, qui sont des transporteurs de neurotransmetteurs dépendants de l'ion sodium. Le transporteur SLC6A19, localisé majoritairement au niveau des reins et de l'intestin (Broer, 2006; Pramod et

al., 2013; Verrey et al., 2005), est spécifique des acides aminés neutres et présente une affinité intermédiaire pour la Gln (Bohmer et al., 2005; Ugawa et al., 2001). Au vu de sa localisation, il est supposé que le transporteur SLC6A19 est le principal responsable de l'absorption de la Gln alimentaire dans l'intestin par les microvillosités intestinales et de la réabsorption rénale par les tubules proximaux (Bohmer et al., 2005; Broer et al., 2011; Verrey et al., 2005). Le transport des acides aminés par SLC6A19 est électrogène et permet ainsi un transport efficace des acides aminés même en présence de gradients de concentrations défavorables (Bohmer et al., 2005; Oppedisano et al., 2011; Uchiyama et al., 2008).

3. *Les transporteurs SLC38 : SNATs*

Les transporteurs SLC38 sont des protéines hautement spécifiques de la glutamine (Broer, 2014; Schioth et al., 2013). La famille SLC38 comprend au total 11 transporteurs, à l'origine classifiés comme systèmes A et N, et que l'on a ensuite appelé SNATs. Parmi cette famille, 6 transporteurs sont spécifiques de la Gln, à savoir : SLC38A1, A2, A3, A5, A7 et A9. Tandis que les transporteurs SLC38A1, A2, A7 et A9 sont omniprésents (Albers et al., 2001; Chaudhry et al., 2002; Hagglund et al., 2011), le transporteur SLC38A3 est exprimé dans le foie, les muscles squelettiques, les reins et le pancréas (Chaudhry et al., 1999) et le transporteur SLC38A5 est exprimé dans l'estomac, le cerveau, le foie, les poumons, l'intestin grêle, la rate, le côlon et les reins (Nakanishi et al., 2001). A la différence des autres membres de la famille SLC38 qui se trouvent sur la membrane plasmique des cellules, le transporteur SLC38A9 est localisé spécifiquement au niveau de la membrane lysosomale. Comme les transporteurs que nous avons pu voir, la famille SLC38 est dépendante de l'ion sodium. L'absorption de la Gln est électrogène pour les transporteurs SLC38A1 et A2. Au contraire, les transporteurs SLC38A3, A5 et A7 sont aussi des échangeurs Na+ / H+ (cation hydrogène) et permettant donc un mécanisme de transport électroneutre (Broer, 2014). Les transporteurs SLC38 vont jouer des rôles différents selon leur localisation. Au sein du cerveau, les transporteurs SLC38 participent au cycle Gln/Glu entre les neurones et les astrocytes (Schioth et al., 2013). En effet, les transporteurs SLC38A3, A5 et A7 libèrent la Gln des astrocytes, tandis que les transporteurs SLC38A1 et A2 permettent son absorption au sein des neurones. Le transporteur SLC38A3 est considéré comme un capteur de l'état nutritionnel de la cellule. En effet, à de faibles doses

plasmatiques de Gln, le transporteur SLC38A3 des cellules β libère de la Gln et permet la sécrétion de glucagon *via* SLC38A2. Cependant, en présence de fortes concentrations de Gln dans le plasma, SLC38A3 accumule la Gln et permet son hydrolyse en Glu, permettant par la suite la production d'ATP (Jenstad and Chaudhry, 2013). Dans le foie, SLC38A1, A2, A3 et A5 régulent la gluconéogenèse et participe au cycle Gln/ alanine entre le foie et le muscle (Kondou et al., 2013). Dans l'intestin, les transporteurs SLC38A1 et A2 permettent le transfert de la Gln de l'intestin vers le sang (Broer, 2008). Au niveau du rein, SLC38A3 participe à l'absorption de la Gln par la circulation (Busque and Wagner, 2009). Enfin au niveau du placenta, SLC38A1 et A2 permettent l'absorption de la Gln au niveau du fœtus pour ensuite être utilisée comme source d'énergie.

4. *Les transporteurs SLC7A5 et SLC7A8 : LAT1/LAT2*

Les transporteurs SLC7A5 et SLC7A8, aussi appelés LAT1 et LAT2 respectivement, sont deux transporteurs appartenant à la famille des SLC7. La famille SLC7 se compose de deux grands groupes : les transporteurs cationiques d'acides aminés et les transporteurs d'acides aminés hétérodimériques dont font partie SLC7A5 et SLC7A8 (Fotiadis et al., 2013). SLC7A5 est majoritairement exprimé au niveau du cerveau, des testicules, de la moelle osseuse et du placenta (Fotiadis et al., 2013; Prasad et al., 1999) mais est aussi retrouvé dans les ovaires, la rate, le côlon, la barrière hémato-encéphalique, le foie fœtal, les muscles squelettiques, le cœur, les poumons, le thymus, les reins et à la surface des lymphocytes activés (Kanai et al., 1998; Yoon et al., 2005). Quant à lui, le transporteur SLC7A8 est principalement exprimé au niveau des reins, du placenta, du cerveau, de la rate, des muscles squelettiques, du petit intestin et des poumons (Fotiadis et al., 2013; Fraga et al., 2005; Pineda et al., 1999; Yoon et al., 2005) mais se retrouve aussi au sein de la prostate, des ovaires, des testicules et du foie fœtal (Park et al., 2005). Au sein de la membrane plasmique SLC7A5 et SLC7A8 forment un hétérodimère avec la glycoprotéine SLC3A2 par la formation d'un pont disulfure entre les deux résidus de cystéine (Kanai et al., 1998). Cependant, seules les sous-unités SLC7A5 et SLC7A8 jouent un rôle dans le transport des acides aminés (Napolitano et al., 2015). Le transporteur SLC7A5 permet l'échange de tous les acides aminés avec une préférence pour l'histidine (Scalise et al., 2018), tandis que SLC7A8 est un transporteur des acides aminés neutres.

Contrairement aux autres transporteurs que nous avons pu voir, ces deux transporteurs fonctionnent indépendamment du sodium et du pH. En effet, le rôle de ces transporteurs antiport est de permettre l'efflux de la glutamine, en utilisant le gradient de glutamine, en échange d'un acide aminé neutre (principalement la leucine). Les transporteurs SLC7A5 et SLC7A8 présentent une asymétrie fonctionnelle. En effet, la tyrosine, la leucine, la phénylalanine, l'isoleucine, la méthionine et la cystéine sont principalement transportées dans l'espace intracellulaire des cellules tandis que la Gln est majoritairement effluée vers l'extérieur (Napolitano et al., 2015). La régulation du transporteur SLC7A5 a beaucoup été étudié au vu de son rôle dans le développement des cancers. En effet, SLC7A5 peut être régulé par le proto-oncogène c-myc, et la sous-expression de c-myc entraine la diminution de l'expression du récepteur SLC7A5 dans les cellules de la prostate (Hayashi et al., 2012). De même, l'insuline régule positivement l'ARNm du transporteur SLC7A5 dans les cellules musculaires squelettiques (Walker et al., 2014). Enfin, le traitement chronique par l'aldostérone entraine une expression à la hausse des transporteurs SLC7A5 et SLC7A8 dans les cellules épithéliales jéjunales (Amaral et al., 2008).

D. Les glutaminases

La glutaminase (Gls) a été décrite pour la première fois en 1935 par Krebs (Krebs, 1935). Dans son étude, il met en évidence l'existence d'au moins deux types de glutaminases différentes par leurs localisations tissulaires et leur capacité à être inhibées par l'acide glutamique : la glutaminase exprimé dans le cerveau et les reins (brain or kidney-type) et la glutaminase exprimée dans le foie (liver-type) (Krebs, 1935). Ce n'est qu'en 1987 que ces enzymes ont pu être purifiées et précisément identifiées chez le rat puis plus tard chez l'Homme (Heini et al., 1987; Smith and Watford, 1988). Sur la base de ces travaux, on distingue deux types de glutaminase, la glutaminase 1 (Gls1) aussi appelé KGA (kidney-type glutaminase) et la glutaminase 2 (Gls2) aussi appelée LGA (liver-type glutaminase). Ces deux enzymes, dérivées de gènes distincts, ont des caractéristiques cinétiques, immunologiques et moléculaires différentes.

1. *La glutaminase 1 (ou KGA)*

i. Structure

La glutaminase 1 est codée par le gène GLS situé sur le chromosome 2 humain (Mock et al., 1989). Ce gène de 82 kb contient 19 exons et existe sous trois types d'épissages alternatifs différents : la KGA, la glutaminase C (GAC) et la GAM (Figure 22) (Elgadi et al., 1999). L'ARNm de la KGA est la transcription primaire de la glutaminase exprimée dans les reins, le cerveau et l'intestin (Shapiro et al., 1991). LA KGA est une protéine de 669 acides aminés. Les 16 premiers acides aminés de la protéine forment une hélice amphipathique qui permet son adressage vers la mitochondrie (Shapiro et al., 1991). Une fois transloquée au sein de la mitochondrie, la séquence d'adressage vers la mitochondrie est coupée par une protéase qui clive également la protéine après l'acide aminé 72 générant ainsi une sous-unité mature de 66kDa (Srinivasan et al., 1995). La variante de la KGA, nommée GAC, est plus courte et est composée de 598 acides aminés. Tout comme la KGA, la GAC est transloquée au niveau de la mitochondrie et possède une sous-unité mature de 58kDa. Les deux protéines partagent 550 acides aminés en communs mais diffèrent par leur région C-terminale. La région centrale contenant le domaine catalytique est hautement conservée des bactéries aux humains (Brown et al., 2008). *In vitro*, les protéines KGA et GAC sont activées par du phosphate inorganique, permettant leur passage de dimères inactifs en tétramères actif (Godfrey et al., 1977). Le dernier sous-type de glutaminase, la GAM, possède une séquence de 169 acides aminés, dont les 72 premiers sont clivés une fois que la protéine se trouve au sein de la mitochondrie, laissant ainsi une protéine tronquée de seulement 11kDa. Compte tenu de sa taille, qui ne lui permet pas d'avoir une activité glutaminase, et de la rareté de sa séquence C-terminale qui correspond à une inclusion d'introns, il n'est pas clair si la GAM existe réellement ou si elle est le résultat d'un défaut génétique des cellules à partir desquelles elle a été isolée (Sammeth et al., 2008).

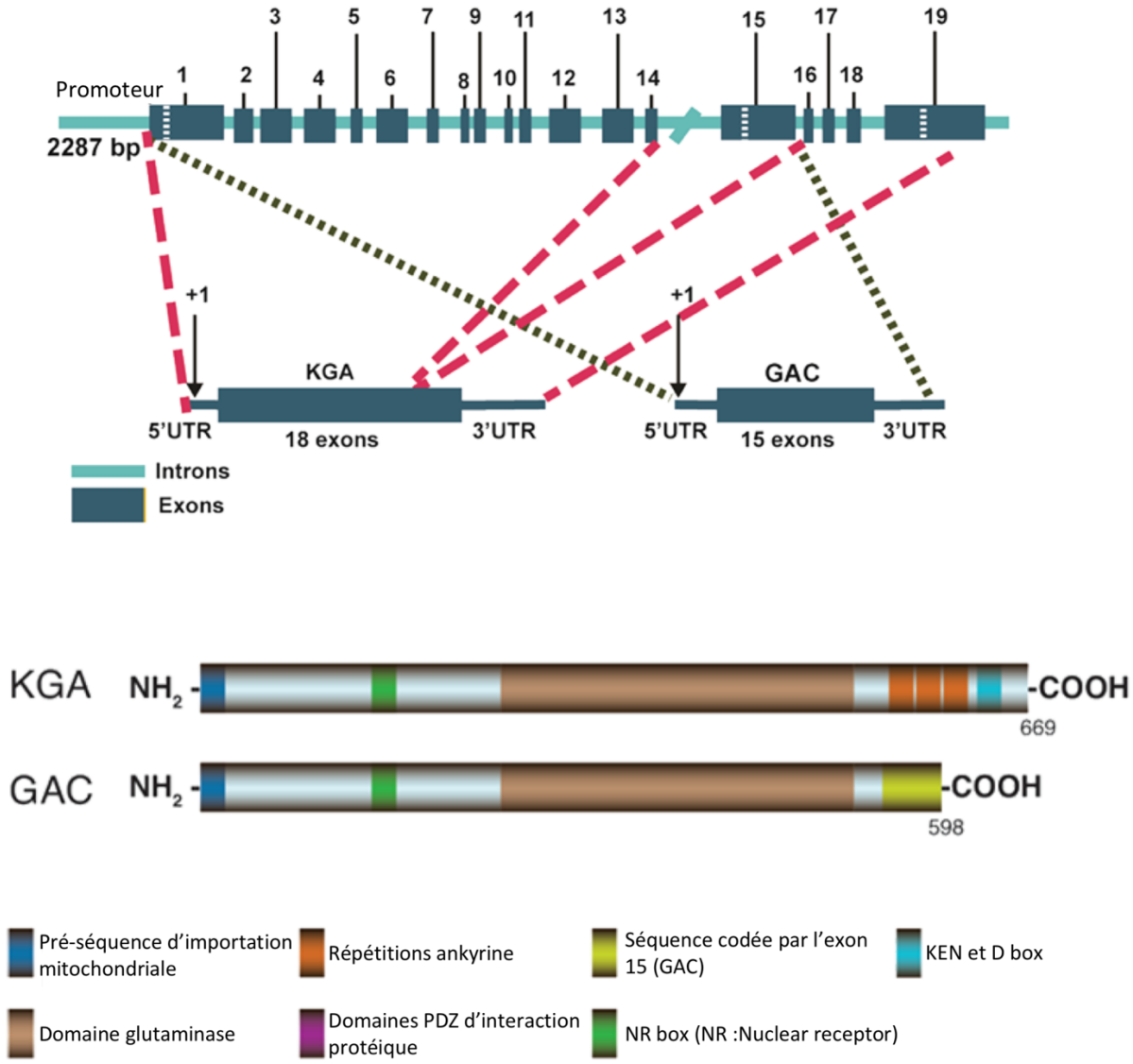

Figure 22 : Structure génomique du gène GLS humain et de ses transcrits alternatifs KGA et GAC. (Campos-Sandoval, 2019)

ii. Fonction

La glutaminase est une enzyme qui permet l'hydrolyse de la Gln pour former du glutamate et de l'ammonium. Le glutamate est ensuite converti en α-kétoglutarate (α-KG), un intermédiaire du cycle de Krebs, pour produire à la fois de l'ATP et des carbones anabolisants pour la synthèse d'acides aminés, de nucléotides et de lipides (Wise and Thompson, 2010). Dans l'organisme la Gls1 joue un rôle essentiel dans divers processus métaboliques, comme l'équilibre redox, la signalisation mTOR (mammalian target of rapamycin), l'apoptose ou encore l'autophagie, mais toutes les fonctions métaboliques de la glutaminase seront détaillées dans la partie suivante (voir IV.B). Au sein du cerveau, la Gln permet 70% de la synthèse du Glu au niveau des neurones et est indispensable pour la transmission synaptique glutamatergique. Chez la souris, la déficience totale du gène Gls1 est létale. En effet, les souris déficientes pour Gls1 sont plus petites, présentent des troubles du comportements empêchant la lactation et une hyperventilation, le tout entrainant leur mort 36h après leur naissance (Masson et al., 2006).

iii. Régulation

Les mécanismes de régulation de la Gls1 ne sont pas encore bien compris. Quelques études ont pu mettre en évidence un lien entre l'oncogène c-myc et la Gln. En effet, la déprivation en Gln induit une apoptose dépendante de l'activité de c-myc dans les cellules humaines (Yuneva et al., 2007). Au sein des cellules cancéreuses, l'expression de la glutaminase est régulée positivement par c-myc *via* les miARN 23a/b (Gao et al., 2009). Rathore *et al.* ont pu démontrer que la Gln permettait l'adressage au niveau du noyau de la sous-unité p65 de NF-κB, qui va alors se lier au promoteur de miR23a et l'inhiber, entrainant ainsi l'expression de la Gls1 (Rathore et al., 2012). De même, la voie mTOR est capable de réguler indirectement l'expression de la Gls1 en améliorant la traduction de la protéine c-myc (Csibi et al., 2014). De plus, L'ARNm de la Gls1 peut être surexprimé en réponse à l'acidose dans les cellules rénales (Laterza and Curthoys, 2000). La glutaminase est aussi régulée *via* la modulation de son activité enzymatique sans modification de son expression protéique (Colombo et al., 2011; Thangavelu et al., 2012; Wang et al., 2010). En effet, la GLS1 est régulée positivement par l'EGF par la signalisation Raf-Mek-Erk (Thangavelu et al., 2012). Par ailleurs, la Gls1 est

modulée au cours du cycle cellulaire par l'APC/C-Cdh1 qui stabilise la GLS1 à la fin de la phase G1 et au cours de la phase S (Moncada et al., 2012). Enfin, au cours des encéphalopathies liées au VIH ou en réponse à l'IFN-α, le facteur de transcription STAT1 est activé et phosphorylé. Ainsi, il est capable de se fixer sur le promoteur de la glutaminase et permet l'augmentation de son expression (Zhao et al., 2013).

2. *La glutaminase 2 (ou LGA)*

La LGA (ou tout simplement glutaminase 2) est codée par le gène Gls2, situé sur le chromosome 12 humain (Aledo et al., 2000). Ce gène de 18 exons qui s'étend sur 18 kb, est principalement retrouvé au niveau foie mais aussi dans le cerveau et le pancréas (Aledo et al., 2000), et existe en deux transcrits appelés GAB et LGA (Figure 23) (Martin-Rufian et al., 2012). L'isoforme GAB est plus longue et est formée de 602 acides aminés, tandis que l'isoforme courte LGA possède 565 acides aminés. Contrairement aux isoformes de la Gls1 qui diffèrent par leurs extrémités C-terminales, les isoformes de la Gls2 diffèrent par leurs extrémités N-terminales. Les protéines LGA et GAB sont principalement exprimées dans le foie, au niveau des mitochondries des cellules. Une fois au sein de la mitochondrie, les résidus N-terminaux de la GAB sont tronqués (Campos-Sandoval et al., 2007; Lee et al., 2014). Dans le cerveau, la Gls2 est retrouvée au sein du noyau des cellules neuronales et astrocytaires (Cardona et al., 2015; Olalla et al., 2002). La Gls 2 est activée par des taux faibles de phosphate et légèrement inhibée par le glutamate. De plus, la Gls2 est activée par l'ammoniac, qui comme nous l'avons vu, inhibe l'enzyme GLS1 (McGivan et al., 1980; Patel and McGivan, 1984). Enfin la Gls2 joue un rôle anti-ongénique via la p53 qui régule positivement la Gls2 et qui permet l'augmentation des processus antioxydants (Hu et al., 2010).

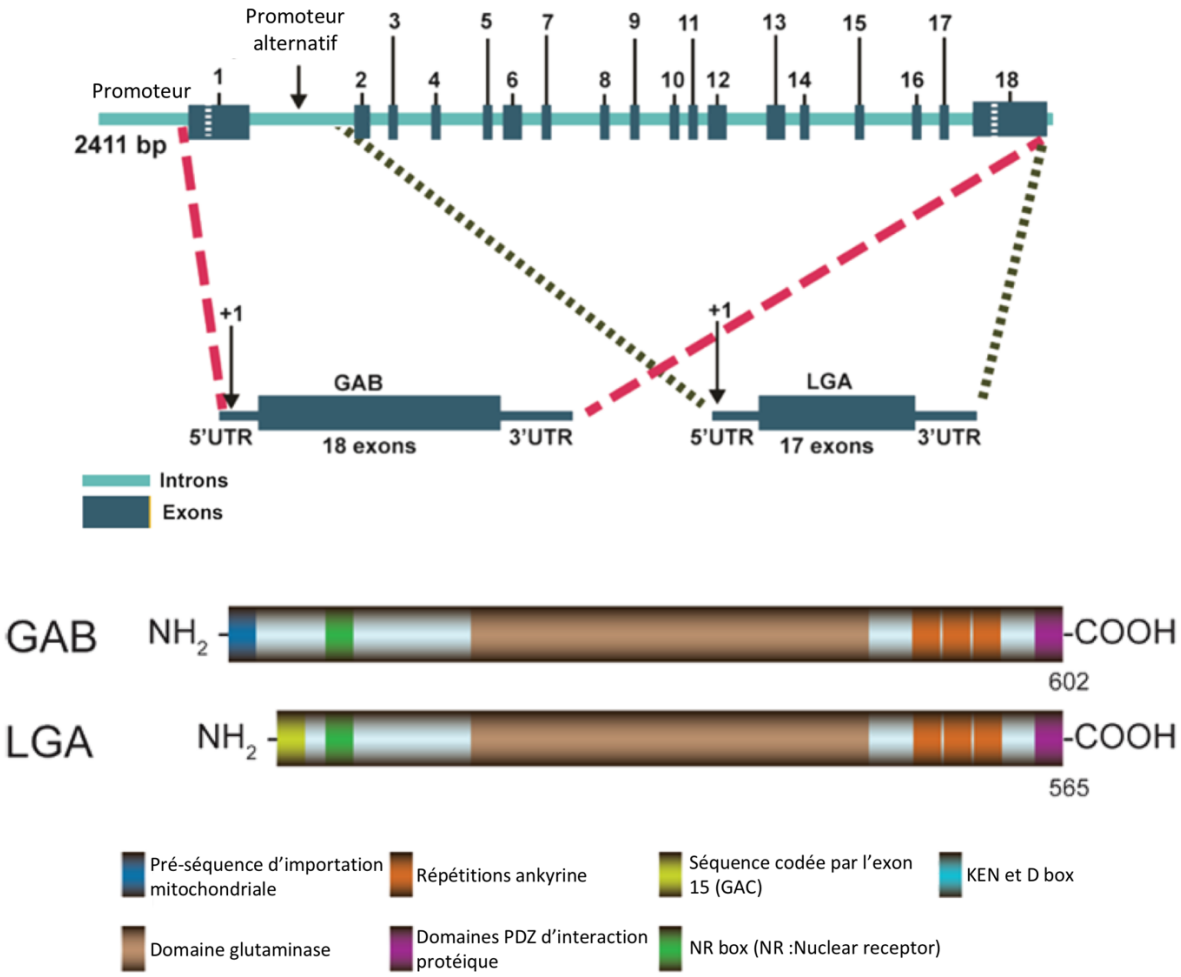

Figure 23 : Structure génomique du gène GLS2 humain et de ses transcrits alternatifs GAB et LGA. (Campos-Sandoval, 2019)

E. Utilisation de la glutamine par les différentes voies métaboliques

Une fois synthétisée et transportée au sein des cellules, la Gln est hydrolysée en Glu et est rapidement utilisée dans de nombreuses voies métaboliques de base nécessaires à la survie, la croissance et la prolifération des cellules (Figure 24). Nous allons détailler les étapes une à une dans la partie qui suit.

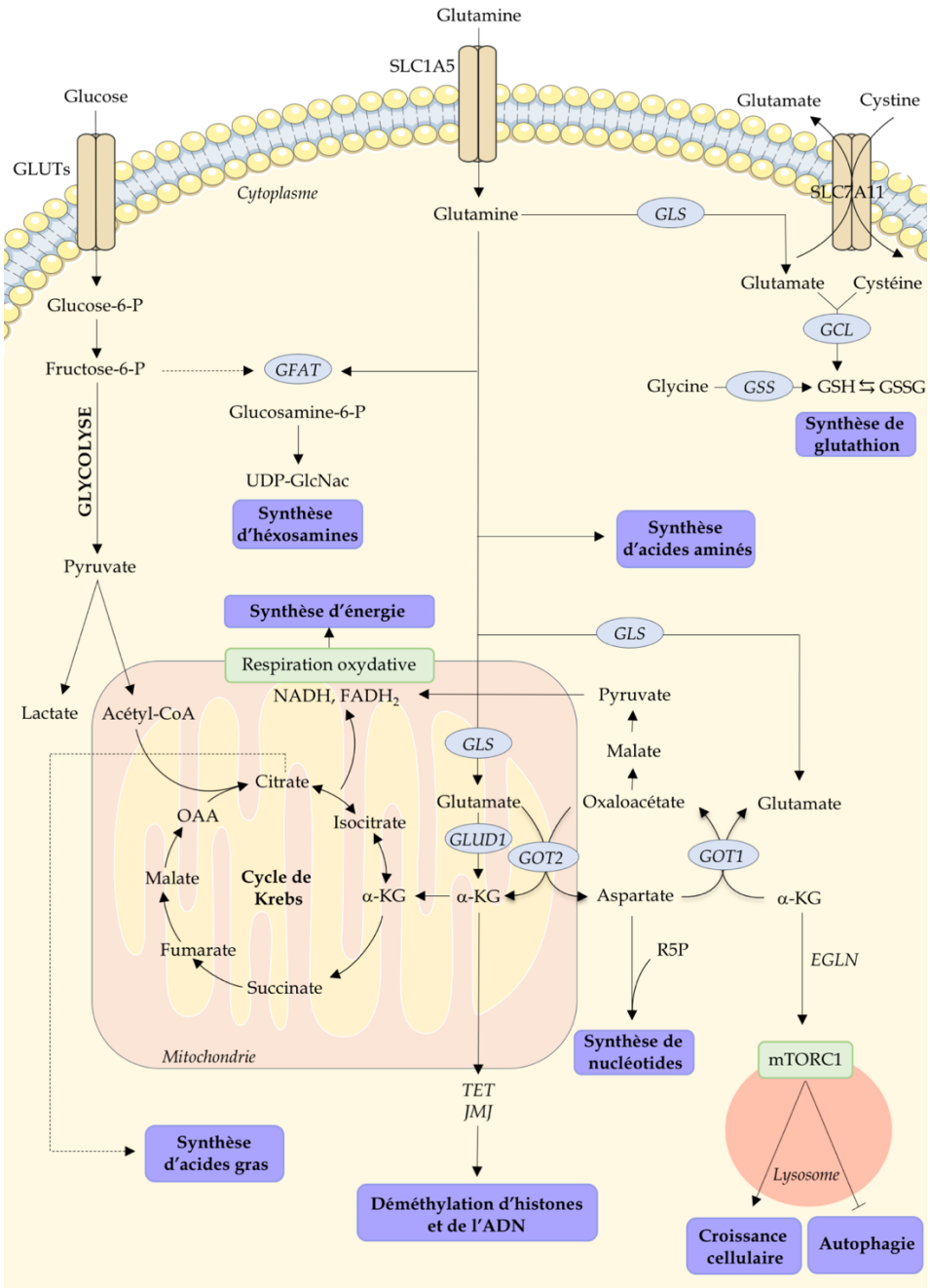

Figure 24 : Utilisation de la Gln par les différentes voies métaboliques.

1. *La synthèse d'énergie*

Au sein de la mitochondrie, la Gln est convertie en Glu et en ammoniac par la Gls1 au cours de la glutaminolyse. Le glutamate ainsi formé va pouvoir être utilisé dans plusieurs voies métaboliques différentes. Entre autres, le Glu va être converti en α-KG (α-kétoglutarate) par l'enzyme glutamate déhydrogénase (Glud1). L'α-KG va pouvoir ainsi entrer dans le cycle de Krebs et entrainer la production de NADH et de $FADH_2$ qui vont pouvoir alimenter la respiration oxydative, et ainsi produire de l'ATP. Environ 24 molécules d'ATP peuvent être synthétisées à partir d'une molécule de Gln (Mazat and Ransac, 2019). De plus, au cours du cycle de Krebs, la Gln va permettre la synthèse de citrate, qui va alors sortir des mitochondries et être indispensable pour la synthèse d'acides gras (voir chapitre I).

2. *La synthèse d'hexosamines*

Afin de maintenir l'homéostasie du RE, la Gln contrôle le repliement et le trafic des protéines en participant à la voie de synthèse des hexosamines. Au cours de cette voie métabolique, le glucose est convertit en fructose-6P (fructose-6-phosphate) qui est majoritairement utilisé par la glycolyse. Le fructose-6P non utilisé par la glycolyse sert, avec la glutamine, de substrat à la GFAT (glutamine-fructose-6-phosphate amidotransférase) pour former du glucosamine-6P. La GFAT catalyse la première étape limitante de la synthèse d'hexosamines et est donc un régulateur clé de cette voie (Chiaradonna et al., 2018). Le produit final de cette voie, l'uridine diphosphate N-acetylglucosamine (UDP-GlcNAc), est utilisé d'une part comme substrat pour les réactions de N et O-glycosylations dans le RE et le golgi respectivement (Freeze and Elbein, 2009), et d'autre part comme substrat pour la réaction d'O-GlcNAcylation catalysée par l'OGT (O-GlcNAc transférase) dans le cytoplasme, le noyau et les mitochondries (Butkinaree et al., 2010). La N-glycosylation permet l'ajout d'un groupement glucidique sur un résidu asparagine des protéines en cours de traduction, tandis que la O-glycosylation permet l'ajout d'un sucre sur les thréonines et/ou serines des protéines, au niveau de sites pouvant également être phosphorylés. Ces modifications post-traductionnelles jouent un rôle majeur dans la modification des fonctions protéiques comme l'activité catalytique, la localisation ou la fonction transcriptionnelle des protéines. Ainsi, la déprivation en Gln peut entraîner un

repliement et un chaperonnage inappropriés des protéines et un stress du RE (Wellen et al., 2010).

3. *La synthèse de nucléotides*

Dans le cytosol, la Gln peut être directement métabolisée afin de synthétiser des nucléotides contribuant ainsi à la synthèse de l'ARN (acide ribonucléique) (Newsholme et al., 1987; Newsholme et al., 2003a). La synthèse de nucléotides nécessite à la fois de la Gln, de l'asparte et du R5P. En effet, la Gln possède deux atomes d'azotes réduits appelés α-azote et γ-azote. Les bases pyrimidiques et puriques contiennent respectivement un et deux atomes de γ-azote dérivés de la Gln. De plus, la Gln contribue à la biosynthèse des nucléotides en fournissant de l'aspartate par deux voies différentes. A la fois au sein du cytosol et de la mitochondrie, le glutamate peut être converti en aspartate par les glutamate-oxaloacétate transaminases (GOT1 dans le cytosol et GOT2 dans la mitochondrie). De plus, au sein de la mitochondrie, l'oxaloacétate (OOA) formé au cours du cycle de Krebs génère de l'aspartate qui soutient la synthèse de nucléotides (Son et al., 2013). L'aspartate sert de source cruciale de carbone pour la synthèse des purines et pyrimidine (Birsoy et al., 2015; Sullivan et al., 2015) et l'apport d'aspartate peut inverser l'arrêt du cycle cellulaire causé par la déprivation en glutamine (Patel et al., 2016). Enfin, le ribose-5-phosphate (R5P) est produit au cours du métabolisme du glucose, par les intermédiaires de la glycolyse et par la voie du pentose phosphate.

4. *La synthèse d'acides aminés*

L'α-azote de la Gln soutient les niveaux de nombreux pools d'acides aminés dans la cellule grâce à l'action des aminotransférases (Hosios et al., 2016). Une fois la Gln hydrolysée en Glu, le carbone et l'azote du Glu peuvent être utilisés afin de produire de la proline, un acide aminé jouant un rôle clé dans la production du collagène de la matrice extracellulaire (Phang et al., 2015). En parallèle, le glutamate est transformé par l'ornithine aminotransferase (OAT) en ornithine qui peut, soit être utilisée dans la voie des polyamines, soit être convertie, après plusieurs réactions en arginine par l'argininosuccinate lyase (ASL). De plus, la transamination

du glutamate permet la synthèse de sérine qui, à son tour, peut être convertie par une série de réactions en glycine ou en cystéine. Comme nous l'avons vu, le glutamate peut aussi produire de l'aspartate *via* l'OOA produit dans le cycle de Krebs ou *via* les transaminases GOT1 et GOT2. L'aspartate est un précurseur de nombreux acides aminés comme la méthionine, la thréonine et la lysine. De plus, l'amidation de l'aspartate permet la synthèse d'asparagine. Enfin, la transamination du glutamate fourni du pyruvate qui peut à son tour donner de l'alanine, de la valine et de l'isoleucine. Dans les cellules cancéreuses la Gln est la source d'au moins 50% des acides aminés non essentiels utilisés pour la synthèse protéique (Altman et al., 2016).

5. *Le contrôle de l'homéostasie redox*

Le métabolisme de la Gln joue un rôle essentiel dans les mécanismes anti-oxydants cellulaires. Les ROS sont générés à partir de plusieurs sources, notamment lors de la respiration oxydative. Plusieurs voies métaboliques impliquant la Gln contrôlent les niveaux de ROS cellulaires. La voie la plus connue dans le contrôle des ROS est la synthèse de glutathion (GSH). Le glutathion est un tripeptide composé d'une molécule de glutamate, d'une cystéine et d'une glycine (Glu-Cys-Gly), et sert à neutraliser les radicaux libres peroxydes. L'apport de la Gln est l'étape limitante de la synthèse du GSH (Welbourne, 1979). De plus, la glutamine est directement et indirectement responsable de l'entrée ou de la conversion des deux autres composants du glutathion. La synthèse du GSH a lieu dans le cytosol. Le glutamate dérivé de la glutamine est condensé à la cystéine par la glutamate-cystéine ligase, puis la glycine est ajoutée par la glutathion synthétase. De plus, le glutamate synthétisé à partir de la Gln sert à importer la cystine extracellulaire, *via* le co-transporteur antiport SLC7A11. Une fois au sein de la cellule la cystine est convertie en cystéine qui peut ensuite être incorporée au glutathion. Enfin, l'oxydation du glutamate permet la génération de NADPH grâce aux enzymes maliques. Ainsi le NADPH est utilisé pour réduire le glutathion oxydé (GSSG) et ainsi protéger les cellules du stress oxydatif (Son et al., 2013).

6. *Le contrôle épigénétique des chromatines*

Outre le rôle de la Gln dans la génération d'énergie et d'éléments constitutifs, le métabolisme de la Gln est capable de produire des co-substrats pour les cascades de régulation cellulaires, notamment pour réguler l'organisation de la chromatine. L'α-KG dérivé de la glutamine est un co-substrat des enzymes dioxygénases permettant de réguler les familles TET (Ten-eleven translocation) et JMJ (jumonji) (Liu et al., 2017; Tahiliani et al., 2009). Les enzymes de la famille TET et JMJ catalysent la déméthylation de l'histone et de l'ADN. De plus, les mutations de perte de fonction de la succinate déshydrogénase (SDH) augmentent le taux de succinate cellulaire, ce qui inhibe la déméthylation de l'ADN et contribue à la tumorigenèse (Letouze et al., 2013; Xiao et al., 2012). Le métabolisme de la Gln joue donc un rôle majeur dans l'expression des gènes grâce à la contribution de l'α-KG et du succinate dans la modification de la structure de la chromatine.

7. *Régulation de la croissance cellulaire et de l'autophagie*

Une fois activée, la voie de signalisation TOR favorise les voies de biosynthèses tout en inhibant les processus de dégradation comme l'autophagie (Laplante and Sabatini, 2012). L'activité mTORC1 est ainsi finement régulée par la glutaminolyse afin d'empêcher toute croissance cellulaire inappropriée. La glutamine régule positivement la voie mTORC1 par la leucine *via* un mécanisme dépendant de la Rag GTPase ainsi que par l'α-KG *via* un mécanisme indépendant de la GTPase, afin de transloquer mTORC1 vers le lysosome (Jewell et al., 2015). En effet, lorsque les taux de Gln sont élevés, l'α-KG est exporté vers le cytosol et active les enzymes EGLN permettant l'activation de la voie mTORC1 et favorisant ainsi la croissance cellulaire et l'inhibition de l'autophagie (Duran et al., 2013; Duran et al., 2012; Villar et al., 2015). De plus, l'inhibition de l'entrée de la Gln, par le blocage du transporteur SLC1A5, conduit à l'inhibition de la signalisation mTORC1 et à l'activation de l'autophagie.

F. Rôle de la glutamine dans l'activation des cellules immunes

La Gln est impliquée dans de nombreuses fonctions clés du système immunitaires. En effet, les dérivés du métabolisme du glucose et de la Gln tels que le succinate, le fumarate, le citrate ainsi que les intermédiaires du cycle de Krebs, participent au contrôle de l'immunité au sein des cellules innées et adaptatives. De plus, il faut noter que l'utilisation de la Gln par les neutrophiles, les macrophages et les lymphocytes est égale ou, dans certaines conditions, supérieure à celle du glucose (Curi et al., 1999) montrant ainsi le rôle essentiel que cet acide aminé peut jouer sur les fonctions immunes.

1. *Glutamine et monocytes/macrophages*

Lors de l'activation des macrophages, le métabolisme du glucose et de la glutamine joue un rôle prédominant. C'est Philip Newsholme, en 1986, qui rapporte pour la première fois que les macrophages utilisent de la Gln (Newsholme et al., 1986). Bien que la Gln joue un rôle au niveau des macrophages M1 en contribuant à la production de succinate (Tannahill et al., 2013), de nombreuses études récentes se sont focalisées sur le rôle de la Gln dans la polarisation M2. En 2015, Jha *et al.* ont montré que le métabolisme de la Gln était l'une des caractéristique du macrophage M2. Près d'un tiers des carbones présents au sein du cycle de Krebs provient de la Gln. La Gln peut modifier la polarisation des macrophages M2 *via* la biosynthèse de l'uridine 5'-diphosphate-N-acétylglucosamine et la N-glycosylation (Jha et al., 2015). En effet, la déprivation *in vitro* de la Gln ainsi que l'inhibition de la N-glycosylation diminue l'expression de plusieurs marqueurs M2 tels que CD206, Irf4, Klf4, Ccl22 et Il4i1. De plus, l'inhibition de la Glutamine synthétase induit la conversion des macrophages M2 vers un profil M1 (Palmieri et al., 2017). Ainsi, une absorption massive de Gln par les macrophages indiquerait la présence d'une population de macrophage anti-inflammatoire (Tavakoli et al., 2017). De même, Liu *et al.* ont récemment démontré que l'inhibition de la Gln *in vitro* par le BPTES, un inhibiteur de Gls1, régule positivement l'expression des marqueurs M1 tels que IL-1β, TNF-α, IL-6 et IL-12, tout en diminuant l'expression des marqueurs M2 tels que Arg1, Ym1, Retnl-α et Mrc1. Ces régulations dépendantes de la Gln seraient dues à la régulation épigénétique des gènes M2 *via* l'α-KG qui régule l'histone déméthylase Jmjd3 (Liu et al., 2017).

Enfin, Davies *et al.* ont pu montrer que les différentes populations de macrophages n'expriment pas les même niveau d'expression de glutaminolyse, suggérant qu'ils utilisent de façon différente cet acide aminé. En effet, dans leurs travaux, les auteurs démontrent que les macrophages péritonéaux dépendent plus fortement de la glutaminolyse que les macrophages dérivés de la moelle osseuse (BMDM) présentent ainsi une capacité mitochondriale doublée (Davies et al., 2017).

2. *Glutamine et neutrophiles*

Outre le glucose, la Gln est un substrat énergétique pour les leucocytes et joue un rôle clé dans la prolifération cellulaire, la réparation tissulaire et dans les voies cellulaires associées à la reconnaissance des pathogènes (Mills et al., 2017). Lors de la phagocytose de bactéries ou de fragments de tissus par les neutrophiles, de nombreux processus cellulaires sont déclenchés *via* des stimuli appropriés, tels que la motilité de la cellule, la sécrétion d'enzymes protéolytiques ainsi que la sécrétion de composés immuno-modulateurs. Les neutrophiles possèdent deux mécanismes bactéricides agissant en coopération, d'une part un mécanisme oxygène indépendant ou le pH du lysosome ainsi que diverses molécules telles que le lysozyme, la lactoferrine, la défensine ou encore des protéines cationiques, lysent les bactéries. D'autre part, un mécanisme dépendant de l'oxygène peut avoir lieu nommé le « burst respiratoire ». Au cours de ce processus, le neutrophile augmente sa consommation d'oxygène pour produire des anions superoxydes *via* la NADPH oxydase. Par la suite, l'anion superoxyde est transformé en perhydrol par la superoxyde dismutase puis en hypochlorite et hypobromite par la myéloperoxydase, ce qui génère une forte activité anti-microbienne. L'ensemble de ces processus conduit à la mort des bactéries et leur dégradation et peut entrainer sur le long terme une inflammation locale. En 1997, le groupe de Curi démontre pour la première fois que la Gln est hautement consommée par les neutrophiles (Curi et al., 1997a; Curi et al., 1997b). L'inhibition de la glutaminase par la 6-diazo-5-oxo-l-norleucine (DON) a pu démontrer le rôle de la Gln dans la production de superoxyde, probablement par la génération d'ATP et la régulation de l'expression des composants du complexe NADPH oxydase (Pithon-Curi et al., 2002). De plus, la Gln peut prévenir les variations d'activité de la

NADPH oxydase et de la production de superoxyde après une stimulation avec de l'adrénaline (Garcia et al., 1999).

3. *Glutamine et lymphocytes*

L'activation des lymphocytes dépend de différentes voies métaboliques. Les métabolites et signaux extracellulaires permettent de moduler le métabolisme énergétique, la prolifération cellulaire ou encore la production de cytokines. C'est le groupe d'Eric Newsholme qui, en 1985, a montré pour la première fois l'importance de l'utilisation de la Gln par les lymphocytes (Newsholme et al., 1985). En effet, la Gln joue un rôle clé dans le fonctionnement des lymphocytes en contrôlant, avec le glucose, leurs fonctions et leur prolifération (Curi et al., 1988). La Gln est essentielle pour la prolifération des lymphocytes T et B, à la synthèse de protéines et d'anticorps, et à la production d'IL-2, une cytokine stimulant la prolifération et la différenciation lymphocytaire.

En effet, les processus de prolifération nécessitent de l'ATP, et la biosynthèse de lipides et nucléotides pour la synthèse d'ARN et d'ADN, des processus sous le contrôle de la Gln. Chez l'Homme, la Gln est capitale pour la différenciation des lymphocytes B en plasmocytes et pour la transformation lymphoblastique (Crawford and Cohen, 1985). Au sein des cellules T effectrices, l'absorption de la Gln, les transporteurs d'acides aminés, et les enzymes métabolisant la Gln sont régulés à la hausse (Carr et al., 2010; Nakaya et al., 2014; Wang et al., 2011). De plus, il a été montré que l'inhibition du transporteur SLC1A5 favorise l'expression de Foxp3, le facteur de transcription des lymphocytes T régulateurs (Treg) (Klysz et al., 2015; Nakaya et al., 2014). De même, l'inhibition de GOT1, une des enzymes permettant la conversion du glutamate en α-KG, entraine un changement de différenciation des Th17 en Treg *via* la méthylation du locus Foxp3 (Xu et al., 2017). Enfin, le groupe de Jeffrey Rathmell a démontré que la déficience en Gls1 spécifiquement au niveau des lymphocytes T diminue l'activation et la prolifération des cellules T et altère la différenciation de Th17 tout en stimulant la différenciation des cellules Th1 et des lymphocytes CD4 cytotoxiques (Johnson et al., 2018). Pour finir, en régulant la synthèse de polyamines, la Gln peut jouer sur l'auto-immunité des cellules T et B et leur confèrent des propriétés anti-tumorales (Hesterberg et al., 2018).

G. Rôle de la glutamine lors de blessures ou maladies graves

La Gln est un acide aminé non essentiel, mais son rôle conditionnellement essentiel lors de maladies et de blessures graves est de plus en plus décrit (Wischmeyer, 2019). Lors de conditions de stress métabolique, la réserve périphérique de glutamine est rapidement libérée pour fournir de l'énergie aux processus métaboliques. La dégradation de la réserve de glutamine contribuerait à la pathologie globale et à la récupération lente des pathologies (Rodas et al., 2012). Les faibles concentrations plasmatiques de Gln chez les patients admis à l'hôpital sont un prédicteur indépendant de décès prématuré. Cependant, il n'est pas clair si la déficience en Gln plasmatique contribue au décès ou s'il s'agit d'un simple marqueur de la gravité de la maladie (Rodas et al., 2012). En 2017, la FDA (Food and Drug Administration) a approuvé l'administration orale de Gln chez les personnes atteintes de drépanocytose afin de réduire les complications aigües (Niihara et al., 2018). De plus, si le corps utilise plus de Gln que les muscle ne peuvent en produire, une fonte musculaire peut survenir. C'est notamment le cas chez les personnes atteintes du SIDA. En période de stress métabolique, la supplémentation en Gln peut soutenir la fonction intestinale, le système immunitaire et d'autres processus essentiels de l'organisme. En effet la supplémentation en Gln fournit des azotes et des carbones, servant de carburant à de nombreuses cellules du corps et permettant ainsi la production d'autres acides aminés et de glucose.

De même, les brulures entrainent une baisse significative des niveaux de Gln et la supplémentation en cet acide aminé permet l'amélioration des résultats (Bongers et al., 2007). Les brulures entrainent une haute réponse inflammatoire et un fort catabolisme menant à des carences nutritionnelles, le tout pouvant mener à un risque élevé d'infection, de défaillance d'organes et de mortalité (Berger and Pantet, 2016). La supplémentation en Gln chez les grands brulés atténue l'atrophie de la muqueuse intestinale pendant la nutrition parentérale (McCauley et al., 1996) et préserve les niveaux extra-intestinaux et intestinaux d'immunoglobuline A (Kudsk et al., 2000). De plus, des données expérimentales ont montré que la supplémentation en Gln réduit les lésions pulmonaires tardives suite à l'inhalation de fumée lors des brulures (Li et al., 2013). La Gln améliore également la fonction cardiaque après une brûlure grave (Yan et al., 2012). Enfin, la supplémentation en Gln peut préserver le métabolisme musculaire en améliorant la sensibilité à l'insuline (Bakalar et al., 2006; Dock-

Nascimento et al., 2012) et en préservant la fonctionnalité de la masse corporelle maigre permettant une amélioration de la condition physique après un long séjour en soin intensif (Jones et al., 2015). Les effets protecteurs de la supplémentation en Gln lors des brulures semblent être liés à une augmentation de l'expression des protéines de choc thermique des organes (Singleton and Wischmeyer, 2007) et à la diminution de la libération de cytokines inflammatoires (Wischmeyer et al., 2001).

Objectifs de mes travaux de thèse

Les maladies cardio-métaboliques telles que l'obésité et l'athérosclérose sont un problème majeur de santé publique dans les pays occidentaux. Les cellules immunes et en particulier les macrophages jouent un rôle clé dans l'initiation et le développement de ces pathologies. En contexte physiologique, les macrophages sont des cellules immunes contrôlant l'homéostasie des tissus. Au cours de pathologies cardio-métaboliques, le changement d'environnement local, principalement dû à la dyslipidémie, entraine un changement métabolique au sein du macrophage qui affecte sa fonction. Les macrophages nécessitent plusieurs substrats afin de fonctionner correctement. Le glucose qui entre dans la cellule par le transporteur GLUT1 et sert pour la glycolyse, les acides gras qui entrent par différents transporteurs notamment CD36 et sont utilisés au cours de la β-oxydation et les acides aminés, et particulièrement la glutamine qui utilise différents transporteurs et est utilisée au cours de la glutaminolyse. La glutamine est l'acide aminé le plus abondant dans le plasma chez l'Homme et la souris. Au cours des pathologies inflammatoires, la demande en Gln augmente et sa synthèse endogène n'est pas suffisante, c'est pourquoi la Gln est un acide aminé dit conditionnellement essentiel.

L'objectif de mes travaux de thèse fut de comprendre le rôle de la glutaminolyse des macrophages au cours de l'obésité et de l'athérosclérose. Nous nous sommes demandé si la conversion de la glutamine en glutamate par l'enzyme Gls1 était modifiée au cours de ces pathologies et quelles pouvaient être les conséquences. Au cours de ces trois ans de thèse, j'ai donc pu étudier l'impact de la glutaminolyse des macrophages sur ces deux pathologies à l'aide de modèles murins. Nous avons ainsi utilisé deux modèles de souris : des souris déficientes pour Gls1 au niveau des cellules myéloïdes ($LyzM^{cre}$ x $Gls1^{fl/fl}$) que nous avons mis sous régime riche en graisses pendant 12 semaines pour engendrer le développement de l'obésité, et des souris $LyzM^{cre}$ x $Gls1^{fl/fl}$ croisées avec des souris $ApoE^{-/-}$ que nous avons mis sous régime riche en cholestérol pour l'étude de l'athérosclérose.

Les résultats obtenus au cours de ma thèse ont permis de mettre en lumière l'effet de la glutaminolyse des macrophages sur l'obésité et l'athérosclérose et permettent d'envisager qu'un apport en glutamate spécifiquement au sein des macrophages pourrait être bénéfique pour les patients atteint de maladies cardio-métaboliques.

Papier 1

Spinal cord macrophage glutaminolysis controls glucose homeostasis by supporting sympathetic tone of thermogenic adipose depots.

Johanna Merlin[1*], Stoyan Ivanov[1*], Alexey Sergushichev[2], Marion Ayrault[1], Nathalie Vaillant[1], Jérome Gilleron[3], Mireille Cormont[3], Jean-Francois Tanti[3], Karine Dumas[3], Michael Ohanna[3], Justine Masson[4], Inna Gaisler-Salomon[4], Stephen Rayport[4], Diane B Re[5], Emmanuel L. Gautier[6], Rodolphe Guinamard[1], Maxim N Artyomov[7], Laurent Yvan-Charvet[1]

*These authors contributed equally to this work

[1]Institut National de la Santé et de la Recherche Médicale (Inserm) U1065, Université Côte d'Azur, Centre Méditerranéen de Médecine Moléculaire (C3M), Atip-Avenir, Fédération Hospitalo-Universitaire (FHU) Oncoage, 06204 Nice, France (J.M., S.I., M.A., N.V, R.G., L.Y.C.)

[2]Computer Technologies Department, ITMO University, Saint Petersburg, Russia (A.S.)

[3]Université Côte d'Azur, Institut National de la Santé et de la Recherche Médicale (Inserm) U1065, Centre Méditerranéen de Médecine Moléculaire (C3M), Team 1 and 7, 06204 Nice, France (J.G., M.C., J.F.T., K.D., M.O.)

[4]Department of Psychiatry, Columbia University, USA; Department of Molecular Therapeutics, NYS Psychiatric Institute, USA (J.M., I.G.S., S.R.)

[5]EHS Department and Motor Neuron Center, Columbia University, 630W 168th Street Suite 16421-B, New York, NY, 10032, USA (D.B.R)

[6]Sorbonne Université, INSERM, UMR_S 1166 ICAN, F-75013 Paris, France (E.G.)

[7]Department of Pathology and Immunology, Washington University School of Medicine, St. Louis, MO, USA (M.N.A.)

Address correspondence to LYC: yvancharvet@unice.fr

Short title: Macrophage glutaminolysis and thermogenesis

Keywords: Macrophage, Glutaminolysis, Thermogenesis, Glucose tolerance, Adipose tissue, Glutamatergic and Sympathetic tones.

Abstract

Adipose tissue dysfunction causes metabolic diseases, including glucose intolerance. Adipose tissue macrophages (ATMs) are important sentinels that control the expandability of visceral adipose tissue and thermogenesis in inguinal and brown adipose depots. The underlying mechanisms that regulate these alterations, however, are still poorly defined. Here, we report that mice with defective macrophage glutaminolysis displayed glucose intolerance independent of excessive visceral fat inflammation and storage. Reduced glucose influx was associated with impaired norepinephrine-dependent thermogenic responses of subcutaneous and brown adipose tissue. This phenomenon was associated with upstream perturbation of neuronal activation in the spinal cords of mice deficient in macrophage glutaminolysis, which is required for activation of sympathetic tone-dependent thermogenesis. Mechanistically, we found that altered glutaminolysis reprogrammed spinal cord macrophage metabolism and limited the fusiform projections of macrophages, which are hallmarks of neuronal contacts, *in vitro* and *in vivo*. Collectively, our study reveals a previously unappreciated homeostatic role for spinal cord macrophage glutaminolysis in the control of sympathetic tone in thermogenic adipose depots. Disruption of these circuits results in metabolic imbalance.

Introduction

Macrophages, which maintain tissue homeostasis and integrity, are present in all organs (Okabe and Medzhitov, 2016). In healthy adipose tissue, macrophages are the numerically dominant immune cell type (Lumeng et al., 2007; Weisberg et al., 2003; Xu et al., 2003). The diverse functions of visceral adipose tissue macrophage (vATM) subsets, ranging from regulation of lipid metabolism to sampling of blood material in visceral white adipose tissue (vWAT), have been documented (Jaitin et al., 2019; Lumeng et al., 2008; Silva et al., 2019; Xu et al., 2013). Macrophages have also been observed in subcutaneous white adipose tissue (ScWAT) and in brown adipose tissue (BAT), where they are involved in nonshivering thermogenesis. Indeed, these macrophages regulate sympathetic tone associated with the high innervation density of these thermogenic adipose depots (Ivanov et al., 2018; Kajimura et al., 2015; Reitman, 2017). Mechanistically, these macrophages can limit sympathetic tone-mediated thermogenesis by expressing PlexinA4, which repulses Sema6A-expressing sympathetic axons, thus controlling BAT neuron density (Wolf et al., 2017). A recent report also suggested that sympathetic neuron-associated macrophages can locally reduce norepinephrine (NE) availability through its uptake and subsequent degradation, which represents an alternative mechanism of thermogenesis regulation (Pirzgalska et al., 2017). However, the metabolic regulation of these processes remains poorly understood.

At the molecular level, macrophage effector functions and metabolic processes are intertwined and constitute integral components of metabolic complications (Artyomov et al., 2016; Mills et al., 2017; Puleston et al., 2017; Stienstra et al., 2017). Perturbation of glutamine metabolism links obesity to inflammation in vWAT (Petrus et al., 2020), and although its use is controversial, glutamine supplementation can improve weight loss and metabolic health (Opara et al., 1996; Laviano et al., 2014; Ramezani Ahmadi et al., 2019). Network integration of parallel *in vitro* high-throughput metabolomic and transcriptomic data has revealed that glutaminolysis is central to alternative macrophage polarization (Jha et al., 2015). This finding could explain why glutamine administration attenuates proinflammatory profiles in the visceral fat of obese patients (Petrus et al., 2020). The role of glutamine in other adipose depots is unknown, but the thermogenic functions of ScWAT and BAT macrophages are unlikely to be linked to their inflammatory status (Fischer et al., 2017; Nguyen et al., 2011; Qiu et al., 2014). Thus, the causal relevance of macrophage glutaminolysis *in vivo*, both at steady state and during metabolic inflammation, remains poorly understood.

Macrophage glutaminolysis relies on the enzyme glutaminase (Gls) 1, which hydrolyzes glutamine into glutamate. To test the causal relationship between modulation of glutamine catabolism, ATM behavior and metabolic homeostasis, we generated and characterized myeloid cell-specific *Gls1*-deficient ($Lyz2^{cre}$ x $Gls1^{flox}$) mice. The elimination of macrophage glutaminolysis in mice resulted in a proinflammatory phenotype in vWAT, which was associated with higher visceral adiposity, but not in other adipose depots upon exposure to a high-fat diet (HFD). However, this phenotype is likely not the culprit of the systemic metabolic perturbations in these mice since glucose intolerance was also observed in $Lyz2^{cre}$ x $Gls1^{flox}$ mice fed a regular chow diet and was associated with impaired homeostatic energy expenditure due to perturbed BAT and ScAT thermogenesis. Malfunction of thermogenic adipose depots was the consequence of reduced sympathetic tone in mice with defective macrophage glutaminolysis and was associated with upstream perturbation of neuronal circuits in the spinal cord. Indeed, the metabolic reprogramming of *Gls1*-deficient spinal cord macrophages promoted a decrease in cell projections and the expression of molecules associated with the microtubule cytoskeleton reorganization machinery. These changes dampened the release of the excitatory neurotransmitter glutamate, which is required for activation of sympathetic tone. Collectively, our findings suggest that macrophage glutaminolysis governs glucose homeostasis through the previously unknown homeostatic role of spinal cord macrophages in the control of glutamatergic neuron activation and subsequent sympathetic tone of thermogenic adipose depots.

Results

Macrophage Gls1 deficiency promotes metabolic imbalance and glucose intolerance. To investigate the potential contribution of macrophage glutaminolysis to energy homeostasis, mice with macrophage-specific Gls1 deficiency ($Mac^{\Delta Gls1}$ mice) and their controls were fed standard chow or a HFD for 12 weeks. $Mac^{\Delta Gls1}$ mice developed normally and exhibited similar body weight gain as control mice, even when the mice were fed a HFD (**Fig. S1A**). Nevertheless, standard chow- and HFD-fed $Mac^{\Delta Gls1}$ mice exhibited a lower respiratory quotient (RQ) profile during the nocturnal period than standard chow- and HFD-fed control mice, as measured by indirect calorimetry (**Fig. 1A**). This finding could explain the lower energy expenditure observed in $Mac^{\Delta Gls1}$ mice fed either standard chow or a HFD (**Fig. 1B**), as food intake was not consistently different between $Mac^{\Delta Gls1}$ mice and control mice under either diet and locomotor activity was similar between genotypes (**Table. S1**). Notably, pair feeding confirmed that the reduced energy expenditure of standard chow-fed $Mac^{\Delta Gls1}$ mice was independent of food intake (**Fig. S1B**). Consistently, the mRNA expression of genes encoding hypothalamic central regulators of food intake, such as *Pomc*, *Agrp*, *Npy* and *Pth2r,* in the hypothalamus was similar between standard chow-fed $Mac^{\Delta Gls1}$ mice and littermate controls (**Fig. S1C**). Consistent with the observation that the $Mac^{\Delta Gls1}$ mice did not have lower RQ profiles during the postabsorptive period (transition to daily phase), when lipid oxidation occurs (**Fig. 1A**), we excluded the possibility that fatty acid metabolism was altered in these mice. First, we observed that increasing fatty acid oxidation by fasting resulted in similar energy expenditure (**Fig. S1B**). Second, plasma free fatty acid levels were similar between standard chow-fed $Mac^{\Delta Gls1}$ mice and their littermates after a fasting/refeeding protocol (**Fig. S1D**). Additionally, a similar percentage of gastrocnemius skeletal muscle oxidative fibers was observed in HFD-fed $Mac^{\Delta Gls1}$ mice and HFD-fed control mice (**Fig. S1E**). Finally, liver morphology (**Fig. S1F**), the levels of plasma alanine transaminase (ALAT) and aspartate transaminase (ASAT), which are hepatotoxicity markers (**Fig. S1G**), and triglyceride content (**Fig. S1H**) were unaltered in $Mac^{\Delta Gls1}$ mice compared to control mice. In contrast, $Mac^{\Delta Gls1}$ mice exhibited a ~20% decrease in glucose oxidation compared to that in control mice when fed standard chow or a HFD (**Table. S1**). We next found that administration of an intraperitoneal bolus of glucose resulted in delayed substrate clearance from the peripheral blood circulation in mice lacking Gls1 in macrophages. This was observed in both standard chow -fed (**Fig. 1C**) and HFD-fed $Mac^{\Delta Gls1}$ mice (**Fig. 1D**). Quantification of the area under the curve confirmed that glucose utilization was perturbed (**Figs 1C and 1D**). Analysis of homeostatic model assessment- insulin resistance (HOMA-IR) indexes suggested that this perturbation occurred with little effect on insulin sensitivity (**Fig. 1E**). Similar insulin levels were observed at baseline and 20 minutes after glucose injection in HFD-fed $Mac^{\Delta Gls1}$ mice (**Fig. S1I**). Thus, impaired glucose tolerance in mice with macrophage glutaminolysis deficiency was most likely the consequence of reduced peripheral glucose clearance.

Brown adipose tissue rather than visceral fat couples macrophage-specific Gls1 deficiency to glycemic control. Increased vATM infiltration and a switch from the alternatively activated phenotype to the proinflammatory phenotype are hallmarks of metainflammation and metabolic perturbations (McNelis and Olefsky, 2014; Odegaard and Chawla, 2015; Rosen and Spiegelman, 2014), and a role for glutamine in vWAT inflammation has recently emerged (Petrus et al., 2020). We first observed that macrophage Gls1 deficiency perturbed glutaminolysis in the vWAT of standard chow-fed mice but not in other adipose depots, as shown by higher glutamine (Gln) and lower glutamate (Glu) levels in vWAT than in other adipose tissues (**Fig. S1K**). Taking advantage of publicly available gene expression datasets (Choi et al., 2015; Fitzgibbons et al., 2011), we also observed that HFD feeding lowered *Gls1* mRNA expression specifically in vWAT and that this decrease paralleled a decrease in the expression of alternatively activated macrophage markers and an increase in the expression of proinflammatory markers (**Fig. S1J**). Thus, we next characterized the

phenotype of vWAT in Mac$^{\Delta Gls1}$ mice to determine whether it is associated with impaired glucose tolerance in these mice. Surprisingly, we did not observe significant changes in fat mass (**Fig. S1L**) or ATM number (**Fig. S1M**) in any adipose depots, including vWAT, of standard chow-fed Mac$^{\Delta Gls1}$ mice. In contrast, we observed specific increases in vWAT mass (**Fig. S1L**) and vATM number (**Fig. S1M**) when Mac$^{\Delta Gls1}$ mice were challenged with a HFD. Morphological examination showed that the vWAT of HFD-fed Mac$^{\Delta Gls1}$ mice contained larger adipocytes and confirmed that macrophage infiltration was enhanced, as illustrated by the appearance of characteristic crown-like structures (**Fig. S1N**). Additionally, an imbalance in the expression of alternatively activated (*Mrc1* and *Retnla*) and proinflammatory (*Cd68*, *Tnf*α, and *Hmox1*) macrophage markers was observed in the vWAT of HFD-fed Mac$^{\Delta Gls1}$ mice (**Fig. S1O**) but not in ScWAT or BAT (**Fig. S1P**). This change was associated with reduced AKT phosphorylation, suggesting that inflammatory cell infiltration participated in local insulin resistance in the vWAT of HFD-fed Mac$^{\Delta Gls1}$ mice (**Fig. S1Q**). To delineate whether this effect can explain the glucose intolerance of Mac$^{\Delta Gls1}$ mice, we next examined the uptake of the radiolabeled D-glucose analog 2-[^{14}C]-deoxyglucose (2-[^{14}C]-DG) in these mice. No significant changes were observed in the total uptake of 2-[^{14}C]-DG in the brain, skeletal muscle, pancreas or ScWAT of standard chow- and HFD-fed control and Mac$^{\Delta Gls1}$ mice (**Fig. 1F, left panel**). Total 2-[^{14}C]-DG incorporation in vWAT was higher in HFD-fed Mac$^{\Delta Gls1}$ than in standard chow-fed Mac$^{\Delta Gls1}$ mice, correlating with vWAT mass, but as expected, the rate constant for net tissue uptake of 2-[^{14}C]-DG was reduced (**Fig. 1F, right panel**). This latter finding was consistent with local insulin resistance observed in the vWAT of HFD-fed Mac$^{\Delta Gls1}$ mice and partially contributed to the glucose intolerance of these mice under HFD conditions. However, this finding could not explain the glucose intolerance observed in standard chow-fed mice. Unexpectedly, both the total uptake and rate constant of 2-[^{14}C]-DG were indeed decreased by two- to three-fold in the intrascapular BAT of standard chow- and HFD-fed Mac$^{\Delta Gls1}$ mice compared to standard chow- and HFD-fed control mice (**Figs. 1F**). Altogether, our observations identify a previously undescribed role of macrophage glutaminolysis in controlling BAT glucose utilization, which most likely participates in improving glucose tolerance through energy dissipation.

Defective macrophage glutaminolysis leads to impaired homeostatic nonshivering thermogenesis. Glucose fuels sympathetic nervous system-induced nonshivering thermogenesis (Orava et al., 2011; Stanford et al., 2013). Thus, we first quantified NE levels in different adipose depots. A decrease in NE levels was observed in both the ScWAT and BAT of standard chow- and HFD-fed Mac$^{\Delta Gls1}$ mice compared to controls (**Fig. 2A**). This change was not observed in vWAT (**Fig. 2A**). To test the *in vivo* relevance of these findings, we next measured heat production in Mac$^{\Delta Gls1}$ mice. Indirect calorimetry measurements (Wolf et al., 2017) showed that standard chow-fed Mac$^{\Delta Gls1}$ mice displayed significantly lower energy dissipation through heat production than their littermate controls (**Fig. 2B**). A trend towards lower heat production was also observed in HFD-fed Mac$^{\Delta Gls1}$ mice during the nocturnal period (**Fig. 2B**). Nonshivering thermogenesis is dependent on the high expression levels of uncoupling protein 1 (*Ucp1*), PR-domain containing 16 (*Prdm16*), type II deiodinase (*Dio2*), peroxisome proliferator–activated receptor coactivator Pgc1α (*Ppargc1*α), cell death activator-A (*Cidea*) and β3 adrenergic receptor (*Adrb3*), which are highly expressed in ScWAT and BAT, to support energy metabolism and shunt energy generated by mitochondria from ATP to thermogenesis (Chechi et al., 2013). Lower expression of *Ucp1*, *Ppargc1*α and *Cidea* was observed in the ScWAT of HFD-fed Mac$^{\Delta Gls1}$ mice than in the HFD-fed control mice (**Fig. S2A**). Further histological analysis of ScWAT revealed fewer clusters of multilocular brown fat-like areas and more unilocular regions in HFD-fed Mac$^{\Delta Gls1}$ mice than in HFD-fed control mice (**Fig. S2B**). Thus, macrophage glutaminolysis participated to some extent in ScWAT browning. More strikingly, downregulation of most of the genes involved in thermogenesis was observed in the BAT of both standard chow- and HFD-fed Mac$^{\Delta Gls1}$ mice compared to that of littermate controls (**Fig. 2C**). Consistently, larger lipid droplets in brown adipocytes were observed in chow- and HFD-fed Mac$^{\Delta Gls1}$ mice than in control animals (**Fig. 2D**). The BAT temperature of Mac$^{\Delta Gls1}$

mice also decreased by approximately 1°C at steady state (**Fig. S2C**). These results suggest that macrophage glutaminolysis dominantly controls nonshivering thermogenesis through local availability of NE in BAT.

Macrophage glutaminolysis controls sympathetic tone independent of macrophage-adipocyte interactions, sympathetic innervation and catecholamine catabolism. Several macrophage-dependent mechanisms are involved in thermogenic function. First, vascular cell adhesion molecule-1 (VCAM-1) on macrophages can directly interact with its ligand integrin α4 (ITGA4) on adipocytes to limit beige adipogenesis (Chung et al., 2017). Consistent with the lack of differential inflammation, we failed to observe changes in the mRNA expression of *Vcam1* and *Itga4* between the ScWAT and BAT of Mac$^{\Delta Gls1}$ mice and those of control mice (**Fig. S3A**). BAT macrophages can also modulate the attraction of sympathetic axons (Wolf et al., 2017), which are known to innervate adipose depots and control NE-dependent thermogenesis (Cannon and Nedergaard, 2004; Nguyen et al., 2014; Nguyen et al., 2018). To address the role of sympathetic tone, we chemically denervated the sympathetic nervous system by injection of 6-hydroxydopamine (6-OHDA), a hydroxylated analog of dopamine (Cao et al., 2019; Nguyen et al., 2017). Treatment with 6-OHDA lowered BAT NE levels to the same extent in control and Mac$^{\Delta Gls1}$ mice (**Fig. 3A**). Consequently, by reducing energy expenditure (**Fig. S3B**) and heat production (**Fig. 3B**), 6-OHDA treatment abolished the differences between control and Mac$^{\Delta Gls1}$ mice. Transcriptomic analysis of genes involved in nonshivering thermogenesis in BAT confirmed that following chemical denervation, the expression of Ucp1, Pgc1α and Prdm16 was similar in both genotypes (**Fig. S3C**). These findings suggest that reduced sympathetic tone in Mac$^{\Delta Gls1}$ mice could be the cause of defective NE-dependent thermogenesis in these mice. However, the trend towards reduced tyrosine hydroxylase (Th) staining in the BAT of CD-fed Mac$^{\Delta Gls1}$ mice compared to that of control mice was nonsignificant, and analysis of axons in the sympathetic autonomic nervous system (Wolf et al., 2017) revealed no difference in sympathetic axon density between HFD-fed Mac$^{\Delta Gls1}$ and HFD-fed control mice (**Fig. 3C**). Consistently, the expression of genes previously shown to control the repulsion of neurons by macrophages, such as the transmembrane semaphorin Sema6a, its ligand Plexin A4 and the transcription regulator methyl-CpG-binding protein 2 (Mecp2) (Wolf et al., 2017), was unaltered in the BAT of Mac$^{\Delta Gls1}$ mice compared to that of control mice (**Fig. 3D**). Similar findings were observed in the ScWAT of Mac$^{\Delta Gls1}$ mice (**Fig. S3D**). The expression of Th was low and not significantly altered in the adipose depots of these mice (**Fig. 3D and Fig. S3D**). Recently, a population of sympathetic neuron-associated macrophages (SAMs) in different adipose depots and in subcutaneous fascia was found to mediate catecholamine catabolism (Camell et al., 2017; Pirzgalska et al., 2017). Low Gls1 mRNA expression was first observed in these SAM populations (**Fig. S3E**). Transcriptomic analysis did not reveal significant changes in genes that regulate catecholamine catabolism between the BAT and ScWAT of standard chow- and HFD-fed Mac$^{\Delta Gls1}$ mice and those of standard chow- and HFD-fed control mice, including the NE transporter Slc6a2 and the monoamine oxidase A (MAOA), which were previously shown to control NE uptake and degradation, respectively (**Fig. 3D and Fig. S3D**). To directly assess the contribution of glutaminolysis to the ability of SAMs to degrade NE, we first visualized SAMs in the subcutaneous fascia based on the expression of CX3CR1 and isolated them by flow cytometry based on the expression of the canonical macrophage markers CD64 and MerTK (**Fig. S3F**). We cultured these cells with exogenous NE in the presence or absence of clorgyline, a selective MAOA inhibitor, as previously described (Camell et al., 2017; Pirzgalska et al., 2017). As expected, MAOA inhibition prevented NE degradation in the culture medium, but Gls1 deficiency had no effect on this process (**Fig. 3E**). Thus, macrophage glutaminolysis controls NE-dependent thermogenesis through a mechanism independent of local inflammation, sympathetic innervation and macrophage catecholamine degradation.

Macrophage glutaminolysis controls spinal cord neuron activation. We next reasoned that sympathetic preganglionic neurons that project to thermogenic adipose depots can be controlled by presynaptic glutamatergic neurons (Morrison and Madden, 2014; Tupone et al.,

2014). These neurons are localized in the intermediolateral nucleus (IML) located between the T2 and T6 segments of the spinal cord (**Fig. 4A**). Quantification of activated neurons by immunoblotting with a c-Fos antibody revealed less neuron activation in the spinal cord of $Mac^{\Delta Gls1}$ mice than in that of control mice (**Fig. 4B**). The level of glutamate, which is a physiological excitatory neurotransmitter, was also decreased in the T2-6 segments of the spinal cord of $Mac^{\Delta Gls1}$ mice compared to controls (**Fig. 4C**). Remarkably, daily *i.p.* administration of glutamate (50 mg/kg) to standard chow-fed $Mac^{\Delta Gls1}$ and littermate control mice for 12 days did not alter body weight (data not shown) but increased postprandial energy expenditure (**Fig. S4A**) and heat production (**Fig. 4D**) in both genotypes and thus rescued the defects observed in $Mac^{\Delta Gls1}$ mice. These observations were mirrored by normalization of NE levels in the BAT of these mice (**Fig. 4E**). We next evaluated whether defective macrophage glutaminolysis plays a role in the spinal cord by investigating the gene expression profile of spinal cord macrophages compared to those of microglia and peritoneal cavity macrophages (PCMs). We sorted these macrophage populations based on the expressed canonical CD64 and CD11b markers (**Fig. S4B**). We confirmed that, similar to microglia (Ajami et al., 2007; Ginhoux et al., 2010; Schulz et al., 2012; Guimaraes et al., 2019), spinal cord macrophages were tissue-resident and not monocyte-derived, as shown by their resistance to radiation and their lack of repopulation after $CX3CR1^{gfp/+}$ (CD45.1) bone marrow transplantation in lethally irradiated CD45.2 control recipients (**Fig. S4C**). Of note, by performing k-means clustering of our gene expression profile data obtained by RNA-seq, we also identified modules containing markers that were expressed by both spinal cord macrophages and microglia (i.e., Cx3cr1) or PCMs (i.e., Cxcl2) and found genes that were not expressed in microglia and PCMs (i.e., Cxcl10, Chil3, Klf4 and Trem3) (**Fig. S4D**). PCA analysis revealed that spinal cord macrophages were transcriptionally distinct from both PCMs and microglia and were strongly impacted by defective glutaminolysis (**Fig. 4F**). Global metabolic transcriptome signatures and topological analyses using CoMBI-T (Jha et al., 2015) also confirmed that defective glutaminolysis metabolically reprogrammed spinal cord macrophages (**Fig. S4E**). To explore the broader effect of Gls1 deficiency on the expression profile of spinal cord macrophages, we constructed a volcano plot. Specifically, 354 genes were upregulated and 124 were downregulated ($-Log_{10}(Pval) > 2$) (**Fig. 4G**). Gene set enrichment analysis (GSEA) of the differentially expressed genes identified 'Microtubule cytoskeleton' and 'Mitochondrion' GO terms as the most enriched terms for genes that were upregulated in glutaminolysis-deficient spinal cord macrophages, while 'Cell projection' and 'Response to stimuli' were enriched for downregulated genes (**Fig. S4F**). To test the *in vivo* relevance of these findings, $Cx3cr1^{GFP/+}$ reporter mice were backcrossed to control and $Mac^{\Delta Gls1}$ mice, and spinal cord tissues were stained for VGLUT3 and DAPI and visualized by confocal microscopy. While control $Cx3cr1^{GFP/+}$ mice exhibited a dense network of fusiform $Cx3cr1^{GFP/+}$ macrophages in the IML region of the spinal cord, $Cx3cr1^{GFP/+}Mac^{\Delta Gls1}$ mice exhibited more rounded $Cx3cr1^{GFP}$ spinal cord macrophages (**Fig. 4H and S4G**). Finally, we cocultured primary $actin^{+}$ neocortical neurons enriched in glutamate with sorted control or Gls1-deficient spinal cord or peritoneal macrophages. As in the *in vivo* experiment, we observed that defective glutaminolysis significantly changed the shape of macrophages; specifically, it decreased the ratio of fusiform to rounded macrophages, suggesting that the macrophages participated in less cellular sensing through their profuse pseudopodia (**Fig. 4I**). Reduced glutamate levels in the coculture medium of Gls1-deficient macrophages was consistent with the lower levels of excitatory neurotransmitters *in vivo* **(Fig. 4J**). Collectively, these data suggest that glutaminolysis deficiency metabolically reprograms spinal cord macrophages, impeding their projections and compromising the glutamatergic tone that governs peripheral thermogenic adipose tissue sympathetic activation.

Discussion

Glutamine links obesity to adipose tissue inflammation (Petrus et al., 2020), but the pathophysiological and causal relevance of this pathway *in vivo* at steady state and during metabolic inflammation remains poorly understood. Using a newly generated genetic mouse model, we first demonstrated a causal role of Gls1-dependent macrophage glutaminolysis in limiting visceral fat inflammation and storage during obesity. Our study also uncovered a novel mechanism by which macrophage glutaminolysis supports glucose tolerance at steady state. Indeed, macrophage glutaminolysis increased glucose oxidation through heat generation and improved homeostatic thermogenesis of subcutaneous and brown adipose depots. This process is increasingly being recognized as a hallmark of metabolic health (Glass and Olefsky, 2012; McNelis and Olefsky, 2014; Murray et al., 2014; Odegaard and Chawla, 2015; Rosen and Spiegelman, 2014; Wynn et al., 2013). Our findings offer a new paradigm explaining how glutaminolysis fine-tunes energy metabolism by playing a previously unrecognized role in spinal cord macrophages, controlling their shape and expression of branching projection genes and supporting glutamatergic transmission, which is required for efficient sympathetic tone-dependent thermogenesis.

When we initiated the present study, we hypothesized that mice with defective macrophage glutaminolysis (i.e., Gls1 deficiency) would induce a switch from an anti-inflammatory to a proinflammatory phenotype in vWAT, leading to *in vivo* fat inflammation and storage, hallmarks of metabolic disease. This hypothesis was driven by observations showing that vATM glutaminolysis is modulated by obesity and inversely associated with the profile of secreted cytokines (Boutens et al., 2018) and that altering macrophage glutamine utilization *in vitro* prevents the promotion of efficient alternative macrophage activation (Jha et al., 2015; Liu et al., 2017). Unlike other adipose depots, WAT was strongly impacted by defective macrophage glutaminolysis, as shown by the increased Gln/Glu ratio in this tissue as well enhanced fat inflammation and storage upon HFD feeding. This finding revealed a causal role of this metabolic pathway in obesity-induced inflammation. The specificity of these regulatory mechanisms for vWAT over other adipose depots requires further investigation. High levels of Gln and Glu in vWAT could provide adequate environmental conditions for these regulatory mechanisms, as was recently shown in the peritoneal cavity (Davies et al., 2017). Consistent with this hypothesis, the mRNA expression of Gls1 in vWAT was high, inversely correlated with the expression of classically activated inflammatory macrophage markers and positively correlated with the expression of alternatively activated macrophage markers. This finding suggests that vATMs may have a specific genetic predisposition to face their local environment. As vATMs are the major immune cells in vWAT, they may specifically interact with visceral adipocytes. For instance, in the vWAT of lean animals, adipocytes constantly release fatty acids into the local microenvironment as sources for macrophage fatty acid oxidation, which is required to support alternative macrophage polarization (Huang et al., 2014). Thus, glutaminolysis may facilitate the generation of anaplerotic reactions to support vATM respiratory burst, as observed in other *in vitro* and *in vivo* settings (Jha et al., 2015; Liu et al., 2017). Downregulation of this pathway upon HFD feeding could reflect perturbed fatty acid oxidation due to a specific program of lysosomal-dependent lipid degradation at the origin of the inflammatory response (Kratz et al., 2014; Xu et al., 2013) or increased recruitment of metabolically immature monocytes from the blood vasculature (Weisberg et al., 2006; (Silva et al., 2019). Although further studies are required to pinpoint the origin of these perturbations, our findings clearly establish that macrophage glutaminolysis causally participates in the crosstalk between vATMs and visceral adipocytes to maintain tissue homeostasis.

Unexpectedly, our results also demonstrate that abrogation of macrophage glutaminolysis in mice results in a broad range of metabolically deleterious effects, particularly impaired glucose tolerance due to lower glucose utilization by thermogenic adipose depots required for nonshivering thermogenesis. Although a switch between alternative and classical macrophage activation is often associated with impaired thermogenesis under conditions of disrupted metabolic homeostasis such as HFD-induced obesity (Ivanov et al., 2018; Reitman,

2017), the present study reveals that reduced thermogenesis occurs under steady state conditions in Mac$^{\Delta Gls1}$ mice independent of any perturbation in ATM activation in thermogenic adipose depots. These findings add to the current debate on the causal contribution of macrophage activation pathways to the regulation of thermogenesis. For instance, alternatively activated macrophages were first reported as a source of catecholamines that act in a paracrine fashion to activate β-adrenergic receptor signaling-dependent thermogenesis in ScWAT and BAT (Nguyen et al., 2011; Qiu et al., 2014). However, this view was recently challenged by Buettner's group, who showed that Th, the rate-limiting enzyme for the synthesis of catecholamines, is not expressed in ATMs (Fischer et al., 2017; Wolf et al., 2017). Additionally, the authors reported that conditioned media obtained from IL-4-stimulated macrophages and chronic *in vivo* IL-4 treatment fail to increase the thermogenic response in adipose tissue (Fischer et al., 2017). Thus, we hypothesized that macrophage glutaminolysis can promote glucose-dependent nonshivering thermogenesis through a different mechanism that may involve sympathetic stimulation (Orava et al., 2011; Stanford et al., 2013). Indeed, an alternative role of macrophages in controlling thermogenesis involves their adhesion to sympathetic neurons that innervate thermogenic adipose depots (Wolf et al., 2017) and their capacity to degrade NE during aging and in obesity (Camell et al., 2017; Pirzgalska et al., 2017). Although we identified defective macrophage glutaminolysis as a critical regulator of the sympathetic tone of thermogenic adipose depots, we did not observe perturbations in the sympathetic innervation of BAT or NE degradation by sympathetic neuron-associated macrophages. Instead, we identified that macrophage glutaminolysis controls the sympathetic tone of thermogenic adipose depots by potentializing the glutamatergic neural pathway stemming from the IML region of the spinal cord located between the T2 and T6 segments, which is known to activate nonshivering thermogenesis under behavioral stress (Morrison and Madden, 2014; Tupone et al., 2014). Thus, our study identified an unprecedented and unexpected role of macrophage glutaminolysis in controlling spinal cord neuron activation required for sympathetic tone-dependent thermogenesis.

Although brain macrophages (i.e., microglia) and intestinal muscularis macrophages are known to communicate with neurons and control their activity (Crotti and Ransohoff, 2016; Muller et al., 2014), reports of interactions between macrophages and spinal nerves are scarce, and their relevance to metabolic function has not yet been investigated. Recent reports have identified populations of nerve-associated macrophages in different body regions and have suggested that these cells exhibit specific transcriptomic profiles depending on the nerve they communicate with (Wang et al., 2020; Ydens et al., 2020). Whether these diverse populations share common metabolic configurations and requirements, particularly the involvement of glutaminolysis, remains to be elucidated. Here, we documented a population of spinal cord macrophages that are present in the IML region of the gray matter, where spinal nerves, especially glutamatergic axons, normally unite. Transcriptomic analysis revealed that these macrophages were significantly distinct from brain microglia in terms of transcriptional machinery and were strongly impacted by defective glutaminolysis, consistent with earlier reports showing that they express lower levels of CD45 (Goldmann et al., 2016) and are metabolically more active than microglia (Zhu et al., 2017). These findings are consistent with divergent gene expression landscapes across different tissue-resident macrophages, supporting the idea of local macrophage adaptation (Gautier et al., 2012; Gosselin et al., 2014; Lavin et al., 2014; Okabe and Medzhitov, 2014). Spinal cord macrophage pseudopodia extending over axons are also morphologically distinct from the finely branching ramifications of brain microglia (Crotti and Ransohoff, 2016), which could offer an explanation for how glutaminolysis impacts these cells. Indeed, our results clearly demonstrated that the transcriptional profiles of spinal cord macrophages were modulated in Mac$^{\Delta Gls1}$ mice; specifically, the expression of genes involved in cell projection and the response to various stimuli was decreased, and the expression of genes associated with the microtubule cytoskeleton and mitochondrion rearrangement was increased. There was no evidence that these cells exhibited a proinflammatory profile. Among the modulated genes, members of the semaphorin and plexin families (i.e., *Sema3g* and *Plxnb3*), which are known to contribute to axonal guidance in the spinal cord (Ducuing et al., 2019), and various genes involved in cilium

and dendrite formation and movement (i.e., *Wdr78*, *Kctd17*, *Syt3*, *Tmem67*, *Plekha8* or *Rhof*), were identified; the changes in these genes require further exploration. Nevertheless, our data clearly revealed altered spindle-shaped spinal cord macrophages in the spinal cords of $Mac^{\Delta Gls1}$ mice, which affected autonomous medullospinal axonal activity, which is critical for sympathetic tone-dependent nonshivering thermogenesis (Morrison and Madden, 2014; Tupone et al., 2014) and metabolic adaptation of thermogenic brown adipose tissue (Chechi et al., 2013).

Collectively, our data reveal that macrophage glutaminolysis acts as a central component of metabolic adaptation at steady state and in HFD-induced obesity through two independent but complementary tissue-dependent roles. First, macrophage glutaminolysis limits visceral fat inflammation and storage in HFD-induced obesity. Second, we identified a previously unknown glutamine-dependent homeostatic role for spinal cord macrophages through which they control medullispinal glutamatergic transmission, favoring sympathetic tone activation in thermogenic adipose depots and glucose homeostasis. Overall, our study helps to elucidate the role of macrophage glutaminolysis in metabolic health and disease.

Figure 1

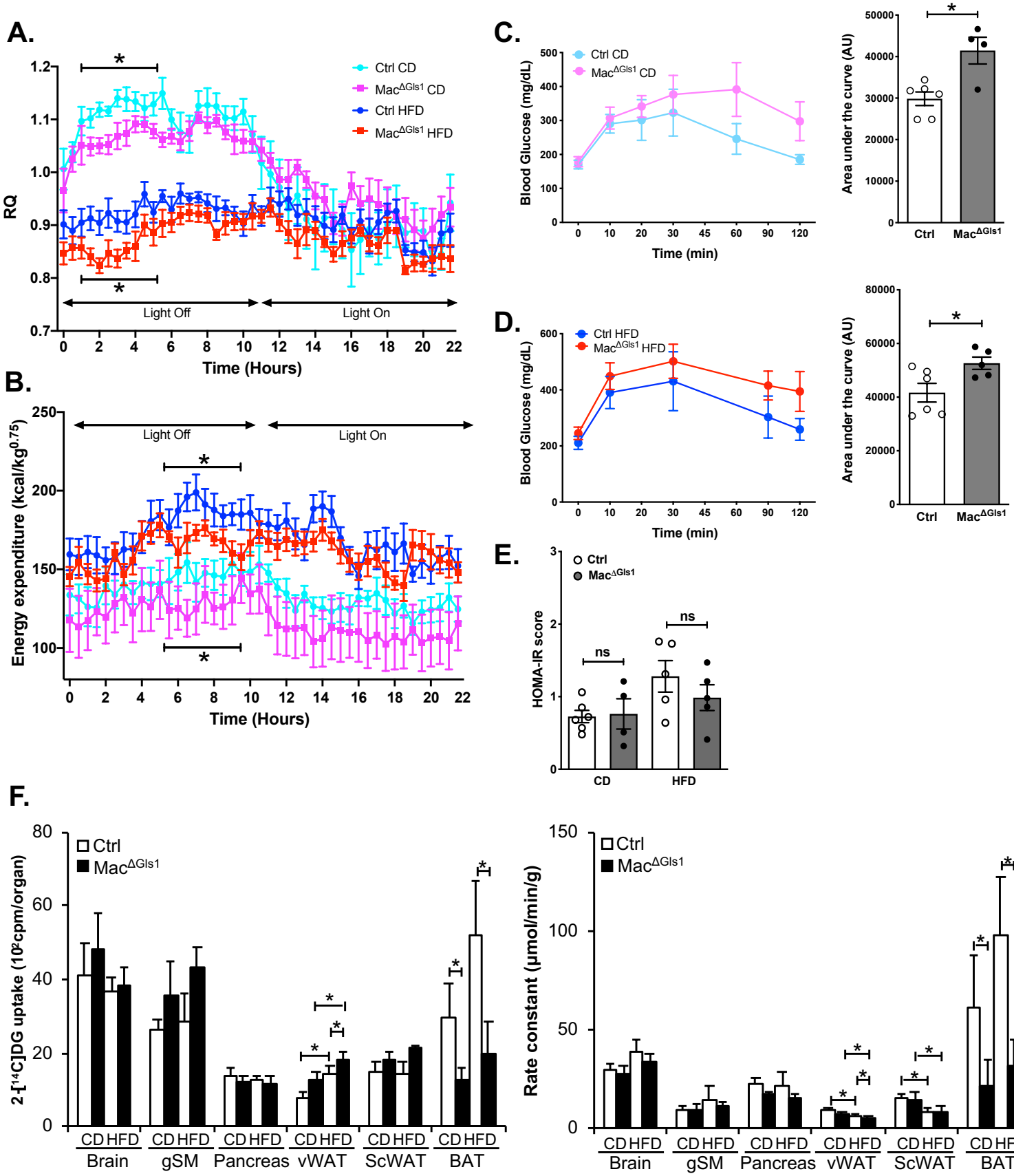
A.
RQ
Time (Hours)
Ctrl CD
Mac$^{\Delta Gls1}$ CD
Ctrl HFD
Mac$^{\Delta Gls1}$ HFD
Light Off
Light On
B.
Energy expenditure (kcal/kg$^{0.75}$)
Time (Hours)
Light Off
Light On
C.
Blood Glucose (mg/dL)
Time (min)
Area under the curve (AU)
Ctrl
Mac$^{\Delta Gls1}$
D.
Blood Glucose (mg/dL)
Time (min)
Area under the curve (AU)
E.
HOMA-IR score
ns
CD
HFD
F.
2-[^{14}C]DG uptake (10^{2}cpm/organ)
Rate constant (µmol/min/g)
CD HFD
Brain
gSM
Pancreas
vWAT
ScWAT
BAT

Figure 1. Macrophage Gls1 deficiency reduces glucose utilization independently of visceral fat inflammation. **(A)** Respiratory quotient and **(B)** whole-body energy expenditure measured by indirect calorimetry in control and Gls1 deficient mice ($Mac^{\Delta Gls1}$) fed for 12 weeks with a standard chow or high-fat diet (CD and HFD, respectively). **(C)** Intraperitoneal glucose tolerance test (ipGTT) performed on fasted CD-fed and **(D)** HFD-fed control and $Mac^{\Delta Gls1}$ mice. Blood glucose concentrations were measured at the indicated time points. Quantifications are calculated as the glucose area under the curve (AUC). **(E)** Insulin resistance index in control and $Mac^{\Delta Gls1}$ mice fed for 12 weeks with a CD or HFD. The insulin resistance index is calculated as fasting insulin x fasting blood glucose/405 and expressed as HOMA-IR score. **(F)** Tissue uptake (left panel) and rate constant (right panel) of 2-[^{14}C]-deoxyglucose (2-[^{14}C]-DG) in CD and HFD-fed control and $Mac^{\Delta Gls1}$ mice (40min after *i.v.* injection of the radiolabeled tracer). All values are means ± SEM and are representative of an experiment of five to seven animals per group. *, $P<0.05$ versus control.

Figure 2

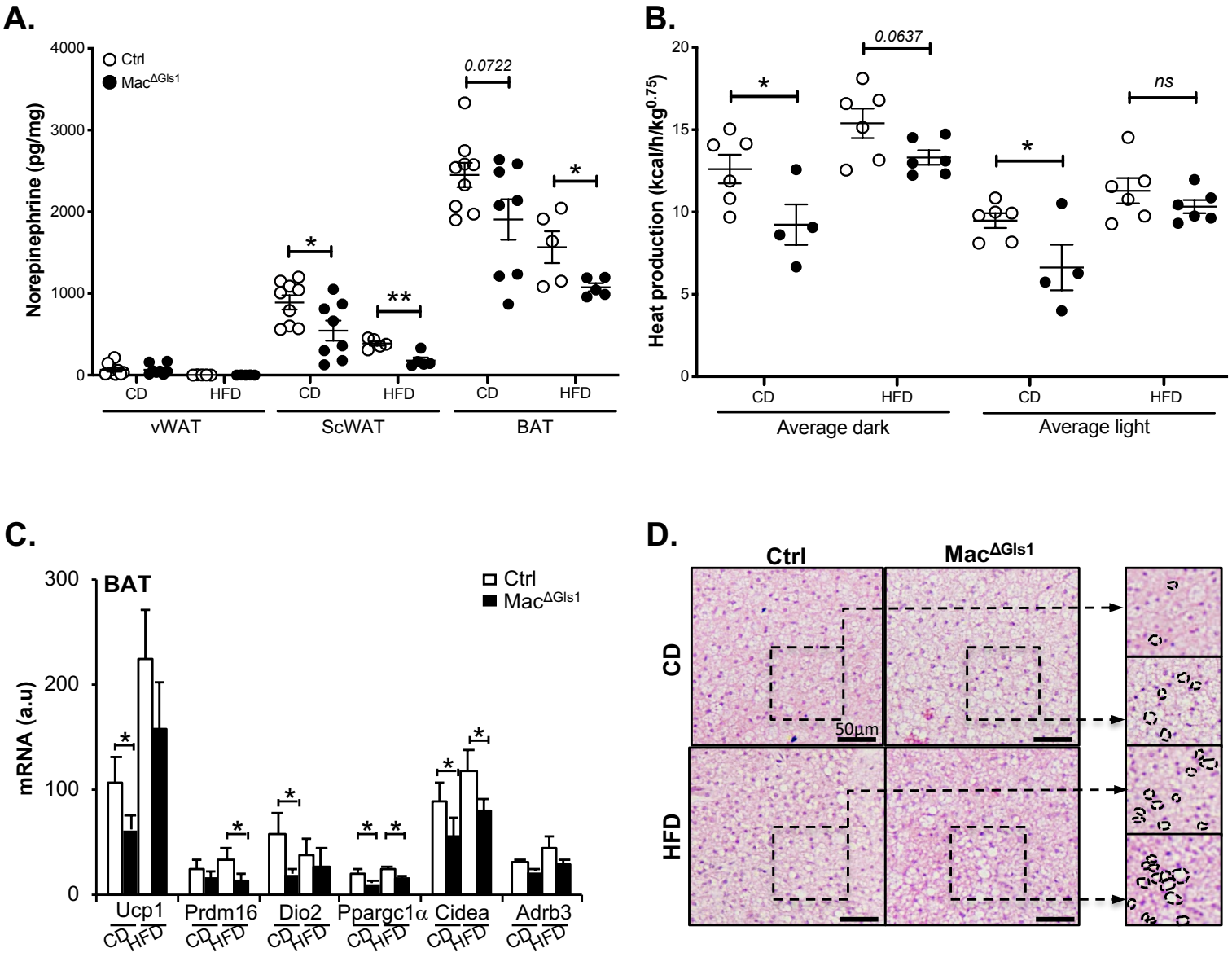

Figure 2. Macrophage-restricted deletion of Gls1 reduces catecholamine levels in thermogenic adipose depots and impairs BAT-dependent thermoregulation. (A) Norepinephrine (NE) levels in visceral and thermogenic adipose tissues of CD and HFD-fed control and Mac$^{\Delta Gls1}$ mice; each dot represents one animal. **(B)** Heat production in these mice calculated by indirect calorimetry and presented as the average values for the light or dark periods during the final 24h of monitoring; each symbol represents an individual mouse. **(C)** Expression of genes encoding molecules involved in thermogenesis in BAT of CD and HFD-fed control and Mac$^{\Delta Gls1}$ mice, assessed by RT-qPCR. **(D)** Histology of hematoxylin- and eosin (H&E)-stained BAT from CD and HFD-fed Mac$^{\Delta Gls1}$ mice and their littermates at the end of the study period. All values are means ± SEM and are representative of at least one experiment (n= 5-9). *, *P*<0.05 versus control.

Figure 3

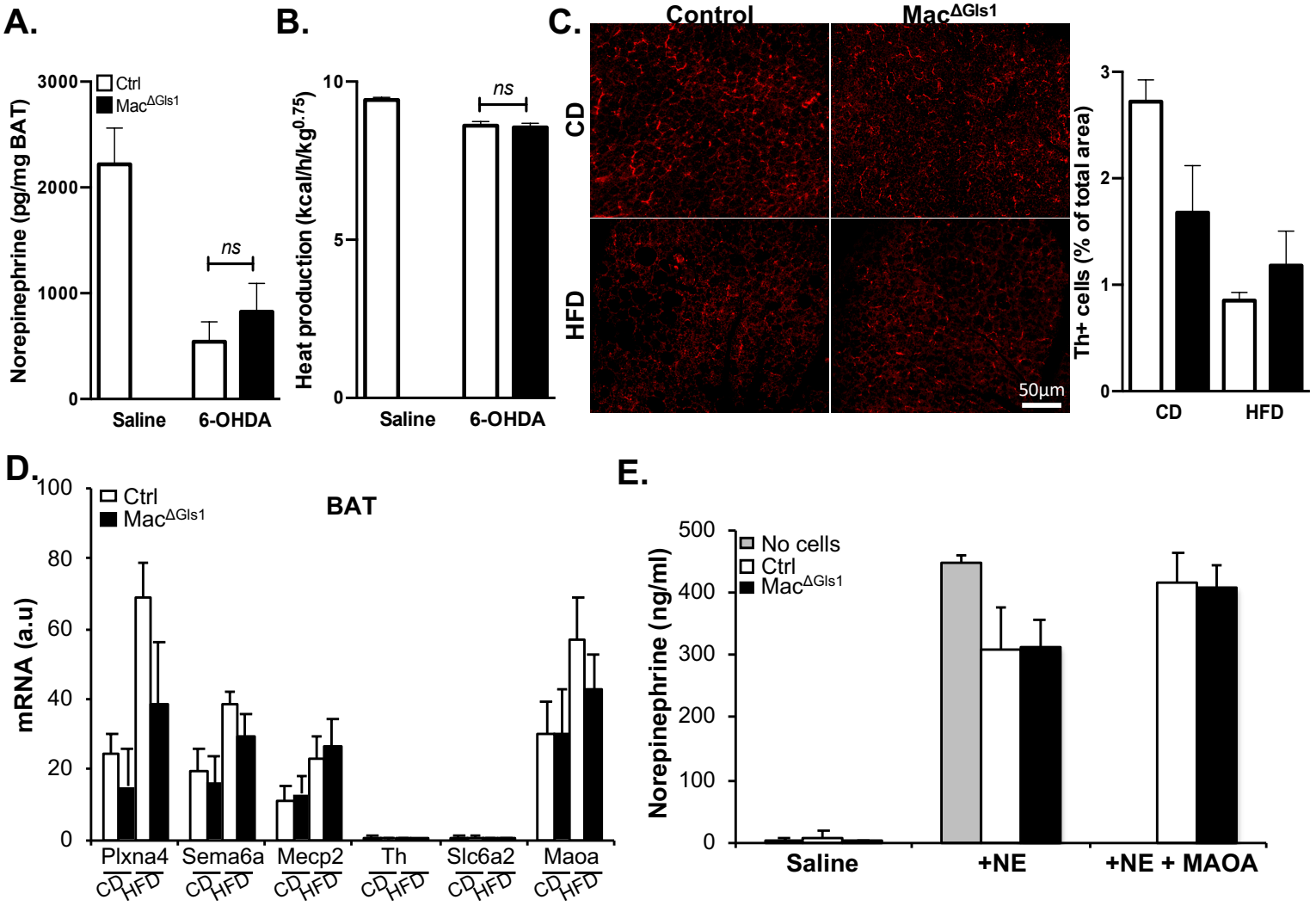

Figure 3. Defective macrophage glutaminolysis impacts the sympathetic tone but does not diminish BAT innervation or NE degradation. Effect of neurochemical sympathectomy of control and Mac$^{\Delta Gls1}$ mice with 6-hydroxydopamine (6-OHDA) on **(A)** BAT NE levels and **(B)** heat production calculated by indirect calorimetry. **(C)** Visualization of tyrosine hydroxylase (Th)$^{+}$ fibers by immunofluorescence microscopy in BAT of CD and HFD-fed control and Mac$^{\Delta Gls1}$ mice. **(D)** RT-qPCR analysis of genes involved in the repulsion of neurons or NE degradation in BAT of CD and HFD-fed control or Mac$^{\Delta Gls1}$ mice. **(E)** NE content in the media of cell-sorted sympathetic neuron-associated macrophages (SAMs) cultured overnight in presence or absence of NE and chlorgyline, a MAOA blocker. All values are means ± SEM and are representative of an experiment of five to seven animals per group. *, P<0.05 versus control.

Figure 4

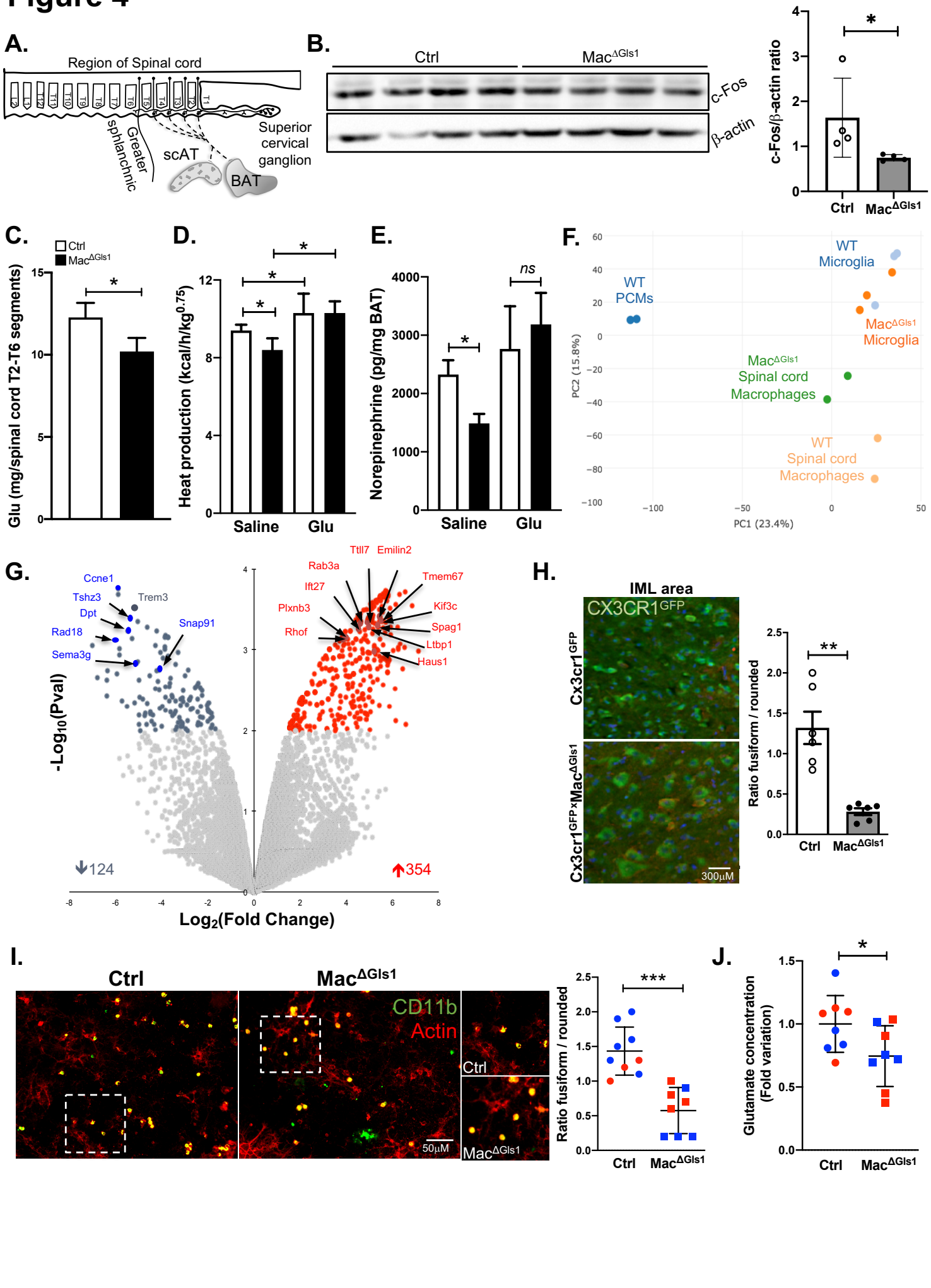
A.
Region of Spinal cord
Greater splanchnic
scAT
BAT
Superior cervical ganglion
B.
Ctrl
Mac^ΔGls1
c-Fos
β-actin
c-Fos/β-actin ratio
C.
Glu (mg/spinal cord T2-T6 segments)
D.
Heat production (kcal/h/kg^0.75)
Saline
Glu
E.
Norepinephrine (pg/mg BAT)
ns
F.
WT Microglia
WT PCMs
Mac^ΔGls1 Microglia
Mac^ΔGls1 Spinal cord Macrophages
WT Spinal cord Macrophages
PC1 (23.4%)
PC2 (15.8%)
G.
Ccne1
Tshz3
Trem3
Dpt
Rad18
Snap91
Sema3g
Ttll7
Emilin2
Rab3a
Ift27
Tmem67
Plxnb3
Kif3c
Rhof
Spag1
Ltbp1
Haus1
-Log10(Pval)
124
354
Log2(Fold Change)
H.
IML area
CX3CR1GFP
Cx3cr1GFP
Cx3cr1GFP×Mac^ΔGls1
300μM
Ratio fusiform / rounded
I.
Ctrl
Mac^ΔGls1
CD11b
Actin
50μM
J.
Glutamate concentration (Fold variation)

Figure 4. Identification and characterization of a role for glutaminolysis in spinal cord macrophages. (A) Schematic illustration showing the sympathetic innervation of thermogenic adipose tissues stemming from the IML region of the spinal cord located between T2 and T6 segments. **(B)** Immunoblot of c-Fos and β-actin of spinal cord T2-T6 segments. The bar graph show densitometry quantification of immunoblots normalized to β-actin. **(C)** Glutamate levels in the spinal cord T2-6 segments of control or $Mac^{\Delta Gls1}$ mice. **(D)** Effect of glutamate supplementation (50mg/kg for 12 days) in control and $Mac^{\Delta Gls1}$ mice on heat production calculated by indirect calorimetry and **(E)** BAT NE levels. **(F)** PCA based on gene expression from RNA-seq of cell sorted control PCMs (blue), control and Gls1-deficient microglia (light blue and orange, respectively) and control and Gls1-deficient spinal cord macrophages (green and light orange, respectively). Each dot represents an independent experiment. **(G)** Volcano plot shows genes differentially expressed between control and Gls1-deficient spinal cord macrophages with differences in expression (*P* value ($-\log_{10}$)) plotted against $\log_2$-fold change (based on RNA-seq data). Genes with significantly different expression (a *P* value of < 0.01) in Gls1-deficient spinal cord macrophages were indicated in red (upregulation) or in blue (downregulation). **(H)** Confocal microscopy of the intermediolateral cell column (IML) of the spinal cord isolated from $CX3CR1^{gfp/+}$ or $CX3CR1^{gfp/+}$ $Mac^{\Delta Gls1}$ mice and quantification of the ratio of fusiform/rounded macrophages. Cells were counterstained with DAPI (nuclear staining). Each dot represents a cell from pooled animals. **(I)** Primary neocortical cultures, enriched in glutamatergic neurons, were incubated for 16 h with PCMs (blue) or cell-sorted spinal cord macrophages (red) and visualized by immunofluorescence microscopy of actin and CD11b (left panel). Spindle-shaped macrophages (i.e., fusiform/rounded ratio) were quantified (right panel). **(J)** Glutamate levels in media, a hallmark of glutamatergic neuron activation, were also quantified. Each dot represents an experiment from an individual mouse. All values are means ± SEM and are representative of an experiment of up to five animals per group. *, *P*<0.05 versus control. **, *P*<0.01 versus control. ***, *P*<0.001 versus control.

Table S1. Effect of Gls1 deficiency on energy metabolism.

	Chow diet			High fat diet		
	Control	**Mac$^{\Delta Gls1}$**	***P***	**Control**	**Mac$^{\Delta Gls1}$**	*P*
Food intake (kcal/day)	17.91±0.76	14.89±1.30	*	19.34±3.65	17.66±3.91	*NS*
EE (kcal/day/kg$^{0.75}$)	135.1±3.1	118.2±3.3	***	171.0±2.2	160.7±1.6	***
Gox (kcal/day/kg$^{0.75}$)	116.6±4.7	95.7±5.3	*	121.8±4.1	93.4±3.5	***
Lox (kcal/day/kg$^{0.75}$)	18.5±1.5	22.5±0.8	*NS*	49.2±2.5	67.2±2.9	***
Locomotor activity (a.u)	109.2±8.4	94.9±7.2	*NS*	72.6±6.3	81.2±6.8	*NS*

Indirect calorimetry parameters (food intake, energy expenditure (EE), glucose oxidation (Gox), lipid oxidation (Lox) and locomotor activity) of control and Mac$^{\Delta Gls1}$ mice fed on CD or HFD for 12 weeks. Data are means ± SEM (n=5-7 per group). *, $P<0.05$; ***, $P<0.001$ versus control.

Supplemental Figure 1

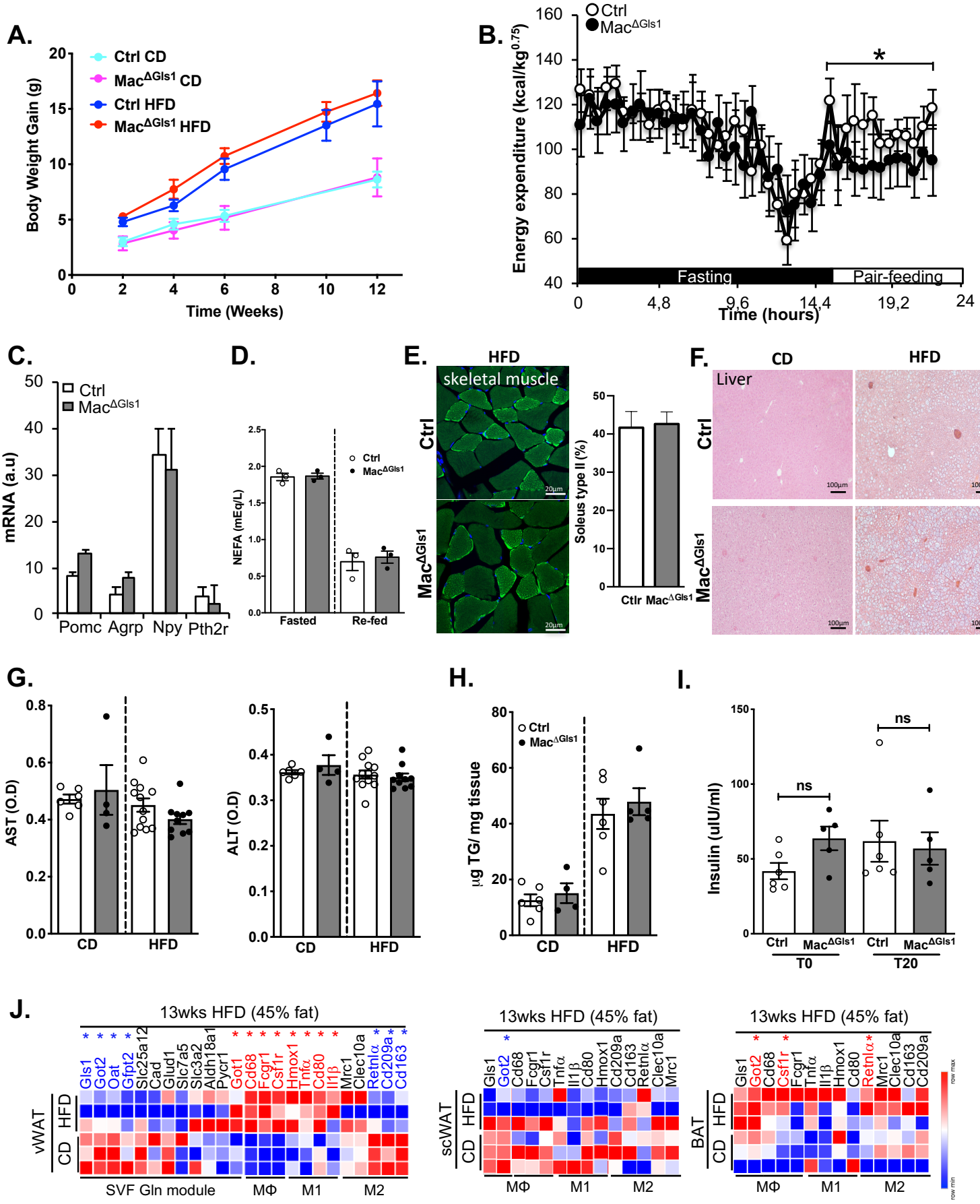

Supplemental Figure 1

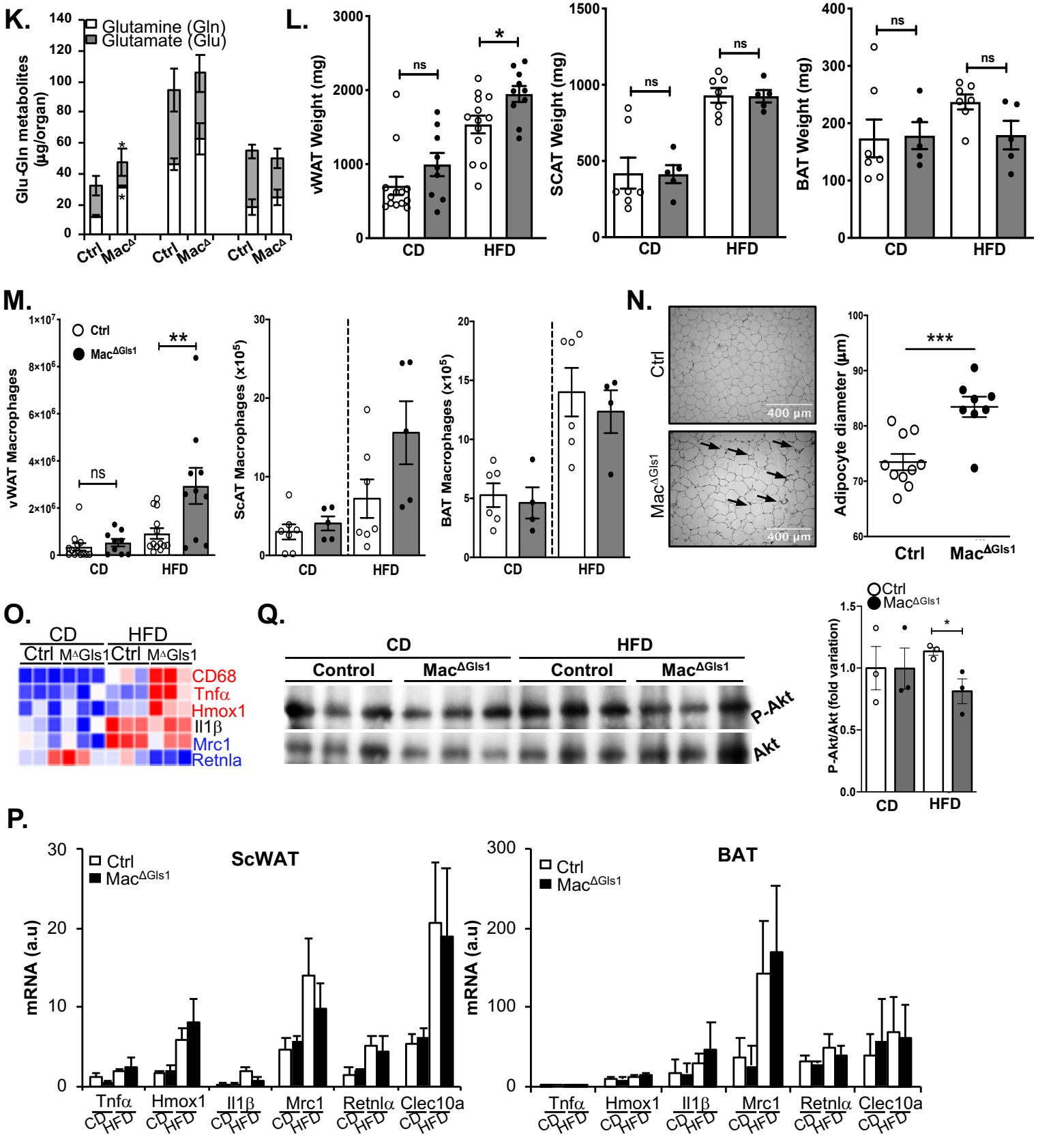

Figure S1. Effect of macrophage glutaminolysis deficiency on metabolic and adipose tissue parameters. (A) Body weight gain of control and $Mac^{\Delta Gls1}$ mice fed a CD or HFD for 12 weeks. **(B)** Whole-body energy expenditure of control and $Mac^{\Delta Gls1}$ mice subjected to fasting and pair-feeding. **(C)** RT-qPCR analysis of genes encoding central feeding regulatory neuropeptides in hypothalami obtained from CD fed control and $Mac^{\Delta Gls1}$ mice. **(D)** Plasma non-esterified fatty acid (NEFA) levels in mice of the indicated genotypes. **(E)** Representative sections of gastrocnemius skeletal muscle immunostained with antibodies against type II MyHC to visualize type II oxidative fibers in HFD-fed control and $Mac^{\Delta Gls1}$ mice. **(F)** Representative H&E staining of liver sections of CD or HFD-fed control and $Mac^{\Delta Gls1}$ mice. Effect of Gls1 deficiency on **(G)** plasma AST and ALT levels and **(H)** liver triglyceride content in mice of the indicated genotypes. **(I)** Plasma insulin concentrations during the ipGTT at time 0 and 20min in HFD-fed control and $Mac^{\Delta Gls1}$ mice. **(J)** Microarray analysis of vWAT, ScWAT and BAT isolated from CD and HFD-fed WT mice (GSE28440) and heatmaps were performed with Phantasus software. Genes labeled in red are significantly upregulated and genes labeled in blue are significantly downregulated. **(K)** Glutamine and glutamate concentrations in adipose depots of CD-fed control or $Mac^{\Delta Gls1}$ mice. **(L)** Weight of different adipose depots (vWAT, ScWAT and BAT) in CD or HFD-fed control and $Mac^{\Delta Gls1}$ mice. Each dot represents one animal. **(M)** Quantification of macrophage numbers in vWAT, ScWAT and BAT analyzed by flow cytometry. Each dot represents one animal. **(N)** Representative H&E staining of vWAT sections and quantification of adipocyte diameter in HFD-fed control and $Mac^{\Delta Gls1}$ mice. **(O)** Expression of anti- and pro-inflammatory genes in the vWAT of CD and HFD-fed control and $Mac^{\Delta Gls1}$ mice, assessed by qPCR. **(P)** RT-qPCR analysis of anti and pro-inflammatory genes in the ScWAT and BAT of the indicated genotypes. **(Q)** Western blot analysis of phospho-Akt and total Akt in the vWAT of CD and HFD-fed control and $Mac^{\Delta Gls1}$ mice. All values are means ± SEM and are representative of an experiment of five to seven animals per group. *, $P<0.05$; **, $P<0.01$; ***, $P<0.001$ versus control.

Supplemental Figure 2

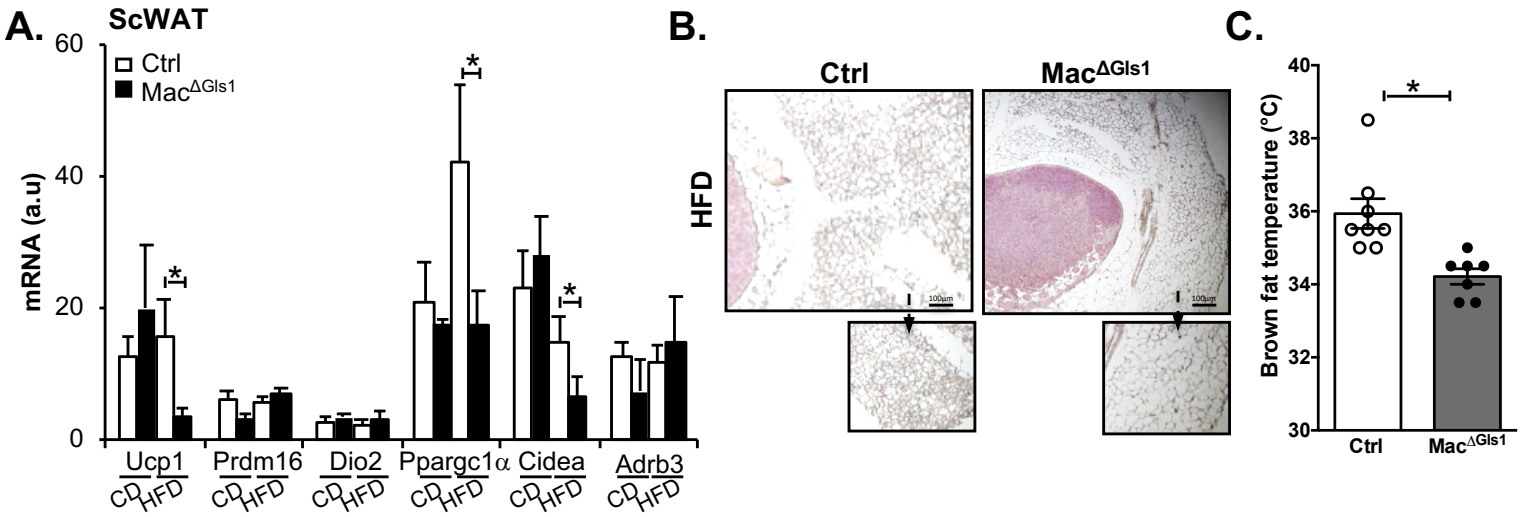

Figure S2. Macrophage Gls1 deficiency causes impairment of ScWAT browning. (A) Expression of genes encoding molecules involved in thermogenesis in ScWAT of CD and HFD-fed control and Mac$^{\Delta Gls1}$ mice, assessed by RT-qPCR. **(B)** Representative H&E staining of ScWAT sections showing clusters of multilocular or unilocular brown fat-like in HFD-fed control or Mac$^{\Delta Gls1}$ mice. **(C)** Changes in BAT temperature in the absence of Gls1 in macrophages. All values are means ± SEM and are representative of at least one experiment (n= 5-9). *, *P*<0.05 versus control.

Supplemental Figure 3

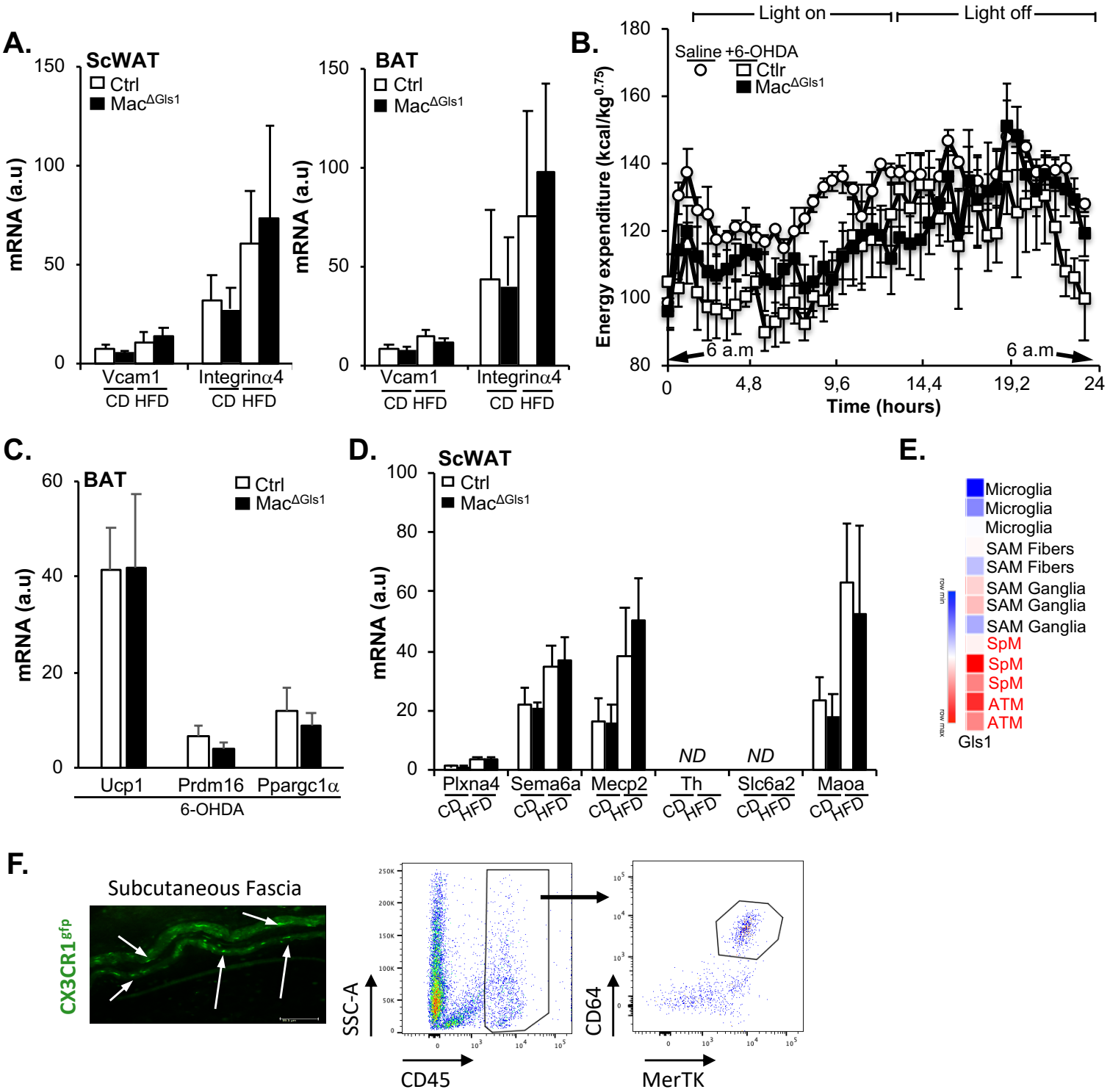

Figure S3. Effect of macrophage glutaminolysis on cell adhesion molecule-dependent browning and its dependence on sympathetic tone. (A) RT-qPCR analysis of genes involved in macrophage-adipocyte adhesion in ScWAT and BAT of CD and HFD-fed control or $Mac^{\Delta Gls1}$ mice. Effect of neurochemical sympathectomy of control and $Mac^{\Delta Gls1}$ mice with 6-hydroxydopamine (6-OHDA) on **(B)** whole-body energy expenditure measured by indirect calorimetry and **(C)** expression of genes encoding molecules involved in BAT thermogenesis assessed by RT-qPCR. **(D)** RT-qPCR analysis of genes involved in the repulsion of neurons or NE degradation in ScWAT of CD and HFD-fed control or $Mac^{\Delta Gls1}$ mice. **(E)** Comparative analysis of Gls1 expression in different macrophage populations from a publicly available dataset (GSE103847). **(F)** Visualization of sympathetic neuron-associated macrophages (SAMs) in the subcutaneous fascia of $CX3CR1^{gfp/+}$ mice (left) and flow cytometry gating strategy for isolation (right). All values are means ± SEM and are representative of an experiment of five to seven animals per group.

Supplemental Figure 4

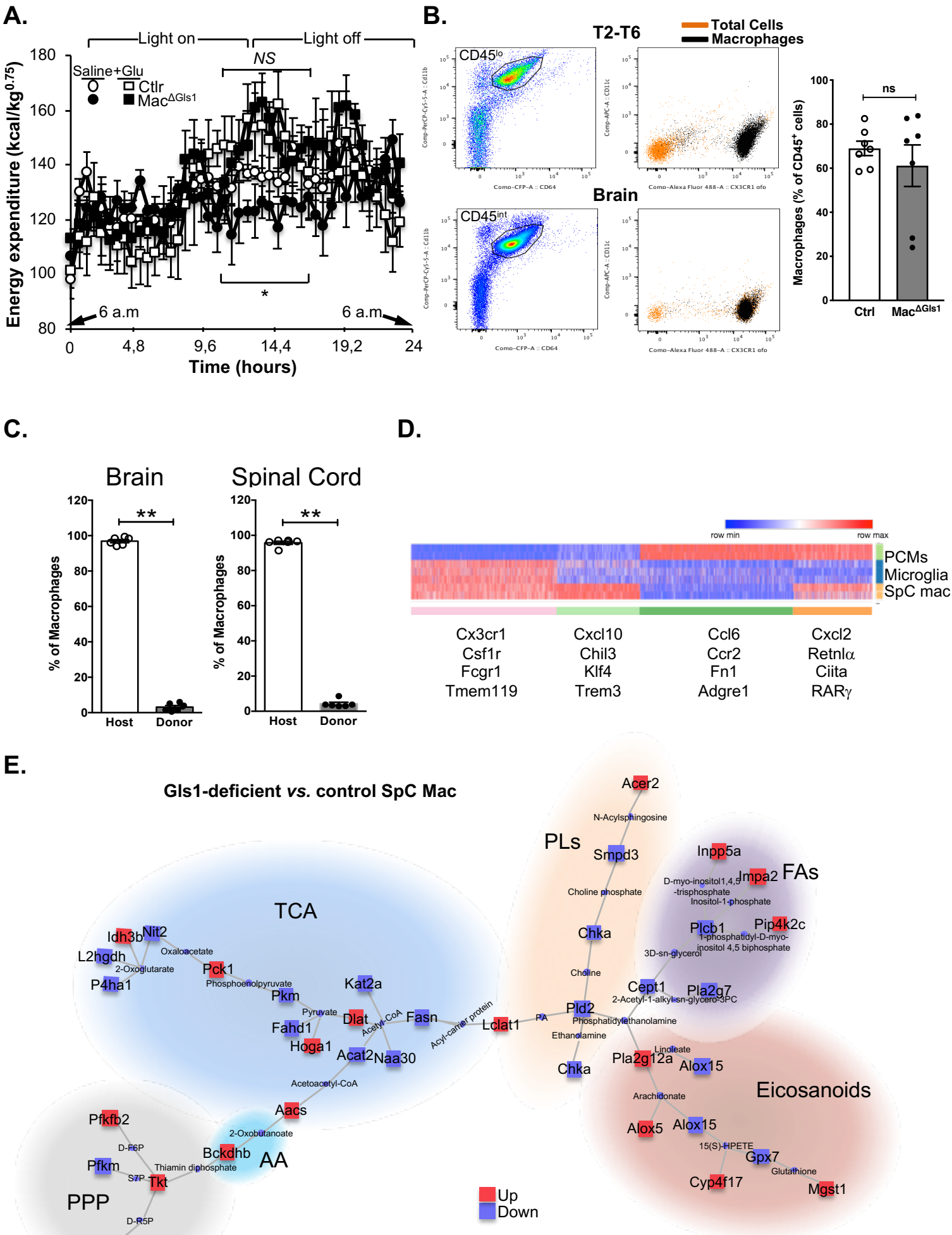

Supplemental Figure 4

F.

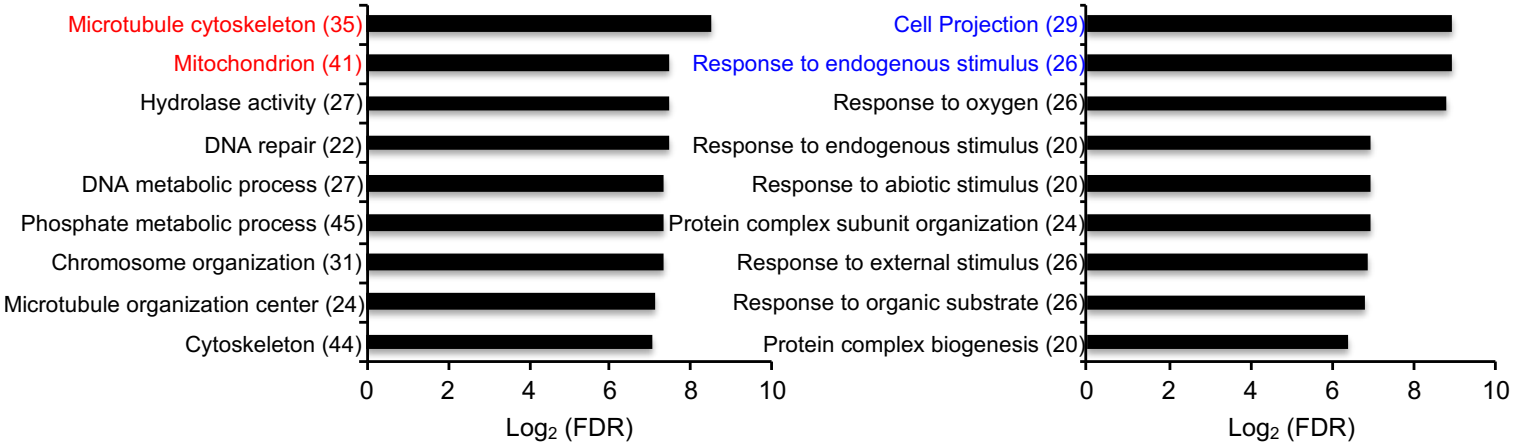

G.

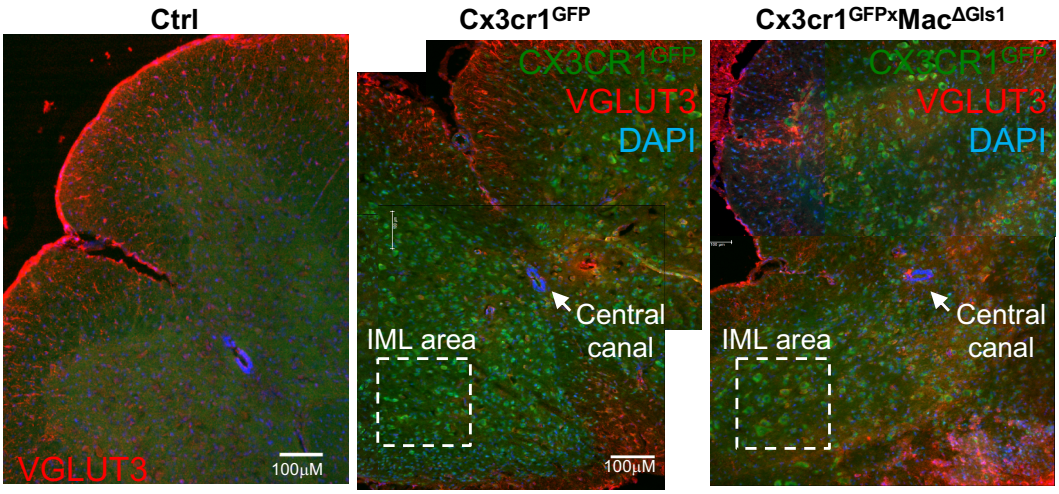

Figure S4. Characterization of Gls1-deficient spinal cord macrophages. (A) Effect of glutamate supplementation on whole-body energy expenditure measured by indirect calorimetry in control and Mac$^{\Delta Gls1}$ mice. **(B)** Gating strategy of brain microglia and spinal cord macrophages by flow cytometry. **(C)** Repopulation experiment after CX3CR1$^{gfp/+}$ (CD45.1) bone marrow transplantation into lethally irradiated CD45.2 control recipients and quantification of the percentage of repopulating microglia (left) and spinal cord macrophages (right) by flow cytometry. **(D)** K-means clustering of genes associated with PCMs, microglia and spinal cord macrophages from RNA-seq dataset of control mice. **(E)** Metabolic pathway analysis from RNAseq data of control and Mac$^{\Delta Gls1}$ spinal cord macrophages using CoMBI-T topological tool. **(F)** Functional annotation enrichment analysis for GO terms from RNAseq analysis of control and Gls1-deficient spinal cord macrophages (upregulated pathway in left panel and downregulated pathway in right panel). **(G)** Confocal microscopy of spinal cord isolated from CX3CR1$^{gfp/+}$ or CX3CR1$^{gfp/+}$ Mac$^{\Delta Gls1}$ mice counterstained with VGLUT3 (spinal cord neuron staining) antibody and DAPI (nuclear staining). All values are means ± SEM and are representative of an experiment of five to seven animals per group. **, *P*<0.005 versus control.

Acknowledgments. We thank Dr Fréderic Labret for assistance with flow cytometry, Dr Véronique Corcelle and her team for assistance in animal facilities and Dr. Marie Irondelle for assistance with confocal microscopy (C3M Imaging Core Facility funded by the Conseil Général Alpes-Maritimes and Région PACA, which belongs to the IBISA Microscopy and Imaging platform Côte d'Azur (MICA). C3M biochemical and Seahorse analyzers were co-funded by the Conseil Général Alpes-Maritimes and Région PACA.

Financial support and sponsorship. This work was supported by grants from the Fondation de France (FDF), the National Agency for Research (ANR) and the European Research Council (ERC) consolidator program (ERC2016COG724838) to L.Y.C.

Disclosures. The authors have declared that no conflict of interest exists.

Author contributions.
L.Y.C conceived the project, designed the experiments and wrote the manuscript. J.M. and S.I. designed the experiments and performed most of the molecular, histological or *in vivo* experiments. M.A., N.V., J.G., K.D., M.O., R.G. helped with experimental design and assisted with data analysis. A.S. and M.N.A helped with bioinformatic data analysis. J.M., I.G.S., and S.R., provided tool materials for *in vivo* studies. M.C., J.F.T., D.B.R., E.L.G., R.G., and M.N.A provided scientific advice and helped with experimental design. L.Y.C. also designed and supervised the study and obtained funding. All authors read, edited, and approved the manuscript.

STAR Methods

Lead Contact and Materials Availability

Lead contact. Further information and requests for resources and reagents should be directed to and will be fulfilled by the Lead Contact, Dr. Laurent Yvan-Charvet (yvancharvet@unice.fr).

Experimental model and subject details

Mice. $Gls1^{fl/fl}$ mice were kindly provided by Pr. Stephen Rayport's lab and have been crossed to $Lyz2^{Cre}$ mice (B6.129P2-Lyz2tm1(cre)Ifo/J, The Jackson Laboratory) and $CX3CR1^{gfp}$ [B6.129P-$Cx3cr1^{tm1Litt}$/J, The Jackson Laboratory) mice. For each experiment, co-housed littermate controls were used. Animal protocols were approved by the Institutional Animal Care and Use Committee of the French Ministry of Higher Education and Research and the Mediterranean Center of Molecular Medicine (Inserm U1065) and were undertaken in accordance with the European Guidelines for Care and Use of Experimental Animals. Animals had free access to food and water and were housed in a controlled environment with a 12-hour light–dark cycle and constant temperature (22°C). Obesity was induced by feeding the mice with a Western diet (TD88137, Ssniff) for 12 weeks. Mice were weighted every two weeks following Western diet induction.

Peritoneal cavity macrophage (PCM) culture. Resident PCMs were obtained by PBS lavage of the peritoneal cavity and macrophages were enriched by 2hour incubation in 96-well flat bottom plates. Cells were then washed 3 times and adherent cells were cultured overnight in complete RPMI 1640 medium (Corning) containing 10mM glucose, 2mM L-glutamine, 100U/ml penicillin/streptomycin, and 10% FBS at 37°C and 5% CO2.

Sympathetic neuron-associated macrophage (SAM) culture. Subcutaneous fascia was carefully excised and digested with collagenase A (1,5mg/ml) for 30minutes. Red blood cells were then lysed, and macrophages enriched by 2hour incubation in 96-well flat bottom plates. Cells were then washed 3 times and adherent cells were cultured overnight in complete RPMI 1640 medium (Corning) containing 10mM glucose, 2mM L-glutamine, 100U/ml penicillin/streptomycin, and 10% FBS at 37°C and 5% CO2.

Brain dissection and cortical neuron dissociation. As previously published (Marcuzzo et al., 2019), whole brains were extracted from P18 mouse embryos and placed in a dissociation medium containing 134 mM Na-isethionate, 2 mM KCl, 8 mM MgCl, 100 µM CaCl2, 23 mM D-glucose, 15 mM Hepes and 1 mM kynurenic acid, pH 7.2. Working with tweezers under a dissection microscope, the hemispheres were carefully separated; the cerebellum, septum, thalamus and hypothalamus were separated from the cortex, followed by the meninges and hippocampus. The cortices were cut into 1-mm3 pieces, digested in XIV protease for 20 min at 37 °C by gentle agitation, and washed with dissociation medium at room temperature three times. The pieces were subsequently mechanically homogenized using fire-polished Pasteur pipettes having three decreasing diameter sizes, and the resulting supernatant containing neurons was collected into a new tube (Hilgenberg and Smith, 2007, Cestèle et al., 2008). The neurons were maintained in a culture medium containing Neurobasal A, 0.5% glutamax, 0.5% penicillin/streptomycin, 2% B27, 10 µg/ml fibroblast growth factor (Thermo Fisher Scientific Inc., Foster City MA, USA) until 28 DIV.

Method details

Mice and treatments. For the glutamate supplementation experiment, mice were *i.p.* injected with 50mg/Kg for 12 consecutive days. For the chemical denervation experiment, mice were subcutaneously injected every 2 days for a week with 10mg/mL of 6-hydroxydopamine (6-OHDA).

Bone marrow transplantation. Bone marrow transplantation was performed as previously described (Gautier et al., 2013). Briefly, WT (CD45.2) and Cx3cr1^{GFP} (CD45.1) were lethally irradiated 16h before transplantation. Then, WT recipient mice were *i.v.* injected with BM from Cx3cr1^{GFP} mice and Cx3cr1^{GFP} recipients were *i.v.* injected with BM from WT mice. Mice were then allowed to recover for five weeks before sacrifice and analysis.

Calorimetry. *In vivo* indirect open circuit calorimetry was performed in metabolic chambers using the Labmaster system (TSE-Systems, Bad Homburg, Germany). The 12-week-old animals were randomly and alternatively placed into experimental chambers at 25°C ± 1 with free access to food and water. Constant airflow (0.5 l/min) was drawn through the chamber and monitored by a mass-sensitive flowmeter. To calculate oxygen consumption (VO_2), carbon dioxide production (VCO_2), and respiratory quotient (RQ: ratio of VCO_2 to VO_2), gas concentrations were monitored at the inlet and outlet of the scaled chambers. Data were collected after 24 hours of adaptation in acclimated singly housed mice. Total metabolic rate (energy expenditure) was calculated from oxygen consumption and carbon dioxide production using Lusk's equation and expressed as watts per kilogram to the 0.75 power of body weight. Glucose, lipid oxidation and heat production were calculated as previously described (Gautier et al., 2013)(Wolf et al., 2017).

Glucose Tolerance Test. Mice were fasted for 6 hours and then injected i.p. with D-Glucose (2g/kg of body weight). Blood samples were collected at different times by tail bleeding after injection (Gautier et al., 2013). Blood glucose was measured with Optium Xceed Glucometer (Abbott). Graphical representations were generated using GraphPad Prism 7 and the area under the curve for each animal was calculated. Blood samples were also collected at time 0 and 20 minutes to determine serum insulin levels using Insulin Mouse Serum Assay kit (Cisbio, PerkinElmer) according to the manufacturer's instructions.

Homeostasis Model Assessment of Insulin Restistance scores. The homeostasis model assessment of insulin resistance (HOMA-IR) scores were calculated from glucose and insulin concentrations obtained from mice after 6 h of fasting. The following equation was used: fasting insulin (ng/mL) x fasting blood glucose (mg/dL)/405.

***In vivo* 2-[^{14}C]-DG uptake.** Uptake of 2-[^{14}C]-DG in peripheral tissues was measured as previously described (Gautier et al., 2013). In brief, 2 µCi 2-[^{14}C]-DG was *i.v.* injected, and blood samples were collected at 5, 10, 20, 30, and 40 min. Blood glucose was monitored through the study period with a glucometer (Roche). After 40 min, brain, skeletal muscle, pancreas and adipose tissues were rapidly dissected, weighed, and homogenized with 5% $HClO_4$ solution. The radioactivity incorporated in both 2-[^{14}C]-DG and its 6-phosphate derivative was measured in the $HClO_4$ extract and expressed as total radioactivity per tissue weight. The rate constant of net tissue uptake of 2-[^{14}C]-DG was also calculated. In brief, the relative glucose uptake was calculated by dividing the area under the blood 2-[^{14}C]-DG disappearance curve (cpm/min/ml) to the steady-state glucose concentration (mM) multiplied by the tissue 2-[^{14}C]-DG (cpm/g tissue or cpm/10^6 cells for the BM) at 40 min.

Western Blotting. BM cells were harvested from mouse femur and tibia and differentiated in the presence of recombinant mouse M-CSF (20 ng/ml; Miltenyi) in complete RPMI 1640 medium (Corning) containing 10mM glucose, 2mM L-glutamine, 100U/ml of penicillin/streptomycin, and 10% FBS for 7 days at 37°C and 5% CO2. Cells were then lysed

in RIPA buffer containing protease inhibitors cocktail (ThermoFisher) and agitated for 1 hour at 4°C before centrifugation at 14000 rpm for 10min at 4°C. Supernatants were sampled and later used for SDS-PAGE. Protein content was evaluated using Pierce™ BCA assay kit (ThermoFisher). Protein samples were resolved on 10% SDS-PAGE gels and were then transferred onto polyvinylidene difluoride membrane using a wet transfer system. Membranes were blocked in 5% (w/v) BSA in Tris-buffered saline-Tween for one hour at room temperature. Membranes were then incubated with primary antibody (anti-cFos antibody (Abcam), anti Phospho-Akt antibody (Cell Signaling Technology) or anti-Akt antibody (Cell Signaling Technology)) followed by the appropriate horseradish peroxidase-conjugated secondary antibody. Anti α-actin mAb (Santa Cruz) was used as loading control. Proteins were detected by substrate HRP (Sigma).

Plasma biochemical parameters. Plasma multi-analyte profiling was performed using a clinical chemistry analyzer (Mindray BS-240 Pro, BioSentec) with the following colorimetric kits: NEFA-HR2 (Fujifilm Wako), triglycerides Reagent (Sigma) and alanine aminotransferase (ALT-0102) and aspartate aminotransferase (AST-0102), all from Biosentec.

Glutamine and glutamate measurements. Tissues were harvested and mechanically disrupted with mammalian ringer buffer solution (Electron Microscopy Sciences). Glutamine and glutamate concentrations were measured using YSI 2050 Biochemistry analyzer. To analyze glutamine and glutamate media content we used a commercially available Glutamine/Glutamate-GloTM Assay (Promega) in accordance with the manufacturer's instructions.

Norepinephrine measurement. Tissues were harvested and mechanically disrupted with mammalian ringer buffer solution (Electron Microscopy Sciences). Norepinephrine concentration was measured using Norepinephrine ELISA Kit (abnova) according to the manufacturer's instructions.

Norepinephrine degradation assay. Sympathetic neuron-associated macrophages **(**SAMs) were cell-sorted from subcutaneous fascia and incubated overnight with the following treatments: Norepinephrine (2µM, Abcam), Chlorgyline (100µM, Abcam). After an overnight incubation period, media were collected, and NE levels were quantified.

Macrophage-Neuron co-culture. We cultured primary neocortical neurons from P18 wild-type embryos, which are enriched in glutamatergic neurons (see above for the method). After 2 weeks of culture, neurons were co-cultured for 16h with PCMs or cell-sorted spinal cord macrophages (see below for the method) in neuron culture medium. The medium was then collected for glutamate quantification, a surrogate of glutamatergic neuron activation. Cells were then washed with PBS and fixed in 4% paraformaldehyde. F-actin was stained overnight at 4°C with Texas Red-X Phalloidin (ThermoScinetific) to visualize cell structure and anti-CD11b APC conjugated (Biolegend) to determine macrophage shape. Digitized images were analyzed with ImageJ and data were expressed as a ratio of fusiform/rounded cells.

Histology. Mice were sacrificed and tissues (epididymal, subcutaneous, brown adipose tissues and liver) were excised and fixed in 4% paraformaldehyde. The tissues were later embedded in paraffin. 6 µm sections were performed using a HM340E microtome (Microm Microtech, Francheville France) and stained with H&E as previously described (Gautier et al., 2013).
- For immunofluorescence, spinal cords were fixed in 4% paraformaldehyde 30% sucrose for 48h and embedded in OCT before sectioning by cryostat. Samples were blocked 30min at room temperature with PBS containing 1% BSA and FC block before incubation with PBS containing 0.2% BSA. Then samples were incubated with either anti-VGLUT3 (Biolegend,

clone 2B9) overnight at 4°C. Next, samples were incubated with secondary antibody (Jackson Immuno Research, anti-mouse IgG Cy5 conjugated) in PBS at RT for 2 hours.
- For immunohistochemistry in paraffin embedded sections: paraffin sections of brown adipose tissue were de-paraffinized and rehydrated by washes in 100% xylene, 100% ethanol, 95% ethanol, 70% ethanol, 50% ethanol, water and then washed in phosphate-buffered saline (PBS). Heat-induced antigen retrieval of sections was carried out IHC Antigen retrieval solution (eBiosciences) and then washed in PBS. Sections were then blocked for 1 hour in blocking buffer (1% BSA, 1% Tween, in PBS), then incubated with anti-Tyrosine hydroxylase alexa fluor 488 conjugated antibody (Abcam) diluted in antibody dilution buffer (1% BSA, 1% Tween, in PBS) overnight at 4°C. Slides were then washed thoroughly and coverslips were mounted with aqueous glue. Sections were observed the following day by fluorescent microscopy.

Adipose tissue cellularity. Cellularity of WAT was determined as previously described (Gautier et al., 2013). Briefly, images of sectionned adipocytes were acquired from a light microscope fitted with a camera, and the measurement of ~400 cell diameters was performed allowing calculation of a mean fat cell weight using the MotionTracking Software (Generous gift from the Zerial Lab MPI-CGB, Dresden, Germany).

Muscle type II fibre type. For tibialis anterior muscle fibre type analysis, sections were immunostained with anti-type II myosin heavy chain (MyHC) monoclonal antibodies (SC-71, 2F7, MHCIIb (BF-F3), Developmental studies hybridoma bank) at 1:500 dilution. The percentage of type II (fast) MyHC fibres were counted per section using Imaris software.

Flow cytometry analysis. Tissues were collected, weighted, shredded with scissors and then incubated for 30 minutes with HBSS medium containing 1.5 mg/ml collagenase A (for adipose tissues) or collagenase D (Roche Diagnostics) at 30°C. The resulting suspension was lysed (BD PharmLyse), centrifuged (400g, 5min at 4°C) and stained for 25 min protected from light. For flow cytometry analysis the following list of antibodies was used: CD45 APC-Cy7 conjugated (clone 30-F11, BD Biosciences), CD64 Brilliant Violet 421 conjugated (clone X54-5/7.1, BioLegend), F4/80 PeCy7 conjugated (clone BM8, BioLegend), CD206 PerCp-Cy5.5 conjugated (clone C068C2, BioLegend), CD301 FITC conjugated (clone ER-MP23, Bio-Rad), Mertk PE conjugated (clone 2B10C42, BioLegend). Cells were then washed, centrifuged and data were acquired on BDFACSCanto flow cytometer. Analysis was performed using FlowJo software (Tree Star).

RNA seq of cell sorted macrophages. After peritoneal lavage with PBS, cells were stained with CD64 Brilliant Violet 421 conjugated (clone X54-5/7.1), ICAM-2 APC conjugated (clone 3C4(MIC2/4)) and CD115 PE conjugated (clone AFS98). These antibodies allowed us to cell-sort the major subset of ICAM2^{+} PCMs (Gautier et al., 2012; Kim et al., 2016). Brain and spinal cord macrophages were purified following tissue digestion with 1.5mg/mL collagenase D in HBSS for 30min at 37°C. Then cells were washed and resuspended in 35% Percoll (Sigma). This solution was gently applied over 70% Percoll and centrifuged for 20min at 2000rpm (room temperature). The middle ring was collected and stained with CD11b Brillant violet 510 conjugated (clone M1/70, BioLegend), CD64 Brilliant Violet 421 conjugated (clone X54-5/7.1, BioLegend), CD45 APC-Cy7 conjugated (clone 30-F11, BD Biosciences), MerTK PE conjugated (clone 2B10C42, BioLegend). Cells were cell sorted on BD FacsAria flow cytometer. Total RNA was extracted with RNeasy Mini Kit (Qiagen) according to the manufacturer's protocol and quality was assessed by Nanodrop (Ozyme). Library construction were conducted as described previously (Jha et al., 2015). Libraries were sequenced at the Centre for Applied Genomics (SickKids, Toronto) using a HiSeq 2500 (Illumina).

Integrated network analyses. PCA analysis, k-means clustering, and volcano plot were performed with Phantasus software (Jha et al., 2015). Significant up and down regulated genes were based on p values and fold change calculated with Phantasus. Network-based integration of metabolite and gene expression datasets was conducted using Shiny Gam as previously described (Jha et al., 2015).

RNA analysis. Total RNA was isolated using the RNeasy Plus Mini kit (QIAGEN) and quantified using a Nanodrop (Ozyme). cDNA was prepared using 10 ng/µl total RNA by a RT-PCR using a high capacity cDNA reverse transcription kit (Applied Biosystems), according to the manufacturer's instructions. Real-time qPCR was performed on cDNA using SYBR Green on StepOne device from Applied Biosystem (France). GAPDH gene expression was used to account for variability in the initial quantities of mRNA. Details on the primers used can be found in Table below.

	Sequences of PCR primers	
	Left (5' to 3')	**Right (5' to 3')**
Adrb3	CAG CCA GCC CTG TTG AAG	CCT TCA TAG CCA TCA AAC CTG
Agrp	AAG CTT TGG CGG AGG TGC TAG AT	AAG CAG GAC TCG TGC AGC CTT ACA
CCL2	CAT CCA CGT GTT GGC TCA	GAT CAT CTT GCT GGT GAA TGA GT
CD68	GAC CTA CAT CAG AGC CCG AGT	CGC CAT GAA TGT CCA CTG
Cidea	TTC AAG GCC GTG TTA AGG A	CCT TTG GTG CTA GGC TTG G
Clec10a	AAA ACC CAA GAG CCT GGT AAA	AGG TGG GTC CAA GAG AGG AT
Dio2	CTG CGC TGT GTC TGG AAC	GGA GCA TCT TCA CCC AGT TT
hmox1	AGG GTC AGG TGT CCA GAG AA	CTT CCA GGG CCG TGT AGA TA
IL1 beta	CAA CCA ACA AGT GAT ATT CTC CAT G	GAT CCA CAC TCT CCA GCT GCA
IL6	GCT ACC AAA CTG GAT ATA ATC AGG A	CCA GGT AGC TAT GGT ACT CCA GAA
Integrin alpha 4 (CD49d)	ACT CCC CAC AGG CCT TTA TT	TCA GTC ACT TCG CAG TTT ATT TG
Maoa	CGG ATA TTC TCA GTC ACC AAT G	ATT TGG CCA GAG CCA CCT A
Mecp2	GAC CAG CTC CAA CAG GAT TC	CCC TGG AGA TCC TGG TCT T
Mrc1	CCA CAG CAT TGA GGA GTT TG	ACA GCT CAT CAT TTG GCT CA
NPY	CCG CTC TGC GAC ACT ACA T	TGT CTC AGG GCT GGA TCT CT
Plxna4	CAG CAA TGT TGT GGT GAT GTT	TAG GAT GGA GAG CGC CTG T
pomc	AGT GCC AGG ACC TCA CCA	CAG CGA GAG GTC GAG TTT G
Ppargc1alpha	TGA AAG GGC CAA ACA GAG AG	GTA AAT CAC ACG CGC TCT T
Prdm16	ACA GGC AGG CTA AGA ACC AG	CGT GGA GAG GAG TGT CTT CAG
Pth2R	CTC TGG CTG ATG CGA GGT	CTG CTA AGA TCG GTG CTT GA
Retnl alpha	CCC TCC ACT GTA ACG AAG ACT C	CAC ACC CAG TAG CAG TCA TCC
Sema6a	CCA GAC GAA CGA GTC CCT AA	TTC TAA AGA GGA TGA TCC AGC AC
Slc6a2	GCG GTT CCC TTA TCT CTG CT	CAG CGT GTA TGG AAT CAG GA
Tyrosine hydroxylase	CCC AAG GGC TTC AGA AGA G	GGG CAT CCT CGA TGA GAC T
TNF alpha	CAC AAG ATG CTG GGA CAG TGA	TCC TTG ATG GTG CAT GA
Ucp1	GGC CTC TAC GAC TCA GTC CA	TAA GCC GGC TGA GAT TCT TGT
Vcam1	TCT TAC CTG TGC GCT GTG AC	ACT GGA TCT TCA GGG AAT GAG T

Quantification and statistical analysis

Statistical analysis.
Data are expressed as mean+/- SEM. Statistical analysis was performed using a 2-tailed t test or ANOVA (with Tukey's post-test analysis) with GraphPad Prism software. A P value ≤ 0.05 was considered as statistically significant.

Data and Code availability. The datasets supporting the current study have not been deposited in a public repository because of a pending patent at the time of submission but are available from the corresponding author on request.

Key resources table

REAGENT or RESOURCE	SOURCE	IDENTIFIER
Antibodies		
Akt (C67E7)	Cell Signaling Technology	4691 RRID:AB_915783
CD115 PE (clone AFS98)	eBioscience	12-1152-82 RRID:AB_465808
CD11b APC (Clone M1/70)	Biolegend	101212 RRID:AB_312795
CD11b Brilliant Violet 510 (cloneM1/70)	Biolegend	101263
CD206 PerCp-Cy5.5 (clone C068C2)	Biolegend	141715
CD301 FITC (clone ER-MP23)	Bio-Rad	MCA2392
CD45 APC-Cy7 (clone 30-F11)	BD Biosciences	557659 RRID:AB_396774
CD64 Brillant Violet 421 (clone X54-5/7.1)	Biolegend	139309 RRID:AB_2562694
c-FOS	Abcam	ab190289 RRID:AB_2737414
F4/80 PE-Cy7 (clone BM8)	Biolegend	123114 RRID:AB_893478
ICAM-2 alexa fluor 647 (clone 3C4(MIC2/4))	Biolegend	105612 RRID:AB_2658040
IgG-Cy5	Jackson Immuno research	715-175-150 RRID:AB_2340819
MerTK PE (clone 2B10C42)	Biolegend	151506 RRID:AB_2617037
Myosin Heavy Chain Type IIA (SC71)	Developmental studies hybridoma bank	SC-71 RRID:AB_2147165
Myosin Heavy Chain Type IIB (BF-F3)	Developmental studies hybridoma bank	BF-F3 RRID:AB_2266724
Phospho-Akt (Ser473)	Cell Signaling Technology	4060 RRID:AB_2315049
Texas Red™-X Phalloidin	Thermofisher	T7471 RRID:AB_2828017.
Tyrosine Hydroxylase	Millipore	AB152 RRID:AB_390204
VGLUT3 (clone 2B9)	Sigma	Discontinued
Chemicals, Peptides, and Recombinant Proteins		
2-Deoxy-D-glucose	Sigma	D6134
6-OHDA	Sigma	162957
B-27 Supplement	Invitrogen	17504-044
bFGF Protein	R&D Biosystems	3139-FB-025
Bovine serum Albumin (BSA)	Sigma	A7030
Bovine serum Albumin (BSA) for neuron culture	Sigma	A8806
Clorgyline	Abcam	ab145646
Collagenase A	Sigma	11088793001
Collagenase D	Sigma	11088882001
D-Glucose	Sigma	G7021

DAPI	Sigma	D9542
Fetal bovine serum	Fisher Scientific	12350273
GlutaMAX-1	Invitrogen,	35050-038
HBSS	Fisher Scientific	14175053
L-Glutamic acid	Sigma	G1251
L-Glutamine	Thermofischer	25030024
Neurobasal-A Medium	Invitrogen	10888-022
PBS 1X	Fisher Scientific	14190169
Penicillin-Streptomycin	Fisher Scientific	15140130
Percoll	Sigma	P1644
PFA 4%	VWR International	9713.1000
Poly-D-Lysine Hydrobromide	Dutscher	354210
Protease from Streptomyces griseus (type XIV)	Sigma	P5147
RPMI medium	Fisher Scientific	31870074
Critical Commercial Assays		
ALT reagent	Biosentec	ALT0102
AST reagent	Biosentec	AST0102
BUN reagent	Biosentec	N.A.
Glutamine/Glutamate-Glo™ Assay	Promega	J8022
High-Capacity cDNA reverse transcription kit	Applied Biosystems	4368814
Insulin Mouse Serum Assay kit	Cisbio	62IN3-PEF
NEFA assay	Fujifilm WAKO	W1W436-91995
Norepinephrine ELISA Kit	Abnova	157KA1891
RNeasy Plus Mini Kit (250)	QIAGEN	74136
Triglycerides assay	Diasys	1 5710 99 10021
Uric Acid Reagent	Biosentec	UA-0102
Deposited Data		
RNAseq	NCBI GEO	GEO: GSE to complete
Experimental Models: Organisms/Strains		
Mouse: CX_3CR1^{GFP}	Jackson Laboratory	005582 RRID:IMSR_JAX:005582
Mouse: Gls1fl/fl	Pr. Stephen Rayport's lab	N.A.
Mouse: $LyzM^{cre}$	Jackson Laboratory	004781 RRID:IMSR_JAX:004781
Oligonucleotides		
See **Table in Method details**		
Software and Algorithms		
FlowJo	Tree Star	N.A.
ImageJ	NIH	N.A.
Phantasus	http://genome.ifmo.ru/phantasus/	N.A.
Prism8	GraphPad	N.A.
StepOne Software v.2.2.2	Applied Biosystem	N.A.
Other		
High Fat Diet	Ssniff	TD88137

References

Artyomov, M.N., A. Sergushichev, and J.D. Schilling. 2016. Integrating immunometabolism and macrophage diversity. *Semin Immunol* 28:417-424.

Boutens, L., G.J. Hooiveld, S. Dhingra, R.A. Cramer, M.G. Netea, and R. Stienstra. 2018. Unique metabolic activation of adipose tissue macrophages in obesity promotes inflammatory responses. *Diabetologia* 61:942-953.

Camell, C.D., J. Sander, O. Spadaro, A. Lee, K.Y. Nguyen, A. Wing, E.L. Goldberg, Y.H. Youm, C.W. Brown, J. Elsworth, M.S. Rodeheffer, J.L. Schultze, and V.D. Dixit. 2017. Inflammasome-driven catecholamine catabolism in macrophages blunts lipolysis during ageing. *Nature* 550:119-123.

Cannon, B., and J. Nedergaard. 2004. Brown adipose tissue: function and physiological significance. *Physiol Rev* 84:277-359.

Cao, Q., J. Jing, X. Cui, H. Shi, and B. Xue. 2019. Sympathetic nerve innervation is required for beigeing in white fat. *Physiol Rep* 7:e14031.

Chechi, K., A.C. Carpentier, and D. Richard. 2013. Understanding the brown adipocyte as a contributor to energy homeostasis. *Trends Endocrinol Metab* 24:408-420.

Choi, M.S., Y.J. Kim, E.Y. Kwon, J.Y. Ryoo, S.R. Kim, and U.J. Jung. 2015. High-fat diet decreases energy expenditure and expression of genes controlling lipid metabolism, mitochondrial function and skeletal system development in the adipose tissue, along with increased expression of extracellular matrix remodelling- and inflammation-related genes. *Br J Nutr* 113:867-877.

Crotti, A., and R.M. Ransohoff. 2016. Microglial Physiology and Pathophysiology: Insights from Genome-wide Transcriptional Profiling. *Immunity* 44:505-515.

Davies, L.C., C.M. Rice, E.M. Palmieri, P.R. Taylor, D.B. Kuhns, and D.W. McVicar. 2017. Peritoneal tissue-resident macrophages are metabolically poised to engage microbes using tissue-niche fuels. *Nat Commun* 8:2074.

Ducuing, H., T. Gardette, A. Pignata, S. Tauszig-Delamasure, and V. Castellani. 2019. Commissural axon navigation in the spinal cord: A repertoire of repulsive forces is in command. *Semin Cell Dev Biol* 85:3-12.

Fischer, K., H.H. Ruiz, K. Jhun, B. Finan, D.J. Oberlin, V. van der Heide, A.V. Kalinovich, N. Petrovic, Y. Wolf, C. Clemmensen, A.C. Shin, S. Divanovic, F. Brombacher, E. Glasmacher, S. Keipert, M. Jastroch, J. Nagler, K.W. Schramm, D. Medrikova, G. Collden, S.C. Woods, S. Herzig, D. Homann, S. Jung, J. Nedergaard, B. Cannon, M.H. Tschop, T.D. Muller, and C. Buettner. 2017. Alternatively activated macrophages do not synthesize catecholamines or contribute to adipose tissue adaptive thermogenesis. *Nat Med* 23:623-630.

Fitzgibbons, T.P., S. Kogan, M. Aouadi, G.M. Hendricks, J. Straubhaar, and M.P. Czech. 2011. Similarity of mouse perivascular and brown adipose tissues and their resistance to diet-induced inflammation. *Am J Physiol Heart Circ Physiol* 301:H1425-1437.

Gautier, E.L., T. Shay, J. Miller, M. Greter, C. Jakubzick, S. Ivanov, J. Helft, A. Chow, K.G. Elpek, S. Gordonov, A.R. Mazloom, A. Ma'ayan, W.J. Chua, T.H. Hansen, S.J. Turley, M. Merad, G.J. Randolph, and C. Immunological Genome. 2012. Gene-expression profiles and transcriptional regulatory pathways that underlie the identity and diversity of mouse tissue macrophages. *Nat Immunol* 13:1118-1128.

Glass, C.K., and J.M. Olefsky. 2012. Inflammation and lipid signaling in the etiology of insulin resistance. *Cell Metab* 15:635-645.

Goldmann, T., P. Wieghofer, M.J. Jordao, F. Prutek, N. Hagemeyer, K. Frenzel, L. Amann, O. Staszewski, K. Kierdorf, M. Krueger, G. Locatelli, H. Hochgerner, R. Zeiser, S. Epelman, F. Geissmann, J. Priller, F.M. Rossi, I. Bechmann, M. Kerschensteiner, S. Linnarsson, S. Jung, and M. Prinz. 2016. Origin, fate and dynamics of macrophages at central nervous system interfaces. *Nat Immunol* 17:797-805.

Gosselin, D., V.M. Link, C.E. Romanoski, G.J. Fonseca, D.Z. Eichenfield, N.J. Spann, J.D. Stender, H.B. Chun, H. Garner, F. Geissmann, and C.K. Glass. 2014. Environment drives selection and function of enhancers controlling tissue-specific macrophage identities. *Cell* 159:1327-1340.

Huang, S.C., B. Everts, Y. Ivanova, D. O'Sullivan, M. Nascimento, A.M. Smith, W. Beatty, L. Love-Gregory, W.Y. Lam, C.M. O'Neill, C. Yan, H. Du, N.A. Abumrad, J.F. Urban, Jr., M.N. Artyomov, E.L. Pearce, and E.J. Pearce. 2014. Cell-intrinsic lysosomal lipolysis is essential for alternative activation of macrophages. *Nat Immunol* 15:846-855.
Ivanov, S., J. Merlin, M.K.S. Lee, A.J. Murphy, and R.R. Guinamard. 2018. Biology and function of adipose tissue macrophages, dendritic cells and B cells. *Atherosclerosis* 271:102-110.
Jaitin, D.A., L. Adlung, C.A. Thaiss, A. Weiner, B. Li, H. Descamps, P. Lundgren, C. Bleriot, Z. Liu, A. Deczkowska, H. Keren-Shaul, E. David, N. Zmora, S.M. Eldar, N. Lubezky, O. Shibolet, D.A. Hill, M.A. Lazar, M. Colonna, F. Ginhoux, H. Shapiro, E. Elinav, and I. Amit. 2019. Lipid-Associated Macrophages Control Metabolic Homeostasis in a Trem2-Dependent Manner. *Cell*
Jha, A.K., S.C. Huang, A. Sergushichev, V. Lampropoulou, Y. Ivanova, E. Loginicheva, K. Chmielewski, K.M. Stewart, J. Ashall, B. Everts, E.J. Pearce, E.M. Driggers, and M.N. Artyomov. 2015. Network integration of parallel metabolic and transcriptional data reveals metabolic modules that regulate macrophage polarization. *Immunity* 42:419-430.
Kajimura, S., B.M. Spiegelman, and P. Seale. 2015. Brown and Beige Fat: Physiological Roles beyond Heat Generation. *Cell Metab* 22:546-559.
Kim, K.W., J.W. Williams, Y.T. Wang, S. Ivanov, S. Gilfillan, M. Colonna, H.W. Virgin, E.L. Gautier, and G.J. Randolph. 2016. MHC II+ resident peritoneal and pleural macrophages rely on IRF4 for development from circulating monocytes. *J Exp Med* 213:1951-1959.
Kratz, M., B.R. Coats, K.B. Hisert, D. Hagman, V. Mutskov, E. Peris, K.Q. Schoenfelt, J.N. Kuzma, I. Larson, P.S. Billing, R.W. Landerholm, M. Crouthamel, D. Gozal, S. Hwang, P.K. Singh, and L. Becker. 2014. Metabolic dysfunction drives a mechanistically distinct proinflammatory phenotype in adipose tissue macrophages. *Cell Metab* 20:614-625.
Lavin, Y., D. Winter, R. Blecher-Gonen, E. David, H. Keren-Shaul, M. Merad, S. Jung, and I. Amit. 2014. Tissue-resident macrophage enhancer landscapes are shaped by the local microenvironment. *Cell* 159:1312-1326.
Liu, P.S., H. Wang, X. Li, T. Chao, T. Teav, S. Christen, G. Di Conza, W.C. Cheng, C.H. Chou, M. Vavakova, C. Muret, K. Debackere, M. Mazzone, H.D. Huang, S.M. Fendt, J. Ivanisevic, and P.C. Ho. 2017. alpha-ketoglutarate orchestrates macrophage activation through metabolic and epigenetic reprogramming. *Nat Immunol* 18:985-994.
Lumeng, C.N., J.L. Bodzin, and A.R. Saltiel. 2007. Obesity induces a phenotypic switch in adipose tissue macrophage polarization. *J Clin Invest* 117:175-184.
Lumeng, C.N., J.B. DelProposto, D.J. Westcott, and A.R. Saltiel. 2008. Phenotypic switching of adipose tissue macrophages with obesity is generated by spatiotemporal differences in macrophage subtypes. *Diabetes* 57:3239-3246.
McNelis, J.C., and J.M. Olefsky. 2014. Macrophages, immunity, and metabolic disease. *Immunity* 41:36-48.
Mills, E.L., B. Kelly, and L.A.J. O'Neill. 2017. Mitochondria are the powerhouses of immunity. *Nat Immunol* 18:488-498.
Morrison, S.F., and C.J. Madden. 2014. Central nervous system regulation of brown adipose tissue. *Compr Physiol* 4:1677-1713.
Muller, P.A., B. Koscso, G.M. Rajani, K. Stevanovic, M.L. Berres, D. Hashimoto, A. Mortha, M. Leboeuf, X.M. Li, D. Mucida, E.R. Stanley, S. Dahan, K.G. Margolis, M.D. Gershon, M. Merad, and M. Bogunovic. 2014. Crosstalk between muscularis macrophages and enteric neurons regulates gastrointestinal motility. *Cell* 158:300-313.
Murray, P.J., J.E. Allen, S.K. Biswas, E.A. Fisher, D.W. Gilroy, S. Goerdt, S. Gordon, J.A. Hamilton, L.B. Ivashkiv, T. Lawrence, M. Locati, A. Mantovani, F.O. Martinez, J.L. Mege, D.M. Mosser, G. Natoli, J.P. Saeij, J.L. Schultze, K.A. Shirey, A. Sica, J. Suttles, I. Udalova, J.A. van Ginderachter, S.N. Vogel, and T.A. Wynn. 2014. Macrophage activation and polarization: nomenclature and experimental guidelines. *Immunity* 41:14-20.
Nguyen, K.D., Y. Qiu, X. Cui, Y.P. Goh, J. Mwangi, T. David, L. Mukundan, F. Brombacher, R.M. Locksley, and A. Chawla. 2011. Alternatively activated macrophages produce catecholamines to sustain adaptive thermogenesis. *Nature* 480:104-108.

Nguyen, N.L., C.L. Barr, V. Ryu, Q. Cao, B. Xue, and T.J. Bartness. 2017. Separate and shared sympathetic outflow to white and brown fat coordinately regulates thermoregulation and beige adipocyte recruitment. *Am J Physiol Regul Integr Comp Physiol* 312:R132-R145.
Nguyen, N.L., J. Randall, B.W. Banfield, and T.J. Bartness. 2014. Central sympathetic innervations to visceral and subcutaneous white adipose tissue. *Am J Physiol Regul Integr Comp Physiol* 306:R375-386.
Nguyen, N.L.T., B. Xue, and T.J. Bartness. 2018. Sensory denervation of inguinal white fat modifies sympathetic outflow to white and brown fat in Siberian hamsters. *Physiol Behav* 190:28-33.
Odegaard, J.I., and A. Chawla. 2015. Type 2 responses at the interface between immunity and fat metabolism. *Curr Opin Immunol* 36:67-72.
Okabe, Y., and R. Medzhitov. 2014. Tissue-specific signals control reversible program of localization and functional polarization of macrophages. *Cell* 157:832-844.
Okabe, Y., and R. Medzhitov. 2016. Tissue biology perspective on macrophages. *Nat Immunol* 17:9-17.
Orava, J., P. Nuutila, M.E. Lidell, V. Oikonen, T. Noponen, T. Viljanen, M. Scheinin, M. Taittonen, T. Niemi, S. Enerback, and K.A. Virtanen. 2011. Different metabolic responses of human brown adipose tissue to activation by cold and insulin. *Cell Metab* 14:272-279.
Pirzgalska, R.M., E. Seixas, J.S. Seidman, V.M. Link, N.M. Sanchez, I. Mahu, R. Mendes, V. Gres, N. Kubasova, I. Morris, B.A. Arus, C.M. Larabee, M. Vasques, F. Tortosa, A.L. Sousa, S. Anandan, E. Tranfield, M.K. Hahn, M. Iannacone, N.J. Spann, C.K. Glass, and A.I. Domingos. 2017. Sympathetic neuron-associated macrophages contribute to obesity by importing and metabolizing norepinephrine. *Nat Med* 23:1309-1318.
Puleston, D.J., M. Villa, and E.L. Pearce. 2017. Ancillary Activity: Beyond Core Metabolism in Immune Cells. *Cell Metab* 26:131-141.
Qiu, Y., K.D. Nguyen, J.I. Odegaard, X. Cui, X. Tian, R.M. Locksley, R.D. Palmiter, and A. Chawla. 2014. Eosinophils and type 2 cytokine signaling in macrophages orchestrate development of functional beige fat. *Cell* 157:1292-1308.
Reitman, M.L. 2017. How Does Fat Transition from White to Beige? *Cell Metab* 26:14-16.
Rosen, E.D., and B.M. Spiegelman. 2014. What we talk about when we talk about fat. *Cell* 156:20-44.
Silva, H.M., A. Bafica, G.F. Rodrigues-Luiz, J. Chi, P.D.A. Santos, B.S. Reis, D.P. Hoytema van Konijnenburg, A. Crane, R.D.N. Arifa, P. Martin, D. Mendes, D.S. Mansur, V.J. Torres, K. Cadwell, P. Cohen, D. Mucida, and J.J. Lafaille. 2019. Vasculature-associated fat macrophages readily adapt to inflammatory and metabolic challenges. *J Exp Med* 216:786-806.
Stanford, K.I., R.J. Middelbeek, K.L. Townsend, D. An, E.B. Nygaard, K.M. Hitchcox, K.R. Markan, K. Nakano, M.F. Hirshman, Y.H. Tseng, and L.J. Goodyear. 2013. Brown adipose tissue regulates glucose homeostasis and insulin sensitivity. *J Clin Invest* 123:215-223.
Stienstra, R., R.T. Netea-Maier, N.P. Riksen, L.A.B. Joosten, and M.G. Netea. 2017. Specific and Complex Reprogramming of Cellular Metabolism in Myeloid Cells during Innate Immune Responses. *Cell Metab* 26:142-156.
Tupone, D., C.J. Madden, and S.F. Morrison. 2014. Autonomic regulation of brown adipose tissue thermogenesis in health and disease: potential clinical applications for altering BAT thermogenesis. *Front Neurosci* 8:14.
Weisberg, S.P., D. McCann, M. Desai, M. Rosenbaum, R.L. Leibel, and A.W. Ferrante, Jr. 2003. Obesity is associated with macrophage accumulation in adipose tissue. *J Clin Invest* 112:1796-1808.
Wolf, Y., S. Boura-Halfon, N. Cortese, Z. Haimon, H. Sar Shalom, Y. Kuperman, V. Kalchenko, A. Brandis, E. David, Y. Segal-Hayoun, L. Chappell-Maor, A. Yaron, and S. Jung. 2017. Brown-adipose-tissue macrophages control tissue innervation and homeostatic energy expenditure. *Nat Immunol* 18:665-674.
Wynn, T.A., A. Chawla, and J.W. Pollard. 2013. Macrophage biology in development, homeostasis and disease. *Nature* 496:445-455.

Xu, H., G.T. Barnes, Q. Yang, G. Tan, D. Yang, C.J. Chou, J. Sole, A. Nichols, J.S. Ross, L.A. Tartaglia, and H. Chen. 2003. Chronic inflammation in fat plays a crucial role in the development of obesity-related insulin resistance. *J Clin Invest* 112:1821-1830.
Xu, X., A. Grijalva, A. Skowronski, M. van Eijk, M.J. Serlie, and A.W. Ferrante, Jr. 2013. Obesity activates a program of lysosomal-dependent lipid metabolism in adipose tissue macrophages independently of classic activation. *Cell Metab* 18:816-830.
Zhu, Y., K. Lyapichev, D.H. Lee, D. Motti, N.M. Ferraro, Y. Zhang, S. Yahn, C. Soderblom, J. Zha, J.R. Bethea, K.L. Spiller, V.P. Lemmon, and J.K. Lee. 2017. Macrophage Transcriptional Profile Identifies Lipid Catabolic Pathways That Can Be Therapeutically Targeted after Spinal Cord Injury. *J Neurosci* 37:2362-2376.

Papier 2

Non-canonical transamination metabolism of glutamine sustains efferocytosis by coupling oxidative stress buffering to oxidative phosphorylation.

Johanna Merlin[1*], Stoyan Ivanov[1*], Alexey Sergushichev[2], Julie Gall[1], Marion Stunault[1], Marion Ayrault[1], Amanda Swain[3], Francois Orange[4], Alexandre Gallerand[1], Emmanuel L. Gautier[5], Thierry Berton[6], Jean-Charles Martin[6], Stefania Carobbio[7], Justine Masson[8], Inna Gaisler-Salomon[8], Pierre Maechler[7], Stephen Rayport[8], Judith C. Sluimer[9], Erik A. L. Biessen[9], Rodolphe R. Guinamard[1], Edward B. Thorp[10], Maxim N. Artyomov[3] and Laurent Yvan-Charvet[1]

*These authors contributed equally to this work

[1]Institut National de la Santé et de la Recherche Médicale (Inserm) U1065, Université Côte d'Azur, Centre Méditerranéen de Médecine Moléculaire (C3M), Atip-Avenir, Fédération Hospitalo-Universitaire (FHU) Oncoage, 06204 Nice, France (J.M., S.I., J.G., M.S., M.A., A.G., R.G., L.Y.C.)

[2]Computer Technologies Department, ITMO University, Saint Petersburg, Russia (A.S.)

[3]Department of Pathology and Immunology, Washington University School of Medicine, St. Louis, MO, USA (A.S., M.N.A.)

[4]Université Côte d'Azur, Centre Commun de Microscopie Appliquée (CCMA), 06108 Nice, France (F.O)

[5]Sorbonne Université, INSERM, UMR_S 1166 ICAN, F-75013 Paris, France (E.L.G).

[6]Centre de Recherche Cardiovasculaire et Nutritionnelle (C2VN), INSERM, Institut National de la Recherche Agricole (INRA), BioMet, Aix-Marseille University, Marseille, France (T.B., J.C.M.)

[7]Department of Cell Physiology and Metabolism; Faculty Diabetes Centre, University of Geneva Medical Centre, Geneva, Switzerland (S.C., P.M.)

[8]Department of Psychiatry, Columbia University, USA; Department of Molecular Therapeutics, NYS Psychiatric Institute, USA (J.M., I.G.S., S.R)

[9]Department of Pathology, Cardiovascular Research Institute Maastricht, Maastricht University Medical Center, Maastricht, the Netherlands (J.C.S., E.A.L.B.)

[10]Department of Pathology, Northwestern University, Feinberg School of Medicine, Chicago, Illinois 60611, USA (E.B.T.)

Address correspondence to LYC: yvancharvet@unice.fr

Key words: Macrophage, Glutaminolysis, Efferocytosis, Interleukin-4 and Atherosclerosis

Summary

Tissue macrophages rely on tightly integrated metabolic rewiring to maintain tissue integrity and continuously clear dying neighboring cells. We identify a critical role for glutaminase (Gls) 1 in promoting apoptotic cell (AC) clearance by macrophages (efferocytosis) after interleukin-4 (IL-4) stimulation or upon multiple rounds of AC exposure. Mice selectively lacking macrophage glutaminolysis showed defective efferocytosis *in vivo* and significant pathologic consequences in atherosclerotic lesions. A strong correlation between Gls1 expression and plaque necrosis was discovered in human atherosclerotic plaque. Most cells utilize glutamate dehydrogenase (Glud1) to fuel α-ketoglutarate (α–KG) into the tricarboxylic acid (TCA) cycle for anapleurosis and epigenetic modifications. However, high-throughput transcriptional and metabolic profiling revealed that macrophage effector and clearance functions rely on a non-canonical transaminase pathway to meet the demand for high energy cytoskeletal rearrangements and cellular detoxification requirements. Thus, our non-biased systems approach identifies that efficient ACs clearance has a previously unknown reliance on non-canonical glutamine metabolism.

Highlights

• Macrophage Gls1 facilitates apoptotic cell (AC) clearance in the presence of IL-4 or during continued clearance of ACs.

• Macrophage-specific glutaminolysis inhibition led to defective efferocytosis in atherosclerotic lesions.

• Glud1 deficiency does not recapitulate the defective efferocytosis of Gls1 deficient macrophages.

• High-throughput profiling revealed that efferocytosis relied on a non-canonical transamination metabolism of glutamine to support the high energy actin dynamics.

Introduction

Clearance of apoptotic cells (ACs) by macrophage (i.e, efferocytosis) prevent the leakage of cellular contents from dying cells to maintain tissue integrity in normal physiology (Kojima et al., 2017; Elliott and Ravichandran, 2016). Impaired efferocytosis in disease can have multiple causes, but defects in multiple AC internalization, a process termed 'continual efferocytosis', has emerged as a culprit of many chronic inflammatory diseases such as atherosclerosis (Wang et al., 2017; Yurdagul et al., 2020). Resolution and repair processes also require the cytokine interleukin-4 (IL-4) (Bosurgi et al., 2017) and an efficient metabolic reprogramming to sustain continual efferocytosis (Han and Ravichandran, 2011). However, these separate observations have never been linked at the molecular level.

Glutamine metabolism is considered as a 'fuel for the immune system' and is routinely used as a component for clinical supplementation in trauma patients. Glutamine is initially hydrolyzed into glutamate by the glutaminase Gls1 in a metabolic process called glutaminolysis (DeBerardinis and Cheng, 2010; O'Neill and Pearce, 2016). This is the most upregulated pathway in alternatively activated macrophages (Jha et al., 2015) but whether it supports the metabolic reprogramming of efferocytosis beyond glucose and fatty acid metabolism is not known (Morioka et al., 2018; Zhang et al., 2019).

Here, we tested the hypothesis that glutaminolysis plays a critical role in macrophage effector function. Mice lacking macrophage Gls1 exhibited defective efferocytosis *in vivo* and significant pathologic consequences in atherosclerotic lesions of fat-fed ApoE$^{-/-}$ mice. This was recapitulated *in vitro* after IL-4 stimulation or upon multiple rounds of AC exposure, which are two physiologic paradigms. Mechanistically, we found that glutamate is channeled into the malate-aspartate shuttle by aspartate aminotransferase (GOT)-dependent transamination in order to meet the demand for cellular detoxification and high energy cytoskeletal rearrangements.

Results

To investigate broader metabolic roles of macrophage Gls1 during effector and clearance functions, mice bearing a conditional allele for glutaminase 1 ($Gls1^{fl/fl}$) in macrophages were generated by crossing to Lysozyme-Cre transgenic mice (LysM-Cre). LysM-Cre x $Gls1^{fl/fl}$ peritoneal cavity macrophages ($Mac^{\Delta Gls1}$ PCMs) efficiently deleted *Gls1* and lowered cellular glutamate levels by 2-fold compared to control macrophages (**Fig. 1a**). Although *Gls1* was expressed to various levels in PCMs, bone marrow (BM) monocytes/macrophages, red pulp macrophages (RPMs), Kupffer cells and microglia (**Fig. S1a**), macrophage numbers were similar in all these tissues in $Mac^{\Delta Gls1}$ mice (**Fig. S1b**). Consistently, proliferation and apoptosis were similar in $Mac^{\Delta Gls1}$ PCMs compared to control cells (**Fig. S1c**). Levels of phospho-S6 and Myc protein, mTORC1 downstream targets, were also unchanged in these cells (**Fig. S1d**) along with absence of transcriptional regulation of rapamycin (mTOR), hypoxia or ferroptosis targets (**Fig. S1e**). This rules out a role for glutaminolysis in macrophage maintenance or development at steady state (Dixon et al., 2012; Nicklin et al., 2009). Consistent with the proposed role for macrophage glutaminolysis in efficient IL-4 response (Jha et al., 2015), we observed an impaired induction of canonical M2 genes (*Clec10a*, *Tgm2*, *Arg1*, *Stab1*, *Sepp1*) (**Fig. S1f**) and cell surface expression of CD206 and CD301 (**Fig. S1g**) in $Mac^{\Delta Gls1}$ PCMs suggesting defective macrophage effector function. Additionally, challenging PCMs with either IL-4, apoptotic cells (ACs) or IL-4 and ACs together revealed that Gls1-dependent glutaminolysis was significantly required for efficient efferocytosis in alternatively activated macrophages as measured by the 28% phagocytic index reduction of $Mac^{\Delta Gls1}$ PCMs after 45 min exposure to apoptotic thymocytes (**Fig. 1b**). Similar findings were confirmed in bone marrow-derived macrophages (BMDMs) (data not shown). To test the impact of glutaminolysis on efferocytosis during heightened metabolic challenge, we challenged Gls1-deficient macrophages to continued clearance of ACs, which mimics tissue states of high cell turnover (Han and Ravichandran, 2011). We performed a validated two-stage efferocytosis experiment in which BMDMs were first incubated for 45min with unlabeled ACs and, after AC removal and one-hour interval, incubated with a second round of labelled ACs (Wang et al., 2017). Consistent with the hypothesis, the percentage of macrophages that had internalized the second round of ACs was significantly decreased in Gls1-deficient macrophages than in controls (**Fig. 1c**). Overexpression of Gls1 in BMDMs using lentiviral particles enhanced efferocytosis in un-stimulated control cells and rescued the defective efferocytosis observed in alternatively activated $Mac^{\Delta Gls1}$ macrophages (**Fig. S1h**). To test the *in vivo* significance, we intravenously injected fluorescently labeled ACs into controls and $Mac^{\Delta Gls1}$ mice. Gls1 deficiency reduced the ability of $CD11b^{lo}F4/80^{high}$ Kupffer cells (KCs) in the liver and to some extent $CD11b^{high}F4/80^{high}$ red pulp macrophages (RPMs) in the spleen to internalize labeled ACs one hour after injection (**Fig. 1d**). These findings provide the first *in vivo* genetic evidence of the pivotal role of Gls1-dependent glutaminolysis during macrophage phagocytic clearance.

To determine the relevance of these observations during disease, we next tested Gls1 requirement in a mouse model of pathological atherosclerosis, in which defective lesional dead cell clearance translates into unstable necrotic core within plaques (Kojima et al., 2017; Tabas, 2010). Taking advantage of publicly available gene expression dataset of high-fat diet (HFD) fed wild-type (WT) and ApoE-deficient mice (Grabner et al., 2009) and computation analysis of metabolic networks (Jha et al., 2015), we first observed a downregulation of Gls1 expression in whole atheromatous plaques that was part of a global metabolic transcriptome signature making up a densely connected core that governs atherosclerotic lesions (**Fig. S2a**). Lower Gls1 expression correlated with an imbalance in markers of classically and alternatively activated macrophages and was inversely correlated to main characteristic of lipid-laden atherosclerotic plaques (i.e, CD36, ABCA1 and ABCG1 expression) (Heatmap, **Fig. S2a**). To monitor glutaminolysis activity in atherosclerotic plaque, we next investigated radiolabeled [^{14}C] glutamine uptake and hydrolysis in aortas extracted from WT and $ApoE^{-/-}$ mice fed on western diet (WD) for 6 weeks. Biomolecular imaging revealed higher glutamine incorporation into Oil Red O^{+} atherosclerotic prone areas, that were enriched in macrophages (**Fig. S2b**).

Nevertheless, quantification of [^{14}C] glutamine conversion into glutamate, after separation by thin-layer chromatography, confirmed lower glutaminase-dependent metabolism in atherosclerotic aorta (**Fig. S2c**). Next, Mac$^{\Delta Gls1}$ mice were crossed onto an atherosclerotic ApoE$^{-/-}$ background. After Western-type diet feeding (12 weeks), there was an approximately 1.7-fold increase in atherosclerosis plaque area in their proximal aortas compared to co-housed control littermates (**Fig. 2a**). Oil red O staining in aortas confirmed higher lipid-rich atherosclerotic plaques in ApoE$^{-/-}$ Mac$^{\Delta Gls1}$ mice (**Fig. 2b**) despite similar plasma lipid levels (**Fig. S2d**). Increased plaque area was also visualized in an independent cohort of ApoE$^{-/-}$ Mac$^{\Delta Gls1}$ mice using non-invasive ultrasound imaging (**Fig. 2c**). These effects were specific to macrophage glutaminolysis since hematopoietic Gls1-deficiency (i.e, generation of Mx1-Cre x Gs1$^{fl/fl}$ mice onto the atherosclerotic ApoE$^{-/-}$ background) recapitulated similar accelerated atherosclerosis than control animals (**Fig. S2e**). Further characterization of atherosclerotic lesions in ApoE$^{-/-}$ Mac$^{\Delta Gls1}$ mice revealed complex plaques containing macrophages (**Fig. S2f**) and necrotic core typified by a greater proportion of TUNEL-positive ACs and reduced ratio of macrophage associated to free AC, a hallmark of defective efferocytosis (**Fig. 2d**). We did not observe significant change in Ki67-positive proliferative cells in ApoE$^{-/-}$ Mac$^{\Delta Gls1}$ mice (**Fig. S2f**). To further support our hypothesis, we *i.p.* injected ApoE$^{-/-}$ Mac$^{\Delta Gls1}$ mice with fluorescent dye labeled apoptotic lymphocytes and examined macrophage efferocytic capacity one hour later. We confirmed the reduced ability of peritoneal macrophages from ApoE$^{-/-}$ Mac$^{\Delta Gls1}$ mice to phagocytose labeled ACs (**Fig. S2g**). To examine clinical significance, we investigated whether Gls1 expression correlated with human atherosclerotic plaque complexity. We found a reduced Gls1 expression in unstable *vs.* stable human carotid artery plaque. Moreover, we established a specific correlation between Gls1 expression and the M2-specific marker Arg1^{+} and an inverse correlation with plaque size, intraplaque hemorrhage (IPH) and necrotic core composition (**Fig. 2e**). Taken together, these results demonstrate that Gls1 contributes to AC engulfment in the pathological process of human and murine atherosclerosis.

To evaluate how IL-4 might couple macrophage glutaminolysis to efferocytosis, we performed an RNA sequencing (RNA-seq) analysis of PCMs after IL-4 complex *i.p* injection. When compared to control PCMs, Gls1-deficient cells had similar transcriptional regulation of genes involved in the sensing of soluble mediators released by ACs ('smell' or 'find-me' signals), the direct contact and recognition of ACs by ligand-receptor interactions ('taste' or 'eat me' signals) and the corpse internalization and processing ('ingestion' and 'digestion' processes) (Han and Ravichandran, 2011) (**Fig. S3a**). Consistently, inversion of alternatively activated controls and Mac$^{\Delta Gls1}$ BMDMs culture media at the initiation of efferocytosis had no impact on AC uptake excluding a role for the generation of an autocrine 'find-me' signal sensors (**Fig. S3b**). Further, alternatively activated Mac$^{\Delta Gls1}$ BMDMs treated only with AC supernatants exhibited similar percentage of fluorescent bead incorporation than control macrophages (**Fig. S3c**). We also investigated whether glutamine or glutamate uptake could serve as a 'smell' signal per se for surrounding cells as recently observed for glucose by-products (Morioka et al., 2018). The similar incorporation of [^{14}C] glutamine in presence or absence of competition with cold glutamine in alternatively activated Mac$^{\Delta Gls1}$ BMDMs first suggested similar glutamine sensing in these cells (**Fig. S3d**). Switching alternatively activated control and Gls1-deficient BMDMs to glutamine or glucose-free medium at the initiation of efferocytosis did not reduce uptake of ACs ruling out this hypothesis (**Fig. S3e**). Nevertheless, we found that intracellular Gls1 mRNA expression was similarly upregulated by IL-4 stimulation or AC ingestion in a validated gene expression dataset (Bosurgi et al., 2017) (**Fig. S3f**). We confirmed this upregulation in a time course experiment (**Fig. S3g**), paralleling a drop in cellular glutamine to glutamate ratio (**Fig. S3h**). We compared the accumulation of fluorescent apoptotic debris 30 min and 6 hours post-efferocytosis. Similar amount of fluorescent apoptotic debris was observed in alternatively activated Mac$^{\Delta Gls1}$ BMDMs compared to controls at 6 hours (**Fig. S3i**), indicating that perturbation in digestion efficiency was unlikely the culprit of the reduced efferocytosis. To distinguish fully internalized from partially engulfed ACs, we next incubated macrophages with prelabeled ACs and after 45 min, sealed and unsealed ACs were detected by CD4/CD8 staining before and after permeabilization, respectively (**Fig. S3j**). We found similar fraction of

$CD4^+CD8^+$ ACs in permeabilized control and Gls1-deficient macrophages but a lower fraction of $CD4^+CD8^+$ ACs in unpermeabilized alternatively activated $Mac^{\Delta Gls1}$ BMDMs, suggesting a defect in the energy-intensive dynamic actin rearrangements to engulf corpse rather than in phagosome sealing (**Fig. 3a**). Consistent with our hypothesis, transmission electron microscopy revealed less membrane ruffling surrounding the $Mac^{\Delta Gls1}$ BMDMs (**Fig. 3b**). Finally, phalloidine (red) immunostaining, 45 min after efferocytosis, revealed a general decrease in the amount of F-actin staining at the leading edge of membrane ruffle formation surrounding the apoptotic cells (green) (**Fig. 3c**). Thus, we identify that glutaminolysis meets the demand for high energy cytoskeletal rearrangement that facilitates the process of corpse engulfment.

To identify glutamine-dependent pathways that support the energy-intensive engulfment process, we traced ^{13}C-labeled glutamine intracellular fate and quantified several metabolites and by-products by liquid chromatography-mass spectrometry. Labeling distribution analyses revealed similar labeling of BC-AA in alternatively activated $Mac^{\Delta Gls1}$ BMDMs within 4 hours of addition of ^{13}C-glutamine (**Fig. 3d**). Consistently, similar amount of BB-AAs, such as leucine and valine, were observed in basal and alternatively activated $Mac^{\Delta Gls1}$ BMDMs (**Fig. S3k**). Consistent with these findings, inhibition of branched chain aminotransferases (BCATs) using Gabapentin (pan competitive inhibitor) or BCATc (BCAT2 selective inhibitor) was insufficient to restore the defective OCR and efferocytic function of alternatively activated $Mac^{\Delta Gls1}$ BMDMs (**Fig. S3l**). We next focused on the urea cycle pathway (**Fig. S3m**). A significant accumulation of unlabeled glutamyl-5-semi-aldehyde (GSA) (**Fig. 3d**) and pyrroline-5-carboxyllate (P5C) (**Fig. S3n**) in alternatively activated $Mac^{\Delta Gls1}$ BMDMs suggested a slower urea cycle turnover. However, we observed similar ^{13}C labeling in urea cycle metabolites (arginine and ornithine), proline or the N-acetylglutamate (NAG) intermediate in these cells (**Fig. 3d**). Quantification of urea cycle metabolites and by-products confirmed these findings (**Fig. S3n**) and ornithine supplementation to feed the urea cycle was not sufficient to rescue the OCR and efferocytosis of $Mac^{\Delta Gls1}$ BMDMs (**Fig. S3o**). Thus, neither higher BCAA catabolism or slower urea cycle turnover could explain the lower energy-dependent engulfment process of Gls1-deficient macrophages. In contrast, lower ^{13}C incorporation into TCA metabolites (succinate, malate, aconitase) and ATP in alternatively activated $Mac^{\Delta Gls1}$ BMDMs within 4 hours of addition of ^{13}C-glutamine supported partially defective TCA cycling in these cells (**Fig. 3d**). Consistently, we provide genetic evidence of reduced basal oxygen consumption rate (OCR) and maximal respiration after FCCP (carbonyl cyanide 4-[trifluoromethoxy] phenylhydrazone) treatment in $Mac^{\Delta Gls1}$ PCMs and BMDMs in comparison to control cells (**Fig. S3p and S3q**). These effects occurred independently of fluctuation in extracellular acidification rate (ECAR), a surrogate of glycolytic activity (**Fig. S3r**). We next addressed whether glutaminolysis could impact OXPHOS after ingestion of ACs. Flux measurements showed that both unstimulated and alternatively activated $Mac^{\Delta Gls1}$ BMDMs that were fed ACs, exhibited a decrease in maximal respiration response (**Fig. 3e and 3f**). These effects were also associated with a drop in ATP production reflecting an inability of these cells to respond to increased energy demand (**Fig. S3s**). Similar to IL-4 stimulation, basal OCR and maximal respiration response were also reduced during continued clearance of ACs (**Fig. 3g**). The decrease in mitochondria metabolism was also associated to higher total and mitochondrial ROS levels in both unstimulated and alternatively activated $Mac^{\Delta Gls1}$ BMDMs (**Fig. S3t**) suggesting a reverse electron transport (RET) by the mitochondrial electron transport chain (ETC). To dissect the origin of the defective OCR in Gls1-deficient macrophages and its causal role on efferocytosis, we used ETC pharmacological inhibitors or we supplemented $Mac^{\Delta Gls1}$ BMDMs with mitochondrial ROS scavengers (**Fig. 3h**). Indeed, mitochondrial redox status has been previously shown to metabolically pre-program macrophage skewing (Jais et al., 2014; Vats et al., 2006). Mitochondrial ROS scavenging by the superoxide dismutase mimetic (Tempol) or the mitochondria-targeted antioxidant coenzyme Q10 (MitoQ) was insufficient to rescue the defective OCR of alternatively activated $Mac^{\Delta Gls1}$ BMDMs, suggesting that mitochondrial ROS production are unlikely the cause but rather the consequence of the metabolic rewiring (**Fig. 3i**). These treatments did also not improve the efferocytic index in $Mac^{\Delta Gls1}$ BMDMs (**Fig. 3j**). We rather observed that direct OCR inhibition by targeting mitochondrial complex II (i.e,

succinate dehydrogenase (SDH)) with 3-Nitropropionic acid (3NPA) or complex III with antimycin A reduced efferocytosis in control cells to the levels of alternatively activated Mac$^{\Delta Gls1}$ BMDMs (**Fig. 3j**). Similar findings were observed during continued clearance of ACs (**Fig. S3u**). Consistent with the reduced OCR and pro-inflammatory properties of Risp knockout macrophages (Zhang et al., 2019), we also confirmed the genetic requirement of complex III to efferocytosis and continued clearance of ACs (**Fig. S3v**). Together, these findings reveal that glutaminolysis couples mitochondrial oxidative phosphorylation to ATP production for efficient efferocytosis.

We next compared differentially expressed genes in alternatively activated Mac$^{\Delta Gls1}$ PCMs to differentially expressed genes in macrophages that have engulfed ACs from a publicly available gene expression dataset (Morioka et al., 2018). Venn diagram revealed a core signature of genes that was commonly regulated by Gls1 deficiency and efferocytosis (**Fig. S4a**). Functional annotation enrichment analysis for GO terms highlighted mitochondria and redox status gene signatures (**Fig. S4a**) that are known to be exquisitely intertwined (Chandel, 2015; O'Neill and Pearce, 2016). Consistently, metabolic pathway enrichment analysis in resting and alternatively activated Mac$^{\Delta Gls1}$ PCMs highlighted down-regulation of KEGG pathways involved in oxidative phosphorylation and GSH synthesis (i.e, NADP, folate and GSH metabolism) (**Fig. S4b**). To dissect the interplay between the mitochondrial metabolic repurposing and the perturbation in antioxidant metabolism in Mac$^{\Delta Gls1}$ macrophages, we performed topological analyses using CoMBI-T profiling analysis (Jha et al., 2015) and compared the predictions to DreamBio that allows direct computational KEGG pathway mapping. CoMBI-T and DreamBio profiling analyses suggested that Mac$^{\Delta Gls1}$ PCM mitochondrial metabolic reprogramming could be linked directly to lower expression of tricarboxylic acid (TCA) cycle and aspartate-arginino-succinate (AAS) shunt genes that are interconnected to glutamine metabolism itself, carbohydrate, hexosamine and fatty acid metabolism (**Fig. 4a and S4c**). CoMBI-T predictions also revealed that the redox status of alternatively activated Mac$^{\Delta Gls1}$ PCMs could be linked to the one carbon cycle-centered module known to support the transsulfuration pathway (i.e, GSH synthesis) (**Fig. 4a**). KEGG mapping with DreamBio offered an alternative visualization of the perturbed transcriptomic pathways in alternatively activated Gls1-deficient macrophages and highlighted additional reactions that are not yet predicted to be connected (**Fig. S4c**). For instance, in contrast to CoMBI-T, DreamBio analysis predicted downregulation of phosphogluconate dehydrogenase (PGD) and malic enzyme (ME1) in alternatively activated Gls1-deficient macrophages. These are two key enzymes that also contribute to NADPH generation to efficiently supply reduced glutathione and maintain macrophages redox status (**Fig. S4c**). Consistent with these observations, the ratio between GSH (reduced glutathione)/GSSG (glutathione disulfide), known to scavenge reactive oxygen species (ROS) (DeBerardinis and Cheng, 2010), was greatly reduced in resting and alternatively activated Mac$^{\Delta Gls1}$ PCMs (**Fig. S4d**). Although total glutathione concentration was decreased to some extent in alternatively activated Mac$^{\Delta Gls1}$ PCMs, the decrease in the NADPH/NADP ratio was more strongly correlated to the GSH/GSSG ratio in resting and alternatively activated Mac$^{\Delta Gls1}$ PCMs (**Fig. S4d**). Altogether, this unique approach helped pinpoint the metabolic origin on how Gls1-dependent glutamine metabolism integrates canonical mitochondrial reprogramming and non-canonical redox status.

We first explored the canonical glutaminolysis pathway that relies on glutamate dehydrogenase (Glud1) to convert glutamate into α-ketoglutarate (α–KG) to fuel the TCA cycle. First, there was no difference in α-KG carbon numbers that originated from ^{13}C-glutamine in alternatively activated Mac$^{\Delta Gls1}$ BMDMs in comparison to the strong decrease detected in malate (**Fig. 3d**). Similar α-KG levels were also observed between controls and Mac$^{\Delta Gls1}$ BMDMs in our metabolomic analysis (data not shown). Consistent with these findings, treatment of control and Mac$^{\Delta Gls1}$ BMDMs with dimethyl α–KG did not rescue the inhibitory effect of Gls1 deficiency or BPTES (a Gls1 inhibitor) on basal OCR (**Fig. S4e**). α–KG-dependent KDM6 and ten-eleven translocation dioxygenase 2 (TET2) activities were also similar between control and Mac$^{\Delta Gls1}$ BMDMs (**Fig. S4f**) and similar expression of KDM6 target genes such as Phf2, Phf8, Jarid2 or

Mina were observed in these cells (**Fig. S4g**). Additionally, treatment of alternatively activated $Mac^{\Delta Gls1}$ BMDMs with a histone demethylase JMJD3 inhibitor (GSK-J4) or a broader DNA methyltransferase inhibitor (azacytidine) did not restore their OCR defect and particularly efferocytosis (**Fig. S4h**). Finally, similar global histone trimethylation modification, assessed by flow cytometry using H3K4me3 and H3K27me3 staining, was observed between controls and $Mac^{\Delta Gls1}$ BMDMs (**Fig. S4i**) and we did not find major transcriptional perturbation of epigenetic enzymes in Gls1-deficient macrophages (**Fig. S4j**). To confirm that α–KG generation through Glud1 was not responsible of the effects observed in Gls1-deficient macrophages, we generated myeloid specific Glud1-deficient mice ($HSC^{\Delta Glud1}$) (**Fig. 4b**). Unexpectedly, higher basal OCR and maximal respiration response (**Fig. 4c**), ATP production rate (**Fig. 4d**) and efferocytosis (**Fig. 4e**) were observed in alternatively activated macrophages genetically deficient in Glud1. An increase in glutathione concentration was also observed in these cells (data not shown). RNA sequencing analysis and functional annotation enrichment analysis for GO terms confirmed changes in transcriptional programs in Glud1-deficient macrophages, including enhanced immune process, whole membrane, cell activation or defense response (**Fig. 4f**). These findings suggest that Glud1 inhibition could redirect glutamate flux to promote efficient mitochondrial reprogramming and support the high energy requirement of efferocytosis. Inhibition of Glud1 with epigallocatechin gallate (EGCG) also exhibited an opposite effect versus Gls1 deficiency with increases in basal OCR and efferocytosis in alternatively activated control macrophages, and to some extent in $Mac^{\Delta Gls1}$ BMDMs (**Fig. 4g**). Altogether, these data suggest that Gls1-deficient macrophages metabolize less glutamate through a non-canonical glutaminolysis pathway to limit the TCA cycle anapleurosis required for efficient efferocytosis.

Based on our topological analyses, we next scrutinized the balance between the utilization of glutamate into the non-canonical GSH synthesis pathway that could prevent ATP leakage by limiting the γ-glutamyl futile cycle or into the non-canonical transaminase-dependent malate-aspartate shuttle that is nested to the AAS shunt to maximize the number of ATP molecules produced in mitochondria (DeBerardinis and Cheng, 2010) (**Fig. 5a**). We first excluded a role of the γ-glutamyl futile cycle in facilitating ATP leakage as we observed similar amount of the pyroglutamate intermediate (also known as PCA or 5-oxoproline) in $Mac^{\Delta Gls1}$ BMDMs despite reduced cystathionine levels (**Fig. S5a**). Treatment with N-acetylcysteine (NAC) to replenish this futile cycle and boost GSH synthesis had also no effect on OCR and efferocytosis in $Mac^{\Delta Gls1}$ BMDMs (**Fig. S5b**). In contrast, scavenging of ROS by direct supplementation of glutathione monoethyl ester (GSH) (**Fig. S5c**) raised basal OCR levels, ATP production and efferocytosis in alternatively activated $Mac^{\Delta Gls1}$ BMDMs to the levels of control macrophages (**Fig. 5b**). These findings suggest that GSH could overcome the perturbation of GSH salvage pathway (i.e, NADPH-producing pathways to recycle GSSG into GSH) in Gls1-deficient macrophages rather than limiting the γ-glutamyl futile cycle. There are several mechanisms of generating NADPH that depend on enzymes present in mitochondria including isocitrate dehydrogenase or malic enzyme. Topological analysis suggested a role of the malate-pyruvate cycling pathway (i.e, reduced ME1 expression) in $Mac^{\Delta Gls1}$ PCMs that directly relies on the malate-aspartate shuttle. Thus, we next inhibited the aspartate aminotransferases (GOT_s)-dependent transamination with aminooxyacetic acid (AOA) (**Fig. 5a**). Interestingly, AOA treatment reduced not only GSH levels (**Fig. S5c**) but also basal OCR and this limited efferocytosis in control macrophages to the levels of alternatively activated $Mac^{\Delta Gls1}$ BMDMs (**Fig. 5c**). Treatment with AOA also inhibited efferocytosis during continued clearance of ACs in control and $Mac^{\Delta Gls1}$ BMDMs (**Fig. S5d**). We validated these observations by showing that reduced expression of Got1 and Got2 by siRNA in BMDMs prevented the engulfment of apoptotic cells (**Fig. S5e**). Finally, AOA treatment also reversed the enhanced efferocytosis observed in alternatively activated Glud1-deficient BMDMs (**Fig. 5d**). Our results reveal that glutaminolysis and non-canonical transaminase pathways are preferentially used to maximize the number of ATP molecules produced in mitochondria for macrophage clearance function, which is linked to the ability of these pathways to power cells with the reducing equivalents necessary to detoxify ROS.

The energy-intensive cytoskeletal rearrangement to engulf corpse may rely on actin dynamics and these processes can be regulated by polymerization and depolymerization steps that can be accelerated by an ATP-dependent nucleation phase of new actin filaments or by small GTPases such as Rac1 and Cdc42 (Caron et al., 1998) (**Fig. S5f**). We indeed observed a slower polarization of G- to F-actin in alternatively activated $Mac^{\Delta Gls1}$ macrophages (**Fig. 5e**). Expression analysis of F-actin dynamic regulators did not reveal major differences in alternatively activated $Mac^{\Delta Gls1}$ PCMs, except thymosin beta-10 (Tmsb10) (**Fig. S5g**), a peptide that binds to ATP-containing actin monomers to limit actin nucleation. However, Tmsb10 protein expression was not altered in alternatively activated $Mac^{\Delta Gls1}$ macrophages (**Fig. S5h**). These findings indicate that transcriptional regulation was unlikely responsible for cytoskeletal rearrangement in Gls1 deficient macrophages. Because pull-down activation assay showed reduced activity of Cdc42 (**Fig. S5h**) and Rac1 (**Fig. S5i**) in alternatively activated $Mac^{\Delta Gls1}$ BMDMs, we next wondered if the conversion of ATP to GTP by mitochondrial nucleoside diphosphate kinase (Ndks) or succinyl-CoA ligases (Suclgs) could modulate small GTPase activity. Among these enzymes, expression of Nme1, Nme6 and Suclg1 was downregulated in alternatively activated $Mac^{\Delta Gls1}$ PCMs (**Fig. S5k**). Nevertheless, overexpression of Nme1/6 or Sucgl1 (**Fig. S5l**) was not sufficient to rescue the defective efferocytosis of alternatively activated $Mac^{\Delta Gls1}$ BMDMs (**Fig. S5m**).

Discussion

Macrophages need to handle a substantial amount of nutrients after ingestion of apoptotic cells (i.e, efferocytosis) to maintain normal tissue function (Han and Ravichandran, 2011). Especially, we and others have demonstrated that efferocytes can adapt their metabolism to face cholesterol and fatty acid overload during this process (A-Gonzalez et al., 2009)(Yvan-Charvet et al., 2010)(Viaud et al., 2018)(Zhang et al., 2019). Increased glucose uptake preceding AC engulfment could also prime continued AC clearance (Morioka et al., 2018). We now uncover that Gls1-dependent glutaminolysis is required to optimize AC clearance upon IL-4 stimulation or continued AC uptake by efficiently reprogramming macrophage metabolism. Indeed, conversion of glutamine through non-canonical transaminase pathways couples oxidative stress buffering to ATP production to meet the demand for high energy actin dyamics and cytoskeletal rearrangements.

Glutamine is considered a conditionally essential amino acid because of its role during conditions of metabolic stress, including injury (DeBerardinis and Cheng, 2010; O'Neill and Pearce, 2016). Glutamine utilization is increased in alternative macrophage polarization (Jha et al., 2015) and could predict macrophage activation profile in aortas of atherosclerotic mouse models (Tavakoli et al., 2017). However, the link between Gls1 and efferocytosis in this setting remains to be elucidated. Strikingly, despite enhanced glutamine utilization in the aortas of atherosclerotic mice, we observed impaired glutamate conversion and reduced Gls1 expression reflecting perturbed glutaminolysis. In our mouse and human datasets, we also observed that Gls1 expression within plaques was positively associated to canonical alternative polarization markers suggesting that glutaminolysis rather than glutamine uptake could predict macrophage profile. Functionally, we also observed that Gls1 expression negatively correlated to necrotic cores suggesting it could become a new imaging tool to assess defective efferocytosis as it is the case with ^{18}F-fluorodeoxyglucose PET imaging to detect inflamed tissues.

Modulation of glutamine metabolism at different steps can lead to strikingly different phenotypes. For instance, it has recently been suggested that glutaminolysis could support α–KG generation to orchestrate the jumonji domain containing-3 (Jmjd3, KDM6B)-dependent epigenetic reprogramming of alternatively activated macrophages *in vitro* (Liu et al., 2017) or promote mTORC1 signaling during Th1 differentiation (Jonhson et al., 2018). In the current setting, we neither observe perturbations of α–KG-dependent epigenetic reprogramming or upregulation of glycolysis and downstream mTOR signaling pathways in glutaminolysis deficient macrophages. Glutamine can be converted through at least two canonical and non-canonical mechanisms involving glutamate dehydrogenase (Glud1) or transaminases, respectively. Unexpectedly, Glud1 deficiency exhibited an opposite effect than Gls1 deficiency on efferocytosis suggesting that efferocytes metabolize glutamine in a manner that is different from the canonical α–KG generation model. Indeed, high-throughput transcriptional and metabolic profiling revealed that macrophage effector and clearance functions rely on a non-canonical transaminase pathway. The transaminase-dependent malate-aspartate shuttle is nested to the AAS shunt and requires glutamate to regenerate NADH, which is used to transfer electrons to the electron transport chain (ETC). This is required to maximize the number of ATP molecules produced in mitochondria and potentially favor NADPH production through ME-dependent malate-pyruvate cycling pathway to support GSH salvage pathway (DeBerardinis and Cheng, 2010). Consistently, all markers of these pathways were downregulated in Gls1-deficient macrophages. Although reduced GSH levels could explain the higher mitochondrial ROS in Gls1-deficient macrophages and mitochondrial redox status has been previously shown to metabolically pre-program macrophage skewing (Jais et al., 2014; Vats et al., 2006), we excluded a causal role of mitochondrial ROS in the metabolic reprogramming and defective efferocytosis of these cells using pharmacological mitochondrial ROS scavengers. Thus, treatment of Gls1-deficient macrophages with GSH most likely improved oxidative phosphorylation and efferocytosis by limiting NADPH consumption, which 'energy value' can be roughly estimated at between 2.5 and 3.5 ATP equivalents for purposes of comparing energy inputs and outputs of metabolic pathways (Stipanuk and Caudill, 2013). The central

role of ATP produced within mitochondria after glutamate is channeled into the malate-aspartate shuttle by aspartate aminotransferase (GOT)-dependent transamination in efferocytes was ultimately highlighted by directly targeting GOTs or mitochondrial complex II and III.

The metabolism of other amino acids has recently emerged to control macrophage effector functions. For example, BB-AAs cause itaconate accumulation, a hallmark of macrophage proinflammatory response (Papathanassiu et al., 2017)(O'Neill and Artyomov 2019). The group led by Tabas et al. have also recently reported that the metabolism of AC-derived arginine or ornithine to putrescine is required for continual efferocytosis by a mechanism involving cytoskeletal rearrangements (Yurdagul et al., 2020) and potentially linked to mitochondrial fission (Wang et al., 2017). This pathway is induced in alternatively activated macrophages (Jha et al., 2015), known to enhance efferocytic response for efficient tissue repair (Bosurgi et al., 2017). Impairment of macrophage glutaminolysis described here is predicted to occur independently of the aforementioned metabolic pathways as similar levels of BB-AAs and putrescine were observed in Gls1-deficient macrophages and inhibition of BCAT or ornithine supplementation did not rescue the defective efferocytosis of these cells. This pathway may contribute to daily clearance of billions of white blood cells to maintain tissue homeostasis as illustrated here in the liver, spleen and peritoneal cavity (Elliott and Ravichandran, 2016) or lead to impaired resolution and tissue necrosis as illustrated in progressing atherosclerosis (Kojima et al., 2017; Tabas, 2010).

The high energy demand for cytoskeletal rearrangements during efferocytosis has previously been suggested but the underlying mechanisms remain poorly understood (Elliott and Ravichandran, 2016). Most of the studies focus on small GTPase such as Rac1 or Cdc42 because they are key regulators of membrane ruffling for AC recognition and internalization (Han and Ravichandran, 2011). However, actin remodeling can also be directly regulated by polymerization and depolymerization steps that are energy-intensive processes. Along with reduced ATP production in Gls1-deficient macrophages, we observed both impaired actin polymerization and reduced Cdc42 and Rac1 activities. Although the link between ATP production and actin polymerization makes intuitive sense, the link with small GTPase activation is less apparent. Nevertheless, blockade of the AAS shunt to limit ATP production clearly recapitulated these observations. Because Rac1 was not regulated at the transcriptional levels, we reasoned that ATP production might directly be linked to GTP production to activate small GTPase (Boissan et al., 2018). However, we did not find evidences that conversion of ATP to GTP by Nme1/6 or Suclg1 could explain modulation of efferocytic response. It is possible that other mechanisms such as regulation of (GTP)-exchange factor (GEF) may be involved and future studies will be required to address this question (Marei and Malliri, 2017).

Collectively, our results reveal a novel dependence on transaminases for metabolism of the glutamine carbon skeleton during key macrophage effector functions that are required for tissue repair. Mechanistically, these reactions orchestrate ATP generation through the ETC in the presence of IL-4 or during continued apoptotic cell clearance. These findings support the larger concept that any process that compromises the metabolic reprogramming and ATP production of efferocytes will likely result in dire pathologic consequences. Conversely, therapeutic interventions to enhance macrophage glutaminolysis and boost efferocytosis may be able to face maladaptive inflammation and necrosis.

Figure 1

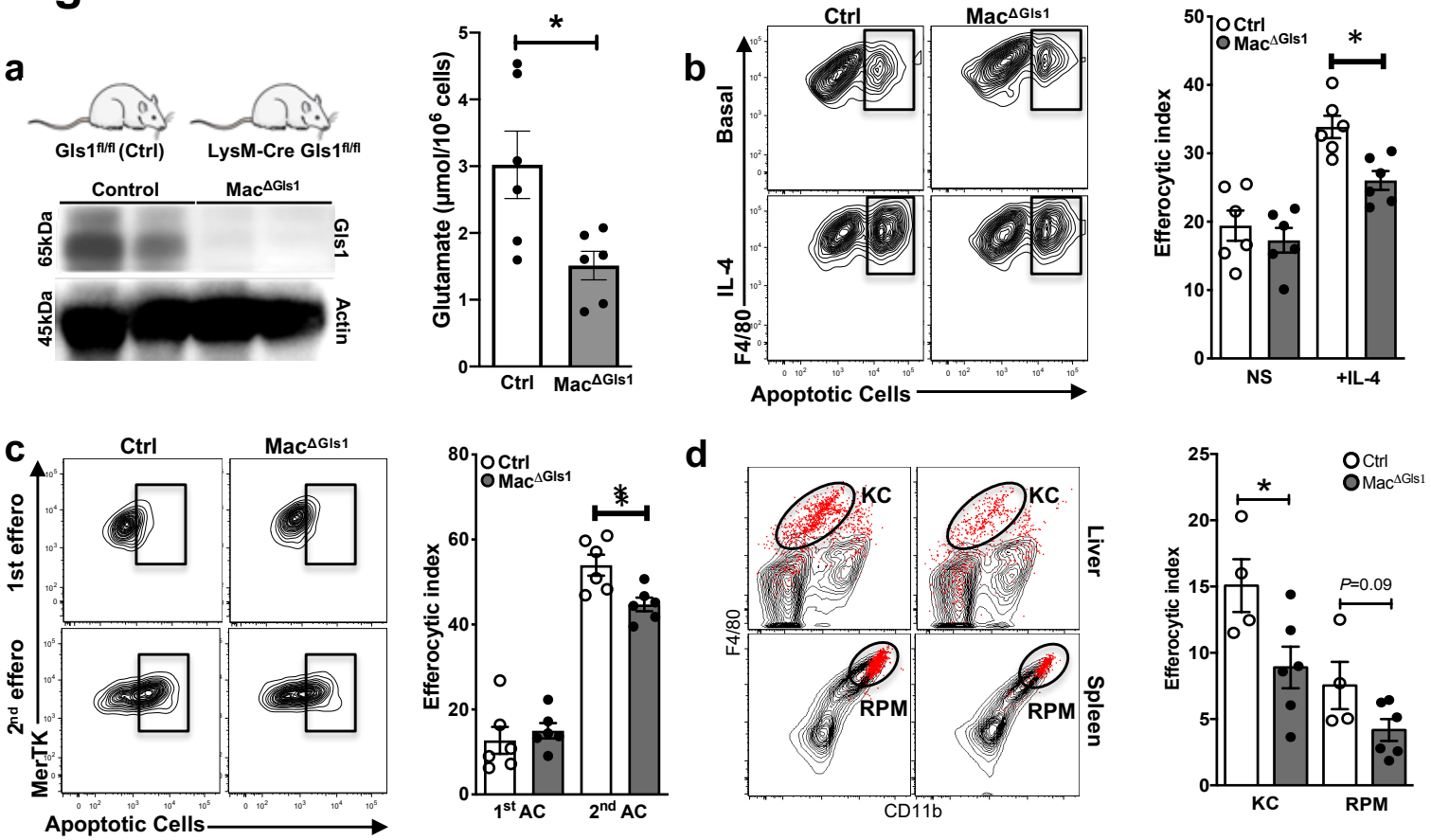

Figure 1: Macrophage-Gls1 deletion impairs efferocytosis *in vitro* and *in vivo*. (a) Western blot of Gls1 protein (left) and Glutamate levels (right) in Control or Mac$^{\Delta Gls1}$ PCMs. **(b)** Efferocytic index gating strategy (left) and quantification (right) measured by flow cytometry after 45min exposure with apoptotic cells (ACs) in BMDMs at steady state or after overnight IL-4 stimulation. Efferocytic index was calculated as follows: (number of macrophages with ACs/total number of macrophages) × 100. **(c)** Efferocytic index gating strategy (Left) and quantification (right) measured by flow cytometry after one (45min) or two (45min + 1-hour rest + 45min) incubations with ACs in control or Mac$^{\Delta Gls1}$ BMDMs. **(d)** Efferocytic index gating strategy (left) and quantification (right) measured by flow cytometry in control or Mac$^{\Delta Gls1}$ Kupffer cells (KC) and red pulp macrophages (RPM) after labelled apoptotic thymocytes i.v. injection. All values are mean ± SEM and are representative of at least one experiment (n=4-6 independent animals). **P*<0.05 *compared to control*.

Figure 2

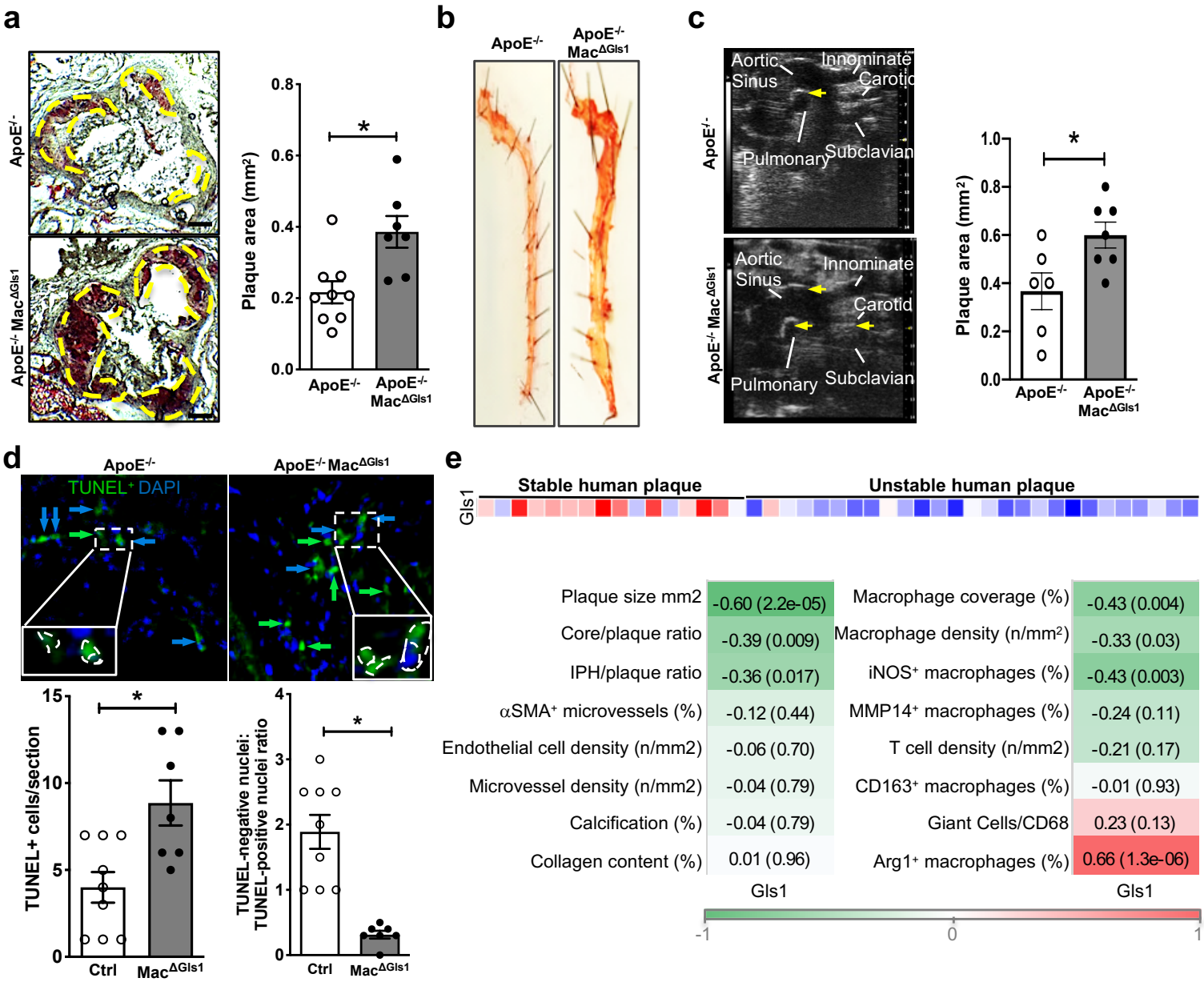

Figure 2: Myeloid-Gls1 deletion impairs efferocytosis in the pathological process of atherosclerosis. (a) Representative sections (left) and quantification (right) of aortic plaques from ApoE$^{-/-}$ or ApoE$^{-/-}$ Mac$^{\Delta Gls1}$ mice (12 weeks WD) stained for Oil Red O and Hematoxylin Eosin. Scale bar: 200□m. **(b)** Oil red O stained descending aortas from ApoE$^{-/-}$ or ApoE$^{-/-}$ Mac$^{\Delta Gls1}$ mice maintained on a WD for 12 weeks. **(c)** Echography (left) and quantification (right) of aortic plaques from ApoE$^{-/-}$ or ApoE$^{-/-}$ Mac$^{\Delta Gls1}$ mice fed for 12 weeks on WD. Arrows indicate plaque areas. **(d)** Representative images (top) and quantification (bottom) of TUNEL^{+} cells in aortic plaques from ApoE$^{-/-}$ or ApoE$^{-/-}$ Mac$^{\Delta Gls1}$ mice (12 weeks WD). Green and blue arrow depict TUNEL negative nuclei and TUNEL-positive nuclei, respectively. **(e)** Correlation between Gls1 expression and human atherosclerotic plaque complexity in the Maastricht Pathology collection. All values are mean ± SEM and are representative of at least one experiment (n=6-9). *P<0.05 *compared to control*.

Figure 3

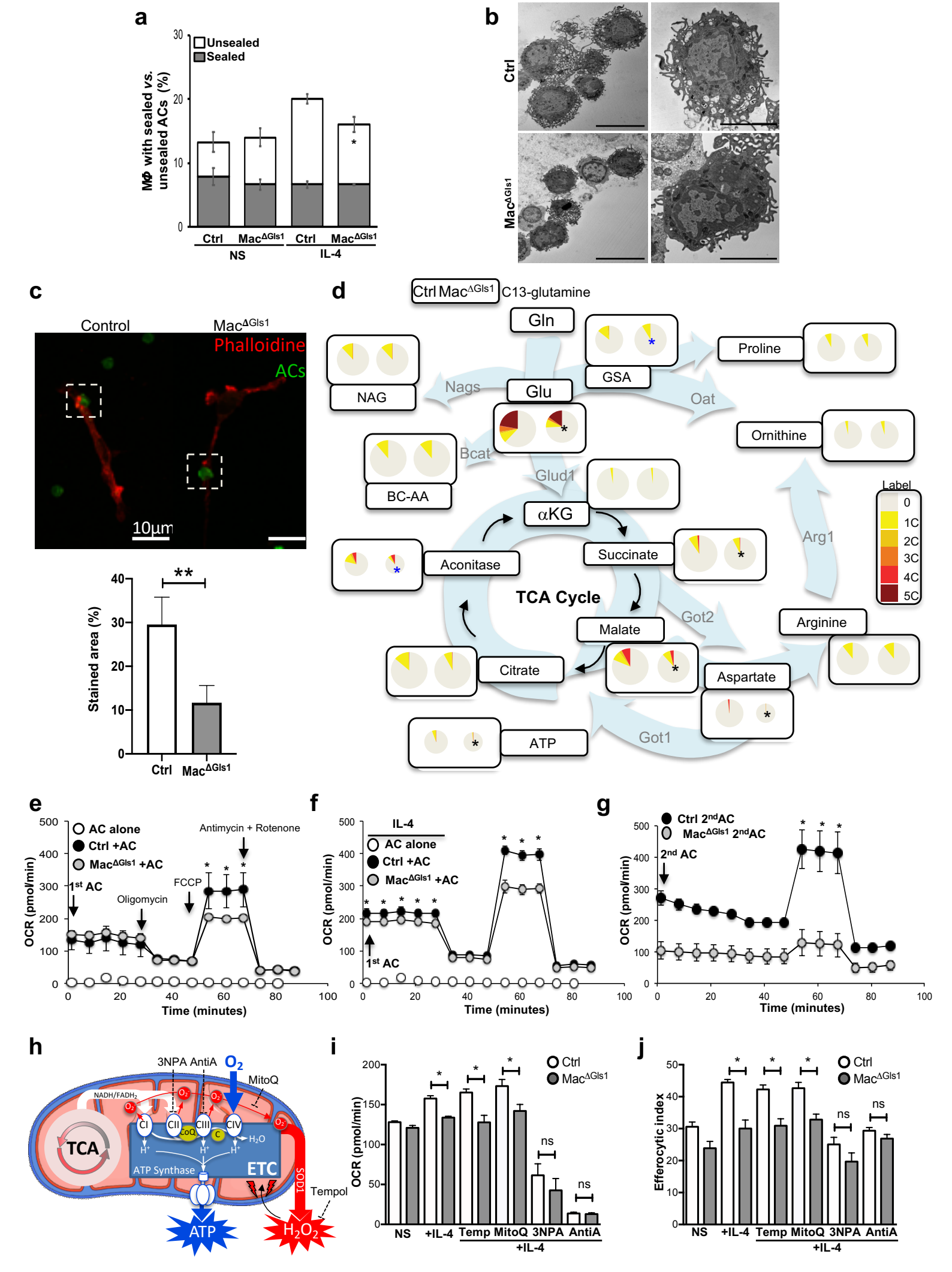
a
Unsealed
Sealed
MΦ with sealed vs. unsealed ACs (%)
Ctrl
MacΔGls1
Ctrl
MacΔGls1
NS
IL-4
b
Ctrl
MacΔGls1
c
Control
MacΔGls1
Phalloidine
ACs
10µm
Stained area (%)
Ctrl
MacΔGls1
d
Ctrl MacΔGls1 C13-glutamine
Gln
NAG
Nags
Glu
GSA
Proline
Oat
Ornithine
Bcat
BC-AA
Glud1
αKG
Aconitase
Succinate
TCA Cycle
Arg1
Got2
Malate
Citrate
Aspartate
Arginine
ATP
Got1
Label
0
1C
2C
3C
4C
5C
e
AC alone
Ctrl +AC
MacΔGls1 +AC
1st AC
Oligomycin
FCCP
Antimycin + Rotenone
OCR (pmol/min)
Time (minutes)
f
IL-4
AC alone
Ctrl +AC
MacΔGls1 +AC
1st AC
OCR (pmol/min)
Time (minutes)
g
Ctrl 2ndAC
MacΔGls1 2ndAC
2nd AC
OCR (pmol/min)
Time (minutes)
h
3NPA AntiA
O2
MitoQ
NADH/FADH2
CI
CII
CIII
CIV
CoQ
C
H2O
H+
TCA
ATP Synthase
ETC
SOD1
Tempol
ATP
H2O2
i
Ctrl
MacΔGls1
OCR (pmol/min)
ns
ns
NS
+IL-4
Temp
MitoQ
3NPA
AntiA
+IL-4
j
Ctrl
MacΔGls1
Efferocytic index
ns
ns
NS
+IL-4
Temp
MitoQ
3NPA
AntiA
+IL-4

Figure 3 Glutamine metabolism supports the high energy requirement of efferocytosis. **(a)** Apoptotic cell internalization quantification in control or $Mac^{\Delta Gls1}$ PCMs stimulated overnight +/- IL-4. **(b)** Transmission electron microscopy imaging of control or $Mac^{\Delta Gls1}$ PCMs. Left scale bar: 10□m. Right scale bar: 5□m. **(c)** Representative images of control or $Mac^{\Delta Gls1}$ BMDMs stimulated overnight with IL-4 and stained for F-actin (Red) and ACs (green). Scale bar: 10µm. **(d)** Carbon fluxes using U-13C-glutamine. U-13C glutamine was added in the medium of non-stimulated and IL-4-treated macrophages. Circle sizes are scaled with respect to pool size for individual metabolites in each condition. Thin black arrows represent known metabolic pathway connections; background arrows indicate deduced major metabolic flows in alternatively activated macrophages. **(e)** OCR measured by Seahorse after one incubation with ACs in control or $Mac^{\Delta Gls1}$ BMDMs in basal conditions or **(f)** stimulated overnight with IL-4. **(g)** OCR measurement after two exposures with ACs in control or $Mac^{\Delta Gls1}$ BMDMs. **(h)** Schematic representation of mitochondria electron transport chain and its pharmacological inhibitors. **(i)** OCR quantification and **(j)** efferocytic index of control or $Mac^{\Delta Gls1}$ BMDMs at steady state or after overnight IL-4 stimulation +/- Tempol, Mitoquinol, 3NPA or antimicyn A. All values are mean ± SEM and are representative of at least one experiment (n=3-9). **P*<0.05 compared *to control*.

Figure 4

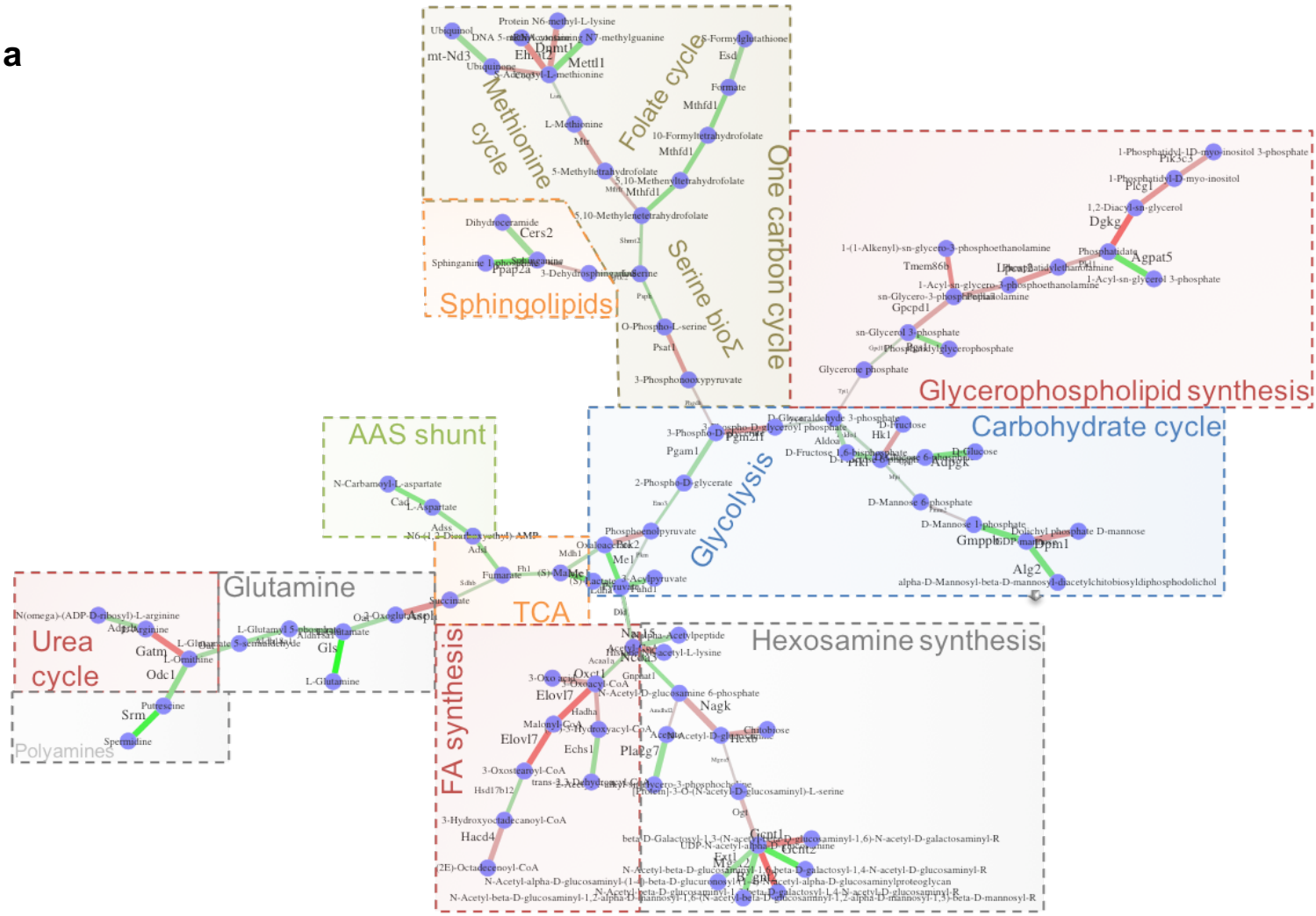
a
Methionine cycle
Folate cycle
One carbon cycle
Serine bioΣ
Sphingolipids
Glycerophospholipid synthesis
Carbohydrate cycle
AAS shunt
Glycolysis
Glutamine
Urea cycle
TCA
Polyamines
FA synthesis
Hexosamine synthesis

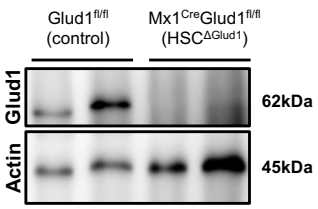
b
Glud1fl/fl (control)
Mx1Cre Glud1fl/fl (HSCΔGlud1)
Glud1
Actin
62kDa
45kDa

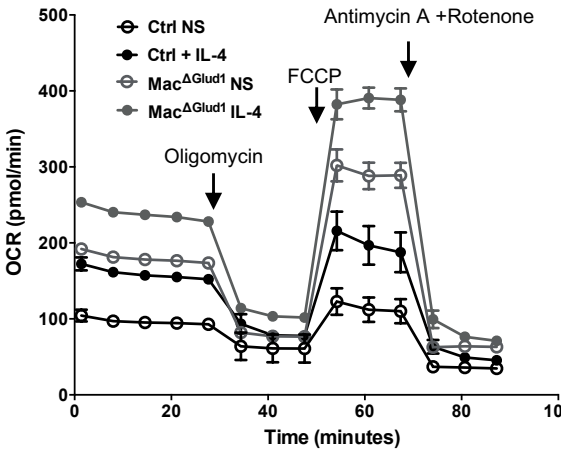
c
Ctrl NS
Ctrl + IL-4
MacΔGlud1 NS
MacΔGlud1 IL-4
Antimycin A +Rotenone
FCCP
Oligomycin
OCR (pmol/min)
Time (minutes)

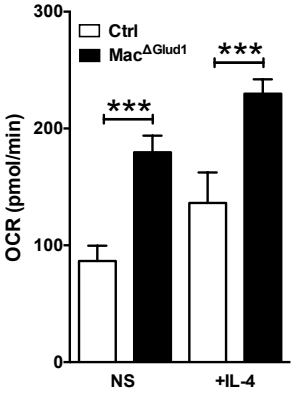
Ctrl
MacΔGlud1
OCR (pmol/min)
NS
+IL-4

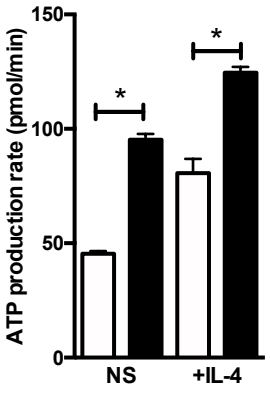
ATP production rate (pmol/min)
NS
+IL-4

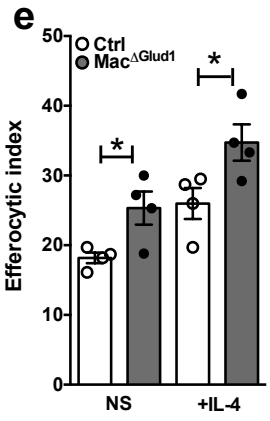
e
Ctrl
MacΔGlud1
Efferocytic index
NS
+IL-4

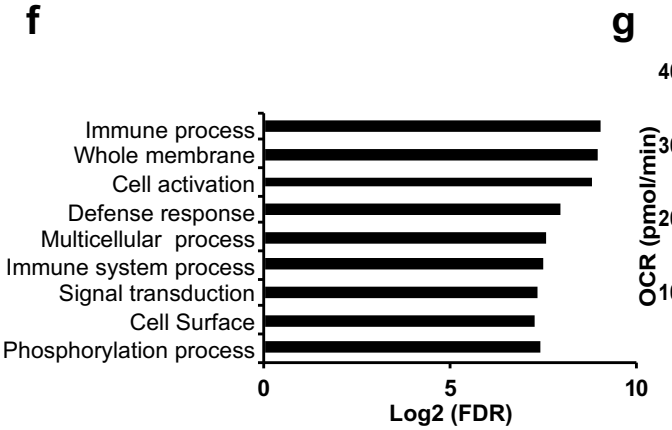
f
Immune process
Whole membrane
Cell activation
Defense response
Multicellular process
Immune system process
Signal transduction
Cell Surface
Phosphorylation process
Log2 (FDR)

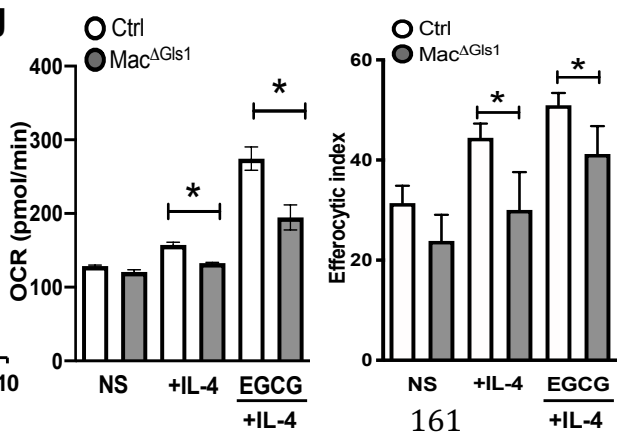
g
Ctrl
MacΔGls1
OCR (pmol/min)
NS
+IL-4
EGCG +IL-4
Efferocytic index

Figure 4: Macrophages utilize a non-canonical glutamine metabolism pathway to promote efficient efferocytosis. (a) CoMBI-T profiling analysis from RNAseq data of alternatively activated Gls1-deficient or sufficient PCMs. **(b)** Glud1 protein expression assessed by Western blotting in control or $HSC^{\Delta Glud1}$ PCMs. **(c)** OCR and **(d)** ATP production rate measured by Seahorse in control or $Mac^{\Delta Glud1}$ BMDMs at steady state or after overnight IL-4 stimulation. **(e)** efferocytic index in control or $Mac^{\Delta Glud1}$ BMDMs at steady state or after overnight IL-4 stimulation. **(f)** RNAseq analysis and functional annotation enrichment analysis for GO terms in control or $Mac^{\Delta Gls1}$ PCMs. **(g)** OCR quantification (left) and efferocytic index (right) from control or $Mac^{\Delta Gls1}$ BMDMs in basal conditions or overnight IL-4 stimulation +/- EGCG. All values are mean ± SEM and are representative of at least one experiment (n=3-8). **P*<0.05, ****P*<0.0005 compared *to control*.

Figure 5

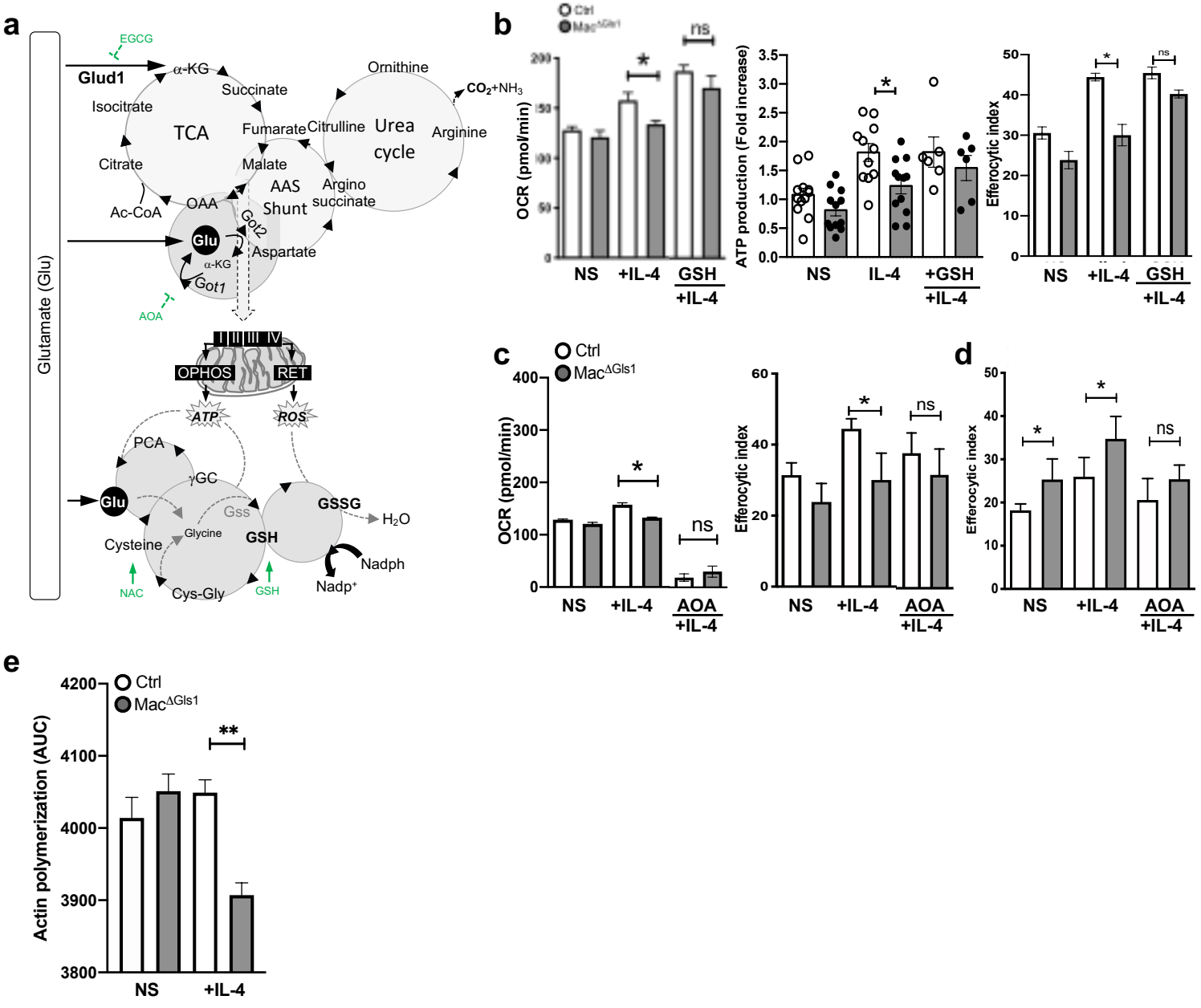

Figure 5: Non-canonical transaminase pathway supports glutamine carbon skeleton metabolism to promote cytoskeletal rearrangement and corpse engulfment. (a) Schematic representation of glutamate incorporation into metabolic cycles. **(b)** OCR quantification (left), ATP production (middle) and efferocytic index (right) in control or Mac$^{\Delta Gls1}$ BMDMs in basal conditions or overnight IL-4 stimulation +/- GSH. **(c)** OCR quantification (left) and efferocytic index (right) in control or Mac$^{\Delta Gls1}$ BMDMs in basal conditions or overnight IL-4 stimulation +/- AOA. **(d)** OCR quantification (left) and efferocytic index (right) in control or Mac$^{\Delta Glud1}$ BMDMs in basal conditions or overnight IL-4 stimulation +/- AOA. **(e)** Actin polymerization assay in control or Mac$^{\Delta Gls1}$ BMDMs in basal condition or following overnight IL-4 stimulation. All values are mean ± SEM and are representative of at least one experiment (n=3-12). **P*<0.05 compared *to control*.

Figure S1

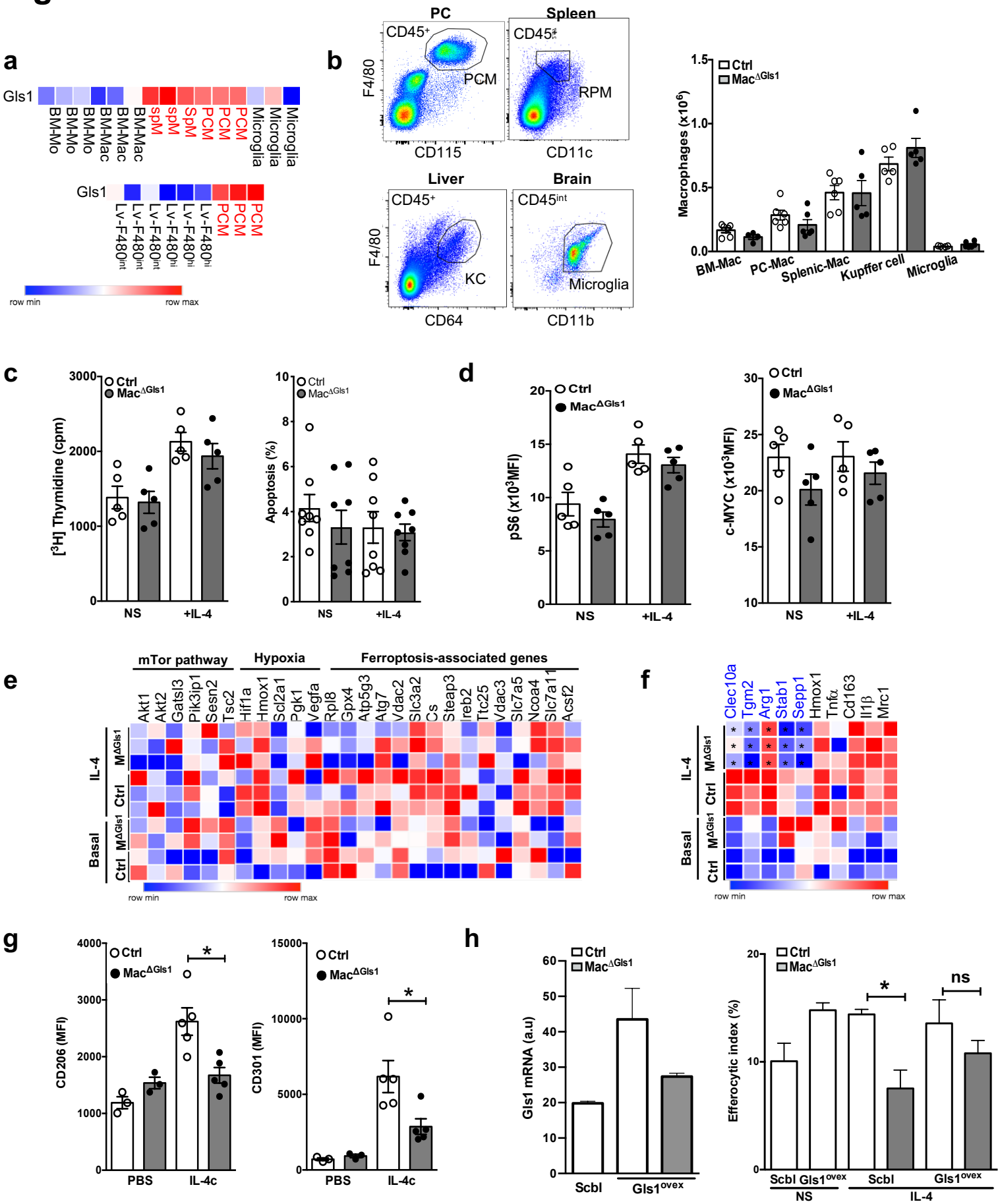
a
Gls1
BM-Mo
BM-Mo
BM-Mo
BM-Mac
BM-Mac
BM-Mac
spM
spM
SpM
PCM
PCM
PCM
Microglia
Microglia
Microglia
Gls1
Lv-F480int
Lv-F480int
Lv-F480int
Lv-F480hi
Lv-F480hi
Lv-F480hi
PCM
PCM
PCM
PCM
row min
row max
b
PC
Spleen
CD45+
PCM
CD45+
RPM
F4/80
CD115
CD11c
Liver
Brain
CD45+
KC
CD45int
Microglia
F4/80
CD64
CD11b
Ctrl
MacΔGls1
Macrophages (x10⁶)
BM-Mac
PC-Mac
Splenic-Mac
Kupffer cell
Microglia
c
Ctrl
MacΔGls1
[³H] Thymidine (cpm)
NS
+IL-4
Apoptosis (%)
d
pS6 (x10³MFI)
c-MYC (x10³MFI)
e
mTor pathway
Hypoxia
Ferroptosis-associated genes
Akt1
Akt2
Gatsl3
Pik3ip1
Sesn2
Tsc2
Hif1a
Hmox1
Scl2a1
Pgk1
Vegfa
Rpl8
Gpx4
Atp5g3
Atg7
Vdac2
Slc3a2
Cs
Steap3
Ireb2
Ttc25
Vdac3
Slc7a5
Ncoa4
Slc7a11
Acsf2
IL-4
Basal
MΔGls1
Ctrl
row min
row max
f
Clec10a
Tgm2
Arg1
Stab1
Sepp1
Hmox1
Tnfα
Cd163
Il1β
Mrc1
g
CD206 (MFI)
PBS
IL-4c
CD301 (MFI)
h
Gls1 mRNA (a.u)
Scbl
Gls1ovex
Efferocytic index (%)
ns
NS
IL-4

Figure S1: GLS1 is dispensable for macrophage homeostasis but supports macrophage effector and clearance functions. (a) Comparative analysis of Gls1 mRNA expression in different macrophage populations from a publicly available dataset (Immgen). **(b)** Macrophage population gating strategy (left) and numbers (right) measured by flow cytometry in multiple mouse tissues (bone marrow, peritoneal cavity, spleen, liver and brain). n= 5-6 **(c)** [^{3}H]-Thymidine incorporation (left) and apoptosis percentage (right) in control or Mac$^{\Delta Gls1}$ BMDMs at steady state or after an overnight stimulation with IL-4. **(d)** Phospho-S6 (left) and c-myc (right) expression measured by flow cytometry in control or Mac$^{\Delta Gls1}$ BMDMs with or without overnight IL-4 stimulation. **(e)** RNAseq of control or Mac$^{\Delta Gls1}$ cell sorted PCMs at steady state or after IL-4 stimulation. **(f)** RNAseq analysis with focus on alternatively activated genes in control or Mac$^{\Delta Gls1}$ PCMs stimulated overnight or not with IL-4. **(g)** CD206 and CD301 expression by flow cytometry in mice injected i.p. with PBS or IL-4-complex. **(h)** qPCR quantification (left) and efferocytic index (right) of Gls1 lentivirus overexpression in control or Mac$^{\Delta Gls1}$ BMDMs stimulated overnight with IL-4. All values are mean ± SEM and are representative of at least one experiment (n=3–13 independent animals). *P<0.05

Figure S2

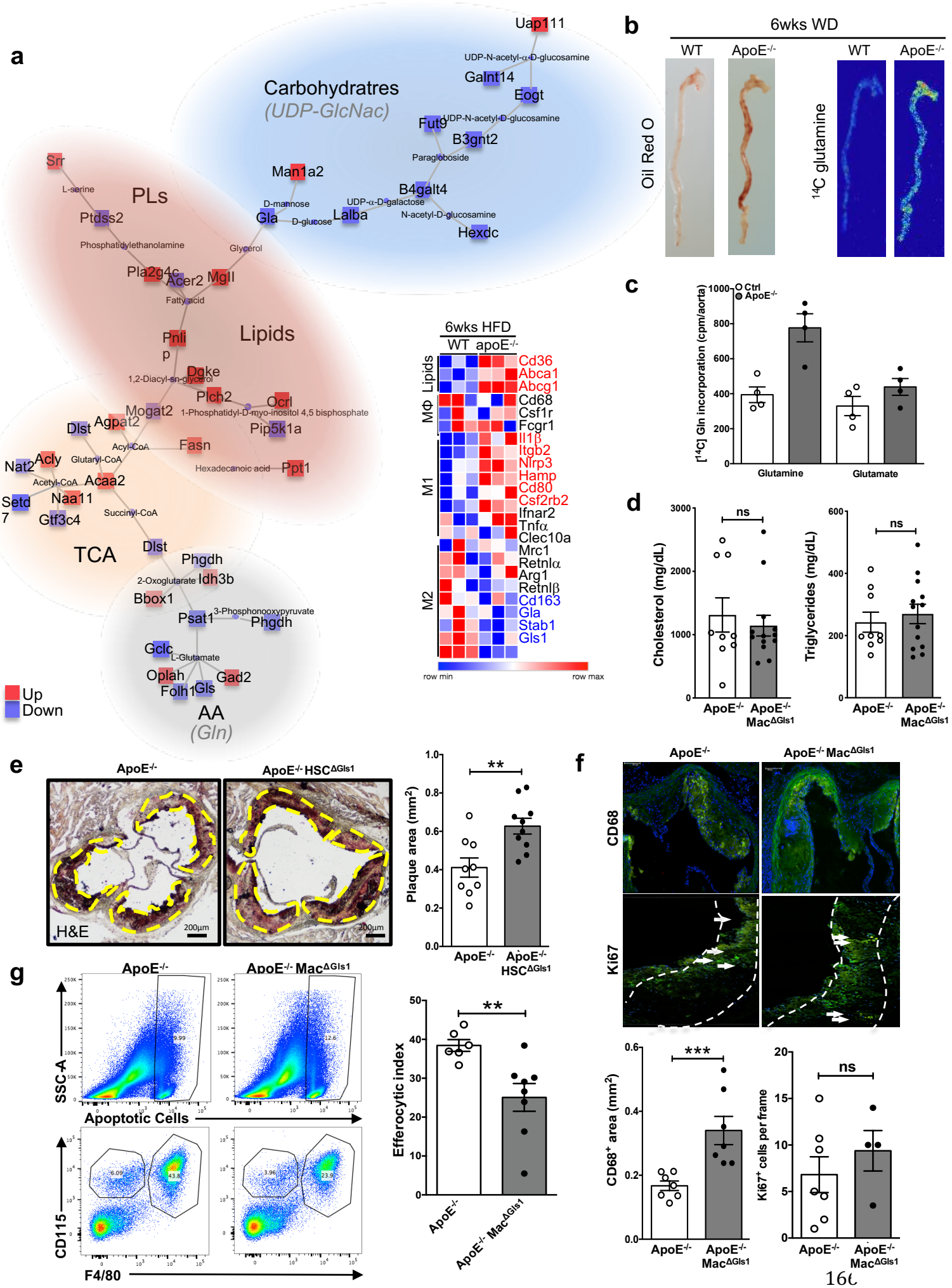
a
Carbohydratres
(UDP-GlcNac)
Uap111
UDP-N-acetyl-α-D-glucosamine
GalNt14
Eogt
UDP-N-acetyl-D-glucosamine
Fut9
B3gnt2
Paraglobboside
Man1a2
B4galt4
D-mannose
UDP-α-D-galactose
Gla
D-glucose
Lalba
N-acetyl-D-glucosamine
Hexdc
Srr
L-serine
PLs
Ptdss2
Phosphatidylethanolamine
Glycerol
Pla2g4c
Acer2
Mgll
Fatty acid
Lipids
Pnlip
Dgke
1,2-Diacyl-sn-glycerol
Plch2
Ocrl
1-Phosphatidyl-D-myo-inositol 4,5 bisphosphate
Mogat2
Dlst
Agpat2
Pip5k1a
Acyl-CoA
Fasn
Nat2
Acly
Glutaryl-CoA
Hexadecanoic acid
Ppt1
Acetyl-CoA
Acaa2
Setd7
Naa11
Gtf3c4
Succinyl-CoA
TCA
Dlst
Phgdh
2-Oxoglutarate
Idh3b
Bbox1
Psat1
3-Phosphonooxypyruvate
Phgdh
Gclc
L-Glutamate
Oplah
Gad2
Folh1
Gls
AA
(Gln)
Up
Down
6wks HFD
WT apoE-/-
Lipids
MΦ
M1
M2
Cd36
Abca1
Abcg1
Cd68
Csf1r
Fcgr1
Il1β
Itgb2
Nlrp3
Hamp
Cd80
Csf2rb2
Ifnar2
Tnfα
Clec10a
Mrc1
Retnlα
Arg1
Retnlβ
Cd163
Gla
Stab1
Gls1
row min
row max
b
6wks WD
WT
ApoE-/-
Oil Red O
14C glutamine
c
Ctrl
ApoE-/-
[14C] Gln incorporation (cpm/aorta)
Glutamine
Glutamate
d
Cholesterol (mg/dL)
Triglycerides (mg/dL)
ns
ApoE-/-
ApoE-/- MacΔGls1
e
ApoE-/-
ApoE-/- HSCΔGls1
H&E
200μm
Plaque area (mm2)
**
ApoE-/-
ApoE-/- HSCΔGls1
f
ApoE-/-
ApoE-/- MacΔGls1
CD68
Ki67
CD68+ area (mm2)
***
Ki67+ cells per frame
ns
g
ApoE-/-
ApoE-/- MacΔGls1
SSC-A
Apoptotic Cells
CD115
F4/80
Efferocytic index
**

Figure S2: Atherosclerosis development relies on GLS1-dependent glutaminolyis. (a) Metabolic pathway (left) and RNAseq analysis (right) of ApoE$^{-/-}$ versus WT mouse aortas (6 weeks on WD) performed with Phantasus software (GSE10000). **(b)** Oil red O staining (left) or ^{14}C glutamine accumulation after i.v. injection (right) in descending aortas extracted from WT and ApoE$^{-/-}$ mice maintained on a WD for 6 weeks. **(c)** ^{14}C glutamine incorporation in aortas obtained from ApoE$^{-/-}$ and ApoE$^{-/-}$ Mac$^{\Delta Gls1}$ mice fed for 6 weeks on WD. **(d)** Cholesterol (left) and triglyceride (right) content in plasma of ApoE$^{-/-}$ and ApoE$^{-/-}$ Mac$^{\Delta Gls1}$ mice. **(e)** Representative sections (left) and quantification (right) of aortic plaques from ApoE$^{-/-}$ or ApoE$^{-/-}$ HSC$^{\Delta Gls1}$ mice (12 weeks WD) stained for Oil Red O and Hematoxylin Eosin. Scale bar: 200□m. **(f)** Representative sections (top) and quantification (bottom) of aortic plaques from ApoE$^{-/-}$ or ApoE$^{-/-}$ Mac$^{\Delta Gls1}$ mice (12 weeks WD) stained for CD68 and Ki67. **(g)** Gating strategy (left) and quantification (right) of PCM efferocytic index in ApoE$^{-/-}$ *and* ApoE$^{-/-}$ Mac$^{\Delta Gls1}$ mice 1-hour after labeled ACs i.p. injection. All values are mean ± SEM and are representative of at least one experiment (n=4–13). ***P*<0.005; ****P*<0.0005 compared *to control*.

Figure S3

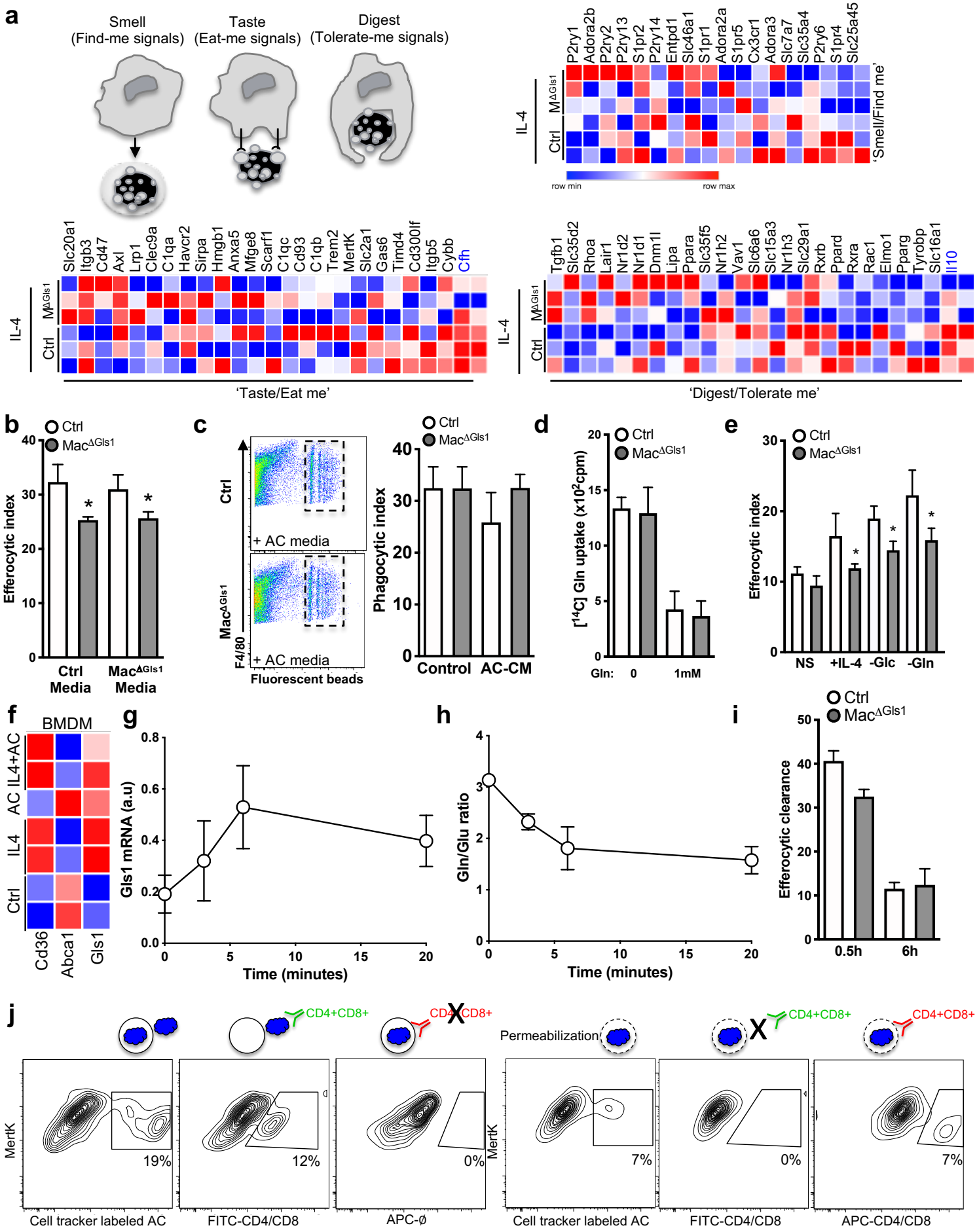
a
Smell
(Find-me signals)
Taste
(Eat-me signals)
Digest
(Tolerate-me signals)
P2ry1 Adora2b P2ry2 P2ry13 S1pr2 P2ry14 Entpd1 Slc46a1 S1pr1 Adora2a S1pr5 Cx3cr1 Adora3 Slc7a7 Slc35a4 P2ry6 S1pr4 Slc25a45
IL-4
MΔGls1
Ctrl
'Smell/Find me'
row min
row max
Slc20a1 Itgb3 Cd47 Axl Lrp1 Clec9a C1qa Havcr2 Sirpa Hmgb1 Anxa5 Mfge8 Scarf1 C1qc Cd93 C1qb Trem2 MertK Slc2a1 Gas6 Timd4 Cd300lf Itgb5 Cybb Cfh
'Taste/Eat me'
Tgfb1 Slc35d2 Rhoa Lair1 Nr1d2 Nr1d1 Dnm1l Lipa Ppara Slc35f5 Nr1h2 Vav1 Slc6a6 Slc15a3 Nr1h3 Slc29a1 Rxrb Ppard Rxra Rac1 Elmo1 Pparg Tyrobp Slc16a1 Il10
'Digest/Tolerate me'
b
Ctrl
MacΔGls1
Efferocytic index
Ctrl Media
MacΔGls1 Media
c
Ctrl
MacΔGls1
+ AC media
F4/80
Fluorescent beads
Phagocytic index
Control
AC-CM
d
[14C] Gln uptake (x10^2cpm)
Gln: 0 1mM
e
Efferocytic index
NS
+IL-4
-Glc
-Gln
f
BMDM
AC IL4+AC
IL4
Ctrl
Cd36
Abca1
Gls1
g
Gls1 mRNA (a.u)
Time (minutes)
h
Gln/Glu ratio
Time (minutes)
i
Efferocytic clearance
0.5h
6h
j
CD4+CD8+
Permeabilization
MertK
19%
12%
0%
7%
0%
7%
Cell tracker labeled AC
FITC-CD4/CD8
APC-Ø
APC-CD4/CD8

Figure S3

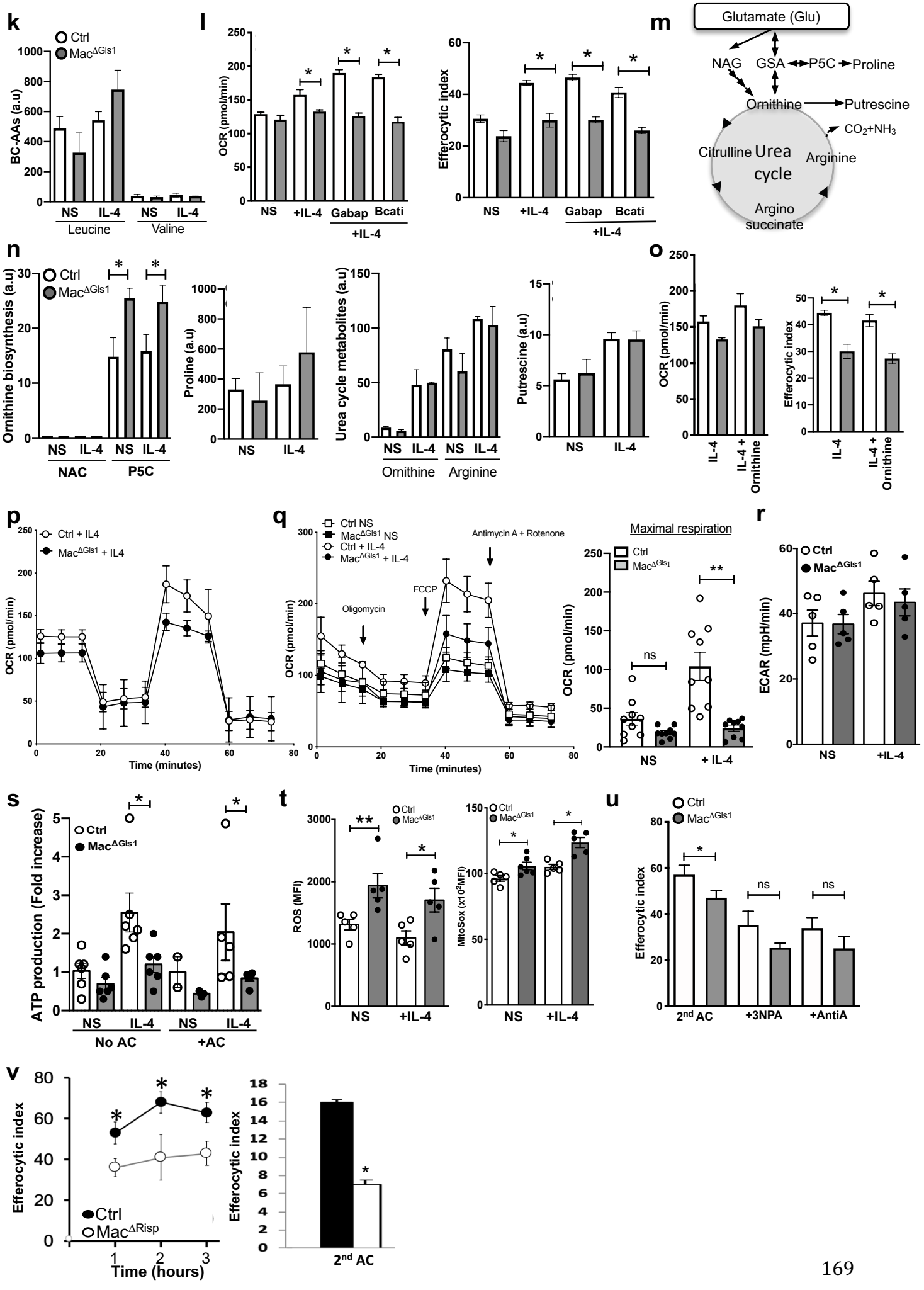
k
Ctrl
MacΔGls1
BC-AAs (a.u)
NS
IL-4
Leucine
Valine
l
OCR (pmol/min)
Efferocytic index
NS
+IL-4
Gabap
Bcati
m
Glutamate (Glu)
NAG
GSA
P5C
Proline
Ornithine
Putrescine
CO2+NH3
Citrulline
Urea cycle
Arginine
Argino succinate
n
Ornithine biosynthesis (a.u)
NAC
P5C
Proline (a.u)
Urea cycle metabolites (a.u)
Ornithine
Arginine
Putrescine (a.u)
o
OCR (pmol/min)
Efferocytic index
IL-4
IL-4 + Ornithine
p
Ctrl + IL4
MacΔGls1 + IL4
OCR (pmol/min)
Time (minutes)
q
Ctrl NS
MacΔGls1 NS
Ctrl + IL-4
MacΔGls1 + IL-4
Antimycin A + Rotenone
FCCP
Oligomycin
Maximal respiration
ns
r
ECAR (mpH/min)
s
ATP production (Fold increase)
No AC
+AC
t
ROS (MFI)
MitoSox (x10²MFI)
u
2nd AC
+3NPA
+AntiA
v
Efferocytic index
Ctrl
MacΔRisp
Time (hours)
2nd AC

Figure S3: Gls1-deficient macrophages have a defect in ATP-dependent corpse engulfment. (a) Schematic representation of efferocytosis steps and RNAseq analysis of "find-me", "eat-me" and "tolerate-me" signals in control and $Mac^{\Delta Gls1}$ PCMs stimulated overnight with IL-4. **(b)** Efferocytic index in control or $Mac^{\Delta Gls1}$ BMDMs stimulated overnight with IL-4 and incubated with either control or $Mac^{\Delta Gls1}$ media during the 45min efferocytosis. **(c)** Beads phagocytosis gating strategy (left) and quantification (right) in control or $Mac^{\Delta Gls1}$ BMDMs stimulated overnight with IL-4 and cultured with either basal or ACs media during the 45min efferocytosis. **(d)** Glutamine uptake in control or $Mac^{\Delta Gls1}$ BMDMs after [^{14}C]-Glutamine exposure. **(e)** Efferocytic index in control or $Mac^{\Delta Gls1}$ BMDMs in either basal condition, overnight IL-4 stimulation, and after a 4-hour glucose or glutamine deprivation. **(f)** Publicly available gene expression datasets analysis of macrophages ingesting apoptotic cells (GSE98169). **(g)** Gls1 mRNA expression and **(h)** Glutamine/Glutamate ratio during efferocytosis in control BMDMs in a time course experiment. **(i)** Clearance of fluorescent apoptotic debris 30min and 6 hours post-efferocytosis in control and $Mac^{\Delta Gls1}$ BMDMs. **(j)** Gating strategy and schematic representation of sealed and unsealed ACs. **(k)** Leucine and Valine levels by liquid chromatography-mass spectrometry in control or $Mac^{\Delta Gls1}$ BMDMs at steady state or after overnight IL-4 stimulation. **(l)** OCR and **(e)** efferocytic index in control or $Mac^{\Delta Gls1}$ BMDMs in basal conditions or stimulated overnight with IL-4 and +/- Gabapentin or Bcat inhibitor. **(m)** Schematic representation of glutamate utilization in the urea cycle. **(n)** Quantification of NAG, P5C, proline, ornithine, arginine and putrescine levels by liquid chromatography-mass spectrometry in control or $Mac^{\Delta Gls1}$ BMDMs in basal condition or following overnight IL-4 treatment. **(o)** OCR quantification (left) and efferocytic index (right) of control or $Mac^{\Delta Gls1}$ BMDMs treated overnight with IL-4 and ornithine. **(p)** OCR measured by Seahorse in control and $Mac^{\Delta Gls1}$ PCMs **(q)** OCR (left) and maximal respiration quantification (left) measured by Seahorse on control or $Mac^{\Delta Gls1}$ BMDMs with or without IL-4 stimulation. **(r)** ECAR measured by Seahorse in control or $Mac^{\Delta Gls1}$ BMDMs with or without overnight IL-4 stimulation. **(s)** ATP production measured by Seahorse in control or $Mac^{\Delta Gls1}$ BMDMs after one or no round of efferocytosis and +/- overnight IL-4 stimulation. **(t)** ROS (left) and Mitosox (right) quantification using flow cytometry in control or $Mac^{\Delta Gls1}$ BMDMs at steady state or following overnight IL-4 stimulation. **(u)** Efferocytic index in control or $Mac^{\Delta Gls1}$ BMDMs after either 2 rounds of efferocytosis or 3NPA +IL-4 or Antimycin A + IL-4 treatments overnight. **(v)** Efferocytic index after one round efferocytosis quantified by microscopy (left) or after two round efferocytosis measured by flow cytometry (right) in control or $Risp^{-/-}$ macrophages. All values are mean ± SEM and are representative of at least one experiment (n=3-9). **P*<0.05, ***P*<0.005 compared *to control*.

Figure S4

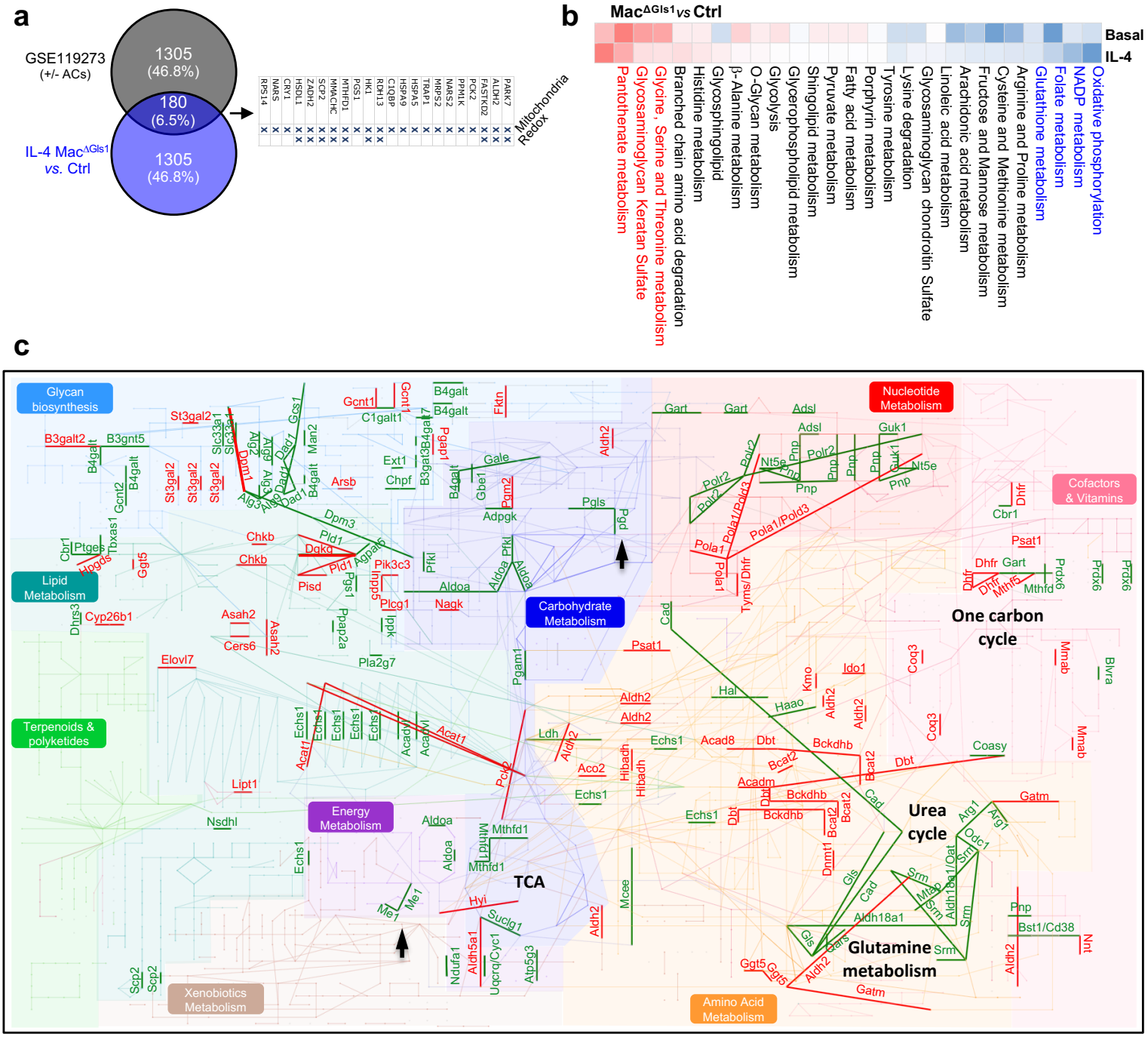
a
GSE119273
(+/- ACs)
1305
(46.8%)
180
(6.5%)
1305
(46.8%)
IL-4 Mac^ΔGls1
vs. Ctrl
RPS14 NARS CRY1 HSDL1 ZADH2 SCP2 MMACHC MTHFD1 PGS1 HK1 CLQBP RDH13 HSPA9 HSPA5 TRAP1 MRPS2 NARS2 PPM1K PCK2 FASTKD2 ALDH2 PARK7
Mitochondria Redox
b
Mac^ΔGls1 vs Ctrl
Basal
IL-4
Pantothenate metabolism
Glycosaminoglycan Keratan Sulfate
Glycine , Serine and Threonine metabolism
Branched chain amino acid degradation
Histidine metabolism
Glycosphingolipid
β-Alanine metabolism
O-Glycan metabolism
Glycolysis
Glycerophospholipid metabolism
Shingolipid metabolism
Pyruvate metabolism
Fatty acid metabolism
Porphyrin metabolism
Tyrosine metabolism
Lysine degradation
Glycosaminoglycan chondroitin Sulfate
Linoleic acid metabolism
Arachidonic acid metabolism
Fructose and Mannose metabolism
Cysteine and Methionine metabolism
Arginine and Proline metabolism
Glutathione metabolism
Folate metabolism
NADP metabolism
Oxidative phosphorylation
c
Glycan biosynthesis
Lipid Metabolism
Terpenoids & polyketides
Xenobiotics Metabolism
Energy Metabolism
Carbohydrate Metabolism
Nucleotide Metabolism
Cofactors & Vitamins
One carbon cycle
Urea cycle
Glutamine metabolism
Amino Acid Metabolism
TCA
d
Ctrl
Mac^ΔGls1
GSH/GSSG ratio
Total glutathione (μM)
NADPH/NADP ratio
NS
+IL-4
IL-4

Figure S4

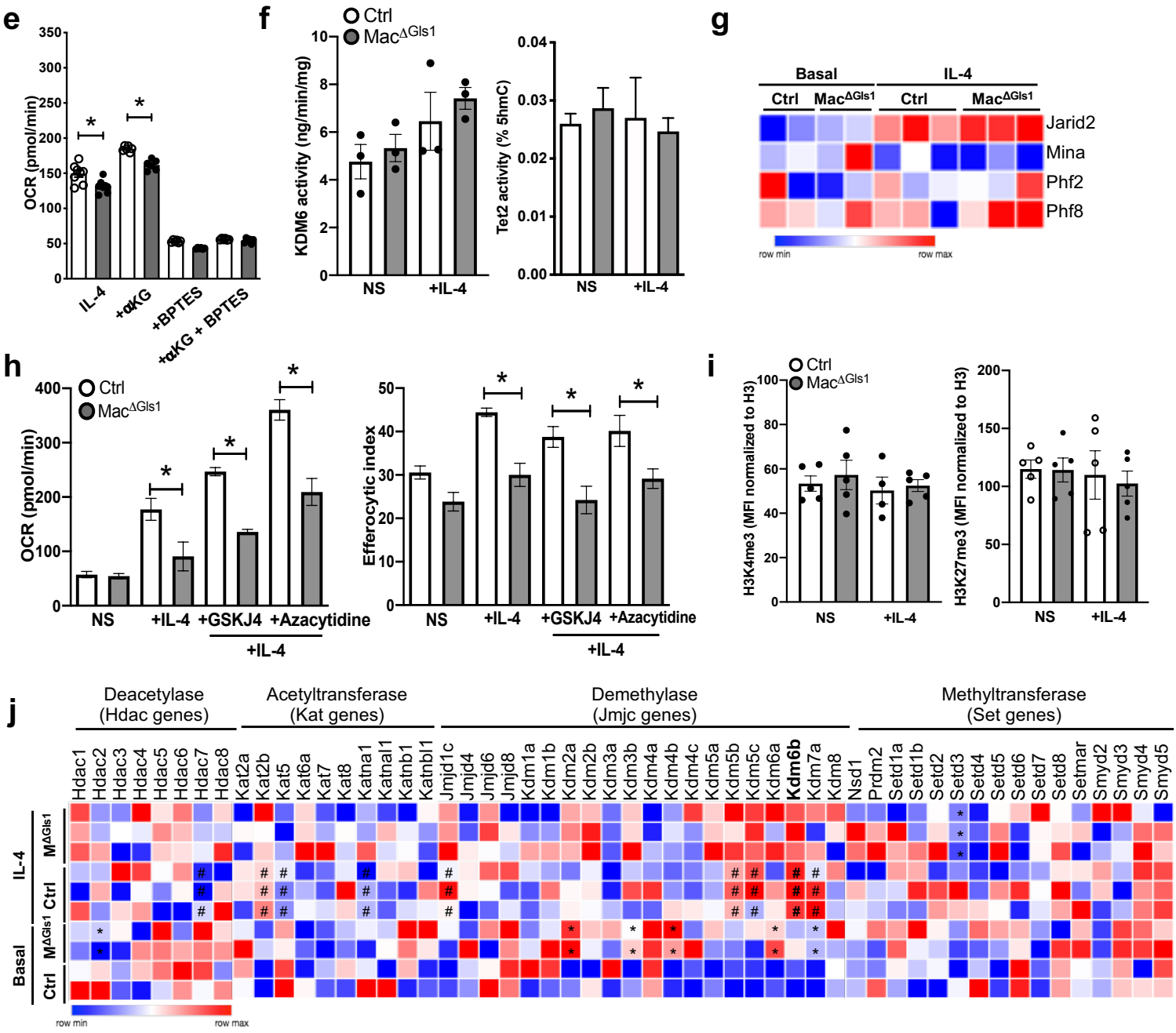
e
OCR (pmol/min)
IL-4
+αKG
+BPTES
+αKG + BPTES
f
Ctrl
MacΔGls1
KDM6 activity (ng/min/mg)
Tet2 activity (% 5hmC)
NS
+IL-4
g
Basal
IL-4
Ctrl
MacΔGls1
Jarid2
Mina
Phf2
Phf8
row min
row max
h
OCR (pmol/min)
Efferocytic index
NS
+IL-4
+GSKJ4
+Azacytidine
i
H3K4me3 (MFI normalized to H3)
H3K27me3 (MFI normalized to H3)
j
Deacetylase (Hdac genes)
Acetyltransferase (Kat genes)
Demethylase (Jmjc genes)
Methyltransferase (Set genes)
Hdac1 Hdac2 Hdac3 Hdac4 Hdac5 Hdac6 Hdac7 Hdac8
Kat2a Kat2b Kat5 Kat6a Kat7 Kat8 Katna1 Katnal1 Katnb1 Katnbl1
Jmjd1c Jmjd4 Jmjd6 Jmjd8 Kdm1a Kdm1b Kdm2a Kdm2b Kdm3a Kdm3b Kdm4a Kdm4b Kdm4c Kdm5a Kdm5b Kdm5c Kdm6a Kdm6b Kdm7a Kdm8
Nsd1 Prdm2 Setd1a Setd1b Setd2 Setd3 Setd4 Setd5 Setd6 Setd7 Setd8 Setmar Smyd2 Smyd3 Smyd4 Smyd5
IL-4
Basal
MΔGls1
Ctrl
row min
row max

Figure S4: GLS1 is essential for macrophage mitochondrial oxidative phosphorylation and redox balance but not epigenetic reprogramming. (a) Venn diagram from publicly available gene datasets (GSE119273). **(b)** Pathway enrichment analysis of RNA-seq profiling in control or $Mac^{\Delta Gls1}$ PCMs in basal conditions or stimulated overnight with IL-4. **(c)** KEGG mapping with DreamBio from RNAseq data of alternatively activated Gls1-deficient or sufficient PCMs. **(d)** GSH/GSSG ratio (left) and total glutathione concentration (middle) in control or $Mac^{\Delta Gls1}$ BMDMs at steady state and NADPH/NADP ratio (right) analyzed by liquid chromatography-mass spectrometry in control or $Mac^{\Delta Gls1}$ BMDMs at steady state or after overnight IL-4 stimulation. **(e)** OCR quantification in control or $Mac^{\Delta Gls1}$ BMDMs stimulated overnight with IL-4 and either □Ketoglutarate, BPTES, or □Ketoglutarate + BPTES. **(f)** KDM6 activity assay (left) and Tet2 activity assay (right) in control or $Mac^{\Delta Gls1}$ BMDMs in basal conditions or stimulated overnight with IL-4. **(g)** RNAseq analysis with focus on KDM6 target genes in control or $Mac^{\Delta Gls1}$ PCMs at steady state or after an overnight stimulation with IL-4. **(h)** OCR quantification (left) and efferocytic index (right) in control or $Mac^{\Delta Gls1}$ BMDMs in basal conditions or after an overnight stimulation with IL-4 and either GSKJ4 or azacytidine. **(i)** Global histone trimethylation modification assessed by flow cytometry using H3K4me3 and H3K27me3 staining in control and $Mac^{\Delta Gls1}$ BMDMs at steady state or stimulated overnight with IL-4. **(j)** RNAseq analysis with focus on epigenetic genes in control or $Mac^{\Delta Gls1}$ PCMs ($M^{\Delta Gls1}$) at steady state or after an overnight stimulation with IL-4. All values are mean ± SEM and are representative of at least one experiment (n=3-8). **P*<0.05 compared *to control*.

Figure S5

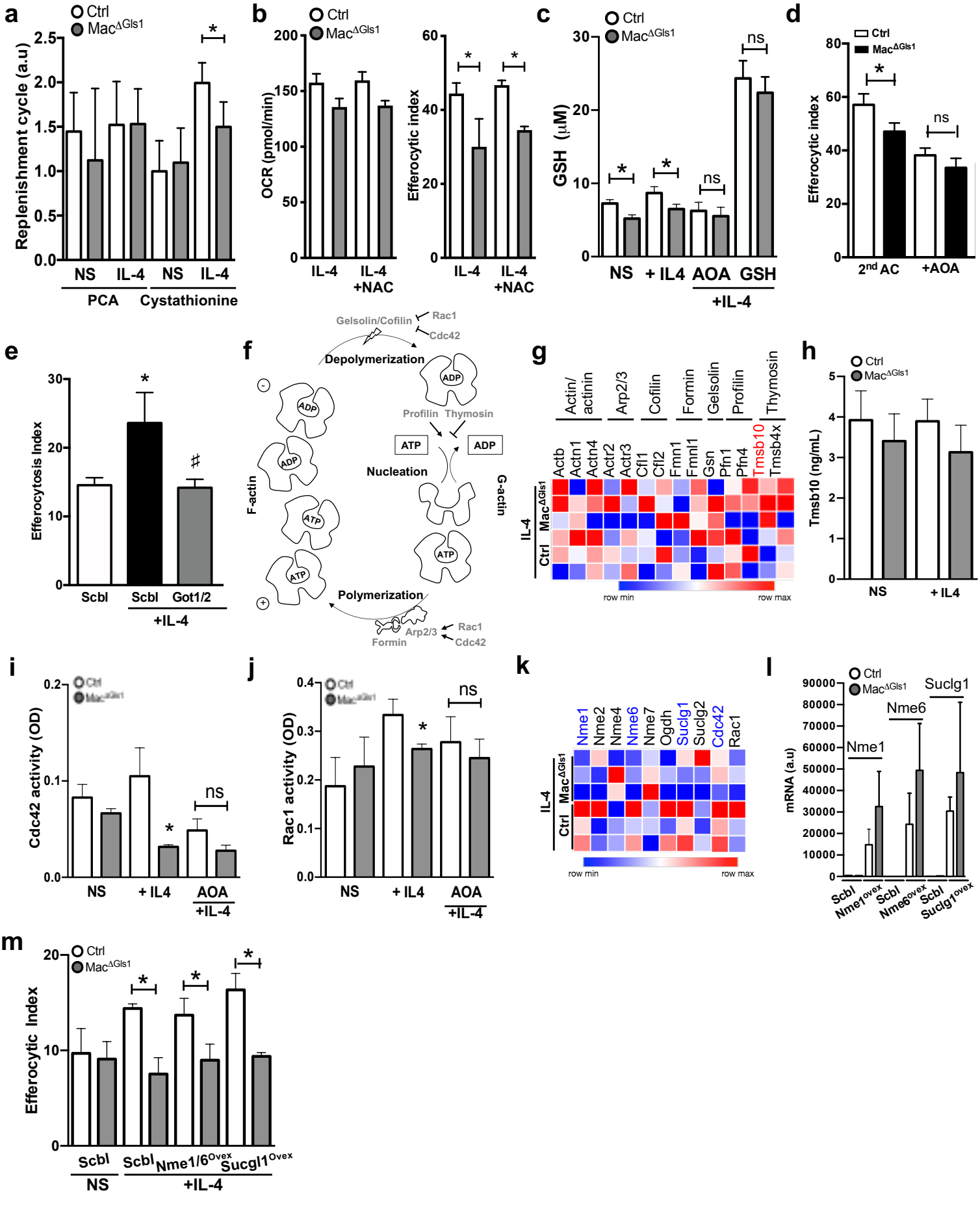
a
Ctrl
Mac^ΔGls1
Replenishment cycle (a.u)
NS
IL-4
NS
IL-4
PCA
Cystathionine
b
OCR (pmol/min)
Efferocytic index
IL-4
IL-4 +NAC
c
GSH (μM)
NS
+ IL4
AOA
GSH
+IL-4
d
Efferocytic index
2nd AC
+AOA
e
Efferocytosis Index
Scbl
Scbl
Got1/2
+IL-4
f
Gelsolin/Cofilin
Rac1
Cdc42
Depolymerization
Profilin
Thymosin
ATP
ADP
Nucleation
F-actin
G-actin
Polymerization
Arp2/3
Formin
g
Actin/ actinin
Arp2/3
Cofilin
Formin
Gelsolin
Profilin
Thymosin
Actb
Actn1
Actn4
Actr2
Actr3
Cfl1
Cfl2
Fmn1
Fmnl1
Gsn
Pfn1
Pfn4
Tmsb10
Tmsb4x
IL-4
Mac^ΔGls1
Ctrl
row min
row max
h
Tmsb10 (ng/mL)
NS
+ IL4
i
Cdc42 activity (OD)
NS
+ IL4
AOA
+IL-4
j
Rac1 activity (OD)
NS
+ IL4
AOA
+IL-4
k
Nme1
Nme2
Nme4
Nme6
Nme7
Ogdh
Suclg1
Suclg2
Cdc42
Rac1
IL-4
Mac^ΔGls1
Ctrl
row min
row max
l
mRNA (a.u)
Nme1
Nme6
Suclg1
Scbl
Nme1^ovex
Scbl
Nme6^ovex
Scbl
Suclg1^ovex
m
Efferocytic Index
Scbl
Scbl
Nme1/6^Ovex
Sucgl1^Ovex
NS
+IL-4

Figure S5: Non-canonical transaminase pathway is essential for actin dynamics and efferocytosis. (a) Effect of Gls1 deficiency on glutathione precursors (PCA, pyroglutamate; cystathionine) as a read out of cellular GSH replenishment. **(b)** OCR quantification (left) and efferocytic index (right) in control or $Mac^{\Delta Gls1}$ BMDMs treated overnight with IL-4 and IL-4 + N-Acetylcysteine (NAC). **(c)** GSH concentration in control or $Mac^{\Delta Gls1}$ BMDMs at steady state or treated overnight with IL-4 and either AOA or GSH. **(d)** Efferocytic index in control or $Mac^{\Delta Gls1}$ BMDMs after either 2 rounds of efferocytosis or AOA + IL-4 overnight treatment. **(e)** Efferocytic index in control or $Mac^{\Delta Gls1}$ BMDMs stimulated overnight or not with IL-4 and transfected with a scramble, or Got1/Got2 siRNA. **(f)** Schematic representation of actin polymerization and depolarization. **(g)** RNAseq analysis with focus on F-actin dynamic regulators in control or $Mac^{\Delta Gls1}$ PCMs stimulated overnight with IL-4. **(h)** Thymosin beta-10 concentration in control or $Mac^{\Delta Gls1}$ BMDMs in basal condition or stimulated overnight with IL-4. **(i)** Cdc42 activity and **(j)** Rac1 activity assay in control or $Mac^{\Delta Gls1}$ BMDMs in basal condition or stimulated overnight with IL-4 +/- AOA. **(k)** RNAseq analysis of ATP-GTP-converting enzymes in control or $Mac^{\Delta Gls1}$ PCMs stimulated overnight with IL-4. **(l)** qPCR quantification and **(m)** efferocytic index of Nme1, Nme6 and Suclg1 lentivirus overexpression in control or $Mac^{\Delta Gls1}$ BMDMs stimulated overnight with IL-4. All values are mean ± SEM and are representative of at least one experiment (n=3-6). **P*<0.05 compared *to control*.

Material and Methods

KEY RESOURCES TABLE

REAGENT or RESOURCE	SOURCE	IDENTIFIER
Antibodies		
Anti-α-actine HRP	Santa Cruz	sc-32251HRP RRID:AB_262054
Anti-CD68 (clone FA-11)	Bio-Rad	MCA1957 RRID:AB_322219
Anti-Glud1	Abcam	ab166618 RRID:AB_2815030.
Anti-Glutaminase	Abcam	ab93434 RRID:AB_10561964
Anti-IL-4 (clone 11B11)	BioXcell	BE0045 RRID:AB_1107707
Anti-Ki67 PE (clone 16A8)	Biolegend	652403 RRID:AB_2561524
Anti-Rat Alexa Fluor 488	ThermoFisher	A-11006 RRID:AB_2534074
c-Myc PE (Clone D84C12)	Cell Signaling	14819S RRID:AB_2798629
CD115 PE (clone AFS98)	eBioscience	12-1152-82 RRID:AB_465808
CD11b Brilliant Violet 510 (cloneM1/70)	Biolegend	101263 RRID:AB_2629529
CD11c APC (clone N418)	BD Biosciences	117309 RRID:AB_313778
CD206 PerCp-Cy5.5 (clone C068C2)	Biolegend	141715 RRID:AB_2561991
CD301 FITC (clone ER-MP23)	Bio-Rad	MCA2392 RRID:AB_872014
CD45 APC-Cy7 (clone 30-F11)	BD Biosciences	557659 RRID:AB_396774
CD64 Brillant Violet 421 (clone X54-5/7.1)	Biolegend	139309 RRID:AB_2562694
F4/80 PE-Cy7 (clone BM8)	Biolegend	123114 RRID:AB_893478
Histone H3 Alexa fluor 647 (clone D1H2)	Cell Signaling	12230S RRID:AB_2797852
ICAM-2 alexa fluor 647 (clone 3C4(MIC2/4))	Biolegend	105612 RRID:AB_2658040
MerTK PE (clone 2B10C42)	Biolegend	151506 RRID:AB_2617037
PD-L2 APC (clone B7-DC)	Biolegend	107210 RRID:AB_2566345
Phalloidine Alexa Fuor 594	InVitrogen	A12381 RRID:AB_2315633
Phospho-S6 Ribosomal Protein (ser235/236) PE (clone D57.2.2E)	Cell Signaling	5316S RRID:AB_10694989
Tri-Methyl-Histone H3 Lys27 Alexa fluor 647 (clone C36B11)	Cell Signaling	12158S RRID:AB_2797834+ E:F
Tri-Methyl-Histone H3 Lys4 Alexa fluor 647 (clone C42D8)	Cell Signaling	12064S RRID:AB_2797813
Chemicals, Peptides, and Recombinant Proteins		
^{13}C glutamine	Sigma	605166
^{14}C glutamine	PerkinElmer	NEC451050UC

^{3}H thymidine	PerkinElmer	NET027E250UC
3NPA	Sigma	164603
aKG	Sigma	349631
Annexin V PE	Biolegend	640908
Antimycin	Sigma	A8674
AOA	Sigma	C13408
Aspartate	Sigma	MAK095
Azacytidine	Sigma	A2385
BCAT inhibitor	Cayman Chemical	9002002
Bovine serum Albumin (BSA)	Sigma	A7030
BPTES	Sigma	SML0601
Cell Trace Violet proliferation kit	ThermoFisher	C34557
CFSE	ThermoFisher	C34570
Collagenase D	Sigma	11088882001
DAPI	Sigma	D9542
Substrate HRP	Sigma	WBKLS0500
EGCG	Sigma	E4143
Eosin	DiaPath	C0363
FCCP	Sigma	C2920
Fetal bovine serum	Fisher Scientific	12350273
Gabapentin	Sigma	G154
GSH	Sigma	G4251
GSK-J4	Sigma	SML0701
HBSS	Fisher Scientific	14175053
Hematoxylin Solution	Sigma	HHS32
High-Capacity cDNA reverse transcription kit	Applied Biosystems	4368814
IL-4	Peprotech	200-04
L-Glutamine	ThermoFisher	25030024
L-ornithine	Sigma	75440
Lipofectamine RNAiMAX	Fisher Scientific	13778150
Lysing buffer	BD Biosciences	555899
M-CSF	Miltenyi	130-101-704
Mitoquinol	Cayman Chemical	89950
MitoSOX Red	Thermofisher	M36008
Mouse Foxp3 Buffer Set	Biosciences	560409
NAC	Sigma	A7250
OCT	TEK	4583-01
Oil Red O	Sigma	O0625
Oligomycin	Sigma	75351
PBS 1X	Fisher Scientific	14190169
Penicillin-Streptomycin	Fisher Scientific	15140130
Percoll	Sigma	P1644
PFA 4%	VWR International	9713.1000
Poly-I:C	Invivogen	TLRL-PIC-5
Protease inhibitor cocktail	Sigma	P8340
RIPA buffer	Cell signaling	9806
RNeasy Plus Mini Kit (250)	QIAGEN	74136
ROS	Thermofisher	C6827

Rotenone	Sigma	R8875
RPMI medium	Fisher Scientific	31870074
Tempol	Sigma	581500
Critical Commercial Assays		
DNA Hydroxymethylation (5-hmC) ELISA	Euromedex	P-1032-96
Glutamine/Glutamate-Glo™ Assay	Promega	J8022
GSH/GSSG-Glo™ Assay	Promega	V6611
KDM6A/ KDM6B Activity	Abcam	ab156910
LabAssay(TM) Cholesterol	Sobioda	W1W294-65801
Rac1 G-LISA	Euromedex	CS-BK128
Triglycerides assay	Diasys	1 5710 99 10021
TUNEL Assay Kit - FITC	Abcam	ab66108
Deposited Data		
RNAseq	NCBI GEO	GEO: GSE to complete
Experimental Models: Organisms/Strains		
Mouse: ApoE KO	Jackson Laboratory	002052 RRID:IMSR_JAX:002052
Mouse: Gls1fl/fl	Pr. Stephen Rayport's lab	N.A.
Mouse: Glud1fl/fl	Pr. Pierre Maechler's lab	N.A.
Mouse: LyzM^{cre}	Jackson Laboratory	004781 RRID:IMSR_JAX:004781
Mouse: Mx1^{cre}	Jackson Laboratory	003556 RRID:IMSR_JAX:003556
Oligonucleotides		
Got1 siRNA	Dharmacon	L-043492-01-0010
Got2 siRNA	Dharmacon	L-043495-01-0010
Scramble siRNA	Dharmacon	D-001810-01-05
Software and Algorithms		
FlowJo	Tree Star	N.A.
ImageJ	NIH	N.A.
Phantasus	http://genome.ifmo.ru/phantasus/	N.A.
Prism8	GraphPad	N.A.
StepOne Software v.2.2.2	Applied Biosystem	N.A.
Other		
Western Diet	Ssniff	TD88137

Human atherosclerosis. Tissue collection was part of the Maastricht Pathology Tissue Collection (MPTC) and further storage and use of the tissue was in line with the Dutch Code for Proper Secondary use of Human Tissue and the local Medical Ethical Committee (protocol number 16-4-181).
Carotid arteries were collected from symptomatic patients undergoing carotid endarterectomy (CEA). Formalin-fixed, paraffin embedded (FFPE) 5mm-segments were alternated with frozen segments for RNA isolation. FFPE segments were then classified as fibrous cap atheroma with or without intraplaque hemorrhage (stable or unstable respectively) according to haematoxylin-eosin (HE) staining.1 Forty-four paired stable and unstable snap-frozen

segments from 22 symptomatic patients undergoing CEA in the Maastricht human plaque study (MaasHPS) were only used for further microarray analysis when both adjacent plaque segments showed the same histological classification. Snap-frozen segments were pulverized and 5-20mg of material was subjected for transcriptomics. RNA isolation was performed by Guanidium Thiocyanate extraction and further purified with the Nucleospin RNA II kit (Macherey-Nagel GmbH&Co). RNA quality and integrity were determined using the Agilent 2100 Bioanalyzer. Biotinylated cRNA was prepared with Illumina TotalPrep RNA Amplification Kit (Ambion, TX, U.S.A) and 750ng cRNA per sample was used for hybridization (Illumina Human Sentrix-8 V2.0, Beadchip®). Scanning was performed on the Illumina Beadstation 500 (Illumina, CA, U.S.A) and image analysis was done using the Illumina Beadstudio v3 Gene expression software. A total of 22,184 human transcripts were analyzed in R Bioconductor lumi package.2 Firstly, a variance stabilizing transformation, which is incorporated in the lumi package, was performed. Secondly, Robust Spline Normalization (RSN) algorithm in lumi package was applied to normalize the data. Differential gene expression analysis was done by using the function lmFit() provided in Limma R package on preprocessed transcriptomics data.3
The 88 adjacent tissue sections were phenotyped extensively for plaque size, necrosis, inflammation (CD68, CD3, arginase, iNOS), SMCs (αSMA), collagen (Sirius red) and angiogenesis (CD31+ microvessel density, newly formed CD105+ microvessels, αSMA+ mature microvessels, Lyve+ lymphatic density). Pearson correlation analysis was performed to assess the association between gene expression and plaque phenotypical traits.

Mice. Gls1$^{fl/fl}$ mice were kindly provided by Pr. Stephen Rayport and have been crossed to Lyz2^{Cre} mice (B6.129P2-Lyz2tm1(cre)Ifo/J, The Jackson Laboratory) or Mx1^{cre} mice (B6.Cg-Tg(Mx1-cre)1Cgn/J) and brought on ApoE-deficient genetic background (B6.129P2-ApoEtm1Unc/J). Mx1^{cre} mice (B6.Cg-Tg(Mx1-cre)1Cgn/J) were also crossed to Glud1 floxed mice (kindly provided by Pr. Pierre Maechler). For each experiment, co-housed littermate controls were used. Animal protocols were approved by the Institutional Animal Care and Use Committee of the French Ministry of Higher Education and Research and the Mediterranean Center of Molecular Medicine (Inserm U1065) and were undertaken in accordance with the European Guidelines for Care and Use of Experimental Animals. Animals had free access to food and water and were housed in a controlled environment with a 12-hour light–dark cycle and constant temperature (22°C). Hyperlipidemia was induced by feeding the mice with a Western diet (TD88137, Ssniff) for 12 weeks. Mice were weighted every two weeks following Western diet induction.

Poly(I:C) induction. Mx1^{cre} mice were i.p. injected with 1mg/mL poly(I:C) three times every two days(Kuhn et al., 1995). Mice were then used for experimentation 3 weeks later.

IL-4c in vivo treatment. Mice were i.p. injected with IL-4 complexed to anti-IL-4 mAb (IL-4c; containing 5 µg of IL-4, PeproTech, and 25 µg of anti-IL-4 clone 11B11, BioXcell). 36 hours later, PCMs were collected and analyzed by flow cytometry.

Cell culture, LPMs and BMDMs generation. BM cells were harvested from mouse femur and tibia and differentiated in the presence of recombinant mouse M-CSF (20 ng/ml; Miltenyi) in complete RPMI 1640 medium (Corning) containing 10mM glucose, 2mM L-glutamine, 100U/ml of penicillin/streptomycin, and 10% FBS for 7 days at 37°C and 5% CO2.

Cell treatments. At day 7 BMDMs were collected, plated and activated overnight as indicated. Peritoneal cells were obtained by peritoneal lavage with 5ml of PBS. Cells were plated and cultured overnight in complete RPMI 1640 medium (Corning) containing 10mM glucose, 2mM L-glutamine, 100U/ml penicillin/streptomycin, and 10% FBS at 37°C and 5% CO2. Cell were incubated overnight with the following treatments: IL-4 (20ng/mL, Peprotech), AOA (200µM, Sigma), Dimethyl-α-ketoglutarate (1mM, Sigma), EGCG (100µM, Sigma), GSH (10mM, Sigma), BPTES (10µM, Sigma), L-ornithine (1mM, Sigma), BCATc inhibitor (20µM, Cayman

Chemical), Gabapentin (10µg/mL, Sigma), GSKJ4 (20µM, Sigma), Azacytidine (100µM, Sigma), 3NPA (1.68mM, Sigma), Antimycin A (0.1µM, Sigma), Tempol (4mM, EMD Millipore), mitoquinol (200nM, Cayman Chemical), NAC (10mM, Sigma), Aspartate (5µg/mL, Sigma). For glutamine and glucose deprivation, glucose or glutamine free media were used, and cells were deprived for 4 hours before the experiments.

siRNA transfection. Cells were transfected with Got1/Got2 siRNA (L-043492-01-0005 and L-043495-01-0005, Dharmacon) or control siRNA (D-001810-01-05, Dharmacon) (referred to as Scbl) at 30 nM using Lipofectamine RNAiMAX (Life Technologies), according to the manufacturer's instructions.

Lentivirus overexpression. Cells were spin-transfected for 90min at 2500 rpm with Gls1, Nme1/Nme6 or suclg1 lentivirus (LVM(VB200119-1197bpk)-C, LVM(VB200120-1064ucb)-C, LVM(VB200120-1213tjc)-C, LVM(VB200120-1214hxx)-C respectively, Vectorbuilder) or control lentivirus (LVM(VB200120-1215tyv)-C, Vectorbuilder) (referred to as Scbl) and used at MOI 10. After 6 hours, cells were washed, and the media replaced with fresh media.

Western Blotting. LPMs were cell-sorted and then lysed in RIPA buffer containing protease inhibitors cocktail (ThermoFisher) and agitated for 1 hour at 4°C before centrifugation at 14000 rpm for 10min at 4°C. Supernatants were sampled and later used for SDS-PAGE. Protein content was evaluated using Pierce™ BCA assay kit (ThermoFisher). Protein samples were resolved on 10% SDS-PAGE gels and were then transferred onto polyvinylidene difluoride membrane using a wet transfer system. Membranes were blocked in 5% (w/v) BSA in Tris-buffered saline-Tween for one hour at room temperature. Membranes were then incubated with primary antibody (anti-Glud1 or anti-Gls1 antibodies (Abcam)) followed by the appropriate horseradish peroxidase-conjugated secondary antibody. Anti α-actin mAb (Santa Cruz) was used as loading control. Proteins were detected by substrate HRP (Sigma).

Analysis of atherosclerotic plaque. Mice were sacrificed and slowly perfused with 10ml of ice-cold PBS. The hearts and aortas were carefully excised and fixed in 4% paraformaldehyde containing 30% sucrose. The aortas were stained with Oil Red O (Sigma- O0625) to evaluate plaque neutral lipid content as previously described (Yun et al., 2017). The hearts were embedded in OCT compound (Gentaur) and stored at –80°C before analysis. 10µm cryosections of the aortic sinus were prepared. Oil Red O staining was used to detect neutral lipid content in the plaque combined with a haematoxylin/eosin staining to analyse tissue architecture. Plaque macrophages were visualized using purified anti-CD68 mAb (clone FA-11, AbD Serotec). Anti-rat Alexa Fluor 488-conjugated antibody (A-11006, Life technologies) was used for detection of CD68 staining. For analysis of plaque macrophage proliferation, anti-Ki67 PE conjugated mAb (clone 16A8, BioLegend) was used. Nuclei were revealed with DAPI counterstaining (2µg/ml). TUNEL staining was performed using the DeadEnd™ Fluorometric TUNEL System (Promega). Plaque area quantification were measured with ImageJ software.

Echography. Animals were fully anesthetized with 1.5% Isoflurane before and during ultrasound scanning. Before all ultrasound scanning, the hair of the mouse chest wall was carefully removed, and warm ultrasound transmission gel was liberally applied to ensure optimal image quality. Echocardiography was performed using a high-frequency Vevo2100 (Visualsonics)-imaging.

Transmission Electronic Microscopy. Cells were observed with transmission electron microscopy (TEM) for ultrastructural analysis. Cells were fixed in a 1.6 % glutataraldehyde solution in 0.1 M sodium phosphate buffer at room temperature (RT) and stored overnight at 4°C. After three rinsing in 0.1 M cacodylate buffer (15 min each), cells were postfixed in a 1 % osmium tetroxide and 1 % potassium ferrocyanide solution in 0.1 M cacodylate buffer for 1 hour at RT. Cells were subsequently dehydrated in a series of acetone baths (90 %, 100% three times, 15 min each) and progressively embedded in Epon 812 resin (acetone / resin 1:1,

100 % resin two times, 2 hours for each bath). Resin blocs were finally left to harden in a 60 °C oven for 2 days. Ultrathin sections (70 nm) were obtained with a Reichert Ultracut S ultramicrotome equipped with a Drukker International diamond knife and collected on 200 mesh copper grids. Sections were stained with lead citrate and uranyl acetate. TEM observations were performed with a JEOL JEM-1400 transmission electron microscope, equipped with a Morada camera, at a 100kV acceleration voltage.

In vitro efferocytosis analysis. BMDMs and PCMs were generated and stimulated as described above.
To generate apoptotic cells (ACs), thymii from C57BL/6J mice were harvested and mechanistically dissociated, filtered on 100µm nylons (Falcon), pelleted and resuspended in RPMI medium supplemented with 10% FBS. Apoptosis was induced by UV exposure at 312nm for 10min and cells were maintained in culture for an additional 2 hours. This method results in 70-90% apoptotis (Yvan-Charvet et al., 2010). ACs were labelled with CellTrace™ Violet Cell Proliferation kit (ThermoFisher) according to the manufacturer's instructions. Fluorescent ACs were washed twice with PBS before use.
For one round efferocytosis: Stained apoptotic cells (ACs) were added at a 5:1 ratio on plated macrophages for 45min.
For two rounds efferocytosis: Unlabelled apoptotic lymphocytes (ACs) were added at a 5:1 ratio on plated macrophages for 45min. Cells were then washed 3 times and macrophages were incubated for 1h. Stained apoptotic lymphocytes (ACs) were then added at a 5:1 ratio on macrophages for 45min.
Cells were washed 3 times and macrophages were stained and analysed for AC content and activation markers by flow cytometry. For Seahorse extracellular flux analysis ACs were injected directly, before drug treatment, during the assay.

Histology. BMDMs and ACs were generated and stimulated as described above. ACs were stained with CellTrace™ CFSE (Invitrogen) for 30min prior to one round efferocytosis. After 15min of efferocytosis, BMDMs were washed with a 37°C heated medium and fixed for 10min at 37°C with 4% paraformaldehyde culture medium. Cells were then saturated for 30min in PBS 10% FBS. Cells were incubated for 30min with Texas Red™-X Phalloidin (Invitrogen). Cells were then washed thoroughly, and coverslips were mounted with aqueous glue. Sections were observed the following day by fluorescent microscopy.

Find-me experiments. To test whether cells had a different ability to sense ACs we applied "taste-me" experiments. BMDMs were generated and stimulated as described above. Immediately before one-round efferocytosis, BMDMs culture medium was either left or inverted between the two genotypes. In the second experiment, immediately before one-round efferocytosis, BMDMs culture medium was either left or replaced by ACs culture medium.

In vivo efferocytosis analysis. ACs were generated as described above. Mice were i.v injected with $2*10^7$ stained ACs and 1 hour later, the spleen and liver were collected and analysed by flow cytometry.

In vitro flow cytometry analysis. Cells were stained for 25 min at 4°C protected from light. For flow cytometry analysis the following list of antibodies was used: MitoSOX™ Red (ThermoFisher), ROS (Thermofisher, CM-H2DCFDA), CD206 PerCp-Cy5.5 conjugated (clone C068C2, BioLegend), PD-L2 APC conjugated (Clone B7-DC, Biolegend), MerTK PE conjugated (clone 2B10C42, BioLegend), CD115 PE conjugated (clone AFS98, eBioscience), CD64 Brillant Violet 421 conjugated (clone X54-5/7.1, BioLegend), F4/80 Pe-Cy7 conjugated (clone BM8, BioLegend), Annexin V (Biolegend), CD4 FITC conjugated (Clone RM4.5), CD8b FITC conjugated (Clone YTS156.7.7). Cells were then washed, centrifuged and data were acquired on BDFACSCanto flow cytometer. Analysis was performed using FlowJo software (Tree Star).

Intracellular flow cytometry. For all intracellular stainings: Phospho-S6 Ribosomal Protein (Ser235/236) PE conjugated (clone D57.2.2E, Cell signaling), c-Myc PE Conjugate (Clone D84C12, Cell signaling), Tri-Methyl-Histone H3 (Lys27) Alexa Fluor® 647 Conjugated (Clone C36B11), Histone H3 (Alexa Fluor® 647 Conjugated (Clone D1H2), Tri-Methyl-Histone H3 (Lys4) Alexa Fluor® 647 conjugated (Clone C42D8), CD4 APC conjugated (Clone RM4.5), CD8b Alexa Fluor® 647 Conjugated (Clone YTS156.7.7). Cells were removed from media, stained for surface, fixed, then stained for intracellular proteins using Foxp3 Transcription Factor Fixation/Permeabilization kit (BD biosciences).

In vivo flow cytometry analysis. Cells were collected from spleen, peritoneal cavity, bone marrow, liver and brain. Splenocytes were extracted by pressing spleens through a stainless-steel grid. Peritoneal and bone marrow leukocytes were harvested by PBS lavage. Liver and brain were cut in small piece and digested for 30min with HBSS medium containing 1,5mg/mL collagenase D (Roche) at 37°C. For liver and microglia preparation, an additional purification step was performed by Percoll gradient. Single-cell suspension was submitted to red blood cell lysis, filtration and centrifugation for 5min at 1,500rpm. Cell suspensions were stained with the appropriate antibodies for 30min on ice protected from light. The following antibodies were used for macrophage flow cytometric analysis: CD11b Brillant Violet 510 conjugated (clone M1/70, BioLegend), CD115 PE conjugated (clone AFS98, eBioscience), CD45 APC-Cy7 conjugated (clone 30-F11, BD Biosciences), CD64 Brillant Violet 421 conjugated (clone X54-5/7.1, BioLegend), CD11c APC conjugated (clone N418, BioLegend), F4/80 Pe-Cy7 conjugated (clone BM8, BioLegend), CD206 PerCp-Cy5.5 conjugated (clone C068C2, BioLegend), CD301 FITC conjugated (clone ER-MP23, Bio-Rad). Cells were then washed, centrifuged and data were acquired on BDFACSCanto flow cytometer. Analysis was performed using FlowJo software (Tree Star).

Seahorse extracellular flux analysis. For extracellular flux assay, 1×10^5 BMDMs or LPMs were plated in a Seahorse Bioscience culture plate. Cells were then incubated overnight with different drugs and metabolites. OCR and ECAR was measured by an XF96 Seahorse Extracellular Flux Analyzer following the manufacturer's instruction. In the seahorse assay, cells were treated with oligomycin (1µM), FCCP (1.5µM), rotenone (1µM) and antimycin A (0.1µM). Each condition was performed in 3 replicates.

RNAseq. PCMs were obtained by lavage as described above. Then cells were stained with CD64 Brilliant Violet 421 conjugated (clone X54-5/7.1), ICAM-2 alexa fluor 647 conjugated (clone 3C4(MIC2/4)) and CD115 PE conjugated (clone AFS98). These antibodies allow us to separate the two subsets of peritoneal macrophages with only the major one expressing ICAM-2 (Gautier et al., 2012; Kim et al., 2016). Cells were cell sorted on BD FacsAria flow cytometer. Total RNA was extracted with RNeasy Mini Kit (Qiagen) according to the manufacturer's protocol and quality was assessed by Nanodrop (Ozyme). Library construction were conducted as described previously (Jha et al., 2015). Libraries were sequenced at the Centre for Applied Genomics (SickKids, Toronto) using a HiSeq 2500 (Illumina).

Integrated network analyses. Network-based integration of metabolite and gene expression datasets was conducted using Shiny Gam as previously described (Jha et al., 2015). We also developed *DreamBio*, a complementary topological tool for Integrated Network Analysis mapped into KEGG pathway. The same strategy than Shiny Gam was used by downloading KEGG REACTION, KEGG ENZYME, KEGG COMPOUND, and KEGG GLYCAN databases (August 2013 version) except that GEPHI GEXF (graph exchange format) was converted from KGML to be analyzed through Sigma library js dedicated to graph drawing. Up and down regulated metabolic genes based on p values calculated with Phantasus (Jha et al., 2015) were mapped into models maintaining all essential KEGG pathway attributes. DreamBio will become soon freely available at http://dreamsession.com/biotest/bioinfo/index.php?w=sigma.

Fluxomics. Metabolite extraction of BMDMs was performed on 2.5 million cells per well using 70°C aqueous 70% ethanol as described previously (Devos et al., 2019). At collection, cells were placed immediately on ice, the media was removed, and cells were washed three times with ice-cold PBS to remove residual media. Intracellular metabolites were extracted twice with hot ethanol. For LCMS, samples where dried under nitrogen flow and reconstituted in a milliQ water/acetonitrile (1:1) mixture for injection using a UPLC Acquity (Waters) separation system coupled with a Xevo G2 ToF (Waters). Compounds were ionized using an electrospray ionization source in negative mode. Data processing was performed in MATLAB (Mathworks, Inc.) using a custom-made in-house protocol. Compound identification was performed using both retention time of authentic standards and accurate mass with an accepted deviation of 0.005 Da. Raw data was converted to netCDF format using Chemstation (Agilent), before processing in MATLAB R2014b (Mathworks, Inc.) using PARADISe software. All MS sample processing and analysis were performed by MS-Omics, Inc. (Copenhagen, Denmark).

Metabolomics. Metabolomics analyses were performed at CriBioM as previously described (Aidoud et al., 2018). Briefly, control and Gls1-deficient BMDMs were treated with or without 20ng/mL IL-4 as indicated in the figure legends. Metabolites were extracted by exposing cells to cold methanol and analyzed by LC-MS.

Typhoon™ Biomolecular Imager. 2µCi of [^{14}C]-labelled glutamine were i.v. injected and mice were sacrificed 15 minutes later. Aortas were harvested and the associated adipose tissue was carefully dissected and removed. Imaging for [^{14}C]-labelled glutamine was performed on Typhoon™ Biomolecular Imager (Amersham). Whole mount staining with Oil Red O paralleled this analysis on the same samples.

Thin-Layer Chromatography (TLC). Aortic tissues were homogenized with 5% HClO4 solution and the radioactivity incorporated in this extract was measured before being dropped on silica-gel POLYGRAM precoated TLC sheets (Sigma). Separation of ^{14}C glutamine and the ^{14}C glutamine-derived glutamate was achieved in hexane/diethylether/formic acid (80:20:1 v/v/v) running buffer. The radioactivity was quantified and expressed as a percentage of ingested radioactivity.

[^{14}C]- Glutamine incorporation. BMDMs were generated and stimulated as described above. Four hours before the experiment, cells were deprived in glutamine or put in presence of medium containing 1mM glutamine. [^{14}C]-Glutamine (1µCi) was added on cells for 18 hours. Cells were collected, centrifuged, washed with PBS, and resuspended in NaOH (0.1N)/SDS (0,1%) before adding scintillation.

[^{3}H]-Thymidine incorporation. BMDMs were generated and stimulated as described above. The day before the experiment, cells were stimulated overnight with IL-4 (20ng/µL). [^{3}H]-Thymidine (1µCi) was added on cells in regular media for 2 hours. Cells were collected, centrifuged, washed with PBS, and resuspended in NaOH (0.1N)/SDS (0,1%) before adding scintillation.

Glutamine and glutamate measurement. To analyse macrophage glutamine and glutamate content we used a commercially available kit Glutamine/Glutamate-Glo™ Assay (Promega) in accordance with the manufacturer's instructions. Briefly, BMDMs and PCMs were incubated as previously described and washed three times with PBS to remove remaining cell culture medium. Cells were then subjected to osmotic lysis with DI water before following the manufacturer's instructions.

Plasma cholesterol and triglycerides content. Plasma cholesterol and triglyceride content was measured with LabAssayTM Cholesterol (Sobioda) and Triglycerides Reagent (Diasys) according to the manufacturer's protocol.

Intracellular GSH/GSSG assay. The reduced glutathione (GSH)/ oxidized glutathione (GSSG) balance was determined using GSH/GSSG-Glo™ Assay (Promega) according to the manufacturer's instructions.

Rac1 and Cdc42 activity assay. Rac1 and Cdc42 activities were determined with Rac1 G-LISA Activation Assay Kit (Cytoskeleton BK128) and Cdc42 G-LISA Activation Assay Kit (Cytoskeleton BK127) according to the manufacturer's instructions.

G-Actin/F-Actin assay. G-Actin/F-Actin activity was determined with G-Actin/F-Actin In Vivo Assay Biochem Kit (Cytoskeleton) according to the manufacturer's instructions.

Actin polymerization assay. Actin polarization activity was determined with Actin Polymerization Biochem Kit (Cytoskeleton) according to the manufacturer's instructions.

KDM6 activity assay. KDM6 activity was determined with KDM6A/ KDM6B Activity Quantification Assay Kit (Abcam) according to the manufacturer's instructions.

Tet2 activity assay. Tet2 activity was determined with MethylFlash Global DNA Hydroxymethylation (5-hmC) ELISA Easy Kit (Epigentek) according to the manufacturer's instructions.

Real-Time qPCR. Total RNA was isolated using the RNeasy Plus Mini kit (QIAGEN) and quantified using a Nanodrop (Ozyme). cDNA was prepared using 10 ng/µl total RNA by a RT-PCR using a high capacity cDNA reverse transcription kit (Applied Biosystems), according to the manufacturer's instructions. Real-time qPCR was performed on cDNA using SYBR Green. qPCRs were performed on StepOne device from Applied Biosystem (France). Samples were performed in triplicates. Results are expressed in arbitrary units. Gls1 (GCACATTATTCACCCGGTAACC; CTGCCCACCCACCATCC, Thermofisher)

Statistics. Data are expressed as mean+/- SEM. Statistical analysis was performed using a 2-tailed t test or ANOVA (with Tukey's post-test analysis) with GraphPad Prism software. A P value ≤ 0.05 was considered as statistically significant.

Acknowledgments. We thank Béatrice Caraveo for computional development of DreamBio, a novel topological tool for Integrated Network Analysis. We thank Samantha Fernandez for the non-invasive study of atheroma plaques by ultrasound echography as part of the European Center for Research in Imaging (Cerimed), Dr Fréderic Labret for assistance with flow cytometry, Dr Véronique Corcelle for assistance in animal facilities and Dr. Marie Irondelle for assistance with confocal microscopy.

Financial support and sponsorship. This work was supported by grants from the Fondation de France (FDF) and the European Research Council (ERC) consolidator program (ERC2016COG724838) to L.Y.C. CCMA electron microscopy equipments have been funded by the Région Sud - Provence-Alpes-Côte d'Azur, the Conseil Départemental des Alpes Maritimes, and the GIS-IBiSA

Conflict of interest: The authors have declared that no conflict of interest exists.

References

A-Gonzalez, N., Bensinger, S.J., Hong, C., Beceiro, S., Bradley, M.N., Zelcer, N., Deniz, J., Ramirez, C., Díaz, M., Gallardo, G., de Galarreta, C.R., Salazar, J., Lopez, F., Edwards, P., Parks, J., Andujar, M., Tontonoz, P., Castrillo, A. Apoptotic cells promote their own clearance and immune tolerance through activation of the nuclear receptor LXR. Immunity. 2009 Aug 21;31(2):245-58.

Aidoud, N., Delplanque, B., Baudry, C., Garcia, C., Moyon, A., Balasse, L., Guillet, B., Antona, C., Darmaun, D., Fraser, K., et al. (2018). A combination of lipidomics, MS imaging, and PET scan imaging reveals differences in cerebral activity in rat pups according to the lipid quality of infant formulas. FASEB J *32*, 4776-4790.

Aspenström, P. (2004). Integration of signalling pathways regulated by small GTPases and calcium. Biochim Biophys Acta *1742*, 51-8.

Bauer, T.M., Murphy, E. (2020). Role of Mitochondrial Calcium and the Permeability Transition Pore in Regulating Cell Death. Circ Res *126*, 280-293.

Boissan M, Schlattner U, Lacombe ML. The NDPK/NME superfamily: state of the art. Lab Invest. 2018 Feb;98(2):164-174.

Bosurgi, L., Cao, Y.G., Cabeza-Cabrerizo, M., Tucci, A., Hughes, L.D., Kong, Y., Weinstein, J.S., Licona-Limon, P., Schmid, E.T., Pelorosso, F., et al. (2017). Macrophage function in tissue repair and remodeling requires IL-4 or IL-13 with apoptotic cells. Science *356*, 1072-1076.

Caron, E., Hall, A. (1998). Identification of two distinct mechanisms of phagocytosis controlled by different Rho GTPases. Science *282*, 1717-21.

Chandel, N.S. (2015). Evolution of Mitochondria as Signaling Organelles. Cell Metab *22*, 204-206.

DeBerardinis, R.J., and Cheng, T. (2010). Q's next: the diverse functions of glutamine in metabolism, cell biology and cancer. Oncogene *29*, 313-324.

Devos, M., Mogilenko, D.A., Fleury, S., Gilbert, B., Becquart, C., Quemener, S., Dehondt, H., Tougaard, P., Staels, B., Bachert, C., et al. (2019). Keratinocyte Expression of A20/TNFAIP3 Controls Skin Inflammation Associated with Atopic Dermatitis and Psoriasis. J Invest Dermatol *139*, 135-145.

Dixon, S.J., Lemberg, K.M., Lamprecht, M.R., Skouta, R., Zaitsev, E.M., Gleason, C.E., Patel, D.N., Bauer, A.J., Cantley, A.M., Yang, W.S., et al. (2012). Ferroptosis: an iron-dependent form of nonapoptotic cell death. Cell *149*, 1060-1072.

Elliott, M.R., and Ravichandran, K.S. (2016). The Dynamics of Apoptotic Cell Clearance. Dev Cell *38*, 147-160.

Fan, J., Ye, J., Kamphorst, J.J., Shlomi, T., Thompson, C.B., and Rabinowitz, J.D. (2014). Quantitative flux analysis reveals folate-dependent NADPH production. Nature *510*, 298-302.

Gautier, E.L., Shay, T., Miller, J., Greter, M., Jakubzick, C., Ivanov, S., Helft, J., Chow, A., Elpek, K.G., Gordonov, S., et al. (2012). Gene-expression profiles and transcriptional regulatory pathways that underlie the identity and diversity of mouse tissue macrophages. Nat Immunol *13*, 1118-1128.

Grabner, R., Lotzer, K., Dopping, S., Hildner, M., Radke, D., Beer, M., Spanbroek, R., Lippert, B., Reardon, C.A., Getz, G.S., et al. (2009). Lymphotoxin beta receptor signaling promotes tertiary lymphoid organogenesis in the aorta adventitia of aged ApoE-/- mice. J Exp Med *206*, 233-248.

Han, C.Z., and Ravichandran, K.S. (2011). Metabolic connections during apoptotic cell engulfment. Cell *147*, 1442-1445.

Jais, A., Einwallner, E., Sharif, O., Gossens, K., Lu, T.T., Soyal, S.M., Medgyesi, D., Neureiter, D., Paier-Pourani, J., Dalgaard, K., et al. (2014). Heme oxygenase-1 drives metaflammation and insulin resistance in mouse and man. Cell *158*, 25-40.

Jha, A.K., Huang, S.C., Sergushichev, A., Lampropoulou, V., Ivanova, Y., Loginicheva, E., Chmielewski, K., Stewart, K.M., Ashall, J., Everts, B., et al. (2015). Network integration of parallel metabolic and transcriptional data reveals metabolic modules that regulate macrophage polarization. Immunity *42*, 419-430.

Johnson, M.O., Wolf, M.M., Madden, M.Z., Andrejeva, G., Sugiura, A., Contreras, D.C., Maseda, D., Liberti, M.V., Paz, K., Kishton, R.J., Johnson, M.E., de Cubas, A.A., Wu, P., Li, G., Zhang, Y., Newcomb, D.C., Wells, A.D., Restifo, N.P., Rathmell, W.K., Locasale, J.W., Davila, M.L., Blazar, B.R., Rathmell, J.C. Distinct Regulation of Th17 and Th1 Cell Differentiation by Glutaminase-Dependent Metabolism. Cell. 2018 Dec 13;175(7):1780-1795.e19.
Kim, K.W., Williams, J.W., Wang, Y.T., Ivanov, S., Gilfillan, S., Colonna, M., Virgin, H.W., Gautier, E.L., and Randolph, G.J. (2016). MHC II+ resident peritoneal and pleural macrophages rely on IRF4 for development from circulating monocytes. J Exp Med *213*, 1951-1959.
Kojima, Y., Weissman, I.L., and Leeper, N.J. (2017). The Role of Efferocytosis in Atherosclerosis. Circulation *135*, 476-489.
Kuhn, R., Schwenk, F., Aguet, M., and Rajewsky, K. (1995). Inducible gene targeting in mice. Science *269*, 1427-1429.
Liu, P.S., Wang, H., Li, X., Chao, T., Teav, T., Christen, S., Di Conza, G., Cheng, W.C., Chou, C.H., Vavakova, M., et al. (2017). alpha-ketoglutarate orchestrates macrophage activation through metabolic and epigenetic reprogramming. Nat Immunol *18*, 985-994.
Marei, H., Malliri, A. GEFs: Dual Regulation of Rac1 Signaling. Small GTPases. 2017 Apr 3;8(2):90-99.
Morioka, S., Perry, J.S.A., Raymond, M.H., Medina, C.B., Zhu, Y., Zhao, L., Serbulea, V., Onengut-Gumuscu, S., Leitinger, N., Kucenas, S., et al. (2018). Efferocytosis induces a novel SLC program to promote glucose uptake and lactate release. Nature *563*, 714-718.
Nicklin, P., Bergman, P., Zhang, B., Triantafellow, E., Wang, H., Nyfeler, B., Yang, H., Hild, M., Kung, C., Wilson, C., et al. (2009). Bidirectional transport of amino acids regulates mTOR and autophagy. Cell *136*, 521-534.
O'Neill, L.A., and Artyomov, M.N. Itaconate: the poster child of metabolic reprogramming in macrophage function. Nat Rev Immunol. 2019 May;19(5):273-281
O'Neill, L.A., and Pearce, E.J. (2016). Immunometabolism governs dendritic cell and macrophage function. J Exp Med *213*, 15-23.
Papathanassiu, A.E., Ko, J.H., Imprialou, M., Bagnati, M., Srivastava, P.K., Vu, H.A., Cucchi, D., McAdoo, S.P., Ananieva, E.A., Mauro, C., Behmoaras, J. BCAT1 controls metabolic reprogramming in activated human macrophages and is associated with inflammatory diseases. Nat Commun. 2017 Jul 12;8:16040.
Stipanuk, M.H and Caudill, M.A. Biochemical, physiological and molecular aspects of human nutrition. 2013 International Book Number: 978-0-323-44181-0.
Tabas, I. (2010). Macrophage death and defective inflammation resolution in atherosclerosis. Nat Rev Immunol *10*, 36-46.
Tavakoli, S., Downs, K., Short, J.D., Nguyen, H.N., Lai, Y., Jerabek, P.A., Goins, B., Toczek, J., Sadeghi, M.M., Asmis, R. Characterization of Macrophage Polarization States Using Combined Measurement of 2-Deoxyglucose and Glutamine Accumulation: Implications for Imaging of Atherosclerosis. Arterioscler Thromb Vasc Biol. 2017 Oct;37(10):1840-1848.
Vats, D., Mukundan, L., Odegaard, J.I., Zhang, L., Smith, K.L., Morel, C.R., Wagner, R.A., Greaves, D.R., Murray, P.J., and Chawla, A. (2006). Oxidative metabolism and PGC-1beta attenuate macrophage-mediated inflammation. Cell Metab *4*, 13-24.
Viaud, M., Ivanov, S., Vujic, N., Duta-Mare, M., Aira, L.E., Barouillet, T., Garcia, E., Orange, F., Dugail, I., Hainault, I., Stehlik, C., Marchetti, S., Boyer, L., Guinamard, R., Foufelle, F., Bochem, A., Hovingh, K.G., Thorp, E.B., Gautier, E.L., Kratky, D., Dasilva-Jardine, P., Yvan-Charvet, L. Lysosomal Cholesterol Hydrolysis Couples Efferocytosis to Anti-Inflammatory Oxysterol Production. Circ Res. 2018 May 11;122(10):1369-1384.
Wang, Y., Subramanian, M., Yurdagul, A. Jr., Barbosa-Lorenzi, V.C., Cai, B., de Juan-Sanz, J., Ryan, T.A., Nomura, M., Maxfield, F.R., Tabas, I. Mitochondrial Fission Promotes the Continued Clearance of Apoptotic Cells by Macrophages. Cell. 2017 Oct 5;171(2):331-345.e22.
Yurdagul, A Jr., Subramanian, M., Wang, X., Crown, S.B., Ilkayeva, O.R., Darville, L., Kolluru, G.K., Rymond, C.C., Gerlach, B.D., Zheng, Z., et al. (2020). Macrophage Metabolism of

Apoptotic Cell-Derived Arginine Promotes Continual Efferocytosis and Resolution of Injury. Cell Metab *31*, 518-533.e10.
Yun, T.J., Lee, J.S., Shim, D., Choi, J.H., and Cheong, C. (2017). Isolation and Characterization of Aortic Dendritic Cells and Lymphocytes in Atherosclerosis. Methods Mol Biol *1559*, 419-437.
Yvan-Charvet, L., Pagler, T.A., Seimon, T.A., Thorp, E., Welch, C.L., Witztum, J.L., Tabas, I., and Tall, A.R. (2010). ABCA1 and ABCG1 protect against oxidative stress-induced macrophage apoptosis during efferocytosis. Circ Res *106*, 1861-1869.
Zhang, S., Weinberg, S., DeBerge, M., Gainullina, A., Schipma, M., Kinchen, J.M., Ben-Sahra, I., Gius, D.R., Yvan-Charvet, L., Chandel, N.S., et al. (2019). Efferocytosis Fuels Requirements of Fatty Acid Oxidation and the Electron Transport Chain to Polarize Macrophages for Tissue Repair. Cell Metab *29*, 443-456 e445.

Discussion

Au cours des maladies cardio-métaboliques comme l'obésité et l'athérosclérose, le métabolisme des macrophages est modifié et joue un rôle majeur sur le développement ou la résolution de la pathologie. Notre étude démontre pour la première fois la fonction *in vivo* de la glutaminolyse des macrophages au cours des maladies cardio-métaboliques. Les résultats sont récapitulés dans les figures 25 et 26 du manuscrit.

I- Rôle de la glutaminolyse des macrophages au cours de l'obésité

Au cours de l'obésité, le nombre de macrophages dans le tissu adipeux augmente et conduit à une inflammation chronique de bas grade favorisant le développement d'une résistance à l'insuline (Bigornia et al., 2012; Lumeng et al., 2007b; Wentworth et al., 2010). En effet, ces macrophages acquièrent un phénotype métabolique contribuant à l'accroissement des lésions et de l'inflammation (Kratz et al., 2014). Des études comparatives ont mis en évidence que le taux de glutamine plasmatique corrélait négativement avec le développement du diabète de type 2 chez l'adulte et de l'obésité chez l'enfant (Cheng et al., 2012; Wahl et al., 2012). Nous nous sommes ainsi intéressés au rôle de la glutaminolyse des macrophages au cours de l'obésité.

Dans notre étude, nous avons pu montrer qu'après 12 semaines de régime riche en graisses, les souris déficientes pour Gls1 dans les macrophages acquièrent un défaut morphologique au niveau du tissu adipeux blanc. En effet, le TA blanc de ces souris devient plus gros et contient plus de macrophages. Nous avons également observé une altération de la polarisation alternative de ceux-ci, et une augmentation des « crown like structures », suggérant une inflammation locale accrue. Ces résultats sont en accord avec les travaux récents de Petrus *et al.*, montrant que la glutamine dans le TA blanc est un régulateur immuno-métabolique jouant sur l'inflammation et l'obésité chez l'Homme (Petrus et al., 2020). Nos travaux établissent ainsi le lien étroit entre les macrophages et les adipocytes dans le TA blanc et les effets de l'environnement local sur les adipocytes. Dans notre étude, il serait intéressant de supplémenter les souris en glutamate afin de regarder si cela restaure

l'activation des macrophages et diminue l'inflammation et l'expansion du TA qui s'en suit. Afin de cibler spécifiquement les macrophages, nous pourrions développer des modèles permettant l'incorporation du glutamate au sein de liposomes ou dans des particules de glucane (Barreby et al., 2019). Bien que risquée, cette approche pourrait nous permettre de restaurer l'utilisation du glutamate dans les macrophages au cours du développement de l'obésité. Ainsi, la régulation du statut inflammatoire des macrophages *in vivo* pourrait contribuer à l'amélioration de l'obésité.

Outre les effets métaboliques au niveau du TA blanc, nos travaux mettent en lumière un effet plus large de la glutaminolyse sur les dépôts adipeux. En effet, les souris déficientes pour Gls1 dans les macrophages présentent une intolérance au glucose causée essentiellement par une diminution de l'utilisation du glucose par le TA brun. Dans notre modèle, la diminution de l'absorption du glucose conduit à une altération de la thermogenèse non frissonnante comme montré précédemment (Labbe et al., 2016; Orava et al., 2011; Ouellet et al., 2012; Putri et al., 2015).

Les macrophages alternativement activés ont dans un premier temps été montrés comme source des catécholamines, pouvant agir sur le TA brun et le TA sous-cutané *via* les récepteurs β adrénergiques pour soutenir la thermogenèse (Nguyen et al., 2011). Cependant, des travaux plus récents ont remis en question ces données en démontrant que les macrophages n'expriment pas la Tyrosine hydroxylase (Th), l'enzyme limitante de la synthèse de catécholamines (Fischer et al., 2017; Wolf et al., 2017), et que le traitement chronique *in vivo* d'IL-4 ne permet pas d'améliorer la thermogenèse (Fischer et al., 2017). Nos travaux sont en accord avec ces derniers et mettent en évidence un défaut de la thermogenèse indépendamment de l'activation des macrophages du TA brun.

Au sein du TA brun, les macrophages sont en contact avec des neurones sympathiques qui relarguent de la norépinephrine (NE), une catécholamine capable de stimuler la thermogenèse (Wolf et al., 2017). Les macrophages associés aux neurones sont capables d'internaliser et dégrader la NE au cours de l'obésité (Pirzgalska et al., 2017). Chez nos souris déficientes pour Gls1, nous avons pu mettre en évidence que les TA brun et beige contenaient des niveaux plus faibles de NE, pouvant être dus à une plus forte utilisation/dégradation de la NE par les macrophages ou à moins de production par les neurones. Notre étude n'a pas révélé

de problème de dégradation de la NE par les macrophages et nous avons alors investigué l'activation des neurones.

Le glutamate est libéré au niveau de la pré-synapse des neurones glutamatergiques de la moelle épinière vers le noyau intermédiaire-latéral (IML) situé entre les segments vertébraux T2 et T6. Ces segments contiennent des neurones sympathiques pré-ganglionnaires qui se projettent vers les dépôts adipeux thermogéniques (Tupone et al., 2014). La dénervation chimique par le 6-OHDA a permis de reproduire le phénotype de nos souris confirmant que la glutaminolyse des macrophages contribue à la thermogenèse du tissu adipeux brun induite par le tonus sympathique. D'une manière intéressante, les neurones glutamatergiques de la moelle épinière sont moins activés dans notre étude. La supplémentation en glutamate a, de même, permis de restaurer la thermogenèse défectueuse des souris Gls1 déficientes, prouvant le rôle clé de la glutaminolyse des macrophages sur l'activation des neurones glutamatergiques en amont des neurones sympathiques. La co-culture de neurones glutamatergiques avec des macrophages de la moelle épinière a mis en évidence le défaut de contact entre les deux types cellulaires. Cette diminution de contact peut être due à l'augmentation des processus de répulsion comme illustré dans le profil de séquençage des macrophages de la moelle épinière. Parmi les voies connues pour réguler ce phénomènes il existe l'axe Slit3-Robo1 (Dun et al., 2019), PlexinA4-Sema6a (Wolf et al., 2017) ou encore la protéine RGM-A (Korner et al., 2019). Le défaut de contact peut aussi être due à la diminution des processus d'attractions ou à des défauts de chimiotaxie des macrophages par l'axe Ccl2/Ccr2 (Kwon et al., 2015), Cx3cl1/Cx3Cr1 (Luo et al., 2019), Mecp2 (Wolf et al., 2017), la nétrine 1 (van Gils et al., 2012) ou Trem2 (Mazaheri et al., 2017). Bien que les gènes Trem3 et Sema3g, identifiés comme sous-exprimé au cours de notre séquençage, ne soient pas connus dans l'interaction neurone/macrophage, une étude plus poussée devra être réalisée. Les perspectives du laboratoire seront donc d'identifier le mécanisme exact d'interaction des macrophages permettant l'activation des neurones glutamatergiques. Le glutamate produit au cours de la glutaminolyse par les macrophages pourrait, de plus, être essentiel à l'activation des neurones au cours de leurs contacts. En effet, dans le cerveau, un échange de glutamine et glutamate se produit entre les neurones et les astrocytes. Un tel cycle pourrait ainsi avoir lieu au sein des macrophages de la moelle épinière, et permettre l'activation neuronale. Il faut cependant noter que les macrophages peuvent être différents selon leur provenance et

localisation (Bleriot et al., 2020), et que la communication entre les neurones et la microglie au sein du cerveau n'est peut-être pas transposable au niveau de la moelle épinière puisque la microglie et les macrophages de la moelle épinière sont deux types bien distincts d'après l'analyse en composante principale (PCA) de notre étude. De même, les macrophages de la moelle épinière et du TA sous-cutané n'ayant pas la même provenance, l'échange de NE entre les neurones et les macrophages expliqué par Pirzgalska *et al.* (Pirzgalska et al., 2017) peut ne pas se reproduire au niveau de la moelle épinière.

Pour conclure, nos travaux ont mis en lumière le rôle essentiel de la glutaminolyse des macrophages, d'une part sur le métabolisme du tissu adipeux blanc au cours de l'obésité, et sur l'activation des neurones glutamatergiques de la moelle épinière conduisant à une thermogenèse non frissonnante efficace. Une étude plus poussée sur les voies de signalisations permettant la communication entre les neurones et macrophages de la moelle épinière est essentielle afin de comprendre le processus exact de notre étude.

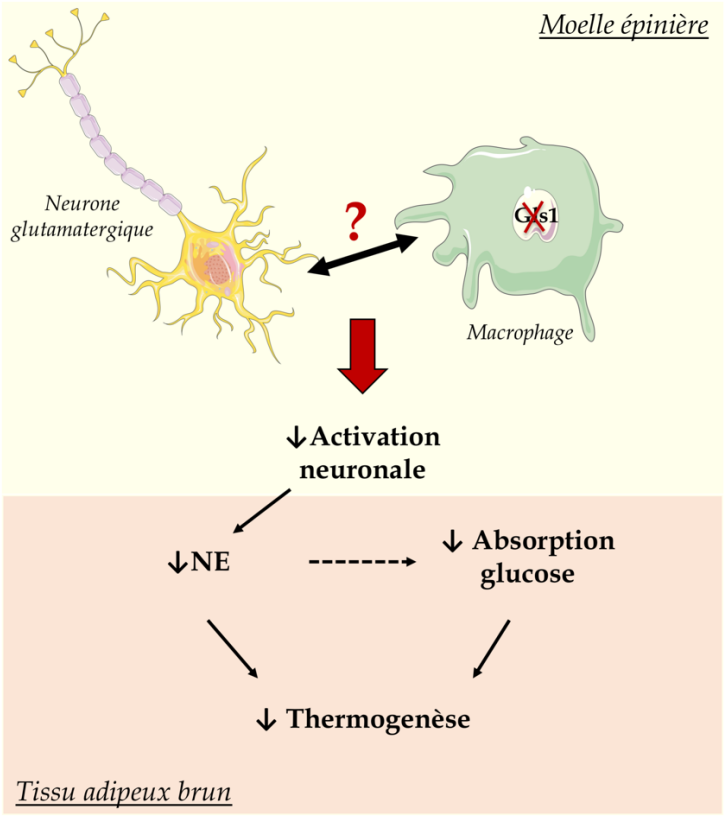

Figure 25 : Schéma récapitulatif : Effet de la déficience pour Gls1 dans les macrophages sur le tissu adipeux brun.

Au sein de la moelle épinière, les macrophages déficients pour Gls1 ont moins d'interaction avec les neurones glutamatergiques par le biais d'un processus encore non élucidé. Ce défaut entraine une perte d'activation des neurones glutamatergiques dans la moelle épinière en amont du tonus sympathique. Les neurones sympathiques se projettent au niveau des dépôts adipeux thermogéniques. Ainsi, le défaut de ce tonus glutamatergique/sympathique conduit à la diminution de norépinephrine au sein du tissu adipeux brun qui contrôle le découplage des oxydations phosphorylantes à partir du glucose. Ensemble, ces processus conduisent à un défaut de thermogénèse dans les souris déficientes pour Gls1 au niveau des macrophages.

II- Rôle de la glutaminolyse des macrophages au cours de l'athérosclérose

Comme nous avons pu le voir, le métabolisme des macrophages joue un rôle clé dans le développement des maladies cardio-métaboliques. Nous nous sommes ainsi demandé si la déficience génétique pour Gls1 dans les macrophages pouvait avoir un effet sur le développement de l'athérosclérose et quels étaient les mécanismes liés.

Au sein des cellules, le glutamate provenant de la glutamine peut être majoritairement utilisé par deux enzymes, Glud1 afin de faire de l'α-KG, ou les transaminases Got1/Got2. En 2017, Liu *et al.* ont montré, par l'inhibition de Gls1 avec du BPTES, que la production d'α-KG à la suite de la glutaminolyse était importante pour l'activation alternative des macrophages et pour le contrôle épigénétique de l'expression des gènes M2 par les JMJ (Liu et al., 2017). Cependant, dans notre modèle d'étude, le niveau de l'α-KG, des métabolites du cycle de Krebs, et les activités des JMJ ne sont pas changés. De plus, suite à la délétion génétique de Glud1 dans les cellules souches hématopoïétiques, nous n'avons pas retrouvé d'altération de la polarisation M2 des macrophages mais bien au contraire une augmentation de celle-ci en comparaison avec les souris sauvages. La différence entre nos modèles peut être due à des mécanismes de compensations au sein de nos souris génétiquement déficientes et aux effets non ciblés du BPTES. En effet, l'étude de Liu *et al*., est essentiellement basée sur l'utilisation d'inhibiteurs pharmacologiques dont les effets non-ciblés peuvent affecter les conclusions. A titre d'exemple, des études récentes ont permis de révéler que l'Etomoxir, largement utilisé pour inhiber Cpt1, présentent des effets non-spécifiques à des concentrations élevées (Divakaruni et al., 2018; Nomura et al., 2016).

L'analyse transcriptionnelle et métabolique des macrophages de nos souris a mis en évidence que la voie des transaminases était altérée dans ce modèle. Les transaminases permettent, entre autres, la génération d'oxaloacétate et ainsi de malate (Curi et al., 2017). Le malate peut soit être transformé en pyruvate et donner du NADH, qui sert pour la chaine de transport d'électrons (ETC), soit repartir dans le cycle de Krebs. Dans notre modèle, du fait de l'altération de la voie des transaminases, la respiration mitochondriale est diminuée. Au cours de la respiration mitochondriale, la chaine respiratoire produit majoritairement de l'ATP et peu de

ROS (Zhao et al., 2019). Dans les cas de perturbations de l'ETC, une majorité des ROS mitochondriaux peuvent être produits au détriment de l'ATP (Zhang et al., 2019; Zhao et al., 2019). Dans notre modèle, la déficience en glutaminolyse altère la respiration mitochondriale et la production d'ATP et conduit à une augmentation de la production de ROS mitochondriaux. De plus, nous avons détecté une diminution de la concentration en GSH qui pourrait également expliquer l'augmentation des ROS dans nos macrophages déficients pour Gls1.

L'utilisation de la glutamine est augmentée dans la polarisation alternative des macrophages (Jha et al., 2015) et nous avons pu montrer, tout comme Liu *et al.* (Liu et al., 2017), que son absence altérait la polarisation M2 des macrophages *in vivo* et *ex vivo*. Au sein de la plaque les macrophages arborent une infinité de polarisation, jouant des rôles pro- ou anti-inflammatoires (Cochain et al., 2018; Fernandez et al., 2019; Kim et al., 2018; Winkels et al., 2018). Nous avons pu montrer que l'absorption de la glutamine au sein des aortes de souris $ApoE^{-/-}$ ayant développées de l'athérosclérose est améliorée. Cela est en accord avec les travaux de Tavakoli et al., qui ont mis en évidence une accumulation accrue de glutamine dans les aortes de souris $Ldlr^{-/-}$ (Tavakoli et al., 2017). Cependant, dans notre étude, la conversion de la glutamine en glutamate est diminuée au sein des aortes de souris $ApoE^{-/-}$, montrant un défaut de glutaminolyse au cours de l'athérosclérose. De même, chez l'Homme, l'expression génique de Gls1 est diminuée dans les plaques instables et corrèle positivement aux marqueurs de polarisation alternative. Cela suggère que la seule présence en glutamine n'est pas suffisante et que la conversion de la glutamine en glutamate par Gls1 est essentielle dans l'activation alternative des macrophages et par conséquent contribuent à la stabilité de la plaque. Ces résultats suggèrent que Gls1 pourrait être un nouveau révélateur des profils des macrophages dans la plaque. Dans leurs travaux, Tavakoli *et al.* proposent de prédire le profil dominant de polarisation des macrophages dans la plaque par de l'autoradiographie *ex vivo*. Une accumulation majoritaire de glutamine au dépend du 2-désoxyglucose suppose une population anti-inflammatoire dominante tandis que l'inverse indique une teneur plus élevée en macrophages pro-inflammatoires (Tavakoli et al., 2017). Cependant, cette méthode ne tient pas compte de la glutaminolyse et de la conversion de la glutamine en glutamate. Afin d'étudier et valider le rôle protecteur de Gls1 au cours de l'athérosclérose, des souris $ApoE^{-/-}$

surexprimant Gls1 sont actuellement sous régime riche en graisses. Selon les résultats, l'étude pourrait aider au développement de nouvelles thérapies ciblant la glutaminolyse.

Nous montrons que chez l'Homme la diminution de l'expression génique de Gls1 corrèle avec l'augmentation du cœur nécrotique dans les aortes, une conséquence d'un défaut efférocytique. Dans notre étude, la déficience en Gls1 dans les macrophages des souris conduit à un défaut d'efférocytose après stimulation à l'IL-4 *in vivo* et *ex vivo*, et à l'augmentation de la taille de la plaque chez les souris athérogène. La diminution de l'efférocytose peut être due à plusieurs mécanismes. En effet, comme nous l'avons vu, l'efférocytose est assurée par les signaux « taste-me », « eat-me », et le post-engloutissement. Dans notre modèle, ni ces signaux, ni la digestion des cellules apoptotiques ne sont dramatiquement changés. Cependant, nous avons mis en lumière une diminution du réseau de filaments d'actine autour de la coupe pendant l'engloutissement de la cellule apoptotique. Le réseau d'actine peut être modifié par plusieurs mécanismes. Le réarrangement du cytosquelette d'actine au cours de l'efférocytose oblige une forte demande énergétique (Elliott and Ravichandran, 2016). Les petites GTPases Rac1 et Cdc42 sont très étudiées au cours de l'athérosclérose car leur diminution entraine des changements d'actine (Proto et al., 2018; Ravichandran and Lorenz, 2007; Yurdagul et al., 2020). Dans notre modèle d'étude, l'activité de Rac1 et Cdc42 est diminuée après stimulation à l'IL-4 et pourrait ainsi expliquer au moins une part du phénomène. De même, la déficience pour Gls1 dans nos souris conduit à une diminution de la production d'ATP. Le lien entre la diminution de l'ATP et la polymérisation de l'actine parait évident, et les résultats préliminaires montre une diminution de la polarisation de l'actine dans nos souris déficientes pour Gls1. Cependant, le lien direct entre la production d'ATP, les petites GTPases, et la polymérisation de l'actine reste à élucider. PAK1 (P21-Activated Kinase 1) est une enzyme pouvant faire une boucle d'autorégulation avec Rac1 et Cdc42, qui eux-mêmes vont réguler la dynamique du cytosquelette (Elliott and Ravichandran, 2016). La phosphorylation de PAK1 par l'ATP entraine l'activation de l'enzyme et pourrait ainsi permettre l'activation de Rac1/Cdc42 (Lo et al., 2020; Meyer Zum Buschenfelde et al., 2018). De nouvelles expériences en cours, visant à invalider Rac1 par des nanoblades, inhiber le site d'activation de l'ATP sur PAK1, et utiliser des macrophages déficients pour PAK1, afin de regarder l'efférocytose et le remaniement de l'actine, pourraient

permettre de mettre en lumière PAK1 comme un lien entre la diminution de l'ATP et le réarrangement du cytosquelette d'actine au cours de l'efférocytose.

Dans le cas où PAK1 n'est pas à l'origine du défaut d'efférocytose, d'autres pistes sont à explorer. En effet, le cytosquelette peut être altéré par des réponses épigénétiques (Fu et al., 2019; Yang et al., 2017; Zacharopoulou et al., 2018). Comme discuté plus haut, la glutamine est maintenant connue pour réguler certains facteurs épigénétiques tels que Tet2 et les KDM6 (Johnson et al., 2018; Liu et al., 2017; Tahiliani et al., 2009). Bien que nous n'ayons pas retrouvé de modifications ni dans l'activité des KDM6 ni de Tet2, ni sur les sites de méthylations connus (H3K27, H3K4), et que les enzymes épigénétiques connues pour affecter le cytosquelette, comme par exemple les KDM2B (Zacharopoulou et al., 2018), ne semblent pas modifiées transcriptionnellement, il est possible qu'il y ait des changements au niveau de leur promoteur, ou de leur activité. Enfin, lors de la conversion de la glutamine en glutamate, du NH_4^+ est produit. Cet ammonium peut avoir plusieurs effets sur la cellule et notamment réguler le pH cytosolique (Watts and Good, 1994). Ce pH peut, par la suite, lui-même avoir un impact sur le cytosquelette d'actine (Kohler et al., 2012). Il se pourrait dans ce cas, que les différences de niveaux de NH_4^+ au sein des macrophages déficients pour Gls1 soient suffisant pour entrainer des défauts de pH et ainsi de réseau d'actine.

Dans l'ensemble, nos résultats démontrent le rôle clé de la glutaminolyse des macrophages au cours de l'athérosclérose. Notre étude montre pour la première fois l'impact des transaminases sur la fonction effectrice des macrophages stimulé à l'IL-4. L'absence de Gls1, et la diminution des transaminases qui s'en suit, conduit à l'altération de la chaine respiratoire augmentant ainsi les ROS mitochondriaux au détriment de l'ATP. Nos résultats montrent le rôle pivot de l'ATP sur le remaniement du cytosquelette d'actine et ainsi de l'efférocytose entrainant par la suite une augmentation de la taille de la plaque d'athérosclérose chez la souris. Ces résultats soutiennent l'importance de la glutaminolyse dans les maladies cardio-vasculaires et pourraient mener au développement de nouvelles thérapies visant à supplémenter les macrophages avec du glutamate afin d'augmenter la fonction effectrice des macrophages, nécessaires au cours de la réparation tissulaire. L'apport du glutamate par des

liposomes pourrait conduire à une supplémentation spécifique des monocytes et des macrophages qui en dérivent par phagocytose.

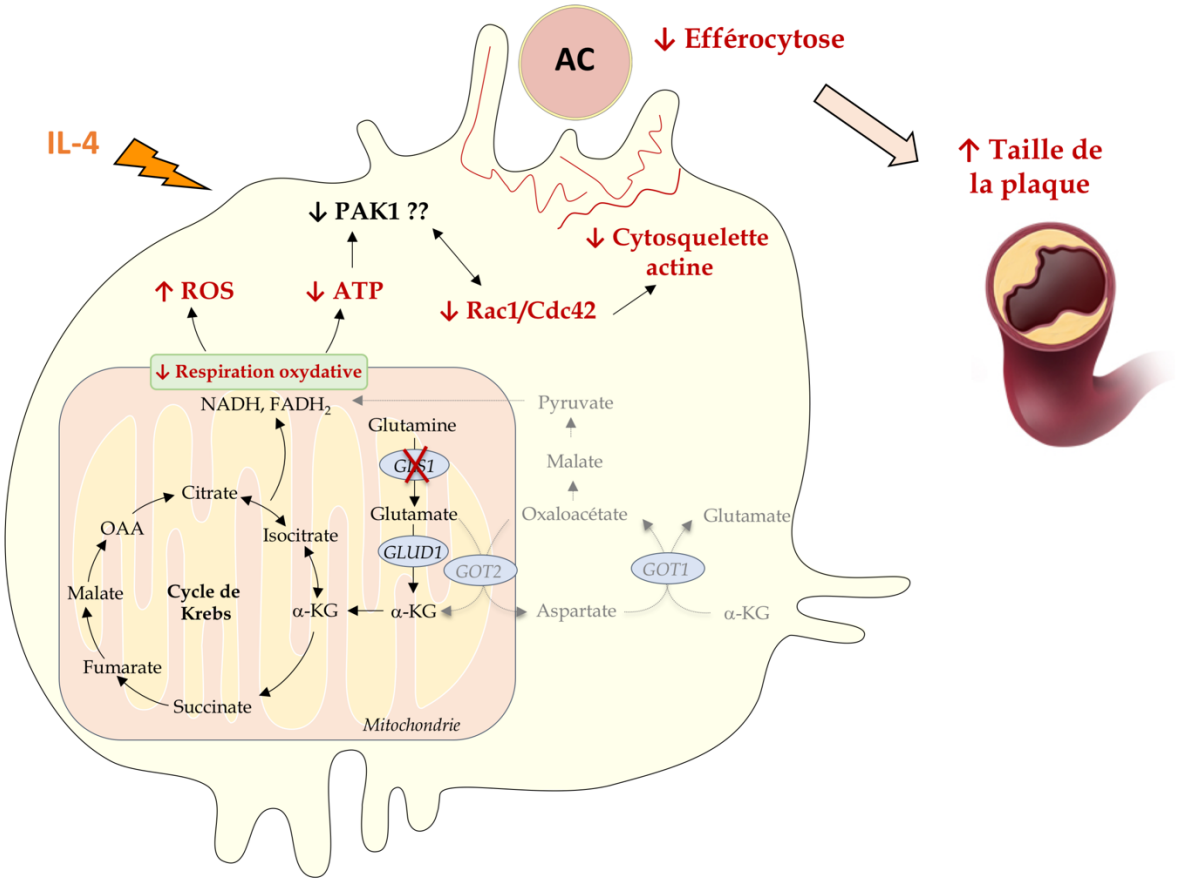

Figure 26 : Schéma récapitulatif : Rôle de la glutaminolyse des macrophages sur le développement de l'athérosclérose.

Au sein des macrophages, la déficience pour Gls1 entraine des changements métaboliques importants. En effet, l'absence de Gls1 entraine une diminution des voies de transaminases (GOT1/GOT2), limitant la production de malate et de pyruvate. Cet effet contribue à un défaut de respiration oxydative au sein des macrophages déficients pour Gls1. La respiration oxydative étant altérée, l'ATP ainsi produit est diminué en déséquilibre avec une augmentation des ROS. La baisse d'ATP pourrait entrainer une perte d'activité de PAK1, une enzyme contrôlée par une phosphorylation dépendante de l'ATP. Ainsi la baisse d'activité de PAK1 entrainerait la diminution des GTPases Rac1 et Cdc42 qui conduit à un réarrangement du cytosquelette d'actine et ainsi à une diminution de l'efférocytose. Ce défaut d'efférocytose par les macrophages entraine alors, in vivo, une diminution de la taille de la plaque d'athérosclérose.

Conclusion

Au cours de ma thèse, j'ai étudié le rôle de Gls1 au sein des macrophages et son impact sur les maladies cardio-métaboliques. Bien que mon travail ouvre de nombreuses perspectives qui devront être approfondies, j'ai pu mettre en évidence le rôle essentiel de la glutaminolyse des macrophages dans deux pathologies importantes que sont l'obésité et l'athérosclérose.

Même si la glutamine est considérée comme un carburant pour le système immunitaire, il n'a toujours pas été montré si la glutaminolyse pouvait avoir un impact sur la fonction des macrophages au sein des tissus cardio-métaboliques. Dans ma première étude, nous avons pu démontrer pour la première fois l'impact du métabolisme des macrophages de la moelle épinière sur la thermogenèse non frissonnante dépendante du glucose *via* l'activation et la projection des neurones sympathiques. Cependant, à ce jour, nous n'avons toujours pas déterminé les mécanismes d'interaction mis en jeu entre les neurones et les macrophages. D'autres expériences telles que le séquençage single-cell nuclei de la moelle épinière ou encore l'étude de la projection des neurones par de la microscopie intravitale, sont prévues afin de déterminer comment les macrophages déficients pour Gls1 impactent la projection des neurones glutamatergiques. Au cours de ma seconde étude, j'ai pu mettre en évidence le rôle central de la glutaminolyse des macrophages dans l'élimination des cellules apoptotiques après stimulation à l'IL-4 ou pendant la clairance continue des cellules apoptotiques. Nous avons pu démontrer que ces fonctions reposaient sur la voie métabolique des transaminases ouvrant ainsi de nouvelles perspectives thérapeutiques pour le contrôle métabolique des macrophages au cours de l'athérosclérose. De plus, il serait intéressant de déterminer comment la baisse d'ATP au sein des macrophages impacte le réseau d'actine au cours de l'efférocytose. Enfin, j'aime à croire que ces différentes réponses mettront en lumière le rôle essentiel de la glutaminolyse des macrophages au cours des maladies cardio-métaboliques et permettront, à long terme, de développer de nouvelles stratégies de traitements afin de contrôler la fonction des macrophages dans ces pathologies et améliorer la survie et le quotidien des patients concernés.

Annexes

Atherosclerosis 271 (2018) 102–110

Contents lists available at ScienceDirect

Atherosclerosis

journal homepage: www.elsevier.com/locate/atherosclerosis

Review article

Biology and function of adipose tissue macrophages, dendritic cells and B cells

Stoyan Ivanov [a], Johanna Merlin [a], Man Kit Sam Lee [b], Andrew J. Murphy [b], Rodolphe R. Guinamard [a, *]

[a] INSERM U1065, Mediterranean Center of Molecular Medicine, University of Nice Sophia-Antipolis, Faculty of Medicine, Nice, France
[b] Haematopoiesis and Leukocyte Biology, Baker Heart and Diabetes Institute, Melbourne, Victoria, Australia

ARTICLE INFO

Article history:
Received 31 August 2017
Received in revised form
22 November 2017
Accepted 12 January 2018
Available online 20 February 2018

Keywords:
Macrophage
Dendritic cell
B cell
Adipose tissue
Obesity

ABSTRACT

The increasing incidence of obesity and its socio-economical impact is a global health issue due to its associated co-morbidities, namely diabetes and cardiovascular disease [1–5]. Obesity is characterized by an increase in adipose tissue, which promotes the recruitment of immune cells resulting in low-grade inflammation and dysfunctional metabolism. Macrophages are the most abundant immune cells in the adipose tissue of mice and humans. The adipose tissue also contains other myeloid cells (dendritic cells (DC) and neutrophils) and to a lesser extent lymphocyte populations, including T cells, B cells, Natural Killer (NK) and Natural Killer T (NKT) cells. While the majority of studies have linked adipose tissue macrophages (ATM) to the development of low-grade inflammation and co-morbidities associated with obesity, emerging evidence suggests for a role of other immune cells within the adipose tissue that may act in part by supporting macrophage homeostasis. In this review, we summarize the current knowledge of the functions ATMs, DCs and B cells possess during steady-state and obesity.

1. Introduction

Phagocytes were first described by Metchnikoff in the 19th century. Among phagocytes, macrophages are the first line of host defense against pathogens, and interest in their functions and ontogeny has since grown tremendously. Recent studies using genetic fate-mapping techniques, show that the pool of tissue resident macrophages is established during embryonic development [6–9]. During adulthood, this population of tissue resident macrophages self-renew via proliferation, independently from circulating blood monocytes [10,11]. However, in the context of inflammation or injury, monocytes infiltrate peripheral tissues and give rise to tissue macrophages [10,12,13]. When these monocyte-derived macrophages (often referred to as “recruited” or “inflammatory” macrophages) are under the influence of their local tissue environment, they can express surface markers typically found on tissue resident macrophages, making it difficult to distinguish between each other.

Although the adipose tissue had long been considered as a storage organ, this view dramatically changed after Spiegelman's group revealed that the adipose tissue was in fact an endocrine organ, capable of secreting inflammatory factors impacting co-morbidities such as insulin resistance [14]. It took almost a decade for the scientific community to gain interest into whether and how the immune system could communicate with adipocytes to promote low-grade inflammation observed in obesity. The first observation of macrophages in the adipose tissue (ATMs) was discovered in the early 2000s [15–17] and was followed 5 years later by the identification of the presence of lymphocytes [18,19]. ATMs are present in the adipose tissue of many vertebrate species, and not exclusively in rodents, primates and humans, even though their numbers vary between different adipose tissue depots [20,21]. Since then the presence of a large diversity of immune cells, including, among others, DCs and B cells, was reported and the field has become an area of intense investigation, and concepts discovered in the immunology field have been tested directly at the level of the adipose tissue, creating what is now known as ‘immunometabolism’.

In this review, we discuss the recent advances made on adipose tissue immune cell homeostasis with a macrophage centric view since these cells are the most abundant population of immune cells in the adipose tissue of mice and humans [22,23].

* Corresponding author.
E-mail addresses: Stoyan.ivanov@unice.fr (S. Ivanov), rguinamard@unice.fr (R.R. Guinamard).

https://doi.org/10.1016/j.atherosclerosis.2018.01.018
0021-9150/

2. Homeostatic and pathological maintenance of adipose tissue resident macrophages

2.1. The diversity and complexity of adipose tissue macrophage origin

The original observation that macrophage infiltration into the white adipose tissue is increased during obesity led to the hypothesis that ATMs originated from bone marrow stem cells [16,17]. However, recent studies argue that ATMs are derived predominantly from primitive yolk-sac progenitors and self-renew via proliferation under homeostatic conditions [24]. Therefore, the relative contribution of embryonic and monocyte-derived macrophages to the total pool of ATMs may vary depending on the local environment. Intriguingly, in other tissues, aging is associated with progressive replacement of embryonic macrophages by monocyte-derived cells and this could also hold true in the adipose tissue since epigenomic alterations control ATM function [25] and that the adipose tissue is known to expand with age. Of note, one of the caveats is the phenotypic distinction between macrophages, monocytes or even dendritic cells (DCs) that remain a technical challenge due to the overlap of cell surface markers. Nevertheless, it appears that embryonic and monocyte-derived macrophages have distinguishable transcriptomic signatures [26]. These findings suggest that it may be possible to identify novel specific markers based on unique functions and mechanisms of regulation of each population. Indeed, such a core transcriptomic signature between tissue resident macrophages, monocytes and DCs in multiple organs [27,28] has led to the identification of more specific markers (i.e. CD64 and MerTK) allowing for the separation of macrophages from monocytes and DCs, helping to develop more robust strategies to analyze the phenotype and function of these cells (Fig. 1 and Table 1). However, this gating strategy still does not distinguish tissues resident macrophages from recruited or monocyte-derived macrophages. Previous studies used a combination of CD11b, F4/80 and CD11c markers to identify ATM subsets [29,30]. This documented 3 distinct populations of ATMs [30], which may not necessarily reflect pure ATMs. However, the current consensus is that CD11c^{+}F4/80^{+} macrophages are likely the more 'inflammatory' subset [31]. The complication in identifying these cells is that recent reports have demonstrated that F4/80 expression is not only restricted to macrophages but also to conventional CD11b^{+} DCs and that the *Emr1* gene coding for F4/80 is found in eosinophils ([32] and Immgen.org). Additionally, the developmental origin of each subset remains currently unknown and requires further investigation. Nevertheless, these pioneering works provide exciting insights into the diversity of ATMs and suggest a potential role during obesity, elaborating new strategies that could be helpful to analyze ATM subsets during steady-state and obesity. So far, studies on the lifespan and origin of ATMs are limited in number. The use of already established models of fate mapping and parabiosis will certainly shed light on the developmental origin and homeostatic maintenance of these cells.

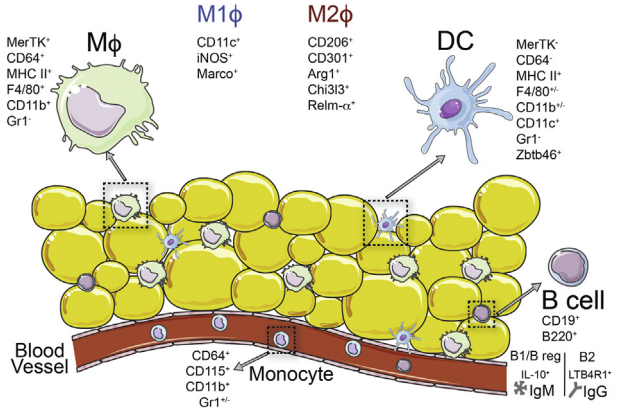

Fig. 1. Topological distribution of macrophages, dendritic cells, monocytes and B cells in the adipose tissue.

2.2. Differentiation and survival of adipose tissue macrophages

Macrophage colony stimulating factor (M-CSF) binds to its receptor CSF-1R and stimulates the differentiation and survival of macrophages in multiple tissues. The *op* mutation, a nucleotide insertion disrupting the coding region of the M-CSF gene, provides a genetic model to test the importance of M-CSF signaling for macrophage development and function [33]. *Op/op* mice have about 70% decrease in the number of F4/80^{+} cells in the adipose tissue. This demonstrates that compared to other tissues, resident macrophages of the adipose tissue do not entirely rely on M-CSF for their maintenance [16], or perhaps this remaining 30% of F4/80^{+} cells in the adipose tissue are not macrophages. However, given the fact that *op/op* mice lack macrophages in different tissues, it is challenging to analyze these mice in the context of a high fat diet (HFD)- induced obesity. The use of op/WT haplodeficient mice did not reveal any remarkable difference compared to control mice in terms of weight gain, although the level of M-CSF was reduced in the adipose tissue under HFD [34]. Recently, the cytokine interleukin (IL)-34 was identified as another ligand for CSF-1R [35,36]. It is known that IL-34 plays a critical role in the maintenance of microglia. IL-34 also controls the induction of macrophages in amphibians [37]. Interestingly, obesity is associated with increased IL-34 serum concentration and mRNA expression in the adipose tissue [38]. ATMs are not completely missing in *op/op* mice, thus it will be interesting to test whether IL-34 is required for the maintenance of these cells under homeostatic and obese conditions.

2.3. Tuned balance between monocyte recruitment and macrophage proliferation/polarization

The chemokine Mcp1 (CCL2) was originally identified as the key soluble mediator for macrophage infiltration into white adipose tissue during obesity [16]. Consistently, serum CCL2 concentrations are increased in mice fed a HFD [39]. However, CCL2 is equally a critical regulator of monocyte egress from the bone marrow to the blood, preceding their infiltration into peripheral tissues [40]. Additionally, CCL2 was recently shown to control the homeostatic maintenance and proliferation of ATMs [41]. Therefore, because of the multiple effects of this chemokine, it remains challenging to know whether increased ATMs during obesity is a consequence of enhanced monocyte mobilization from the bone marrow, increased monocyte recruitment or whether it is due to direct CCL2 function on local proliferation of ATMs.

Similarly, the integrin CD11b regulates the recruitment of monocytes to adipose tissue during obesity as CD11b deficient mice have reduced ATM content [42]. In contrast to CCL2, ATMs lacking CD11b favor 'alternatively' activated macrophage, and have enhanced proliferation due to activation of STAT6, downstream of IL-4 signaling [42]. Indeed, Th2 cytokines IL-4 and IL-13 (known to promote the proliferation of peritoneal macrophages [11]) also control the proliferation of ATMs in a mechanism that requires IL-6 [43]. Another illustration of the involvement of STAT6 signaling in ATM homeostasis is reported with the appetite-reducing

Table 1
Markers used to define macrophage pattern in lean and obese fat.

	Markers	Notes
Adipose tissue macrophages	MerTk CD64 F4/80	General ATM markers
Anti-inflammatory (M2)	Arg1 CD163 CD206 CD301 Chi3L3 PD-L2 Relm-α IL-4Rα IL-10	ATMs predominantly express M2 markers in lean adipose tissue
Pro-inflammatory (M1)	iNOS CD11c CD86 CCR2 Marco TLR4 IL-1β IL-6 IL-12 TNFα	ATMs switch to pro-inflammatory phenotype in obese adipose tissue

neuropeptide FF (NPFF) known to promote the proliferation of ATMs after binding to its receptor NPFFR2 along with their alternatively activated state. The underlying mechanism relies on the regulation of STAT6 through its stabilization and the prevention of pSTAT6 degradation [44].

In a healthy and obese adipose tissue, the regulation of ATM pool is currently inexplicable. Adipose tissue expansion is correlated with increased number of ATMs. Whether this increase is due to local proliferation of resident ATMs or recruitment of monocytes from the blood circulation is unclear. Monocyte recruitment to adipose tissue may be a consequence of insufficient proliferation of resident ATMs and an urgent need to fill the empty niche. An alternative explanation could be that monocyte recruitment to adipose tissue prevents resident ATM proliferation. Since CCL2-CCR2 axis controls both monocyte egress from bone marrow and ATM proliferation in the adipose tissue it seems that proliferation and recruitment are interconnected [40,41]. The same scenario is observed in atherosclerosis where monocyte recruitment and macrophage proliferation in the plaque both contribute to disease progression [45,46]. A better understanding of these mechanisms may offer alternative therapeutic opportunities. Indeed, development of obesity is tightly associated with a switch in the polarization of adipose tissue macrophages towards an M1 phenotype (classically activated macrophages), which is correlated with increased tissue inflammation and damage [29,47]. The current view postulates that M1 macrophages are inflammatory compared to alternatively activated M2 macrophages (anti-inflammatory) that have been implicated in tissue repair and wound healing. However, excessive alternative activation of macrophages may lead to a pro-fibrotic phenotype of the adipose tissue and induce its dysregulation by limiting expansion [48].

As discussed above, the mechanisms controlling the size of the pool of ATMs are still not clearly established. Recently, Boulenouar and colleagues added another layer to ATM pool size control by showing that adipose tissue residing type1 innate lymphoid cells (AT1-ILCs) are critical regulators of ATMs [49]. AT1-ILCs eliminate ATMs (preferentially phenotypic M2s) during homeostatic conditions. This mechanism relies on the expression of perforin by AT1-ILCs. During obesity this interaction is impaired and the pool of ATMs expand [49].

2.4. Control of macrophage polarization by environmental cues: role of insulin signaling

Obesity is associated with alteration of the host metabolism and often results in insulin resistance. Insulin is naturally produced by pancreatic beta cells to help the absorption of glucose from the blood and, in the adipose tissue, glucose is in turn converted into triglycerides for storage. Pioneering studies have shown that insulin also binds to its receptor on macrophages to induce a signaling cascade that limits fatty acid-induced foam cell formation [50] and endoplasmic reticulum (ER)-stress induced apoptosis [51]. We will not discuss the role of the insulin signaling pathway in macrophages in depth since excellent reviews have been published on this topic [52,53]. However, emerging evidence suggests that insulin and insulin-like receptor signaling may also have a central role in the metabolic reprograming of macrophages to promote their activation [54,55]. In the context of obesity, it was recently demonstrated, using a mouse model of ablation of insulin-like receptor in macrophages, that Igf1 signaling promotes alternative M2 macrophage polarization. Igfr1 deficient mice develop increased body weight and fat pads in comparison to control animals [56]. This is mirrored by accumulation of pro-inflammatory macrophages in the adipose tissue under conditions of high fat diet (HFD) [56]. Similar observations are reported using myeloid cell specific deletion of Sirtuin 6. These mice have higher macrophage recruitment in the adipose tissue paralleled by M1 polarization [57]. Sirtuin 6 is known to control insulin sensitivity but it remains to be determined whether the effects observed in Sirtuin 6 deficient macrophages rely on modulation of the insulin signaling pathway. The contribution of macrophage ER stress to metabolic disease progression was recently addressed by Bo Shan and colleagues [58]. Macrophage specific deletion of the innate sensor IRE1α, a central player during ER-stress, induces adipose tissue macrophage M2 polarization and rescues HFD-induced obesity and insulin resistance [58].

Lipolysis in the adipose tissue generate fatty acids (FAs) and ATMs are constantly exposed to these FAs that have been released. Metabolic analysis of macrophages revealed that pro-inflammatory M1 macrophages preferentially use glycolysis in comparison to M2 macrophages that utilize both glucose and FAs for oxidative

phosphorylation [59]. Macrophages utilize the membrane receptor CD36 to internalize substrates that are further degraded via the lysosomal acid lipase (LAL) to fuel fatty acid oxidation. In the lean fat, ATMs have an M2 phenotype (Table 1) which might suggest that these cells rely on fatty acid oxidation for their metabolic demands. During obesity, ATMs progressive switch to an M1 phenotype is accompanied by high intracellular lipid content suggesting that lipotoxicity is a key player in the generation of adipose tissue inflammation [60]. However, it remains unknown as to whether the excess accumulation of lipids in ATMs is a key event at the origin of M1 polarization or that M1 ATMs do not have the capacity to utilize lipids as energetic substrates and therefore accumulate in excess.

3. Function of ATMs during obesity

3.1. Diversity of adipose tissue depots

Two major classes of adipocytes are described: white and brown adipocytes. These cells have distinct progenitors and functions. The main role of white adipose tissue is to store fatty acids, which is typically expanded during obesity. In contrast, brown adipocytes burn substrates in order to generate heat and play a key role during adaptive thermogenesis. The brown fat is located on the back of the mice, in the interscapular region. Recently, a third type of adipocytes sharing characteristics of both white and brown adipocytes was found. These cells are named beige adipocytes and their presence was observed in subcutaneous adipose tissue of humans. In rodents, visceral adipose tissue is mainly composed of white adipocytes while subcutaneous fat contains both beige and white adipocytes. The cellular composition varies between adipose tissue depots and their function and regulation during obesity is differential [61].

3.2. Role of visceral ATMs during obesity

The adipose tissue can respond to nutrient fluctuations by expanding or contracting in order to adapt to modifications of energy intake and demand. Visceral ATMs play a key role during obesity to amplify inflammation [62]. Although most of the original studies have focused on the contribution of local cytokine secretion by macrophages to the low-grade inflammation in obesity, following works have established an association between this systemic inflammation and the degree of insulin resistance [16,63]. These works have been extensively reviewed elsewhere [64–70]. Nevertheless, a study has pushed the concept forward by showing that activation of TLR4 on macrophages leads to NLRP3 inflammasome dependent release of IL-1β and this is at the origin of enhanced monocyte and neutrophil production/mobilization from the bone marrow [31]. Increased circulating monocyte counts are associated with obesity and diabetes [71], along with accelerated atherosclerosis both in mice [72,73] and in humans [74,75].

Therefore, it is tempting to develop strategies to reduce adipose tissue monocyte recruitment to abolish inflammation and improve cardiometabolic complications. Indeed, mice deficient for the chemokine receptor CCR2 and its ligand CCL2 or CD11b all exhibit reduced adipose tissue inflammation and this is associated with better insulin sensitivity and reduced adipose tissue inflammation [76,77].

3.3. Role of subcutaneous and brown ATMs in thermogenesis

Importantly, ATMs play a critical role in the induction of adaptive thermogenesis [78]. Adaptive thermogenesis, characterized by Ucp1 (uncoupling protein 1) increase in adipocytes, is induced by cold environmental temperature and is dependent on the secretion of the cytokines IL-4 and IL-13 by innate lymphoid cells and eosinophils [79]. These cytokines promote M2 polarization of ATMs [79,80]. The central role of ATMs in this mechanism was demonstrated through clodronate liposome depletion of macrophages and genetic deletion of IL-4Rα (common receptor for IL-4 and IL-13) specifically in myeloid cells (*Lyz2 x IL4ra* flox mouse) completely blunted adipocyte *Ucp1* expression and heat generation [58,79,81]. Surprisingly, M2 macrophages participated in this mechanism by secreting norepinephrine [81] (Fig. 2). This finding revealed an intriguing and novel function of ATMs and suggested their ability to control non-shivering thermogenesis in the context of cold exposure. Given the well-established beneficial effect of adaptive thermogenesis on host metabolism, this provides a new pathway to consider for the development of pharmaceutical approaches aimed at preventing obesity and its related complications. However, this concept was recently challenged by Christoph Buettner's group [82]. Using tyrosine hydroxylase (Th) (the rate limiting enzyme for the synthesis of catecholamines, including among others norepinephrine) reporter mice (Th^{Cre}: r26-tdTomato), the authors demonstrated that Th is not expressed in ATMs. Additionally, while Th is detected in neurons, its expression is completely absent in brown ATMs after cold exposure, a condition that requires brown adipose activation via catecholamines production [82]. Incubation of primary adipocytes with conditioned medium of IL-4 stimulated macrophages failed to induce Ucp1 protein expression. 2-Photon microscopy analysis of brown adipose tissue in Th^{Cre}: r26-tdTomato (visualization of neurons) crossed with $CX3CR1^{gfp}$ mice (visualization of macrophages) further revealed that some brown ATMs are intimately associated with neurons [83]. Although the factors required for this interaction remain to be elucidated, it seems to be critical for brown adipose tissue innervation. Selective deletion of the nuclear transcription factor *Mecp2* (methyl-CpG-binding protein 2) in macrophages, a murine model of Rett syndrome, resulted in decreased *Th* mRNA expression in brown adipose tissue and generally impaired innervation of this tissue [83]. This led to spontaneous obesity in mice lacking macrophage *Mecp2* compared to control animals. Mechanistically, Mecp2-deficient mice showed decreased heat production and decreased *Ucp1* expression. Additionally, adipose tissue macrophages possess a set of genes that control norepinephrine levels by regulating its degradation [84]. Similar findings are reported in a population of macrophages associated with sympathetic neurons and by controlling norepinephrine degradation influences adipose tissue

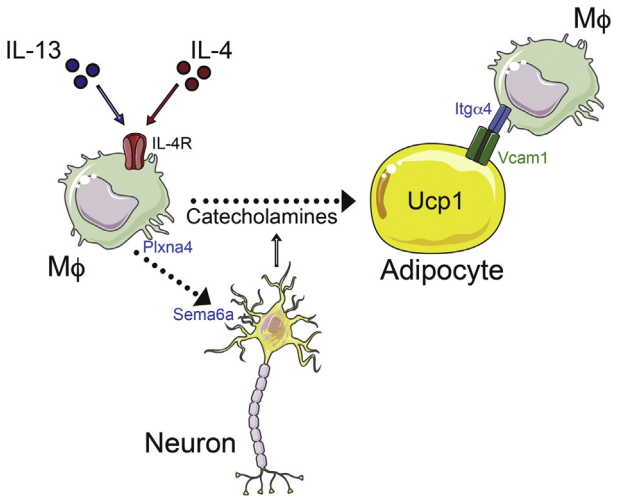

Fig. 2. Mechanisms leading to adipose tissue beiging and thermogenesis.

thermogenesis [85].

As discussed above, obesity is associated with increased macrophage ER stress [58]. Modulation of macrophage polarization in mice lacking IRE1α also correlated with increased brown and beige fat activation and higher energy expenditure. Indeed, both Th and Ucp1 expression are increased in the brown adipose tissue of IRE1α δεfιχιεντ mice [58]. How insulin signaling and altered ER stress are linked to increased activation of beige and brown adipose tissue remains unknown. One could imagine that soluble factors are altered and would eventually lead to pronounced norepinephrine secretion. Alternatively, cell contact might also be involved in the control of adipocyte expansion and/or the induction of beiging program. Indeed, the interactions between ATMs and adipocytes via VCAM1 and its ligand the integrin α4 (Itga4) controls the expression of *Ucp1* in adipocytes [86] (Fig. 2). Using inducible deletion of *Itga4* in hematopoietic cells revealed that this integrin controls the accumulation of macrophages in visceral and subcutaneous adipose tissue depots. Interestingly, while the population of M2 macrophages defined by the expression of the marker CD206 is not affected, adipose tissue M1 macrophages ($CD206^{-}$ $iNOS^{+}$) are dramatically reduced when integrin α4 is deficient. The absence of this contact-interaction between ATMs and adipocytes increases *Ucp1* expression in adipocytes [86].

4. Heterogeneity of adipose tissue dendritic cells: is there a role for DCs in obesity?

4.1. Dendritic cell nomenclature

Discovered in the early 1970s by Ralph Steinman [87–89], DCs have traditionally been known for their function for antigen presentation and initiation of T cell response [90]. Two different types of DCs have been further identified: myeloid DC (mDC) and plasmacytoid DC (pDC). These two DC populations have distinct cell morphology as demonstrated by electron microscopy, and express specific cell markers allowing for their specific identification and analysis. Indeed, mDCs are characterized by a large cytoplasm and a number of dendrites, while pDCs are smaller and round shaped. Additionally, mDCs are characterized by high expression of the integrin CD11c and the major histocompatibility complex II (MHC II). On the other hand, pDCs express lower levels of MHC II and possess membrane molecules, B220 and siglec H, which can be selectively deleted in BDCA2-DTR mice following administration of diphtheria toxin (reviewed in Ref. [91]). Upon stimulation, peripheral mDCs are mobilized and migrated to their corresponding draining lymph nodes to activate the T cell compartment. This migration relies on their expression of the chemokine receptor CCR7 [92] and its interaction with the chemokine CCL21 expressed by lymphatic endothelial cells. Interestingly, CCR7 expression enables the separation of DCs from macrophages as they do not express this receptor and are therefore unable to migrate via the lymphatic vasculature. Two major subsets of mDCs according to their cell surface expression of the molecules CD8, CD11b, CD24, CD103 and Sirpα were defined (reviewed in Ref. [93]). Indeed, $CD11b^{+}$ $CD103^{-}$ (here referred to as $CD11b^{+}$ DCs) and $CD103^{+}CD11b^{-}$ ($CD103^{+}$ DCs) have been identified in peripheral tissues. The gut, where a population of $CD11b^{+}CD103^{+}$ have been described, makes an exception [94,95]. The transcription factors controlling the development of both subsets were defined as well. IRF8 (Interferon Regulatory Factor 8) and BATF3 (Basic leucine zipper transcriptional factor ATF-like 3) control the development of the $CD8^{+}$ and $CD103^{+}$ DC, whereas mice deficient for this transcription factor are devoid of this population [96–98]. Concerning the transcriptional control of $CD11b^{+}$ DCs, the transcription factor IRF4 emerged as an indispensable player for their development in multiple tissues [99–103]. However, heterogeneity exists in IRF4-dependent DCs and subsets have been identified according to their Notch2 or Klf4 (Kruppel-like factor 4) dependency. These two subsets of $CD11b^{+}$ DCs play a critical role in the control of bacterial intestinal and helminth infections, respectively [104–106].

4.2. Specific adipose tissue dendritic cell signature

The majority of adipose tissue DCs (80–90%) express CD11b [107,108]. Adipose tissue DCs also express CD11c, MHC II and the co-stimulatory molecules CD40 and CD80 [108]. However, adipose tissue DCs do not express CD64 and MerTK, allowing for the separation from ATMs [107,108]. Using the $CD11c^{cre}$ x $Irf4^{fl/fl}$ mice, $CD11b^{+}$ DCs are ablated to various degrees in various tissues [99–103], but are almost completely ablated in the adipose tissue [107]. Interestingly, when we analyzed data generated by the Immgen consortium we found that the few adipose tissue $CD103^{+}$ DCs express XCR1 and IRF8 but low BATF3 expression in comparison to $CD11b^{+}$ DCs (Fig. 3A). The population of $CD11b^{+}$ adipose tissue DCs expresses IRF4 and Sirpα but have low Notch2 expression compared to $CD103^{+}$ adipose tissue DCs (Fig. 3A). Whether DCs extracted from different adipose tissue depots (visceral versus subcutaneous) may have different signatures and properties, is currently unknown. One major difference between subcutaneous and perigonadal fat is the absence of lymph nodes in the latter one. In subcutaneous adipose tissue, DCs detect the lymphatic content that leaks out due to inherent permeability of lymphatic collector vessels and initiate a T cell response [109]. Yet to our knowledge, lymphatic collector vessels are not reported in the perigonadal fat, and thus the function of the resident DC is enigmatic as is the nature (if any) of the antigen they sample.

4.3. Adipose tissue dendritic cells and obesity

A role for adipose tissue DCs has been recently proposed in the context of obesity, noted by their prominent expansion [110–112]. The recruitment of adipose tissue DCs, particularly the $CD11b^{+}$ subset to the adipose tissue during HFD induced obesity requires the chemokine CCR7 and to a lesser degree CCR2 [108]. Even though CCR7-deficient mice are protected against obesity and insulin resistance, it remains unclear whether this is due to defective DC recruitment or to a modification in T and B cell subsets, known to also express CCR7 [108,111]. Thus, whether and how adipose tissue DCs contribute to inflammation in the context of obesity remains incompletely understood. Recent evidence suggests that adipose tissue DCs could be involved in the induction of T_H17 response via their production of the cytokines IL-1β, IL-6 and IL-23 [113,114]. However, future experiments will be required to address

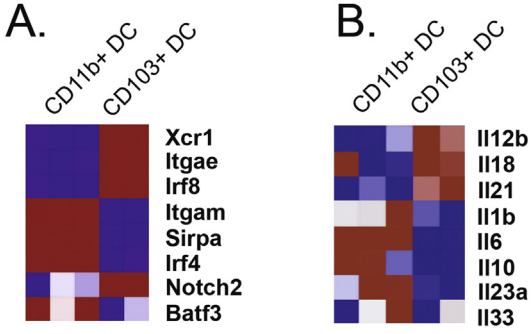

Fig. 3. Comparative analysis of adipose tissue dendritic cell subsets. Data were downloaded from the Immgen consortium database.

whether this effect is truly DC dependent and if so, which DC subsets are involved. Indeed, gating strategies of adipose tissue DCs (DC are identified as CD11c$^+$ F4/80$^-$ cells) could lead to contamination by NK cells that express CD11c and the particular signature of the minor subset of CD103$^+$ DC could be masked in studies analyzing all DC subsets since CD11b$^+$ DCs account for 80–90% of adipose tissue DCs. Indeed, when we interrogated the data from Immgen, we found that at the transcriptomic level CD11b$^+$ DC expressed more IL-1β, IL-6 and IL-23 mRNA (Fig. 3B), which could also influence T_H17 maturation. Intriguingly, Th1 polarizing cytokines (IL-12 and IL-18) were predominantly found in CD103$^+$ DCs (Fig. 3B). Even though this subset is present at low frequencies at steady state, its regulation in the course of obesity is not addressed. Obesity is characterized by Th1 inflammation and therefore it will be of interest to use BATF3-deficient mice to analyze the disease in the absence of CD103$^+$ DCs. Moreover, this subset of DC is already a well-established player for the development of diabetes [115] and could be at the origin of obesity induced inflammation.

5. Emerging role of adipose tissue B cells

B-cell subsets are intricate regulators of immune response. They directly shape T-cell repertoire via antigen presentation but also indirectly via immunoglobulin (Ig) secretion and their targeting to DCs and macrophages in the form of immune complexes. Further, B cells play a critical role in setting up normal intestinal microbiotic flora and by doing so impact integrity and metabolic capacity of epitheliums [116]. Therefore, and not surprisingly, B-cell role during obesity is complex and is only starting to get appreciated.

B cells can be developmentally and functionally separated into B-1 and conventional B-2 B cells. Like tissue resident macrophages, B-1 but not B-2 cell precursors are found in the yolk sac and are maintained predominantly in the adult pleural and peritoneal cavities via self-renewal, as opposed to BM precursor dependent replenishment of B-2 cells [117]. B-1 cells are known for their role in participating in early immunoglobulin production following pathogen encounter, but they are responsible for the stable secretion of natural IgM that are present in germ free mice and in the absence of immunization. B-2 cells are the main players of germinal center reaction and IgG production while both populations participate in microbiota driven IgA production.

5.1. Adipose tissue B cells and obesity

Diet-induced obesity leads to a significant accumulation of B cells in the visceral adipose tissue while B-cell overall mRNA core signature decreases due to over representation of macrophages (Fig. 4). This accumulation mostly concerns B2-cells and isotype switched B cells. While a precise phenotyping of AT B cells is still missing, AT B2 cells are characterized by elevated leukotriene B4 receptor 1 (LTB4R1) expression that participates in their local recruitment to adipose tissue [118]. Further described B-cell changes during diet induced obesity include IgM and IgG2c systemic and local increase and a gradual loss of IL-10$^+$ B cells as well as their lower IL-10 production.

B-cell role in IR is supported by the analysis of μ heavy-chain knockout mice (deficient for B cells) and of CD20 treated mice (depleted mostly of B2 cells) that both show protection against diet induced obesity and manifested strong decrease in inflammatory cytokines production (IFNγ and TNFα) and improved ability to handle glucose [119].

5.2. Local role of adipose tissue B cells in obesity

The ability of adipose tissue B cells to locally produce IL-10, as well as their frequency, decrease rapidly during the course of obesity. Interestingly, specific deletion of IL-10 production in these cells led to amplified inflammation during HFD and increased metabolic disorder [120]. These findings provided evidence of a local role of B cells in obesity and associated metabolic disorders. Mechanistically, the authors show that adoptive transfer of IL-10 sufficient, but not IL-10 deficient B cells, significantly decreased the production of pro-inflammatory cytokines (TNFα, CCL2) and the activation of T cells (CD44 expression and IFNγ production) in diet induced obesity [120]. This situation is unique because in other tissues, such as the intestine, IL-10 is produced mainly by tissue resident macrophages. For example, macrophage specific deletion of IL-10 or its receptor (IL-10Rα) leads to gut permeability and spontaneous colitis [121].

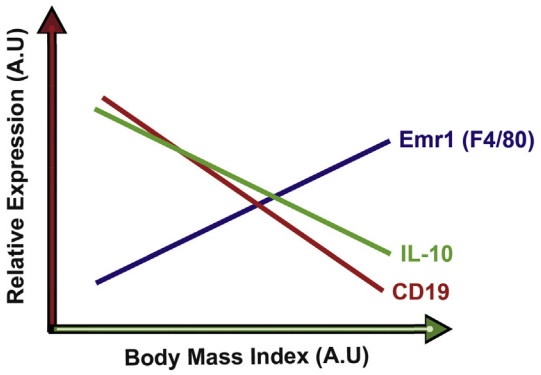

Fig. 4. Fluctuation of *CD19*, *Emr1* and *IL-10* mRNA expression in adipose tissue according to modulation of body mass index.

5.3. Systemic role of adipose tissue B cells in obesity

These data suggest that the local production of IL-10 by adipose tissue B cells may play a protective role during obesity. Further, lack of MHC-I and II in B cells is necessary for B-cell induction of insulin resistance and suggested that a direct presentation to T cells was necessary for B-cell negative impact. Alternatively, lack of T-cell help also blunts IgG production and therefore it remains possible that B-cell negative role during obesity is mediated via secreted Igs. Indeed, it was shown that IgG2c and IgM were increased during diet-induced obesity. IgG2c production has previously been shown to rely on B-cell autonomous sensing of TLR agonist while during obesity, IgM increase was shown to depend on TLR signaling [122].

As dissected in atherosclerosis models, B cell production of pathologic IgG is associated with diet-induced obesity, glucose intolerance and inflammation [119]. Importantly IgG negative impact is transferable and Fc-dependent echoes the negative impact of activating Fcγ receptor during obesity [123]. At the molecular level, the Fc portion of IgG binds to Fcγ receptors expressed on macrophages to induce the secretion of pro-inflammatory TNFα [119], IgG and FcgR also regulates antigen presentation by DCs [124]. Also, IgG negative role could be restricted to antigen binding part of immunoglobulins and independent from FcγR according to yet to be described modalities [125].

The impact of IgM induction during obesity merits specific comments. It was originally shown that B-1 cells could protect from diet-induced obesity via IgM production [126]. However, these findings have been recently debated as IgM transfer did not influence obesity outcome [119]. Interestingly, IgM levels are strongly correlated in both humans and mice with CD5L (AIM); produced mainly by macrophages [127]. During obesity both serum IgM and AIM levels increase, and it has been shown that IgM associates itself

with AIM to stabilize and prevent its degradation [128]. Such effect may have metabolic consequences since AIM is produced by ATMs and binds to CD36 on adipocytes where it induces lipolysis [129]. Besides stability, IgM and AIM might be handled differently when isolated or associated together. Thus, AIM bound to IgM inhibits Fc dependent IgM internalization by follicular dendritic cells in lymphoid organs [127]. However, it is currently unknown whether and how IgM affects AIM dependent lipolysis. The established ability of IgM to recognize oxidized lipids could be the regulator of this process. Is it surprising to find this dual function of IgG and IgM in obesity? Perhaps not, as one can legitimately draw a comparison between the role of B cells in atherosclerotic cardiovascular disease. The role of B cells during atherosclerosis is subset dependent. B-1 cells are atheroprotective and this effect is due to the production of natural IgMs [130,131]. By contrast, B2 cells play an atherogenic role via the production of pathogenic IgGs [132]. Therefore, better characterization of the role of each subset of B cells during obesity will help to understand their respective contribution to the overall pathology.

In summary, adipose tissue B cells control the local environment by secreting soluble factors (such as IL-10), but also contributing to systemic inflammation via their production of IgGs and potentially IgM.

6. Concluding remarks

Despite recent progress in dissecting the contribution of inflammation during obesity, we still lack many pieces of the puzzle. Many studies have addressed the role of ATMs, DCs and B cells, in the context of obesity and provided considerable insights about their functions and the production of specific soluble mediators. However, all these cell types co-exist and constantly interact in the adipose tissue, contributing both separately and cooperatively to maintain tissue homeostasis and prevent disease. The current challenge is to develop an integrative approach to predict how a deletion/modulation of a unique cell type, pathway or gene will affect the other cell partners and adipose tissue as a whole. Therefore, better understanding of their origin, development and function will be of huge importance for the successful development of therapeutic approaches.

Conflict of interest

The authors declared they do not have anything todisclose regarding conflict of interest with respect to this manuscript.

Acknowledgments

We apologize to colleagues whose works could not be cited due to space constraints. For additional lecture please refer to the following list of reviews [64–70].

AJM is supported by a career development fellowship from the NHMRC (APP1085752), a future leader fellowship from the National Heart Foundation (100440). RRG is supported by Centre National de la Recherche Scientifique (CNRS). SI is supported by Institut National de la Santé et de la Recherche Médicale (INSERM) and Agence Nationale de la Recherche (ANR-17-CE14-0017-01).

References

[1] K.M. Flegal, C.L. Ogden, Use of projection analyses and obesity trends-reply, J. Am. Med. Assoc. 316 (2016) 1317.
[2] M. Ng, T. Fleming, M. Robinson, et al., Global, regional, and national prevalence of overweight and obesity in children and adults during 1980-2013: a systematic analysis for the Global Burden of Disease Study 2013, Lancet 384 (2014) 766–781.
[3] D. Withrow, D.A. Alter, The economic burden of obesity worldwide: a systematic review of the direct costs of obesity, Obes. Rev. 12 (2011) 131–141.
[4] A.G. Tsai, D.F. Williamson, H.A. Glick, Direct medical cost of overweight and obesity in the USA: a quantitative systematic review, Obes. Rev. 12 (2011) 50–61.
[5] Y.C. Wang, K. McPherson, T. Marsh, et al., Health and economic burden of the projected obesity trends in the USA and the UK, Lancet 378 (2011) 815–825.
[6] C. Schulz, E. Gomez Perdiguero, L. Chorro, et al., A lineage of myeloid cells independent of Myb and hematopoietic stem cells, Science 336 (2012) 86–90.
[7] S. Yona, K.W. Kim, Y. Wolf, et al., Fate mapping reveals origins and dynamics of monocytes and tissue macrophages under homeostasis, Immunity 38 (2013) 79–91.
[8] F. Ginhoux, M. Greter, M. Leboeuf, et al., Fate mapping analysis reveals that adult microglia derive from primitive macrophages, Science 330 (2010) 841–845.
[9] S. Epelman, K.J. Lavine, A.E. Beaudin, et al., Embryonic and adult-derived resident cardiac macrophages are maintained through distinct mechanisms at steady state and during inflammation, Immunity 40 (2014) 91–104.
[10] D. Hashimoto, A. Chow, C. Noizat, et al., Tissue-resident macrophages self-maintain locally throughout adult life with minimal contribution from circulating monocytes, Immunity 38 (2013) 792–804.
[11] S.J. Jenkins, D. Ruckerl, G.D. Thomas, et al., IL-4 directly signals tissue-resident macrophages to proliferate beyond homeostatic levels controlled by CSF-1, J. Exp. Med. 210 (2013) 2477–2491.
[12] C.C. Bain, C.A. Hawley, H. Garner, et al., Long-lived self-renewing bone marrow-derived macrophages displace embryo-derived cells to inhabit adult serous cavities, Nat. Commun. 7 (2016) ncomms11852.
[13] C.L. Scott, F. Zheng, P. De Baetselier, et al., Bone marrow-derived monocytes give rise to self-renewing and fully differentiated Kupffer cells, Nat. Commun. 7 (2016) 10321.
[14] G.S. Hotamisligil, N.S. Shargill, B.M. Spiegelman, Adipose expression of tumor necrosis factor-alpha: direct role in obesity-linked insulin resistance, Science 259 (1993) 87–91.
[15] S.R. Bornstein, M. Abu-Asab, A. Glasow, et al., Immunohistochemical and ultrastructural localization of leptin and leptin receptor in human white adipose tissue and differentiating human adipose cells in primary culture, Diabetes 49 (2000) 532–538.
[16] S.P. Weisberg, D. McCann, M. Desai, et al., Obesity is associated with macrophage accumulation in adipose tissue, J. Clin. Invest. 112 (2003) 1796–1808.
[17] H. Xu, G.T. Barnes, Q. Yang, et al., Chronic inflammation in fat plays a crucial role in the development of obesity-related insulin resistance, J. Clin. Invest. 112 (2003) 1821–1830.
[18] U. Kintscher, M. Hartge, K. Hess, et al., T-lymphocyte infiltration in visceral adipose tissue: a primary event in adipose tissue inflammation and the development of obesity-mediated insulin resistance, Arterioscler. Thromb. Vasc. Biol. 28 (2008) 1304–1310.
[19] H. Wu, S. Ghosh, X.D. Perrard, et al., T-cell accumulation and regulated on activation, normal T cell expressed and secreted upregulation in adipose tissue in obesity, Circulation 115 (2007) 1029–1038.
[20] S.F. Hassnain Waqas, A. Noble, A.C. Hoang, et al., Adipose tissue macrophages develop from bone marrow-independent progenitors in Xenopus laevis and mouse, J. Leukoc. Biol. 102 (2017) 845–855.
[21] G. Ampem, H. Azegrouz, A. Bacsadi, et al., Adipose tissue macrophages in non-rodent mammals: a comparative study, Cell Tissue Res. 363 (2016) 461–478.
[22] O. Osborn, J.M. Olefsky, The cellular and signaling networks linking the immune system and metabolism in disease, Nat. Med. 18 (2012) 363–374.
[23] A. Chawla, K.D. Nguyen, Y.P. Goh, Macrophage-mediated inflammation in metabolic disease, Nat. Rev. Immunol. 11 (2011) 738–749.
[24] S.F. Hassnain Waqas, A. Noble, A.C. Hoang, et al., Adipose tissue macrophages develop from bone marrow-independent progenitors in Xenopus laevis and mouse, J. Leukoc. Biol. 102 (3) (2017 Sep) 845–855.
[25] R. Fan, A. Toubal, S. Goni, et al., Loss of the co-repressor GPS2 sensitizes macrophage activation upon metabolic stress induced by obesity and type 2 diabetes, Nat. Med. 22 (2016) 780–791.
[26] J. Leid, J. Carrelha, H. Boukarabila, et al., Primitive embryonic macrophages are required for coronary development and maturation, Circ. Res. 118 (2016) 1498–1511.
[27] E.L. Gautier, T. Shay, J. Miller, et al., Gene-expression profiles and transcriptional regulatory pathways that underlie the identity and diversity of mouse tissue macrophages, Nat. Immunol. 13 (2012) 1118–1128.
[28] J.C. Miller, B.D. Brown, T. Shay, et al., Deciphering the transcriptional network of the dendritic cell lineage, Nat. Immunol. 13 (2012) 888–899.
[29] C.N. Lumeng, J.B. DelProposto, D.J. Westcott, et al., Phenotypic switching of adipose tissue macrophages with obesity is generated by spatiotemporal differences in macrophage subtypes, Diabetes 57 (2008) 3239–3246.
[30] X. Xu, A. Grijalva, A. Skowronski, et al., Obesity activates a program of lysosomal-dependent lipid metabolism in adipose tissue macrophages independently of classic activation, Cell Metabol. 18 (2013) 816–830.
[31] P.R. Nagareddy, M. Kraakman, S.L. Masters, et al., Adipose tissue macrophages promote myelopoiesis and monocytosis in obesity, Cell Metabol. 19 (2014) 821–835.
[32] F. Ginhoux, K. Liu, J. Helft, et al., The origin and development of nonlymphoid

tissue CD103+ DCs, J. Exp. Med. 206 (2009) 3115–3130.
[33] M.G. Cecchini, M.G. Dominguez, S. Mocci, et al., Role of colony stimulating factor-1 in the establishment and regulation of tissue macrophages during postnatal development of the mouse, Development 120 (1994) 1357–1372.
[34] S. Sugita, Y. Kamei, J. Oka, et al., Macrophage-colony stimulating factor in obese adipose tissue: studies with heterozygous op/+ mice, Obesity 15 (2007) 1988–1995.
[35] Y. Wang, K.J. Szretter, W. Vermi, et al., IL-34 is a tissue-restricted ligand of CSF1R required for the development of Langerhans cells and microglia, Nat. Immunol. 13 (2012) 753–760.
[36] M. Greter, I. Lelios, P. Pelczar, et al., Stroma-derived interleukin-34 controls the development and maintenance of langerhans cells and the maintenance of microglia, Immunity 37 (2012) 1050–1060.
[37] L. Grayfer, J. Robert, Distinct functional roles of amphibian (Xenopus laevis) colony-stimulating factor-1- and interleukin-34-derived macrophages, J. Leukoc. Biol. 98 (2015) 641–649.
[38] E.J. Chang, S.K. Lee, Y.S. Song, et al., IL-34 is associated with obesity, chronic inflammation, and insulin resistance, J. Clin. Endocrinol. Metab. 99 (2014) E1263–E1271.
[39] C. Zheng, Q. Yang, J. Cao, et al., Local proliferation initiates macrophage accumulation in adipose tissue during obesity, Cell Death Dis. 7 (2016) e2167.
[40] N.V. Serbina, E.G. Pamer, Monocyte emigration from bone marrow during bacterial infection requires signals mediated by chemokine receptor CCR2, Nat. Immunol. 7 (2006) 311–317.
[41] S.U. Amano, J.L. Cohen, P. Vangala, et al., Local proliferation of macrophages contributes to obesity-associated adipose tissue inflammation, Cell Metabol. 19 (2014) 162–171.
[42] C. Zheng, Q. Yang, C. Xu, et al., CD11b regulates obesity-induced insulin resistance via limiting alternative activation and proliferation of adipose tissue macrophages, Proc. Natl. Acad. Sci. U. S. A. 112 (2015) E7239–E7248.
[43] J. Braune, U. Weyer, C. Hobusch, et al., IL-6 regulates M2 polarization and local proliferation of adipose tissue macrophages in obesity, J. Immunol. 198 (2017) 2927–2934.
[44] S.F.H. Waqas, A.C. Hoang, Y.T. Lin, et al., Neuropeptide FF increases M2 activation and self-renewal of adipose tissue macrophages, J. Clin. Invest. 127 (9) (2017 Sep 1) 3559.
[45] G.J. Randolph, Mechanisms that regulate macrophage burden in atherosclerosis, Circ. Res. 114 (2014) 1757–1771.
[46] C.S. Robbins, I. Hilgendorf, G.F. Weber, et al., Local proliferation dominates lesional macrophage accumulation in atherosclerosis, Nat. Med. 19 (2013) 1166–1172.
[47] C.N. Lumeng, J.L. Bodzin, A.R. Saltiel, Obesity induces a phenotypic switch in adipose tissue macrophage polarization, J. Clin. Invest. 117 (2007) 175–184.
[48] K. Sun, J. Tordjman, K. Clement, et al., Fibrosis and adipose tissue dysfunction, Cell Metabol. 18 (2013) 470–477.
[49] S. Boulenouar, X. Michelet, D. Duquette, et al., Adipose type one innate lymphoid cells regulate macrophage homeostasis through targeted cytotoxicity, Immunity 46 (2017) 273–286.
[50] C.P. Liang, S. Han, H. Okamoto, et al., Increased CD36 protein as a response to defective insulin signaling in macrophages, J. Clin. Invest. 113 (2004) 764–773.
[51] S. Han, C.P. Liang, T. DeVries-Seimon, et al., Macrophage insulin receptor deficiency increases ER stress-induced apoptosis and necrotic core formation in advanced atherosclerotic lesions, Cell Metabol. 3 (2006) 257–266.
[52] I. Tabas, A. Tall, D. Accili, The impact of macrophage insulin resistance on advanced atherosclerotic plaque progression, Circ. Res. 106 (2010) 58–67.
[53] C. Rask-Madsen, C.R. Kahn, Tissue-specific insulin signaling, metabolic syndrome, and cardiovascular disease, Arterioscler. Thromb. Vasc. Biol. 32 (2012) 2052–2059.
[54] I.F. Charo, Macrophage polarization and insulin resistance: PPARgamma in control, Cell Metabol. 6 (2007) 96–98.
[55] E. Vergadi, E. Ieronymaki, K. Lyroni, et al., Akt signaling pathway in macrophage activation and m1/m2 polarization, J. Immunol. 198 (2017) 1006–1014.
[56] O. Spadaro, C.D. Camell, L. Bosurgi, et al., IGF1 shapes macrophage activation in response to immunometabolic challenge, Cell Rep. 19 (2017) 225–234.
[57] Y. Lee, S.O. Ka, H.N. Cha, et al., Myeloid Sirtuin 6 deficiency causes insulin resistance in high-fat diet-fed mice by eliciting macrophage polarization toward an M1 phenotype, Diabetes 66 (10) (2017 Oct) 2659–2668.
[58] B. Shan, X. Wang, Y. Wu, et al., The metabolic ER stress sensor IRE1alpha suppresses alternative activation of macrophages and impairs energy expenditure in obesity, Nat. Immunol. 18 (2017) 519–529.
[59] S.C. Huang, B. Everts, Y. Ivanova, et al., Cell-intrinsic lysosomal lipolysis is essential for alternative activation of macrophages, Nat. Immunol. 15 (2014) 846–855.
[60] X. Prieur, C.Y. Mok, V.R. Velagapudi, et al., Differential lipid partitioning between adipocytes and tissue macrophages modulates macrophage lipotoxicity and M2/M1 polarization in obese mice, Diabetes 60 (2011) 797–809.
[61] D.A. Kaminski, T.D. Randall, Adaptive immunity and adipose tissue biology, Trends Immunol. 31 (2010) 384–390.
[62] D. Mathis, Immunological goings-on in visceral adipose tissue, Cell Metabol. 17 (2013) 851–859.
[63] R. Cancello, C. Henegar, N. Viguerie, et al., Reduction of macrophage infiltration and chemoattractant gene expression changes in white adipose tissue of morbidly obese subjects after surgery-induced weight loss, Diabetes 54 (2005) 2277–2286.
[64] L. Boutens, R. Stienstra, Adipose tissue macrophages: going off track during obesity, Diabetologia 59 (2016) 879–894.
[65] A.A. Hill, W. Reid Bolus, A.H. Hasty, A decade of progress in adipose tissue macrophage biology, Immunol. Rev. 262 (2014) 134–152.
[66] J.M. Olefsky, C.K. Glass, Macrophages, inflammation, and insulin resistance, Annu. Rev. Physiol. 72 (2010) 219–246.
[67] D.L. Morris, K. Singer, C.N. Lumeng, Adipose tissue macrophages: phenotypic plasticity and diversity in lean and obese states, Curr. Opin. Clin. Nutr. Metab. Care 14 (2011) 341–346.
[68] G. Martinez-Santibanez, C.N. Lumeng, Macrophages and the regulation of adipose tissue remodeling, Annu. Rev. Nutr. 34 (2014) 57–76.
[69] G. Chinetti-Gbaguidi, B. Staels, Macrophage polarization in metabolic disorders: functions and regulation, Curr. Opin. Lipidol. 22 (2011) 365–372.
[70] M.J. Kraakman, A.J. Murphy, K. Jandeleit-Dahm, et al., Macrophage polarization in obesity and type 2 diabetes: weighing down our understanding of macrophage function? Front. Immunol. 5 (2014) 470.
[71] H.S. Schipper, R. Nuboer, S. Prop, et al., Systemic inflammation in childhood obesity: circulating inflammatory mediators and activated CD14++ monocytes, Diabetologia 55 (2012) 2800–2810.
[72] A.J. Murphy, M. Akhtari, S. Tolani, et al., ApoE regulates hematopoietic stem cell proliferation, monocytosis, and monocyte accumulation in atherosclerotic lesions in mice, J. Clin. Invest. 121 (2011) 4138–4149.
[73] L. Yvan-Charvet, T. Pagler, E.L. Gautier, et al., ATP-binding cassette transporters and HDL suppress hematopoietic stem cell proliferation, Science 328 (2010) 1689–1693.
[74] K. Nasir, E. Guallar, A. Navas-Acien, et al., Relationship of monocyte count and peripheral arterial disease: results from the National Health and Nutrition Examination Survey 1999-2002, Arterioscler. Thromb. Vasc. Biol. 25 (2005) 1966–1971.
[75] C.M. Chapman, J.P. Beilby, B.M. McQuillan, et al., Monocyte count, but not C-reactive protein or interleukin-6, is an independent risk marker for subclinical carotid atherosclerosis, Stroke 35 (2004) 1619–1624.
[76] H. Kanda, S. Tateya, Y. Tamori, et al., MCP-1 contributes to macrophage infiltration into adipose tissue, insulin resistance, and hepatic steatosis in obesity, J. Clin. Invest. 116 (2006) 1494–1505.
[77] S.P. Weisberg, D. Hunter, R. Huber, et al., CCR2 modulates inflammatory and metabolic effects of high-fat feeding, J. Clin. Invest. 116 (2006) 115–124.
[78] M.L. Reitman, How does fat transition from white to beige? Cell Metabol. 26 (2017) 14–16.
[79] Y. Qiu, K.D. Nguyen, J.I. Odegaard, et al., Eosinophils and type 2 cytokine signaling in macrophages orchestrate development of functional beige fat, Cell 157 (2014) 1292–1308.
[80] R.R. Rao, J.Z. Long, J.P. White, et al., Meteorin-like is a hormone that regulates immune-adipose interactions to increase beige fat thermogenesis, Cell 157 (2014) 1279–1291.
[81] K.D. Nguyen, Y. Qiu, X. Cui, et al., Alternatively activated macrophages produce catecholamines to sustain adaptive thermogenesis, Nature 480 (2011) 104–108.
[82] K. Fischer, H.H. Ruiz, K. Jhun, et al., Alternatively activated macrophages do not synthesize catecholamines or contribute to adipose tissue adaptive thermogenesis, Nat. Med. 23 (2017) 623–630.
[83] Y. Wolf, S. Boura-Halfon, N. Cortese, et al., Brown-adipose-tissue macrophages control tissue innervation and homeostatic energy expenditure, Nat. Immunol. 18 (2017) 665–674.
[84] C.D. Camell, J. Sander, O. Spadaro, et al., Inflammasome-driven catecholamine catabolism in macrophages blunts lipolysis during ageing, Nature 550 (2017) 119–123.
[85] R.M. Pirzgalska, E. Seixas, J.S. Seidman, et al., Sympathetic neuron-associated macrophages contribute to obesity by importing and metabolizing norepinephrine, Nat. Med. 23 (2017) 1309–1318.
[86] K.J. Chung, A. Chatzigeorgiou, M. Economopoulou, et al., A self-sustained loop of inflammation-driven inhibition of beige adipogenesis in obesity, Nat. Immunol. 18 (2017) 654–664.
[87] R.M. Steinman, Z.A. Cohn, Identification of a novel cell type in peripheral lymphoid organs of mice. I. Morphology, quantitation, tissue distribution, J. Exp. Med. 137 (1973) 1142–1162.
[88] R.M. Steinman, Z.A. Cohn, Identification of a novel cell type in peripheral lymphoid organs of mice. II. Functional properties in vitro, J. Exp. Med. 139 (1974) 380–397.
[89] R.M. Steinman, D.S. Lustig, Z.A. Cohn, Identification of a novel cell type in peripheral lymphoid organs of mice. 3. Functional properties in vivo, J. Exp. Med. 139 (1974) 1431–1445.
[90] R.M. Steinman, M.D. Witmer, Lymphoid dendritic cells are potent stimulators of the primary mixed leukocyte reaction in mice, Proc. Natl. Acad. Sci. U. S. A. 75 (1978) 5132–5136.
[91] M. Swiecki, M. Colonna, The multifaceted biology of plasmacytoid dendritic cells, Nat. Rev. Immunol. 15 (2015) 471–485.
[92] R. Forster, A. Schubel, D. Breitfeld, et al., CCR7 coordinates the primary immune response by establishing functional microenvironments in secondary lymphoid organs, Cell 99 (1999) 23–33.
[93] T.L. Murphy, G.E. Grajales-Reyes, X. Wu, et al., Transcriptional control of dendritic cell development, Annu. Rev. Immunol. 34 (2016) 93–119.

[94] M. Bogunovic, F. Ginhoux, J. Helft, et al., Origin of the lamina propria dendritic cell network, Immunity 31 (2009) 513–525.
[95] C. Varol, A. Vallon-Eberhard, E. Elinav, et al., Intestinal lamina propria dendritic cell subsets have different origin and functions, Immunity 31 (2009) 502–512.
[96] K. Hildner, B.T. Edelson, W.E. Purtha, et al., Batf3 deficiency reveals a critical role for CD8alpha+ dendritic cells in cytotoxic T cell immunity, Science 322 (2008) 1097–1100.
[97] S. Hambleton, S. Salem, J. Bustamante, et al., IRF8 mutations and human dendritic-cell immunodeficiency, N. Engl. J. Med. 365 (2011) 127–138.
[98] P. Tailor, T. Tamura, H.C. Morse 3rd, et al., The BXH2 mutation in IRF8 differentially impairs dendritic cell subset development in the mouse, Blood 111 (2008) 1942–1945.
[99] A. Schlitzer, N. McGovern, P. Teo, et al., IRF4 transcription factor-dependent CD11b+ dendritic cells in human and mouse control mucosal IL-17 cytokine responses, Immunity 38 (2013) 970–983.
[100] E.K. Persson, H. Uronen-Hansson, M. Semmrich, et al., IRF4 transcription-factor-dependent CD103(+)CD11b(+) dendritic cells drive mucosal T helper 17 cell differentiation, Immunity 38 (2013) 958–969.
[101] J.W. Williams, M.Y. Tjota, B.S. Clay, et al., Transcription factor IRF4 drives dendritic cells to promote Th2 differentiation, Nat. Commun. 4 (2013) 2990.
[102] B. Vander Lugt, A.A. Khan, J.A. Hackney, et al., Transcriptional programming of dendritic cells for enhanced MHC class II antigen presentation, Nat. Immunol. 15 (2014) 161–167.
[103] Y. Gao, S.A. Nish, R. Jiang, et al., Control of T helper 2 responses by transcription factor IRF4-dependent dendritic cells, Immunity 39 (2013) 722–732.
[104] A.T. Satpathy, C.G. Briseno, J.S. Lee, et al., Notch2-dependent classical dendritic cells orchestrate intestinal immunity to attaching-and-effacing bacterial pathogens, Nat. Immunol. 14 (2013) 937–948.
[105] R. Tussiwand, B. Everts, G.E. Grajales-Reyes, et al., Klf4 expression in conventional dendritic cells is required for T helper 2 cell responses, Immunity 42 (2015) 916–928.
[106] K.L. Lewis, M.L. Caton, M. Bogunovic, et al., Notch2 receptor signaling controls functional differentiation of dendritic cells in the spleen and intestine, Immunity 35 (2011) 780–791.
[107] S. Ivanov, J.P. Scallan, K.W. Kim, et al., CCR7 and IRF4-dependent dendritic cells regulate lymphatic collecting vessel permeability, J. Clin. Invest. 126 (2016) 1581–1591.
[108] K.W. Cho, B.F. Zamarron, L.A. Muir, et al., Adipose tissue dendritic cells are independent contributors to obesity-induced inflammation and insulin resistance, J. Immunol. 197 (2016) 3650–3661.
[109] E.L. Kuan, S. Ivanov, E.A. Bridenbaugh, et al., Collecting lymphatic vessel permeability facilitates adipose tissue inflammation and distribution of antigen to lymph node-homing adipose tissue dendritic cells, J. Immunol. 194 (2015) 5200–5210.
[110] H. Frikke-Schmidt, B.F. Zamarron, R.W. O'Rourke, et al., Weight loss independent changes in adipose tissue macrophage and T cell populations after sleeve gastrectomy in mice, Mol. Metabol. 6 (2017) 317–326.
[111] J. Hellmann, B.E. Sansbury, C.R. Holden, et al., CCR7 maintains nonresolving lymph node and adipose inflammation in obesity, Diabetes 65 (2016) 2268–2281.
[112] M. Stefanovic-Racic, X. Yang, M.S. Turner, et al., Dendritic cells promote macrophage infiltration and comprise a substantial proportion of obesity-associated increases in CD11c+ cells in adipose tissue and liver, Diabetes 61 (2012) 2330–2339.
[113] A. Bertola, T. Ciucci, D. Rousseau, et al., Identification of adipose tissue dendritic cells correlated with obesity-associated insulin-resistance and inducing Th17 responses in mice and patients, Diabetes 61 (2012) 2238–2247.
[114] Y. Chen, J. Tian, X. Tian, et al., Adipose tissue dendritic cells enhances inflammation by prompting the generation of Th17 cells, PLoS One 9 (2014) e92450.
[115] S.T. Ferris, J.A. Carrero, J.F. Mohan, et al., A minor subset of Batf3-dependent antigen-presenting cells in islets of Langerhans is essential for the development of autoimmune diabetes, Immunity 41 (2014) 657–669.
[116] N. Shulzhenko, A. Morgun, W. Hsiao, et al., Crosstalk between B lymphocytes, microbiota and the intestinal epithelium governs immunity versus metabolism in the gut, Nat. Med. 17 (2011) 1585–1593.
[117] N. Baumgarth, B-1 cell heterogeneity and the regulation of natural and antigen-induced IgM production, Front. Immunol. 7 (2016) 324.
[118] W. Ying, J. Wollam, J.M. Ofrecio, et al., Adipose tissue B2 cells promote insulin resistance through leukotriene LTB4/LTB4R1 signaling, J. Clin. Invest. 127 (2017) 1019–1030.
[119] D.A. Winer, S. Winer, L. Shen, et al., B cells promote insulin resistance through modulation of T cells and production of pathogenic IgG antibodies, Nat. Med. 17 (2011) 610–617.
[120] S. Nishimura, I. Manabe, S. Takaki, et al., Adipose natural regulatory B cells negatively control adipose tissue inflammation, Cell Metabol. (2013 Oct 22) pii: S1550-4131(13)00386-0.
[121] E. Zigmond, B. Bernshtein, G. Friedlander, et al., Macrophage-restricted interleukin-10 receptor deficiency, but not IL-10 deficiency, causes severe spontaneous colitis, Immunity 40 (2014) 720–733.
[122] C. Pasare, R. Medzhitov, Control of B-cell responses by Toll-like receptors, Nature 438 (2005) 364–368.
[123] L. van Beek, I.O. Vroegrijk, S. Katiraei, et al., FcRgamma-chain deficiency reduces the development of diet-induced obesity, Obesity 23 (2015) 2435–2444.
[124] A. Bergtold, D.D. Desai, A. Gavhane, et al., Cell surface recycling of internalized antigen permits dendritic cell priming of B cells, Immunity 23 (2005) 503–514.
[125] A.D. van Dam, L. van Beek, A.C.M. Pronk, et al., IgG is elevated in obese white adipose tissue but does not induce glucose intolerance via Fcgamma-receptor or complement, Int. J. Obes. (Lond). 42 (2) (2018 Feb) 260–269.
[126] D.B. Harmon, P. Srikakulapu, J.L. Kaplan, et al., Protective role for B-1b B cells and IgM in obesity-associated inflammation, glucose intolerance, and insulin resistance, Arterioscler. Thromb. Vasc. Biol. 36 (2016) 682–691.
[127] S. Arai, N. Maehara, Y. Iwamura, et al., Obesity-associated autoantibody production requires AIM to retain the immunoglobulin M immune complex on follicular dendritic cells, Cell Rep. 3 (2013) 1187–1198.
[128] T. Kai, T. Yamazaki, S. Arai, et al., Stabilization and augmentation of circulating AIM in mice by synthesized IgM-Fc, PLoS One 9 (2014), e97037.
[129] J. Kurokawa, S. Arai, K. Nakashima, et al., Macrophage-derived AIM is endocytosed into adipocytes and decreases lipid droplets via inhibition of fatty acid synthase activity, Cell Metabol. 11 (2010) 479–492.
[130] T. Kyaw, C. Tay, S. Krishnamurthi, et al., B1a B lymphocytes are atheroprotective by secreting natural IgM that increases IgM deposits and reduces necrotic cores in atherosclerotic lesions, Circ. Res. 109 (2011) 830–840.
[131] H. Hosseini, Y. Li, P. Kanellakis, et al., Toll-like receptor (TLR)4 and MyD88 are essential for atheroprotection by peritoneal B1a B cells, J. Am. Heart Assoc. 5 (2016).
[132] A.P. Sage, D. Tsiantoulas, L. Baker, et al., BAFF receptor deficiency reduces the development of atherosclerosis in mice—brief report, Arterioscler. Thromb. Vasc. Biol. 32 (2012) 1573–1576.

Le sommeil protège-t-il nos vaisseaux sanguins ?

Laurent Yvan-Charvet, Johanna Merlin

Inserm U1065, Université Côte d'Azur, Centre méditerranéen de médecine moléculaire (C3M), Atip-avenir, Fédération hospitalo-universitaire Oncoage, 06204 Nice, France.
yvancharvet@unice.fr

> L'industrialisation de nos sociétés a entraîné de profonds changements dans notre mode de vie. Parallèlement, on observe une nette augmentation de l'incidence de multiples maladies inflammatoires chroniques. C'est en particulier vrai pour l'athérosclérose, la cause majeure des maladies cardio-vasculaires, qui sont responsables de plus de 30 % des décès dans le monde. L'athérosclérose est considérée comme une maladie inflammatoire chronique, caractérisée par la formation de plaques d'athérome suite à un dépôt de lipides, en particulier de cholestérol, dans la paroi des grosses et moyennes artères. Ces lipides, suite à leur modification biochimique, induisent une réaction inflammatoire locale qui perturbe la cicatrisation et favorise le recrutement de monocytes circulants, conduisant à une accumulation de macrophages inflammatoires gorgés de lipides, à l'origine du développement de la plaque d'athérome. Il n'est donc pas étonnant qu'une alimentation inadaptée à nos nouveaux modes de vie sédentaire ait été incriminée dans le développement des maladies cardio-vasculaires [1]. Mais qu'entendons-nous vraiment par « mode de vie » ? Par définition, le mode de vie d'un individu inclut tout ce qu'il fait, du réveil au coucher, et même pendant qu'il dort. Chacun se rappelle les conseils avisés de ses parents ou grands-parents « d'avoir une bonne nuit de sommeil pour récupérer ». Mais que cachent vraiment ces observations empiriques ? Des études épidémiologiques ont confirmé la pertinence des conseils de nos aïeux, en faisant le lien entre durée et/ou qualité du sommeil et prévalence des maladies cardio-vasculaires [2-3]. Ainsi, il a été proposé qu'une nuit idéale pour nos artères serait d'environ 7 heures de sommeil. Bien entendu, les besoins peuvent différer d'un individu à l'autre. A cause de l'augmentation du temps de travail, l'accroissement du travail posté ou l'utilisation de dispositifs électroniques qui tend à changer la durée et la qualité du sommeil dans nos modes de vie modernes, il a été estimé qu'un français sur trois dort moins de 6 heures par nuit. Mais quels sont les mécanismes liant le manque de sommeil et l'athérosclérose ?

Afin de comprendre comment le sommeil protège contre les maladies cardio-vasculaires, McAlpine *et al.* ont étudié l'effet de la fragmentation du sommeil dans un modèle préclinique murin [4]. Des animaux susceptibles de développer des plaques d'athérome ont ainsi été tenus éveillés de manière intermittente par le déplacement d'une barre au fond des cages d'élevage, et comparés à des animaux qui avaient un cycle de sommeil normal. Ces auteurs ont ainsi prouvé que les souris ayant un sommeil fragmenté développaient plus de plaques d'athérome, un phénomène accompagné par une infiltration très importante de macrophages. Étonnamment, ce phénotype était associé à un état inflammatoire chronique caractérisé par une augmentation du nombre de globules blancs dans le sang, en particulier des monocytes et des polynucléaires neutrophiles, secondaire à une production accrue de ces cellules dans la moelle osseuse. Bien que l'association entre maladies cardio-vasculaires et taux élevé de leucocytes (hyperleucocytose) et monocytes (monocytose) dans le sang soit bien établie [1], l'existence d'un sommeil fragmenté n'avait pas été mise en évidence comme facteur de risque dans l'apparition de ces anomalies avant cette étude.

Dans leur article de synthèse paru en 2015, Nahrendorf et Swirski, derniers signataires de cette étude récente rapportant les résultats chez la souris, faisaient un premier bilan des arguments scientifiques permettant de relier le mode de vie dans nos sociétés industrialisées à l'existence d'une inflammation chronique à bas bruit, qui aboutit à une production accrue de globules blancs [1]. Ces auteurs discutaient du rôle de l'obésité (déséquilibre entre prise alimentaire excessive et sédentarité), de changements du microbiote liés également en grande partie à notre alimentation, et du stress psychique induisant la libération de corticostéroïdes ou de catécholamines [1]. En se fondant sur l'existence d'une régulation circadienne des polynucléaires neutrophiles et des monocytes, et sur le fait que les troubles du sommeil observés chez les individus souffrant d'apnées du sommeil étaient associés à une inflammation chronique (augmentation systémique du taux de cytokines inflammatoires), les auteurs présentaient déjà l'hypothèse d'un lien entre sommeil fragmenté et surproduction de globules blancs comme un mécanisme potentiel du développement des complications cardio-vasculaires [1]. Quatre ans plus tard, non seulement ils valident leur hypothèse, mais de plus, ils identifient un nouveau mécanisme qui

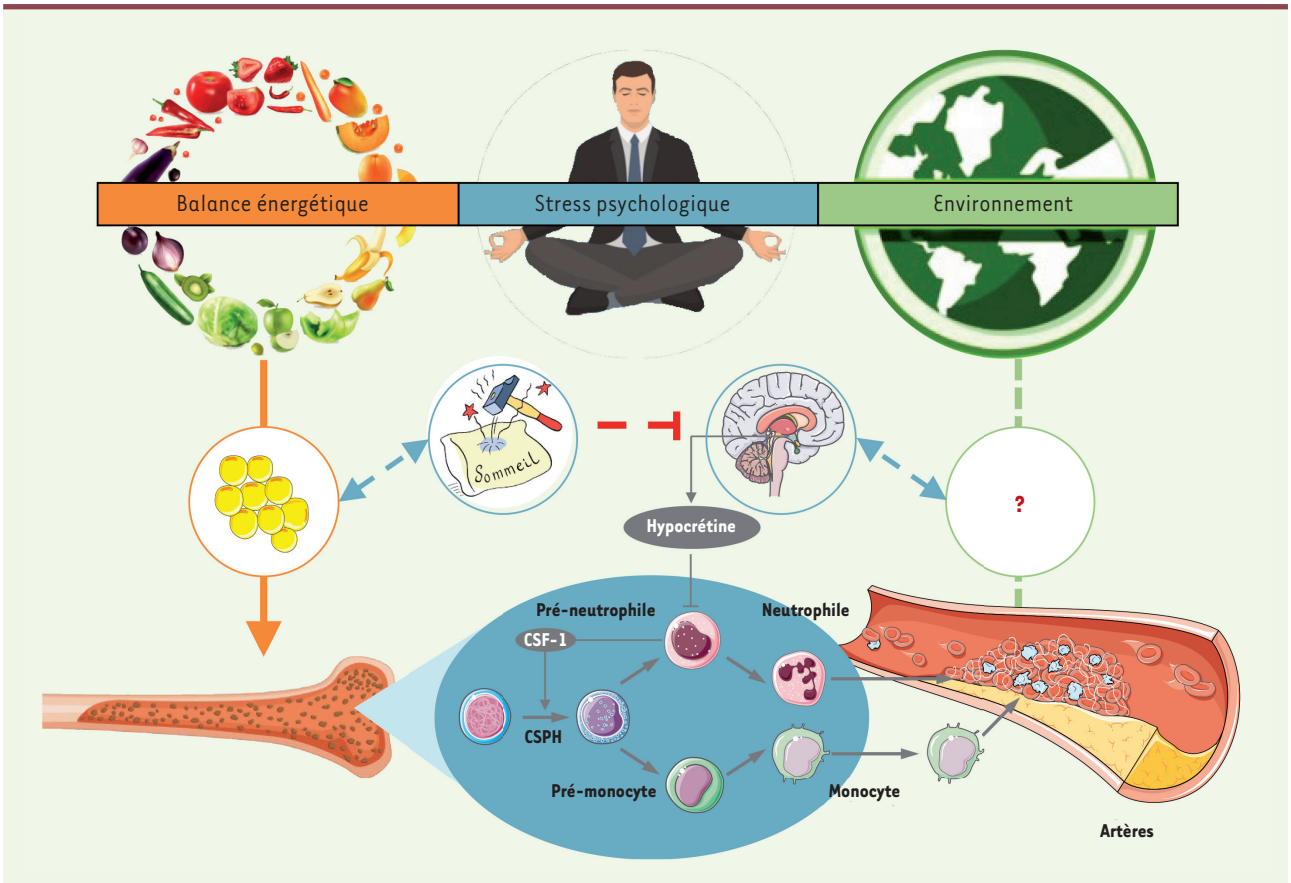

Figure 1. ***Le sommeil fragmenté nuit à nos artères.*** Les sociétés industrialisées ont connu de profonds changements du mode de vie, concernant notamment notre équilibre énergétique, le stress psychique, et l'environnement. Le lien entre ces changements et la forte augmentation de l'incidence de multiples maladies inflammatoires chroniques n'est pas encore complètement élucidé. Dans une étude récente chez la souris, McAlpine *et al.* montrent que le sommeil fragmenté, d'ailleurs souvent associé au stress psychique dans les sociétés humaines, détériore les artères. En soumettant des souris, dans un modèle préclinique, à un protocole de fragmentation du sommeil, les auteurs ont pu mettre en évidence une diminution de la sécrétion d'hypocrétine, une hormone également connue sous le nom d'orexine, par des neurones localisés dans l'hypothalamus. Cette hormone agit sur des cellules pré-neutrophiles de la moelle osseuse. En inhibant la synthèse du facteur de croissance CSF-1 (ou M-CSF, pour *macrophage colony-stimulating factor*) par ces cellules, l'hypocrétine limite la production de monocytes et polynucléaires neutrophiles (des cellules impliquées dans l'inflammation), à partir des cellules souches progénitrices hématopoïétiques (CSPH). La diminution de la sécrétion d'hypocrétine lors d'un sommeil fragmenté entraîne au contraire une production excessive de monocytes et de polynucléaires neutrophiles, qui s'accumulent dans les artères, favorisant la formation de plaques d'athérome. Il n'est pas exclu que d'autres mécanismes, en rapport avec les effets métaboliques de l'hypocrétine, contribuent à la détérioration de la paroi artérielle en cas de sommeil fragmenté.

enrichit nos connaissances sur la complexité du contrôle de la production des globules blancs dans la moelle osseuse.

Le stress émotionnel, lié à une activité excessive de l'amygdale cérébrale, a été associé à une augmentation de l'activité de la moelle osseuse et une inflammation à bas bruit, qui prédisent les événements cardio-vasculaires [5]. Cependant, McAlpine *et al.* n'ont pas mis en évidence de modifications de la concentration du cortisol dans le sang ou de l'activité du système nerveux sympathique, ce qui indiquait que le sommeil fragmenté stimule l'hématopoïèse par un nouveau mécanisme [4]. Les auteurs ont également exclu un rôle du microbiote intestinal en montrant que l'augmentation de l'hématopoïèse liée à un sommeil fragmenté était maintenue après l'administration d'antibiotiques à large spectre. C'est en analysant l'expression des gènes de l'hypothalamus impliqués dans le contrôle du sommeil que les auteurs ont identifié une diminution de la production d'hypocrétine, également appelée orexine, un neurotransmetteur excitateur stimulant l'appétit et l'état d'éveil [6]. Les auteurs ont établi une corrélation entre la diminution des taux plasmatiques d'hypocrétine et l'augmentation de la production de globules blancs dans la moelle osseuse [4]. Intrigués par cette observation, ils ont alors produit des souris mutantes chez lesquelles le gène de l'hypocrétine avait été

invalidé, et ont ainsi pu montrer que la déficience en hypocrétine augmentait la production des polynucléaires neutrophiles et des monocytes en accélérant la prolifération et la différenciation des cellules hématopoïétiques progénitrices de la moelle osseuse. En produisant des souris déficientes en hypocrétine dans un modèle de susceptibilité à l'athérosclérose, les auteurs ont également montré, chez ces souris, l'aggravation de la maladie athéromateuse associée à une accumulation de polynucléaires neutrophiles, de monocytes, et de macrophages dans les plaques d'athérome. Chez ces souris mutantes, la perfusion d'hypocrétine par une mini-pompe osmotique limite l'augmentation de l'hématopoïèse et le développement de l'athérosclérose induits par un sommeil fragmenté. Les auteurs concluent que la sécrétion hormonale d'hypocrétine pendant le sommeil serait un mécanisme central de protection contre la survenue de complications cardio-vasculaires.

Pour tenter de comprendre les mécanismes moléculaires sous-jacents, les auteurs ont trié 14 populations cellulaires différentes de la moelle osseuse. Ils ont trouvé que seuls les polynucléaires neutrophiles exprimaient l'ARNm du récepteur de l'hypocrétine, et que parmi ces cellules, les pré-neutrophiles l'exprimaient de manière encore plus abondante [4]. Mais quelle est le rôle de ces cellules ? Les pré-neutrophiles synthétisent le facteur de stimulation des colonies de macrophages (CSF-1, également appelé M-CSF, pour *macrophage colony- stimulating factor*), qui est impliqué dans la production des globules blancs de la lignée myélomonocytaire à partir des cellules souches hématopoïétiques [7]. McAlpine *et al*. ont montré un effet inhibiteur de l'hypocrétine sur la production de CSF-1 par les pré-neutrophiles *in vitro*, et chez les souris déficientes pour l'hypocrétine, une augmentation de la production de CSF-1 par les pré-neutrophiles *ex vivo* et dans la moelle osseuse *in vivo* [4]. Ils ont également confirmé ce mécanisme de contrôle de l'hématopoïèse pendant le sommeil en invalidant CSF-1 dans la moelle osseuse de souris susceptibles à l'athérosclérose et en les soumettant à un sommeil fragmenté : ces souris étaient alors protégées contre l'augmentation de l'hématopoïèse et le développement d'une athérosclérose induits par un sommeil fragmenté. Cependant, d'autres mécanismes d'action de l'hypocrétine sur l'hématopoïèse sont possibles, en particulier du fait de ses effets métaboliques [6].

La diminution de la prise alimentaire chez les souris soumises à un sommeil fragmenté, malgré un poids corporel identique [4], suggère que leur dépense énergétique est diminuée et leur métabolisme altéré. Ces résultats sont à mettre en parallèle avec l'apparition d'une obésité et d'une intolérance au glucose tardive chez les souris déficientes en hypocrétine, et avec la plus grande incidence de l'obésité et de l'intolérance au glucose chez les patients narcoleptiques par déficience en hypocrétine [6]. L'absence d'effet du sommeil fragmenté sur la tolérance au glucose dans l'étude de McAlpine *et al*. [4] pourrait donc être expliquée par le fait que l'étude a été réalisée chez de jeunes souris. Bien que les mécanismes de la reprogrammation du métabolisme des cellules souches hématopoïétiques de la moelle osseuse soient encore mal connus, cette reprogrammation métabolique a été récemment impliquée dans de nombreuses maladies chroniques inflammatoires, induites entre autres par un régime riche en graisse ou une obésité d'origine génétique par déficience en leptine [8, 9]. Il n'est donc pas exclu qu'une telle reprogrammation des cellules hématopoïétiques soit liée aux effets métaboliques de la diminution d'hypocrétine observée chez les souris soumises à un sommeil fragmenté.

L'utilisation de corticostéroïdes et de médicaments anti-inflammatoires non stéroïdiens dans des maladies chroniques inflammatoires a été scrutée par les instances de santé pour leur effet faible mais potentiellement délétère sur le risque cardio-vasculaire. A l'inverse, l'essai clinique CANTOS ciblant la cytokine inflammatoire interleukine-1β a fourni des résultats encourageants pour réduire le risque cardio-vasculaire dans une population à haut risque [10]. Par ailleurs, compte-tenu des résultats récents de l'étude de McAlpine *et al*. chez la souris, que penser d'une éventuelle utilisation thérapeutique d'antagonistes du récepteur de l'hypocrétine, actuellement en développement en tant que médicaments contre l'insomnie ?

Outre les perspectives thérapeutiques pour diminuer le risque cardio-vasculaire lié aux troubles du sommeil, l'étude de McAlpine *et al*. ouvre des perspectives plus larges concernant les conséquences de notre mode de vie pour la santé [4]. Dans un article paru récemment, Latz prône une politique agressive d'éducation et de taxation pour réduire des facteurs de risque cardio-vasculaire bien connus tels que la « malbouffe » et la consommation excessive d'alcool ou de tabac [9]. Mais à l'heure de l'engouement collectif pour la consommation de produits issus de l'agriculture « biologique » et d'une prise de conscience de l'impact de l'environnement sur la santé par les pouvoirs publics, qu'en est-il de la prise en considération des autres facteurs de risque cardio-vasculaire ? Le livre du Dr Michel Lallement, paru en 2017, a mis en perspective « les 3 clés de la santé » : alimentation, psychisme (incluant les émotions), et environnement [11]. Mais que sait-on vraiment par exemple de l'impact de la pollution de l'air ou des perturbateurs endocriniens sur nos artères ? Le journal *Le Monde* a récemment révélé la conclusion d'une étude selon laquelle 107 766 années de vie en bonne santé seraient perdues chaque année en Ile-de-France à cause des nuisances sonores liées aux transports, dont on commence à mesurer les conséquences sur la qualité du sommeil, en particulier sa fragmentation. Les résultats de l'étude de McAlpine *et al*. publiés récemment pourraient donc contribuer à une véritable prise de conscience collective. ◊

Does sleep preserve blood vessels?

LIENS D'INTÉRÊT

Les auteurs déclarent n'avoir aucun lien d'intérêt concernant les données publiées dans cet article.

RÉFÉRENCES

1. Nahrendorf M, Swirski FK. Lifestyle effects on hematopoiesis and atherosclerosis. *Circ Res* 2015 ; 116 : 884-94.
2. Tobaldini E, Fiorelli EM, Solbiati M, *et al.* Short sleep duration and cardiometabolic risk: from pathophysiology to clinical evidence. *Nat Rev Cardiol* 2019 ; 16 : 213-24.
3. Cappuccio FP, Miller MA. Sleep and cardio-metabolic disease. *Curr Cardiol Rep* 2017 ; 19 : 110.
4. McAlpine CS, Kiss MG, Rattik S, *et al.* Sleep modulates haematopoiesis and protects against atherosclerosis. *Nature* 2019 ; 566 : 383-7.
5. Tawakol A, Ishai A, Takx RA, *et al.* Relation between resting amygdalar activity and cardiovascular events: a longitudinal and cohort study. *Lancet* 2017 ; 389 : 834-45.
6. Sakurai T. The role of orexin in motivated behaviours. *Nat Rev Neurosci* 2014 ; 15 : 719-31.
7. Mossadegh-Keller N, Sarrazin S, *et al.* M-CSF instructs myeloid lineage fate in single haematopoietic stem cells. *Nature* 2013 ; 497 : 239-43.
8. Yvan-Charvet L, Swirski FK. Is defective cholesterol efflux an integral inflammatory component in myelopoiesis-driven cardiovascular diseases? *Eur Heart J* 2018 ; 39 : 2168-71.
9. Christ A, Latz E. The Western lifestyle has lasting effects on metainflammation. *Nat Rev Immunol* 2019 ; 19 : 267-8.
10. Ridker PM, Everett BM, Thuren T, *et al.* Antiinflammatory therapy with Canakinumab for atherosclerotic disease. *N Engl J Med* 2017 ; 377 : 1119-31.
11. Lallement M. *Les trois clés de la santé.* Donnemarie-Dontilly : Éditions Mosaïque-Santé, 2017.

NOUVELLE

Un nouveau talon d'Achille du bacille de la tuberculose

Claude Gutierrez, Olivier Neyrolles

Institut de pharmacologie et biologie structurale (IPBS), université de Toulouse, CNRS, UPS, 205 route de Narbonne, 31000 Toulouse, France.
claude.gutierrez@ipbs.fr

› La tuberculose, infection principalement pulmonaire due à la bactérie *Mycobacterium tuberculosis*, est la maladie infectieuse due à un agent unique la plus meurtrière à l'échelle mondiale[1]. L'expansion de souches de *M. tuberculosis* multi-résistantes, voire totalement résistantes, aux antibiotiques fait craindre l'apparition d'une pandémie incontrôlable. Ainsi, bien que la tuberculose soit, dans l'imaginaire collectif, une maladie associée au passé, elle reste un problème de santé majeur, et la recherche de nouvelles pistes thérapeutiques est plus que jamais nécessaire. Dans une étude récente, menée par un consortium associant notre équipe et deux équipes du Laboratoire européen de biologie moléculaire (EMBL) à Hambourg et de l'Institut Francis Crick à Londres, nous avons identifié une nouvelle piste thérapeutique, fondée sur l'activation d'un système toxine/antitoxine (TA) pouvant entraîner le « suicide » des cellules de *M. tuberculosis* [1].

[1] Rapport de l'Organisation mondiale de la santé 2018.

Les systèmes toxine/antitoxine

Chez les bactéries, les systèmes TA sont des modules formés d'un gène codant une toxine protéique, capable d'intoxiquer la cellule productrice en bloquant un processus essentiel de son métabolisme (synthèse des protéines par exemple), et d'un élément d'immunité contre cette toxine, l'antitoxine, qui peut, en inhibant la production et/ou l'activité de la toxine, protéger la bactérie productrice [2, 3]. Ces systèmes sont regroupés en diverses familles (de I à VI) selon la nature de l'antitoxine (protéine ou ARN), et le mécanisme d'inactivation de la toxine. Par exemple, dans les systèmes TA de type II, les plus étudiés, l'antitoxine est une protéine qui se lie directement à la toxine pour l'inactiver. Pour les systèmes TA de type IV, la toxine est aussi une protéine, mais elle empêche l'action de la toxine sans interaction directe avec celle-ci. La clé du fonctionnement des systèmes TA est que la toxine et l'antitoxine sont stables en conditions physiologiques standard, mais que l'antitoxine est déstabilisée dans certaines conditions de stress, libérant l'activité de la toxine qui bloque alors la croissance ou peut même entraîner la mort des bactéries soumises au stress. Initialement identifiés comme des systèmes « d'addiction » à des plasmides, les systèmes TA sont présents dans la plupart des génomes bactériens, et ils participent à diverses fonctions biologiques, dont la stabilisation de réplicons ou d'îlots génomiques, la lutte contre les infections par les bactériophages, ou l'entrée en persistance des bactéries. Cependant, le rôle effectif de la plupart des systèmes TA reste une question ouverte [4, 5]. Ceci est particulièrement vrai pour *M. tuberculosis*, dont le génome est très riche en systèmes TA. En effet, on retrouve dans le génome de *M. tuberculosis* plus de 80 systèmes TA, principalement de type II, dont un grand nombre sont portés par des îlots génomiques acquis par transfert horizontal chez l'ancêtre de *M. tuberculosis* [6].

https://doi.org/10.1051/medsci/2019145

Review

Myeloid Cell Diversity and Impact of Metabolic Cues during Atherosclerosis

Alexandre Gallerand †, Marion I. Stunault †, Johanna Merlin †, Rodolphe R. Guinamard, Laurent Yvan-Charvet, Stoyan Ivanov *

Mediterranean center of molecular medicine (C3M)–Université Côte d'Azur–INSERM U1065, Team 13, Nice, 06200, France

† These authors contributed equally to this work.

* Correspondence: Stoyan Ivanov, Email: Stoyan.ivanov@unice.fr.

ABSTRACT

Myeloid cells are key contributors to tissue, immune and metabolic homeostasis and their alteration fuels inflammation and associated disorders such as atherosclerosis. Conversely, in a classical chicken-and-egg situation, systemic and local metabolism, together with receptor-mediated activation, regulate intracellular metabolism and reprogram myeloid cell functions. Those regulatory loops are notable during the development of atherosclerotic lesions. Therefore, understanding the intricate metabolic mechanisms regulating myeloid cell biology could lead to innovative approaches to prevent and treat cardiovascular diseases. In this review, we will attempt to summarize the different metabolic factors regulating myeloid cell homeostasis and contribution to atherosclerosis, the most frequent cardiovascular disease.

KEYWORDS: macrophage; monocyte; dendritic cell; metabolism; atherosclerosis

INTRODUCTION

Atherosclerosis is a major vascular disease that continuously spreads worldwide. Atherosclerosis contributes to cardiovascular disease (CVD)-related deaths, estimated to account for more than 17 million deaths per year worldwide, making this pathology a major public health issue. Atherosclerosis is described as a metabolic disease associated with a chronic low-grade inflammation linked to lipid accumulation in the intima of large and medium-sized arteries, which favors plaque formation [1,2]. Since the 1950's, mounting evidence linked cholesterol metabolism to atherosclerosis development. Atherosclerotic patients not only showed increased serum cholesterol levels, and more specifically cholesterol present in the low-density lipoproteins fraction (LDL), but also accumulation of cholesterol in macrophage foam cells pointing out to cholesterol as a culprit of immunometabolic perturbations in the establishment and development of atherosclerosis. LDL-cholesterol levels are now considered as an independent risk factor for CVDs [3,4].

Received: 29 June 2020
Accepted: 10 August 2020
Published: 17 August 2020

Interestingly, LDL accumulation into the arterial wall is associated with inflammatory signals which trigger the attraction of myeloid cells such as dendritic cells (DC), neutrophils, macrophages and monocytes [5]. Advanced atherosclerotic plaques are complex structures containing lipids, necrotic cores, calcification zones and immune cells [6]. Plaque growth increases arterial stiffness and could be responsible for disturbed blood flow, while their rupture can lead to ischaemic strokes and transient cerebral ischaemic attacks [7].

During the past two decades, tremendous progress has been made highlighting the involvement of immune cells at all stages of the disease including plaque initiation, development and rupture. Particularly, the accumulation of myeloid cells in human atheromatous plaques is a strong marker of plaque instability and predictor of negative outcome [8,9]. The respective role of the different myeloid cell types in the establishment and progression of the disease has since been thoroughly investigated using pre-clinical mouse models. Monocytes, which enter atheromatous plaques from the blood circulation and differentiate into macrophages, are the main culprits of atherosclerosis development. Further mechanistic complexity came later with the realization of the involvement of neutrophils and DCs in the disease, the latter driving and bringing adaptative immunity in the picture.

Myeloid cell precursors have diverse origins: some emerge from hematopoiesis in the bone marrow, while others arise from primitive embryonic structures [10]. Their functional diversity is thought to be acquired via the action of tissue-specific cues but little is known on how this local developmental imprinting of myeloid cells takes place [11]. This observation particularly stands regarding myeloid cell immunometabolism, as microenvironmental signals can trigger rapid metabolic adaptations to adjust the immune response. In atherosclerosis, myeloid cell metabolism influences plaque development [12]. For example, under inflammatory conditions, macrophages display increased glycolytic metabolism and Glut1 expression, the main myeloid cell glucose transporter [13]. Monocytes and macrophages from atherosclerotic patients show increased mitochondrial oxygen consumption rate (OCR). Together these findings suggest a global change in metabolic activation state [14].

A metabolomics-based analysis of human carotid plaques revealed a correlation between plaque metabolic signatures, namely elevated glycolysis and low fatty-acid oxidation, and the presence of plaque instability features [15]. This observation strongly suggests that intra-plaque metabolic cues may determine the outcome of the disease. A better understanding of how metabolites affect in situ myeloid cell activation would help for the design of new therapeutic approaches to prevent and treat atherosclerosis. In this review, we will address how metabolic signals impact on myeloid cell diversity and function in the context of atherosclerosis.

IMMUNE CELL DIVERSITY IN PLAQUES

Pioneering studies revealed that human plaques contain a variety of immune cells. These observations were repeated in mouse pre-clinical models of atherosclerosis development, namely Ldlr$^{-/-}$ and ApoE$^{-/-}$ mice. Although wild-type mice are protected against the disease, high cholesterol diet feeding of Ldlr$^{-/-}$ and ApoE$^{-/-}$ mice promotes hypercholesterolemia and atherosclerosis development. Descriptions of plaque immune cells were initially based on immunochemistry and demonstrated the presence of macrophages, B and T cells in plaque lesions [16]. Nevertheless, the limited number of parameters available was not adapted to grasp the full spectrum of immune cells residing in advanced plaques. With the improvement of flow cytometry, the number of parameters simultaneously analyzed progressively increased and a further complexity in plaque immune cell populations emerged [17,18]. Single-cell RNA-Seq and Cytometry by Time of Flight (CyTOF) technologies further extended our ability to discover and characterize new tissue-resident immune populations and their activation states. This technological leap offered a new perspective to decipher in greater depth immune cell diversity in atherosclerotic plaques [19]. In the past two years, multiple studies applied single-cell RNA-Seq techniques to human plaque samples from endarterectomy patients [20], and to aortic cells extracted from wild-type and atherosclerotic mice [18,21–25]. This generated an extensive characterization of the blood vessel-residing immune landscape in health and disease (**Tables 1 and 2**). Interestingly, only a small number of myeloid cells (of which around 70% were monocytes) were observed at steady state in the aortic wall of wild-type mice [25]. It seems reasonable that monocytes crawling on endothelial cells were the main population of immune cells detected in those studies. Leukocyte diversity was shown to greatly increase in the aorta during atherosclerosis development, as neutrophils, T cells, B cells and NK cells were also identified in Ldlr$^{-/-}$and ApoE$^{-/-}$ mice fed a chow or a high fat diet [21,22,24]. This diversity was also observed in human samples [20,22].

Table 1. Recent single-cell based studies assessing plaque composition.

References	Samples
Kim K et al., 2018 [23]	LdlR$^{-/-}$ mice; 12 weeks HFD; aortic CD45^{+} cells
Cochain C et al., 2018 [21]	LdlR$^{-/-}$ mice; 12 weeks HFD; aortic CD45^{+} cells
Winkels H et al., 2018 [22]	LdlR$^{-/-}$ mice; 12 weeks CD or HFD; aortic CD45^{+} cells
	Transcriptomic data; 126 samples from the biobank of Karolinska Endarterectomies
Fernandez DM et al., 2019 [20]	Endarterectomy plaque samples
Cole JE et al., 2018 [24]	ApoE$^{-/-}$ mice; CD or HFD 12 weeks; aortic CD45^{+} cells
Kalluri AS et al., 2019 [25]	WT digested aorta

Table 2. Summary of the reported plaque leukocyte proportions across the reports mentioned in Table 1.

Refs	Samples	Method	Macrophages	Monocytes	Dendritic cells			Neutrophils	T cells		B cells	NK cells
					pDC	cDC1	cDC2		$CD4^+$	$CD8^+$		
[23]	Male $LdlR^{-/-}$ HFD 12 weeks	Single cell RNA-Seq	83.9%*	ND	ND	2.2%*	6.9%*	ND	3%*		ND	ND
[21]	Male $LdlR^{-/-}$ HFD 11 weeks	Single cell RNA-Seq	28.9%	12.3%	14.9%			2%	8.7%	19.6%	2%	4%
	Male $LdlR^{-/-}$ HFD 20 weeks		49.6%	ND	14.2%			ND	8.5%	16.8%	2.1%*	2.4%*
[22]	Male $LdlR^{-/-}$ CD	Single cell RNA-Seq	13.6%	Myeloid cells: 6.2%					54.1%		24.4%	1.7%
	Male $LdlR^{-/-}$ HFD 12 weeks		27%	Myeloid cells: 21.1%					45.8%		4%	2.1%
	Female $ApoE^{-/-}$ CD		4.9%	Myeloid cells: 10.3%					60.6%		21.9%	2.4%
	Female $ApoE^{-/-}$ HFD 12 weeks		9.6%	Myeloid cells: 12.6%					49%		27.2%	1.6%
	Human	Bulk RNA-Seq deconvolution	50%*	12%	ND			ND	20%*		10%*	5%
[20]	Human	CyTOF	10.6%	2.5%	0.4%	0.1%	ND	0.1%	31.6%	31.1%	2.6%	4.1%
	Human	CITE-Seq	16%	ND	6%*	1.5%*	ND	ND	20%*	26%*	8% *	11%*
[24]	$ApoE^{-/-}$ sex unspecified CD	CyTOF	60%	2.5%	0.25%	1.6%	8.5%	2.5%	3%	3%	8%	1%
	$ApoE^{-/-}$ sex unspecified HFD 12 weeks		57%	7%	1%	1.8%	6.5%	4%	3%	3%	5%	0.75%
[25]	Female WT CD	Single cell RNA-Seq	23%*	73.4%*	3.3%*			ND	ND		ND	ND

When possible, we reported the proportion of each cell type among total leukocytes as indicated by the authors. Stars (*) indicate missing information that was estimated and completed using the Single-Cell Explorer software (Artyomov Lab, Washington University St Louis). WT = Wild-Type. CD = Chow Diet. HFD = High Fat Diet. ND = Not Determined.

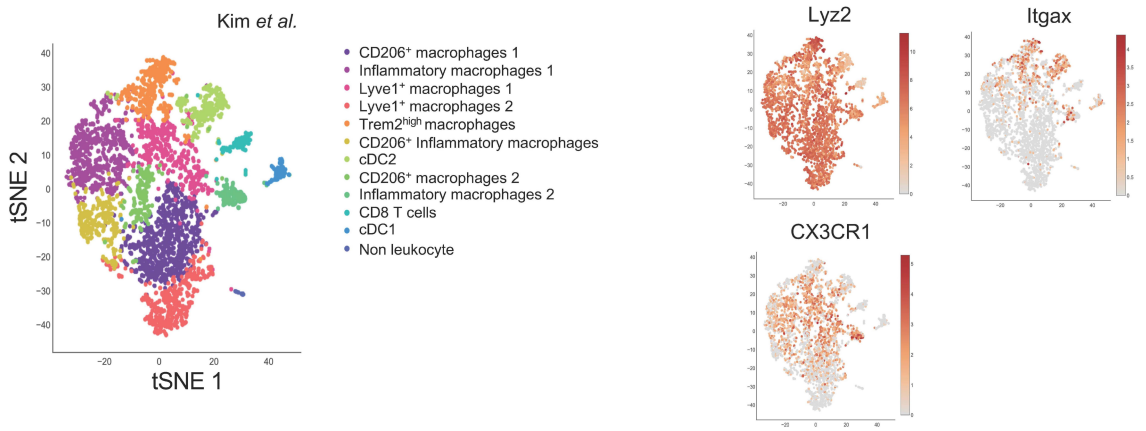

A **B**

Figure 1. Single-Cell approaches highlight plaque immune cell diversity. (**A**) Single-Cell RNA-Seq of aortic CD45^{+} cells from Ldlr$^{-/-}$ mice fed a HFD for 12 weeks. Data from Kim et al. [23] (GSM3215435) were analyzed using the Single-Cell Explorer software. **List of markers used**: CD206^{+} Macrophages: Fcgr1, Itgam, Mafb, Mrc1. Inflammatory macrophages: Fcgr1, Itgam, Mafb, NLRP3, IL1b, Nfkbia. Lyve1^{+} macrophages: Fcgr1, Itgam, Mafb, Lyve1. TREM2^{high} macrophages: Fcgr1, Itgam, Mafb, TREM2, ABCG1, Lpl, Lipa. CD206^{+} Inflammatory macrophages: Fcgr1, Itgam, Mafb, Mrc1, NLRP3, IL1b (low), Nfkbia, TNF. CD8 T cells: Lck, CD3, CD8. cDC2: Zbtb46, Itgax, Flt3, Itgam (+), Itgae (−). cDC1: Zbtb46, Itgax, Flt3, Itgam (−), Itgae, IRF8. Non leukocyte: Ptprpc (−). (**B**) Expression pattern of genes used for targeted Cre expression in myeloid cells.

However, the relative proportion of each cell type reported by different single-cell studies shows significant fluctuations. In mice, macrophages were reported to represent from 9 to 80% of the aortic leukocyte pool and, inversely, T cells represented from 3 to 60% of leukocytes. The same variations were observed in human samples (Table 2). These differences could be explained by multiple factors, and notably differences in tissue digestion technique, leukocyte purification method, and the markers and transcripts used for cell type identification. The entry of atherosclerosis research in the single cell RNA-Seq era could therefore benefit from a universal experimental pipeline that would facilitate comparison between studies. A first step toward this direction could consist in generating a meta-analysis of the data from the studies summarized in Table 1 to characterize plaque composition. A meta-analysis study was recently published and evidenced the immune cell diversity in plaque and the markers allowing to define each population [26].

These studies illustrate that single-cell approaches are amongst the most powerful tools to precisely identify cell subsets as well as their respective metabolic demands. Myeloid cells were broadly shown to represent a significant part (up to 90%) of immune cells in atherosclerotic lesions [23]. Here, we will briefly discuss the identity and origin of plaque resident myeloid cells.

Monocytes

Monocytes are short-lived mononuclear phagocytes that are generated in the bone marrow (BM) during hematopoiesis [27,28]. They rely on CSF1R (Colony Stimulating Factor 1 Receptor) signaling for their development and survival [29,30]. Among leukocytes, which have been positively correlated with cardiovascular events in humans [31–33], monocytes play a pivotal role in atherosclerosis development. Hypercholesterolemia, a key component of atherosclerosis, has been associated with increased circulating monocyte numbers (monocytosis) in mice, rabbits, swines and humans [34–36].

Circulating monocytes are identified as $CD11b^{+}$ $CD115^{+}$ cells, and exist as two functionally distinct subsets in both mice and humans: classical monocytes, identified as $Ly6C^{high}$ in mice and $CD14^{high}$ $CD16^{low}$ in humans, and non-classical monocytes, identified as $Ly6C^{low}$ and $CD14^{low}$ $CD16^{high}$ [37]. An additional human population of $CD14^{+}CD16^{+}$ monocytes has also been documented. Developmentally, $Ly6C^{low}$ monocytes were proposed to arise from $Ly6C^{high}$ monocytes [38,39]. $Ly6C^{low}$ monocytes require the transcription factor Nr4a1 (Nur77) for their maturation [40], they are commonly referred to as “patrolling monocytes”, as they are closely associated to the endothelium which they survey in order to remove dead endothelial cells [41,42].

$Ly6C^{high}$ monocytes are also called “inflammatory” monocytes, as they accumulate during infections and are preferentially recruited to inflamed tissues [38]. They display a high expression of CCR2 [43,44], the main chemokine receptor governing monocyte recruitment to inflammatory sites [45] as well as into atherosclerotic plaques. Plaque initiation is driven by $Ly6C^{high}$ monocyte recruitment to the intima of the endothelial wall [46–50]. Their inflammatory nature seems to be supported by the fact that osteopetrotic mice, which lack functional CSF1 (Colony Stimulating Factor 1) and therefore monocytes [51], are protected against hypercholesterolemia-induced atherosclerosis [52–54]. In 1998, two independent studies documented the key role played by monocyte recruitment to atheromatous lesions through the CCL2-CCR2 chemotactic axis, as mice deficient for CCR2 [55] or its ligand CCL2 [56] also displayed reduced atherosclerotic lesions. Monocyte chemotaxis in atherosclerosis was further characterized in 2007, as Tacke and colleagues provided evidence of the relative contribution of CCR2, CCR5 and CX3CR1 for monocyte recruitment into plaques [47]. CX3CR1 is highly expressed on $Ly6C^{low}$ monocytes and remains detectable on $Ly6C^{high}$ monocyte subset [57]. In contrast, CCR2 is predominantly expressed by the $Ly6C^{high}$ population [57].

Understanding the roles played by metabolism in monocyte biology is of key importance considering the limitations of current therapies. Indeed, limiting monocyte recruitment to the plaque seems to be a reasonable strategy for reducing the development of atherosclerotic lesions. Complementarily, new anti-inflammatory approaches have recently

gained great interest. Indeed, lowering the inflammatory response has emerged as a novel therapeutic target to decrease CVDs related death and comorbidities. Interleukine-6 (IL-6) and IL-1β are two well-established pro-inflammatory mediators and their levels are increased during atherosclerosis progression [58]. Among those two, the pro-inflammatory cytokine IL-1β emerged as a major mediator of atherosclerosis development [59–61]. Surprisingly, IL-1β signaling was also shown to be an important component of plaque remodeling and stability [62]. The Canakinumab Anti-inflammatory Thrombosis Outcome Study (CANTOS) trial showed that patients treated with the IL-1β-targeting monoclonal antibody Canakinumab had a lowered cardiovascular-event-related mortality rate. However, Canakinumab treatment induced various side effects and increased susceptibility to infections, resulting in no overall survival benefits and underlining the urgent need for other therapeutic approaches [63,64].

Macrophages

Macrophages are highly phagocytic cells that can be identified through their co-expression of CD64 and MerTK [11]. Macrophages are ubiquitously present across organs and play key roles both in health and disease [11]. A key function of tissue-resident macrophage is the removal of dead cells, a process named efferocytosis [65]. Every day around 0.4% of the total estimated number of 3.7×10^{13} cells dye in the adult human body [66]. Although all macrophage populations perform efferocytosis, they also display tissue-specific functions such as heme detoxification and iron handling in the spleen, surfactant clearing in the lungs or thermogenesis regulation in brown adipose tissue [67,68]. This functional heterogeneity can partly be explained by the developmental origin of macrophages. Microglia, the population of brain resident macrophages, arise from yolk sac precursors present at early developmental stages [69,70]. Alveolar pulmonary macrophages originate from foetal liver progenitors [71] while the population of gut macrophages derives from bone marrow precursors [72]. Consequently, embryonically-derived macrophages and monocyte-derived macrophages often coexist in adult tissues [73,74]. Like monocytes, tissue-resident macrophages rely on CSF1R signalling, which can bind either IL-34 or CSF1, for their maintenance. Interestingly, a tissue specificity for either ligand has been observed among tissue-resident macrophages, as microglia rely on IL-34 while large peritoneal macrophages rely exclusively on CSF1 [75,76]. Furthermore, macrophage heterogeneity can be attributed to local environmental features, even between subsets that share a common developmental origin [11].

Atheromatous plaque macrophages are monocyte-derived macrophages with the ability to proliferate in situ following their recruitment and differentiation. The understanding of macrophage diversity in metabolic disorders and inflammatory diseases is of particular

interest during atherosclerosis, as multiple macrophage subsets with specific immune profiles and functions have been observed within the plaque [18,21–23] (Figure 1A). Our knowledge on plaque macrophage diversity was previously restricted to pro-inflammatory "M1" macrophages, anti-inflammatory "M2" macrophages, and foam cells which were considered inflammatory cells [5]. The in situ identification of these subsets was based on immunohistochemistry approaches, while their functions were explored using in vitro models. However, new single cell methods have now revealed more layers of complexity in plaque macrophage subsets [18,21–23]. Notably, the single-cell RNA-Seq dataset from Kim and colleagues [23], which displays the greater myeloid cell enrichment, shows the existence of several distinct populations of inflammatory and anti-inflammatory subsets. Surprisingly, expression of the archetypical anti-inflammatory macrophage marker CD206 also appears on populations expressing inflammatory markers (Figure 1A). Two macrophage populations expressed high levels of Lyve1, a marker associated with tissue-resident macrophages [77] which were also identified by Cochain et al. [21] (Figure 1A). This new technology also allowed a detailed in vivo characterization of foam cells, identified as Trem2^{high} macrophages [23,78,79].

Single cell studies now pave the way to understanding plaque macrophage biology. Further investigation is needed to determine how these different subsets participate to inflammation or its resolution via efferocytosis and plaque remodelling [19]. To establish the developmental connection between plaque macrophage populations and their particular localization and metabolic demands is of crucial significance to understand the pathological mechanisms occurring during atherosclerosis progression.

Dendritic Cells

DCs are professional antigen presenting cells (APC). Two major DCs populations have been identified in mice and humans: the conventional (cDCs) and the plasmacytoid dendritic cells (pDCs). Both human and mouse cDCs highly and selectively express the transcription factor Zbtb46 (Zinc finger and BTB domain containing 46) [80,81]. Zbtb46 is not expressed by other myeloid cells such as macrophages, monocytes or neutrophils. In mice, cDCs populations highly express CD11c and MHC II and two main subsets have been identified in lymphoid and non-lymphoid tissues. In lymphoid tissues, cDC1s express CD8, CD24 and XCR1 while cDC2s are characterized by CD4 and Sirpα expression [82]. In the majority of nonlymphoid tissues, cDC1s are described as CD103$^+$ XCR1$^+$ and cDC2s as CD11b$^+$ Sirpα$^+$. cDC1 and cDC2 require specific transcription factors for their development. cDC1 depend on BATF3 (Basic Leucine Zipper activating transcription factor–like transcription factor 3) and IRF8 (IFN regulatory factor 8) while cDC2 rely on IRF4 and Notch2 for their development and maintenance [82]. A key feature of cDCs is their high

capacity to capture antigens in peripheral tissues and subsequently migrate to local draining lymph nodes to initiate the adaptive immune response. Another major function of cDCs is the production of pro-inflammatory cytokine such as IL-6, TNFα and IL-1 following activation of innate immunity receptors. This cytokine production leads to immune cell recruitment and mobilization and allows for specific and efficient immune responses. On the other hand, pDCs essentially release type 1 interferons (IFN-I), both IFNα and IFNβ, in response to virus infections [83]. Their potential implication in atherosclerosis is suggested by the fact that IFN-I decreases macrophage phagocytic abilities [84] and that IFNAR-deficient animals have decreased plaque area and macrophage content [85].

In the context of atherosclerosis, cDCs contribute to chronic inflammation by attracting and activating T cells [86]. The production of CCL17 by mature cDCs contributes to $CD4^+$ T cells and regulatory T cells (Tregs) migration and recruitment to plaques. CCL17 deletion leads to a slower atherosclerosis progression and a decreased number of macrophages and T cells in plaques [87]. The presence of $CD4^+$ T cells with a phenotype of antigen activated ($CD44^+$) cells was documented in mouse atherosclerotic models [17]. $CD4^+$ T cells stimulation requires a peptide loading on major histocompatibility complex (MHC II), selectively expressed by antigen presenting cells. The cDC antigen presentation function seems to play a pivotal role in the progression of atherosclerosis. Nevertheless, and despite recent progress in the field, the nature of the antigen (peptide or lipid) remains to be fully understood. For instance, ApoB (the core protein in LDL) reactive $CD4^+$ T cells were identified in pre-clinical atherosclerotic models [17] and humans [88]. Immunization strategies were developed using ApoB epitopes and those demonstrated atheroprotective effect, illustrated by reduced plaque area, when conjugated to appropriate adjuvants [89,90]. This protection was associated with increased IL-10 production, an anti-inflammatory cytokine mainly secreted by regulatory T cells (Tregs). In atherosclerotic patients, an oligoclonal T cell repertoire was observed in comparison to healthy patients [91,92]. This observation further supports the relevance of antigen presentation during disease development. Recently, the generation of MHC II tetramers loaded with ApoB-derived peptide revealed that the majority of ApoB-recognizing T cells are T regs [88]. Moreover, the deletion of two important costimulatory molecules: CD80 and CD86 in mice DCs decreased T-cell activation/infiltration in plaques [93] demonstrating that cDCs play a crucial role during disease development.

In advanced plaques, apoptotic cell accumulation due to defective efferocytosis leads to DNGR-1 activation (dendritic cell NK lectin group receptor-1) on $CD8a^+$ cDC1s, which blunts IL-10 production, therefore contributing to atherosclerosis aggravation [94]. However, the mechanisms underlying the defective efferocytosis in DCs are still unknown and need to be deciphered. In conclusion, DCs, as pivotal players

linking innate and adaptive immunity, offer new insights that may lead to new therapeutic targets and notably vaccination strategies.

Neutrophils

Neutrophils are associated with the early inflammatory response [95]. Neutrophils have been shown to either be able to directly affect atherogenesis [96], or contribute to pathology onset by driving immune cell entry in atherosclerotic lesions [97] and by promoting plaque rupture [98] respectively. This suggests an important crosstalk between neutrophils and other immune and stromal cells.

Growing evidence suggests that neutrophils play a pivotal role in the initiation of atherosclerosis. Neutrophil adhesion to the endothelial wall through CCL3 and CCL5 binding on CCR1, CCR3 or CCR5 triggers neutrophils extravasation and their entry into plaques [99]. There, activated neutrophils release granule proteins containing chemotactic “alarmins”, such as cathelicidin/LL-37 in Human (CRAMP in mice), Human α-defensins (human neutrophil peptides, HNPs), azurocidin (HBP, CAP37) and serprocidins (elastase, cathepsin G, proteinase-3), inducing leukocytes attraction and recruitment to the site of inflammation (for review see [100]). In addition, S100A8/A9, a cytoplasmic protein, reduces neutrophils rolling on the endothelial wall and activates β2 integrin to facilitate leukocyte extravasation and entry to the site of inflammation [101]. Interestingly, alarmins have also been reported to contribute to the activation of inflammasomes such as NLRP3 [102]. NLRP3 activation leads to IL-1β and IL-18 production and to the HMGB1 alarmin (High-mobility group box 1 protein) release, creating a loop that amplifies innate immune responses [103]. NLRP3 inflammasome activation then increases neutrophil recruitment to inflammatory sites leading to the activation of neutrophil extracellular traps (NETs) [104]. NETs are web-like fiber structures released by neutrophils and made of extracellular chromatin, nuclear proteins, and serine proteases. NETs are known to increase monocyte recruitment to inflamed sites and trigger reactive oxygen species (ROS) and proinflammatory cytokines release by macrophages [105,106]. In this context, NETs may promote type I interferon (IFN-I) release from pDCs contributing therefore to atherosclerosis progression and suggesting an essential crosstalk between neutrophils and pDCs [107].

Neutrophils have been found at sites of plaque rupture in patients with acute coronary syndrome [108]. Interestingly, neutrophils are essentially located in the unstable layers of human atherosclerotic lesions with a high inflammatory activity and also correlated to the elevated numbers of monocytes found in these regions [99]. In addition, NETs are thought to be involved in plaque destabilization through the induction of endothelial cell wall cytotoxicity in humans [109,110]. Neutrophils are the main producer of myeloperoxidase (MPO) [111]. MPO is a heme-containing peroxidase that catalyzes the formation of reactive oxygen species intermediates [112] that induce macrophage cholesterylester

accumulation and foam cell formation, leading to atherosclerosis aggravation [113]. Recent studies have highlighted that neutrophils undergo transcriptional regulations under inflammatory conditions and NETosis [114,115]. The significance of NETs during atherosclerosis was extensively described in a recent manuscript [115].

Mouse Models

Mouse Cre-Lox systems have extensively been used to explore the role of myeloid cell functions in atherosclerosis. $Lyz2^{Cre}$, $CX3CR1^{Cre}$ and $CD11c^{Cre}$ mice were the most commonly used to study macrophages and neutrophils, monocytes, and dendritic cells respectively. Although these genes are dominantly expressed by the aforementioned cell types, some well-documented overlaps in their expression exist between myeloid cell types. Single-cell sequencing approaches have now brought to light the subset-specific expression pattern of these genes within the plaque (Figure 1B), which may allow more specific targeting of myeloid subsets within plaques and reinterpretation of previously generated data.

As expected, $Lyz2^{Cre}$ appears to be virtually ubiquitously expressed across plaque resident myeloid cells. Although CX3CR1 expression is only restricted to certain myeloid subsets within the plaque, most macrophages are monocyte-derived cells which therefore expressed CX3CR1-driven Cre at an earlier differentiation stage. However, the use of inducible $CX3CR1^{CreERT2}$ models gives more flexibility to the model. As an example, Lin and colleagues recently used $Cx3cr1^{CreERT2\text{-}IRES\text{-}YFP/+}Rosa26^{fl\text{-}tdTomato/+}$ mice in a fate-mapping and single-cell approach [18]. The authors induced Cre expression when plaques were established, immediately prior to plaque regression induction in order to differentially characterize $CX3CR1^{+}$ plaque cells and cells derived from $CX3CR1^{+}$ precursors [18]. $CD11c^{Cre}$ mice were extensively used to characterize DCs functions in health and disease. However, CD11c was also shown to be expressed by $Ly6C^{low}$ monocytes [57] which can, to a lower extent than $Ly6C^{high}$ monocytes, infiltrate atheromatous lesions [47]. As shown in Figure 1B, plaque expression of CD11c is not restricted to DCs, but also concerns certain macrophage subsets including the now well identified $TREM2^{high}$ foam cells [23,78,79]. $CD11c^{Cre}$ mice could therefore be a valuable model to study foam cell metabolism during atherosclerosis.

METABOLIC PHENOTYPE OF PLAQUE IMMUNE CELLS

Atherosclerosis progression is accompanied by a modulation of systemic and plaque metabolites. Recently, non-invasive imaging techniques, commonly used in oncology, were deployed to predict rupture-prone plaques. Positron emission tomography (PET) is traditionally employed to investigate myocardial reperfusion. PET/CT studies revealed an accumulation of the glucose analog 18F-fluoro-2-deoxy-d-glucose (18F-FDG) in atherosclerotic lesions in humans [116]. This suggested increased glucose avidity and potentially metabolization in

plaque residing cells. A metabolomic analysis performed on iliac-femoral arteries extracted from control and atherogenic rabbits revealed an increased abundance of glycolysis and pentose phosphate pathway (PPP) metabolites in plaque-enriched vessels [117]. Whether these metabolites accumulate in specific immune or stromal cell-type remains to be established. In the following section we will discuss the impact of myeloid cell glucose metabolism on plaque development.

Lipid Handling

Monocytes

Hypercholesterolemia, the predominant metabolic feature of cardiovascular diseases, is known to influence hematopoiesis and induce a differentiation bias of hematopoietic stem cells (HSCs) towards the myeloid lineage. Indeed, HSCs obtained from ABCA1$^{-/-}$ ABCG1$^{-/-}$ mice, lacking transporters involved in cholesterol efflux, display increased proliferation and myelopoiesis switch [118]. This phenomenon is amplified in ApoE$^{-/-}$ mice, one of the most commonly used murine models of hypercholesterolemia-induced atherosclerosis [119]. Taken together, recent data on cholesterol-related myelopoiesis exacerbation suggest that an increase in cellular cholesterol content promotes membrane lipid raft formation in HSCs, thus promoting the stabilization of chemokine and cytokine receptors at the cell surface and signal HSCs to quit quiescence [118,120–122].

Emerging immunometabolism-centered studies have mainly focused on macrophages, while only a few studies investigated monocyte metabolic requirements. This may partly be explained by technical difficulty of using undifferentiated monocytes in *in vitro* cultures. Recent studies pointed towards lipid metabolism as an important factor of monocyte homeostasis. Using a BM transplant approach, Babaev and colleagues reported a decreased CCR2 expression on blood monocytes from Ldlr$^{-/-}$ mice with FABP5$^{-/-}$ (Fatty-acid binding protein) hematopoietic compartment, suggesting a chemotaxis-dependent proatherogenic role of myeloid FABP5 expression [123]. FABPs regulate intracellular lipid traffic and control their access to specific organelles. By contrast, FABP4 deletion in immune cells had no impact on plaque development [123]. ApoE$^{-/-}$ mice with myeloid-specific deletion of lipoprotein lipase (Lpl) displayed decreased plaque development [124]. Lpl hydrolyzes circulating TGs and control their levels. Impaired monocyte generation and differentiation to macrophages were observed in a mouse model of Lpl deficiency and were attributed to Lpl-dependent regulation of CSF1R signaling [125]. Interestingly, FABP5 and Lpl mRNA were highly and selectively expressed in Trem2^{+} foam cells (Figure 2A,B). This could suggest that the atheroprotective effects of myeloid-specific deletion of Lpl might not be caused solely by monocytes but could additionally be the consequence of foam cell dysfunction.

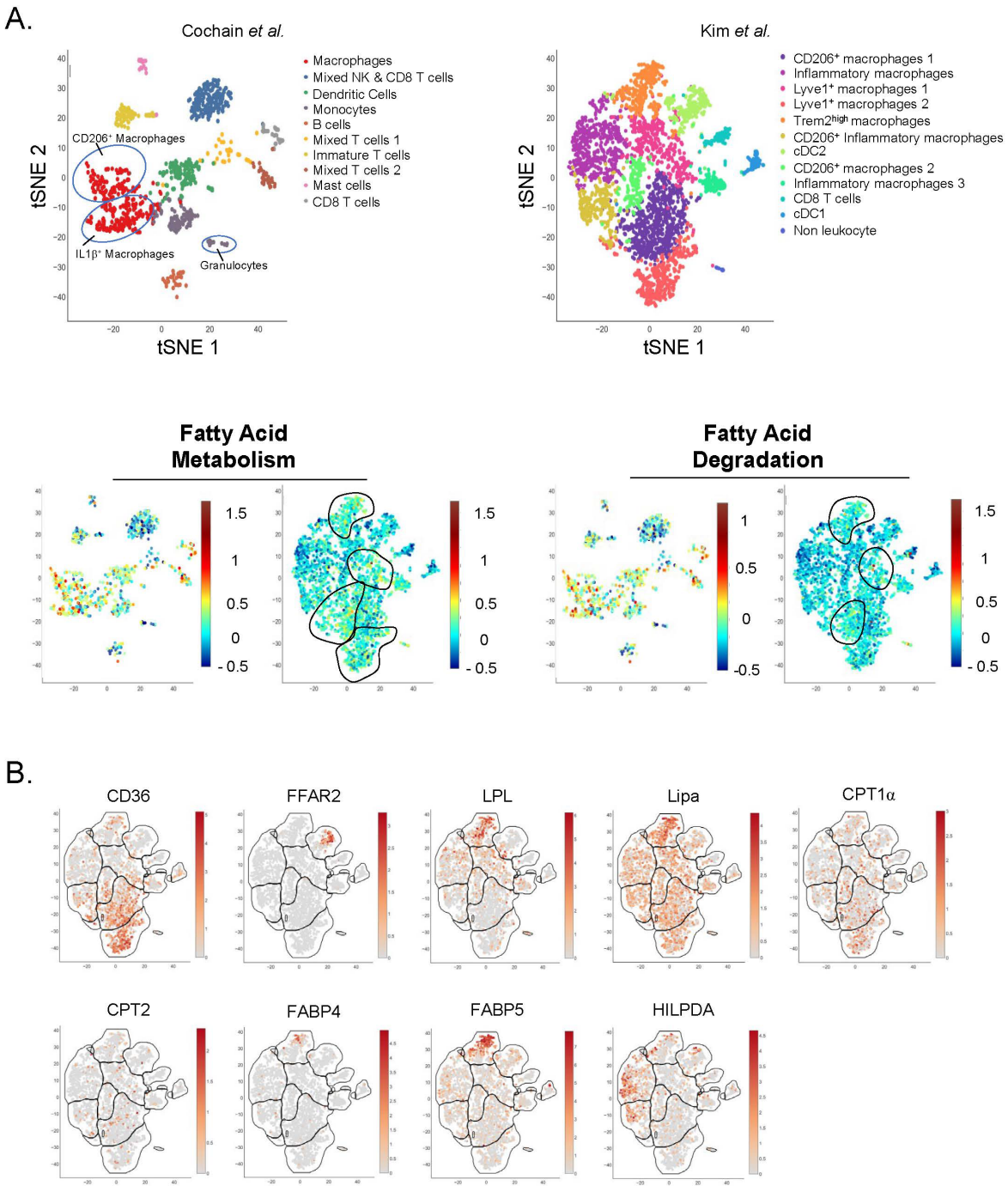

Figure 2. Single-Cell analysis of plaque immune cell lipid metabolism. **(A,B)** Single-Cell RNA-Seq of aortic CD45⁺ cells from Ldlr$^{-/-}$ mice fed a HFD for (left) 11 weeks or (right) 12 weeks. Data from (left) Cochain et al. [21] (GSE97310) and (right) Kim et al. [23] (GSM3215435) were analyzed using the Single-Cell Explorer software (Artyomov lab). **(A)** Leukocyte clusters and corresponding KEGG Metabolic Pathway analysis. Fatty-Acid metabolism: KEGG mmu01212. Fatty-Acid degradation: KEGG mmu00071. **List of markers used in Cochain et al.**: Macrophages (mixed subsets): Itgam, Fcgr1, MerTK. Mixed NK and CD8 T cells: CD3, CD8, Klrb1c, Ncr1, Gzmb. Dendritic Cells (mixed subsets): Itgax, Ciita, Zbtb46. Monocytes: Itgam, Fcgr1, Ly6C, CCR2. B cells: Ciita, CD19, CD79α/β. Mixed T cells: Lck, CD3, CD4, CD8, Rag1. Immature T cells: Lck (−), CD3(+), Rag1 (−), CD4 (−), CD8 (−). Mast cells: Furin, Il1rl1. CD8 T cells: Lck, CD3, CD8. **Markers used in Kim et al. are in the legend for Figure 1A.** **(B)** Expression pattern of genes involved in lipid metabolism (Kim et al. [23] (GSM3215435)).

The importance of monocyte lipid metabolism was challenged by recent data. Jordan and colleagues observed a decrease in blood monocyte numbers during fasting in humans. This effect could not be reverted by fat supplementation in mice, while carbohydrate and protein supplementation both restored blood monocyte counts [126]. However, this modulation of monocyte counts was attributed to modulations of CCL2 production through a liver-BM axis, and not to monocyte cell-intrinsic mechanisms. Nevertheless, monocytes from fasted mice were in a pronounced quiescent metabolic state in comparison to controls, as extracellular flux analysis of these cells showed reduction in both oxygen consumption rate and extracellular acidification rate. This was associated with up-regulation of inositol triphosphate metabolism and suppression of serine and glutathione metabolism. Overall, this metabolic adaptation of monocytes to fasting was associated with improved outcomes in models of chronic inflammatory diseases [126].

As atherosclerosis is associated with numerous systemic metabolic alterations, these exciting results support the urgent need to identify the dietary-related metabolic mechanisms controlling monocyte inflammatory and migratory potentials in this disease. Indeed, both qualitative and quantitative diet modulations could then be envisioned as non-invasive prophylactic therapies for patients presenting monocytosis and metabolic syndrome.

Macrophages

Lipid-laden macrophages were first described inside of atherosclerotic lesions in the late 1970s [127]. These macrophages, called foam cells, take up excessive cholesterol and oxidized LDL (oxLDL) particles via their scavenger receptors, which leads to the intracellular formation of lipid droplets [128–131]. The presence of these cells is considered as a hallmark of atherosclerosis, and foamy macrophages have historically been held culprit for plaque progression.

Intracellular accumulation of cholesterol has been linked to foam cell formation, cytokine production and atherosclerosis progression in a mouse model of defective cholesterol efflux [132]. Atherosclerosis progression has been associated with the formation of cholesterol crystals, which results from reduced esterification of free cholesterol [133]. These crystals can trigger inflammation through the activation of the NLRP3 inflammasome and subsequent IL-1β maturation, which have lately been a major focus of atherosclerosis research [134]. These results support a beneficial role for cholesterol efflux, which is mediated through the liver X receptor (LXR)-regulated transcriptional control of among others the cholesterol transporters ABCA1 and ABCG1. Mice deficient for LXRα and LXRβ display the formation of atheromatous lesions containing foam cells even in the absence of diet-induced hypercholesterolemia [135]. Subsequently, attempts have been made to decrease intracellular cholesterol accumulation and foam cell formation by the use of synthetic

LXR agonists which have proven to be beneficial in pre-clinical models of atherosclerosis [136–138]. Consistently, myeloid-specific deletion of the LXR-regulated ABCA1/G1 cholesterol transporters was shown to exacerbate atherosclerosis development [139]. Alternatively activated (M2) human monocytes and macrophages were reported to be less responsive to LXR agonists [140]. Interestingly, they also displayed less foam cell traits despite decreased ABCA1 expression. This was countered by an improved cholesterol esterification capacity (an anti-inflammatory mechanism) [141], suggesting that efficient cholesterol handling may be more valuable than cholesterol efflux [140]. PPARα stimulation positively regulates ABCA1 expression [142]. Additionally, PPARγ activation also increases ABCA1 expression via LXR [143]. PPARα prevents foam cell formation and decreases plaque development [144,145]. PPARγ agonist also decreased foam cell formation [144]. The role of PPARs in macrophage biology and atherosclerosis is extensively reviewed in [146,147]. However, whether and how precisely PPARs affect specifically different myeloid cell populations in plaque remains to be defined. We recently reported that lysosomal acid lipase (LIPA)-dependent cholesterol hydrolysis promotes macrophage efferocytic capacity [148]. LIPA is expressed by all plaque macrophage subsets and is particularly enriched in foam cells (Figure 2B). The relevance of our observations linking LIPA activity and efferocytosis to atherosclerosis needs to be further investigated, as multiple studies reported a correlation between LIPA variants and coronary artery disease [149,150].

Macrophage foam cell formation is regulated by natural antibodies recognizing modified LDL particles and apolipoproteins. Indeed, the inhibition of oxLDL uptake by oxLDL-specific natural IgMs, which mask oxidized epitopes, decreases foam cell formation, inflammation and atherosclerosis development [151–153]. The production of oxLDL-specific antibodies, both of the IgM and IgG isotype, occurs during the development of atherosclerosis [154]. IgG-containing immune complexes are recognized by FcγR receptors, and $ApoE^{-/-}$ mice deficient for FcγRIIb/CD32b, a low affinity inhibitory receptor, showed reduced plaque lipid content suggesting lower foam cell formation [155]. This was associated with an overall increase in plaque stability, as well as in circulating levels of oxLDL and IgG-ApoB immune complexes, suggesting a lower uptake of these particles by macrophages [155]. Foam cell formation was also reported to be induced by ApoA1-specific IgG in vitro [156]. Although atherosclerosis-associated IgMs and IgGs display different roles in foam cell formation, only the former are robustly associated with a (protective) role in the development of the disease [157].

In macrophages, a consequence of foam cell formation could be lipid overload-induced toxicity, which may hypothetically be a determinant of plaque necrosis. Both fatty acid metabolism and degradation pathways are enriched in plaque macrophages (Figure 2A). The hypoxia-inducible lipid-droplet-associated (Hilpda) protein has emerged as a key player in lipid

droplet handling. Its role as a lipid-sensor and inhibitor of ATGL (the rate limiting enzyme of adipose tissue lipolysis) promotes lipid accumulation into lipid droplets and foam cell formation [158]. In plaques, Hilpda mRNA was preferentially expressed in inflammatory macrophages (Figure 2B). This Hilpda-mediated lipid storage was reported to be necessary for the maintenance of macrophage viability upon lipid overload, suggesting a beneficial role for lipid storage in terms of survival [159]. Nevertheless, Hilpda deficiency was shown to decrease atherosclerosis development and plaque lipid content, without affecting plaque macrophage apoptosis [159]. The authors attributed this phenotype to the Hilpda-dependent macrophage lipid accumulation and production of prostaglandin E2, which promotes vascular inflammation [160].

Overall, previous reports point towards a proatherogenic role for foam cells. However, the emergence of omics approaches led recent studies to challenge this view. Foamy peritoneal macrophages extracted from $Ldlr^{-/-}$ mice fed a high cholesterol diet surprisingly showed a LXR-mediated down-regulation of genes associated with inflammatory responses and chemotaxis [161]. A turning point in foam cell research was reached by Kim and colleagues, who developed a strategy to isolate and characterize plaque foam cells using a lipid probe-based strategy [23]. Surprisingly, their results showed that foam cells only represent around 10% of aortic macrophages in atherosclerotic mice, although this proportion may vary depending on isolation efficiency. Moreover, both bulk and single cell RNA-Seq approaches showed that foamy macrophages are rather anti-inflammatory in comparison to non-foamy plaque macrophages. As discussed earlier, this is of particular interest in the context of the recent CANTOS trial, as NLRP3 and IL-1β expression were clearly a feature of non-foamy macrophages [23]. While previous studies relied greatly on in vitro models to analyze macrophage lipid metabolism and foam cell formation, this innovative approach may have supplied the methodology to further characterize foam cells in vivo. As discussed earlier, studying macrophages in the context of their micro-environment has repeatedly proven to be the key to understanding their biology.

In vitro studies revealed that IL-4 induces a specific metabolic profile in macrophages. These cells are named alternatively activated (M2) macrophages and rely on fatty acid oxidation for their metabolic needs [162]. Seminal studies demonstrated that fatty acid oxidation inhibition in macrophages prevents their M2 phenotype. This concept was recently challenged by the demonstration that etomoxir, a specific Cpt1a inhibitor, has “off-target” effects even at fairly low concentrations [163,164]. Genetic Cpt2-deletion failed to affect macrophage alternative polarization, further challenging the previously established dogma [165]. Cpt1 and Cpt2 mRNA were detected in plaque-resident myeloid cells without a subset-specific signature (Figure 2B). Whether plaque resident macrophages rely on fatty oxidation and Cpt1 remains currently unknown. Importantly, macrophage alternative activation depends on CD36, a membrane receptor for long

chain fatty acids [162]. Single-cell RNA-Seq analysis revealed that CD36 is highly expressed in Lyve1^{+} plaque resident macrophages (Figure 2B). Of interest, Lyve1 is a canonical M2 activation marker which, together with CD36 expression, might help identifying the real in vivo alternatively activated macrophage relying on fatty acid oxidation (at least in the context of the plaque). CD36 is involved in non-classical monocyte patrolling during atherosclerosis induction [166]. Previous reports demonstrated that CD36 plays a crucial role during atherosclerosis development but it remains unclear how CD36 governs plaque myeloid cell metabolism [167–170]. For instance, CD36 signaling is involved in ROS generation and controls macrophage cytoskeleton organization [171].

Dendritic cells

One of the major proofs of DCs implication in atherosclerosis development is their impact on cholesterol homeostasis. Indeed, DC depletion in hyperlipidemic CD11c-DTR ApoE$^{-/-}$ mice leads to increased hypercholesterolemia but no change in atherosclerosis due to lower DC-driven T-cell activation, suggesting that there is a close relationship between DCs and cholesterol homeostasis. CD11c expression in plaque is not restricted to DCs, and this function might be shared with CD11c-expressing macrophages (Figure 1B). Increasing DC survival by overexpressing Bcl2 leads to decreased cholesterol plasma levels [172]. However, long term DC depletion led to a progressive myeloproliferative syndrome, highlighting an indirect impact on the hematopoietic system [173]. Additionally, in Ldlr-deficient mice, DCs in atherosclerotic lesions have been shown to capture oxLDL contributing to foam cell formation and therefore to atherosclerosis progression [174].

Despite the fact that pDCs are present in a relatively low frequency in human and mouse atherosclerotic plaques, this cell type also plays a role in atherosclerosis development. pDCs numbers are increased in aortas of ApoE$^{-/-}$ and Ldlr$^{-/-}$ mice fed a high-fat diet [24,175]. Intriguingly, ApoE$^{-/-}$ mice depleted in pDCs display decreased lipid-containing area, lower T cell activation and lower macrophage accumulation in the plaque [176]. In addition, when treated with oxLDL, pDCs show increased phagocytic capacity as well as a stimulated antigen-specific T cell response [177]. Genetic pDC depletion, following diptheria toxin administraton in BDCA2-DTR atherogenic mice, led to increased lesion area [175]. Moreover, TLR-induced IFN-I production by pDCs is triggered by neutrophils NETs in human atherosclerotic plaque [178]. All together, these data suggest that pDCs might be interesting targets in controlling the evolution of atherosclerosis. However, pDCs role in atherosclerosis is still under debate due to the opposite effects the antibody used against pDC bone marrow stromal cell antigen-2/PDCA1 has on Ldlr$^{-/-}$ and ApoE$^{-/-}$ mouse [176,177,179].

Neutrophils

Cholesterol metabolism appears to play a key role in neutrophil biology, as both $Ldlr^{-/-}$ and $ApoE^{-/-}$ mice fed a high fat diet display increased blood neutrophil numbers [119]. Cholesterol efflux receptors such as ABCA1/ABCG1 notably regulate neutrophil adhesion and activation [180]. Moreover, neutrophil accumulation and NETosis have also been found in the context of defective cholesterol efflux induced by ABCA1 and ABCG1 deficiency [181] (for review see [182]). Additionally, inhibition of cholesterol efflux in myeloid progenitors led to increased neutrophil production while a disruption in the chemotactic axis CXCL12-CXCR4 in the BM led to neutrophilia and therefore amplified lesion formation [97]. Moreover, mice fed a high-fat diet show significant increase in circulating neutrophil numbers [183]. However, surprisingly, epidemiological studies in humans have shown a positive correlation between elevated numbers of circulating neutrophils and cardiovascular events, independently from serum cholesterol levels [184]. In addition, fatty acids have also been proposed to be involved in neutrophils metabolic demands. Indeed, fatty acid receptors including free fatty acid receptor-1 (FFAR1/GPR40), free fatty acid receptor 2 (FFAR2/GPR43), and GPR84 are expressed on neutrophils [185]. However, short term fasting in humans had no effect on circulating neutrophil levels [126]. Cell-autonomous effects of lipids on neutrophils and their relevance in atherosclerosis require further investigations.

Glucose Metabolism in Myeloid Cells

Monocytes

Unlike tissue-resident immune cells, monocytes need to quickly adapt to their new environment after blood vessel extravasation and entry into peripheral tissues. This seems critical in atherogenic conditions, as recent evidence suggests that monocytes might contribute to the onset of the disease due to their sensitivity to the plaque micro-environment, rather than to a preexisting inflammatory phenotype. Notably, Williams and colleagues showed that newly-recruited monocytes lose motility as they differentiate into macrophages within the plaque, thus reducing their capacity to reach apoptotic cells located deeper within the plaque and perform efferocytosis [186]. This rapid adaptation probably requires an adjustment of metabolic pathways to the locally available substrates.

In humans, glucose metabolism disorders such as *diabetes mellitus* have been associated with cardiovascular diseases, though the underlying cellular mechanisms remain unclear [187,188]. The use of the glucose analog 18F-FDG in PET-CT imaging has brought to light a correlation between acute coronary syndrome and 18F-FDG accumulation (representative of glucose avidity) in the bone marrow and the spleen (the later probably reflecting extramedullary hematopoiesis) in at least two independent cohorts [189]. Interestingly, Oburoglu and colleagues showed

that in vitro (human $CD34^+$ cells) and in vivo (newborn mice), administration of 2-deoxyglucose, a partially non metabolizable glucose analog used to inhibit glycolysis, restricted myeloid differentiation while promoting erythroid differentiation of HSCs [190]. Consistently, using chimeric pre-clinical models of atherosclerosis, our group previously reported a decrease in myelopoiesis and plaque development in mice with partial deficiency for Glut1, the main glucose transporter in the hematopoietic compartment [191]. Increased glucose levels in diabetic mice drive myelopoiesis, further supporting the evidence that glucose metabolism favors myeloid cells generation [192]. Interestingly, Jordan and colleagues reported a direct relation between food intake and systemic CCL2 levels, which allows for monocyte egress from the bone marrow compartment to the blood circulation [126]. This effect was mainly attributed to glucose metabolism, as the authors observed a positive correlation between blood monocyte counts and the quantity of gavage-administered glucose. Furthermore, monocyte mobilization could be inhibited by gavage with 2-deoxyglucose [126]. As discussed earlier, the CCL2-CCR2 chemotactic axis governs monocyte recruitment to atherosclerotic plaques and progression of the diseases [47]. Importantly, monocyte CCR2 expression strongly associates with vascular wall inflammation in patients with CVD risk [193]. However, whether glucose affects chemokine receptor expression on monocytes and facilitates their entry into inflamed plaques remains to be explored. In a pre-clinical plaque regression model, it was demonstrated that lowering plasma glucose concentration prevents monocyte entry into the inflamed plaque and improves pathology resolution [192]. Nevertheless, whether glucose lowering therapies affect monocyte CCR2 expression and their ability to enter into plaques and differentiate into macrophages also requires further investigations.

Macrophages

Macrophages rely on the membrane transporter Glut1, encoded by Slc2a1, for glucose entry. Slc2a1 is ubiquitously expressed among plaque myeloid cells (Figure 3A,B). However, transcriptomic analysis revealed an enrichment in transcripts related to glycolysis and PPP pathways in macrophages and DCs (Figure 3A,B). Glut1 is solely responsible for glucose entry into macrophages, as its ablation using genetic models demonstrated that other members of this family of transporters cannot substitute its absence [194]. Thus, $Lyz2^{cre} \times Slc2a1^{fl/fl}$ animals have minimal glucose entry associated with decreased levels of many glycolysis and PPP-related metabolites [194]. Compensatory mechanisms led to increased tricarboxylic acid cycle (TCA) metabolites in Glut1-deficent macrophages in comparison to controls [194]. Interestingly, when crossed to atherogenic $Ldlr^{-/-}$ mice, $Lyz2^{cre} \times Slc2a1^{fl/fl} \times Ldlr^{-/-}$ animals had similar plaque size as control mice [194]. Macrophage content, quantified by MOMA2 staining, remained similar as well. However, mice with Glut1-deficient myeloid

cells had an elevated frequency of necrotic core per plaque that paired with a partial deficiency in efferocytosis [194]. This observation was confirmed in another study using the same genetic model [195]. Indeed, efferocytosis triggers a specific metabolic reprogramming of macrophages that relies mainly on glycolysis [195] and lowering glucose concentration, or pharmacological or genetic Glut1-inhibition all efficiently alter macrophage efferocytosis [195]. Glut1 expression is increased following macrophage TLR4 stimulation with LPS to facilitate glucose entry [196], though the relevance of this observation for plaque formation or maintenance requires further investigation. LPS also leads to accelerated glucose flux and increased glycolysis and PPP activation. This is supported by the transcriptional regulation of key enzymes involved in the aforementioned pathways. Thus, LPS increases the expression of two critical enzymes (HK3 and PFKFB3) involved in glycolysis, and this is paralleled by increased pro-inflammatory cytokine production [13]. In plaques, HK3 is found mainly in a population of $Trem2^{+}$ macrophages, while PFKFB3 expression is higher in inflammatory macrophages (Figure 3B). Four HK (hexokinase) isoforms have been identified. Interestingly, HK1 was not enriched in a specific plaque immune subset, while HK2 is highly expressed in inflammatory macrophages (Figure 3B). Again, the biological significance of this observation needs further work. However, macrophage-specific Glut1 overexpression, despite increasing glucose entry and metabolization, failed to generate an increased pro-inflammatory cytokine production [13]. Plaque size, macrophage content and necrotic core area were similar between control and macrophage-Glut1 overexpressing animals [13]. This observation is surprising since increased glucose levels in mice have been associated with a macrophage pro-inflammatory phenotype and disease severity. Taken together, these observations suggest that glucose flux through Glut1 contributes to myeloid cells activation during atherosclerosis, but this is not sufficient to fully explain the pro-inflammatory phenotype of plaque macrophages. Macrophage alternative polarization also requires efficient glucose metabolism [197]. Blocking pyruvate mitochondrial entry and subsequent TCA incorporation leads to decreased ATP production [197]. This is consistent with the role of glucose in TCA cycle activation and ATP generation. Inhibition of the enzyme Acly, playing a key role in Acetyl-CoA generation, prevents macrophage alternative polarization in murine macrophages [198]. The human relevance of this observation was challenged in a recent report using pharmacological inhibitors and genetic approaches [199]. However, whether those pathways affect particularly the metabolic rewiring of a specific subset of plaque resident myeloid cells remains to be defined.

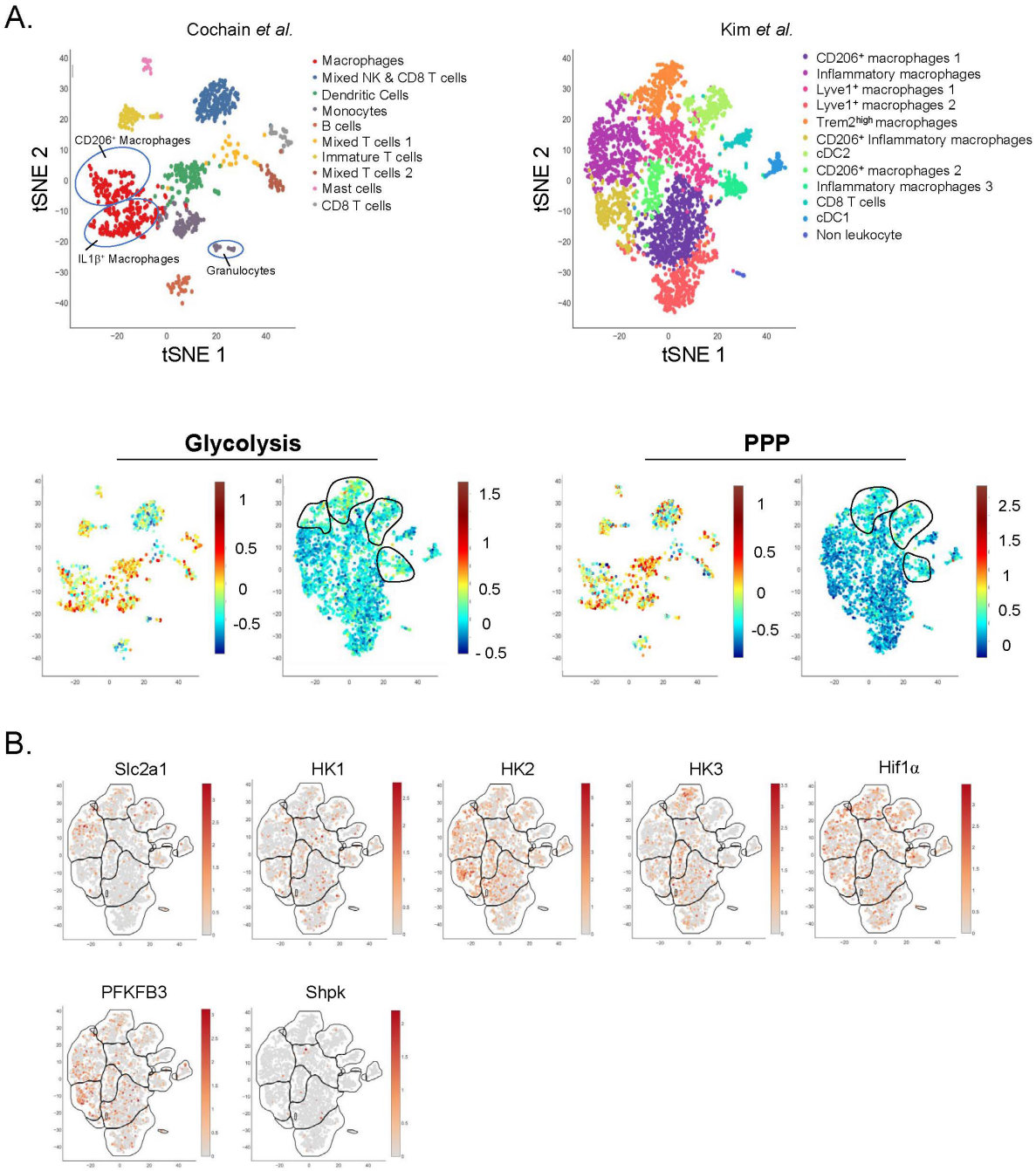

Figure 3. Single-Cell analysis of plaque immune cell glucose metabolism. (**A**,**B**) Single-Cell RNA-Seq of aortic CD45^{+} cells from Ldlr$^{-/-}$ mice fed a HFD for (left) 11 weeks or (right) 12 weeks. Data from (left) Cochain et al. [21] (GSE97310) and (right) Kim et al. [23] (GSM3215435) were analyzed using the Single-Cell Explorer software (Artyomov lab). (**A**) Leukocyte clusters and corresponding KEGG Metabolic Pathway analysis. Glycolysis: KEGG mmu00010. Pentose Phosphate Pathway: KEGG mmu00030. The lists of markers used to identify subsets are in the legend of Figures 1 and 2. (**B**) Expression pattern of genes involved in glucose metabolism (Kim et al. [23] (GSM3215435)).

Interestingly, Folco and colleagues reported no modulations in glucose uptake when stimulating human primary macrophages with pro-inflammatory cytokines [200]. However, glucose uptake was increased in hypoxic conditions, along with increased HK2 expression, while HK1

expression remained unchanged. Immuno-histochemical analysis of human atherosclerotic lesions showed a colocalization of HK2 with the transcription factor HIF-1α (Hypoxia-inducible factor-1), a well-established regulator of glycolysis [200]. Hif-1α mRNA is ubiquitously expressed among plaque resident immune cells, most of which also express HK2 but not HK1, thus supporting these observations (Figure 3B). Advanced plaques contain hypoxic regions due to restricted blood supply and Hif-1a expression was detected in mouse and human plaques [201–204]. Conditional deletion of Hif-1α in myeloid cells ($Lyz2^{cre}$ × $Hif\text{-}1\alpha^{fl/fl}$ mice) didn't impact plaque size [205]. However, when Hif-1α was deleted in CD11c-expressing cells, an increased plaque area was documented, suggesting that this transcription factor mainly operates in CD11c-positive cells that could be DCs or a subset of macrophages (Figure 1B) [205]. $CD11c^{cre}$ × $Hif\text{-}1\alpha^{fl/fl}$ mice displayed increased necrotic core area that might result from defective glucose-driven efferocytosis [205]. However, a recent report demonstrated that $Lyz2^{cre}$ × $Hif\text{-}1\alpha^{fl/fl}$ mice have less plaque lesions when compared to control mice [206]. Surprisingly, Hif-1α deficient mice displayed less apoptotic cells and blunted glucose uptake [206].

LPS also regulates glucose flux into the PPP. LPS decreased the expression of the enzyme Shpk (CARKL) involved in the non-oxidative branch of the PPP [207]. Conversely, IL-4 induced CARKL expression is required for optimal macrophage alternative polarization. CARKL genetic deficiency forces glucose flux into the glycolysis pathway at a level similar to the one seen upon LPS challenge [207]. Shpk expression is not restricted to a selective myeloid cell population in plaques (Figure 3B). In advanced plaque, macrophage local proliferation contributes to plaque growth [208] and one would expect that the PPP pathway, involved in nucleotide generation, is highly activated. This was not yet documented to our knowledge. Interestingly, a recent report demonstrated that hypercholesterolemia suppressed the PPP in macrophages [209]. Whether this mechanism occurs in plaque during atherosclerosis development remains to be tested.

Dendritic cells

Several populations of DCs have been identified in plaques, both in mice and humans (**Table 2 and Figure 1**). However, little is known about the metabolic configuration of plaque resident DCs. Following TLR4 activation with LPS, DCs rapidly undergo a metabolic switch towards glycolysis [210,211]. LPS exposure increases glucose consumption rate and increases Glut1 expression in DCs [210]. This is paralleled by augmented nitric oxide (NO) production that subsequently decreases oxidative phosphorylation (OXPHOS) activity, ATP levels and mitochondrial activity. Consistently, activated DCs show less oxygen consumption rate than resting DCs [210]. Thus, NO seems to play a pivotal role in metabolic regulation [211]. In DCs, endogenous nitric oxide production inhibits OXPHOS and commit those cells to glucose metabolism and aerobic

glycolysis similar to the Warburg effect described in tumor cells [211]. Additionally, LPS-induced NO production contributes to DCs induced death following activation [211]. This glycolytic reprogramming that happens within minutes after TLR stimulation is called the “glycolytic burst” and leads to *de novo* fatty acid synthesis needed for inflammatory cytokine production [212]. In addition, glucose restriction decreases activated-DC maturation, life span and cytokine secretion.

As compared to the rapid increase in glucose flux, Glut1 upregulation in DCs takes hours to build up following TLR stimulation. Therefore, exogenous glucose internalization seems unlikely to be the source required during early DC activation. This lag was recently solved by Thwe and colleagues who showed that intracellular glycogen reserves fuel DCs metabolic demands during early DC activation and that glycogen metabolism is required by these cells to initiate proper immune effector responses [213]. Of note, high glucose concentration increased the oxLDL-uptake capacity of DCs and augmented their IL-6 and IL-12 secretion while decreasing their IL-10 production [214].

Neutrophils

Unlike macrophages and monocytes, little is known about neutrophil metabolic configuration in health and disease. This might be explained by the difficulty to analyze these cells ex vivo. Moreover, single-cell RNA-Seq analysis on neutrophils is rather difficult because these cells typically possess lower number of transcripts when compared to T cells and macrophages. Neutrophils have long been thought to mainly rely on glycolytic metabolism [215], but neutrophils are able to switch from glycolysis to different metabolic pathways such as OXPHOS [216,217]. Increased glycemia favors granulopoiesis and neutrophil release in the blood circulation [191,192]. How modulation of plasma glucose levels impacts on neutrophil chemotaxis, especially their recruitment, retention and survival in the atherosclerotic plaque, is another exciting question.

Amino Acids

In addition to glucose and lipids, amino acids are a source of energy for immune cells. Amino acids are essential metabolites for protein synthesis that act as intermediates in metabolic pathways. Amino acids modulate immune cell functions such as activation, differentiation, proliferation, gene expression, redox status or cytokine production. However, the role of amino acids on immune cell functions during atherosclerosis remains poorly understood.

In vitro studies have demonstrated the impact of glutamine metabolism on macrophage polarization [218,219]. More recently, Tavakoli et al. highlighted increased glutamine accumulation in aortas obtained from $Ldlr^{-/-}$ mice. In this study, the autoradiography shows a non-homogenous glutamine accumulation that diverges according to macrophage activation profile. The combination of 2-deoxyglucose and glutamine accumulation

within the aorta could predict the dominant macrophage polarization profile within the plaque. Indeed, a greater accumulation of glutamine than 2-deoxyglucose supposes a dominant anti-inflammatory population while the opposite indicates a higher content of pro-inflammatory macrophages. This study is one of the first to suggest a role for glutamine on plaque macrophage functions [220].

Besides glutamine, arginine is a key metabolite in vascular function and tone due to its role in the production of nitric oxide (NO). Indeed, arginine is metabolized both by arginase 1 (Arg1) and inducible nitric oxide synthase (iNOS) to produce ornithine and urea or NO respectively. As those two enzymes compete for the same substrate, the use of arginine by Arg1 limits NO production, a macrophage pro-atherogenic factor [221]. In $Ldlr^{-/-}$ mice, microarray analysis showed an increase Arg1 expression in carotid artery during early atherosclerotic lesions. Moreover, Arg1 deficiency promoted NO synthesis upon lipid loading. Hematopoietic Arg1 deletion induced increase foam cell formation in the peritoneum. However, after 10 weeks of western diet, Arg1 deficiency in $Ldlr^{-/-}$ mice had no effect on the plaque size nor on the plaque composition [222]. Similarly, in $Ldlr^{-/-}$ mice deficient for Arg1 specifically in myeloid cells, Yurdagul et al. did not observe any phenotypic difference within the plaque. However, in a regression model, the authors demonstrated defective efferocytosis within the plaque leading to impaired regression, increased necrotic core area and decreased cap thickness. In addition, ornithine produced by Arg1 can be subsequently metabolized to putrescine by ODC (ornithine decarboxylase) [223,224]. Putrescine supplementation improves plaque macrophage efferocytosis leading to reduced lesion and necrotic core size, as well as cap thickness [225]. Conversely, $ApoE^{-/-}$ mice deficient for iNOS in the bone marrow compartment have reduced atheromatous lesions showing that leukocyte mediates the pro-atherogenic effect of iNOS in mice [226].

CONCLUSIONS AND FUTURE DIRECTIONS

The field of immunometabolism is a rapidly expanding one that provides new insights on the role of specific metabolites in immune cells during health and disease. Atherosclerosis is characterized by increased plasma glucose and cholesterol concentrations, and we only recently started to appreciate how precisely these two metabolites impact on plaque resident myeloid cell functions and on their generation from bone marrow-derived precursors. The precise circuits incorporating glucose in macrophages, monocytes, DCs and neutrophils remain to be fully understood. Eventually this might help to apprehend how metabolism supports key functions specific for each population. For example, understanding how metabolism guides monocyte recruitment to plaques as well as their retention or eventual egress will be of significant importance for the field. Regarding macrophages, we recently learned that glucose metabolism sustains one of their key functions: the removal of

apoptotic cells [194,195]. Whether glucose modulates macrophage motility in plaque or their interaction with the extracellular matrix remains to be elucidated. Recent reports demonstrated that DCs cytokine production is tightly regulated by their metabolic configuration [227]. Glucose metabolism regulates DCs migration via regulation of the key chemokine receptor CCR7 [228,229]. Of note, the role of CCR7 during atherosclerosis remains debated with studies reporting that CCR7-deficient mice display smaller [230], similar [231] and increased [232] plaque area. One might wonder whether this mechanism occurs during atherosclerosis as well. Specific metabolic configuration might be required for efficient peptide presentation to conventional T cells via MHC II or lipids to NKT (Natural Killer T) cells via CD1d. Another crucial question is whether the way of metabolite incorporation in myeloid cells affects their intracellular distribution. Apoptotic cell ingestion by myeloid cells leads to internalization of metabolites contained in the dying cell [225]. Thus, the efferocytes need to either incorporate these metabolites into their circuits, store them in specialized compartments or expulse them in the interstitial space where they could be used by neighbor cells.

Single-Cell RNA-Seq moved the field forward toward a better understanding of the immune diversity and functions in atherosclerotic plaque. Nevertheless, the predictions generated via this technique need in detail in situ validation. Recently, an elegant approach was validated to investigate single-cell metabolism in local environment [233]. This new technical advance will be helpful to investigate whether different myeloid cell populations residing in plaque possess a unique enzymatic profile. These analyses could also reveal a zonation in plaque enzyme and metabolite distribution. The field will benefit from our future ability to dose locally metabolites at the scale of the milieu surrounding a cell as well as cellular micro-compartmentalization. This, together with our ability to measure enzymatic activities and at the same scale will certainly make our task of making sense of metabolism an easier one. Our computing ability to integrate all those parameters will also facilitate the large-scale understanding of deciphering how access and competition for nutrients shape immunity and to what extent this can be used as new therapeutic handles.

AUTHOR CONTRIBUTIONS

AG and SI outlined the manuscript. AG, MIS, JM and SI wrote the manuscript. AG generated the figures and tables. RRG, LYC and SI edited the manuscript. All authors approved the final submission of the manuscript.

CONFLICTS OF INTEREST

The authors have no disclosure and conflict of interest to declare.

FUNDING

AG is supported by the French government, through the UCAJedi Investments in the Future projects managed by the National Research Agency (ANR) with the reference number ANR-15-IDEX-01. RRG is supported by Centre National de la Recherche Scientifique (CNRS). LYC is supported by grants from the European Research Council (ERC) consolidator program (ERC2016COG724838). SI is supported by Institut National de la Sante et de la Recherche Medicale (INSERM) and Agence Nationale de la Recherche (ANR-17-CE14-0017-01 and ANR-19-ECVD-0005-01).

REFERENCES

1. Libby P, Lichtman AH, Hansson GK. Immune effector mechanisms implicated in atherosclerosis: from mice to humans. Immunity. 2013;38(6):1092-104.
2. Kobiyama K, Ley K. Atherosclerosis. Circ Res. 2018;123(10):1118-20.
3. Fredrickson DS, Lees RS. A System for Phenotyping Hyperlipoproteinemia. Circulation. 1965;31:321-7.
4. Dawber TR, Moore FE, Mann GV. Coronary heart disease in the Framingham study. Am J Public Health Nations Health. 1957;47(4 Pt 2):4-24.
5. Moore KJ, Tabas I. Macrophages in the pathogenesis of atherosclerosis. Cell. 2011;145(3):341-55.
6. Otsuka F, Joner M, Prati F, Virmani R, Narula J. Clinical classification of plaque morphology in coronary disease. Nat Rev Cardiol. 2014;11(7):379-89.
7. Tabas I. Heart disease: Death-defying plaque cells. Nature. 2016;536(7614):32-3.
8. Davies MJ, Richardson PD, Woolf N, Katz DR, Mann J. Risk of thrombosis in human atherosclerotic plaques: role of extracellular lipid, macrophage, and smooth muscle cell content. Br Heart J. 1993;69(5):377-81.
9. Virmani R, Kolodgie FD, Burke AP, Farb A, Schwartz SM. Lessons from sudden coronary death: a comprehensive morphological classification scheme for atherosclerotic lesions. Arterioscler Thromb Vasc Biol. 2000;20(5):1262-75.
10. Guilliams M, Ginhoux F, Jakubzick C, Naik SH, Onai N, Schraml BU, et al. Dendritic cells, monocytes and macrophages: a unified nomenclature based on ontogeny. Nat Rev Immunol. 2014;14(8):571-8.
11. Gautier EL, Shay T, Miller J, Greter M, Jakubzick C, Ivanov S, et al. Gene-expression profiles and transcriptional regulatory pathways that underlie the identity and diversity of mouse tissue macrophages. Nat Immunol. 2012;13(11):1118-28.
12. Tabas I, Bornfeldt KE. Intracellular and Intercellular Aspects of Macrophage Immunometabolism in Atherosclerosis. Circ Res. 2020;126(9):1209-27.
13. Nishizawa T, Kanter JE, Kramer F, Barnhart S, Shen X, Vivekanandan-Giri A, et al. Testing the role of myeloid cell glucose flux in inflammation and atherosclerosis. Cell Rep. 2014;7(2):356-65.
14. Shirai T, Nazarewicz RR, Wallis BB, Yanes RE, Watanabe R, Hilhorst M, et al. The glycolytic enzyme PKM2 bridges metabolic and inflammatory dysfunction in coronary artery disease. J Exp Med. 2016;213(3):337-54.

15. Tomas L, Edsfeldt A, Mollet IG, Perisic Matic L, Prehn C, Adamski J, et al. Altered metabolism distinguishes high-risk from stable carotid atherosclerotic plaques. Eur Heart J. 2018;39(24):2301-10.
16. Jonasson L, Holm J, Skalli O, Bondjers G, Hansson GK. Regional accumulations of T cells, macrophages, and smooth muscle cells in the human atherosclerotic plaque. Arteriosclerosis. 1986;6(2):131-8.
17. Koltsova EK, Garcia Z, Chodaczek G, Landau M, McArdle S, Scott SR, et al. Dynamic T cell-APC interactions sustain chronic inflammation in atherosclerosis. J Clin Invest. 2012;122(9):3114-26.
18. Lin JD, Nishi H, Poles J, Niu X, McCauley C, Rahman K, et al. Single-cell analysis of fate-mapped macrophages reveals heterogeneity, including stem-like properties, during atherosclerosis progression and regression. JCI Insight. 2019;4(4):e124574.
19. Williams JW, Winkels H, Durant CP, Zaitsev K, Ghosheh Y, Ley K. Single Cell RNA Sequencing in Atherosclerosis Research. Circ Res. 2020;126(9):1112-26.
20. Fernandez DM, Rahman AH, Fernandez NF, Chudnovskiy A, Amir ED, Amadori L, et al. Single-cell immune landscape of human atherosclerotic plaques. Nat Med. 2019;25(10):1576-88.
21. Cochain C, Vafadarnejad E, Arampatzi P, Pelisek J, Winkels H, Ley K, et al. Single-Cell RNA-Seq Reveals the Transcriptional Landscape and Heterogeneity of Aortic Macrophages in Murine Atherosclerosis. Circ Res. 2018;122(12):1661-74.
22. Winkels H, Ehinger E, Vassallo M, Buscher K, Dinh HQ, Kobiyama K, et al. Atlas of the Immune Cell Repertoire in Mouse Atherosclerosis Defined by Single-Cell RNA-Sequencing and Mass Cytometry. Circ Res. 2018;122(12):1675-88.
23. Kim K, Shim D, Lee JS, Zaitsev K, Williams JW, Kim KW, et al. Transcriptome Analysis Reveals Nonfoamy Rather Than Foamy Plaque Macrophages Are Proinflammatory in Atherosclerotic Murine Models. Circ Res. 2018;123(10):1127-42.
24. Cole JE, Park I, Ahern DJ, Kassiteridi C, Danso Abeam D, Goddard ME, et al. Immune cell census in murine atherosclerosis: cytometry by time of flight illuminates vascular myeloid cell diversity. Cardiovasc Res. 2018;114(10):1360-71.
25. Kalluri AS, Vellarikkal SK, Edelman ER, Nguyen L, Subramanian A, Ellinor PT, et al. Single-Cell Analysis of the Normal Mouse Aorta Reveals Functionally Distinct Endothelial Cell Populations. Circulation. 2019;140(2):147-63.
26. Zernecke A, Winkels H, Cochain C, Williams JW, Wolf D, Soehnlein O, et al. Meta-Analysis of Leukocyte Diversity in Atherosclerotic Mouse Aortas. Circ Res. 2020;127(3):402-26.
27. Wolf AA, Yanez A, Barman PK, Goodridge HS. The Ontogeny of Monocyte Subsets. Front Immunol. 2019;10:1642.
28. Jakubzick CV, Randolph GJ, Henson PM. Monocyte differentiation and antigen-presenting functions. Nat Rev Immunol. 2017;17(6):349-62.
29. Dai XM, Ryan GR, Hapel AJ, Dominguez MG, Russell RG, Kapp S, et al. Targeted disruption of the mouse colony-stimulating factor 1 receptor gene results in

osteopetrosis, mononuclear phagocyte deficiency, increased primitive progenitor cell frequencies, and reproductive defects. Blood. 2002;99(1):111-20.
30. Guilliams M, Thierry GR, Bonnardel J, Bajenoff M. Establishment and Maintenance of the Macrophage Niche. Immunity. 2020;52(3):434-51.
31. Friedman GD, Klatsky AL, Siegelaub AB. The leukocyte count as a predictor of myocardial infarction. N Engl J Med. 1974;290(23):1275-8.
32. Barron HV, Cannon CP, Murphy SA, Braunwald E, Gibson CM. Association between white blood cell count, epicardial blood flow, myocardial perfusion, and clinical outcomes in the setting of acute myocardial infarction: a thrombolysis in myocardial infarction 10 substudy. Circulation. 2000;102(19):2329-34.
33. Cannon CP, McCabe CH, Wilcox RG, Bentley JH, Braunwald E. Association of white blood cell count with increased mortality in acute myocardial infarction and unstable angina pectoris. OPUS-TIMI 16 Investigators. Am J Cardiol. 2001;87(5):636-9,A10.
34. Averill LE, Meagher RC, Gerrity RG. Enhanced monocyte progenitor cell proliferation in bone marrow of hyperlipemic swine. Am J Pathol. 1989;135(2):369-77.
35. Feldman DL, Mogelesky TC, Liptak BF, Gerrity RG. Leukocytosis in rabbits with diet-induced atherosclerosis. Arterioscler Thromb. 1991;11(4):985-94.
36. Lessner SM, Prado HL, Waller EK, Galis ZS. Atherosclerotic lesions grow through recruitment and proliferation of circulating monocytes in a murine model. Am J Pathol. 2002;160(6):2145-55.
37. Geissmann F, Jung S, Littman DR. Blood monocytes consist of two principal subsets with distinct migratory properties. Immunity. 2003;19(1):71-82.
38. Sunderkotter C, Nikolic T, Dillon MJ, Van Rooijen N, Stehling M, Drevets DA, et al. Subpopulations of mouse blood monocytes differ in maturation stage and inflammatory response. J Immunol. 2004;172(7):4410-7.
39. Chong SZ, Evrard M, Devi S, Chen J, Lim JY, See P, et al. CXCR4 identifies transitional bone marrow premonocytes that replenish the mature monocyte pool for peripheral responses. J Exp Med. 2016;213(11):2293-314.
40. Hanna RN, Carlin LM, Hubbeling HG, Nackiewicz D, Green AM, Punt JA, et al. The transcription factor NR4A1 (Nur77) controls bone marrow differentiation and the survival of Ly6C- monocytes. Nat Immunol. 2011;12(8):778-85.
41. Auffray C, Fogg D, Garfa M, Elain G, Join-Lambert O, Kayal S, et al. Monitoring of blood vessels and tissues by a population of monocytes with patrolling behavior. Science. 2007;317(5838):666-70.
42. Carlin LM, Stamatiades EG, Auffray C, Hanna RN, Glover L, Vizcay-Barrena G, et al. Nr4a1-dependent Ly6C(low) monocytes monitor endothelial cells and orchestrate their disposal. Cell. 2013;153(2):362-75.
43. Weber C, Belge KU, von Hundelshausen P, Draude G, Steppich B, Mack M, et al. Differential chemokine receptor expression and function in human monocyte subpopulations. J Leukoc Biol. 2000;67(5):699-704.
44. Palframan RT, Jung S, Cheng G, Weninger W, Luo Y, Dorf M, et al. Inflammatory chemokine transport and presentation in HEV: a remote

control mechanism for monocyte recruitment to lymph nodes in inflamed tissues. J Exp Med. 2001;194(9):1361-73.

45. Dyer DP, Medina-Ruiz L, Bartolini R, Schuette F, Hughes CE, Pallas K, et al. Chemokine Receptor Redundancy and Specificity Are Context Dependent. Immunity. 2019;50(2):378-89.e5.
46. Swirski FK, Libby P, Aikawa E, Alcaide P, Luscinskas FW, Weissleder R, et al. Ly-6Chi monocytes dominate hypercholesterolemia-associated monocytosis and give rise to macrophages in atheromata. J Clin Invest. 2007;117(1):195-205.
47. Tacke F, Alvarez D, Kaplan TJ, Jakubzick C, Spanbroek R, Llodra J, et al. Monocyte subsets differentially employ CCR2, CCR5, and CX3CR1 to accumulate within atherosclerotic plaques. J Clin Invest. 2007;117(1):185-94.
48. Imhof BA, Aurrand-Lions M. Adhesion mechanisms regulating the migration of monocytes. Nat Rev Immunol. 2004;4(6):432-44.
49. Ley K, Laudanna C, Cybulsky MI, Nourshargh S. Getting to the site of inflammation: the leukocyte adhesion cascade updated. Nat Rev Immunol. 2007;7(9):678-89.
50. Verweij SL, Duivenvoorden R, Stiekema LCA, Nurmohamed NS, van der Valk FM, Versloot M, et al. CCR2 expression on circulating monocytes is associated with arterial wall inflammation assessed by 18F-FDG PET/CT in patients at risk for cardiovascular disease. Cardiovasc Res. 2018;114(3):468-75.
51. Yoshida H, Hayashi S, Kunisada T, Ogawa M, Nishikawa S, Okamura H, et al. The murine mutation osteopetrosis is in the coding region of the macrophage colony stimulating factor gene. Nature. 1990;345(6274):442-4.
52. Qiao JH, Tripathi J, Mishra NK, Cai Y, Tripathi S, Wang XP, et al. Role of macrophage colony-stimulating factor in atherosclerosis: studies of osteopetrotic mice. Am J Pathol. 1997;150(5):1687-99.
53. Smith JD, Trogan E, Ginsberg M, Grigaux C, Tian J, Miyata M. Decreased atherosclerosis in mice deficient in both macrophage colony-stimulating factor (op) and apolipoprotein E. Proc Natl Acad Sci U S A. 1995;92(18):8264-8.
54. Rajavashisth T, Qiao JH, Tripathi S, Tripathi J, Mishra N, Hua M, et al. Heterozygous osteopetrotic (op) mutation reduces atherosclerosis in LDL receptor- deficient mice. J Clin Invest. 1998;101(12):2702-10.
55. Boring L, Gosling J, Cleary M, Charo IF. Decreased lesion formation in CCR2$^{-/-}$ mice reveals a role for chemokines in the initiation of atherosclerosis. Nature. 1998;394(6696):894-7.
56. Gu L, Okada Y, Clinton SK, Gerard C, Sukhova GK, Libby P, et al. Absence of monocyte chemoattractant protein-1 reduces atherosclerosis in low density lipoprotein receptor-deficient mice. Mol Cell. 1998;2(2):275-81.
57. Ingersoll MA, Spanbroek R, Lottaz C, Gautier EL, Frankenberger M, Hoffmann R, et al. Comparison of gene expression profiles between human and mouse monocyte subsets. Blood. 2010;115(3):e10-9.
58. Ait-Oufella H, Taleb S, Mallat Z, Tedgui A. Recent advances on the role of cytokines in atherosclerosis. Arterioscler Thromb Vasc Biol. 2011;31(5):969-79.

59. Galea J, Armstrong J, Gadsdon P, Holden H, Francis SE, Holt CM. Interleukin-1 beta in coronary arteries of patients with ischemic heart disease. Arterioscler Thromb Vasc Biol. 1996;16(8):1000-6.
60. Kirii H, Niwa T, Yamada Y, Wada H, Saito K, Iwakura Y, et al. Lack of interleukin-1beta decreases the severity of atherosclerosis in ApoE-deficient mice. Arterioscler Thromb Vasc Biol. 2003;23(4):656-60.
61. Isoda K, Sawada S, Ishigami N, Matsuki T, Miyazaki K, Kusuhara M, et al. Lack of interleukin-1 receptor antagonist modulates plaque composition in apolipoprotein E-deficient mice. Arterioscler Thromb Vasc Biol. 2004;24(6):1068-73.
62. Gomez D, Baylis RA, Durgin BG, Newman AAC, Alencar GF, Mahan S, et al. Interleukin-1beta has atheroprotective effects in advanced atherosclerotic lesions of mice. Nat Med. 2018;24(9):1418-29.
63. Ridker PM, MacFadyen JG, Everett BM, Libby P, Thuren T, Glynn RJ, et al. Relationship of C-reactive protein reduction to cardiovascular event reduction following treatment with canakinumab: a secondary analysis from the CANTOS randomised controlled trial. Lancet. 2018;391(10118):319-28.
64. Ridker PM, Everett BM, Thuren T, MacFadyen JG, Chang WH, Ballantyne C, et al. Antiinflammatory Therapy with Canakinumab for Atherosclerotic Disease. N Engl J Med. 2017;377(12):1119-31.
65. Doran AC, Yurdagul A Jr, Tabas I. Efferocytosis in health and disease. Nat Rev Immunol. 2020;20(4):254-67.
66. Bianconi E, Piovesan A, Facchin F, Beraudi A, Casadei R, Frabetti F, et al. An estimation of the number of cells in the human body. Ann Hum Biol. 2013;40(6):463-71.
67. Wolf Y, Boura-Halfon S, Cortese N, Haimon Z, Sar Shalom H, Kuperman Y, et al. Brown-adipose-tissue macrophages control tissue innervation and homeostatic energy expenditure. Nat Immunol. 2017;18(6):665-74.
68. Kohyama M, Ise W, Edelson BT, Wilker PR, Hildner K, Mejia C, et al. Role for Spi-C in the development of red pulp macrophages and splenic iron homeostasis. Nature. 2009;457(7227):318-21.
69. Schulz C, Gomez Perdiguero E, Chorro L, Szabo-Rogers H, Cagnard N, Kierdorf K, et al. A lineage of myeloid cells independent of Myb and hematopoietic stem cells. Science. 2012;336(6077):86-90.
70. Gomez Perdiguero E, Klapproth K, Schulz C, Busch K, Azzoni E, Crozet L, et al. Tissue-resident macrophages originate from yolk-sac-derived erythro-myeloid progenitors. Nature. 2015;518(7540):547-51.
71. Guilliams M, De Kleer I, Henri S, Post S, Vanhoutte L, De Prijck S, et al. Alveolar macrophages develop from fetal monocytes that differentiate into long-lived cells in the first week of life via GM-CSF. J Exp Med. 2013;210(10):1977-92.
72. Bain CC, Mowat AM. Macrophages in intestinal homeostasis and inflammation. Immunol Rev. 2014;260(1):102-17.
73. Epelman S, Lavine KJ, Beaudin AE, Sojka DK, Carrero JA, Calderon B, et al. Embryonic and adult-derived resident cardiac macrophages are maintained through distinct mechanisms at steady state and during inflammation. Immunity. 2014;40(1):91-104.

74. Silva HM, Bafica A, Rodrigues-Luiz GF, Chi J, Santos PDA, Reis BS, et al. Vasculature-associated fat macrophages readily adapt to inflammatory and metabolic challenges. J Exp Med. 2019;216(4):786-806.
75. Wang Y, Szretter KJ, Vermi W, Gilfillan S, Rossini C, Cella M, et al. IL-34 is a tissue-restricted ligand of CSF1R required for the development of Langerhans cells and microglia. Nat Immunol. 2012;13(8):753-60.
76. Ivanov S, Gallerand A, Gros M, Stunault MI, Merlin J, Vaillant N, et al. Mesothelial cell CSF1 sustains peritoneal macrophage proliferation. Eur J Immunol. 2019;49(11):2012-8.
77. Chakarov S, Lim HY, Tan L, Lim SY, See P, Lum J, et al. Two distinct interstitial macrophage populations coexist across tissues in specific subtissular niches. Science. 2019;363(6432):eaau0964.
78. Cochain C, Saliba AE, Zernecke A. Letter by Cochain et al Regarding Article, "Transcriptome Analysis Reveals Nonfoamy Rather Than Foamy Plaque Macrophages Are Proinflammatory in Atherosclerotic Murine Models". Circ Res. 2018;123(11):e48-9.
79. Kim K, Choi JH. Response by Kim and Choi to Letter Regarding Article, "Transcriptome Analysis Reveals Nonfoamy Rather Than Foamy Plaque Macrophages Are Proinflammatory in Atherosclerotic Murine Models". Circ Res. 2018;123(11):e50.
80. Satpathy AT, Kc W, Albring JC, Edelson BT, Kretzer NM, Bhattacharya D, et al. Zbtb46 expression distinguishes classical dendritic cells and their committed progenitors from other immune lineages. J Exp Med. 2012;209(6):1135-52.
81. Meredith MM, Liu K, Darrasse-Jeze G, Kamphorst AO, Schreiber HA, Guermonprez P, et al. Expression of the zinc finger transcription factor zDC (Zbtb46, Btbd4) defines the classical dendritic cell lineage. J Exp Med. 2012;209(6):1153-65.
82. Murphy TL, Grajales-Reyes GE, Wu X, Tussiwand R, Briseno CG, Iwata A, et al. Transcriptional Control of Dendritic Cell Development. Annu Rev Immunol. 2016;34:93-119.
83. Doring Y, Zernecke A. Plasmacytoid dendritic cells in atherosclerosis. Front Physiol. 2012;3:230.
84. Jensen J, Vazquez-Torres A, Balish E. Poly(I.C)-induced interferons enhance susceptibility of SCID mice to systemic candidiasis. Infect Immun. 1992;60(11):4549-57.
85. Thacker SG, Zhao W, Smith CK, Luo W, Wang H, Vivekanandan-Giri A, et al. Type I interferons modulate vascular function, repair, thrombosis, and plaque progression in murine models of lupus and atherosclerosis. Arthritis Rheum. 2012;64(9):2975-85.
86. Ait-Oufella H, Sage AP, Mallat Z, Tedgui A. Adaptive (T and B cells) immunity and control by dendritic cells in atherosclerosis. Circ Res. 2014;114(10):1640-60.
87. Weber C, Meiler S, Doring Y, Koch M, Drechsler M, Megens RT, et al. CCL17-expressing dendritic cells drive atherosclerosis by restraining regulatory T cell homeostasis in mice. J Clin Invest. 2011;121(7):2898-910.
88. Kimura T, Kobiyama K, Winkels H, Tse K, Miller J, Vassallo M, et al. Regulatory CD4(+) T Cells Recognize Major Histocompatibility Complex Class II Molecule-

Restricted Peptide Epitopes of Apolipoprotein B. Circulation. 2018;138(11):1130-43.

89. Kimura T, Tse K, McArdle S, Gerhardt T, Miller J, Mikulski Z, et al. Atheroprotective vaccination with MHC-II-restricted ApoB peptides induces peritoneal IL-10-producing CD4 T cells. Am J Physiol Heart Circ Physiol. 2017;312(4):H781-90.
90. Tse K, Gonen A, Sidney J, Ouyang H, Witztum JL, Sette A, et al. Atheroprotective Vaccination with MHC-II Restricted Peptides from ApoB-100. Front Immunol. 2013;4:493.
91. Lin Z, Qian S, Gong Y, Ren J, Zhao L, Wang D, et al. Deep sequencing of the T cell receptor beta repertoire reveals signature patterns and clonal drift in atherosclerotic plaques and patients. Oncotarget. 2017;8(59):99312-22.
92. Paulsson G, Zhou X, Tornquist E, Hansson GK. Oligoclonal T cell expansions in atherosclerotic lesions of apolipoprotein E-deficient mice. Arterioscler Thromb Vasc Biol. 2000;20(1):10-7.
93. Buono C, Pang H, Uchida Y, Libby P, Sharpe AH, Lichtman AH. B7-1/B7-2 costimulation regulates plaque antigen-specific T-cell responses and atherogenesis in low-density lipoprotein receptor-deficient mice. Circulation. 2004;109(16):2009-15.
94. Haddad Y, Lahoute C, Clement M, Laurans L, Metghalchi S, Zeboudj L, et al. The Dendritic Cell Receptor DNGR-1 Promotes the Development of Atherosclerosis in Mice. Circ Res. 2017;121(3):234-43.
95. Nathan C. Neutrophils and immunity: challenges and opportunities. Nat Rev Immunol. 2006;6(3):173-82.
96. Doring Y, Drechsler M, Wantha S, Kemmerich K, Lievens D, Vijayan S, et al. Lack of neutrophil-derived CRAMP reduces atherosclerosis in mice. Circ Res. 2012;110(8):1052-6.
97. Zernecke A, Bot I, Djalali-Talab Y, Shagdarsuren E, Bidzhekov K, Meiler S, et al. Protective role of CXC receptor 4/CXC ligand 12 unveils the importance of neutrophils in atherosclerosis. Circ Res. 2008;102(2):209-17.
98. Naruko T, Ueda M, Haze K, van der Wal AC, van der Loos CM, Itoh A, et al. Neutrophil infiltration of culprit lesions in acute coronary syndromes. Circulation. 2002;106(23):2894-900.
99. Rotzius P, Thams S, Soehnlein O, Kenne E, Tseng CN, Bjorkstrom NK, et al. Distinct infiltration of neutrophils in lesion shoulders in ApoE$^{-/-}$ mice. Am J Pathol. 2010;177(1):493-500.
100. Yang, Han Z, Oppenheim JJ. Alarmins and immunity. Immunol Rev. 2017;280(1):41-56.
101. Pruenster M, Kurz AR, Chung KJ, Cao-Ehlker X, Bieber S, Nussbaum CF, et al. Extracellular MRP8/14 is a regulator of beta2 integrin-dependent neutrophil slow rolling and adhesion. Nat Commun. 2015;6:6915.
102. Chen Q, Jin Y, Zhang K, Li H, Chen W, Meng G, et al. Alarmin HNP-1 promotes pyroptosis and IL-1beta release through different roles of NLRP3 inflammasome via P2X7 in LPS-primed macrophages. Innate Immun. 2014;20(3):290-300.

103. Willingham SB, Allen IC, Bergstralh DT, Brickey WJ, Huang MT, Taxman DJ, et al. NLRP3 (NALP3, Cryopyrin) facilitates in vivo caspase-1 activation, necrosis, and HMGB1 release via inflammasome-dependent and -independent pathways. J Immunol. 2009;183(3):2008-15.
104. Kahlenberg JM, Carmona-Rivera C, Smith CK, Kaplan MJ. Neutrophil extracellular trap-associated protein activation of the NLRP3 inflammasome is enhanced in lupus macrophages. J Immunol. 2013;190(3):1217-26.
105. Soehnlein O, Zernecke A, Eriksson EE, Rothfuchs AG, Pham CT, Herwald H, et al. Neutrophil secretion products pave the way for inflammatory monocytes. Blood. 2008;112(4):1461-71.
106. Qi H, Yang S, Zhang L. Neutrophil Extracellular Traps and Endothelial Dysfunction in Atherosclerosis and Thrombosis. Front Immunol. 2017;8:928.
107. Schuster S, Hurrell B, Tacchini-Cottier F. Crosstalk between neutrophils and dendritic cells: a context-dependent process. J Leukoc Biol. 2013;94(4):671-5.
108. Narula J, Kolodgie FD, Virmani R. Apoptosis and cardiomyopathy. Curr Opin Cardiol. 2000;15(3):183-8.
109. Denny MF, Yalavarthi S, Zhao W, Thacker SG, Anderson M, Sandy AR, et al. A distinct subset of proinflammatory neutrophils isolated from patients with systemic lupus erythematosus induces vascular damage and synthesizes type I IFNs. J Immunol. 2010;184(6):3284-97.
110. Chavez-Sanchez L, Espinosa-Luna JE, Chavez-Rueda K, Legorreta-Haquet MV, Montoya-Diaz E, Blanco-Favela F. Innate immune system cells in atherosclerosis. Arch Med Res. 2014;45(1):1-14.
111. van Leeuwen M, Gijbels MJ, Duijvestijn A, Smook M, van de Gaar MJ, Heeringa P, et al. Accumulation of myeloperoxidase-positive neutrophils in atherosclerotic lesions in LDLR$^{-/-}$ mice. Arterioscler Thromb Vasc Biol. 2008;28(1):84-9.
112. Aratani Y. Myeloperoxidase: Its role for host defense, inflammation, and neutrophil function. Arch Biochem Biophys. 2018;640:47-52.
113. Podrez EA, Schmitt D, Hoff HF, Hazen SL. Myeloperoxidase-generated reactive nitrogen species convert LDL into an atherogenic form in vitro. J Clin Invest. 1999;103(11):1547-60.
114. Khan MA, Palaniyar N. Transcriptional firing helps to drive NETosis. Sci Rep. 2017;7:41749.
115. Doring Y, Libby P, Soehnlein O. Neutrophil Extracellular Traps Participate in Cardiovascular Diseases: Recent Experimental and Clinical Insights. Circ Res. 2020;126(9):1228-41.
116. Sriranjan RS, Tarkin JM, Evans NR, Le EPV, Chowdhury MM, Rudd JHF. Atherosclerosis imaging using PET: Insights and applications. Br J Pharmacol. 2019. doi: 10.1111/bph.14868
117. Yamashita A, Zhao Y, Matsuura Y, Yamasaki K, Moriguchi-Goto S, Sugita C, et al. Increased metabolite levels of glycolysis and pentose phosphate pathway in rabbit atherosclerotic arteries and hypoxic macrophage. PLoS One. 2014;9(1):e86426.

118. Yvan-Charvet L, Pagler T, Gautier EL, Avagyan S, Siry RL, Han S, et al. ATP-binding cassette transporters and HDL suppress hematopoietic stem cell proliferation. Science. 2010;328(5986):1689-93.
119. Murphy AJ, Akhtari M, Tolani S, Pagler T, Bijl N, Kuo CL, et al. ApoE regulates hematopoietic stem cell proliferation, monocytosis, and monocyte accumulation in atherosclerotic lesions in mice. J Clin Invest. 2011;121(10):4138-49.
120. Wang M, Subramanian M, Abramowicz S, Murphy AJ, Gonen A, Witztum J, et al. Interleukin-3/granulocyte macrophage colony-stimulating factor receptor promotes stem cell expansion, monocytosis, and atheroma macrophage burden in mice with hematopoietic ApoE deficiency. Arterioscler Thromb Vasc Biol. 2014;34(5):976-84.
121. Morgan PK, Fang L, Lancaster GI, Murphy AJ. Hematopoiesis is regulated by cholesterol efflux pathways and lipid rafts: connections with cardiovascular diseases. J Lipid Res. 2020;61(5):667-75.
122. Hermetet F, Buffiere A, Aznague A, Pais de Barros JP, Bastie JN, Delva L, et al. High-fat diet disturbs lipid raft/TGF-beta signaling-mediated maintenance of hematopoietic stem cells in mouse bone marrow. Nat Commun. 2019;10(1):523.
123. Babaev VR, Runner RP, Fan D, Ding L, Zhang Y, Tao H, et al. Macrophage Mal1 deficiency suppresses atherosclerosis in low-density lipoprotein receptor-null mice by activating peroxisome proliferator-activated receptor-gamma-regulated genes. Arterioscler Thromb Vasc Biol. 2011;31(6):1283-90.
124. Takahashi M, Yagyu H, Tazoe F, Nagashima S, Ohshiro T, Okada K, et al. Macrophage lipoprotein lipase modulates the development of atherosclerosis but not adiposity. J Lipid Res. 2013;54(4):1124-34.
125. Chang CL, Garcia-Arcos I, Nyren R, Olivecrona G, Kim JY, Hu Y, et al. Lipoprotein Lipase Deficiency Impairs Bone Marrow Myelopoiesis and Reduces Circulating Monocyte Levels. Arterioscler Thromb Vasc Biol. 2018;38(3):509-19.
126. Jordan S, Tung N, Casanova-Acebes M, Chang C, Cantoni C, Zhang D, et al. Dietary Intake Regulates the Circulating Inflammatory Monocyte Pool. Cell. 2019;178(5):1102-14.e17.
127. Fowler S, Shio H, Haley NJ. Characterization of lipid-laden aortic cells from cholesterol-fed rabbits. IV. Investigation of macrophage-like properties of aortic cell populations. Lab Invest. 1979;41(4):372-8.
128. Brown MS, Goldstein JL. Lipoprotein metabolism in the macrophage: implications for cholesterol deposition in atherosclerosis. Annu Rev Biochem. 1983;52:223-61.
129. Brown MS, Goldstein JL. A receptor-mediated pathway for cholesterol homeostasis. Science. 1986;232(4746):34-47.
130. Suzuki H, Kurihara Y, Takeya M, Kamada N, Kataoka M, Jishage K, et al. A role for macrophage scavenger receptors in atherosclerosis and susceptibility to infection. Nature. 1997;386(6622):292-6.
131. Kunjathoor VV, Febbraio M, Podrez EA, Moore KJ, Andersson L, Koehn S, et al. Scavenger receptors class A-I/II and CD36 are the principal receptors

responsible for the uptake of modified low density lipoprotein leading to lipid loading in macrophages. J Biol Chem. 2002;277(51):49982-8.

132. Yvan-Charvet L, Ranalletta M, Wang N, Han S, Terasaka N, Li R, et al. Combined deficiency of ABCA1 and ABCG1 promotes foam cell accumulation and accelerates atherosclerosis in mice. J Clin Invest. 2007;117(12):3900-8.
133. Accad M, Smith SJ, Newland DL, Sanan DA, King LE Jr, Linton MF, et al. Massive xanthomatosis and altered composition of atherosclerotic lesions in hyperlipidemic mice lacking acyl CoA:cholesterol acyltransferase 1. J Clin Invest. 2000;105(6):711-9.
134. Duewell P, Kono H, Rayner KJ, Sirois CM, Vladimer G, Bauernfeind FG, et al. NLRP3 inflammasomes are required for atherogenesis and activated by cholesterol crystals. Nature. 2010;464(7293):1357-61.
135. Schuster GU, Parini P, Wang L, Alberti S, Steffensen KR, Hansson GK, et al. Accumulation of foam cells in liver X receptor-deficient mice. Circulation. 2002;106(9):1147-53.
136. Larrede S, Quinn CM, Jessup W, Frisdal E, Olivier M, Hsieh V, et al. Stimulation of cholesterol efflux by LXR agonists in cholesterol-loaded human macrophages is ABCA1-dependent but ABCG1-independent. Arterioscler Thromb Vasc Biol. 2009;29(11):1930-6.
137. Calkin AC, Tontonoz P. Liver × receptor signaling pathways and atherosclerosis. Arterioscler Thromb Vasc Biol. 2010;30(8):1513-8.
138. Bischoff ED, Daige CL, Petrowski M, Dedman H, Pattison J, Juliano J, et al. Non-redundant roles for LXRalpha and LXRbeta in atherosclerosis susceptibility in low density lipoprotein receptor knockout mice. J Lipid Res. 2010;51(5):900-6.
139. Westerterp M, Murphy AJ, Wang M, Pagler TA, Vengrenyuk Y, Kappus MS, et al. Deficiency of ATP-binding cassette transporters A1 and G1 in macrophages increases inflammation and accelerates atherosclerosis in mice. Circ Res. 2013;112(11):1456-65.
140. Chinetti-Gbaguidi G, Baron M, Bouhlel MA, Vanhoutte J, Copin C, Sebti Y, et al. Human atherosclerotic plaque alternative macrophages display low cholesterol handling but high phagocytosis because of distinct activities of the PPARgamma and LXRalpha pathways. Circ Res. 2011;108(8):985-95.
141. Vats D, Mukundan L, Odegaard JI, Zhang L, Smith KL, Morel CR, et al. Oxidative metabolism and PGC-1beta attenuate macrophage-mediated inflammation. Cell Metab. 2006;4(1):13-24.
142. Chinetti G, Lestavel S, Bocher V, Remaley AT, Neve B, Torra IP, et al. PPAR-alpha and PPAR-gamma activators induce cholesterol removal from human macrophage foam cells through stimulation of the ABCA1 pathway. Nat Med. 2001;7(1):53-8.
143. Chawla A, Boisvert WA, Lee CH, Laffitte BA, Barak Y, Joseph SB, et al. A PPAR gamma-LXR-ABCA1 pathway in macrophages is involved in cholesterol efflux and atherogenesis. Mol Cell. 2001;7(1):161-71.
144. Li AC, Binder CJ, Gutierrez A, Brown KK, Plotkin CR, Pattison JW, et al. Differential inhibition of macrophage foam-cell formation and atherosclerosis in mice by PPARalpha, beta/delta, and gamma. J Clin Invest. 2004;114(11):1564-76.

145. Babaev VR, Ishiguro H, Ding L, Yancey PG, Dove DE, Kovacs WJ, et al. Macrophage expression of peroxisome proliferator-activated receptor-alpha reduces atherosclerosis in low-density lipoprotein receptor-deficient mice. Circulation. 2007;116(12):1404-12.
146. Rigamonti E, Chinetti-Gbaguidi G, Staels B. Regulation of macrophage functions by PPAR-alpha, PPAR-gamma, and LXRs in mice and men. Arterioscler Thromb Vasc Biol. 2008;28(6):1050-9.
147. Dubois V, Eeckhoute J, Lefebvre P, Staels B. Distinct but complementary contributions of PPAR isotypes to energy homeostasis. J Clin Invest. 2017;127(4):1202-14.
148. Viaud M, Ivanov S, Vujic N, Duta-Mare M, Aira LE, Barouillet T, et al. Lysosomal Cholesterol Hydrolysis Couples Efferocytosis to Anti-Inflammatory Oxysterol Production. Circ Res. 2018;122(10):1369-84.
149. Wild PS, Zeller T, Schillert A, Szymczak S, Sinning CR, Deiseroth A, et al. A genome-wide association study identifies LIPA as a susceptibility gene for coronary artery disease. Circ Cardiovasc Genet. 2011;4(4):403-12.
150. Evans TD, Zhang X, Clark RE, Alisio A, Song E, Zhang H, et al. Functional Characterization of LIPA (Lysosomal Acid Lipase) Variants Associated With Coronary Artery Disease. Arterioscler Thromb Vasc Biol. 2019;39(12):2480-91.
151. Horkko S, Bird DA, Miller E, Itabe H, Leitinger N, Subbanagounder G, et al. Monoclonal autoantibodies specific for oxidized phospholipids or oxidized phospholipid-protein adducts inhibit macrophage uptake of oxidized low-density lipoproteins. J Clin Invest. 1999;103(1):117-28.
152. Tsimikas S, Miyanohara A, Hartvigsen K, Merki E, Shaw PX, Chou MY, et al. Human oxidation-specific antibodies reduce foam cell formation and atherosclerosis progression. J Am Coll Cardiol. 2011;58(16):1715-27.
153. Que X, Hung MY, Yeang C, Gonen A, Prohaska TA, Sun X, et al. Oxidized phospholipids are proinflammatory and proatherogenic in hypercholesterolaemic mice. Nature. 2018;558(7709):301-6.
154. Palinski W, Tangirala RK, Miller E, Young SG, Witztum JL. Increased autoantibody titers against epitopes of oxidized LDL in LDL receptor-deficient mice with increased atherosclerosis. Arterioscler Thromb Vasc Biol. 1995;15(10):1569-76.
155. Harmon EY, Fronhofer V, 3rd, Keller RS, Feustel PJ, Zhu X, Xu H, et al. Anti-inflammatory immune skewing is atheroprotective: Apoe$^{-/-}$FcgammaRIIb$^{-/-}$ mice develop fibrous carotid plaques. J Am Heart Assoc. 2014;3(6):e001232.
156. Pagano S, Magenta A, D'Agostino M, Martino F, Barilla F, Satta N, et al. Anti-ApoA-1 IgGs in Familial Hypercholesterolemia Display Paradoxical Associations with Lipid Profile and Promote Foam Cell Formation. J Clin Med. 2019;8(12):2035.
157. van den Berg VJ, Vroegindewey MM, Kardys I, Boersma E, Haskard D, Hartley A, et al. Anti-Oxidized LDL Antibodies and Coronary Artery Disease: A Systematic Review. Antioxidants (Basel). 2019;8(10):484.
158. van Dierendonck X, de la Rosa Rodriguez MA, Georgiadi A, Mattijssen F, Dijk W, van Weeghel M, et al. HILPDA Uncouples Lipid Droplet Accumulation in

Adipose Tissue Macrophages from Inflammation and Metabolic Dysregulation. Cell Rep. 2020;30(6):1811-22.e6.

159. Maier A, Wu H, Cordasic N, Oefner P, Dietel B, Thiele C, et al. Hypoxia-inducible protein 2 Hig2/Hilpda mediates neutral lipid accumulation in macrophages and contributes to atherosclerosis in apolipoprotein E-deficient mice. FASEB J. 2017;31(11):4971-84.
160. Gomez I, Foudi N, Longrois D, Norel X. The role of prostaglandin E2 in human vascular inflammation. Prostaglandins Leukot Essent Fatty Acids. 2013;89(2-3):55-63.
161. Spann NJ, Garmire LX, McDonald JG, Myers DS, Milne SB, Shibata N, et al. Regulated accumulation of desmosterol integrates macrophage lipid metabolism and inflammatory responses. Cell. 2012;151(1):138-52.
162. Huang SC, Everts B, Ivanova Y, O'Sullivan D, Nascimento M, Smith AM, et al. Cell-intrinsic lysosomal lipolysis is essential for alternative activation of macrophages. Nat Immunol. 2014;15(9):846-55.
163. Divakaruni AS, Hsieh WY, Minarrieta L, Duong TN, Kim KKO, Desousa BR, et al. Etomoxir Inhibits Macrophage Polarization by Disrupting CoA Homeostasis. Cell Metab. 2018;28(3):490-503.e7.
164. Mogilenko DA, Haas JT, L'Homme L, Fleury S, Quemener S, Levavasseur M, et al. Metabolic and Innate Immune Cues Merge into a Specific Inflammatory Response via the UPR. Cell. 2019;177(5):1201-16.e19.
165. Nomura M, Liu J, Rovira, II, Gonzalez-Hurtado E, Lee J, Wolfgang MJ, et al. Fatty acid oxidation in macrophage polarization. Nat Immunol. 2016;17(3):216-7.
166. Marcovecchio PM, Thomas GD, Mikulski Z, Ehinger E, Mueller KAL, Blatchley A, et al. Scavenger Receptor CD36 Directs Nonclassical Monocyte Patrolling Along the Endothelium During Early Atherogenesis. Arterioscler Thromb Vasc Biol. 2017;37(11):2043-52.
167. Febbraio M, Podrez EA, Smith JD, Hajjar DP, Hazen SL, Hoff HF, et al. Targeted disruption of the class B scavenger receptor CD36 protects against atherosclerotic lesion development in mice. J Clin Invest. 2000;105(8):1049-56.
168. Seimon TA, Nadolski MJ, Liao X, Magallon J, Nguyen M, Feric NT, et al. Atherogenic lipids and lipoproteins trigger CD36-TLR2-dependent apoptosis in macrophages undergoing endoplasmic reticulum stress. Cell Metab. 2010;12(5):467-82.
169. Kuchibhotla S, Vanegas D, Kennedy DJ, Guy E, Nimako G, Morton RE, et al. Absence of CD36 protects against atherosclerosis in ApoE knock-out mice with no additional protection provided by absence of scavenger receptor A I/II. Cardiovasc Res. 2008;78(1):185-96.
170. Sheedy FJ, Grebe A, Rayner KJ, Kalantari P, Ramkhelawon B, Carpenter SB, et al. CD36 coordinates NLRP3 inflammasome activation by facilitating intracellular nucleation of soluble ligands into particulate ligands in sterile inflammation. Nat Immunol. 2013;14(8):812-20.
171. Park YM, Febbraio M, Silverstein RL. CD36 modulates migration of mouse and human macrophages in response to oxidized LDL and may contribute to macrophage trapping in the arterial intima. J Clin Invest. 2009;119(1):136-45.

172. Gautier EL, Huby T, Saint-Charles F, Ouzilleau B, Pirault J, Deswaerte V, et al. Conventional dendritic cells at the crossroads between immunity and cholesterol homeostasis in atherosclerosis. Circulation. 2009;119(17):2367-75.
173. Birnberg T, Bar-On L, Sapoznikov A, Caton ML, Cervantes-Barragan L, Makia D, et al. Lack of conventional dendritic cells is compatible with normal development and T cell homeostasis, but causes myeloid proliferative syndrome. Immunity. 2008;29(6):986-97.
174. Paulson KE, Zhu SN, Chen M, Nurmohamed S, Jongstra-Bilen J, Cybulsky MI. Resident intimal dendritic cells accumulate lipid and contribute to the initiation of atherosclerosis. Circ Res. 2010;106(2):383-90.
175. Yun TJ, Lee JS, Machmach K, Shim D, Choi J, Wi YJ, et al. Indoleamine 2,3-Dioxygenase-Expressing Aortic Plasmacytoid Dendritic Cells Protect against Atherosclerosis by Induction of Regulatory T Cells. Cell Metab. 2016;23(5):852-66.
176. Macritchie N, Grassia G, Sabir SR, Maddaluno M, Welsh P, Sattar N, et al. Plasmacytoid dendritic cells play a key role in promoting atherosclerosis in apolipoprotein E-deficient mice. Arterioscler Thromb Vasc Biol. 2012;32(11):2569-79.
177. Doring Y, Manthey HD, Drechsler M, Lievens D, Megens RT, Soehnlein O, et al. Auto-antigenic protein-DNA complexes stimulate plasmacytoid dendritic cells to promote atherosclerosis. Circulation. 2012;125(13):1673-83.
178. Chen HJ, Tas SW, de Winther MPJ. Type-I interferons in atherosclerosis. J Exp Med. 2020;217(1):e20190459.
179. Daissormont IT, Christ A, Temmerman L, Sampedro Millares S, Seijkens T, Manca M, et al. Plasmacytoid dendritic cells protect against atherosclerosis by tuning T-cell proliferation and activity. Circ Res. 2011;109(12):1387-95.
180. Oh H, Mohler ER, 3rd, Tian A, Baumgart T, Diamond SL. Membrane cholesterol is a biomechanical regulator of neutrophil adhesion. Arterioscler Thromb Vasc Biol. 2009;29(9):1290-7.
181. Westerterp M, Fotakis P, Ouimet M, Bochem AE, Zhang H, Molusky MM, et al. Cholesterol Efflux Pathways Suppress Inflammasome Activation, NETosis, and Atherogenesis. Circulation. 2018;138(9):898-912.
182. Yvan-Charvet L, Ng LG. Granulopoiesis and Neutrophil Homeostasis: A Metabolic, Daily Balancing Act. Trends Immunol. 2019;40(7):598-612.
183. Yvan-Charvet L, Welch C, Pagler TA, Ranalletta M, Lamkanfi M, Han S, et al. Increased inflammatory gene expression in ABC transporter-deficient macrophages: free cholesterol accumulation, increased signaling via toll-like receptors, and neutrophil infiltration of atherosclerotic lesions. Circulation. 2008;118(18):1837-47.
184. Guasti L, Dentali F, Castiglioni L, Maroni L, Marino F, Squizzato A, et al. Neutrophils and clinical outcomes in patients with acute coronary syndromes and/or cardiac revascularisation. A systematic review on more than 34,000 subjects. Thromb Haemost. 2011;106(4):591-9.
185. Milligan G, Alvarez-Curto E, Hudson BD, Prihandoko R, Tobin AB. FFA4/GPR120: Pharmacology and Therapeutic Opportunities. Trends Pharmacol Sci. 2017;38(9):809-21.

186. Williams JW, Martel C, Potteaux S, Esaulova E, Ingersoll MA, Elvington A, et al. Limited Macrophage Positional Dynamics in Progressing or Regressing Murine Atherosclerotic Plaques-Brief Report. Arterioscler Thromb Vasc Biol. 2018;38(8):1702-10.
187. Ross S, Gerstein HC, Eikelboom J, Anand SS, Yusuf S, Pare G. Mendelian randomization analysis supports the causal role of dysglycaemia and diabetes in the risk of coronary artery disease. Eur Heart J. 2015;36(23):1454-62.
188. Ahmad OS, Morris JA, Mujammami M, Forgetta V, Leong A, Li R, et al. A Mendelian randomization study of the effect of type-2 diabetes on coronary heart disease. Nat Commun. 2015;6:7060.
189. Emami H, Singh P, MacNabb M, Vucic E, Lavender Z, Rudd JH, et al. Splenic metabolic activity predicts risk of future cardiovascular events: demonstration of a cardiosplenic axis in humans. JACC Cardiovasc Imaging. 2015;8(2):121-30.
190. Oburoglu L, Tardito S, Fritz V, de Barros SC, Merida P, Craveiro M, et al. Glucose and glutamine metabolism regulate human hematopoietic stem cell lineage specification. Cell Stem Cell. 2014;15(2):169-84.
191. Sarrazy V, Viaud M, Westerterp M, Ivanov S, Giorgetti-Peraldi S, Guinamard R, et al. Disruption of Glut1 in Hematopoietic Stem Cells Prevents Myelopoiesis and Enhanced Glucose Flux in Atheromatous Plaques of ApoE(−/−) Mice. Circ Res. 2016;118(7):1062-77.
192. Nagareddy PR, Murphy AJ, Stirzaker RA, Hu Y, Yu S, Miller RG, et al. Hyperglycemia promotes myelopoiesis and impairs the resolution of atherosclerosis. Cell Metab. 2013;17(5):695-708.
193. van der Valk FM, Kuijk C, Verweij SL, Stiekema LCA, Kaiser Y, Zeerleder S, et al. Increased haematopoietic activity in patients with atherosclerosis. Eur Heart J. 2017;38(6):425-32.
194. Freemerman AJ, Zhao L, Pingili AK, Teng B, Cozzo AJ, Fuller AM, et al. Myeloid Slc2a1-Deficient Murine Model Revealed Macrophage Activation and Metabolic Phenotype Are Fueled by GLUT1. J Immunol. 2019;202(4):1265-86.
195. Morioka S, Perry JSA, Raymond MH, Medina CB, Zhu Y, Zhao L, et al. Efferocytosis induces a novel SLC program to promote glucose uptake and lactate release. Nature. 2018;563(7733):714-8.
196. Fukuzumi M, Shinomiya H, Shimizu Y, Ohishi K, Utsumi S. Endotoxin-induced enhancement of glucose influx into murine peritoneal macrophages via GLUT1. Infect Immun. 1996;64(1):108-12.
197. Huang SC, Smith AM, Everts B, Colonna M, Pearce EL, Schilling JD, et al. Metabolic Reprogramming Mediated by the mTORC2-IRF4 Signaling Axis Is Essential for Macrophage Alternative Activation. Immunity. 2016;45(4):817-30.
198. Covarrubias AJ, Aksoylar HI, Yu J, Snyder NW, Worth AJ, Iyer SS, et al. Akt-mTORC1 signaling regulates Acly to integrate metabolic input to control of macrophage activation. Elife. 2016;5:e11612.
199. Namgaladze D, Zukunft S, Schnutgen F, Kurrle N, Fleming I, Fuhrmann D, et al. Polarization of Human Macrophages by Interleukin-4 Does Not Require ATP-Citrate Lyase. Front Immunol. 2018;9:2858.

200. Folco EJ, Sheikine Y, Rocha VZ, Christen T, Shvartz E, Sukhova GK, et al. Hypoxia but not inflammation augments glucose uptake in human macrophages: Implications for imaging atherosclerosis with ^{18}fluorine-labeled 2-deoxy-D-glucose positron emission tomography. J Am Coll Cardiol. 2011;58(6):603-14.
201. Sluimer JC, Gasc JM, van Wanroij JL, Kisters N, Groeneweg M, Sollewijn Gelpke MD, et al. Hypoxia, hypoxia-inducible transcription factor, and macrophages in human atherosclerotic plaques are correlated with intraplaque angiogenesis. J Am Coll Cardiol. 2008;51(13):1258-65.
202. Bjornheden T, Levin M, Evaldsson M, Wiklund O. Evidence of hypoxic areas within the arterial wall in vivo. Arterioscler Thromb Vasc Biol. 1999;19(4):870-6.
203. Vink A, Schoneveld AH, Lamers D, Houben AJ, van der Groep P, van Diest PJ, et al. HIF-1 alpha expression is associated with an atheromatous inflammatory plaque phenotype and upregulated in activated macrophages. Atherosclerosis. 2007;195(2):e69-75.
204. Parathath S, Mick SL, Feig JE, Joaquin V, Grauer L, Habiel DM, et al. Hypoxia is present in murine atherosclerotic plaques and has multiple adverse effects on macrophage lipid metabolism. Circ Res. 2011;109(10):1141-52.
205. Chaudhari SM, Sluimer JC, Koch M, Theelen TL, Manthey HD, Busch M, et al. Deficiency of HIF1alpha in Antigen-Presenting Cells Aggravates Atherosclerosis and Type 1 T-Helper Cell Responses in Mice. Arterioscler Thromb Vasc Biol. 2015;35(11):2316-25.
206. Aarup A, Pedersen TX, Junker N, Christoffersen C, Bartels ED, Madsen M, et al. Hypoxia-Inducible Factor-1alpha Expression in Macrophages Promotes Development of Atherosclerosis. Arterioscler Thromb Vasc Biol. 2016;36(9):1782-90.
207. Haschemi A, Kosma P, Gille L, Evans CR, Burant CF, Starkl P, et al. The sedoheptulose kinase CARKL directs macrophage polarization through control of glucose metabolism. Cell Metab. 2012;15(6):813-26.
208. Robbins CS, Hilgendorf I, Weber GF, Theurl I, Iwamoto Y, Figueiredo JL, et al. Local proliferation dominates lesional macrophage accumulation in atherosclerosis. Nat Med. 2013;19(9):1166-72.
209. Van den Bossche J, Baardman J, Otto NA, van der Velden S, Neele AE, van den Berg SM, et al. Mitochondrial Dysfunction Prevents Repolarization of Inflammatory Macrophages. Cell Rep. 2016;17(3):684-96.
210. Krawczyk CM, Holowka T, Sun J, Blagih J, Amiel E, DeBerardinis RJ, et al. Toll-like receptor-induced changes in glycolytic metabolism regulate dendritic cell activation. Blood. 2010;115(23):4742-9.
211. Everts B, Amiel E, van der Windt GJ, Freitas TC, Chott R, Yarasheski KE, et al. Commitment to glycolysis sustains survival of NO-producing inflammatory dendritic cells. Blood. 2012;120(7):1422-31.
212. Amiel E, Everts B, Fritz D, Beauchamp S, Ge B, Pearce EL, et al. Mechanistic target of rapamycin inhibition extends cellular lifespan in dendritic cells by preserving mitochondrial function. J Immunol. 2014;193(6):2821-30.
213. Thwe PM, Pelgrom LR, Cooper R, Beauchamp S, Reisz JA, D'Alessandro A, et al. Cell-Intrinsic Glycogen Metabolism Supports Early Glycolytic

Reprogramming Required for Dendritic Cell Immune Responses. Cell Metab. 2017;26(3):558-67.e5.

214. Lu H, Yao K, Huang D, Sun A, Zou Y, Qian J, et al. High glucose induces upregulation of scavenger receptors and promotes maturation of dendritic cells. Cardiovasc Diabetol. 2013;12:80.
215. Borregaard N, Herlin T. Energy metabolism of human neutrophils during phagocytosis. J Clin Invest. 1982;70(3):550-7.
216. Riffelmacher T, Clarke A, Richter FC, Stranks A, Pandey S, Danielli S, et al. Autophagy-Dependent Generation of Free Fatty Acids Is Critical for Normal Neutrophil Differentiation. Immunity. 2017;47(3):466-80.e5.
217. Rodriguez-Espinosa O, Rojas-Espinosa O, Moreno-Altamirano MM, Lopez-Villegas EO, Sanchez-Garcia FJ. Metabolic requirements for neutrophil extracellular traps formation. Immunology. 2015;145(2):213-24.
218. Jha AK, Huang SC, Sergushichev A, Lampropoulou V, Ivanova Y, Loginicheva E, et al. Network integration of parallel metabolic and transcriptional data reveals metabolic modules that regulate macrophage polarization. Immunity. 2015;42(3):419-30.
219. Liu PS, Wang H, Li X, Chao T, Teav T, Christen S, et al. alpha-ketoglutarate orchestrates macrophage activation through metabolic and epigenetic reprogramming. Nat Immunol. 2017;18(9):985-94.
220. Tavakoli S, Downs K, Short JD, Nguyen HN, Lai Y, Jerabek PA, et al. Characterization of Macrophage Polarization States Using Combined Measurement of 2-Deoxyglucose and Glutamine Accumulation: Implications for Imaging of Atherosclerosis. Arterioscler Thromb Vasc Biol. 2017;37(10):1840-8.
221. Sonoki T, Nagasaki A, Gotoh T, Takiguchi M, Takeya M, Matsuzaki H, et al. Coinduction of nitric-oxide synthase and arginase I in cultured rat peritoneal macrophages and rat tissues in vivo by lipopolysaccharide. J Biol Chem. 1997;272(6):3689-93.
222. Ren B, Van Kampen E, Van Berkel TJ, Cruickshank SM, Van Eck M. Hematopoietic arginase 1 deficiency results in decreased leukocytosis and increased foam cell formation but does not affect atherosclerosis. Atherosclerosis. 2017;256:35-46.
223. Kierszenbaum F, Wirth JJ, McCann PP, Sjoerdsma A. Impairment of macrophage function by inhibitors of ornithine decarboxylase activity. Infect Immun. 1987;55(10):2461-4.
224. Tarasenko TN, Singh LN, Chatterji-Len M, Zerfas PM, Cusmano-Ozog K, McGuire PJ. Kupffer cells modulate hepatic fatty acid oxidation during infection with PR8 influenza. Biochim Biophys Acta. 2015;1852(11):2391-401.
225. Yurdagul A, Jr., Subramanian M, Wang X, Crown SB, Ilkayeva OR, Darville L, et al. Macrophage Metabolism of Apoptotic Cell-Derived Arginine Promotes Continual Efferocytosis and Resolution of Injury. Cell Metab. 2020;31(3):518-33.e10.
226. Ponnuswamy P, Ostermeier E, Schrottle A, Chen J, Huang PL, Ertl G, et al. Oxidative stress and compartment of gene expression determine

proatherosclerotic effects of inducible nitric oxide synthase. Am J Pathol. 2009;174(6):2400-10.

227. Everts B, Amiel E, Huang SC, Smith AM, Chang CH, Lam WY, et al. TLR-driven early glycolytic reprogramming via the kinases TBK1-IKKvarepsilon supports the anabolic demands of dendritic cell activation. Nat Immunol. 2014;15(4):323-32.
228. Guak H, Al Habyan S, Ma EH, Aldossary H, Al-Masri M, Won SY, et al. Glycolytic metabolism is essential for CCR7 oligomerization and dendritic cell migration. Nat Commun. 2018;9(1):2463.
229. Liu J, Zhang X, Chen K, Cheng Y, Liu S, Xia M, et al. CCR7 Chemokine Receptor-Inducible lnc-Dpf3 Restrains Dendritic Cell Migration by Inhibiting HIF-1alpha-Mediated Glycolysis. Immunity. 2019;50(3):600-15.e15.
230. Luchtefeld M, Grothusen C, Gagalick A, Jagavelu K, Schuett H, Tietge UJ, et al. Chemokine receptor 7 knockout attenuates atherosclerotic plaque development. Circulation. 2010;122(16):1621-8.
231. Potteaux S, Gautier EL, Hutchison SB, van Rooijen N, Rader DJ, Thomas MJ, et al. Suppressed monocyte recruitment drives macrophage removal from atherosclerotic plaques of Apoe$^{-/-}$ mice during disease regression. J Clin Invest. 2011;121(5):2025-36.
232. Wan W, Lionakis MS, Liu Q, Roffe E, Murphy PM. Genetic deletion of chemokine receptor Ccr7 exacerbates atherogenesis in ApoE-deficient mice. Cardiovasc Res. 2013;97(3):580-8.
233. Miller A, Nagy C, Knapp B, Laengle J, Ponweiser E, Groeger M, et al. Exploring Metabolic Configurations of Single Cells within Complex Tissue Microenvironments. Cell Metab. 2017;26(5):788-800.e6.

How to cite this article:
Gallerand A, Stunault MI, Merlin J, Guinamard RR, Yvan-Charvet L, Ivanov S. Myeloid Cell Diversity and Impact of Metabolic Cues during Atherosclerosis. Immunometabolism. 2020;2(4):e200028. https://doi.org/10.20900/immunometab20200028

Références bibliographiques

(1994). Randomised trial of cholesterol lowering in 4444 patients with coronary heart disease: the Scandinavian Simvastatin Survival Study (4S). Lancet *344*, 1383-1389.

Ahmadian, M., Duncan, R.E., Jaworski, K., Sarkadi-Nagy, E., and Sul, H.S. (2007). Triacylglycerol metabolism in adipose tissue. Future Lipidol *2*, 229-237.

Akakura, S., Singh, S., Spataro, M., Akakura, R., Kim, J.I., Albert, M.L., and Birge, R.B. (2004). The opsonin MFG-E8 is a ligand for the alphavbeta5 integrin and triggers DOCK180-dependent Rac1 activation for the phagocytosis of apoptotic cells. Exp Cell Res *292*, 403-416.

Aktan, F. (2004). iNOS-mediated nitric oxide production and its regulation. Life Sci *75*, 639-653.

Albers, A., Broer, A., Wagner, C.A., Setiawan, I., Lang, P.A., Kranz, E.U., Lang, F., and Broer, S. (2001). Na+ transport by the neural glutamine transporter ATA1. Pflugers Arch *443*, 92-101.

Albert, M.L., Kim, J.I., and Birge, R.B. (2000). alphavbeta5 integrin recruits the CrkII-Dock180-rac1 complex for phagocytosis of apoptotic cells. Nat Cell Biol *2*, 899-905.

Alberti, K.G., Eckel, R.H., Grundy, S.M., Zimmet, P.Z., Cleeman, J.I., Donato, K.A., Fruchart, J.C., James, W.P., Loria, C.M., Smith, S.C., Jr*., et al.* (2009). Harmonizing the metabolic syndrome: a joint interim statement of the International Diabetes Federation Task Force on Epidemiology and Prevention; National Heart, Lung, and Blood Institute; American Heart Association; World Heart Federation; International Atherosclerosis Society; and International Association for the Study of Obesity. Circulation *120*, 1640-1645.

Alberts, A.W. (1988). Discovery, biochemistry and biology of lovastatin. Am J Cardiol *62*, 10J-15J.

Aledo, J.C., Gomez-Fabre, P.M., Olalla, L., and Marquez, J. (2000). Identification of two human glutaminase loci and tissue-specific expression of the two related genes. Mamm Genome *11*, 1107-1110.

Altman, B.J., Stine, Z.E., and Dang, C.V. (2016). From Krebs to clinic: glutamine metabolism to cancer therapy. Nat Rev Cancer *16*, 619-634.

Amano, S.U., Cohen, J.L., Vangala, P., Tencerova, M., Nicoloro, S.M., Yawe, J.C., Shen, Y., Czech, M.P., and Aouadi, M. (2014). Local proliferation of macrophages contributes to obesity-associated adipose tissue inflammation. Cell Metab *19*, 162-171.

Amaral, J.S., Pinho, M.J., and Soares-da-Silva, P. (2008). Genomic regulation of intestinal amino acid transporters by aldosterone. Mol Cell Biochem *313*, 1-10.

Ameer, F., Scandiuzzi, L., Hasnain, S., Kalbacher, H., and Zaidi, N. (2014). De novo lipogenesis in health and disease. Metabolism *63*, 895-902.

An, Z., Li, J., Yu, J., Wang, X., Gao, H., Zhang, W., Wei, Z., Zhang, J., Zhang, Y., Zhao, J.*, et al.* (2019). Neutrophil extracellular traps induced by IL-8 aggravate atherosclerosis via activation NF-kappaB signaling in macrophages. Cell Cycle *18*, 2928-2938.

Anunciado-Koza, R., Ukropec, J., Koza, R.A., and Kozak, L.P. (2008). Inactivation of UCP1 and the glycerol phosphate cycle synergistically increases energy expenditure to resist diet-induced obesity. J Biol Chem *283*, 27688-27697.

Aouadi, M., Tencerova, M., Vangala, P., Yawe, J.C., Nicoloro, S.M., Amano, S.U., Cohen, J.L., and Czech, M.P. (2013). Gene silencing in adipose tissue macrophages regulates whole-body metabolism in obese mice. Proc Natl Acad Sci U S A *110*, 8278-8283.

Arai, S., Shelton, J.M., Chen, M., Bradley, M.N., Castrillo, A., Bookout, A.L., Mak, P.A., Edwards, P.A., Mangelsdorf, D.J., Tontonoz, P.*, et al.* (2005). A role for the apoptosis inhibitory factor AIM/Spalpha/Api6 in atherosclerosis development. Cell Metab *1*, 201-213.

Auffray, C., Fogg, D., Garfa, M., Elain, G., Join-Lambert, O., Kayal, S., Sarnacki, S., Cumano, A., Lauvau, G., and Geissmann, F. (2007). Monitoring of blood vessels and tissues by a population of monocytes with patrolling behavior. Science *317*, 666-670.

Baardman, J., and Lutgens, E. (2020). Regulatory T Cell Metabolism in Atherosclerosis. Metabolites *10*.

Badimon, L., Vilahur, G., and Padro, T. (2009). Lipoproteins, platelets and atherothrombosis. Rev Esp Cardiol *62*, 1161-1178.

Bae, Y.S., Lee, J.H., Choi, S.H., Kim, S., Almazan, F., Witztum, J.L., and Miller, Y.I. (2009). Macrophages generate reactive oxygen species in response to minimally oxidized low-density lipoprotein: toll-like receptor 4- and spleen tyrosine kinase-dependent activation of NADPH oxidase 2. Circ Res *104*, 210-218, 221p following 218.

Bailes, B.K. (2002). Diabetes mellitus and its chronic complications. AORN J *76*, 266-276, 278-282; quiz 283-266.

Bak, L.K., Schousboe, A., and Waagepetersen, H.S. (2006). The glutamate/GABA-glutamine cycle: aspects of transport, neurotransmitter homeostasis and ammonia transfer. J Neurochem *98*, 641-653.

Bakalar, B., Duska, F., Pachl, J., Fric, M., Otahal, M., Pazout, J., and Andel, M. (2006). Parenterally administered dipeptide alanyl-glutamine prevents worsening of insulin sensitivity in multiple-trauma patients. Crit Care Med *34*, 381-386.

Barreau, C., Labit, E., Guissard, C., Rouquette, J., Boizeau, M.L., Gani Koumassi, S., Carriere, A., Jeanson, Y., Berger-Muller, S., Dromard, C.*, et al.* (2016). Regionalization of browning revealed by whole subcutaneous adipose tissue imaging. Obesity (Silver Spring) *24*, 1081-1089.

Barreby, E., Sulen, A., and Aouadi, M. (2019). Glucan-Encapsulated siRNA Particles (GeRPs) for Specific Gene Silencing in Adipose Tissue Macrophages. Methods Mol Biol *1951*, 49-57.

Bartness TJ, S.C. (2005). Innervation of brown adipose tissue and its role in thermogenesis. Can J Diabetes *29*, 420–428.

Basu, D., and Goldberg, I.J. (2020). Regulation of lipoprotein lipase-mediated lipolysis of triglycerides. Curr Opin Lipidol *31*, 154-160.

Bennett, C.L., Djulbegovic, B., Norris, L.B., and Armitage, J.O. (2013). Colony-stimulating factors for febrile neutropenia during cancer therapy. N Engl J Med *368*, 1131-1139.

Berg, A.H., Combs, T.P., Du, X., Brownlee, M., and Scherer, P.E. (2001). The adipocyte-secreted protein Acrp30 enhances hepatic insulin action. Nat Med *7*, 947-953.

Berger, M.M., and Pantet, O. (2016). Nutrition in burn injury: any recent changes? Curr Opin Crit Care *22*, 285-291.

Bernstein, D.L., Hulkova, H., Bialer, M.G., and Desnick, R.J. (2013). Cholesteryl ester storage disease: review of the findings in 135 reported patients with an underdiagnosed disease. J Hepatol *58*, 1230-1243.

Bertholet, A.M., Kazak, L., Chouchani, E.T., Bogaczynska, M.G., Paranjpe, I., Wainwright, G.L., Betourne, A., Kajimura, S., Spiegelman, B.M., and Kirichok, Y. (2017). Mitochondrial Patch Clamp of Beige Adipocytes Reveals UCP1-Positive and UCP1-Negative Cells Both Exhibiting Futile Creatine Cycling. Cell Metab *25*, 811-822 e814.

Bigornia, S.J., Farb, M.G., Mott, M.M., Hess, D.T., Carmine, B., Fiscale, A., Joseph, L., Apovian, C.M., and Gokce, N. (2012). Relation of depot-specific adipose inflammation to insulin resistance in human obesity. Nutr Diabetes *2*, e30.

Birsoy, K., Wang, T., Chen, W.W., Freinkman, E., Abu-Remaileh, M., and Sabatini, D.M. (2015). An Essential Role of the Mitochondrial Electron Transport Chain in Cell Proliferation Is to Enable Aspartate Synthesis. Cell *162*, 540-551.

Biswas, S.K., and Mantovani, A. (2010). Macrophage plasticity and interaction with lymphocyte subsets: cancer as a paradigm. Nat Immunol *11*, 889-896.

Bittner, V.A., Szarek, M., Aylward, P.E., Bhatt, D.L., Diaz, R., Edelberg, J.M., Fras, Z., Goodman, S.G., Halvorsen, S., Hanotin, C*., et al.* (2020). Effect of Alirocumab on Lipoprotein(a) and Cardiovascular Risk After Acute Coronary Syndrome. J Am Coll Cardiol *75*, 133-144.

Bjorklund, M.M., Hollensen, A.K., Hagensen, M.K., Dagnaes-Hansen, F., Christoffersen, C., Mikkelsen, J.G., and Bentzon, J.F. (2014). Induction of atherosclerosis in mice and hamsters without germline genetic engineering. Circ Res *114*, 1684-1689.

Bjorntorp, P., and Sjostrom, L. (1978). Carbohydrate storage in man: speculations and some quantitative considerations. Metabolism *27*, 1853-1865.

Bleriot, C., Chakarov, S., and Ginhoux, F. (2020). Determinants of Resident Tissue Macrophage Identity and Function. Immunity *52*, 957-970.

Blomqvist, B.I., Hammarqvist, F., von der Decken, A., and Wernerman, J. (1995). Glutamine and alpha-ketoglutarate prevent the decrease in muscle free glutamine concentration and influence protein synthesis after total hip replacement. Metabolism *44*, 1215-1222.

Bode, B.P. (2001). Recent molecular advances in mammalian glutamine transport. J Nutr *131*, 2475S-2485S; discussion 2486S-2477S.

Bogdanis, G.C., Nevill, M.E., Boobis, L.H., and Lakomy, H.K. (1996). Contribution of phosphocreatine and aerobic metabolism to energy supply during repeated sprint exercise. J Appl Physiol (1985) *80*, 876-884.

Bohmer, C., Broer, A., Munzinger, M., Kowalczuk, S., Rasko, J.E., Lang, F., and Broer, S. (2005). Characterization of mouse amino acid transporter B0AT1 (slc6a19). Biochem J *389*, 745-751.

Bolsoni-Lopes, A., and Alonso-Vale, M.I. (2015). Lipolysis and lipases in white adipose tissue - An update. Arch Endocrinol Metab *59*, 335-342.

Bongers, T., Griffiths, R.D., and McArdle, A. (2007). Exogenous glutamine: the clinical evidence. Crit Care Med *35*, S545-552.

Born GVR, S.G. (1997). Vascular endothelium. Physiology, pathology and therapeutic opportunities. GVR Born and G Schwartz Eds.

Bornstein, S.R., Abu-Asab, M., Glasow, A., Path, G., Hauner, H., Tsokos, M., Chrousos, G.P., and Scherbaum, W.A. (2000). Immunohistochemical and ultrastructural localization of leptin and leptin receptor in human white adipose tissue and differentiating human adipose cells in primary culture. Diabetes *49*, 532-538.

Boyle, J.J., Johns, M., Kampfer, T., Nguyen, A.T., Game, L., Schaer, D.J., Mason, J.C., and Haskard, D.O. (2012). Activating transcription factor 1 directs Mhem atheroprotective macrophages through coordinated iron handling and foam cell protection. Circ Res *110*, 20-33.

Broer, A., Brookes, N., Ganapathy, V., Dimmer, K.S., Wagner, C.A., Lang, F., and Broer, S. (1999). The astroglial ASCT2 amino acid transporter as a mediator of glutamine efflux. J Neurochem *73*, 2184-2194.

Broer, A., Juelich, T., Vanslambrouck, J.M., Tietze, N., Solomon, P.S., Holst, J., Bailey, C.G., Rasko, J.E., and Broer, S. (2011). Impaired nutrient signaling and body weight control in a Na+ neutral amino acid cotransporter (Slc6a19)-deficient mouse. J Biol Chem *286*, 26638-26651.

Broer, S. (2006). The SLC6 orphans are forming a family of amino acid transporters. Neurochem Int *48*, 559-567.

Broer, S. (2008). Apical transporters for neutral amino acids: physiology and pathophysiology. Physiology (Bethesda) *23*, 95-103.

Broer, S. (2014). The SLC38 family of sodium-amino acid co-transporters. Pflugers Arch *466*, 155-172.

Brown, G., Singer, A., Proudfoot, M., Skarina, T., Kim, Y., Chang, C., Dementieva, I., Kuznetsova, E., Gonzalez, C.F., Joachimiak, A*., et al.* (2008). Functional and structural characterization of four glutaminases from Escherichia coli and Bacillus subtilis. Biochemistry *47*, 5724-5735.

Brown, S., Heinisch, I., Ross, E., Shaw, K., Buckley, C.D., and Savill, J. (2002). Apoptosis disables CD31-mediated cell detachment from phagocytes promoting binding and engulfment. Nature *418*, 200-203.

Buchholz, A.C., and Bugaresti, J.M. (2005). A review of body mass index and waist circumference as markers of obesity and coronary heart disease risk in persons with chronic spinal cord injury. Spinal Cord *43*, 513-518.

Busch, K., Klapproth, K., Barile, M., Flossdorf, M., Holland-Letz, T., Schlenner, S.M., Reth, M., Hofer, T., and Rodewald, H.R. (2015). Fundamental properties of unperturbed haematopoiesis from stem cells in vivo. Nature *518*, 542-546.

Busque, S.M., and Wagner, C.A. (2009). Potassium restriction, high protein intake, and metabolic acidosis increase expression of the glutamine transporter SNAT3 (Slc38a3) in mouse kidney. Am J Physiol Renal Physiol *297*, F440-450.

Butkinaree, C., Park, K., and Hart, G.W. (2010). O-linked beta-N-acetylglucosamine (O-GlcNAc): Extensive crosstalk with phosphorylation to regulate signaling and transcription in response to nutrients and stress. Biochim Biophys Acta *1800*, 96-106.

Cai, B., Thorp, E.B., Doran, A.C., Sansbury, B.E., Daemen, M.J., Dorweiler, B., Spite, M., Fredman, G., and Tabas, I. (2017). MerTK receptor cleavage promotes plaque necrosis and defective resolution in atherosclerosis. J Clin Invest *127*, 564-568.

Camell, C.D., Sander, J., Spadaro, O., Lee, A., Nguyen, K.Y., Wing, A., Goldberg, E.L., Youm, Y.H., Brown, C.W., Elsworth, J*., et al.* (2017). Inflammasome-driven catecholamine catabolism in macrophages blunts lipolysis during ageing. Nature *550*, 119-123.

Campbell, J.H., and Campbell, G.R. (1994). Cell biology of atherosclerosis. J Hypertens Suppl *12*, S129-132.

Campos-Sandoval, J.A., Lopez de la Oliva, A.R., Lobo, C., Segura, J.A., Mates, J.M., Alonso, F.J., and Marquez, J. (2007). Expression of functional human glutaminase in baculovirus system: affinity purification, kinetic and molecular characterization. Int J Biochem Cell Biol *39*, 765-773.

Campos-Sandoval, J.A., Martin-Rufián, M. & Márquez, J. (2019). GLS (Glutaminase). Atlas Genet Cytogenet Oncol Haematol.

Cannon, C.P., Blazing, M.A., Giugliano, R.P., McCagg, A., White, J.A., Theroux, P., Darius, H., Lewis, B.S., Ophuis, T.O., Jukema, J.W*., et al.* (2015). Ezetimibe Added to Statin Therapy after Acute Coronary Syndromes. N Engl J Med *372*, 2387-2397.

Cannon, C.P., Braunwald, E., McCabe, C.H., Rader, D.J., Rouleau, J.L., Belder, R., Joyal, S.V., Hill, K.A., Pfeffer, M.A., Skene, A.M*., et al.* (2004). Intensive versus moderate lipid lowering with statins after acute coronary syndromes. N Engl J Med *350*, 1495-1504.

Caputa, G., Castoldi, A., and Pearce, E.J. (2019). Metabolic adaptations of tissue-resident immune cells. Nat Immunol *20*, 793-801.

Cardona, C., Sanchez-Mejias, E., Davila, J.C., Martin-Rufian, M., Campos-Sandoval, J.A., Vitorica, J., Alonso, F.J., Mates, J.M., Segura, J.A., Norenberg, M.D*., et al.* (2015). Expression of Gls and Gls2 glutaminase isoforms in astrocytes. Glia *63*, 365-382.

Carey, B.W., Finley, L.W., Cross, J.R., Allis, C.D., and Thompson, C.B. (2015). Intracellular alpha-ketoglutarate maintains the pluripotency of embryonic stem cells. Nature *518*, 413-416.

Carlin, L.M., Stamatiades, E.G., Auffray, C., Hanna, R.N., Glover, L., Vizcay-Barrena, G., Hedrick, C.C., Cook, H.T., Diebold, S., and Geissmann, F. (2013). Nr4a1-dependent Ly6C(low) monocytes monitor endothelial cells and orchestrate their disposal. Cell *153*, 362-375.

Carmena, R. (2019). Primary Mixed Dyslipidemias - Encyclopedia of Endocrine Diseases. Elsevier *1*, 314-319.

Carr, E.L., Kelman, A., Wu, G.S., Gopaul, R., Senkevitch, E., Aghvanyan, A., Turay, A.M., and Frauwirth, K.A. (2010). Glutamine uptake and metabolism are coordinately regulated by ERK/MAPK during T lymphocyte activation. J Immunol *185*, 1037-1044.

Cecchini, M.G., Dominguez, M.G., Mocci, S., Wetterwald, A., Felix, R., Fleisch, H., Chisholm, O., Hofstetter, W., Pollard, J.W., and Stanley, E.R. (1994). Role of colony stimulating factor-1 in the establishment and regulation of tissue macrophages during postnatal development of the mouse. Development *120*, 1357-1372.

Chan, J., Karere, G. M., Cox, L. A., & VandeBerg, J. L (2015). Animal Models of Diet-induced Hypercholesterolemia. Hypercholesterolemia.

Chang, M.K., Bergmark, C., Laurila, A., Horkko, S., Han, K.H., Friedman, P., Dennis, E.A., and Witztum, J.L. (1999). Monoclonal antibodies against oxidized low-density lipoprotein bind to apoptotic cells and inhibit their phagocytosis by elicited macrophages: evidence that oxidation-specific epitopes mediate macrophage recognition. Proc Natl Acad Sci U S A *96*, 6353-6358.

Chaudhry, F.A., Reimer, R.J., Krizaj, D., Barber, D., Storm-Mathisen, J., Copenhagen, D.R., and Edwards, R.H. (1999). Molecular analysis of system N suggests novel physiological roles in nitrogen metabolism and synaptic transmission. Cell *99*, 769-780.

Chaudhry, F.A., Schmitz, D., Reimer, R.J., Larsson, P., Gray, A.T., Nicoll, R., Kavanaugh, M., and Edwards, R.H. (2002). Glutamine uptake by neurons: interaction of protons with system a transporters. J Neurosci *22*, 62-72.

Chechi, K., Nedergaard, J., and Richard, D. (2014). Brown adipose tissue as an anti-obesity tissue in humans. Obes Rev *15*, 92-106.

Chen, H., Charlat, O., Tartaglia, L.A., Woolf, E.A., Weng, X., Ellis, S.J., Lakey, N.D., Culpepper, J., Moore, K.J., Breitbart, R.E*., et al.* (1996). Evidence that the diabetes gene encodes the leptin receptor: identification of a mutation in the leptin receptor gene in db/db mice. Cell *84*, 491-495.

Chen, Y., Pan, R., and Pfeifer, A. (2016). Fat tissues, the brite and the dark sides. Pflugers Arch *468*, 1803-1807.

Cheng, S., Rhee, E.P., Larson, M.G., Lewis, G.D., McCabe, E.L., Shen, D., Palma, M.J., Roberts, L.D., Dejam, A., Souza, A.L*., et al.* (2012). Metabolite profiling identifies pathways associated with metabolic risk in humans. Circulation *125*, 2222-2231.

Cheruvu, P.K., Finn, A.V., Gardner, C., Caplan, J., Goldstein, J., Stone, G.W., Virmani, R., and Muller, J.E. (2007). Frequency and distribution of thin-cap fibroatheroma and ruptured plaques in human coronary arteries: a pathologic study. J Am Coll Cardiol *50*, 940-949.

Chiaradonna, F., Ricciardiello, F., and Palorini, R. (2018). The Nutrient-Sensing Hexosamine Biosynthetic Pathway as the Hub of Cancer Metabolic Rewiring. Cells *7*.

Chinetti-Gbaguidi, G., Baron, M., Bouhlel, M.A., Vanhoutte, J., Copin, C., Sebti, Y., Derudas, B., Mayi, T., Bories, G., Tailleux, A*., et al.* (2011). Human atherosclerotic plaque alternative macrophages display low cholesterol handling but high phagocytosis because of distinct activities of the PPARgamma and LXRalpha pathways. Circ Res *108*, 985-995.

Chistiakov, D.A., Bobryshev, Y.V., Nikiforov, N.G., Elizova, N.V., Sobenin, I.A., and Orekhov, A.N. (2015). Macrophage phenotypic plasticity in atherosclerosis: The associated features and the peculiarities of the expression of inflammatory genes. Int J Cardiol *184*, 436-445.

Cinti, S., Mitchell, G., Barbatelli, G., Murano, I., Ceresi, E., Faloia, E., Wang, S., Fortier, M., Greenberg, A.S., and Obin, M.S. (2005). Adipocyte death defines macrophage localization and function in adipose tissue of obese mice and humans. J Lipid Res *46*, 2347-2355.

Cochain, C., Vafadarnejad, E., Arampatzi, P., Pelisek, J., Winkels, H., Ley, K., Wolf, D., Saliba, A.E., and Zernecke, A. (2018). Single-Cell RNA-Seq Reveals the Transcriptional Landscape and Heterogeneity of Aortic Macrophages in Murine Atherosclerosis. Circ Res *122*, 1661-1674.

Cole, J.E., Park, I., Ahern, D.J., Kassiteridi, C., Danso Abeam, D., Goddard, M.E., Green, P., Maffia, P., and Monaco, C. (2018). Immune cell census in murine atherosclerosis: cytometry by time of flight illuminates vascular myeloid cell diversity. Cardiovasc Res *114*, 1360-1371.

Colin, S., Chinetti-Gbaguidi, G., and Staels, B. (2014). Macrophage phenotypes in atherosclerosis. Immunol Rev *262*, 153-166.

Collins, R.G., Velji, R., Guevara, N.V., Hicks, M.J., Chan, L., and Beaudet, A.L. (2000). P-Selectin or intercellular adhesion molecule (ICAM)-1 deficiency substantially protects against atherosclerosis in apolipoprotein E-deficient mice. J Exp Med *191*, 189-194.

Colombo, S.L., Palacios-Callender, M., Frakich, N., Carcamo, S., Kovacs, I., Tudzarova, S., and Moncada, S. (2011). Molecular basis for the differential use of glucose and glutamine in cell proliferation as revealed by synchronized HeLa cells. Proc Natl Acad Sci U S A *108*, 21069-21074.

Combadiere, C., Potteaux, S., Rodero, M., Simon, T., Pezard, A., Esposito, B., Merval, R., Proudfoot, A., Tedgui, A., and Mallat, Z. (2008). Combined inhibition of CCL2, CX3CR1, and CCR5 abrogates Ly6C(hi) and Ly6C(lo) monocytosis and almost abolishes atherosclerosis in hypercholesterolemic mice. Circulation *117*, 1649-1657.

Cordeiro Gomes, A., Hara, T., Lim, V.Y., Herndler-Brandstetter, D., Nevius, E., Sugiyama, T., Tani-Ichi, S., Schlenner, S., Richie, E., Rodewald, H.R.*, et al.* (2016). Hematopoietic Stem Cell Niches Produce Lineage-Instructive Signals to Control Multipotent Progenitor Differentiation. Immunity *45*, 1219-1231.

Costales, P., Castellano, J., Revuelta-Lopez, E., Cal, R., Aledo, R., Llampayas, O., Nasarre, L., Juarez, C., Badimon, L., and Llorente-Cortes, V. (2013). Lipopolysaccharide downregulates CD91/low-density lipoprotein receptor-related protein 1 expression through SREBP-1 overexpression in human macrophages. Atherosclerosis *227*, 79-88.

Crawford, J., and Cohen, H.J. (1985). The essential role of L-glutamine in lymphocyte differentiation in vitro. J Cell Physiol *124*, 275-282.

Csibi, A., Lee, G., Yoon, S.O., Tong, H., Ilter, D., Elia, I., Fendt, S.M., Roberts, T.M., and Blenis, J. (2014). The mTORC1/S6K1 pathway regulates glutamine metabolism through the eIF4B-dependent control of c-Myc translation. Curr Biol *24*, 2274-2280.

Cumano, A., and Godin, I. (2007). Ontogeny of the hematopoietic system. Annu Rev Immunol *25*, 745-785.

Curi, R., de Siqueira Mendes, R., de Campos Crispin, L.A., Norata, G.D., Sampaio, S.C., and Newsholme, P. (2017). A past and present overview of macrophage metabolism and functional outcomes. Clin Sci (Lond) *131*, 1329-1342.

Curi, R., Newsholme, P., and Newsholme, E.A. (1988). Metabolism of pyruvate by isolated rat mesenteric lymphocytes, lymphocyte mitochondria and isolated mouse macrophages. Biochem J *250*, 383-388.

Curi, R., Newsholme, P., Pithon-Curi, T.C., Pires-de-Melo, M., Garcia, C., Homem-de-Bittencourt Junior, P.I., and Guimaraes, A.R. (1999). Metabolic fate of glutamine in lymphocytes, macrophages and neutrophils. Braz J Med Biol Res *32*, 15-21.

Curi, T.C., de Melo, M.P., de Azevedo, R.B., and Curi, R. (1997a). Glutamine utilization by rat neutrophils. Biochem Soc Trans *25*, 249S.

Curi, T.C., De Melo, M.P., De Azevedo, R.B., Zorn, T.M., and Curi, R. (1997b). Glutamine utilization by rat neutrophils: presence of phosphate-dependent glutaminase. Am J Physiol *273*, C1124-1129.

Cutolo, M., Sulli, A., Pizzorni, C., Seriolo, B., and Straub, R.H. (2001). Anti-inflammatory mechanisms of methotrexate in rheumatoid arthritis. Ann Rheum Dis *60*, 729-735.

Cybulsky, M.I., and Gimbrone, M.A., Jr. (1991). Endothelial expression of a mononuclear leukocyte adhesion molecule during atherogenesis. Science *251*, 788-791.

Cypess, A.M., Lehman, S., Williams, G., Tal, I., Rodman, D., Goldfine, A.B., Kuo, F.C., Palmer, E.L., Tseng, Y.H., Doria, A.*, et al.* (2009). Identification and importance of brown adipose tissue in adult humans. N Engl J Med *360*, 1509-1517.

Dai, X.M., Ryan, G.R., Hapel, A.J., Dominguez, M.G., Russell, R.G., Kapp, S., Sylvestre, V., and Stanley, E.R. (2002). Targeted disruption of the mouse colony-stimulating factor 1 receptor gene results in osteopetrosis, mononuclear phagocyte deficiency, increased primitive progenitor cell frequencies, and reproductive defects. Blood *99*, 111-120.

Dansky, H.M., Barlow, C.B., Lominska, C., Sikes, J.L., Kao, C., Weinsaft, J., Cybulsky, M.I., and Smith, J.D. (2001). Adhesion of monocytes to arterial endothelium and initiation of atherosclerosis are critically dependent on vascular cell adhesion molecule-1 gene dosage. Arterioscler Thromb Vasc Biol *21*, 1662-1667.

Davies, L.C., Rice, C.M., Palmieri, E.M., Taylor, P.R., Kuhns, D.B., and McVicar, D.W. (2017). Peritoneal tissue-resident macrophages are metabolically poised to engage microbes using tissue-niche fuels. Nat Commun *8*, 2074.

de Meis, L. (2003). Brown adipose tissue Ca2+-ATPase: uncoupled ATP hydrolysis and thermogenic activity. J Biol Chem *278*, 41856-41861.

de Meis, L., Arruda, A.P., da Costa, R.M., and Benchimol, M. (2006). Identification of a Ca2+-ATPase in brown adipose tissue mitochondria: regulation of thermogenesis by ATP and Ca2+. J Biol Chem *281*, 16384-16390.

Deitmer, J.W., Broer, A., and Broer, S. (2003). Glutamine efflux from astrocytes is mediated by multiple pathways. J Neurochem *87*, 127-135.

Divakaruni, A.S., Hsieh, W.Y., Minarrieta, L., Duong, T.N., Kim, K.K.O., Desousa, B.R., Andreyev, A.Y., Bowman, C.E., Caradonna, K., Dranka, B.P.*, et al.* (2018). Etomoxir Inhibits Macrophage Polarization by Disrupting CoA Homeostasis. Cell Metab *28*, 490-503 e497.

Dock-Nascimento, D.B., Aguilar-Nascimento, J.E., and Linetzky Waitzberg, D. (2012). Ingestion of glutamine and maltodextrin two hours preoperatively improves insulin sensitivity after surgery: a randomized, double blind, controlled trial. Rev Col Bras Cir *39*, 449-455.

Doring, Y., Libby, P., and Soehnlein, O. (2020). Neutrophil Extracellular Traps Participate in Cardiovascular Diseases: Recent Experimental and Clinical Insights. Circ Res *126*, 1228-1241.

Dun, X.P., Carr, L., Woodley, P.K., Barry, R.W., Drake, L.K., Mindos, T., Roberts, S.L., Lloyd, A.C., and Parkinson, D.B. (2019). Macrophage-Derived Slit3 Controls Cell Migration and Axon Pathfinding in the Peripheral Nerve Bridge. Cell Rep *26*, 1458-1472 e1454.

Duran, R.V., MacKenzie, E.D., Boulahbel, H., Frezza, C., Heiserich, L., Tardito, S., Bussolati, O., Rocha, S., Hall, M.N., and Gottlieb, E. (2013). HIF-independent role of prolyl hydroxylases in the cellular response to amino acids. Oncogene *32*, 4549-4556.

Duran, R.V., Oppliger, W., Robitaille, A.M., Heiserich, L., Skendaj, R., Gottlieb, E., and Hall, M.N. (2012). Glutaminolysis activates Rag-mTORC1 signaling. Mol Cell *47*, 349-358.

Elgadi, K.M., Meguid, R.A., Qian, M., Souba, W.W., and Abcouwer, S.F. (1999). Cloning and analysis of unique human glutaminase isoforms generated by tissue-specific alternative splicing. Physiol Genomics *1*, 51-62.

Elizabeth G. Nabel, M.D., and Eugene Braunwald, M.D. (2012). A Tale of Coronary Artery Disease and Myocardial Infarction. N Engl J Med.

Elliott, M.R., Chekeni, F.B., Trampont, P.C., Lazarowski, E.R., Kadl, A., Walk, S.F., Park, D., Woodson, R.I., Ostankovich, M., Sharma, P.*, et al.* (2009). Nucleotides released by apoptotic cells act as a find-me signal to promote phagocytic clearance. Nature *461*, 282-286.

Elliott, M.R., Koster, K.M., and Murphy, P.S. (2017). Efferocytosis Signaling in the Regulation of Macrophage Inflammatory Responses. J Immunol *198*, 1387-1394.

Elliott, M.R., and Ravichandran, K.S. (2016). The Dynamics of Apoptotic Cell Clearance. Dev Cell *38*, 147-160.

Enerback, S., Jacobsson, A., Simpson, E.M., Guerra, C., Yamashita, H., Harper, M.E., and Kozak, L.P. (1997). Mice lacking mitochondrial uncoupling protein are cold-sensitive but not obese. Nature *387*, 90-94.

Erbel, C., Tyka, M., Helmes, C.M., Akhavanpoor, M., Rupp, G., Domschke, G., Linden, F., Wolf, A., Doesch, A., Lasitschka, F.*, et al.* (2015). CXCL4-induced plaque macrophages can be specifically identified by co-expression of MMP7+S100A8+ in vitro and in vivo. Innate Immun *21*, 255-265.

Fadok, V.A., Bratton, D.L., Frasch, S.C., Warner, M.L., and Henson, P.M. (1998). The role of phosphatidylserine in recognition of apoptotic cells by phagocytes. Cell Death Differ *5*, 551-562.

Fadok, V.A., de Cathelineau, A., Daleke, D.L., Henson, P.M., and Bratton, D.L. (2001). Loss of phospholipid asymmetry and surface exposure of phosphatidylserine is required for phagocytosis of apoptotic cells by macrophages and fibroblasts. J Biol Chem *276*, 1071-1077.

Fadok, V.A., Voelker, D.R., Campbell, P.A., Cohen, J.J., Bratton, D.L., and Henson, P.M. (1992). Exposure of phosphatidylserine on the surface of apoptotic lymphocytes triggers specific recognition and removal by macrophages. J Immunol *148*, 2207-2216.

Fang, H., and Judd, R.L. (2018). Adiponectin Regulation and Function. Compr Physiol *8*, 1031-1063.

Fantuzzi, G., and Faggioni, R. (2000). Leptin in the regulation of immunity, inflammation, and hematopoiesis. J Leukoc Biol *68*, 437-446.

Fazio, S., Babaev, V.R., Murray, A.B., Hasty, A.H., Carter, K.J., Gleaves, L.A., Atkinson, J.B., and Linton, M.F. (1997). Increased atherosclerosis in mice reconstituted with apolipoprotein E null macrophages. Proc Natl Acad Sci U S A *94*, 4647-4652.

Febbraio, M., Podrez, E.A., Smith, J.D., Hajjar, D.P., Hazen, S.L., Hoff, H.F., Sharma, K., and Silverstein, R.L. (2000). Targeted disruption of the class B scavenger receptor CD36 protects against atherosclerotic lesion development in mice. J Clin Invest *105*, 1049-1056.

Feng, B., Yao, P.M., Li, Y., Devlin, C.M., Zhang, D., Harding, H.P., Sweeney, M., Rong, J.X., Kuriakose, G., Fisher, E.A.*, et al.* (2003). The endoplasmic reticulum is the site of cholesterol-induced cytotoxicity in macrophages. Nat Cell Biol *5*, 781-792.

Feng, B., Zhang, T., and Xu, H. (2013). Human adipose dynamics and metabolic health. Ann N Y Acad Sci *1281*, 160-177.

Fernandez, D.M., Rahman, A.H., Fernandez, N.F., Chudnovskiy, A., Amir, E.D., Amadori, L., Khan, N.S., Wong, C.K., Shamailova, R., Hill, C.A.*, et al.* (2019). Single-cell immune landscape of human atherosclerotic plaques. Nat Med *25*, 1576-1588.

Fielding, C.J., and Fielding, P.E. (1995). Molecular physiology of reverse cholesterol transport. J Lipid Res *36*, 211-228.

Fink, S.L., and Cookson, B.T. (2005). Apoptosis, pyroptosis, and necrosis: mechanistic description of dead and dying eukaryotic cells. Infect Immun *73*, 1907-1916.

Finn, A.V., Nakano, M., Polavarapu, R., Karmali, V., Saeed, O., Zhao, X., Yazdani, S., Otsuka, F., Davis, T., Habib, A.*, et al.* (2012). Hemoglobin directs macrophage differentiation and prevents foam cell formation in human atherosclerotic plaques. J Am Coll Cardiol *59*, 166-177.

Fischer, K., Ruiz, H.H., Jhun, K., Finan, B., Oberlin, D.J., van der Heide, V., Kalinovich, A.V., Petrovic, N., Wolf, Y., Clemmensen, C.*, et al.* (2017). Alternatively activated macrophages do not synthesize catecholamines or contribute to adipose tissue adaptive thermogenesis. Nat Med *23*, 623-630.

Flaherty, S.E., 3rd, Grijalva, A., Xu, X., Ables, E., Nomani, A., and Ferrante, A.W., Jr. (2019). A lipase-independent pathway of lipid release and immune modulation by adipocytes. Science *363*, 989-993.

Flynn, M.C., Kraakman, M.J., Tikellis, C., Lee, M.K.S., Hanssen, N.M.J., Kammoun, H.L., Pickering, R.J., Dragoljevic, D., Al-Sharea, A., Barrett, T.J*., et al.* (2020). Transient Intermittent Hyperglycemia Accelerates Atherosclerosis by Promoting Myelopoiesis. Circ Res *127*, 877-892.

Folco, E.J., Rocha, V.Z., Lopez-Ilasaca, M., and Libby, P. (2009). Adiponectin inhibits pro-inflammatory signaling in human macrophages independent of interleukin-10. J Biol Chem *284*, 25569-25575.

Fotiadis, D., Kanai, Y., and Palacin, M. (2013). The SLC3 and SLC7 families of amino acid transporters. Mol Aspects Med *34*, 139-158.

Fraga, S., Pinho, M.J., and Soares-da-Silva, P. (2005). Expression of LAT1 and LAT2 amino acid transporters in human and rat intestinal epithelial cells. Amino Acids *29*, 229-233.

Franck, G., Mawson, T.L., Folco, E.J., Molinaro, R., Ruvkun, V., Engelbertsen, D., Liu, X., Tesmenitsky, Y., Shvartz, E., Sukhova, G.K*., et al.* (2018). Roles of PAD4 and NETosis in Experimental Atherosclerosis and Arterial Injury: Implications for Superficial Erosion. Circ Res *123*, 33-42.

Freemerman, A.J., Johnson, A.R., Sacks, G.N., Milner, J.J., Kirk, E.L., Troester, M.A., Macintyre, A.N., Goraksha-Hicks, P., Rathmell, J.C., and Makowski, L. (2014). Metabolic reprogramming of macrophages: glucose transporter 1 (GLUT1)-mediated glucose metabolism drives a proinflammatory phenotype. J Biol Chem *289*, 7884-7896.

Freemerman, A.J., Zhao, L., Pingili, A.K., Teng, B., Cozzo, A.J., Fuller, A.M., Johnson, A.R., Milner, J.J., Lim, M.F., Galanko, J.A*., et al.* (2019). Myeloid Slc2a1-Deficient Murine Model Revealed Macrophage Activation and Metabolic Phenotype Are Fueled by GLUT1. J Immunol *202*, 1265-1286.

Freeze, H.H., and Elbein, A.D. (2009). Glycosylation Precursors. In Essentials of Glycobiology, nd, A. Varki, R.D. Cummings, J.D. Esko, H.H. Freeze, P. Stanley, C.R. Bertozzi, G.W. Hart, and M.E. Etzler, eds. (Cold Spring Harbor (NY)).

Friedman, J. (2016). The long road to leptin. J Clin Invest *126*, 4727-4734.

Fu, C., Li, Q., Zou, J., Xing, C., Luo, M., Yin, B., Chu, J., Yu, J., Liu, X., Wang, H.Y*., et al.* (2019). JMJD3 regulates CD4 T cell trafficking by targeting actin cytoskeleton regulatory gene Pdlim4. J Clin Invest *129*, 4745-4757.

Gao, P., Tchernyshyov, I., Chang, T.C., Lee, Y.S., Kita, K., Ochi, T., Zeller, K.I., De Marzo, A.M., Van Eyk, J.E., Mendell, J.T*., et al.* (2009). c-Myc suppression of miR-23a/b enhances mitochondrial glutaminase expression and glutamine metabolism. Nature *458*, 762-765.

Gao, R., Shi, H., Chang, S., Gao, Y., Li, X., Lv, C., Yang, H., Xiang, H., Yang, J., Xu, L*., et al.* (2019). The selective NLRP3-inflammasome inhibitor MCC950 reduces myocardial fibrosis and improves cardiac remodeling in a mouse model of myocardial infarction. Int Immunopharmacol *74*, 105575.

Garcia, C., Pithon-Curi, T.C., de Lourdes Firmano, M., Pires de Melo, M., Newsholme, P., and Curi, R. (1999). Effects of adrenaline on glucose and glutamine metabolism and superoxide production by rat neutrophils. Clin Sci (Lond) *96*, 549-555.

Gardai, S.J., Bratton, D.L., Ogden, C.A., and Henson, P.M. (2006). Recognition ligands on apoptotic cells: a perspective. J Leukoc Biol *79*, 896-903.

Gardai, S.J., McPhillips, K.A., Frasch, S.C., Janssen, W.J., Starefeldt, A., Murphy-Ullrich, J.E., Bratton, D.L., Oldenborg, P.A., Michalak, M., and Henson, P.M. (2005). Cell-surface calreticulin initiates clearance of viable or apoptotic cells through trans-activation of LRP on the phagocyte. Cell *123*, 321-334.

Gautier, E.L., Huby, T., Witztum, J.L., Ouzilleau, B., Miller, E.R., Saint-Charles, F., Aucouturier, P., Chapman, M.J., and Lesnik, P. (2009). Macrophage apoptosis exerts divergent effects on atherogenesis as a function of lesion stage. Circulation *119*, 1795-1804.

Gebuhrer, V., Murphy, J.F., Bordet, J.C., Reck, M.P., and McGregor, J.L. (1995). Oxidized low-density lipoprotein induces the expression of P-selectin (GMP140/PADGEM/CD62) on human endothelial cells. Biochem J *306 (Pt 1)*, 293-298.

Geissmann, F., Gordon, S., Hume, D.A., Mowat, A.M., and Randolph, G.J. (2010a). Unravelling mononuclear phagocyte heterogeneity. Nat Rev Immunol *10*, 453-460.

Geissmann, F., Jung, S., and Littman, D.R. (2003). Blood monocytes consist of two principal subsets with distinct migratory properties. Immunity *19*, 71-82.

Geissmann, F., Manz, M.G., Jung, S., Sieweke, M.H., Merad, M., and Ley, K. (2010b). Development of monocytes, macrophages, and dendritic cells. Science *327*, 656-661.

Gerards, A.H., de Lathouder, S., de Groot, E.R., Dijkmans, B.A., and Aarden, L.A. (2003). Inhibition of cytokine production by methotrexate. Studies in healthy volunteers and patients with rheumatoid arthritis. Rheumatology (Oxford) *42*, 1189-1196.

Getz, G.S., and Reardon, C.A. (2009). Apoprotein E as a lipid transport and signaling protein in the blood, liver, and artery wall. J Lipid Res *50 Suppl*, S156-161.

Ghiselli, G., Schaefer, E.J., Gascon, P., and Breser, H.B., Jr. (1981). Type III hyperlipoproteinemia associated with apolipoprotein E deficiency. Science *214*, 1239-1241.

Gillotte-Taylor, K., Boullier, A., Witztum, J.L., Steinberg, D., and Quehenberger, O. (2001). Scavenger receptor class B type I as a receptor for oxidized low density lipoprotein. J Lipid Res *42*, 1474-1482.

Gimbrone, M.A., Jr., Topper, J.N., Nagel, T., Anderson, K.R., and Garcia-Cardena, G. (2000). Endothelial dysfunction, hemodynamic forces, and atherogenesis. Ann N Y Acad Sci *902*, 230-239; discussion 239-240.

Ginhoux, F., Greter, M., Leboeuf, M., Nandi, S., See, P., Gokhan, S., Mehler, M.F., Conway, S.J., Ng, L.G., Stanley, E.R*., et al.* (2010). Fate mapping analysis reveals that adult microglia derive from primitive macrophages. Science *330*, 841-845.

Ginhoux, F., and Guilliams, M. (2016). Tissue-Resident Macrophage Ontogeny and Homeostasis. Immunity *44*, 439-449.

Ginhoux, F., and Jung, S. (2014). Monocytes and macrophages: developmental pathways and tissue homeostasis. Nat Rev Immunol *14*, 392-404.

Gleissner, C.A., Sanders, J.M., Nadler, J., and Ley, K. (2008). Upregulation of aldose reductase during foam cell formation as possible link among diabetes, hyperlipidemia, and atherosclerosis. Arterioscler Thromb Vasc Biol *28*, 1137-1143.

Gleissner, C.A., Shaked, I., Erbel, C., Bockler, D., Katus, H.A., and Ley, K. (2010a). CXCL4 downregulates the atheroprotective hemoglobin receptor CD163 in human macrophages. Circ Res *106*, 203-211.

Gleissner, C.A., Shaked, I., Little, K.M., and Ley, K. (2010b). CXC chemokine ligand 4 induces a unique transcriptome in monocyte-derived macrophages. J Immunol *184*, 4810-4818.

Godfrey, S., Kuhlenschmidt, T., and Curthoys, P. (1977). Correlation between activation and dimer formation of rat renal phosphate-dependent glutaminase. J Biol Chem *252*, 1927-1931.

Goldstein, J.L., Ho, Y.K., Basu, S.K., and Brown, M.S. (1979). Binding site on macrophages that mediates uptake and degradation of acetylated low density lipoprotein, producing massive cholesterol deposition. Proc Natl Acad Sci U S A *76*, 333-337.

Golozoubova, V., Hohtola, E., Matthias, A., Jacobsson, A., Cannon, B., and Nedergaard, J. (2001). Only UCP1 can mediate adaptive nonshivering thermogenesis in the cold. FASEB J *15*, 2048-2050.

Gomaraschi, M., Bonacina, F., and Norata, G.D. (2019). Lysosomal Acid Lipase: From Cellular Lipid Handler to Immunometabolic Target. Trends Pharmacol Sci *40*, 104-115.

Gordon, S. (2003). Alternative activation of macrophages. Nat Rev Immunol *3*, 23-35.

Gosling, J., Slaymaker, S., Gu, L., Tseng, S., Zlot, C.H., Young, S.G., Rollins, B.J., and Charo, I.F. (1999). MCP-1 deficiency reduces susceptibility to atherosclerosis in mice that overexpress human apolipoprotein B. J Clin Invest *103*, 773-778.

Gosselin, D., Link, V.M., Romanoski, C.E., Fonseca, G.J., Eichenfield, D.Z., Spann, N.J., Stender, J.D., Chun, H.B., Garner, H., Geissmann, F*., et al.* (2014). Environment drives selection and function of enhancers controlling tissue-specific macrophage identities. Cell *159*, 1327-1340.

Grundy, S.M. (2016). Dyslipidaemia in 2015: Advances in treatment of dyslipidaemia. Nat Rev Cardiol *13*, 74-75.

Gu, L., Okada, Y., Clinton, S.K., Gerard, C., Sukhova, G.K., Libby, P., and Rollins, B.J. (1998). Absence of monocyte chemoattractant protein-1 reduces atherosclerosis in low density lipoprotein receptor-deficient mice. Mol Cell *2*, 275-281.

Gude, D.R., Alvarez, S.E., Paugh, S.W., Mitra, P., Yu, J., Griffiths, R., Barbour, S.E., Milstien, S., and Spiegel, S. (2008). Apoptosis induces expression of sphingosine kinase 1 to release sphingosine-1-phosphate as a "come-and-get-me" signal. FASEB J *22*, 2629-2638.

Guilliams, M., De Kleer, I., Henri, S., Post, S., Vanhoutte, L., De Prijck, S., Deswarte, K., Malissen, B., Hammad, H., and Lambrecht, B.N. (2013). Alveolar macrophages develop from fetal monocytes that differentiate into long-lived cells in the first week of life via GM-CSF. J Exp Med *210*, 1977-1992.

Guo, J., de Waard, V., Van Eck, M., Hildebrand, R.B., van Wanrooij, E.J., Kuiper, J., Maeda, N., Benson, G.M., Groot, P.H., and Van Berkel, T.J. (2005). Repopulation of apolipoprotein E knockout mice with CCR2-deficient bone marrow progenitor cells does not inhibit ongoing atherosclerotic lesion development. Arterioscler Thromb Vasc Biol *25*, 1014-1019.

Guyenet, S.J., and Schwartz, M.W. (2012). Clinical review: Regulation of food intake, energy balance, and body fat mass: implications for the pathogenesis and treatment of obesity. J Clin Endocrinol Metab *97*, 745-755.

Ha, Y.C., Calvert, G.D., McIntosh, G.H., and Barter, P.J. (1981). A physiologic role for the esterified cholesterol transfer protein: in vivo studies in rabbits and pigs. Metabolism *30*, 380-383.

Haberle, J., Gorg, B., Rutsch, F., Schmidt, E., Toutain, A., Benoist, J.F., Gelot, A., Suc, A.L., Hohne, W., Schliess, F*., et al.* (2005). Congenital glutamine deficiency with glutamine synthetase mutations. N Engl J Med *353*, 1926-1933.

Haberle, J., Gorg, B., Toutain, A., Rutsch, F., Benoist, J.F., Gelot, A., Suc, A.L., Koch, H.G., Schliess, F., and Haussinger, D. (2006). Inborn error of amino acid synthesis: human glutamine synthetase deficiency. J Inherit Metab Dis *29*, 352-358.

Haberle, J., Shahbeck, N., Ibrahim, K., Hoffmann, G.F., and Ben-Omran, T. (2011). Natural course of glutamine synthetase deficiency in a 3 year old patient. Mol Genet Metab *103*, 89-91.

Haczeyni, F., Bell-Anderson, K.S., and Farrell, G.C. (2018). Causes and mechanisms of adipocyte enlargement and adipose expansion. Obes Rev *19*, 406-420.

Hagglund, M.G., Sreedharan, S., Nilsson, V.C., Shaik, J.H., Almkvist, I.M., Backlin, S., Wrange, O., and Fredriksson, R. (2011). Identification of SLC38A7 (SNAT7) protein as a glutamine transporter expressed in neurons. J Biol Chem *286*, 20500-20511.

Hamilton, J.A., Myers, D., Jessup, W., Cochrane, F., Byrne, R., Whitty, G., and Moss, S. (1999). Oxidized LDL can induce macrophage survival, DNA synthesis, and enhanced proliferative response to CSF-1 and GM-CSF. Arterioscler Thromb Vasc Biol *19*, 98-105.

Han, J., Lee, J.E., Jin, J., Lim, J.S., Oh, N., Kim, K., Chang, S.I., Shibuya, M., Kim, H., and Koh, G.Y. (2011). The spatiotemporal development of adipose tissue. Development *138*, 5027-5037.

Hanna, R.N., Carlin, L.M., Hubbeling, H.G., Nackiewicz, D., Green, A.M., Punt, J.A., Geissmann, F., and Hedrick, C.C. (2011). The transcription factor NR4A1 (Nur77) controls bone marrow differentiation and the survival of Ly6C- monocytes. Nat Immunol *12*, 778-785.

Hanna, R.N., Cekic, C., Sag, D., Tacke, R., Thomas, G.D., Nowyhed, H., Herrley, E., Rasquinha, N., McArdle, S., Wu, R.*, et al.* (2015). Patrolling monocytes control tumor metastasis to the lung. Science *350*, 985-990.

Hansson, G.K. (2005). Inflammation, atherosclerosis, and coronary artery disease. N Engl J Med *352*, 1685-1695.

Hansson, G.K., and Hermansson, A. (2011). The immune system in atherosclerosis. Nat Immunol *12*, 204-212.

Hao, W., and Friedman, A. (2014). The LDL-HDL profile determines the risk of atherosclerosis: a mathematical model. PLoS One *9*, e90497.

Harms, M., and Seale, P. (2013). Brown and beige fat: development, function and therapeutic potential. Nat Med *19*, 1252-1263.

Haschemi, A., Kosma, P., Gille, L., Evans, C.R., Burant, C.F., Starkl, P., Knapp, B., Haas, R., Schmid, J.A., Jandl, C.*, et al.* (2012). The sedoheptulose kinase CARKL directs macrophage polarization through control of glucose metabolism. Cell Metab *15*, 813-826.

Hashimoto, D., Chow, A., Noizat, C., Teo, P., Beasley, M.B., Leboeuf, M., Becker, C.D., See, P., Price, J., Lucas, D.*, et al.* (2013). Tissue-resident macrophages self-maintain locally throughout adult life with minimal contribution from circulating monocytes. Immunity *38*, 792-804.

Havekes, L., de Wit, E., Leuven, J.G., Klasen, E., Utermann, G., Weber, W., and Beisiegel, U. (1986). Apolipoprotein E3-Leiden. A new variant of human apolipoprotein E associated with familial type III hyperlipoproteinemia. Hum Genet *73*, 157-163.

Hayashi, K., Jutabha, P., Endou, H., and Anzai, N. (2012). c-Myc is crucial for the expression of LAT1 in MIA Paca-2 human pancreatic cancer cells. Oncol Rep *28*, 862-866.

Heinecke, J.W. (2012). The not-so-simple HDL story: A new era for quantifying HDL and cardiovascular risk? Nat Med *18*, 1346-1347.

Heini, H.G., Gebhardt, R., Brecht, A., and Mecke, D. (1987). Purification and characterization of rat liver glutaminase. Eur J Biochem *162*, 541-546.

Hesterberg, R.S., Cleveland, J.L., and Epling-Burnette, P.K. (2018). Role of Polyamines in Immune Cell Functions. Med Sci (Basel) *6*.

Hobbs, H.H., Russell, D.W., Brown, M.S., and Goldstein, J.L. (1990). The LDL receptor locus in familial hypercholesterolemia: mutational analysis of a membrane protein. Annu Rev Genet *24*, 133-170.

Hochreiter-Hufford, A., and Ravichandran, K.S. (2013). Clearing the dead: apoptotic cell sensing, recognition, engulfment, and digestion. Cold Spring Harb Perspect Biol *5*, a008748.

Hoeffel, G., Chen, J., Lavin, Y., Low, D., Almeida, F.F., See, P., Beaudin, A.E., Lum, J., Low, I., Forsberg, E.C*., et al.* (2015). C-Myb(+) erythro-myeloid progenitor-derived fetal monocytes give rise to adult tissue-resident macrophages. Immunity *42*, 665-678.

Hoeffel, G., and Ginhoux, F. (2018). Fetal monocytes and the origins of tissue-resident macrophages. Cell Immunol *330*, 5-15.

Hoeffel, G., Wang, Y., Greter, M., See, P., Teo, P., Malleret, B., Leboeuf, M., Low, D., Oller, G., Almeida, F*., et al.* (2012). Adult Langerhans cells derive predominantly from embryonic fetal liver monocytes with a minor contribution of yolk sac-derived macrophages. J Exp Med *209*, 1167-1181.

Hoffmann, P.R., deCathelineau, A.M., Ogden, C.A., Leverrier, Y., Bratton, D.L., Daleke, D.L., Ridley, A.J., Fadok, V.A., and Henson, P.M. (2001). Phosphatidylserine (PS) induces PS receptor-mediated macropinocytosis and promotes clearance of apoptotic cells. J Cell Biol *155*, 649-659.

Hollands, M.A., and Cawthorne, M.A. (1981). Important sites of lipogenesis in the mouse other than liver and white adipose tissue. Biochem J *196*, 645-647.

Hosios, A.M., Hecht, V.C., Danai, L.V., Johnson, M.O., Rathmell, J.C., Steinhauser, M.L., Manalis, S.R., and Vander Heiden, M.G. (2016). Amino Acids Rather than Glucose Account for the Majority of Cell Mass in Proliferating Mammalian Cells. Dev Cell *36*, 540-549.

Hu, W., Zhang, C., Wu, R., Sun, Y., Levine, A., and Feng, Z. (2010). Glutaminase 2, a novel p53 target gene regulating energy metabolism and antioxidant function. Proc Natl Acad Sci U S A *107*, 7455-7460.

Huang, S.C., Everts, B., Ivanova, Y., O'Sullivan, D., Nascimento, M., Smith, A.M., Beatty, W., Love-Gregory, L., Lam, W.Y., O'Neill, C.M*., et al.* (2014). Cell-intrinsic lysosomal lipolysis is essential for alternative activation of macrophages. Nat Immunol *15*, 846-855.

Ignatowski, A. (1909). Ueber die Wirkung der tierschen Einweisse auf der Aorta. Virchow's Arch Pathol Anat 198:248.

Indiveri, C., Abruzzo, G., Stipani, I., and Palmieri, F. (1998). Identification and purification of the reconstitutively active glutamine carrier from rat kidney mitochondria. Biochem J *333 (Pt 2)*, 285-290.

Ingersoll, M.A., Spanbroek, R., Lottaz, C., Gautier, E.L., Frankenberger, M., Hoffmann, R., Lang, R., Haniffa, M., Collin, M., Tacke, F*., et al.* (2010). Comparison of gene expression profiles between human and mouse monocyte subsets. Blood *115*, e10-19.

Ishibashi, S., Brown, M.S., Goldstein, J.L., Gerard, R.D., Hammer, R.E., and Herz, J. (1993). Hypercholesterolemia in low density lipoprotein receptor knockout mice and its reversal by adenovirus-mediated gene delivery. J Clin Invest *92*, 883-893.

Ishibashi, S., Goldstein, J.L., Brown, M.S., Herz, J., and Burns, D.K. (1994). Massive xanthomatosis and atherosclerosis in cholesterol-fed low density lipoprotein receptor-negative mice. J Clin Invest *93*, 1885-1893.

Ivanov, S., Merlin, J., Lee, M.K.S., Murphy, A.J., and Guinamard, R.R. (2018). Biology and function of adipose tissue macrophages, dendritic cells and B cells. Atherosclerosis *271*, 102-110.

Jakubzick, C., Gautier, E.L., Gibbings, S.L., Sojka, D.K., Schlitzer, A., Johnson, T.E., Ivanov, S., Duan, Q., Bala, S., Condon, T*., et al.* (2013). Minimal differentiation of classical monocytes as they survey steady-state tissues and transport antigen to lymph nodes. Immunity *39*, 599-610.

Jenstad, M., and Chaudhry, F.A. (2013). The Amino Acid Transporters of the Glutamate/GABA-Glutamine Cycle and Their Impact on Insulin and Glucagon Secretion. Front Endocrinol (Lausanne) *4*, 199.

Jeppesen, J., and Kiens, B. (2012). Regulation and limitations to fatty acid oxidation during exercise. J Physiol *590*, 1059-1068.

Jewell, J.L., Kim, Y.C., Russell, R.C., Yu, F.X., Park, H.W., Plouffe, S.W., Tagliabracci, V.S., and Guan, K.L. (2015). Metabolism. Differential regulation of mTORC1 by leucine and glutamine. Science *347*, 194-198.

Jha, A.K., Huang, S.C., Sergushichev, A., Lampropoulou, V., Ivanova, Y., Loginicheva, E., Chmielewski, K., Stewart, K.M., Ashall, J., Everts, B*., et al.* (2015). Network integration of parallel metabolic and transcriptional data reveals metabolic modules that regulate macrophage polarization. Immunity *42*, 419-430.

Jia, T., Serbina, N.V., Brandl, K., Zhong, M.X., Leiner, I.M., Charo, I.F., and Pamer, E.G. (2008). Additive roles for MCP-1 and MCP-3 in CCR2-mediated recruitment of inflammatory monocytes during Listeria monocytogenes infection. J Immunol *180*, 6846-6853.

Jiang, X.C., Masucci-Magoulas, L., Mar, J., Lin, M., Walsh, A., Breslow, J.L., and Tall, A. (1993). Down-regulation of mRNA for the low density lipoprotein receptor in transgenic mice containing the gene for human cholesteryl ester transfer protein. Mechanism to explain accumulation of lipoprotein B particles. J Biol Chem *268*, 27406-27412.

Joe, A.W., Yi, L., Even, Y., Vogl, A.W., and Rossi, F.M. (2009). Depot-specific differences in adipogenic progenitor abundance and proliferative response to high-fat diet. Stem Cells *27*, 2563-2570.

Johnson, M.O., Wolf, M.M., Madden, M.Z., Andrejeva, G., Sugiura, A., Contreras, D.C., Maseda, D., Liberti, M.V., Paz, K., Kishton, R.J*., et al.* (2018). Distinct Regulation of Th17 and Th1 Cell Differentiation by Glutaminase-Dependent Metabolism. Cell *175*, 1780-1795 e1719.

Jonas, A. (2000). Lecithin cholesterol acyltransferase. Biochim Biophys Acta *1529*, 245-256.

Jones, C., Eddleston, J., McCairn, A., Dowling, S., McWilliams, D., Coughlan, E., and Griffiths, R.D. (2015). Improving rehabilitation after critical illness through outpatient physiotherapy classes and essential amino acid supplement: A randomized controlled trial. J Crit Care *30*, 901-907.

Judge, D.P., Biery, N.J., Keene, D.R., Geubtner, J., Myers, L., Huso, D.L., Sakai, L.Y., and Dietz, H.C. (2004). Evidence for a critical contribution of haploinsufficiency in the complex pathogenesis of Marfan syndrome. J Clin Invest *114*, 172-181.

Jukema, J.W., Bruschke, A.V., van Boven, A.J., Reiber, J.H., Bal, E.T., Zwinderman, A.H., Jansen, H., Boerma, G.J., van Rappard, F.M., Lie, K.I*., et al.* (1995). Effects of lipid lowering by pravastatin on progression and regression of coronary artery disease in symptomatic men with normal to moderately elevated serum cholesterol levels. The Regression Growth Evaluation Statin Study (REGRESS). Circulation *91*, 2528-2540.

Jung, H., Bhangoo, S., Banisadr, G., Freitag, C., Ren, D., White, F.A., and Miller, R.J. (2009). Visualization of chemokine receptor activation in transgenic mice reveals peripheral activation of CCR2 receptors in states of neuropathic pain. J Neurosci *29*, 8051-8062.

Jung, H., Mithal, D.S., Park, J.E., and Miller, R.J. (2015). Localized CCR2 Activation in the Bone Marrow Niche Mobilizes Monocytes by Desensitizing CXCR4. PLoS One *10*, e0128387.

Kadl, A., Meher, A.K., Sharma, P.R., Lee, M.Y., Doran, A.C., Johnstone, S.R., Elliott, M.R., Gruber, F., Han, J., Chen, W*., et al.* (2010). Identification of a novel macrophage phenotype that develops in response to atherogenic phospholipids via Nrf2. Circ Res *107*, 737-746.

Kamei, N., Tobe, K., Suzuki, R., Ohsugi, M., Watanabe, T., Kubota, N., Ohtsuka-Kowatari, N., Kumagai, K., Sakamoto, K., Kobayashi, M*., et al.* (2006). Overexpression of monocyte chemoattractant protein-1 in adipose tissues causes macrophage recruitment and insulin resistance. J Biol Chem *281*, 26602-26614.

Kanai, Y., Clemencon, B., Simonin, A., Leuenberger, M., Lochner, M., Weisstanner, M., and Hediger, M.A. (2013). The SLC1 high-affinity glutamate and neutral amino acid transporter family. Mol Aspects Med *34*, 108-120.

Kanai, Y., Segawa, H., Miyamoto, K., Uchino, H., Takeda, E., and Endou, H. (1998). Expression cloning and characterization of a transporter for large neutral amino acids activated by the heavy chain of 4F2 antigen (CD98). J Biol Chem *273*, 23629-23632.

Kang, K., Reilly, S.M., Karabacak, V., Gangl, M.R., Fitzgerald, K., Hatano, B., and Lee, C.H. (2008). Adipocyte-derived Th2 cytokines and myeloid PPARdelta regulate macrophage polarization and insulin sensitivity. Cell Metab *7*, 485-495.

Kazak, L., Chouchani, E.T., Jedrychowski, M.P., Erickson, B.K., Shinoda, K., Cohen, P., Vetrivelan, R., Lu, G.Z., Laznik-Bogoslavski, D., Hasenfuss, S.C*., et al.* (2015). A creatine-driven substrate cycle enhances energy expenditure and thermogenesis in beige fat. Cell *163*, 643-655.

Kazak, L., Chouchani, E.T., Stavrovskaya, I.G., Lu, G.Z., Jedrychowski, M.P., Egan, D.F., Kumari, M., Kong, X., Erickson, B.K., Szpyt, J*., et al.* (2017). UCP1 deficiency causes brown fat respiratory chain depletion and sensitizes mitochondria to calcium overload-induced dysfunction. Proc Natl Acad Sci U S A *114*, 7981-7986.

Keipert, S., Kutschke, M., Ost, M., Schwarzmayr, T., van Schothorst, E.M., Lamp, D., Brachthauser, L., Hamp, I., Mazibuko, S.E., Hartwig, S*., et al.* (2017). Long-Term Cold Adaptation Does Not Require FGF21 or UCP1. Cell Metab *26*, 437-446 e435.

Kekuda, R., Prasad, P.D., Fei, Y.J., Torres-Zamorano, V., Sinha, S., Yang-Feng, T.L., Leibach, F.H., and Ganapathy, V. (1996). Cloning of the sodium-dependent, broad-scope, neutral amino acid transporter Bo from a human placental choriocarcinoma cell line. J Biol Chem *271*, 18657-18661.

Khan, B.V., Parthasarathy, S.S., Alexander, R.W., and Medford, R.M. (1995). Modified low density lipoprotein and its constituents augment cytokine-activated vascular cell adhesion molecule-1 gene expression in human vascular endothelial cells. J Clin Invest *95*, 1262-1270.

Kidani, Y., and Bensinger, S.J. (2012). Liver X receptor and peroxisome proliferator-activated receptor as integrators of lipid homeostasis and immunity. Immunol Rev *249*, 72-83.

Kim, J.W., Tchernyshyov, I., Semenza, G.L., and Dang, C.V. (2006). HIF-1-mediated expression of pyruvate dehydrogenase kinase: a metabolic switch required for cellular adaptation to hypoxia. Cell Metab *3*, 177-185.

Kim, K., Shim, D., Lee, J.S., Zaitsev, K., Williams, J.W., Kim, K.W., Jang, M.Y., Seok Jang, H., Yun, T.J., Lee, S.H*., et al.* (2018). Transcriptome Analysis Reveals Nonfoamy Rather Than Foamy Plaque Macrophages Are Proinflammatory in Atherosclerotic Murine Models. Circ Res *123*, 1127-1142.

Kim, S.M., Lun, M., Wang, M., Senyo, S.E., Guillermier, C., Patwari, P., and Steinhauser, M.L. (2014). Loss of white adipose hyperplastic potential is associated with enhanced susceptibility to insulin resistance. Cell Metab *20*, 1049-1058.

Klerkx, A.H., de Grooth, G.J., Zwinderman, A.H., Jukema, J.W., Kuivenhoven, J.A., and Kastelein, J.J. (2004). Cholesteryl ester transfer protein concentration is associated with progression of atherosclerosis and response to pravastatin in men with coronary artery disease (REGRESS). Eur J Clin Invest *34*, 21-28.

Klysz, D., Tai, X., Robert, P.A., Craveiro, M., Cretenet, G., Oburoglu, L., Mongellaz, C., Floess, S., Fritz, V., Matias, M.I*., et al.* (2015). Glutamine-dependent alpha-ketoglutarate production regulates the balance between T helper 1 cell and regulatory T cell generation. Sci Signal *8*, ra97.

Knowles, J.W., and Maeda, N. (2000). Genetic modifiers of atherosclerosis in mice. Arterioscler Thromb Vasc Biol *20*, 2336-2345.

Kobayashi, J., Miyashita, K., Nakajima, K., and Mabuchi, H. (2015). Hepatic Lipase: a Comprehensive View of its Role on Plasma Lipid and Lipoprotein Metabolism. J Atheroscler Thromb *22*, 1001-1011.

Kockx, M.M., and Herman, A.G. (2000). Apoptosis in atherosclerosis: beneficial or detrimental? Cardiovasc Res *45*, 736-746.

Koelwyn, G.J., Corr, E.M., Erbay, E., and Moore, K.J. (2018). Regulation of macrophage immunometabolism in atherosclerosis. Nat Immunol *19*, 526-537.

Kohler, S., Schmoller, K.M., Crevenna, A.H., and Bausch, A.R. (2012). Regulating contractility of the actomyosin cytoskeleton by pH. Cell Rep *2*, 433-439.

Kojima, Y., Volkmer, J.P., McKenna, K., Civelek, M., Lusis, A.J., Miller, C.L., Direnzo, D., Nanda, V., Ye, J., Connolly, A.J*., et al.* (2016). CD47-blocking antibodies restore phagocytosis and prevent atherosclerosis. Nature *536*, 86-90.

Komura, H., Miksa, M., Wu, R., Goyert, S.M., and Wang, P. (2009). Milk fat globule epidermal growth factor-factor VIII is down-regulated in sepsis via the lipopolysaccharide-CD14 pathway. J Immunol *182*, 581-587.

Kondou, H., Kawai, M., Tachikawa, K., Kimoto, A., Yamagata, M., Koinuma, T., Yamazaki, M., Nakayama, M., Mushiake, S., Ozono, K*., et al.* (2013). Sodium-coupled neutral amino acid transporter 4 functions as a regulator of protein synthesis during liver development. Hepatol Res *43*, 1211-1223.

Korner, A., Schlegel, M., Kaussen, T., Gudernatsch, V., Hansmann, G., Schumacher, T., Giera, M., and Mirakaj, V. (2019). Sympathetic nervous system controls resolution of inflammation via regulation of repulsive guidance molecule A. Nat Commun *10*, 633.

Kraakman, M.J., Murphy, A.J., Jandeleit-Dahm, K., and Kammoun, H.L. (2014). Macrophage polarization in obesity and type 2 diabetes: weighing down our understanding of macrophage function? Front Immunol *5*, 470.

Kratz, M., Coats, B.R., Hisert, K.B., Hagman, D., Mutskov, V., Peris, E., Schoenfelt, K.Q., Kuzma, J.N., Larson, I., Billing, P.S*., et al.* (2014). Metabolic dysfunction drives a mechanistically distinct proinflammatory phenotype in adipose tissue macrophages. Cell Metab *20*, 614-625.

Krebs, H.A. (1935). Metabolism of amino-acids: The synthesis of glutamine from glutamic acid and ammonia, and the enzymic hydrolysis of glutamine in animal tissues. Biochem J *29*, 1951-1969.

Krieger, M. (1999). Charting the fate of the "good cholesterol": identification and characterization of the high-density lipoprotein receptor SR-BI. Annu Rev Biochem *68*, 523-558.

Kubo, T., Imanishi, T., Takarada, S., Kuroi, A., Ueno, S., Yamano, T., Tanimoto, T., Matsuo, Y., Masho, T., Kitabata, H.*, et al.* (2007). Assessment of culprit lesion morphology in acute myocardial infarction: ability of optical coherence tomography compared with intravascular ultrasound and coronary angioscopy. J Am Coll Cardiol *50*, 933-939.

Kubota, N., Terauchi, Y., Yamauchi, T., Kubota, T., Moroi, M., Matsui, J., Eto, K., Yamashita, T., Kamon, J., Satoh, H.*, et al.* (2002). Disruption of adiponectin causes insulin resistance and neointimal formation. J Biol Chem *277*, 25863-25866.

Kudsk, K.A., Wu, Y., Fukatsu, K., Zarzaur, B.L., Johnson, C.D., Wang, R., and Hanna, M.K. (2000). Glutamine-enriched total parenteral nutrition maintains intestinal interleukin-4 and mucosal immunoglobulin A levels. JPEN J Parenter Enteral Nutr *24*, 270-274; discussion 274-275.

Kuhnast, S., van der Tuin, S.J., van der Hoorn, J.W., van Klinken, J.B., Simic, B., Pieterman, E., Havekes, L.M., Landmesser, U., Luscher, T.F., Willems van Dijk, K.*, et al.* (2015). Anacetrapib reduces progression of atherosclerosis, mainly by reducing non-HDL-cholesterol, improves lesion stability and adds to the beneficial effects of atorvastatin. Eur Heart J *36*, 39-48.

Kunjathoor, V.V., Febbraio, M., Podrez, E.A., Moore, K.J., Andersson, L., Koehn, S., Rhee, J.S., Silverstein, R., Hoff, H.F., and Freeman, M.W. (2002). Scavenger receptors class A-I/II and CD36 are the principal receptors responsible for the uptake of modified low density lipoprotein leading to lipid loading in macrophages. J Biol Chem *277*, 49982-49988.

Kwon, M.J., Shin, H.Y., Cui, Y., Kim, H., Thi, A.H., Choi, J.Y., Kim, E.Y., Hwang, D.H., and Kim, B.G. (2015). CCL2 Mediates Neuron-Macrophage Interactions to Drive Proregenerative Macrophage Activation Following Preconditioning Injury. J Neurosci *35*, 15934-15947.

Labbe, S.M., Caron, A., Chechi, K., Laplante, M., Lecomte, R., and Richard, D. (2016). Metabolic activity of brown, "beige," and white adipose tissues in response to chronic adrenergic stimulation in male mice. Am J Physiol Endocrinol Metab *311*, E260-268.

Labow, B.I., Souba, W.W., and Abcouwer, S.F. (2001). Mechanisms governing the expression of the enzymes of glutamine metabolism--glutaminase and glutamine synthetase. J Nutr *131*, 2467S-2474S; discussion 2486S-2467S.

Lachmann, H.J., Kone-Paut, I., Kuemmerle-Deschner, J.B., Leslie, K.S., Hachulla, E., Quartier, P., Gitton, X., Widmer, A., Patel, N., Hawkins, P.N.*, et al.* (2009). Use of canakinumab in the cryopyrin-associated periodic syndrome. N Engl J Med *360*, 2416-2425.

Lampropoulou, V., Sergushichev, A., Bambouskova, M., Nair, S., Vincent, E.E., Loginicheva, E., Cervantes-Barragan, L., Ma, X., Huang, S.C., Griss, T.*, et al.* (2016). Itaconate Links Inhibition of Succinate Dehydrogenase with Macrophage Metabolic Remodeling and Regulation of Inflammation. Cell Metab *24*, 158-166.

Laplante, M., and Sabatini, D.M. (2012). mTOR signaling in growth control and disease. Cell *149*, 274-293.

Laterza, O.F., and Curthoys, N.P. (2000). Effect of acidosis on the properties of the glutaminase mRNA pH-response element binding protein. J Am Soc Nephrol *11*, 1583-1588.

Lauber, K., Bohn, E., Krober, S.M., Xiao, Y.J., Blumenthal, S.G., Lindemann, R.K., Marini, P., Wiedig, C., Zobywalski, A., Baksh, S.*, et al.* (2003). Apoptotic cells induce migration of phagocytes via caspase-3-mediated release of a lipid attraction signal. Cell *113*, 717-730.

Lavin, Y., Winter, D., Blecher-Gonen, R., David, E., Keren-Shaul, H., Merad, M., Jung, S., and Amit, I. (2014). Tissue-resident macrophage enhancer landscapes are shaped by the local microenvironment. Cell *159*, 1312-1326.

Lea, S., Plumb, J., Metcalfe, H., Spicer, D., Woodman, P., Fox, J.C., and Singh, D. (2014). The effect of peroxisome proliferator-activated receptor-gamma ligands on in vitro and in vivo models of COPD. Eur Respir J *43*, 409-420.

Lee, C.S., Penberthy, K.K., Wheeler, K.M., Juncadella, I.J., Vandenabeele, P., Lysiak, J.J., and Ravichandran, K.S. (2016). Boosting Apoptotic Cell Clearance by Colonic Epithelial Cells Attenuates Inflammation In Vivo. Immunity *44*, 807-820.

Lee, M.W., Odegaard, J.I., Mukundan, L., Qiu, Y., Molofsky, A.B., Nussbaum, J.C., Yun, K., Locksley, R.M., and Chawla, A. (2015). Activated type 2 innate lymphoid cells regulate beige fat biogenesis. Cell *160*, 74-87.

Lee, Y.T., Lin, H.Y., Chan, Y.W., Li, K.H., To, O.T., Yan, B.P., Liu, T., Li, G., Wong, W.T., Keung, W.*, et al.* (2017). Mouse models of atherosclerosis: a historical perspective and recent advances. Lipids Health Dis *16*, 12.

Lee, Y.Z., Yang, C.W., Chang, H.Y., Hsu, H.Y., Chen, I.S., Chang, H.S., Lee, C.H., Lee, J.C., Kumar, C.R., Qiu, Y.Q.*, et al.* (2014). Discovery of selective inhibitors of Glutaminase-2, which inhibit mTORC1, activate autophagy and inhibit proliferation in cancer cells. Oncotarget *5*, 6087-6101.

Lepper, C., and Fan, C.M. (2010). Inducible lineage tracing of Pax7-descendant cells reveals embryonic origin of adult satellite cells. Genesis *48*, 424-436.

Leto, D., and Saltiel, A.R. (2012). Regulation of glucose transport by insulin: traffic control of GLUT4. Nat Rev Mol Cell Biol *13*, 383-396.

Letouze, E., Martinelli, C., Loriot, C., Burnichon, N., Abermil, N., Ottolenghi, C., Janin, M., Menara, M., Nguyen, A.T., Benit, P.*, et al.* (2013). SDH mutations establish a hypermethylator phenotype in paraganglioma. Cancer Cell *23*, 739-752.

Leung, Y.Y., Yao Hui, L.L., and Kraus, V.B. (2015). Colchicine--Update on mechanisms of action and therapeutic uses. Semin Arthritis Rheum *45*, 341-350.

Lhotak, S., Gyulay, G., Cutz, J.C., Al-Hashimi, A., Trigatti, B.L., Richards, C.D., Igdoura, S.A., Steinberg, G.R., Bramson, J., Ask, K.*, et al.* (2016). Characterization of Proliferating Lesion-Resident Cells During All Stages of Atherosclerotic Growth. J Am Heart Assoc *5*.

Li, A.C., and Glass, C.K. (2002). The macrophage foam cell as a target for therapeutic intervention. Nat Med *8*, 1235-1242.

Li, W., Qiu, X., Wang, J., Li, H., Sun, Y., Zhang, F., Jin, H., Fu, J., and Xia, Z. (2013). The therapeutic efficacy of glutamine for rats with smoking inhalation injury. Int Immunopharmacol *16*, 248-253.

Libby, P., and Everett, B.M. (2019). Novel Antiatherosclerotic Therapies. Arterioscler Thromb Vasc Biol *39*, 538-545.

Liu, J., Thewke, D.P., Su, Y.R., Linton, M.F., Fazio, S., and Sinensky, M.S. (2005). Reduced macrophage apoptosis is associated with accelerated atherosclerosis in low-density lipoprotein receptor-null mice. Arterioscler Thromb Vasc Biol *25*, 174-179.

Liu, P.S., Wang, H., Li, X., Chao, T., Teav, T., Christen, S., Di Conza, G., Cheng, W.C., Chou, C.H., Vavakova, M.*, et al.* (2017). alpha-ketoglutarate orchestrates macrophage activation through metabolic and epigenetic reprogramming. Nat Immunol *18*, 985-994.

Lo, K.A., and Sun, L. (2013). Turning WAT into BAT: a review on regulators controlling the browning of white adipocytes. Biosci Rep *33*.

Lo, L.H., Dong, R., Lyu, Q., and Lai, K.O. (2020). The Protein Arginine Methyltransferase PRMT8 and Substrate G3BP1 Control Rac1-PAK1 Signaling and Actin Cytoskeleton for Dendritic Spine Maturation. Cell Rep *31*, 107744.

Longo, M., Zatterale, F., Naderi, J., Parrillo, L., Formisano, P., Raciti, G.A., Beguinot, F., and Miele, C. (2019). Adipose Tissue Dysfunction as Determinant of Obesity-Associated Metabolic Complications. Int J Mol Sci *20*.

Lopez, D. (2008). Inhibition of PCSK9 as a novel strategy for the treatment of hypercholesterolemia. Drug News Perspect *21*, 323-330.

Lorenzatti, A., and Servato, M.L. (2018). Role of Anti-inflammatory Interventions in Coronary Artery Disease: Understanding the Canakinumab Anti-inflammatory Thrombosis Outcomes Study (CANTOS). Eur Cardiol *13*, 38-41.

Lumeng, C.N., Bodzin, J.L., and Saltiel, A.R. (2007a). Obesity induces a phenotypic switch in adipose tissue macrophage polarization. J Clin Invest *117*, 175-184.

Lumeng, C.N., DelProposto, J.B., Westcott, D.J., and Saltiel, A.R. (2008). Phenotypic switching of adipose tissue macrophages with obesity is generated by spatiotemporal differences in macrophage subtypes. Diabetes *57*, 3239-3246.

Lumeng, C.N., Deyoung, S.M., Bodzin, J.L., and Saltiel, A.R. (2007b). Increased inflammatory properties of adipose tissue macrophages recruited during diet-induced obesity. Diabetes *56*, 16-23.

Luo, P., Chu, S.F., Zhang, Z., Xia, C.Y., and Chen, N.H. (2019). Fractalkine/CX3CR1 is involved in the cross-talk between neuron and glia in neurological diseases. Brain Res Bull *146*, 12-21.

Lv, Z., Bian, Z., Shi, L., Niu, S., Ha, B., Tremblay, A., Li, L., Zhang, X., Paluszynski, J., Liu, M.*, et al.* (2015). Loss of Cell Surface CD47 Clustering Formation and Binding Avidity to SIRPalpha Facilitate Apoptotic Cell Clearance by Macrophages. J Immunol *195*, 661-671.

Maeda, N., Shimomura, I., Kishida, K., Nishizawa, H., Matsuda, M., Nagaretani, H., Furuyama, N., Kondo, H., Takahashi, M., Arita, Y.*, et al.* (2002). Diet-induced insulin resistance in mice lacking adiponectin/ACRP30. Nat Med *8*, 731-737.

Mao, Y., and Finnemann, S.C. (2015). Regulation of phagocytosis by Rho GTPases. Small GTPases *6*, 89-99.

Marotti, K.R., Castle, C.K., Murray, R.W., Rehberg, E.F., Polites, H.G., and Melchior, G.W. (1992). The role of cholesteryl ester transfer protein in primate apolipoprotein A-I metabolism. Insights from studies with transgenic mice. Arterioscler Thromb *12*, 736-744.

Martens, J.S., Reiner, N.E., Herrera-Velit, P., and Steinbrecher, U.P. (1998). Phosphatidylinositol 3-kinase is involved in the induction of macrophage growth by oxidized low density lipoprotein. J Biol Chem *273*, 4915-4920.

Martin-Rufian, M., Tosina, M., Campos-Sandoval, J.A., Manzanares, E., Lobo, C., Segura, J.A., Alonso, F.J., Mates, J.M., and Marquez, J. (2012). Mammalian glutaminase Gls2 gene encodes two functional alternative transcripts by a surrogate promoter usage mechanism. PLoS One *7*, e38380.

Martinet, W., Schrijvers, D.M., and De Meyer, G.R. (2011). Necrotic cell death in atherosclerosis. Basic Res Cardiol *106*, 749-760.

Masson, J., Darmon, M., Conjard, A., Chuhma, N., Ropert, N., Thoby-Brisson, M., Foutz, A.S., Parrot, S., Miller, G.M., Jorisch, R.*, et al.* (2006). Mice lacking brain/kidney phosphate-activated glutaminase have impaired glutamatergic synaptic transmission, altered breathing, disorganized goal-directed behavior and die shortly after birth. J Neurosci *26*, 4660-4671.

Mattson, M.P. (2010). Perspective: Does brown fat protect against diseases of aging? Ageing Res Rev *9*, 69-76.

Maximow, A. (1909). Der Lymphozyt als gemeinsame Stammzelle der verschiedenen Blutelemente in der embryonalen Entwicklung und im postfetalen Leben der Säugetiere. Folia Haematol pp. 125-134.

Mazaheri, F., Snaidero, N., Kleinberger, G., Madore, C., Daria, A., Werner, G., Krasemann, S., Capell, A., Trumbach, D., Wurst, W.*, et al.* (2017). TREM2 deficiency impairs chemotaxis and microglial responses to neuronal injury. EMBO Rep *18*, 1186-1198.

Mazat, J.P., and Ransac, S. (2019). The Fate of Glutamine in Human Metabolism. The Interplay with Glucose in Proliferating Cells. Metabolites *9*.

McCauley, R., Heel, K.A., Barker, P.R., and Hall, J. (1996). The effect of branched-chain amino acid-enriched parenteral nutrition on gut permeability. Nutrition *12*, 176-179.

McGivan, J.D., and Bungard, C.I. (2007). The transport of glutamine into mammalian cells. Front Biosci *12*, 874-882.

McGivan, J.D., Lacey, J.H., and Joseph, S.K. (1980). Localization and some properties of phosphate-dependent glutaminase in disrupted liver mitochondria. Biochem J *192*, 537-542.

McGrath, K.E., Frame, J.M., and Palis, J. (2015). Early hematopoiesis and macrophage development. Semin Immunol *27*, 379-387.

Meyer, C.W., Willershauser, M., Jastroch, M., Rourke, B.C., Fromme, T., Oelkrug, R., Heldmaier, G., and Klingenspor, M. (2010). Adaptive thermogenesis and thermal conductance in wild-type and UCP1-KO mice. Am J Physiol Regul Integr Comp Physiol *299*, R1396-1406.

Meyer Zum Buschenfelde, U., Brandenstein, L.I., von Elsner, L., Flato, K., Holling, T., Zenker, M., Rosenberger, G., and Kutsche, K. (2018). RIT1 controls actin dynamics via complex formation with RAC1/CDC42 and PAK1. PLoS Genet *14*, e1007370.

Michelucci, A., Cordes, T., Ghelfi, J., Pailot, A., Reiling, N., Goldmann, O., Binz, T., Wegner, A., Tallam, A., Rausell, A*., et al.* (2013). Immune-responsive gene 1 protein links metabolism to immunity by catalyzing itaconic acid production. Proc Natl Acad Sci U S A *110*, 7820-7825.

Mills, E.L., Kelly, B., Logan, A., Costa, A.S.H., Varma, M., Bryant, C.E., Tourlomousis, P., Dabritz, J.H.M., Gottlieb, E., Latorre, I*., et al.* (2016). Succinate Dehydrogenase Supports Metabolic Repurposing of Mitochondria to Drive Inflammatory Macrophages. Cell *167*, 457-470 e413.

Mills, E.L., Kelly, B., and O'Neill, L.A.J. (2017). Mitochondria are the powerhouses of immunity. Nat Immunol *18*, 488-498.

Mineo, P.M., Cassell, E.A., Roberts, M.E., and Schaeffer, P.J. (2012). Chronic cold acclimation increases thermogenic capacity, non-shivering thermogenesis and muscle citrate synthase activity in both wild-type and brown adipose tissue deficient mice. Comp Biochem Physiol A Mol Integr Physiol *161*, 395-400.

Mock, B., Kozak, C., Seldin, M.F., Ruff, N., D'Hoostelaere, L., Szpirer, C., Levan, G., Seuanez, H., O'Brien, S., and Banner, C. (1989). A glutaminase (gis) gene maps to mouse chromosome 1, rat chromosome 9, and human chromosome 2. Genomics *5*, 291-297.

Moncada, S., Higgs, E.A., and Colombo, S.L. (2012). Fulfilling the metabolic requirements for cell proliferation. Biochem J *446*, 1-7.

Monemdjou, S., Hofmann, W.E., Kozak, L.P., and Harper, M.E. (2000). Increased mitochondrial proton leak in skeletal muscle mitochondria of UCP1-deficient mice. Am J Physiol Endocrinol Metab *279*, E941-946.

Moore, K.J., Koplev, S., Fisher, E.A., Tabas, I., Bjorkegren, J.L.M., Doran, A.C., and Kovacic, J.C. (2018). Macrophage Trafficking, Inflammatory Resolution, and Genomics in Atherosclerosis: JACC Macrophage in CVD Series (Part 2). J Am Coll Cardiol *72*, 2181-2197.

Morioka, S., Perry, J.S.A., Raymond, M.H., Medina, C.B., Zhu, Y., Zhao, L., Serbulea, V., Onengut-Gumuscu, S., Leitinger, N., Kucenas, S.*, et al.* (2018). Efferocytosis induces a novel SLC program to promote glucose uptake and lactate release. Nature *563*, 714-718.

Mosser, D.M. (2003). The many faces of macrophage activation. J Leukoc Biol *73*, 209-212.

Mosser, D.M., and Edwards, J.P. (2008). Exploring the full spectrum of macrophage activation. Nat Rev Immunol *8*, 958-969.

Mottillo, E.P., Balasubramanian, P., Lee, Y.H., Weng, C., Kershaw, E.E., and Granneman, J.G. (2014). Coupling of lipolysis and de novo lipogenesis in brown, beige, and white adipose tissues during chronic beta3-adrenergic receptor activation. J Lipid Res *55*, 2276-2286.

Munzberg, H., Flier, J.S., and Bjorbaek, C. (2004). Region-specific leptin resistance within the hypothalamus of diet-induced obese mice. Endocrinology *145*, 4880-4889.

Myers, M.G., Jr., Leibel, R.L., Seeley, R.J., and Schwartz, M.W. (2010). Obesity and leptin resistance: distinguishing cause from effect. Trends Endocrinol Metab *21*, 643-651.

N, A.G., Bensinger, S.J., Hong, C., Beceiro, S., Bradley, M.N., Zelcer, N., Deniz, J., Ramirez, C., Diaz, M., Gallardo, G.*, et al.* (2009). Apoptotic cells promote their own clearance and immune tolerance through activation of the nuclear receptor LXR. Immunity *31*, 245-258.

Nagareddy, P.R., Kraakman, M., Masters, S.L., Stirzaker, R.A., Gorman, D.J., Grant, R.W., Dragoljevic, D., Hong, E.S., Abdel-Latif, A., Smyth, S.S.*, et al.* (2014). Adipose tissue macrophages promote myelopoiesis and monocytosis in obesity. Cell Metab *19*, 821-835.

Naghavi, M., Libby, P., Falk, E., Casscells, S.W., Litovsky, S., Rumberger, J., Badimon, J.J., Stefanadis, C., Moreno, P., Pasterkamp, G.*, et al.* (2003). From vulnerable plaque to vulnerable patient: a call for new definitions and risk assessment strategies: Part I. Circulation *108*, 1664-1672.

Nagy, C., and Haschemi, A. (2015). Time and Demand are Two Critical Dimensions of Immunometabolism: The Process of Macrophage Activation and the Pentose Phosphate Pathway. Front Immunol *6*, 164.

Nakanishi, T., Hatanaka, T., Huang, W., Prasad, P.D., Leibach, F.H., Ganapathy, M.E., and Ganapathy, V. (2001). Na+- and Cl--coupled active transport of carnitine by the amino acid transporter ATB(0,+) from mouse colon expressed in HRPE cells and Xenopus oocytes. J Physiol *532*, 297-304.

Nakashima, Y., Plump, A.S., Raines, E.W., Breslow, J.L., and Ross, R. (1994). ApoE-deficient mice develop lesions of all phases of atherosclerosis throughout the arterial tree. Arterioscler Thromb *14*, 133-140.

Nakaya, M., Xiao, Y., Zhou, X., Chang, J.H., Chang, M., Cheng, X., Blonska, M., Lin, X., and Sun, S.C. (2014). Inflammatory T cell responses rely on amino acid transporter ASCT2 facilitation of glutamine uptake and mTORC1 kinase activation. Immunity *40*, 692-705.

Napolitano, L., Scalise, M., Galluccio, M., Pochini, L., Albanese, L.M., and Indiveri, C. (2015). LAT1 is the transport competent unit of the LAT1/CD98 heterodimeric amino acid transporter. Int J Biochem Cell Biol *67*, 25-33.

Nawrocki, A.R., Rajala, M.W., Tomas, E., Pajvani, U.B., Saha, A.K., Trumbauer, M.E., Pang, Z., Chen, A.S., Ruderman, N.B., Chen, H.*, et al.* (2006). Mice lacking adiponectin show decreased hepatic insulin sensitivity and reduced responsiveness to peroxisome proliferator-activated receptor gamma agonists. J Biol Chem *281*, 2654-2660.

Nedergaard, J., Bengtsson, T., and Cannon, B. (2007). Unexpected evidence for active brown adipose tissue in adult humans. Am J Physiol Endocrinol Metab *293*, E444-452.

Newsholme, E.A., Crabtree, B., and Ardawi, M.S. (1985). Glutamine metabolism in lymphocytes: its biochemical, physiological and clinical importance. Q J Exp Physiol *70*, 473-489.

Newsholme, P., Curi, R., Gordon, S., and Newsholme, E.A. (1986). Metabolism of glucose, glutamine, long-chain fatty acids and ketone bodies by murine macrophages. Biochem J *239*, 121-125.

Newsholme, P., Gordon, S., and Newsholme, E.A. (1987). Rates of utilization and fates of glucose, glutamine, pyruvate, fatty acids and ketone bodies by mouse macrophages. Biochem J *242*, 631-636.

Newsholme, P., Lima, M.M., Procopio, J., Pithon-Curi, T.C., Doi, S.Q., Bazotte, R.B., and Curi, R. (2003a). Glutamine and glutamate as vital metabolites. Braz J Med Biol Res *36*, 153-163.

Newsholme, P., Procopio, J., Lima, M.M., Pithon-Curi, T.C., and Curi, R. (2003b). Glutamine and glutamate--their central role in cell metabolism and function. Cell Biochem Funct *21*, 1-9.

Nguyen, K.D., Qiu, Y., Cui, X., Goh, Y.P., Mwangi, J., David, T., Mukundan, L., Brombacher, F., Locksley, R.M., and Chawla, A. (2011). Alternatively activated macrophages produce catecholamines to sustain adaptive thermogenesis. Nature *480*, 104-108.

Nicholls, S.J., Ballantyne, C.M., Barter, P.J., Chapman, M.J., Erbel, R.M., Libby, P., Raichlen, J.S., Uno, K., Borgman, M., Wolski, K.*, et al.* (2011). Effect of two intensive statin regimens on progression of coronary disease. N Engl J Med *365*, 2078-2087.

Niihara, Y., Miller, S.T., Kanter, J., Lanzkron, S., Smith, W.R., Hsu, L.L., Gordeuk, V.R., Viswanathan, K., Sarnaik, S., Osunkwo, I.*, et al.* (2018). A Phase 3 Trial of l-Glutamine in Sickle Cell Disease. N Engl J Med *379*, 226-235.

Nissen, S.E., Nicholls, S.J., Sipahi, I., Libby, P., Raichlen, J.S., Ballantyne, C.M., Davignon, J., Erbel, R., Fruchart, J.C., Tardif, J.C*., et al.* (2006). Effect of very high-intensity statin therapy on regression of coronary atherosclerosis: the ASTEROID trial. JAMA *295*, 1556-1565.

Nomura, M., Liu, J., Rovira, II, Gonzalez-Hurtado, E., Lee, J., Wolfgang, M.J., and Finkel, T. (2016). Fatty acid oxidation in macrophage polarization. Nat Immunol *17*, 216-217.

O'Neill, L.A. (2015). A broken krebs cycle in macrophages. Immunity *42*, 393-394.

O'Neill, L.A. (2016). A Metabolic Roadblock in Inflammatory Macrophages. Cell Rep *17*, 625-626.

Ocana-Guzman, R., Torre-Bouscoulet, L., and Sada-Ovalle, I. (2016). TIM-3 Regulates Distinct Functions in Macrophages. Front Immunol *7*, 229.

Odegaard, J.I., Ricardo-Gonzalez, R.R., Goforth, M.H., Morel, C.R., Subramanian, V., Mukundan, L., Red Eagle, A., Vats, D., Brombacher, F., Ferrante, A.W*., et al.* (2007). Macrophage-specific PPARgamma controls alternative activation and improves insulin resistance. Nature *447*, 1116-1120.

Oka, K., Sawamura, T., Kikuta, K., Itokawa, S., Kume, N., Kita, T., and Masaki, T. (1998). Lectin-like oxidized low-density lipoprotein receptor 1 mediates phagocytosis of aged/apoptotic cells in endothelial cells. Proc Natl Acad Sci U S A *95*, 9535-9540.

Olalla, L., Gutierrez, A., Campos, J.A., Khan, Z.U., Alonso, F.J., Segura, J.A., Marquez, J., and Aledo, J.C. (2002). Nuclear localization of L-type glutaminase in mammalian brain. J Biol Chem *277*, 38939-38944.

Oldenborg, P.A., Gresham, H.D., and Lindberg, F.P. (2001). CD47-signal regulatory protein alpha (SIRPalpha) regulates Fcgamma and complement receptor-mediated phagocytosis. J Exp Med *193*, 855-862.

Oppedisano, F., Pochini, L., Broer, S., and Indiveri, C. (2011). The B degrees AT1 amino acid transporter from rat kidney reconstituted in liposomes: kinetics and inactivation by methylmercury. Biochim Biophys Acta *1808*, 2551-2558.

Orava, J., Nuutila, P., Lidell, M.E., Oikonen, V., Noponen, T., Viljanen, T., Scheinin, M., Taittonen, M., Niemi, T., Enerback, S*., et al.* (2011). Different metabolic responses of human brown adipose tissue to activation by cold and insulin. Cell Metab *14*, 272-279.

Orkin, S.H., and Zon, L.I. (2008). Hematopoiesis: an evolving paradigm for stem cell biology. Cell *132*, 631-644.

Ouellet, V., Labbe, S.M., Blondin, D.P., Phoenix, S., Guerin, B., Haman, F., Turcotte, E.E., Richard, D., and Carpentier, A.C. (2012). Brown adipose tissue oxidative metabolism contributes to energy expenditure during acute cold exposure in humans. J Clin Invest *122*, 545-552.

Ouimet, M., Franklin, V., Mak, E., Liao, X., Tabas, I., and Marcel, Y.L. (2011). Autophagy regulates cholesterol efflux from macrophage foam cells via lysosomal acid lipase. Cell Metab *13*, 655-667.

Oxender, D.L., and Christensen, H.N. (1963). Evidence for two types of mediation of neutral and amino-acid transport in Ehrlich cells. Nature *197*, 765-767.

Paalvast, Y., Gerding, A., Wang, Y., Bloks, V.W., van Dijk, T.H., Havinga, R., Willems van Dijk, K., Rensen, P.C.N., Bakker, B.M., Kuivenhoven, J.A*., et al.* (2017). Male apoE*3-Leiden.CETP mice on high-fat high-cholesterol diet exhibit a biphasic dyslipidemic response, mimicking the changes in plasma lipids observed through life in men. Physiol Rep *5*.

Pagler, T.A., Rhode, S., Neuhofer, A., Laggner, H., Strobl, W., Hinterndorfer, C., Volf, I., Pavelka, M., Eckhardt, E.R., van der Westhuyzen, D.R*., et al.* (2006). SR-BI-mediated high density lipoprotein (HDL) endocytosis leads to HDL resecretion facilitating cholesterol efflux. J Biol Chem *281*, 11193-11204.

Palis, J., Robertson, S., Kennedy, M., Wall, C., and Keller, G. (1999). Development of erythroid and myeloid progenitors in the yolk sac and embryo proper of the mouse. Development *126*, 5073-5084.

Palis, J., and Yoder, M.C. (2001). Yolk-sac hematopoiesis: the first blood cells of mouse and man. Exp Hematol *29*, 927-936.

Palmieri, E.M., Menga, A., Martin-Perez, R., Quinto, A., Riera-Domingo, C., De Tullio, G., Hooper, D.C., Lamers, W.H., Ghesquiere, B., McVicar, D.W*., et al.* (2017). Pharmacologic or Genetic Targeting of Glutamine Synthetase Skews Macrophages toward an M1-like Phenotype and Inhibits Tumor Metastasis. Cell Rep *20*, 1654-1666.

Papandreou, I., Cairns, R.A., Fontana, L., Lim, A.L., and Denko, N.C. (2006). HIF-1 mediates adaptation to hypoxia by actively downregulating mitochondrial oxygen consumption. Cell Metab *3*, 187-197.

Park, D., Tosello-Trampont, A.C., Elliott, M.R., Lu, M., Haney, L.B., Ma, Z., Klibanov, A.L., Mandell, J.W., and Ravichandran, K.S. (2007). BAI1 is an engulfment receptor for apoptotic cells upstream of the ELMO/Dock180/Rac module. Nature *450*, 430-434.

Park, S.Y., Kim, J.K., Kim, I.J., Choi, B.K., Jung, K.Y., Lee, S., Park, K.J., Chairoungdua, A., Kanai, Y., Endou, H*., et al.* (2005). Reabsorption of neutral amino acids mediated by amino acid transporter LAT2 and TAT1 in the basolateral membrane of proximal tubule. Arch Pharm Res *28*, 421-432.

Park, Y.M., Febbraio, M., and Silverstein, R.L. (2009). CD36 modulates migration of mouse and human macrophages in response to oxidized LDL and may contribute to macrophage trapping in the arterial intima. J Clin Invest *119*, 136-145.

Patel, D., Menon, D., Bernfeld, E., Mroz, V., Kalan, S., Loayza, D., and Foster, D.A. (2016). Aspartate Rescues S-phase Arrest Caused by Suppression of Glutamine Utilization in KRas-driven Cancer Cells. J Biol Chem *291*, 9322-9329.

Patel, M., and McGivan, J.D. (1984). Partial purification and properties of rat liver glutaminase. Biochem J *220*, 583-590.

Paulson, K.E., Zhu, S.N., Chen, M., Nurmohamed, S., Jongstra-Bilen, J., and Cybulsky, M.I. (2010). Resident intimal dendritic cells accumulate lipid and contribute to the initiation of atherosclerosis. Circ Res *106*, 383-390.

Pelleymounter, M.A., Cullen, M.J., Baker, M.B., Hecht, R., Winters, D., Boone, T., and Collins, F. (1995). Effects of the obese gene product on body weight regulation in ob/ob mice. Science *269*, 540-543.

Pentikainen, M.O., Oorni, K., Ala-Korpela, M., and Kovanen, P.T. (2000). Modified LDL - trigger of atherosclerosis and inflammation in the arterial intima. J Intern Med *247*, 359-370.

Periasamy, M., Maurya, S.K., Sahoo, S.K., Singh, S., Sahoo, S.K., Reis, F.C.G., and Bal, N.C. (2017). Role of SERCA Pump in Muscle Thermogenesis and Metabolism. Compr Physiol *7*, 879-890.

Petrus, P., Lecoutre, S., Dollet, L., Wiel, C., Sulen, A., Gao, H., Tavira, B., Laurencikiene, J., Rooyackers, O., Checa, A*., et al.* (2020). Glutamine Links Obesity to Inflammation in Human White Adipose Tissue. Cell Metab *31*, 375-390 e311.

Phang, J.M., Liu, W., Hancock, C.N., and Fischer, J.W. (2015). Proline metabolism and cancer: emerging links to glutamine and collagen. Curr Opin Clin Nutr Metab Care *18*, 71-77.

Piedrahita, J.A., Zhang, S.H., Hagaman, J.R., Oliver, P.M., and Maeda, N. (1992). Generation of mice carrying a mutant apolipoprotein E gene inactivated by gene targeting in embryonic stem cells. Proc Natl Acad Sci U S A *89*, 4471-4475.

Pineda, M., Fernandez, E., Torrents, D., Estevez, R., Lopez, C., Camps, M., Lloberas, J., Zorzano, A., and Palacin, M. (1999). Identification of a membrane protein, LAT-2, that Co-expresses with 4F2 heavy chain, an L-type amino acid transport activity with broad specificity for small and large zwitterionic amino acids. J Biol Chem *274*, 19738-19744.

Pinel, C., Coxam, V., Mignon, M., Taillandier, D., Cubizolles, C., Lebecque, P., Darmaun, D., and Meynial-Denis, D. (2006). Alterations in glutamine synthetase activity in rat skeletal muscle are associated with advanced age. Nutrition *22*, 778-785.

Pingitore, P., Pochini, L., Scalise, M., Galluccio, M., Hedfalk, K., and Indiveri, C. (2013). Large scale production of the active human ASCT2 (SLC1A5) transporter in Pichia pastoris--functional and kinetic asymmetry revealed in proteoliposomes. Biochim Biophys Acta *1828*, 2238-2246.

Pirzgalska, R.M., Seixas, E., Seidman, J.S., Link, V.M., Sanchez, N.M., Mahu, I., Mendes, R., Gres, V., Kubasova, N., Morris, I.*, et al.* (2017). Sympathetic neuron-associated macrophages contribute to obesity by importing and metabolizing norepinephrine. Nat Med *23*, 1309-1318.

Pithon-Curi, T.C., Levada, A.C., Lopes, L.R., Doi, S.Q., and Curi, R. (2002). Glutamine plays a role in superoxide production and the expression of p47phox, p22phox and gp91phox in rat neutrophils. Clin Sci (Lond) *103*, 403-408.

Plump, A.S., Smith, J.D., Hayek, T., Aalto-Setala, K., Walsh, A., Verstuyft, J.G., Rubin, E.M., and Breslow, J.L. (1992). Severe hypercholesterolemia and atherosclerosis in apolipoprotein E-deficient mice created by homologous recombination in ES cells. Cell *71*, 343-353.

Poirier, S., Mayer, G., Benjannet, S., Bergeron, E., Marcinkiewicz, J., Nassoury, N., Mayer, H., Nimpf, J., Prat, A., and Seidah, N.G. (2008). The proprotein convertase PCSK9 induces the degradation of low density lipoprotein receptor (LDLR) and its closest family members VLDLR and ApoER2. J Biol Chem *283*, 2363-2372.

Poissonnet, C.M., Burdi, A.R., and Garn, S.M. (1984). The chronology of adipose tissue appearance and distribution in the human fetus. Early Hum Dev *10*, 1-11.

Pond, C.M. (1992). An evolutionary and functional view of mammalian adipose tissue. Proc Nutr Soc *51*, 367-377.

Pramod, A.B., Foster, J., Carvelli, L., and Henry, L.K. (2013). SLC6 transporters: structure, function, regulation, disease association and therapeutics. Mol Aspects Med *34*, 197-219.

Prasad, P.D., Wang, H., Huang, W., Kekuda, R., Rajan, D.P., Leibach, F.H., and Ganapathy, V. (1999). Human LAT1, a subunit of system L amino acid transporter: molecular cloning and transport function. Biochem Biophys Res Commun *255*, 283-288.

Pridans, C., Raper, A., Davis, G.M., Alves, J., Sauter, K.A., Lefevre, L., Regan, T., Meek, S., Sutherland, L., Thomson, A.J.*, et al.* (2018). Pleiotropic Impacts of Macrophage and Microglial Deficiency on Development in Rats with Targeted Mutation of the Csf1r Locus. J Immunol *201*, 2683-2699.

Prieur, X., Mok, C.Y., Velagapudi, V.R., Nunez, V., Fuentes, L., Montaner, D., Ishikawa, K., Camacho, A., Barbarroja, N., O'Rahilly, S.*, et al.* (2011). Differential lipid partitioning between adipocytes and tissue macrophages modulates macrophage lipotoxicity and M2/M1 polarization in obese mice. Diabetes *60*, 797-809.

Proto, J.D., Doran, A.C., Gusarova, G., Yurdagul, A., Jr., Sozen, E., Subramanian, M., Islam, M.N., Rymond, C.C., Du, J., Hook, J.*, et al.* (2018). Regulatory T Cells Promote Macrophage Efferocytosis during Inflammation Resolution. Immunity *49*, 666-677 e666.

Puleston, D.J., Buck, M.D., Klein Geltink, R.I., Kyle, R.L., Caputa, G., O'Sullivan, D., Cameron, A.M., Castoldi, A., Musa, Y., Kabat, A.M.*, et al.* (2019). Polyamines and eIF5A Hypusination Modulate Mitochondrial Respiration and Macrophage Activation. Cell Metab *30*, 352-363 e358.

Putri, M., Syamsunarno, M.R., Iso, T., Yamaguchi, A., Hanaoka, H., Sunaga, H., Koitabashi, N., Matsui, H., Yamazaki, C., Kameo, S.*, et al.* (2015). CD36 is indispensable for thermogenesis under conditions of fasting and cold stress. Biochem Biophys Res Commun *457*, 520-525.

Qiao, J.H., Tripathi, J., Mishra, N.K., Cai, Y., Tripathi, S., Wang, X.P., Imes, S., Fishbein, M.C., Clinton, S.K., Libby, P.*, et al.* (1997). Role of macrophage colony-stimulating factor in atherosclerosis: studies of osteopetrotic mice. Am J Pathol *150*, 1687-1699.

Qiu, Y., Nguyen, K.D., Odegaard, J.I., Cui, X., Tian, X., Locksley, R.M., Palmiter, R.D., and Chawla, A. (2014). Eosinophils and type 2 cytokine signaling in macrophages orchestrate development of functional beige fat. Cell *157*, 1292-1308.

Rafieian-Kopaei, M., Setorki, M., Doudi, M., Baradaran, A., and Nasri, H. (2014). Atherosclerosis: process, indicators, risk factors and new hopes. Int J Prev Med *5*, 927-946.

Rahman, M.S., Murphy, A.J., and Woollard, K.J. (2017). Effects of dyslipidaemia on monocyte production and function in cardiovascular disease. Nat Rev Cardiol *14*, 387-400.

Ramkumar, S., Raghunath, A., and Raghunath, S. (2016). Statin Therapy: Review of Safety and Potential Side Effects. Acta Cardiol Sin *32*, 631-639.

Randolph, G.J. (2008). Emigration of monocyte-derived cells to lymph nodes during resolution of inflammation and its failure in atherosclerosis. Curr Opin Lipidol *19*, 462-468.

Randolph, G.J. (2014). Mechanisms that regulate macrophage burden in atherosclerosis. Circ Res *114*, 1757-1771.

Rao, R.R., Long, J.Z., White, J.P., Svensson, K.J., Lou, J., Lokurkar, I., Jedrychowski, M.P., Ruas, J.L., Wrann, C.D., Lo, J.C.*, et al.* (2014). Meteorin-like is a hormone that regulates immune-adipose interactions to increase beige fat thermogenesis. Cell *157*, 1279-1291.

Rathore, M.G., Saumet, A., Rossi, J.F., de Bettignies, C., Tempe, D., Lecellier, C.H., and Villalba, M. (2012). The NF-kappaB member p65 controls glutamine metabolism through miR-23a. Int J Biochem Cell Biol *44*, 1448-1456.

Ravichandran, K.S., and Lorenz, U. (2007). Engulfment of apoptotic cells: signals for a good meal. Nat Rev Immunol *7*, 964-974.

Ray, K.K., Stoekenbroek, R.M., Kallend, D., Nishikido, T., Leiter, L.A., Landmesser, U., Wright, R.S., Wijngaard, P.L.J., and Kastelein, J.J.P. (2019). Effect of 1 or 2 Doses of Inclisiran on Low-Density Lipoprotein Cholesterol Levels: One-Year Follow-up of the ORION-1 Randomized Clinical Trial. JAMA Cardiol.

Reiner, Z., Guardamagna, O., Nair, D., Soran, H., Hovingh, K., Bertolini, S., Jones, S., Coric, M., Calandra, S., Hamilton, J.*, et al.* (2014). Lysosomal acid lipase deficiency--an under-recognized cause of dyslipidaemia and liver dysfunction. Atherosclerosis *235*, 21-30.

Ricquier, D., and Kader, J.C. (1976). Mitochondrial protein alteration in active brown fat: a soidum dodecyl sulfate-polyacrylamide gel electrophoretic study. Biochem Biophys Res Commun *73*, 577-583.

Ridker, P.M., Everett, B.M., Pradhan, A., MacFadyen, J.G., Solomon, D.H., Zaharris, E., Mam, V., Hasan, A., Rosenberg, Y., Iturriaga, E.*, et al.* (2019). Low-Dose Methotrexate for the Prevention of Atherosclerotic Events. N Engl J Med *380*, 752-762.

Ridker, P.M., Everett, B.M., Thuren, T., MacFadyen, J.G., Chang, W.H., Ballantyne, C., Fonseca, F., Nicolau, J., Koenig, W., Anker, S.D.*, et al.* (2017). Antiinflammatory Therapy with Canakinumab for Atherosclerotic Disease. N Engl J Med *377*, 1119-1131.

Ridker, P.M., Rose, L.M., Kastelein, J.J.P., Santos, R.D., Wei, C., Revkin, J., Yunis, C., Tardif, J.C., Shear, C.L., Studies of, P.I.*, et al.* (2018). Cardiovascular event reduction with PCSK9 inhibition among 1578 patients with familial hypercholesterolemia: Results from the SPIRE randomized trials of bococizumab. J Clin Lipidol *12*, 958-965.

Rius, J., Guma, M., Schachtrup, C., Akassoglou, K., Zinkernagel, A.S., Nizet, V., Johnson, R.S., Haddad, G.G., and Karin, M. (2008). NF-kappaB links innate immunity to the hypoxic response through transcriptional regulation of HIF-1alpha. Nature *453*, 807-811.

Robbins, C.S., Chudnovskiy, A., Rauch, P.J., Figueiredo, J.L., Iwamoto, Y., Gorbatov, R., Etzrodt, M., Weber, G.F., Ueno, T., van Rooijen, N.*, et al.* (2012). Extramedullary hematopoiesis generates Ly-6C(high) monocytes that infiltrate atherosclerotic lesions. Circulation *125*, 364-374.

Robbins, C.S., Hilgendorf, I., Weber, G.F., Theurl, I., Iwamoto, Y., Figueiredo, J.L., Gorbatov, R., Sukhova, G.K., Gerhardt, L.M., Smyth, D.*, et al.* (2013). Local proliferation dominates lesional macrophage accumulation in atherosclerosis. Nat Med *19*, 1166-1172.

Roche-Molina, M., Sanz-Rosa, D., Cruz, F.M., Garcia-Prieto, J., Lopez, S., Abia, R., Muriana, F.J., Fuster, V., Ibanez, B., and Bernal, J.A. (2015). Induction of sustained hypercholesterolemia by single adeno-associated virus-mediated gene transfer of mutant hPCSK9. Arterioscler Thromb Vasc Biol *35*, 50-59.

Rodas, P.C., Rooyackers, O., Hebert, C., Norberg, A., and Wernerman, J. (2012). Glutamine and glutathione at ICU admission in relation to outcome. Clin Sci (Lond) *122*, 591-597.

Rodriguez-Prados, J.C., Traves, P.G., Cuenca, J., Rico, D., Aragones, J., Martin-Sanz, P., Cascante, M., and Bosca, L. (2010). Substrate fate in activated macrophages: a comparison between innate, classic, and alternative activation. J Immunol *185*, 605-614.

Rosenfeld, M.E., Polinsky, P., Virmani, R., Kauser, K., Rubanyi, G., and Schwartz, S.M. (2000). Advanced atherosclerotic lesions in the innominate artery of the ApoE knockout mouse. Arterioscler Thromb Vasc Biol *20*, 2587-2592.

Rosenwald, M., Perdikari, A., Rulicke, T., and Wolfrum, C. (2013). Bi-directional interconversion of brite and white adipocytes. Nat Cell Biol *15*, 659-667.

Roth, E. (2008). Nonnutritive effects of glutamine. J Nutr *138*, 2025S-2031S.

Ruperto, N., Brunner, H.I., Quartier, P., Constantin, T., Wulffraat, N., Horneff, G., Brik, R., McCann, L., Kasapcopur, O., Rutkowska-Sak, L.*, et al.* (2012). Two randomized trials of canakinumab in systemic juvenile idiopathic arthritis. N Engl J Med *367*, 2396-2406.

Sabatine, M.S., Giugliano, R.P., Keech, A., Honarpour, N., Wang, H., Liu, T., Wasserman, S.M., Scott, R., Sever, P.S., and Pedersen, T.R. (2016). Rationale and design of the Further cardiovascular OUtcomes Research with PCSK9 Inhibition in subjects with Elevated Risk trial. Am Heart J *173*, 94-101.

Sacks, F.M., Pfeffer, M.A., Moye, L.A., Rouleau, J.L., Rutherford, J.D., Cole, T.G., Brown, L., Warnica, J.W., Arnold, J.M., Wun, C.C.*, et al.* (1996). The effect of pravastatin on coronary events after myocardial infarction in patients with average cholesterol levels. Cholesterol and Recurrent Events Trial investigators. N Engl J Med *335*, 1001-1009.

Sage, A.P., Tsiantoulas, D., Binder, C.J., and Mallat, Z. (2019). The role of B cells in atherosclerosis. Nat Rev Cardiol *16*, 180-196.

Sammeth, M., Foissac, S., and Guigo, R. (2008). A general definition and nomenclature for alternative splicing events. PLoS Comput Biol *4*, e1000147.

Samokhvalov, I.M., Samokhvalova, N.I., and Nishikawa, S. (2007). Cell tracing shows the contribution of the yolk sac to adult haematopoiesis. Nature *446*, 1056-1061.

Sastrasinh, S., and Sastrasinh, M. (1989). Glutamine transport in submitochondrial particles. Am J Physiol *257*, F1050-1058.

Sather, S., Kenyon, K.D., Lefkowitz, J.B., Liang, X., Varnum, B.C., Henson, P.M., and Graham, D.K. (2007). A soluble form of the Mer receptor tyrosine kinase inhibits macrophage clearance of apoptotic cells and platelet aggregation. Blood *109*, 1026-1033.

Scalise, M., Galluccio, M., Console, L., Pochini, L., and Indiveri, C. (2018). The Human SLC7A5 (LAT1): The Intriguing Histidine/Large Neutral Amino Acid Transporter and Its Relevance to Human Health. Front Chem *6*, 243.

Schaefer, E.J., Gregg, R.E., Ghiselli, G., Forte, T.M., Ordovas, J.M., Zech, L.A., and Brewer, H.B., Jr. (1986). Familial apolipoprotein E deficiency. J Clin Invest *78*, 1206-1219.

Scheja, L., and Heeren, J. (2019). The endocrine function of adipose tissues in health and cardiometabolic disease. Nat Rev Endocrinol *15*, 507-524.

Scherer, P.E., Williams, S., Fogliano, M., Baldini, G., and Lodish, H.F. (1995). A novel serum protein similar to C1q, produced exclusively in adipocytes. J Biol Chem *270*, 26746-26749.

Schioth, H.B., Roshanbin, S., Hagglund, M.G., and Fredriksson, R. (2013). Evolutionary origin of amino acid transporter families SLC32, SLC36 and SLC38 and physiological, pathological and therapeutic aspects. Mol Aspects Med *34*, 571-585.

Schmoker, J.D., Terrien, C., 3rd, McPartland, K.J., Boyum, J., Wellman, G.C., Trombley, L., and Kinne, J. (2009). Cerebrovascular response to continuous cold perfusion and hypothermic circulatory arrest. J Thorac Cardiovasc Surg *137*, 459-464.

Schultze, J.L., Mass, E., and Schlitzer, A. (2019). Emerging Principles in Myelopoiesis at Homeostasis and during Infection and Inflammation. Immunity *50*, 288-301.

Schulz, C., Gomez Perdiguero, E., Chorro, L., Szabo-Rogers, H., Cagnard, N., Kierdorf, K., Prinz, M., Wu, B., Jacobsen, S.E., Pollard, J.W*., et al.* (2012). A lineage of myeloid cells independent of Myb and hematopoietic stem cells. Science *336*, 86-90.

Scott, T., and Owens, M.D. (2008). Thrombocytes respond to lipopolysaccharide through Toll-like receptor-4, and MAP kinase and NF-kappaB pathways leading to expression of interleukin-6 and cyclooxygenase-2 with production of prostaglandin E2. Mol Immunol *45*, 1001-1008.

Seale, P., Bjork, B., Yang, W., Kajimura, S., Chin, S., Kuang, S., Scime, A., Devarakonda, S., Conroe, H.M., Erdjument-Bromage, H*., et al.* (2008). PRDM16 controls a brown fat/skeletal muscle switch. Nature *454*, 961-967.

Seita, J., and Weissman, I.L. (2010). Hematopoietic stem cell: self-renewal versus differentiation. Wiley Interdiscip Rev Syst Biol Med *2*, 640-653.

Serbina, N.V., and Pamer, E.G. (2006). Monocyte emigration from bone marrow during bacterial infection requires signals mediated by chemokine receptor CCR2. Nat Immunol *7*, 311-317.

Shabalina, I.G., Hoeks, J., Kramarova, T.V., Schrauwen, P., Cannon, B., and Nedergaard, J. (2010). Cold tolerance of UCP1-ablated mice: a skeletal muscle mitochondria switch toward lipid oxidation with marked UCP3 up-regulation not associated with increased basal, fatty acid- or ROS-induced uncoupling or enhanced GDP effects. Biochim Biophys Acta *1797*, 968-980.

Shan, L., Pang, L., Zhang, R., Murgolo, N.J., Lan, H., and Hedrick, J.A. (2008). PCSK9 binds to multiple receptors and can be functionally inhibited by an EGF-A peptide. Biochem Biophys Res Commun *375*, 69-73.

Shapiro, R.A., Farrell, L., Srinivasan, M., and Curthoys, N.P. (1991). Isolation, characterization, and in vitro expression of a cDNA that encodes the kidney isoenzyme of the mitochondrial glutaminase. J Biol Chem *266*, 18792-18796.

Shaw, P.X., Horkko, S., Tsimikas, S., Chang, M.K., Palinski, W., Silverman, G.J., Chen, P.P., and Witztum, J.L. (2001). Human-derived anti-oxidized LDL autoantibody blocks uptake of oxidized LDL by macrophages and localizes to atherosclerotic lesions in vivo. Arterioscler Thromb Vasc Biol *21*, 1333-1339.

Shepherd, J., Cobbe, S.M., Ford, I., Isles, C.G., Lorimer, A.R., MacFarlane, P.W., McKillop, J.H., and Packard, C.J. (1995). Prevention of coronary heart disease with pravastatin in men with

hypercholesterolemia. West of Scotland Coronary Prevention Study Group. N Engl J Med *333*, 1301-1307.

Shi, C., Jia, T., Mendez-Ferrer, S., Hohl, T.M., Serbina, N.V., Lipuma, L., Leiner, I., Li, M.O., Frenette, P.S., and Pamer, E.G. (2011). Bone marrow mesenchymal stem and progenitor cells induce monocyte emigration in response to circulating toll-like receptor ligands. Immunity *34*, 590-601.

Shi, H., Kokoeva, M.V., Inouye, K., Tzameli, I., Yin, H., and Flier, J.S. (2006). TLR4 links innate immunity and fatty acid-induced insulin resistance. J Clin Invest *116*, 3015-3025.

Sica, A., and Mantovani, A. (2012). Macrophage plasticity and polarization: in vivo veritas. J Clin Invest *122*, 787-795.

Singleton, K.D., and Wischmeyer, P.E. (2007). Glutamine's protection against sepsis and lung injury is dependent on heat shock protein 70 expression. Am J Physiol Regul Integr Comp Physiol *292*, R1839-1845.

Smith, E.M., and Watford, M. (1988). Rat hepatic glutaminase: purification and immunochemical characterization. Arch Biochem Biophys *260*, 740-751.

Smith, W.S., Broadbridge, R., East, J.M., and Lee, A.G. (2002). Sarcolipin uncouples hydrolysis of ATP from accumulation of Ca2+ by the Ca2+-ATPase of skeletal-muscle sarcoplasmic reticulum. Biochem J *361*, 277-286.

Solomon, D.H., Liu, C.C., Kuo, I.H., Zak, A., and Kim, S.C. (2016). Effects of colchicine on risk of cardiovascular events and mortality among patients with gout: a cohort study using electronic medical records linked with Medicare claims. Ann Rheum Dis *75*, 1674-1679.

Son, J., Lyssiotis, C.A., Ying, H., Wang, X., Hua, S., Ligorio, M., Perera, R.M., Ferrone, C.R., Mullarky, E., Shyh-Chang, N*., et al.* (2013). Glutamine supports pancreatic cancer growth through a KRAS-regulated metabolic pathway. Nature *496*, 101-105.

Spalding, K.L., Arner, E., Westermark, P.O., Bernard, S., Buchholz, B.A., Bergmann, O., Blomqvist, L., Hoffstedt, J., Naslund, E., Britton, T*., et al.* (2008). Dynamics of fat cell turnover in humans. Nature *453*, 783-787.

Srinivasan, M., Kalousek, F., Farrell, L., and Curthoys, N.P. (1995). Role of the N-terminal 118 amino acids in the processing of the rat renal mitochondrial glutaminase precursor. J Biol Chem *270*, 1191-1197.

Stary, H.C., Chandler, A.B., Dinsmore, R.E., Fuster, V., Glagov, S., Insull, W., Jr., Rosenfeld, M.E., Schwartz, C.J., Wagner, W.D., and Wissler, R.W. (1995). A definition of advanced types of atherosclerotic lesions and a histological classification of atherosclerosis. A report from the Committee on Vascular Lesions of the Council on Arteriosclerosis, American Heart Association. Arterioscler Thromb Vasc Biol *15*, 1512-1531.

Stein, M., Keshav, S., Harris, N., and Gordon, S. (1992). Interleukin 4 potently enhances murine macrophage mannose receptor activity: a marker of alternative immunologic macrophage activation. J Exp Med *176*, 287-292.

Strong, J.P., Malcom, G.T., McMahan, C.A., Tracy, R.E., Newman, W.P., 3rd, Herderick, E.E., and Cornhill, J.F. (1999). Prevalence and extent of atherosclerosis in adolescents and young adults: implications for prevention from the Pathobiological Determinants of Atherosclerosis in Youth Study. JAMA *281*, 727-735.

Subbanagounder, G., Wong, J.W., Lee, H., Faull, K.F., Miller, E., Witztum, J.L., and Berliner, J.A. (2002). Epoxyisoprostane and epoxycyclopentenone phospholipids regulate monocyte chemotactic protein-1 and interleukin-8 synthesis. Formation of these oxidized phospholipids in response to interleukin-1beta. J Biol Chem *277*, 7271-7281.

Suganami, T., Nishida, J., and Ogawa, Y. (2005). A paracrine loop between adipocytes and macrophages aggravates inflammatory changes: role of free fatty acids and tumor necrosis factor alpha. Arterioscler Thromb Vasc Biol *25*, 2062-2068.

Sullivan, L.B., Gui, D.Y., Hosios, A.M., Bush, L.N., Freinkman, E., and Vander Heiden, M.G. (2015). Supporting Aspartate Biosynthesis Is an Essential Function of Respiration in Proliferating Cells. Cell *162*, 552-563.

Suzuki, H., Kurihara, Y., Takeya, M., Kamada, N., Kataoka, M., Jishage, K., Ueda, O., Sakaguchi, H., Higashi, T., Suzuki, T*., et al.* (1997). A role for macrophage scavenger receptors in atherosclerosis and susceptibility to infection. Nature *386*, 292-296.

Swirski, F.K., Nahrendorf, M., Etzrodt, M., Wildgruber, M., Cortez-Retamozo, V., Panizzi, P., Figueiredo, J.L., Kohler, R.H., Chudnovskiy, A., Waterman, P*., et al.* (2009). Identification of splenic reservoir monocytes and their deployment to inflammatory sites. Science *325*, 612-616.

Swirski, F.K., Pittet, M.J., Kircher, M.F., Aikawa, E., Jaffer, F.A., Libby, P., and Weissleder, R. (2006). Monocyte accumulation in mouse atherogenesis is progressive and proportional to extent of disease. Proc Natl Acad Sci U S A *103*, 10340-10345.

Tabas, I. (2010). Macrophage death and defective inflammation resolution in atherosclerosis. Nat Rev Immunol *10*, 36-46.

Tacke, F., Alvarez, D., Kaplan, T.J., Jakubzick, C., Spanbroek, R., Llodra, J., Garin, A., Liu, J., Mack, M., van Rooijen, N*., et al.* (2007). Monocyte subsets differentially employ CCR2, CCR5, and CX3CR1 to accumulate within atherosclerotic plaques. J Clin Invest *117*, 185-194.

Tahiliani, M., Koh, K.P., Shen, Y., Pastor, W.A., Bandukwala, H., Brudno, Y., Agarwal, S., Iyer, L.M., Liu, D.R., Aravind, L*., et al.* (2009). Conversion of 5-methylcytosine to 5-hydroxymethylcytosine in mammalian DNA by MLL partner TET1. Science *324*, 930-935.

Taleb, S., Tedgui, A., and Mallat, Z. (2015). IL-17 and Th17 cells in atherosclerosis: subtle and contextual roles. Arterioscler Thromb Vasc Biol *35*, 258-264.

Tannahill, G.M., Curtis, A.M., Adamik, J., Palsson-McDermott, E.M., McGettrick, A.F., Goel, G., Frezza, C., Bernard, N.J., Kelly, B., Foley, N.H*., et al.* (2013). Succinate is an inflammatory signal that induces IL-1beta through HIF-1alpha. Nature *496*, 238-242.

Tardif, J.C., Kouz, S., Waters, D.D., Bertrand, O.F., Diaz, R., Maggioni, A.P., Pinto, F.J., Ibrahim, R., Gamra, H., Kiwan, G.S*., et al.* (2019). Efficacy and Safety of Low-Dose Colchicine after Myocardial Infarction. N Engl J Med *381*, 2497-2505.

Tavakoli, S., and Asmis, R. (2012). Reactive oxygen species and thiol redox signaling in the macrophage biology of atherosclerosis. Antioxid Redox Signal *17*, 1785-1795.

Tavakoli, S., Downs, K., Short, J.D., Nguyen, H.N., Lai, Y., Jerabek, P.A., Goins, B., Toczek, J., Sadeghi, M.M., and Asmis, R. (2017). Characterization of Macrophage Polarization States Using Combined Measurement of 2-Deoxyglucose and Glutamine Accumulation: Implications for Imaging of Atherosclerosis. Arterioscler Thromb Vasc Biol *37*, 1840-1848.

Thangavelu, K., Pan, C.Q., Karlberg, T., Balaji, G., Uttamchandani, M., Suresh, V., Schuler, H., Low, B.C., and Sivaraman, J. (2012). Structural basis for the allosteric inhibitory mechanism of human kidney-type glutaminase (KGA) and its regulation by Raf-Mek-Erk signaling in cancer cell metabolism. Proc Natl Acad Sci U S A *109*, 7705-7710.

Thomas, D., and Apovian, C. (2017). Macrophage functions in lean and obese adipose tissue. Metabolism *72*, 120-143.

Thomas, G.D., Hanna, R.N., Vasudevan, N.T., Hamers, A.A., Romanoski, C.E., McArdle, S., Ross, K.D., Blatchley, A., Yoakum, D., Hamilton, B.A*., et al.* (2016). Deleting an Nr4a1 Super-Enhancer Subdomain Ablates Ly6C(low) Monocytes while Preserving Macrophage Gene Function. Immunity *45*, 975-987.

Thorp, E.B. (2010). Mechanisms of failed apoptotic cell clearance by phagocyte subsets in cardiovascular disease. Apoptosis *15*, 1124-1136.

Tilg, H., and Moschen, A.R. (2006). Adipocytokines: mediators linking adipose tissue, inflammation and immunity. Nat Rev Immunol *6*, 772-783.

Torres-Zamorano, V., Leibach, F.H., and Ganapathy, V. (1998). Sodium-dependent homo- and hetero-exchange of neutral amino acids mediated by the amino acid transporter ATB degree. Biochem Biophys Res Commun *245*, 824-829.

Townsend, L.K., Knuth, C.M., and Wright, D.C. (2017). Cycling our way to fit fat. Physiol Rep *5*.

Trayhurn, P., and Wood, I.S. (2004). Adipokines: inflammation and the pleiotropic role of white adipose tissue. Br J Nutr *92*, 347-355.

Truman, L.A., Ford, C.A., Pasikowska, M., Pound, J.D., Wilkinson, S.J., Dumitriu, I.E., Melville, L., Melrose, L.A., Ogden, C.A., Nibbs, R*., et al.* (2008). CX3CL1/fractalkine is released from apoptotic lymphocytes to stimulate macrophage chemotaxis. Blood *112*, 5026-5036.

Tsai, R.K., and Discher, D.E. (2008). Inhibition of "self" engulfment through deactivation of myosin-II at the phagocytic synapse between human cells. J Cell Biol *180*, 989-1003.

Tsou, C.L., Peters, W., Si, Y., Slaymaker, S., Aslanian, A.M., Weisberg, S.P., Mack, M., and Charo, I.F. (2007). Critical roles for CCR2 and MCP-3 in monocyte mobilization from bone marrow and recruitment to inflammatory sites. J Clin Invest *117*, 902-909.

Tsujita, K., Sugiyama, S., Sumida, H., Shimomura, H., Yamashita, T., Yamanaga, K., Komura, N., Sakamoto, K., Oka, H., Nakao, K*., et al.* (2015). Impact of Dual Lipid-Lowering Strategy With Ezetimibe and Atorvastatin on Coronary Plaque Regression in Patients With Percutaneous Coronary Intervention: The Multicenter Randomized Controlled PRECISE-IVUS Trial. J Am Coll Cardiol *66*, 495-507.

Tupone, D., Madden, C.J., and Morrison, S.F. (2014). Autonomic regulation of brown adipose tissue thermogenesis in health and disease: potential clinical applications for altering BAT thermogenesis. Front Neurosci *8*, 14.

Uchiyama, T., Fujita, T., Gukasyan, H.J., Kim, K.J., Borok, Z., Crandall, E.D., and Lee, V.H. (2008). Functional characterization and cloning of amino acid transporter B(0,+) (ATB(0,+)) in primary cultured rat pneumocytes. J Cell Physiol *214*, 645-654.

Ueha, S., Shand, F.H., and Matsushima, K. (2011). Myeloid cell population dynamics in healthy and tumor-bearing mice. Int Immunopharmacol *11*, 783-788.

Ugawa, S., Sunouchi, Y., Ueda, T., Takahashi, E., Saishin, Y., and Shimada, S. (2001). Characterization of a mouse colonic system B(0+) amino acid transporter related to amino acid absorption in colon. Am J Physiol Gastrointest Liver Physiol *281*, G365-370.

Ukropec, J., Anunciado, R.P., Ravussin, Y., Hulver, M.W., and Kozak, L.P. (2006). UCP1-independent thermogenesis in white adipose tissue of cold-acclimated Ucp1-/- mice. J Biol Chem *281*, 31894-31908.

Ussar, S., Lee, K.Y., Dankel, S.N., Boucher, J., Haering, M.F., Kleinridders, A., Thomou, T., Xue, R., Macotela, Y., Cypess, A.M*., et al.* (2014). ASC-1, PAT2, and P2RX5 are cell surface markers for white, beige, and brown adipocytes. Sci Transl Med *6*, 247ra103.

Utsunomiya-Tate, N., Endou, H., and Kanai, Y. (1996). Cloning and functional characterization of a system ASC-like Na+-dependent neutral amino acid transporter. J Biol Chem *271*, 14883-14890.

Vaidya, K., Arnott, C., Martinez, G.J., Ng, B., McCormack, S., Sullivan, D.R., Celermajer, D.S., and Patel, S. (2018). Colchicine Therapy and Plaque Stabilization in Patients With Acute Coronary Syndrome: A CT Coronary Angiography Study. JACC Cardiovasc Imaging *11*, 305-316.

Van der Donckt, C., Roth, L., Vanhoutte, G., Blockx, I., Bink, D.I., Ritz, K., Pintelon, I., Timmermans, J.P., Bauters, D., Martinet, W*., et al.* (2015a). Fibrillin-1 impairment enhances blood-brain barrier permeability and xanthoma formation in brains of apolipoprotein E-deficient mice. Neuroscience *295*, 11-22.

Van der Donckt, C., Van Herck, J.L., Schrijvers, D.M., Vanhoutte, G., Verhoye, M., Blockx, I., Van Der Linden, A., Bauters, D., Lijnen, H.R., Sluimer, J.C*., et al.* (2015b). Elastin fragmentation in atherosclerotic mice leads to intraplaque neovascularization, plaque rupture, myocardial infarction, stroke, and sudden death. Eur Heart J *36*, 1049-1058.

van der Vorst, E.P., Doring, Y., and Weber, C. (2015). Chemokines and their receptors in Atherosclerosis. J Mol Med (Berl) *93*, 963-971.

van der Wal, A.C., Becker, A.E., van der Loos, C.M., and Das, P.K. (1994). Site of intimal rupture or erosion of thrombosed coronary atherosclerotic plaques is characterized by an inflammatory process irrespective of the dominant plaque morphology. Circulation *89*, 36-44.

Van Eck, M., Herijgers, N., Vidgeon-Hart, M., Pearce, N.J., Hoogerbrugge, P.M., Groot, P.H., and Van Berkel, T.J. (2000). Accelerated atherosclerosis in C57Bl/6 mice transplanted with ApoE-deficient bone marrow. Atherosclerosis *150*, 71-80.

van Furth, R., Cohn, Z.A., Hirsch, J.G., Humphrey, J.H., Spector, W.G., and Langevoort, H.L. (1972). The mononuclear phagocyte system: a new classification of macrophages, monocytes, and their precursor cells. Bull World Health Organ *46*, 845-852.

van Gils, J.M., Derby, M.C., Fernandes, L.R., Ramkhelawon, B., Ray, T.D., Rayner, K.J., Parathath, S., Distel, E., Feig, J.L., Alvarez-Leite, J.I*., et al.* (2012). The neuroimmune guidance cue netrin-1 promotes atherosclerosis by inhibiting the emigration of macrophages from plaques. Nat Immunol *13*, 136-143.

Van Herck, J.L., De Meyer, G.R., Martinet, W., Van Hove, C.E., Foubert, K., Theunis, M.H., Apers, S., Bult, H., Vrints, C.J., and Herman, A.G. (2009). Impaired fibrillin-1 function promotes features of plaque instability in apolipoprotein E-deficient mice. Circulation *120*, 2478-2487.

van Hout, G.P., Bosch, L., Ellenbroek, G.H., de Haan, J.J., van Solinge, W.W., Cooper, M.A., Arslan, F., de Jager, S.C., Robertson, A.A., Pasterkamp, G*., et al.* (2017). The selective NLRP3-inflammasome inhibitor MCC950 reduces infarct size and preserves cardiac function in a pig model of myocardial infarction. Eur Heart J *38*, 828-836.

van Leeuwen, M., Gijbels, M.J., Duijvestijn, A., Smook, M., van de Gaar, M.J., Heeringa, P., de Winther, M.P., and Tervaert, J.W. (2008). Accumulation of myeloperoxidase-positive neutrophils in atherosclerotic lesions in LDLR-/- mice. Arterioscler Thromb Vasc Biol *28*, 84-89.

van Marken Lichtenbelt, W.D., Vanhommerig, J.W., Smulders, N.M., Drossaerts, J.M., Kemerink, G.J., Bouvy, N.D., Schrauwen, P., and Teule, G.J. (2009). Cold-activated brown adipose tissue in healthy men. N Engl J Med *360*, 1500-1508.

Vats, D., Mukundan, L., Odegaard, J.I., Zhang, L., Smith, K.L., Morel, C.R., Wagner, R.A., Greaves, D.R., Murray, P.J., and Chawla, A. (2006). Oxidative metabolism and PGC-1beta attenuate macrophage-mediated inflammation. Cell Metab *4*, 13-24.

Verreck, F.A., de Boer, T., Langenberg, D.M., Hoeve, M.A., Kramer, M., Vaisberg, E., Kastelein, R., Kolk, A., de Waal-Malefyt, R., and Ottenhoff, T.H. (2004). Human IL-23-producing type 1 macrophages promote but IL-10-producing type 2 macrophages subvert immunity to (myco)bacteria. Proc Natl Acad Sci U S A *101*, 4560-4565.

Verrey, F., Ristic, Z., Romeo, E., Ramadan, T., Makrides, V., Dave, M.H., Wagner, C.A., and Camargo, S.M. (2005). Novel renal amino acid transporters. Annu Rev Physiol *67*, 557-572.

Viaud, M., Ivanov, S., Vujic, N., Duta-Mare, M., Aira, L.E., Barouillet, T., Garcia, E., Orange, F., Dugail, I., Hainault, I.*, et al.* (2018). Lysosomal Cholesterol Hydrolysis Couples Efferocytosis to Anti-Inflammatory Oxysterol Production. Circ Res *122*, 1369-1384.

Villar, V.H., Merhi, F., Djavaheri-Mergny, M., and Duran, R.V. (2015). Glutaminolysis and autophagy in cancer. Autophagy *11*, 1198-1208.

Virchow, R. (1856). Der atheromatose Prozess der Arterien. Wien Med Wochenschr.

Virmani, R., Burke, A.P., Kolodgie, F.D., and Farb, A. (2002). Vulnerable plaque: the pathology of unstable coronary lesions. J Interv Cardiol *15*, 439-446.

Wahl, S., Yu, Z., Kleber, M., Singmann, P., Holzapfel, C., He, Y., Mittelstrass, K., Polonikov, A., Prehn, C., Romisch-Margl, W.*, et al.* (2012). Childhood obesity is associated with changes in the serum metabolite profile. Obes Facts *5*, 660-670.

Walker, D.K., Drummond, M.J., Dickinson, J.M., Borack, M.S., Jennings, K., Volpi, E., and Rasmussen, B.B. (2014). Insulin increases mRNA abundance of the amino acid transporter SLC7A5/LAT1 via an mTORC1-dependent mechanism in skeletal muscle cells. Physiol Rep *2*, e00238.

Wang, J.B., Erickson, J.W., Fuji, R., Ramachandran, S., Gao, P., Dinavahi, R., Wilson, K.F., Ambrosio, A.L., Dias, S.M., Dang, C.V.*, et al.* (2010). Targeting mitochondrial glutaminase activity inhibits oncogenic transformation. Cancer Cell *18*, 207-219.

Wang, Q.A., Tao, C., Gupta, R.K., and Scherer, P.E. (2013). Tracking adipogenesis during white adipose tissue development, expansion and regeneration. Nat Med *19*, 1338-1344.

Wang, R., Dillon, C.P., Shi, L.Z., Milasta, S., Carter, R., Finkelstein, D., McCormick, L.L., Fitzgerald, P., Chi, H., Munger, J.*, et al.* (2011). The transcription factor Myc controls metabolic reprogramming upon T lymphocyte activation. Immunity *35*, 871-882.

Wang, S., Pan, M.H., Hung, W.L., Tung, Y.C., and Ho, C.T. (2019). From white to beige adipocytes: therapeutic potential of dietary molecules against obesity and their molecular mechanisms. Food Funct *10*, 1263-1279.

Wang, W., and Seale, P. (2016). Control of brown and beige fat development. Nat Rev Mol Cell Biol *17*, 691-702.

Wang, Y., and Watford, M. (2007). Glutamine, insulin and glucocorticoids regulate glutamine synthetase expression in C2C12 myotubes, Hep G2 hepatoma cells and 3T3 L1 adipocytes. Biochim Biophys Acta *1770*, 594-600.

Wanschel, A., Seibert, T., Hewing, B., Ramkhelawon, B., Ray, T.D., van Gils, J.M., Rayner, K.J., Feig, J.E., O'Brien, E.R., Fisher, E.A.*, et al.* (2013). Neuroimmune guidance cue Semaphorin 3E is expressed in atherosclerotic plaques and regulates macrophage retention. Arterioscler Thromb Vasc Biol *33*, 886-893.

Watts, B.A., 3rd, and Good, D.W. (1994). Effects of ammonium on intracellular pH in rat medullary thick ascending limb: mechanisms of apical membrane NH4+ transport. J Gen Physiol *103*, 917-936.

Wei, Q., and Frenette, P.S. (2018). Niches for Hematopoietic Stem Cells and Their Progeny. Immunity *48*, 632-648.

Weinstock, A., Brown, E.J., Garabedian, M.L., Pena, S., Sharma, M., Lafaille, J., Moore, K.J., and Fisher, E.A. (2019). Single-Cell RNA Sequencing of Visceral Adipose Tissue Leukocytes Reveals that Caloric Restriction Following Obesity Promotes the Accumulation of a Distinct Macrophage Population with Features of Phagocytic Cells. Immunometabolism *1*.

Weisberg, S.P., McCann, D., Desai, M., Rosenbaum, M., Leibel, R.L., and Ferrante, A.W., Jr. (2003). Obesity is associated with macrophage accumulation in adipose tissue. J Clin Invest *112*, 1796-1808.

Welbourne, T.C. (1979). Ammonia production and glutamine incorporation into glutathione in the functioning rat kidney. Can J Biochem *57*, 233-237.

Wellen, K.E., and Hotamisligil, G.S. (2003). Obesity-induced inflammatory changes in adipose tissue. J Clin Invest *112*, 1785-1788.

Wellen, K.E., Lu, C., Mancuso, A., Lemons, J.M., Ryczko, M., Dennis, J.W., Rabinowitz, J.D., Coller, H.A., and Thompson, C.B. (2010). The hexosamine biosynthetic pathway couples growth factor-induced glutamine uptake to glucose metabolism. Genes Dev *24*, 2784-2799.

Wentworth, J.M., Naselli, G., Brown, W.A., Doyle, L., Phipson, B., Smyth, G.K., Wabitsch, M., O'Brien, P.E., and Harrison, L.C. (2010). Pro-inflammatory CD11c+CD206+ adipose tissue macrophages are associated with insulin resistance in human obesity. Diabetes *59*, 1648-1656.

Westerterp, M., Murphy, A.J., Wang, M., Pagler, T.A., Vengrenyuk, Y., Kappus, M.S., Gorman, D.J., Nagareddy, P.R., Zhu, X., Abramowicz, S.*, et al.* (2013). Deficiency of ATP-binding cassette transporters A1 and G1 in macrophages increases inflammation and accelerates atherosclerosis in mice. Circ Res *112*, 1456-1465.

Westerterp, M., van der Hoogt, C.C., de Haan, W., Offerman, E.H., Dallinga-Thie, G.M., Jukema, J.W., Havekes, L.M., and Rensen, P.C. (2006). Cholesteryl ester transfer protein

decreases high-density lipoprotein and severely aggravates atherosclerosis in APOE*3-Leiden mice. Arterioscler Thromb Vasc Biol *26*, 2552-2559.

Wiktor-Jedrzejczak, W., and Gordon, S. (1996). Cytokine regulation of the macrophage (M phi) system studied using the colony stimulating factor-1-deficient op/op mouse. Physiol Rev *76*, 927-947.

Wilborn, C., Beckham, J., Campbell, B., Harvey, T., Galbreath, M., La Bounty, P., Nassar, E., Wismann, J., and Kreider, R. (2005). Obesity: prevalence, theories, medical consequences, management, and research directions. J Int Soc Sports Nutr *2*, 4-31.

Williams, K.J., and Tabas, I. (1995). The response-to-retention hypothesis of early atherogenesis. Arterioscler Thromb Vasc Biol *15*, 551-561.

Williams, K.V., and Kelley, D.E. (2000). Metabolic consequences of weight loss on glucose metabolism and insulin action in type 2 diabetes. Diabetes Obes Metab *2*, 121-129.

Winkels, H., Ehinger, E., Vassallo, M., Buscher, K., Dinh, H.Q., Kobiyama, K., Hamers, A.A.J., Cochain, C., Vafadarnejad, E., Saliba, A.E.*, et al.* (2018). Atlas of the Immune Cell Repertoire in Mouse Atherosclerosis Defined by Single-Cell RNA-Sequencing and Mass Cytometry. Circ Res *122*, 1675-1688.

Wischmeyer, P.E. (2019). The glutamine debate in surgery and critical care. Curr Opin Crit Care *25*, 322-328.

Wischmeyer, P.E., Kahana, M., Wolfson, R., Ren, H., Musch, M.M., and Chang, E.B. (2001). Glutamine reduces cytokine release, organ damage, and mortality in a rat model of endotoxemia. Shock *16*, 398-402.

Wise, D.R., and Thompson, C.B. (2010). Glutamine addiction: a new therapeutic target in cancer. Trends Biochem Sci *35*, 427-433.

Wolf, Y., Boura-Halfon, S., Cortese, N., Haimon, Z., Sar Shalom, H., Kuperman, Y., Kalchenko, V., Brandis, A., David, E., Segal-Hayoun, Y.*, et al.* (2017). Brown-adipose-tissue macrophages control tissue innervation and homeostatic energy expenditure. Nat Immunol *18*, 665-674.

Wu, Z., Puigserver, P., Andersson, U., Zhang, C., Adelmant, G., Mootha, V., Troy, A., Cinti, S., Lowell, B., Scarpulla, R.C.*, et al.* (1999). Mechanisms controlling mitochondrial biogenesis and respiration through the thermogenic coactivator PGC-1. Cell *98*, 115-124.

Xiao, M., Yang, H., Xu, W., Ma, S., Lin, H., Zhu, H., Liu, L., Liu, Y., Yang, C., Xu, Y.*, et al.* (2012). Inhibition of alpha-KG-dependent histone and DNA demethylases by fumarate and succinate that are accumulated in mutations of FH and SDH tumor suppressors. Genes Dev *26*, 1326-1338.

Xu, H., Barnes, G.T., Yang, Q., Tan, G., Yang, D., Chou, C.J., Sole, J., Nichols, A., Ross, J.S., Tartaglia, L.A.*, et al.* (2003). Chronic inflammation in fat plays a crucial role in the development of obesity-related insulin resistance. J Clin Invest *112*, 1821-1830.

Xu, H., Jiang, J., Chen, W., Li, W., and Chen, Z. (2019). Vascular Macrophages in Atherosclerosis. J Immunol Res *2019*, 4354786.

Xu, T., Stewart, K.M., Wang, X., Liu, K., Xie, M., Ryu, J.K., Li, K., Ma, T., Wang, H., Ni, L.*, et al.* (2017). Metabolic control of TH17 and induced Treg cell balance by an epigenetic mechanism. Nature *548*, 228-233.

Yamamoto, R., Morita, Y., Ooehara, J., Hamanaka, S., Onodera, M., Rudolph, K.L., Ema, H., and Nakauchi, H. (2013). Clonal analysis unveils self-renewing lineage-restricted progenitors generated directly from hematopoietic stem cells. Cell *154*, 1112-1126.

Yamauchi, T., Kamon, J., Minokoshi, Y., Ito, Y., Waki, H., Uchida, S., Yamashita, S., Noda, M., Kita, S., Ueki, K.*, et al.* (2002). Adiponectin stimulates glucose utilization and fatty-acid oxidation by activating AMP-activated protein kinase. Nat Med *8*, 1288-1295.

Yan, H., Zhang, Y., Lv, S.J., Wang, L., Liang, G.P., Wan, Q.X., and Peng, X. (2012). Effects of glutamine treatment on myocardial damage and cardiac function in rats after severe burn injury. Int J Clin Exp Pathol *5*, 651-659.

Yang, C., Li, Y.S., Wang, Q.X., Huang, K., Wei, J.W., Wang, Y.F., Zhou, J.H., Yi, K.K., Zhang, K.L., Zhou, B.C.*, et al.* (2017). EGFR/EGFRvIII remodels the cytoskeleton via epigenetic silencing of AJAP1 in glioma cells. Cancer Lett *403*, 119-127.

Yang, L., Brooks, C.R., Xiao, S., Sabbisetti, V., Yeung, M.Y., Hsiao, L.L., Ichimura, T., Kuchroo, V., and Bonventre, J.V. (2015). KIM-1-mediated phagocytosis reduces acute injury to the kidney. J Clin Invest *125*, 1620-1636.

Yoon, J.H., Kim, I.J., Kim, H., Kim, H.J., Jeong, M.J., Ahn, S.G., Kim, S.A., Lee, C.H., Choi, B.K., Kim, J.K.*, et al.* (2005). Amino acid transport system L is differently expressed in human normal oral keratinocytes and human oral cancer cells. Cancer Lett *222*, 237-245.

Yuneva, M., Zamboni, N., Oefner, P., Sachidanandam, R., and Lazebnik, Y. (2007). Deficiency in glutamine but not glucose induces MYC-dependent apoptosis in human cells. J Cell Biol *178*, 93-105.

Yurdagul, A., Jr., Subramanian, M., Wang, X., Crown, S.B., Ilkayeva, O.R., Darville, L., Kolluru, G.K., Rymond, C.C., Gerlach, B.D., Zheng, Z.*, et al.* (2020). Macrophage Metabolism of Apoptotic Cell-Derived Arginine Promotes Continual Efferocytosis and Resolution of Injury. Cell Metab *31*, 518-533 e510.

Yvan-Charvet, L., Pagler, T.A., Seimon, T.A., Thorp, E., Welch, C.L., Witztum, J.L., Tabas, I., and Tall, A.R. (2010). ABCA1 and ABCG1 protect against oxidative stress-induced macrophage apoptosis during efferocytosis. Circ Res *106*, 1861-1869.

Zacharopoulou, N., Tsapara, A., Kallergi, G., Schmid, E., Tsichlis, P.N., Kampranis, S.C., and Stournaras, C. (2018). The epigenetic factor KDM2B regulates cell adhesion, small rho GTPases, actin cytoskeleton and migration in prostate cancer cells. Biochim Biophys Acta Mol Cell Res *1865*, 587-597.

Zannis, V.I., and Breslow, J.L. (1985). Genetic mutations affecting human lipoprotein metabolism. Adv Hum Genet *14*, 125-215, 383-126.

Zannis, V.I., Chroni, A., Kypreos, K.E., Kan, H.Y., Cesar, T.B., Zanni, E.E., and Kardassis, D. (2004). Probing the pathways of chylomicron and HDL metabolism using adenovirus-mediated gene transfer. Curr Opin Lipidol *15*, 151-166.

Zernecke, A., Winkels, H., Cochain, C., Williams, J.W., Wolf, D., Soehnlein, O., Robbins, C.S., Monaco, C., Park, I., McNamara, C.A*., et al.* (2020). Meta-Analysis of Leukocyte Diversity in Atherosclerotic Mouse Aortas. Circ Res *127*, 402-426.

Zhang, S., Weinberg, S., DeBerge, M., Gainullina, A., Schipma, M., Kinchen, J.M., Ben-Sahra, I., Gius, D.R., Yvan-Charvet, L., Chandel, N.S*., et al.* (2019). Efferocytosis Fuels Requirements of Fatty Acid Oxidation and the Electron Transport Chain to Polarize Macrophages for Tissue Repair. Cell Metab *29*, 443-456 e445.

Zhao, L., Huang, Y., and Zheng, J. (2013). STAT1 regulates human glutaminase 1 promoter activity through multiple binding sites in HIV-1 infected macrophages. PLoS One *8*, e76581.

Zhao, R.Z., Jiang, S., Zhang, L., and Yu, Z.B. (2019). Mitochondrial electron transport chain, ROS generation and uncoupling (Review). Int J Mol Med *44*, 3-15.

Zheng, C., Yang, Q., Cao, J., Xie, N., Liu, K., Shou, P., Qian, F., Wang, Y., and Shi, Y. (2016). Local proliferation initiates macrophage accumulation in adipose tissue during obesity. Cell Death Dis *7*, e2167.

Zizzo, G., and Cohen, P.L. (2013). IL-17 stimulates differentiation of human anti-inflammatory macrophages and phagocytosis of apoptotic neutrophils in response to IL-10 and glucocorticoids. J Immunol *190*, 5237-5246.

Zizzo, G., Hilliard, B.A., Monestier, M., and Cohen, P.L. (2012). Efficient clearance of early apoptotic cells by human macrophages requires M2c polarization and MerTK induction. J Immunol *189*, 3508-3520.